Waikato Regional Council Technical Report 2016/19

Mapping residence times in west coast estuaries of the Waikato region

www.waikatoregion.govt.nz
ISSN 2230-4355 (Print)
ISSN 2230-4363 (Online)

Waikato
REGIONAL COUNCIL
Te Kaunihera ā Rohe o Waikato

Prepared by:
Dougal Greer, Ed Atkin, Shaw Mead, Tim Haggitt and Sam O'Neill
eCoast

For:
Waikato Regional Council
Private Bag 3038
Waikato Mail Centre
HAMILTON 3240

August 2016

Document #: 8997234

Peer reviewed by:
Hannah Jones and
Stephen Hunt Date August 2016

Approved for release by:
Dominique Noiton Date September 2016

Disclaimer

This technical report has been prepared for the use of Waikato Regional Council as a reference document and as such does not constitute Council's policy.

The accuracy of information and model simulations presented in this document is entirely reliant on the accuracy and completeness of available information. Furthermore, the models described in this document may not be suitable for any purpose(s) other than those specified.

Council requests that if excerpts or inferences are drawn from this document for further use by individuals or organisations, due care should be taken to ensure that the appropriate context has been preserved, and is accurately reflected and referenced in any subsequent spoken or written communication.

While Waikato Regional Council has exercised all reasonable skill and care in controlling the contents of this report, Council accepts no liability in contract, tort or otherwise, for any loss, damage, injury or expense (whether direct, indirect or consequential) arising out of the provision of this information or its use by you or any other party.

Mapping Residence Times in West Coast Estuaries of the Waikato Region

Report prepared for Waikato Regional Council, August 2016

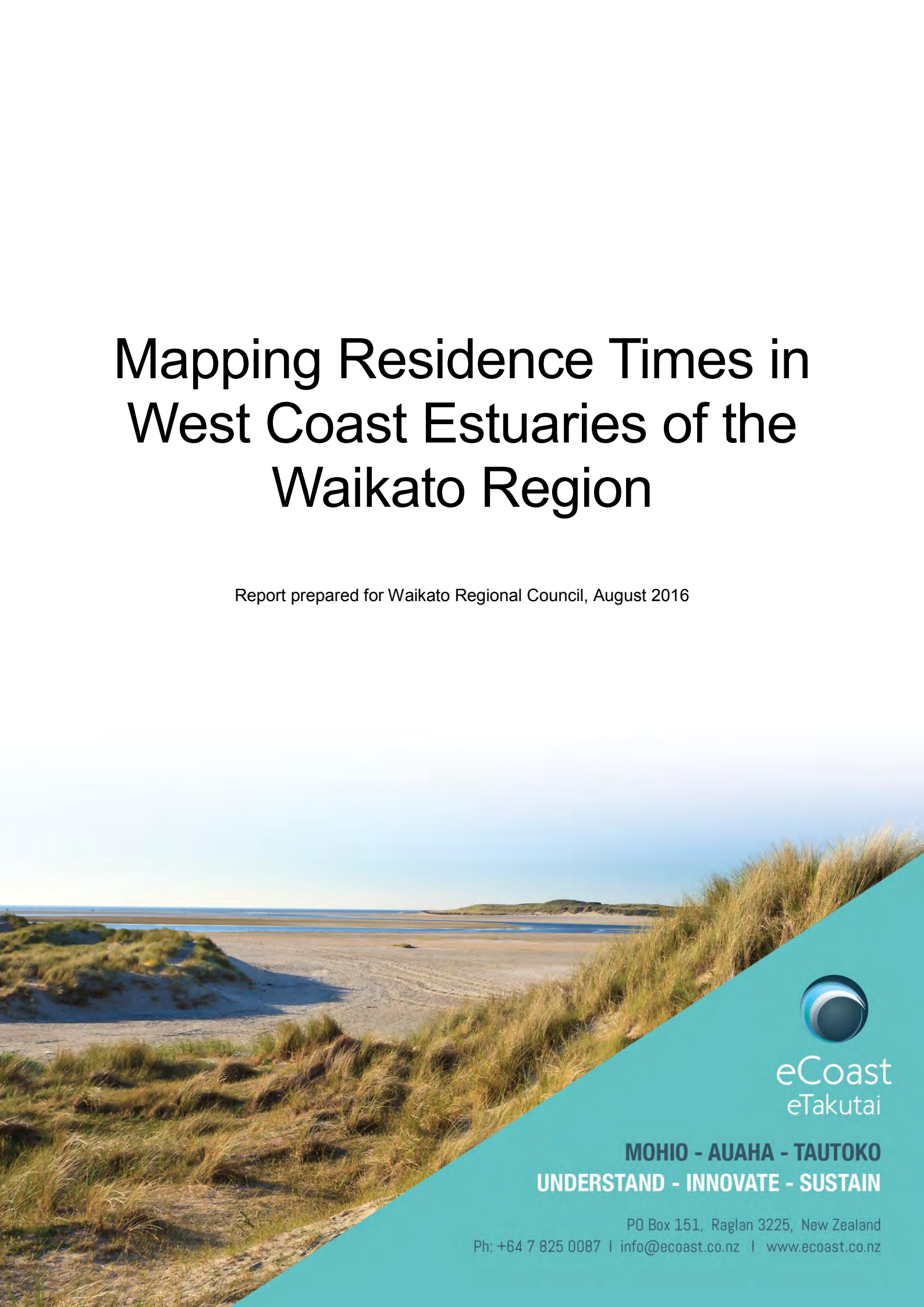

eCoast
eTakutai

MOHIO - AUAHA - TAUTOKO
UNDERSTAND - INNOVATE - SUSTAIN

PO Box 151, Raglan 3225, New Zealand
Ph: +64 7 825 0087 | info@ecoast.co.nz | www.ecoast.co.nz

Mapping Residence Times in West Coast Estuaries of the Waikato Region

Report Status

Version	Date	Status	Approved by
V1	10/04/2016	Draft	JCB
V2	25/05/2016	Final	JCB

It is the responsibility of the reader to verify the version number of this report.

Authors

Dougal Greer, *MSc*

Ed Atkin, *HND, MSc (Hons)*

Shaw Mead *BSc, MSc (Hons), PhD*

Tim Haggitt *BSc, MSc (Hons), PhD*

Sam O'Neill *BSc, MSc (Hons)*

Executive Summary

Quantifying residence times in estuaries (i.e. how long water is retained within different parts of these water bodies) can improve our understanding of the fate of discharges within estuarine systems. Until now, relatively little work has been undertaken to investigate how long water takes to flow through estuaries on the Waikato region's west coast. This report describes the development of a methodology, or proof-of-concept, for mapping residence times in the seven largest estuaries along the Waikato west coast, namely Waikato River estuary, Whaingaroa (Raglan) Harbour, Aotea Harbour, Kawhia Harbour, Marokopa River estuary, Awakino River estuary and Mokau River estuary.

This study involved the development of hydrodynamic models, which were then used to estimate residence times in the seven estuaries. The main body of this report describes the use of the hydrodynamic models to calculate residence times. Detailed descriptions of the fieldwork programme, and of the development and calibration of the models, are included as appendices.

The fieldwork was undertaken between 17th August 2015 and 16th December 2015. The data collected included current speed, water level, salinity, temperature, and topographic and bathymetric (sea floor topography) data in each of the seven estuaries. In Whaingaroa Harbour only salinity and temperature data were collected because there were already sea level, current and bathymetric data available.

The instruments were deployed for six weeks in each estuary with checks made in the middle of the deployments to download the data and clean the instruments where possible. Bathymetric data were collected by hydrographic survey undertaken using a jet ski fitted with a depth sounder and using an RTK GPS system where it was practical to do so. Topographic (intertidal and foreshore) data were collected on foot at Marokopa, Awakino and Mokau River estuaries. At the other estuaries sufficient topographic data already exists in the form of LiDAR data.

The field data have been used to develop partially calibrated hydrodynamic models for each estuary. Estimating freshwater input into the estuaries was achieved in one of two ways, depending on the type of estuary. For the drowned river valley type estuaries (Whaingaroa, Aotea and Kawhia Harbours), the INCA catchment model was used to simulate daily river flow based on measured meteorological data and land use data specific to each sub-catchment. The model was calibrated against available gauged flow data. Modelled river flow was replaced with measured data, where available. For the tidal river type estuaries (Waikato River, Marokopa River, Awakino River and Mokau River estuaries), which are fed by a single

river, measured data from flow gauges and deployed instruments was used to estimate daily river flow.

The hydrodynamic modelling was undertaken using Delft-Flow and used a nesting procedure known as Domain Decomposition (DD) to create a series of 2D models. In each estuary modelled sea level, currents and salinity were assessed against measured data to determine the accuracy of the model.

The Waikato River estuary was the most challenging of the estuaries to simulate. The riverine effect on sea level was well represented and currents were in phase, but current speeds were under-estimated by the model.

The three drowned river valley estuaries (Whaingaroa, Kawhia and Aotea Harbours) calibrated quite well for currents and sea level. It should be noted that these estuaries are complex and dendritic, and more field data would have been useful for a more comprehensive calibration. In particular, there was only one calibration site in Aotea Harbour.

In the three tidal river estuaries to the south (Marokopa, Awakino and Mokau River estuaries), agreement between measured and modelled data for sea level, currents and salinity was variable, possibly because salinity stratification may be an important process in these estuaries (which cannot be simulated using a 2D model).

Although the models could be improved, they have been used to provide a first-order estimate of residence times for the seven estuaries. The methodology for estimating residence times involves the instantaneous uniform release of a conservative tracer within the estuary after a suitable spin up time. The release area is defined as the area inshore of a line drawn across the estuary mouth. The tracer is tracked throughout the remainder of the model run and does not affect the modelled hydrodynamics. As the estuary is inundated by water introduced from the sea and the surrounding rivers, the concentration of the tracer is reduced. Once the tracer concentration in a given cell falls below a predefined threshold of the original value (set at 95% for this study) the cell is considered to have been flushed. The tidal signal is removed from the time series of tracer concentration in each cell using low pass filtering prior to calculating residence time. For each estuary, residence times were investigated under low, medium and high river flow scenarios.

The results highlight the reduced residence time in the tidal river estuaries compared with the drowned river valley estuaries. Overall, increased river flow led to decreased residence time. The tidal river estuary residence times are more sensitive to river flow than drowned river valley estuaries. In general, larger estuaries had longer residence times than smaller estuaries.

For the tidal river estuaries, the residence time was longer in the Waikato and Mokau River estuaries than in Awakino or Marokopa River estuaries. For all of the tidal river estuaries under medium flow conditions, residence times were less than three days and less than one day for most of the Marokopa and Awakino River estuaries.

For the drowned river valley estuaries under medium flow conditions, the longest residence times were observed in Whaingaroa Harbour (35 to 45 days in the upper estuary) followed by Kawhia Harbour (30 to 35 days in the upper estuary). The difference in residence times can likely be attributed to increased flushing due to the larger tidal prism for Kawhia Harbour compared with Whaingaroa Harbour, relative to their high tide volumes. Aotea Harbour had a residence time of 10 to 15 days throughout the main body of the estuary under medium flow conditions. This study indicates that in the drowned river valley estuaries there is a gradient in residence times from the mouth to the upper estuary with longer residence times in the upper estuary.

A sensitivity analysis investigated the effect of wind, tidal release times, and residence time thresholds on residence times in Whaingaroa Harbour. Prevailing south-westerly and north-easterly winds resulted in decreased residence times, and the choice of residence time threshold had a marked effect on estimated residence time. This sensitivity analysis highlights that the residence times estimated in this study should be interpreted with caution. Whilst the results are likely to be useful for assessing the relative difference in residence time between estuaries and between different parts of the estuaries, further work is required to assess the validity of the results as absolute measures of residence times.

It is important to note that this study provides a proof-of-concept only for mapping residence times in estuaries. The hydrodynamic models were relatively simple and only partially calibrated. As such, the results are considered indicative, but the models and methodology can be refined in the future to improve the accuracy of the residence time estimates. For example, the hydrodynamic models could be refined by extending the models to 3D (particularly in estuaries where stratification is likely to be an important process), and by further model calibration and validation, which would require the collection of more field data. Furthermore, refining the catchment models (e.g. by measuring river flow in ungauged catchments) would improve estimates of freshwater inputs to the estuaries, which would likely improve the residence time estimates. Further work is also required to investigate methodologies that use alternative definitions of residence times and/or the dilution of freshwater in estuaries, and to place each of these different definitions of residence times in the appropriate context(s) for resource management.

Contents

Figures

Tables

1 Introduction

Quantifying residence times in estuaries (i.e. how long water is retained within different parts of these water bodies) can improve our understanding of the fate of discharges within estuarine systems. Until now, relatively little work has been undertaken to investigate how long water takes to flow through estuaries on the Waikato region's west coast.

This study presented here provides proof of concept for determining residence times in the seven largest estuaries along the Waikato west coast, namely Waikato River estuary, Whaingaroa (Raglan) Harbour, Aotea Harbour, Kawhia Harbour, Marokopa River estuary, Awakino River estuary and Mokau River estuary. The locations of each of these estuaries are shown in Figure 1.1.

This study involved the development of hydrodynamic models, which were then used to estimate residence times in the estuaries. Fieldwork was also undertaken to collect data suitable for developing the hydrodynamic models.

The fieldwork involved measuring current speeds, water level, salinity, temperature, topographic and bathymetric (sea floor topography) data and is described in Appendix A. The data from the fieldwork campaign has been used to develop numerical models of each estuary (Appendix B). The models simulate inflow into the estuaries from rivers and streams, and are used here to describe how efficiently different parts of the estuaries are flushed with introduced water from the ocean or from rivers.

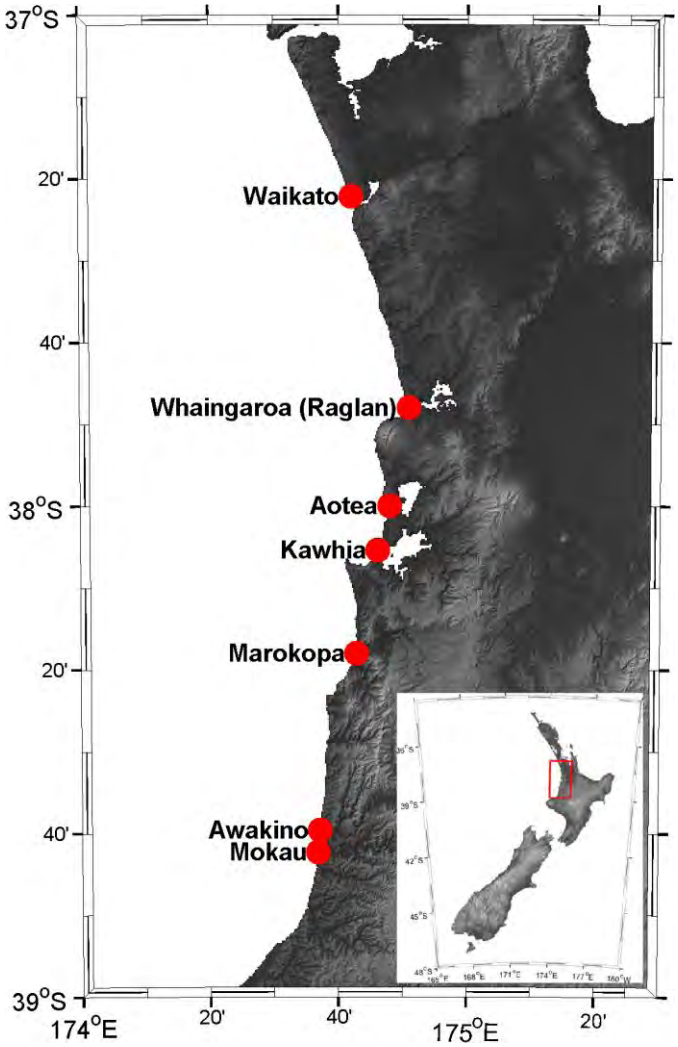

Figure 1.1: Locations of the seven estuaries modelled in this study (image: Courtesy NASA/JPL-Caltech).

2 Residence Times

The aim of this work was to develop a methodology for the calculation of residence times in estuaries in the Waikato. The capacity for an estuary to flush is spatially variable, and a suitable metric needs to reflect this if it is to be used to identify regions of an estuary which are most at risk from inflowing pollutants from surrounding rivers. We use the concept of 'residence time', generally defined as *the required time to flush a given fraction (e.g. 95%) of a conservative constituent from the modelled part of an estuary t*o quantify this. Residence time is discussed further in Section 2.2.

The estuaries in this study comprise of four tidal river estuaries (Waikato River estuary, Marokopa River estuary, Awakino River estuary and Mokau River estuary) and three drowned river valley estuaries (Whaingaroa (Raglan) Harbour, Aotea Harbour and Kawhia Harbour). The calculation of residence time makes use of the calibrated hydrodynamic models described in Appendix B and these models are briefly summarised in Section 2.1.

The majority of this section examines the variability in residence times within each estuary. In the plotted results that follow colour scales representative of residence times are consistent for each estuary, but differ between estuaries. The final part of this section (Section 2.11) uses a consistent colour scheme to compare residence items between estuaries.

2.1 Summary of Hydrodynamic Modelling

This section provides a short summary of the hydrodynamic models used to calculate residence times in this study and they are described in detail in Appendix B.

The modelling methodology used an open source hydrodynamic model called Delft3D-Flow (Deltares, 2013). The hydrodynamic models were 2D and simulated sea level, currents, salinity and river flow taken from gauged data, where it was available, and a purpose built calibrated catchment model. The models were driven by tides, wind, atmospheric pressure and salinity boundaries. The models did not include temperature. The modelling setup used a system of dynamically coupled nested rectilinear model grids using a process known as Domain Decomposition (DD). The system of bathymetric grids started with a common large scale west coast grid which covered the Waikato west coast in its entirety and beyond. Within this, a series of nested grids were embedded which led to high-resolution local bathymetric grids for each of the seven estuaries. Bathymetry data was sourced from bathymetry surveys undertaken as part of this project (Appendix A), digitised data from aerial photography, multibeam data, LIDAR data, hydrographic charts and GEBCO data (Becker *et al.* 2009).

The hydrodynamic models were calibrated by comparing model output with measured sea levels, current and salinity time series data from the fieldwork component of this project

(Appendix A) and from other studies. The calibration process made use of skill scores for quantifying model error.

The results of the hydrodynamic modelling were used to calculate estuary volume at high and low tide, estuary surface area at high and low tide, tidal prism and mean daily river flow. Mean river flow was calculated based on 7 years of flow data from 2008 until 2015. These metrics are presented in Table 2.1. These physical descriptors show that the tidal river estuaries are quite different in form to the drowned river valley estuaries. The tidal river estuaries have a larger daily river flow relative to the tidal prism and estuary volume. Also the difference in surface area between high and low tide is larger for the drowned river valley estuaries.

Table 2.1: Summary of physical characteristics of the seven estuaries.

Estuary	High Tide Area (km^2)	Low Tide Area (km^2)	High Tide Volume (m^3)	Low Tide Volume (m^3)	Tidal Prism (m^3)	Mean Daily River Flow ($m^3\ day^{-1}$)
Waikato River estuary	18.03	12.39	54.124×10^6	18.486×10^6	35.637×10^6	32.763×10^6
Whaingaroa (Raglan) Harbour	32.96	9.01	101.442×10^6	30.215×10^6	71.227×10^6	1.281×10^6
Aotea harbour	32	6	81.444×10^6	13.663×10^6	67.781×10^6	1.328×10^6
Kawhia Harbour	68	18	205.862×10^6	41.326×10^6	164.536×10^6	1.530×10^6
Marokopa River estuary	0.60	0.38	1.024×10^6	0.329×10^6	0.695×10^6	4.929×10^6
Awakino River estuary	0.60	0.35	1.379×10^6	0.381×10^6	0.998×10^6	1.745×10^6
Mokau River estuary	1.66	0.64	4.407×10^6	0.922×10^6	3.485×10^6	4.238×10^6

2.2 Defining the Residence Time

The definition of residence time varies, and this has been repeatedly noted by various authors (e.g. Sheldon and Alber, 2002 and Zimmerman, 1976). Here we use the concept of Estuarine Residence Time (ERT) provided by Miller and McPherson (1991) which they define as:

> *[The] time to flush a given fraction (e.g. 95%) of a conservative constituent from the modelled part of an estuary.*

In reality many pollutants are not conservative. For example, suspended solids can settle out and nutrients can be taken up through biological and chemical processes. However, the use of a conservative tracer provides a broad measure of the spatial variability in residence time throughout an estuary.

Other methodologies have calculated residence time using box models which compartmentalise estuaries into sub-regions and calculate residence times for each box (e.g. Sheldon and Alber, 2002). With the advent of high resolution numerical models for simulating hydrodynamic processes, residence time may be frequently calculated at the resolution of the hydrodynamic model. This is commonly achieved using a Lagrangian approach which involves releasing simulated particles and tracking them until they leave the estuary (e.g. Liu *et al.*, 2007, Defne and Ganju, 2014 and Aikman and Lanerolle, 2004). This approach places emphasis on the time taken for water released at a given location in an estuary to leave the estuary. This can be a valuable metric especially when considering estuary wide processes such as algal blooms.

However, here we are concerned with how long it takes for a given location in the estuary to be flushed with water introduced from other sources. To achieve this, we have followed a Eulerian approach used by Pokavanich and Alosairi (2014) and Lee and Park (2013). This method involves the instantaneous uniform release of a conservative tracer within the estuary after a suitable spin up time. The release area was defined as the area inshore of a line drawn across the estuary mouth. The tracer was tracked throughout the remainder of the model run. The tracer did not affect the hydrodynamics of the model. As the estuary was inundated by water introduced from the sea and the surrounding rivers, the concentration of the tracer reduced. Any of the tracer that exited the estuary on the outgoing tide could re-enter on subsequent incoming tides. Once the tracer concentration in a given cell fell below a predefined threshold the cell was considered to have been flushed. We used a threshold of 95%.

The decrease in tracer concentration in a given cell was not monotonic, but rather oscillated mainly due to tidal effects and also due to wind and pressure effects. The tidal signal was removed using low pass filtering. This was achieved by using orthogonal wavelet

decomposition with a threshold period of 12 hours. This left the monotonically decreasing signal of tracer concentration which was compared with the threshold to establish the residence time in each cell. For each estuary, residence time was calculated for different river flow conditions with no wind (see Section 2.3). A sensitivity analysis was used to explore the effect of wind, release time (relative to tidal phase) and different residence time thresholds (Section 3.3).

2.3 River Flow Boundary Conditions

Residence times are expected to change under different meteorological and oceanographic conditions. Among these, river flow conditions are expected to change the rate at which estuary water is replaced. For each estuary, residence times were investigated under different flow rates corresponding to low, medium and high river flow taken to be the 90th (Q10), 50th (Q50 or median) and 10th (Q90) percentile flows respectively. Flow rates were calculated from complete years of data. Available data for calculating flow rates differed from location to location. Calculations of low, medium and high flows used gauged river flow (Figure 2.1) scaled to account for inflow from the entire catchment, and modelled river flows where this was not available (Appendix B). The flow rates are summarised in Table 2.2. The flows were applied as uniform river flow in the models which were used to calculate residence times. While this is not an entirely realistic representation of river flow, particularly for estuaries with longer residence times, it served the purpose of illustrating the effect of different flow conditions on residence time.

For the Waikato River estuary, flow conditions were estimated from data recorded by the Mercer flow gauge (see Figure 2.1) which was also used to create model boundary conditions. Flow rates were established by analysis of flow rates between 1 Jan 2002 and 1 Jan 2015.

In Whaingaroa Harbour percentile flows for the Waingaro River were estimated by analyses of flow data recorded by the Waingaro flow gauge (Figure 2.1) between 1 Jan 2002 and 1 Jan 2015. Relative flow rates for the other 14 rivers included in the model were estimated by examination of modelled river flow (Appendix B). Median flow rates were calculated for each of the 15 rivers to establish the flow for each river relative to the modelled Waingaro flow. The corresponding low, medium and high flow rates were estimated by scaling these values relative to flow rates calculated from the gauged Waingaro River flow.

There is no gauged river flow in Aotea Harbour so modelled river flow data (from 2007 to 2015 inclusive) were used to estimate low, medium and high flow. Median flows were calculated for each of the 25 rivers and streams included in the model.

Low, medium and high flow rates for Kawhia Habrour were calculated using the same method that was used for Whaingaroa Harbour. In this case median flows were calculated from the

modelled river flow and scaled using percentile flow rates from the Oparau flow gauge (2008 to 2014 inclusive).

For the Marokopa River estuary the flow data from the Marokopa flow gauge (Figure 2.1) was used to estimate low, medium and high flow rates in the river. Flows were calculated from the scaled river flow from 2007 to 2015 inclusive that was used in the hydrodynamic model.

Both Awakino and Mokau low medium and high flows were calculated from the Awakino flow gauge data (2007 to 2015 inclusive) that was scaled for use in the hydrodynamic model.

Table 2.2: Total riverine discharge (m^3 s^{-1}) used in scenarios for each estuary.

Estuary	Low (Q90) Flow	Medium (Q50) Flow	High (Q10) Flow
Waikato River estuary	219	339	628
Whaingaroa (Raglan) Harbour	1.2	5.3	25.7
Aotea harbour	0.9	4.4	15.4
Kawhia Harbour	4.1	11.8	39.89
Marokopa River estuary	4.4	13.0	56.8
Awakino River estuary	3.8	11.2	49
Mokau River estuary	9.2	27.2	119.1

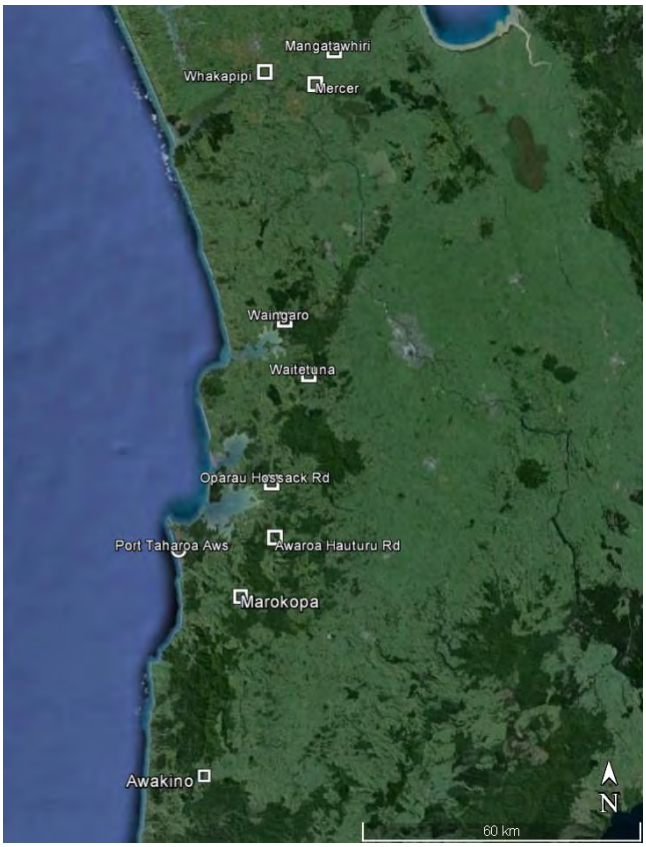

Figure 2.1: River flow gauges and a single AWS (Port Taharoa) used in this study.

2.4 Waikato River Estuary

The Waikato River estuary is fed by the Waikato River, the longest river in New Zealand. Though this is a tidal river estuary, the tidal influence of the river extends beyond the upstream model boundary and can be seen in the flow gauge record at the Mercer tide gauge (see Figure 2.1) some 43 km from the estuary mouth. Residence time maps are shown for each flow condition (low, medium and high flow) in Figure 2.2, Figure 2.3 and Figure 2.4. At a constant low flow, the residence time was at its maximum of approximately 4.5 days at the mouth of the harbour and < 0.5 days at the upstream boundary of the river. For the medium and high flow cases the residence times reduced such that for high flows almost all cells in the estuary had a residence time < 2.5 days.

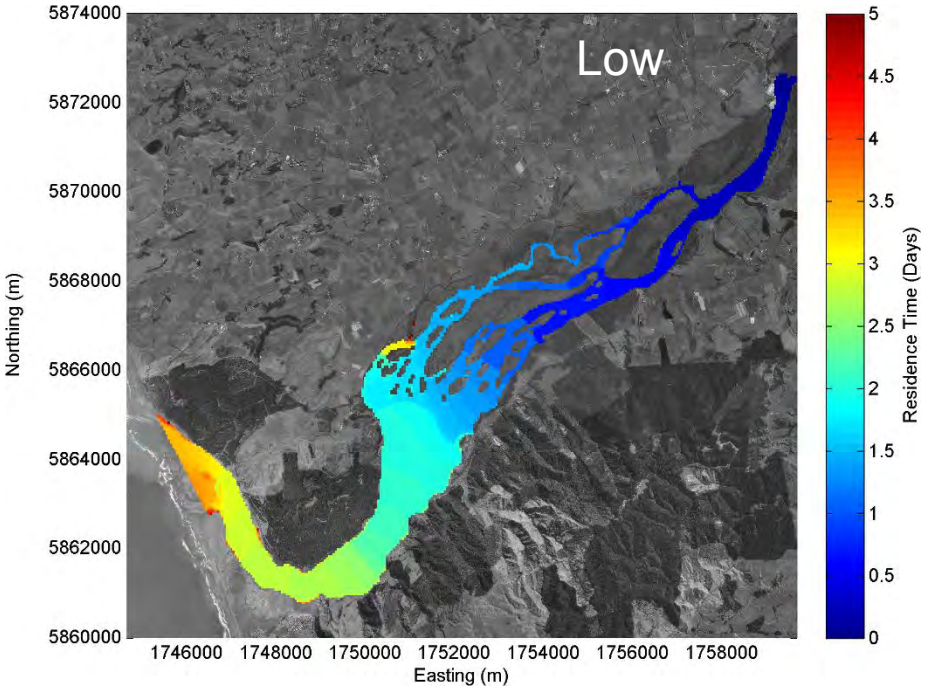

Figure 2.2: Residence time for the Waikato River estuary calculated using low flow. The tracer was released at high tide during mid-range tides.

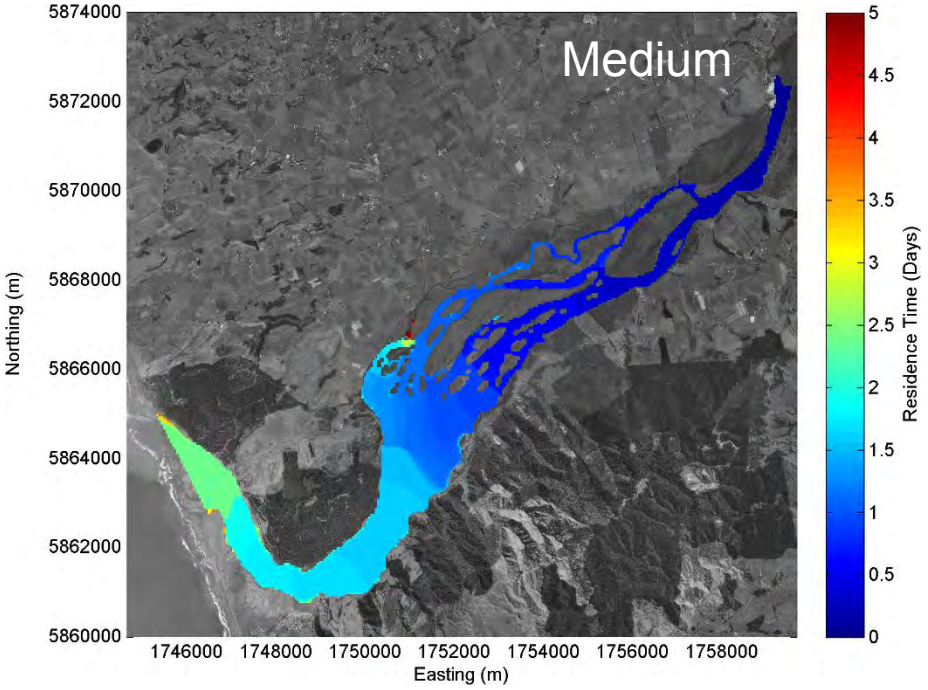

Figure 2.3: Residence time for the Waikato River estuary calculated using medium flow. The tracer was released at high tide during mid-range tides.

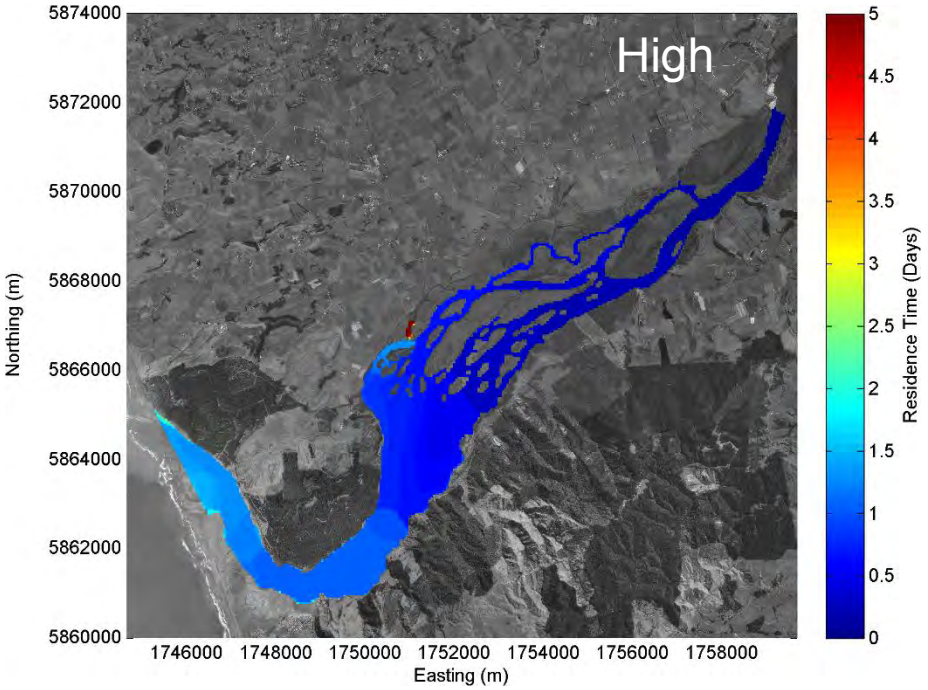

Figure 2.4: Residence time for the Waikato River estuary calculated using high flow. The tracer was released at high tide during mid-range tides.

2.5 Whaingaroa (Raglan) Harbour

The hydrodynamic model of Whaingaroa Harbour is fed by 15 rivers and streams. Of the total catchment area, 60% is accounted for by the Waitetuna and Waingaro Rivers which are received at the estuary head (see Figure 2.5). Residence time maps for low, medium and high flows are shown in Figure 2.6 to Figure 2.8.

During low flows the longest residence times occur in the head of the estuary which took a long time to be flushed. In this scenario, residence times in the head were up to 45 days whereas at the mouth of the estuary residence times were approximately 18 days. For the medium flow case, the residence time in the head of the estuary decreased, particularly near the major river mouths, however; residence time increased to approximately 25 days near the mouth. For the high flow case the residence times continued to decrease to approximately 30 days in the head of the estuary although at the estuary mouth the residence times remained at similar levels to the medium flow case.

The Whaingaroa Harbour model was also used in this study to explore the effects of release times with respect to tidal phase and spring and neap tides as well as the effects of wind and residence time threshold on residence times. The results of this investigation are presented in Section 3.

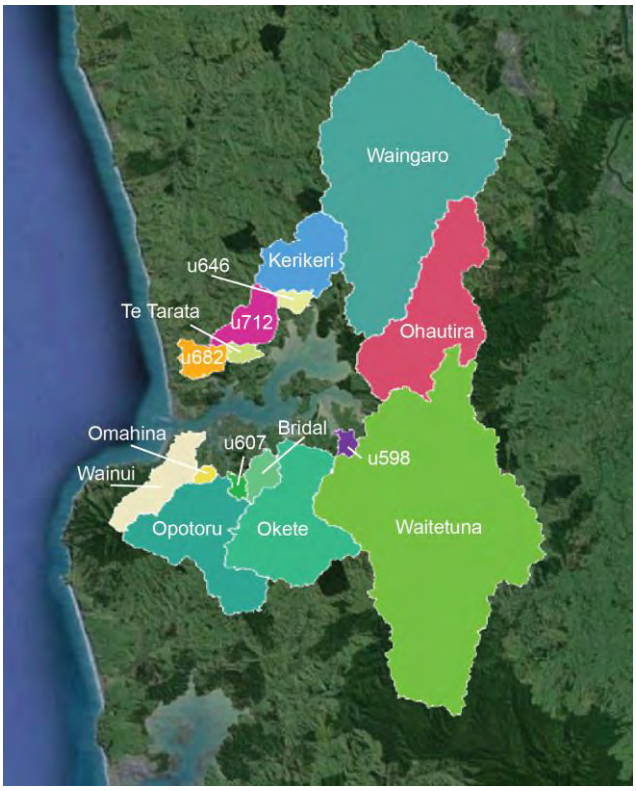

Figure 2.5. The 15 largest sub-catchments of the Raglan Harbour used in this study.

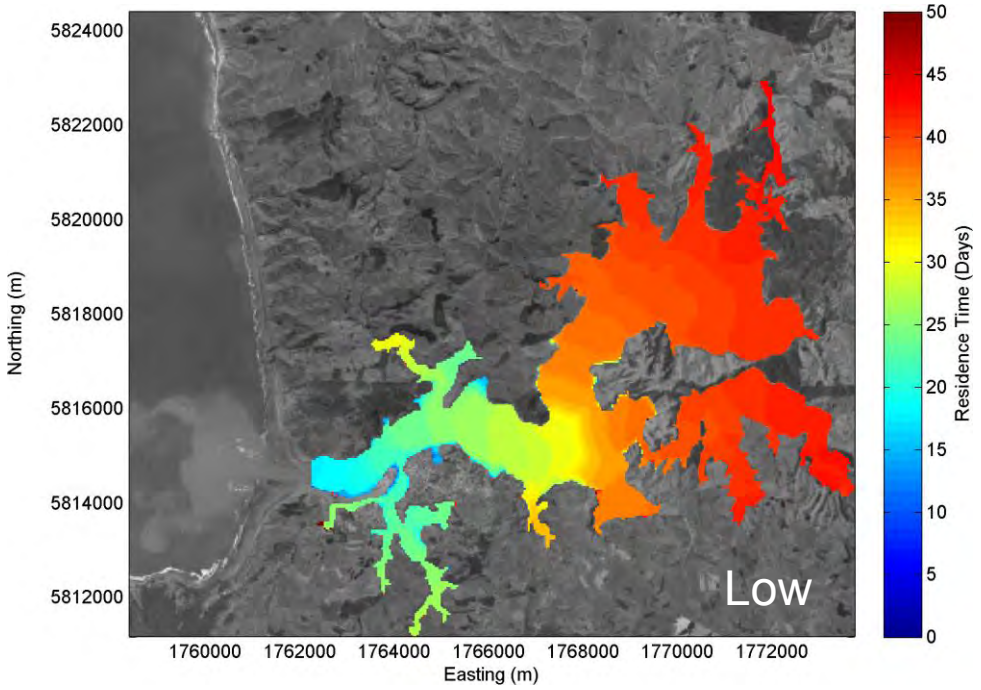

Figure 2.6: Residence time for Whaingaroa Harbour calculated using low flow. The tracer was released at high tide during mid-range tides.

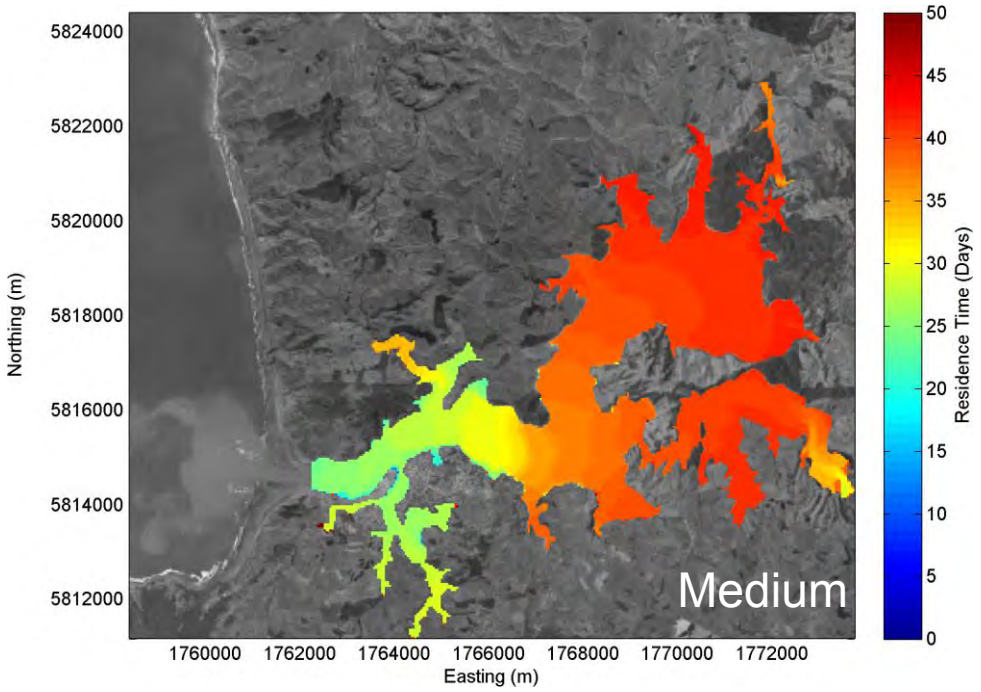

Figure 2.7: Residence time for Whaingaroa Harbour calculated using medium flow. The tracer was released at high tide during mid-range tides.

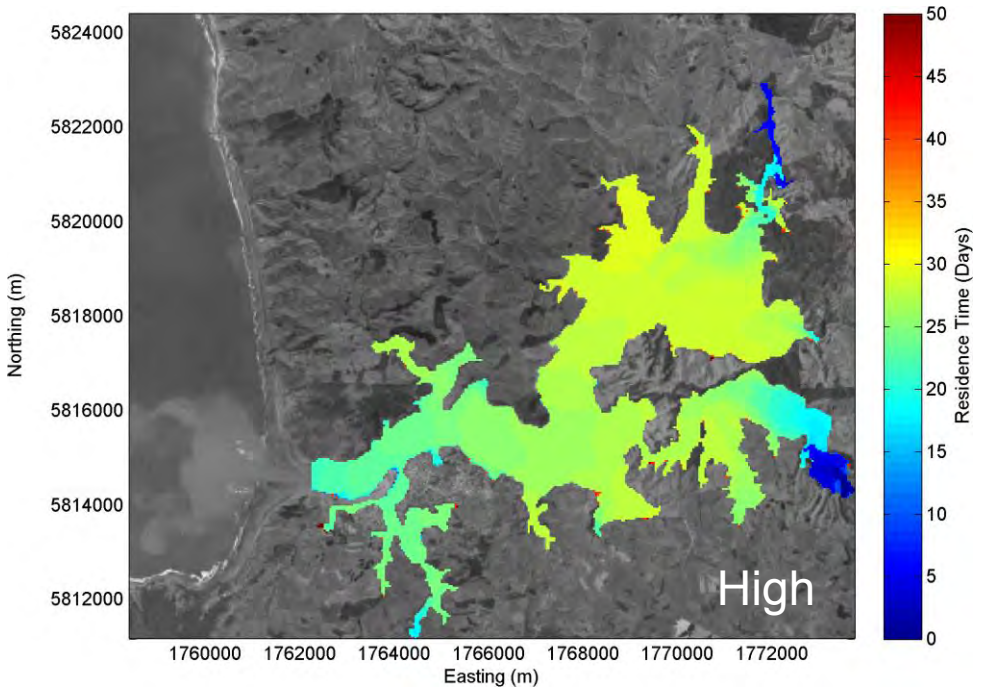

Figure 2.8: Residence time for Whaingaroa Harbour calculated using high flow. The tracer was released at high tide during mid-range tides.

2.6 Aotea Harbour

The hydrodynamic model of Aotea Harbour simulated inflow from 25 rivers and streams. Of these, the Makomako, Te Maari and Pakoka Rivers (Figure 2.9) are the 3 largest and account for 71% of the catchment area. Residence times maps for low, medium and high flows are shown in Figure 2.10 to Figure 2.12. A small model anomaly is apparent in these results which shows a small patch of high residence times near the estuary mouth. This is due to a small landlocked area in the model bathymetry that was not readily flushed by the model.

The spatial variability in residence times for Aotea Harbour are similar to those in Whaingaroa and Kawhia Harbours with an overall trend of increased residence times towards the head of the estuary. However, residence times are generally shorter in Aotea Harbour than in the other two since it is considerably smaller in volume (see Table 2.1). As river flows increased the residence time at the estuary mouth increased while it decreased towards the estuary head.

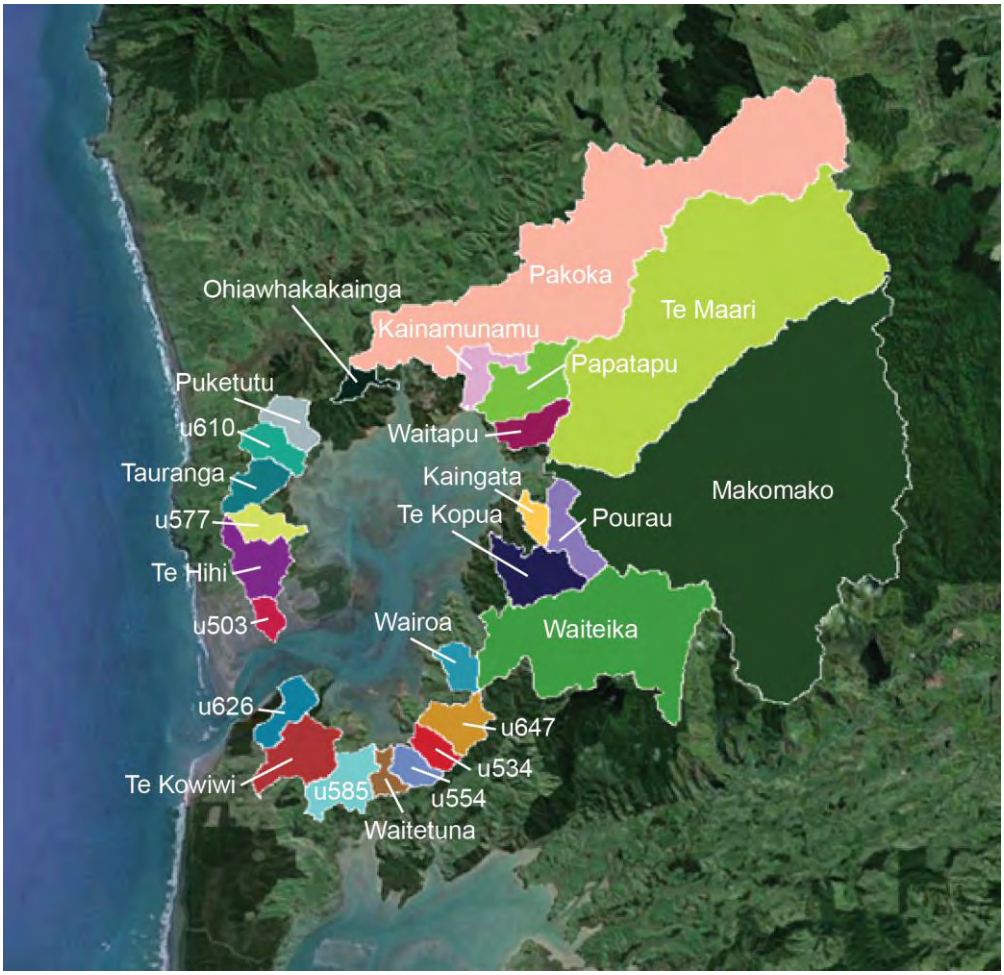

Figure 2.9. The 25 largest sub-catchments of the Aotea Harbour to be modelled in this study.

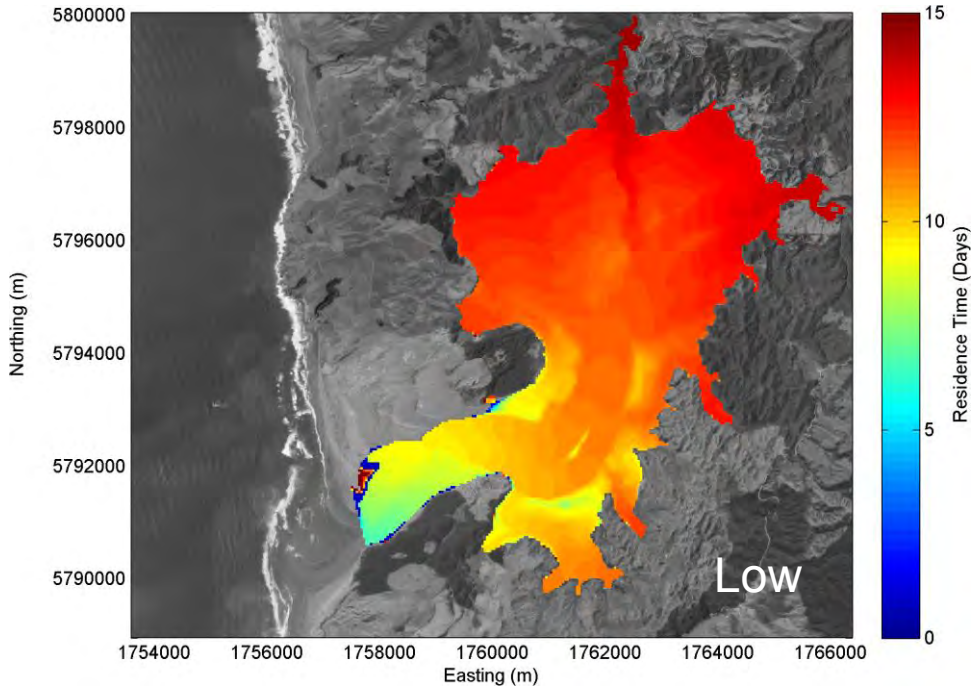

Figure 2.10: Residence time for Aotea Harbour calculated using low flow. The tracer was released at high tide during mid-range tides.

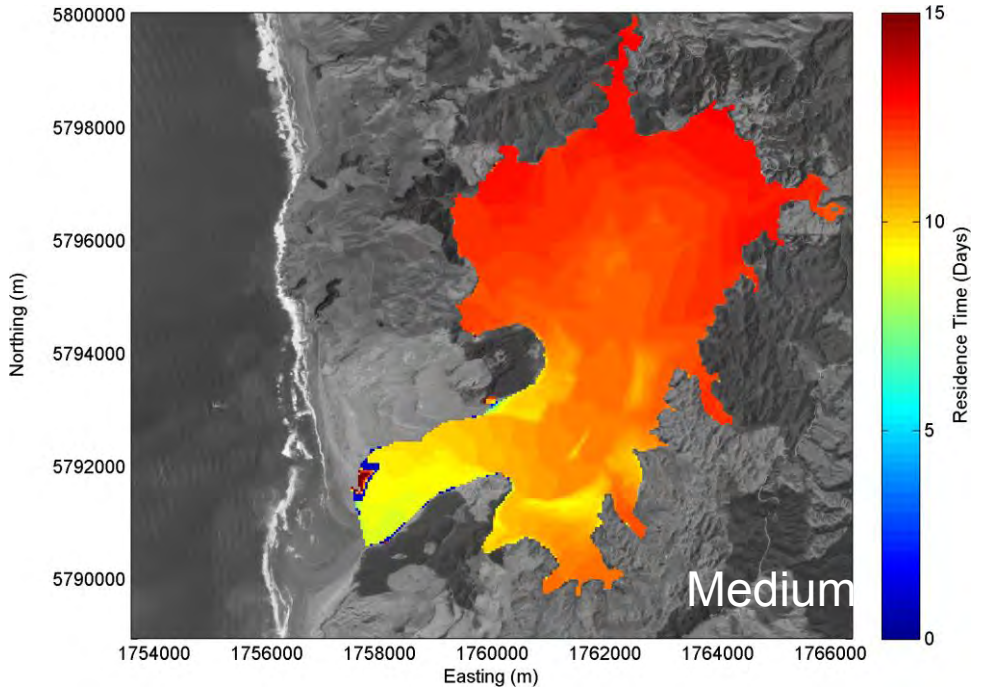

Figure 2.11: Residence time for Aotea Harbour calculated using medium flow. The tracer was released at high tide during mid-range tides.

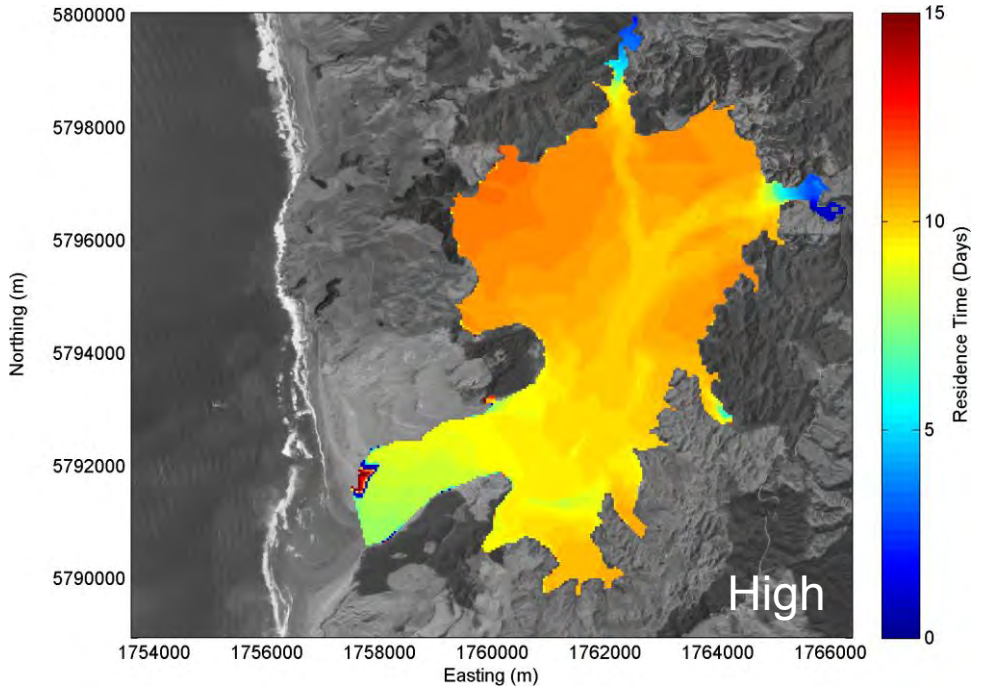

Figure 2.12: Residence time for Aotea Harbour calculated using high flow. The tracer was released at high tide during mid-range tides.

2.7 Kawhia Harbour

The Kawhia Harbour model is fed by 21 rivers and streams. The two largest of these are the Oparau and Awaroa Rivers (see Figure 2.13) which account for 53% of the total catchment area. Residence time maps for low, medium and high flows are shown in Figure 2.14 and Figure 2.16.

As with the Whaingaroa and Aotea Harbours, during low flows, residence times increased towards the head of the estuary with maximum residence times occurring near the mouths of the largest rivers (approximately 33 days). This is larger than for Aotea Harbour, but less than Whaingaroa Harbour. Unlike the other two harbours, the residence time at the harbour mouth did not increase with increased river flow. However, the residence time at the head of the estuary did decrease with increased river flow such that for the Q90 flow scenario the maximum residence time in the head of the estuary was approximately 23 days.

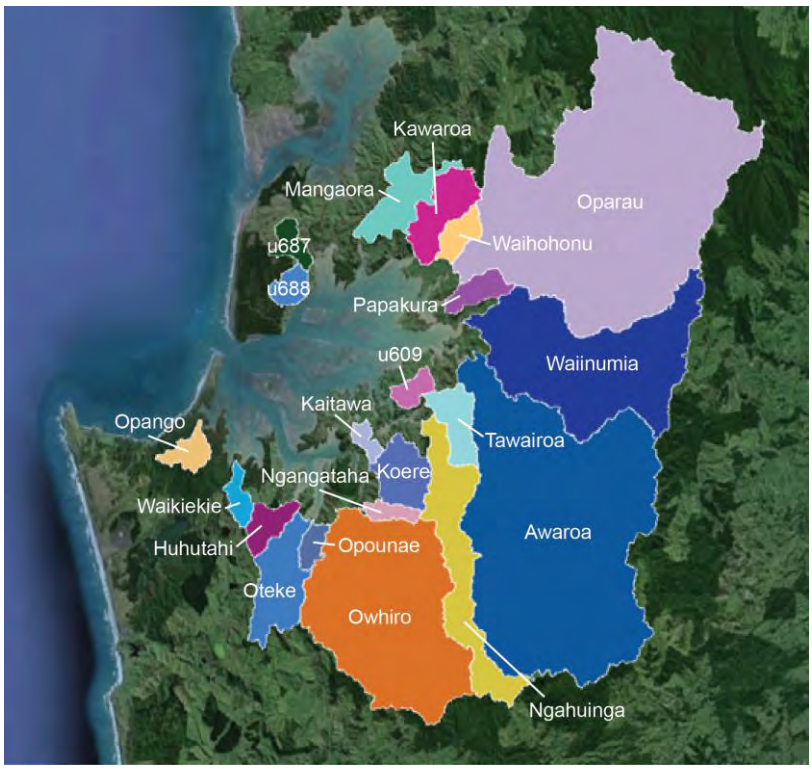

Figure 2.13. The 21 largest sub-catchments of the Kawhia Harbour to be modelled in this study.

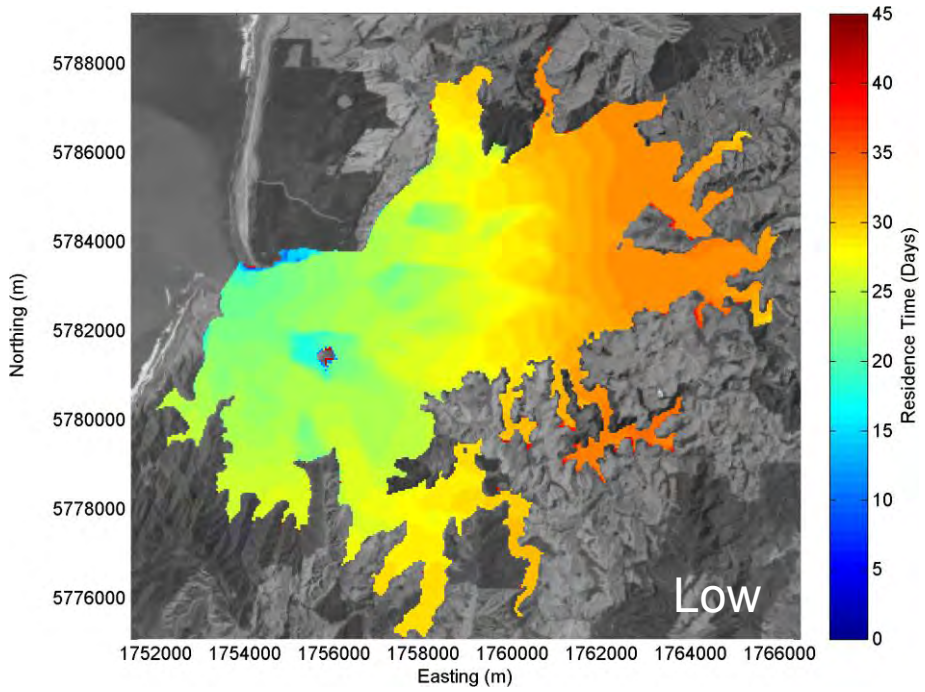

Figure 2.14: Residence time for Kawhia Harbour calculated using low flow. The tracer was released at high tide during mid-range tides.

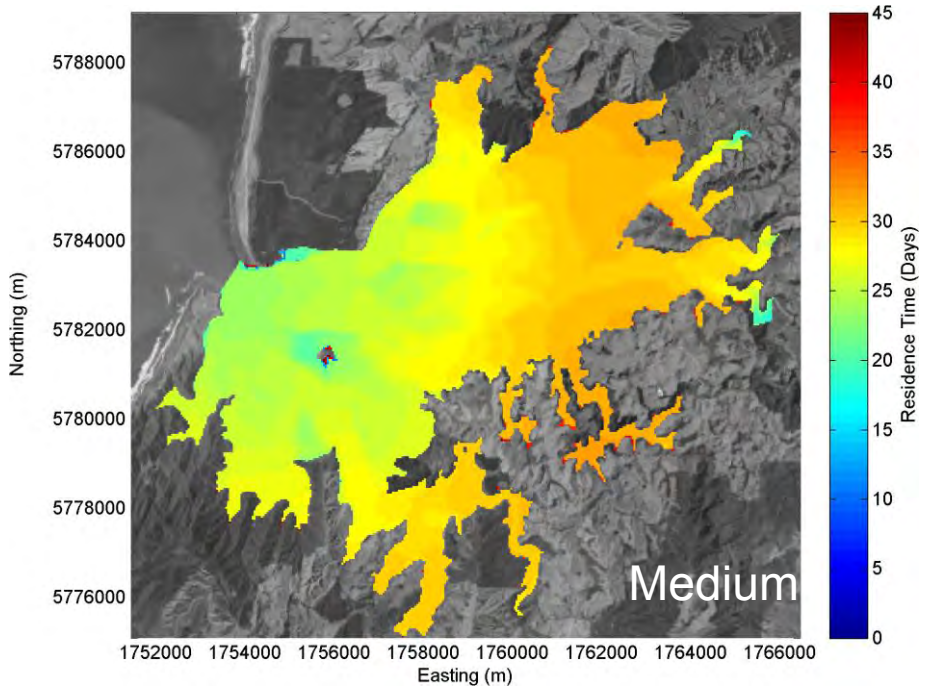

Figure 2.15: Residence time for Kawhia Harbour calculated using medium flow. The tracer was released at high tide during mid-range tides.

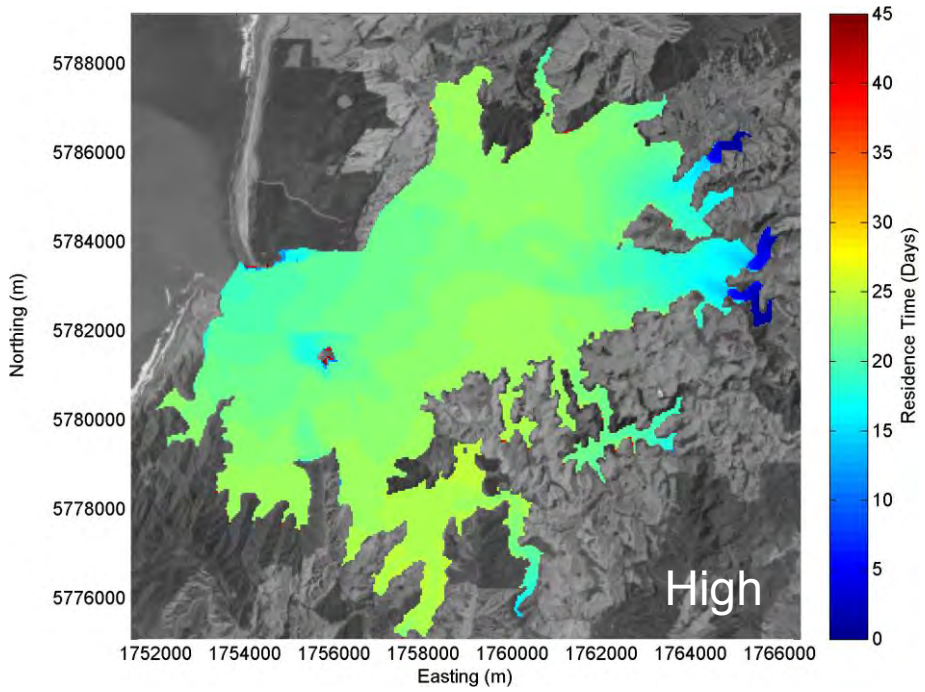

Figure 2.16: Residence time for Kawhia Harbour calculated using high flow. The tracer was released at high tide during mid-range tides.

2.8 Marokopa River Estuary

With a high tide volume of 1024 mega litres at full tide, Marokoa River estuary is the smallest of the seven estuaries though it is similar in shape and form to Awakino River estuary. It is fed by the Marokopa River which drains a 364 km^2 catchment. The residence time maps for the low, medium and high flows are shown in Figure 2.17, Figure 2.18 and Figure 2.19.

Overall the residence times are reasonably low across the model domain for all flow scenarios. For the low flow scenario residence times were less than 2 days across the bulk of the model domain. For the medium and high cases, the residence times are largely < 1 day.

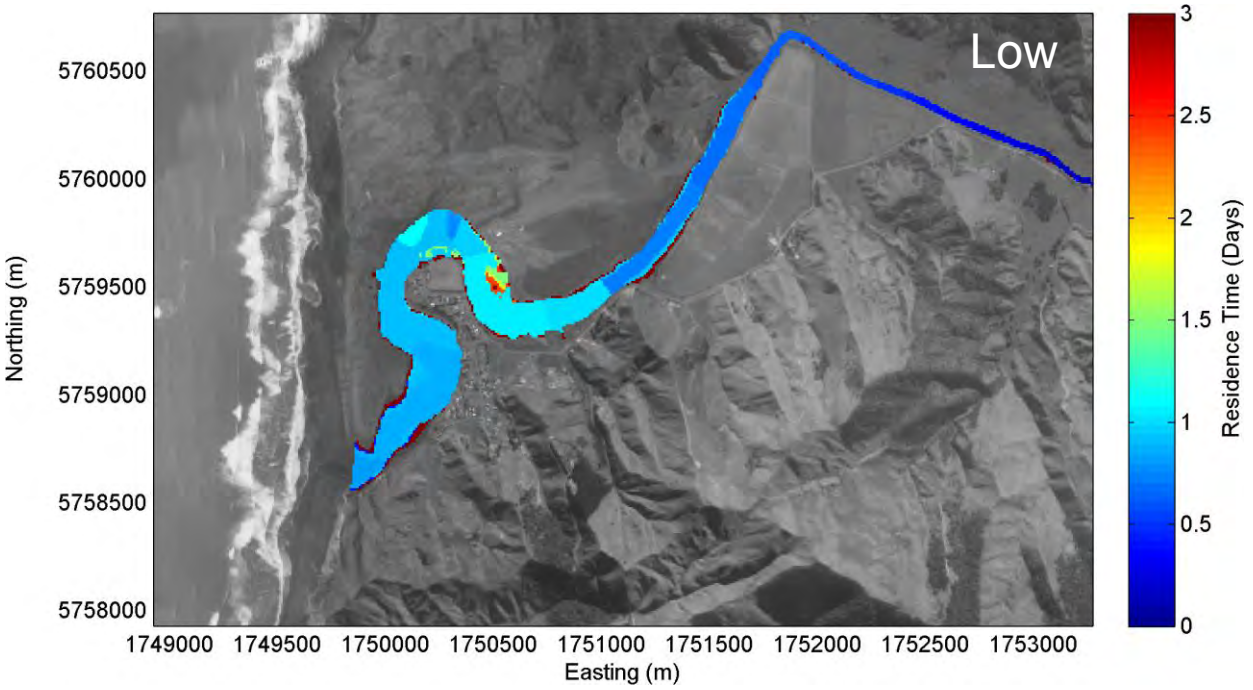

Figure 2.17: Residence time for the Marokopa River estuary calculated using low flow. The tracer was released at high tide during mid-range tides.

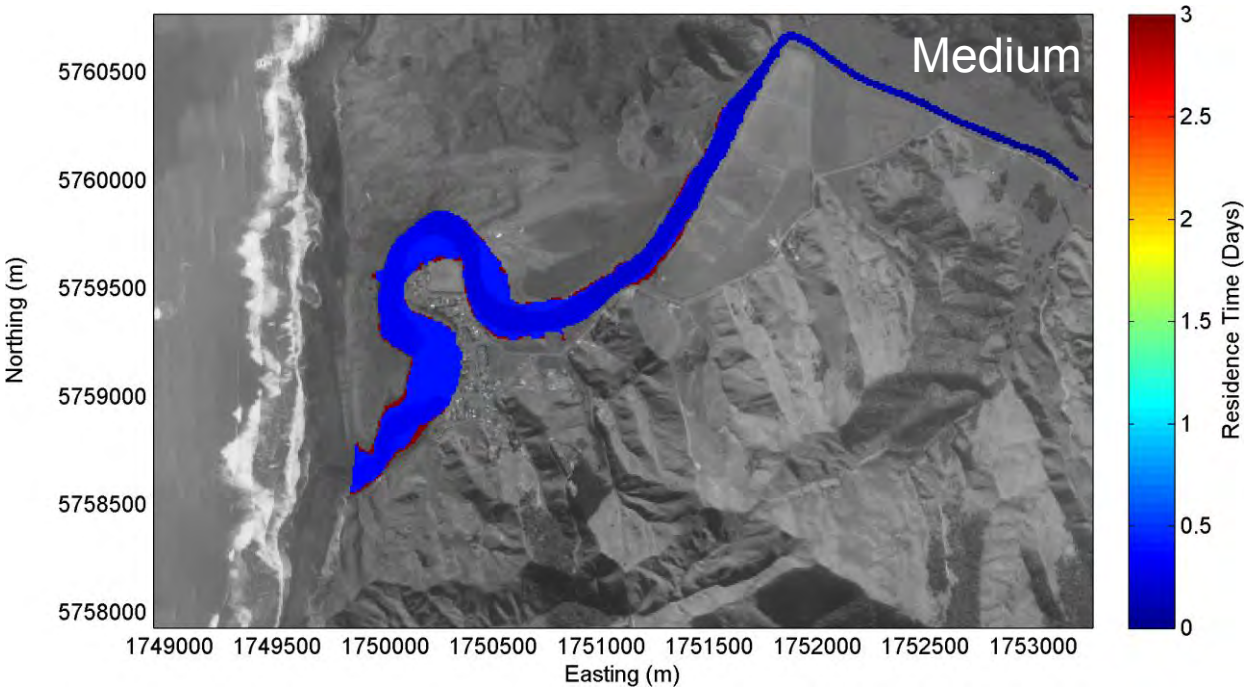

Figure 2.18: Residence time for the Marokopa River estuary calculated using medium flow. The tracer was released at high tide during mid-range tides.

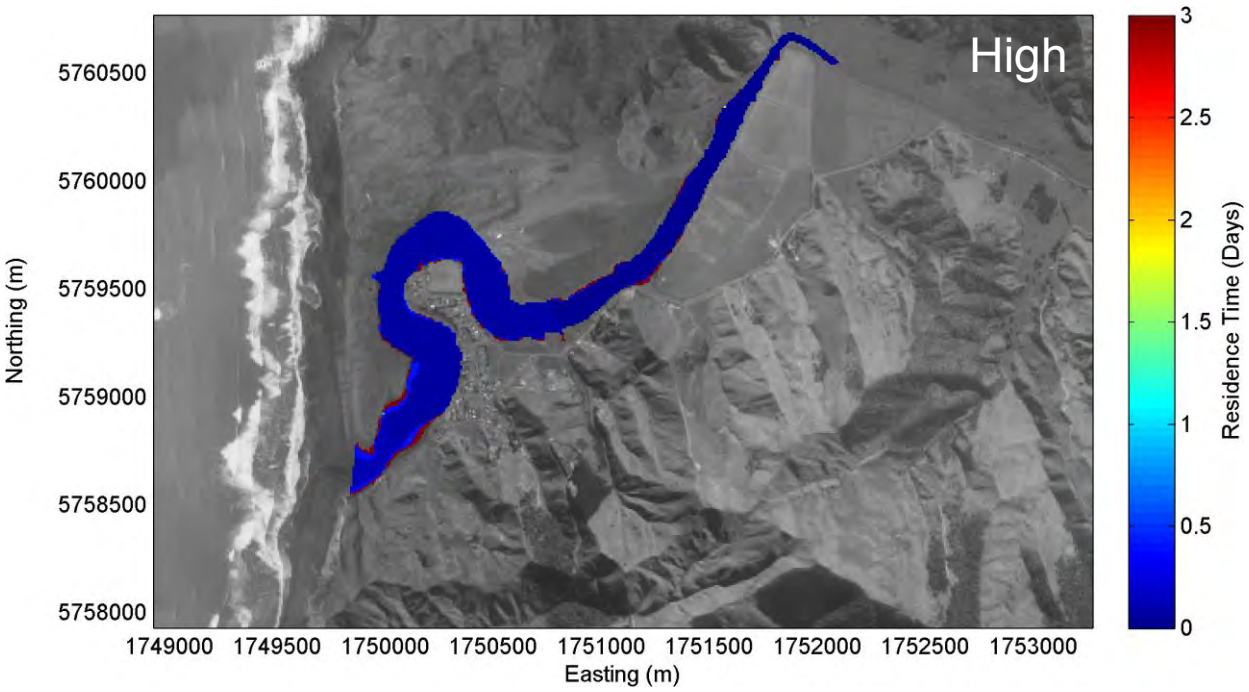

Figure 2.19: Residence time for the Marokopa River estuary calculated using high flow. The tracer was released at high tide during mid-range tides.

2.9 Awakino River Estuary

The Awakino River is similar in shape to the Marokopa River estuary though with a high tide volume of 1379 mega litres it is slightly larger. It is fed by the Awakino River which drains a 383 km^2 catchment. The residence time maps for the low, medium and high flows are shown in Figure 2.20, Figure 2.21 and Figure 2.22.

For tidal river estuaries such as this, residence times are strongly affected by river flow. As with Marokopa, in the low flow scenario, residence times were under 3 days for the bulk of the estuary with the largest residence times in the middle section of the estuary and lower residence times near the head and the mouth of the estuary. Under medium flow, residence times were largely <.1 days and even shorter for the high flow conditions.

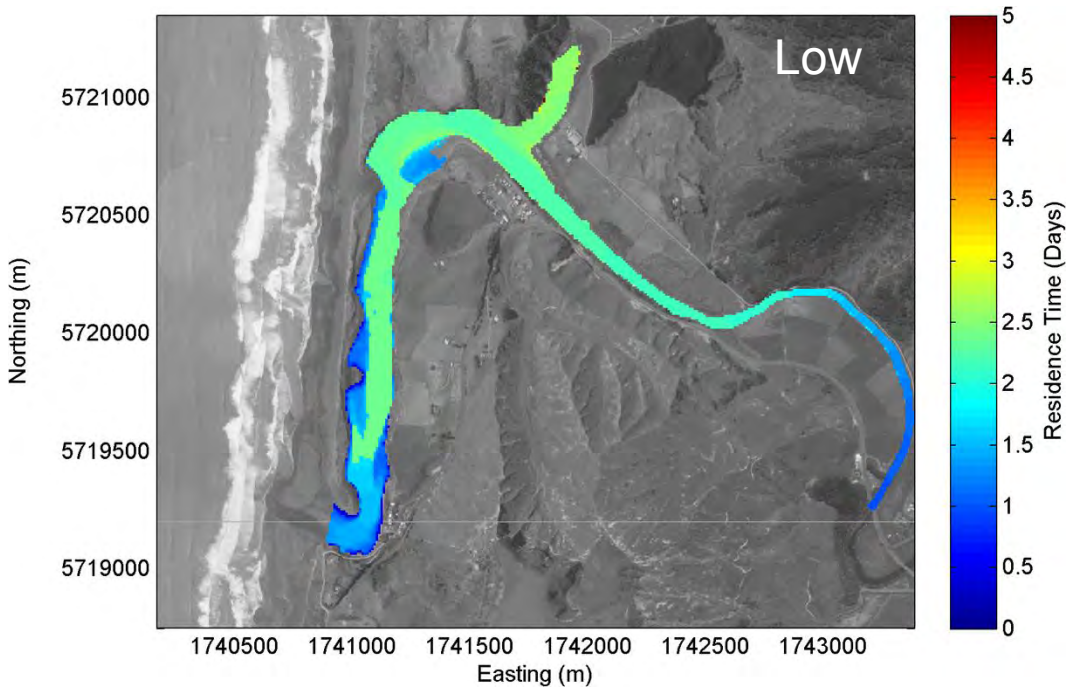

Figure 2.20: Residence time for the Awakino River estuary calculated using low flow. The tracer was released at high tide during mid-range tides.

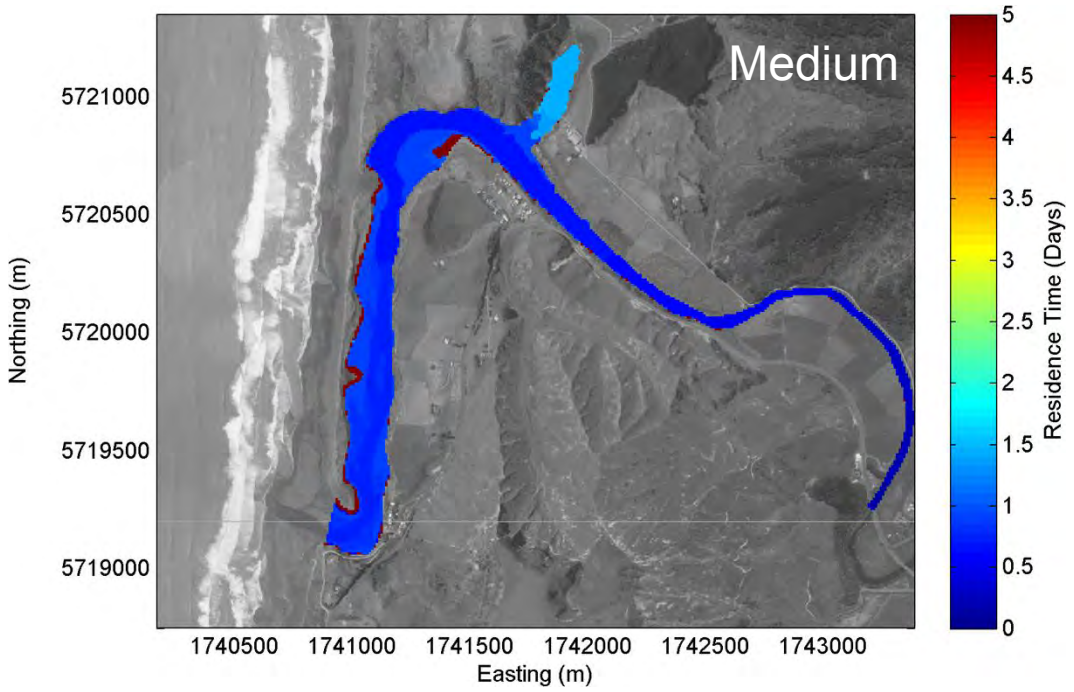

Figure 2.21: Residence time for the Awakino River estuary calculated using medium flow. The tracer was released at high tide during mid-range tides.

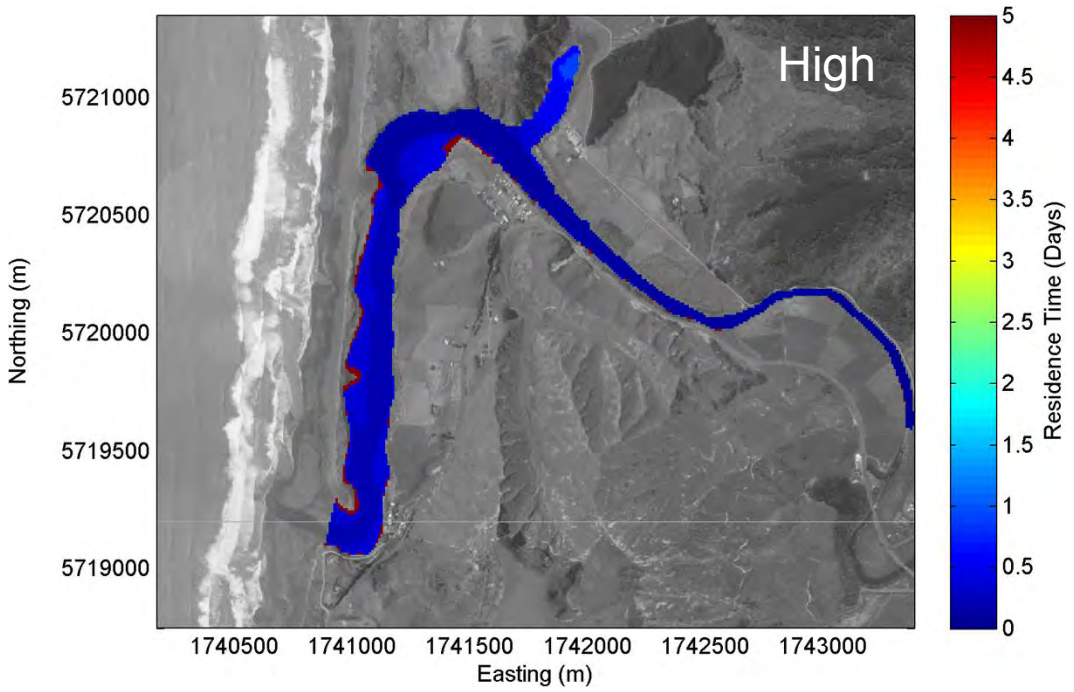

Figure 2.22: Residence time for the Awakino River estuary calculated using high flow. The tracer was released at high tide during mid-range tides.

2.10 Mokau River Estuary

Mokau River estuary is the largest of the three tidal river estuaries in the southern west coast of the Waikato region with a high tide volume of 4407 mega litres. It is fed by the Mokau River which drains a 1444 km^2 catchment.

Residence times for the Mokau River estuary under low flow conditions are larger than those for Marokopa and Awakino River estuaries. The largest residence times are in the centre of the estuary and are generally < 4 days. Residence times are mainly <2.5 days for the medium flow and <1 day for high flows.

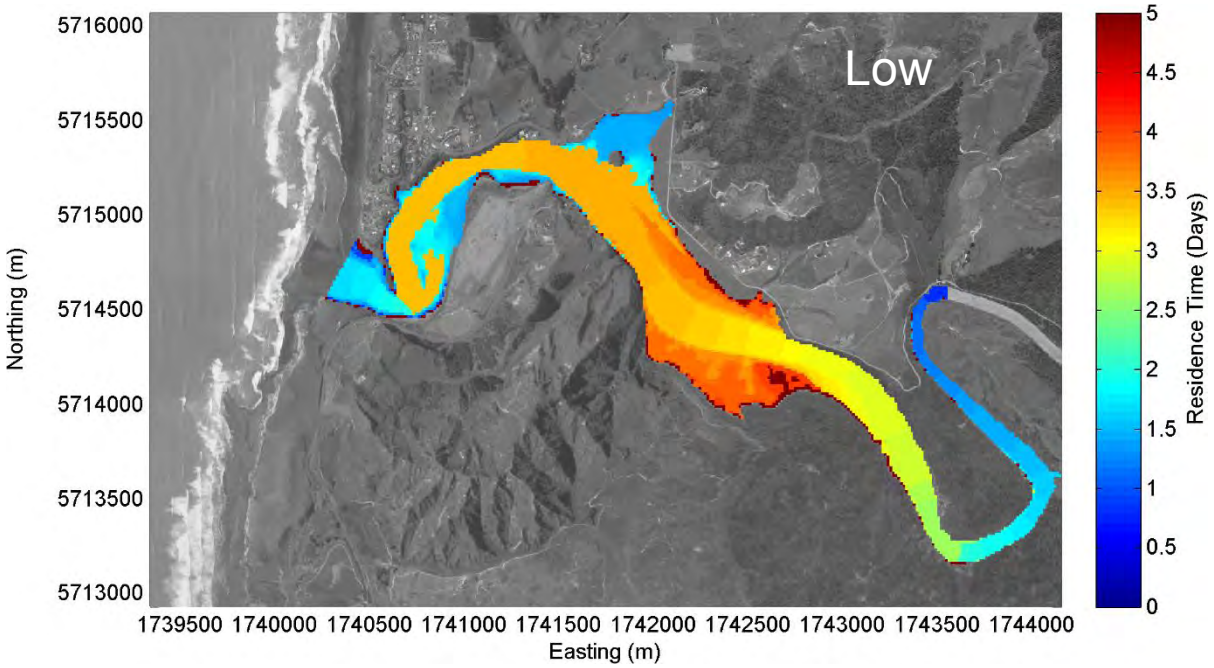

Figure 2.23: Residence time for the Mokau River estuary calculated using low flow. The tracer was released at high tide during mid-range tides.

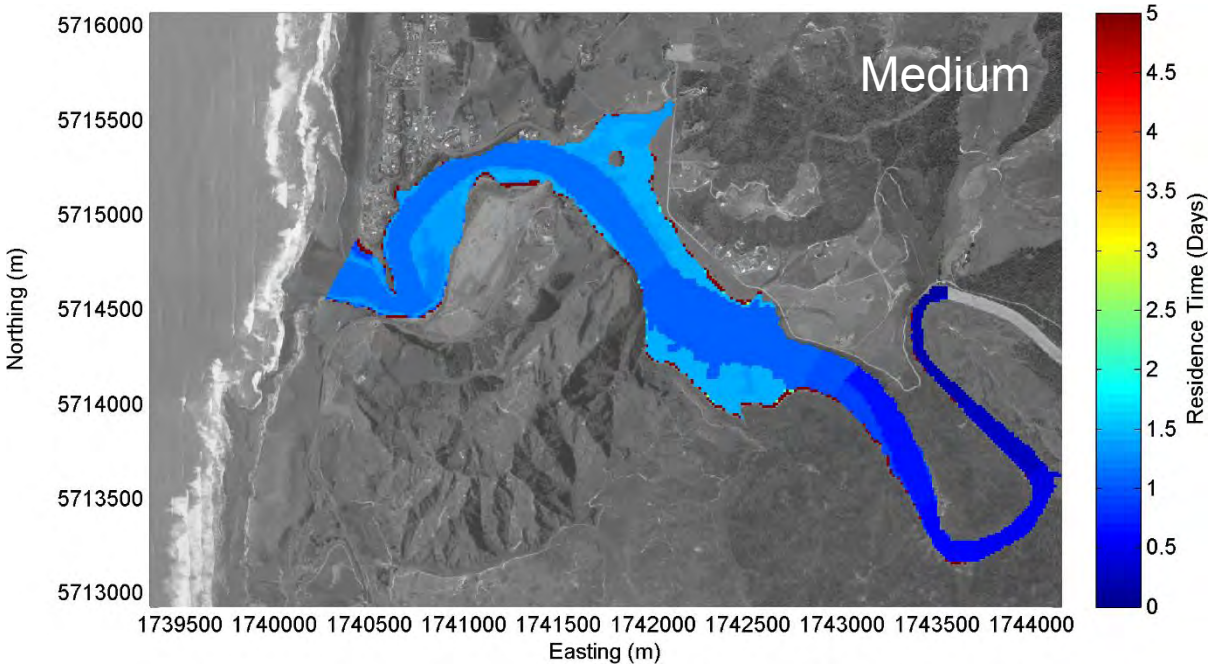

Figure 2.24: Residence time for the Mokau River estuary calculated using medium flow. The tracer was released at high tide during mid-range tides.

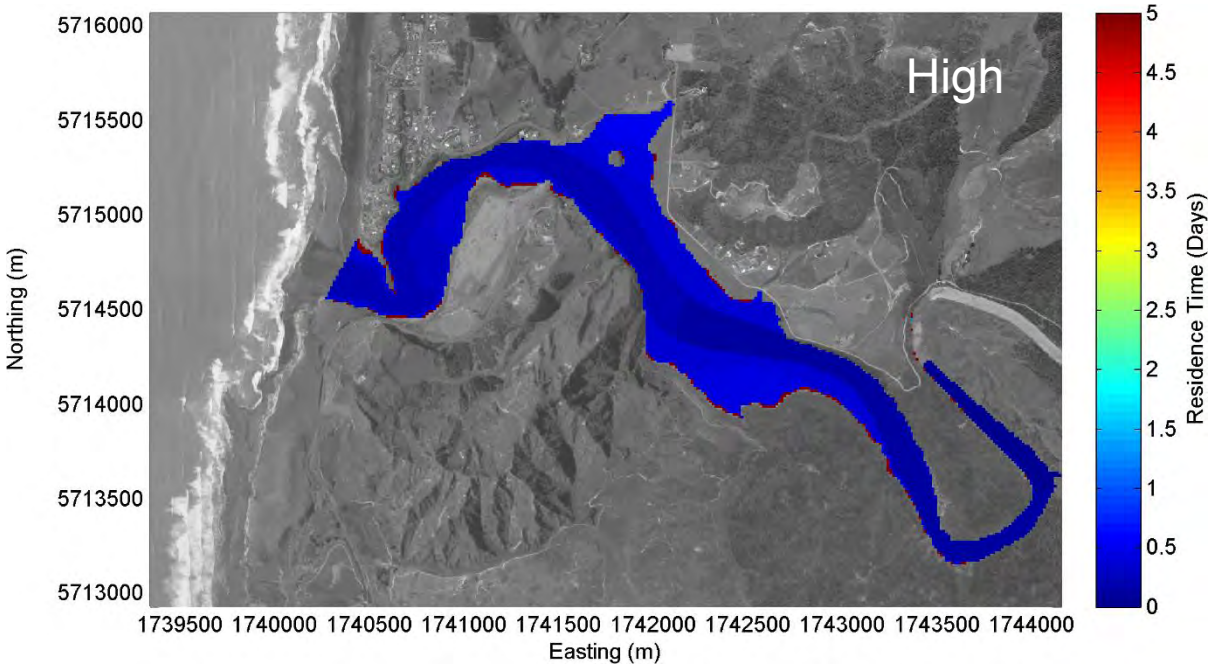

Figure 2.25: Residence time for the Mokau River estuary calculated using high flow. The tracer was released at high tide during mid-range tides.

2.11 Comparison Between Estuaries

In the previous analysis, residence times were presented using scales that were optimised to highlight the variability in residence time within each estuary under different flow conditions. Here we present residence times under medium flow conditions for each estuary using a common scale to highlight the variability between each estuary. These results are shown in Figure 2.26 to Figure 2.32.

The results highlight the reduced residence time in the tidal river estuaries compared with the drowned river valley estuaries. It is also evident that larger estuaries had longer residence times than smaller ones. In particular, the residence time was longer in the Waikato and Mokau River estuaries than in Awakino or Marokopa River estuaries. But for all of the tidal river estuaries residence times were less than 3 days throughout and less than 1 day for most of Marokopa and Awakino River estuaries.

For the drowned river valley estuaries under medium flow conditions, the longest modelled residence times were observed in Whaingaroa Harbour (35-45 days in the heads) followed by Kawhia Harbour (30 – 35 days in the heads) despite the fact that the high tide volume of the latter (205.862 x 10^6 m^3) is more than double that of the former (101.442 x 10^6 m^3). The difference in residence times can likely be attributed increased flushing due to the larger tidal prism for Kawhia Harbour (164.536 x 10^6 m^3) compared with Whaingaroa Harbour (71.227 x

10^6 m^3) relative to their high tide volumes. Aotea Harbour had a residence time of 10 – 15 days throughout the main body of the estuary under medium flow conditions, less than both Whaingaroa and Kawhia Harbours.

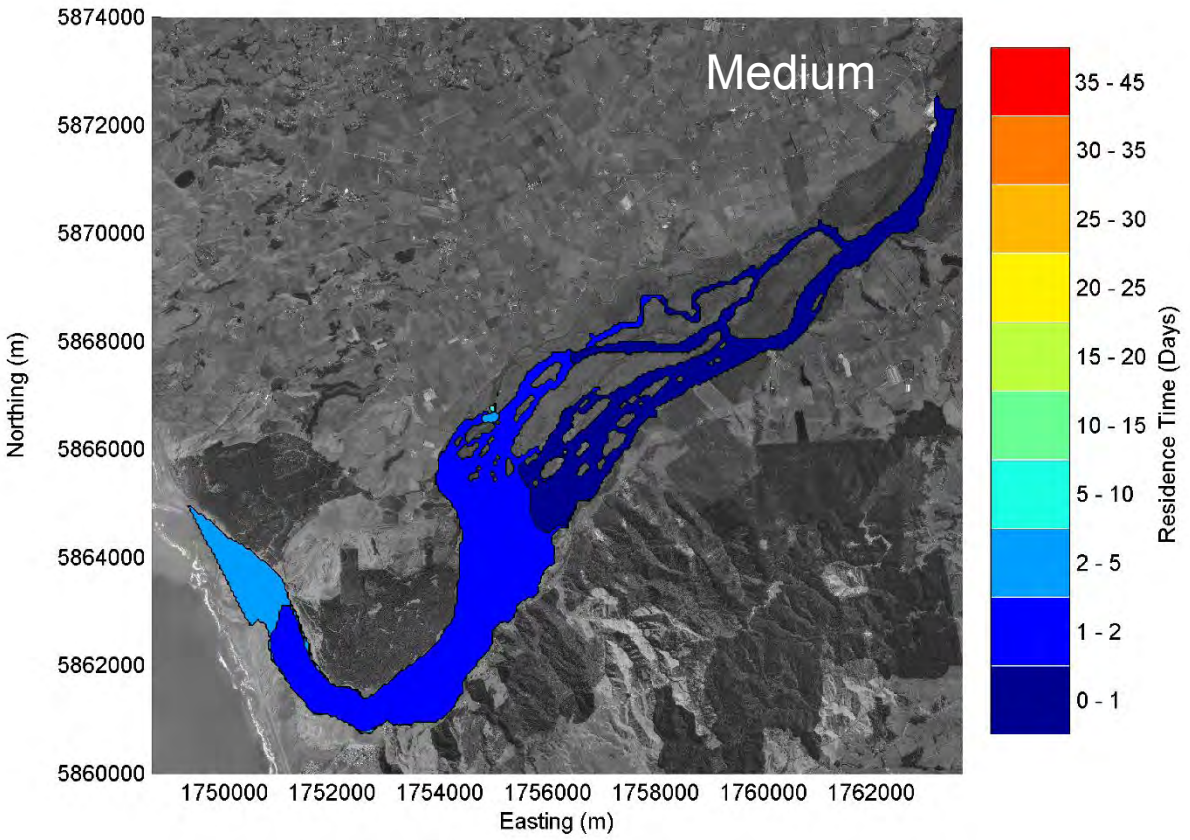

Figure 2.26: Residence times for Waikato River estuary under medium flow conditions.

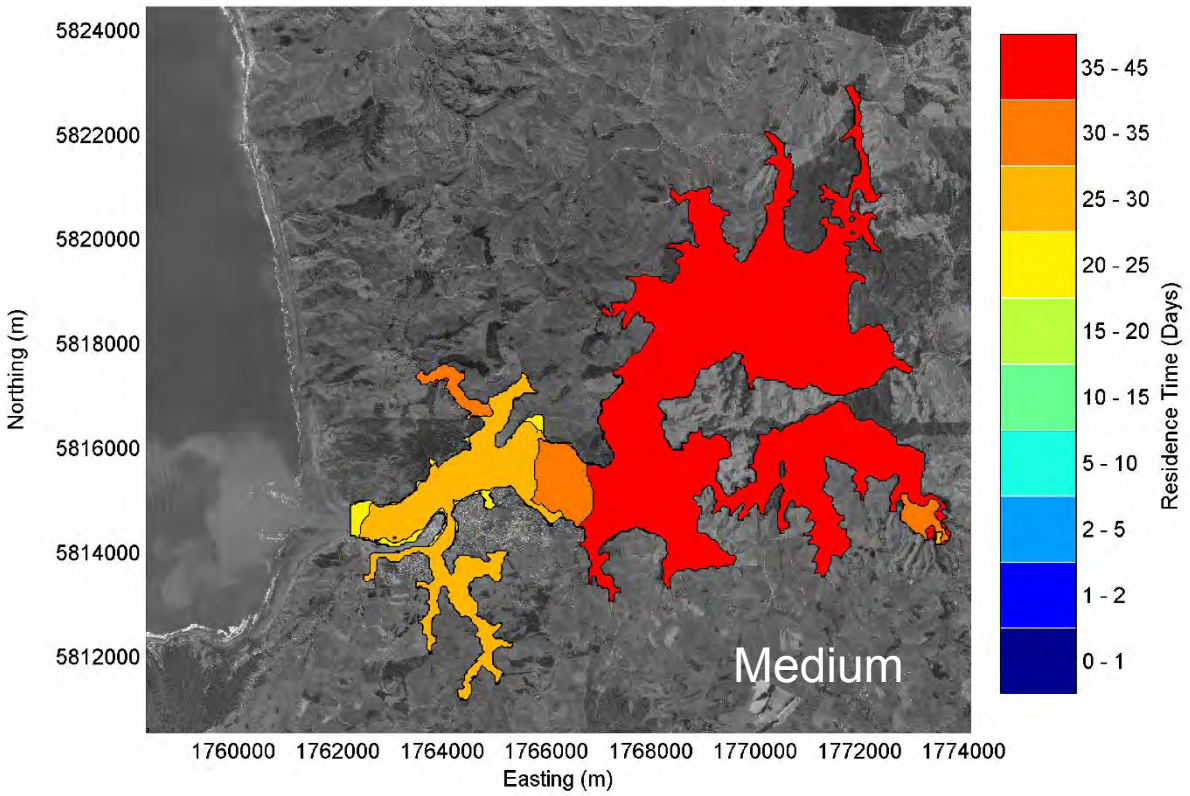

Figure 2.27: Residence times for Whaingaroa Harbour under medium flow conditions.

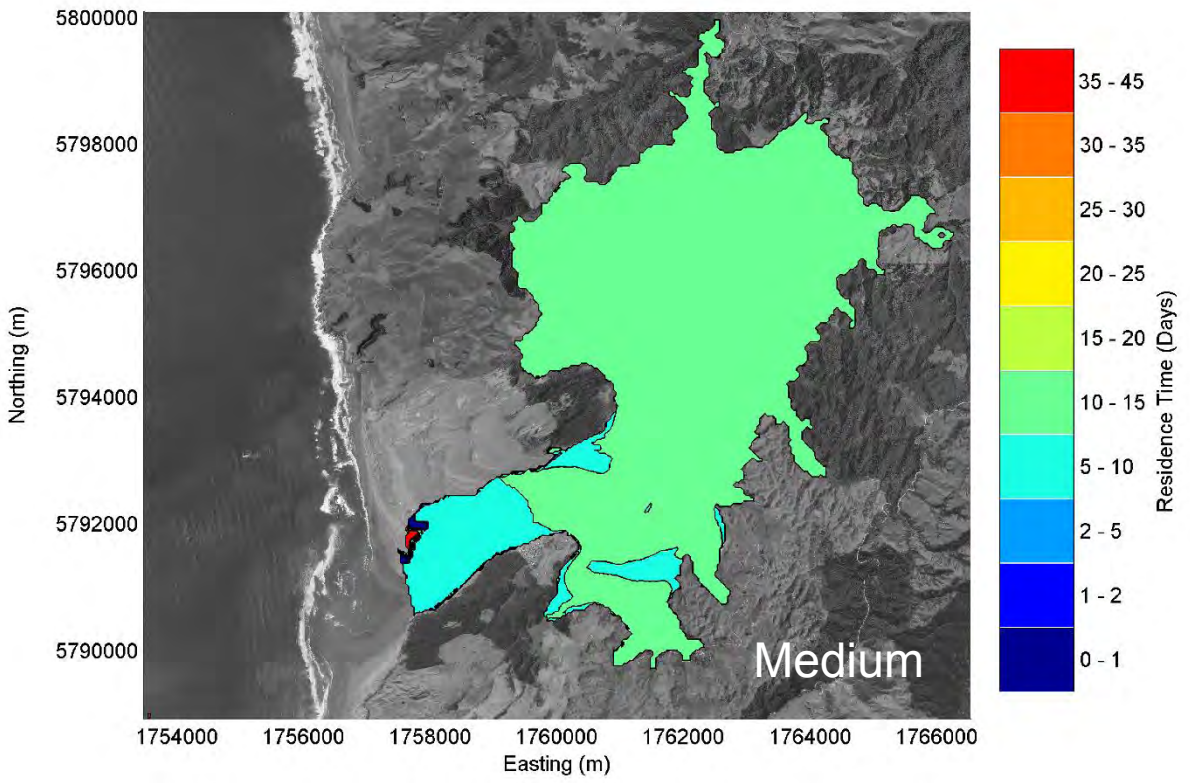

Figure 2.28: Residence times for Aotea Harbour under medium flow conditions.

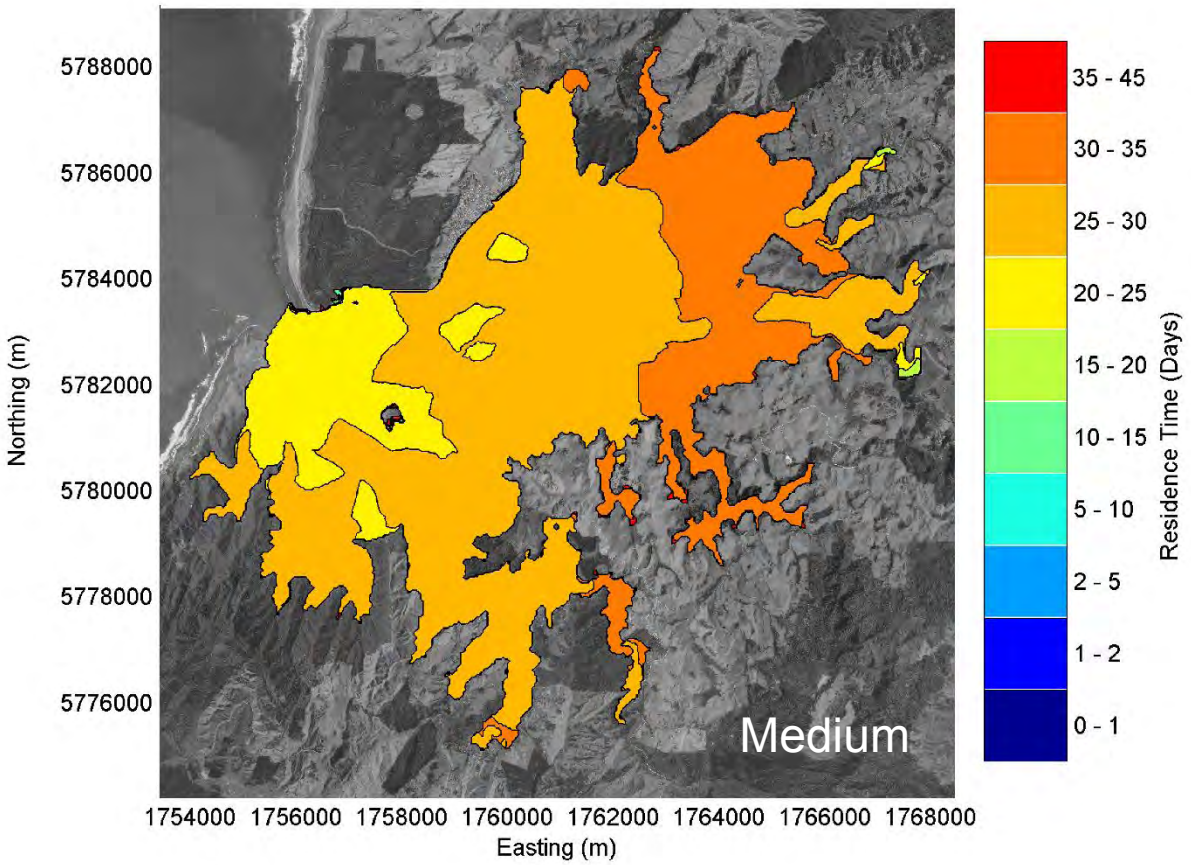

Figure 2.29: Residence times for Kawhia Harbour under medium flow conditions.

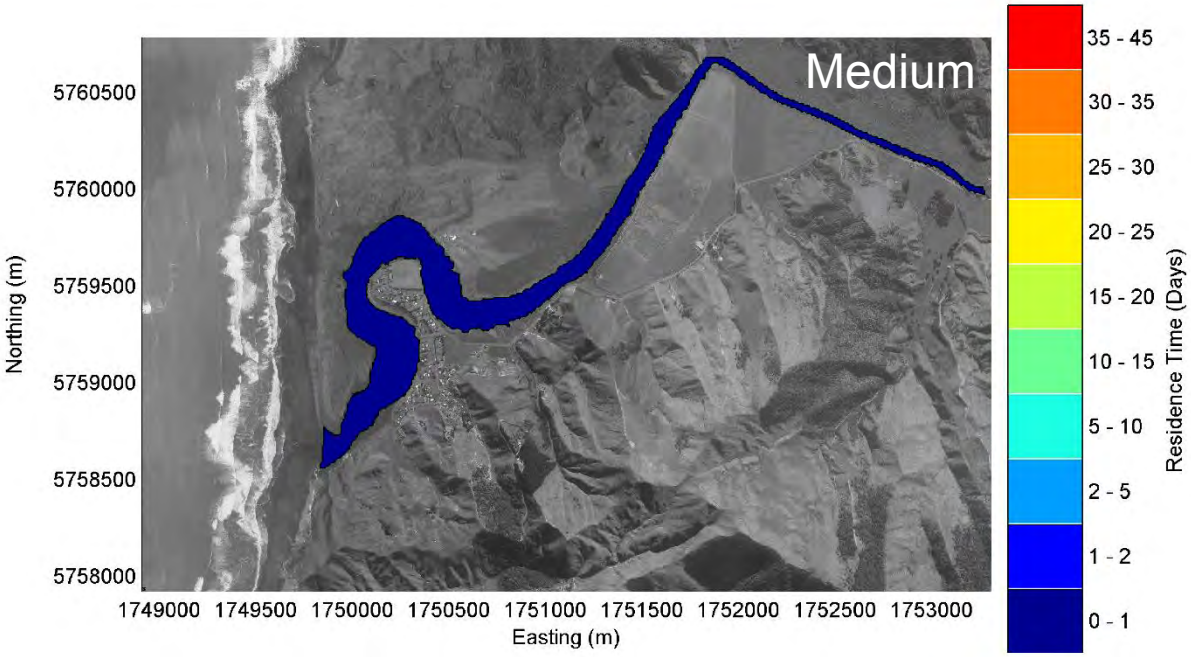

Figure 2.30: Residence times for Marokopa River estuary under medium flow conditions.

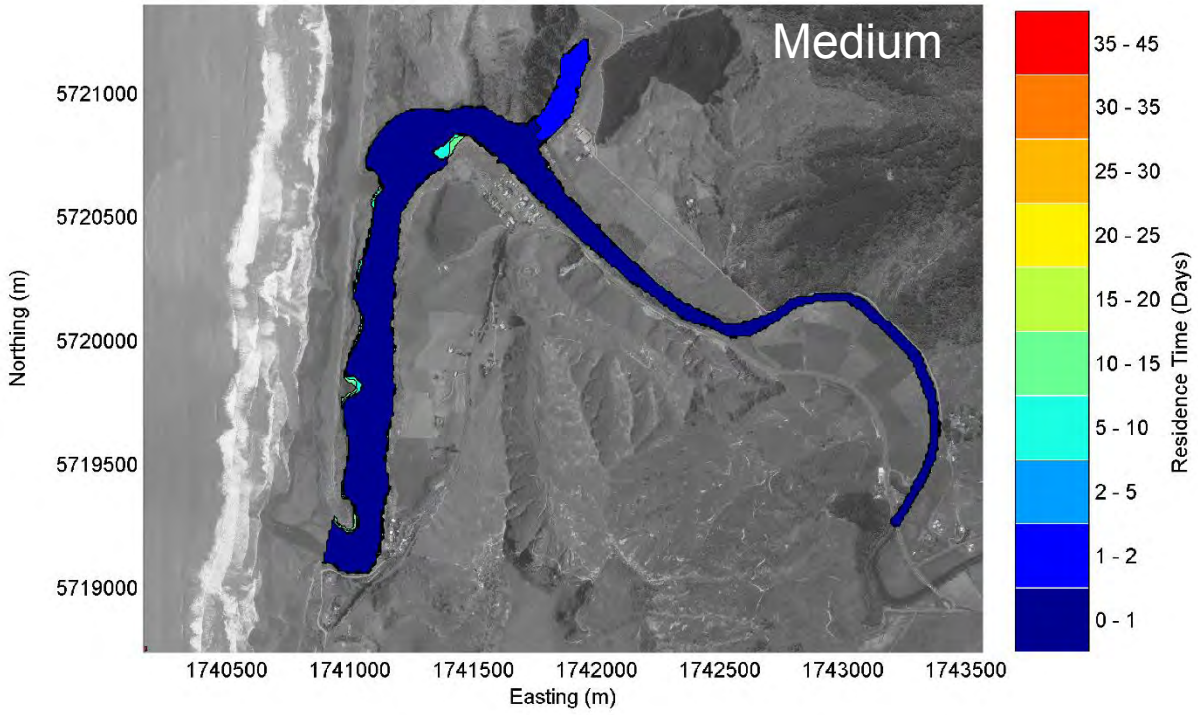

Figure 2.31: Residence times for Awakino River estuary under medium flow conditions.

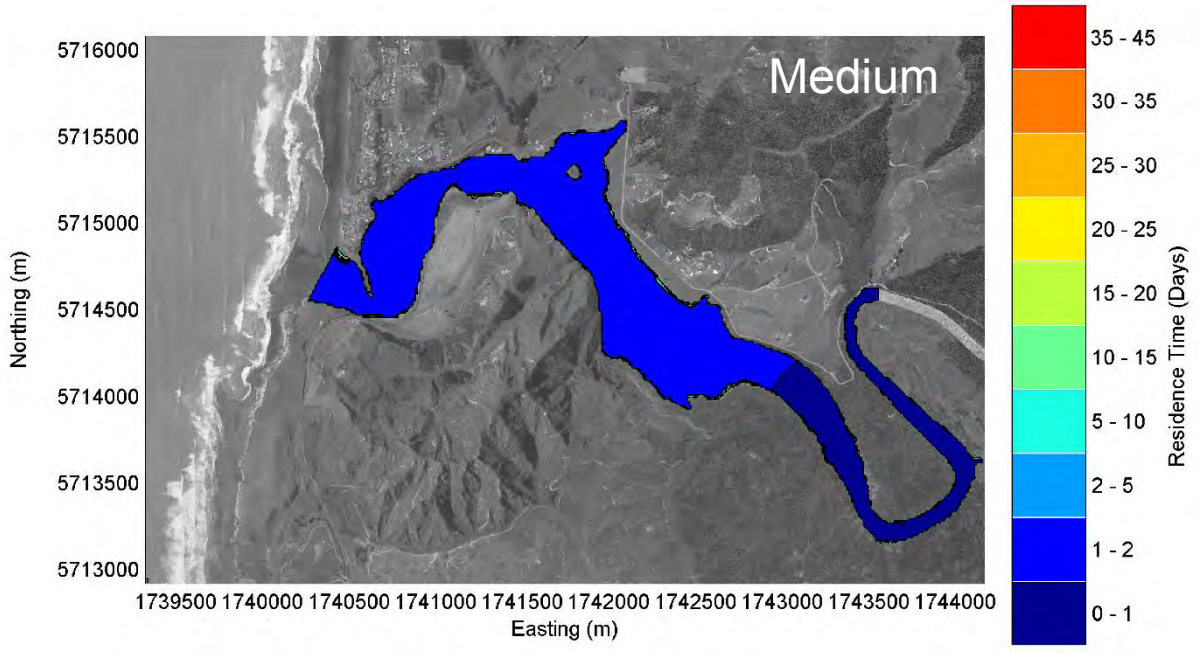

Figure 2.32: Residence times for Mokau River estuary under medium flow conditions.

3 Sensitivity Analysis

The residence times presented in the previous section are focused on the effects of different rivers flows on spatially variable residence times for each of the seven estuaries. Here we use the Whaingaroa Harbour as a case study to explore the effects of other variables on residence times. Specifically, this investigation looks at the effect of release time with respect to tidal phase, wind and residence time thresholds on residence times.

3.1 Tidal Influences on Residence Times

Calculating residence times based on a tracer released at a specific point in time requires that the release time be consistent across scenarios. The release time used for the scenarios in Section 2, corresponded to high tide release during a period between spring and neap tides. Here the effect of releasing a tracer under medium flow conditions at high tide on a spring tide (Figure 3.2), high tide during neap tides (Figure 3.3) and at low tide on a spring tide (Figure 3.4) are considered. The tidal phases at which these releases took place are shown in Figure 3.1.

It could be expected that the increased tidal excursion of spring tides would lead to decreased residence times. However, the spring high tide release shows overall higher residence times than in the case of the neap high tide release. This is because the time scale of residence times in the harbour are of the order of 20 to 50 days which covers several spring neap cycles. The release on the spring high tide is followed by a period of neap tides, and the opposite is true for the neap high tide release.

The release at low tide resulted in lower residence times than for the high tide releases where they were reduced by up to 5 days. In the estuary mouth, the residence times were reduced to <1 day. This is because there is a smaller volume of water in the estuary at low tide and consequently a smaller quantity of tracer was released in the estuary.

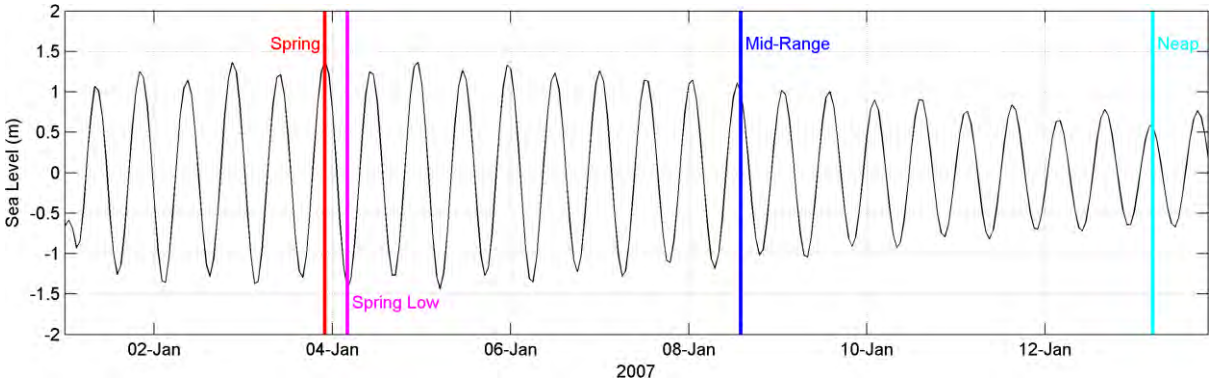

Figure 3.1: Tracer release times for exploring the sensitivity of residence times to tide phase.

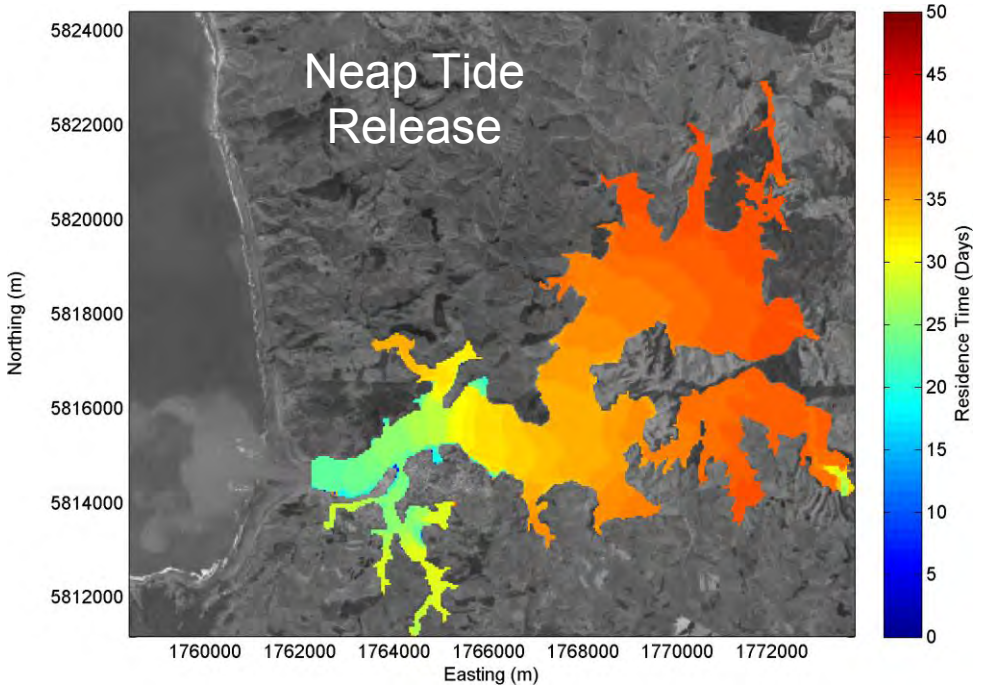

Figure 3.2: Residence time for Whaingaroa Harbour calculated using medium flow. The tracer was released at high tide during neap tides.

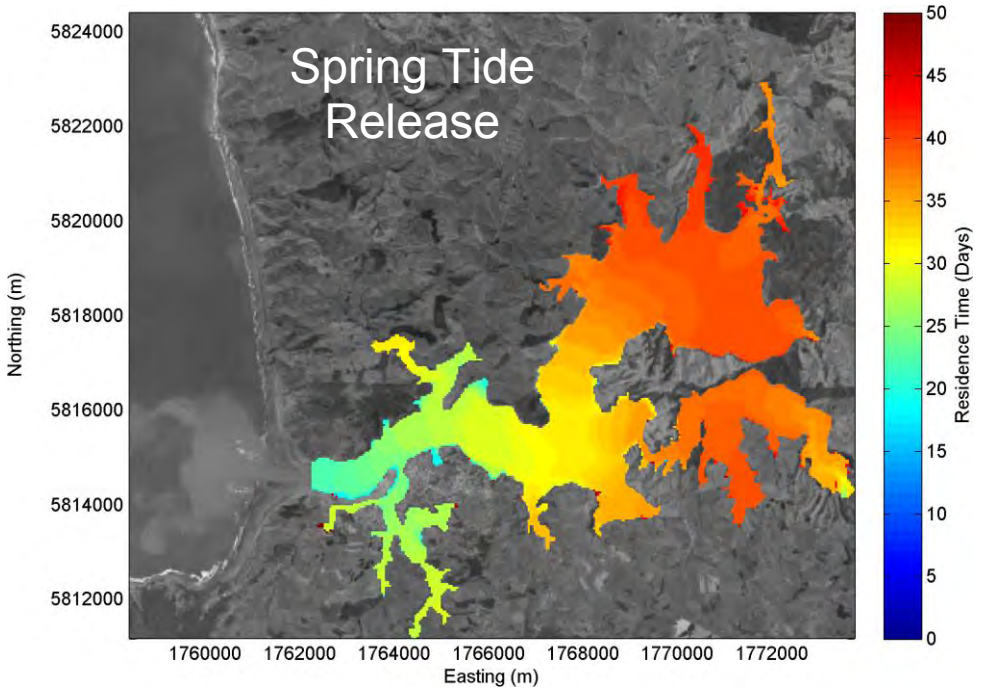

Figure 3.3: Residence time for Whaingaroa Harbour calculated using medium flow. The tracer was released at high tide during spring tides.

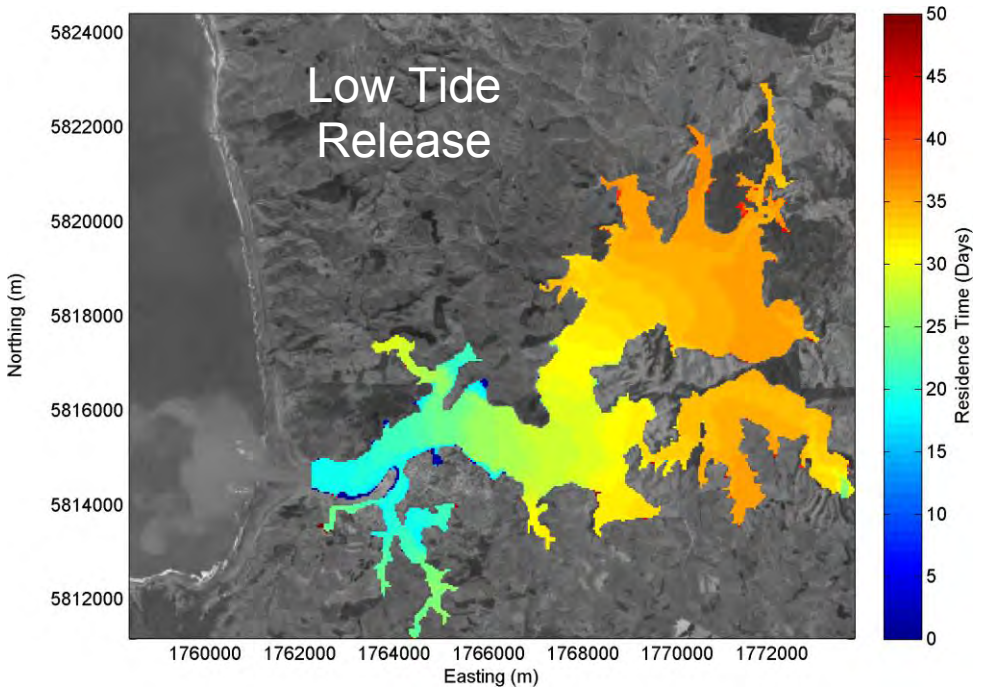

Figure 3.4: Residence time for Whaingaroa Harbour calculated using medium flow. The tracer was released at low tide during spring tides.

3.2 Effect of Wind on Residence Times

Winds are likely to have a considerable effect on circulation and consequently residence times for each estuary. This is particularly true for larger estuaries where the flushing of the estuaries happens over longer time scales. Two wind scenarios were run based on analysis of long term wind data from the Port Taharoa AWS (Figure 2.1). A wind rose (Figure 3.5) shows the two prevailing wind conditions for the region are SW and NE with median wind speeds of 6 and 3 m/s respectively. The results for these two scenarios are shown in Figure 3.6 and Figure 3.7. In both cases the residence time of the harbour was reduced compared with the corresponding scenario with no wind (Figure 2.7).

The south-westerly wind case caused a slight overall reduction in residence time of approximately 2 days when compared with the equivalent no wind scenario (Figure 2.7). The north-easterly event caused a more dramatic reduction of approximately 6 days against the no wind case.

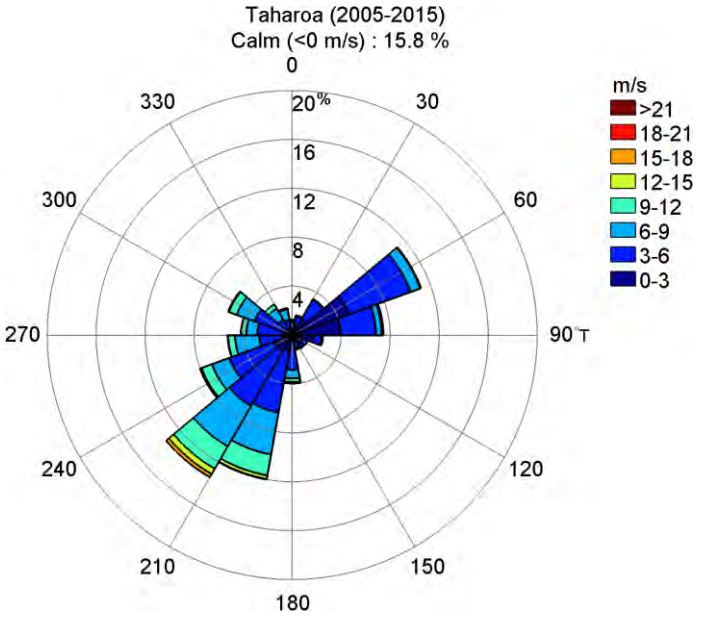

Figure 3.5: Wind rose showing wind records from the Taharoa AWS for complete years from 2002 until 2015.

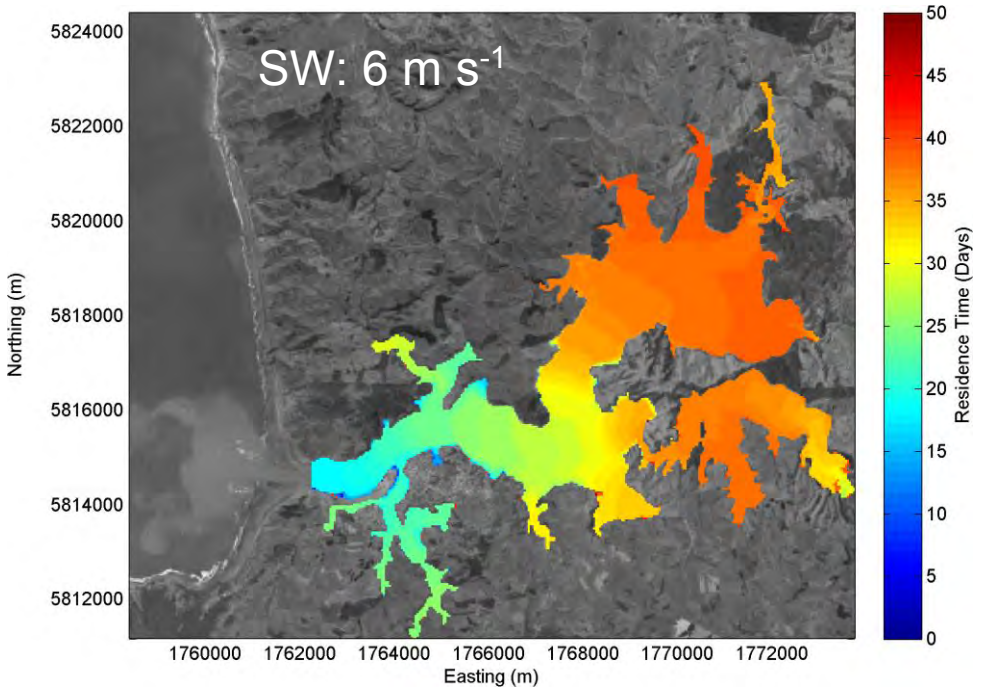

Figure 3.6: Residence time for Whaingaroa Harbour calculated using medium flow under south westerly wind. The tracer was released at high tide during mid-range tides.

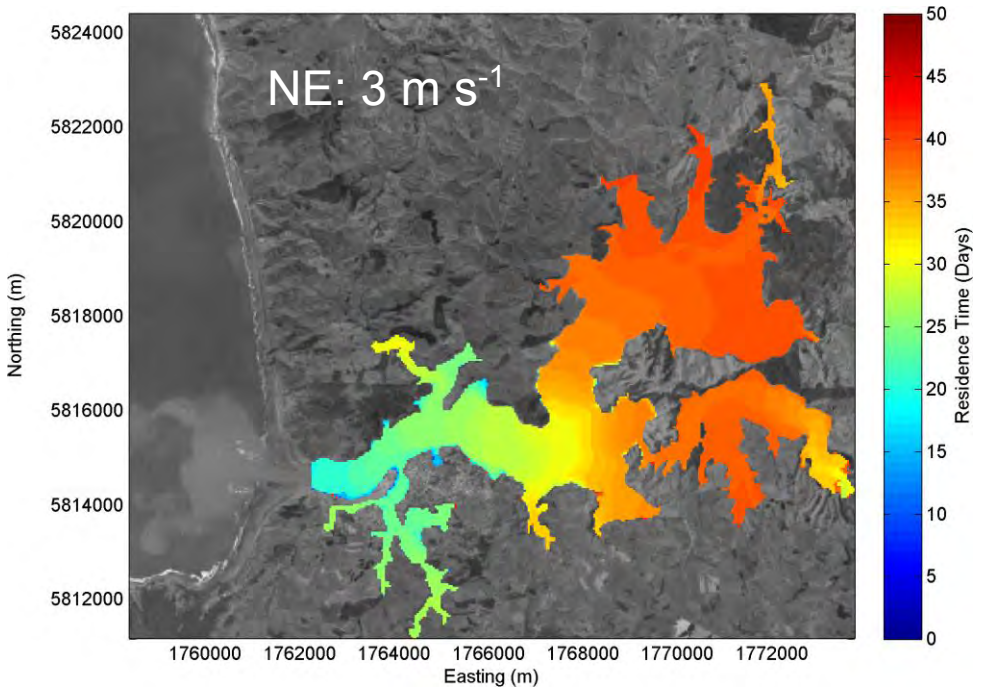

Figure 3.7: Residence time for Whaingaroa Harbour calculated using medium flow under north easterly wind. The tracer was released at high tide during mid-range tides.

3.3 The Effects of Altered Residence Time Thresholds

As discussed in Section 2.2, a cell in the model was considered flushed when the tide averaged concentration was reduced to 5% of the original tracer concentration, but other thresholds can be used (Sheldon and Alber, 2002). To examine the effect of threshold choice on residence time, results of a single scenario were post-processed using different thresholds. The scenario that was used for this was a high tide release during mid-range tides using medium flow rates. The thresholds used were 33%, 20%, 10% and 5% and the results are shown in Figure 3.8 to Figure 3.11.

As expected residence times got longer using lower thresholds as it took longer for the tracer concentration to reduce to the threshold value. However, for each threshold the pattern of spatial variability in residence times remained consistent with longer residence times in the head of the estuary than at the estuary mouth. Using a 33% threshold residence times were < 20 days in nearly all cells, for 20% this number rises to approximately 25 days, for 10% this rises to 30 days and finally for a 5% threshold, residence times are less than 45 days throughout the estuary.

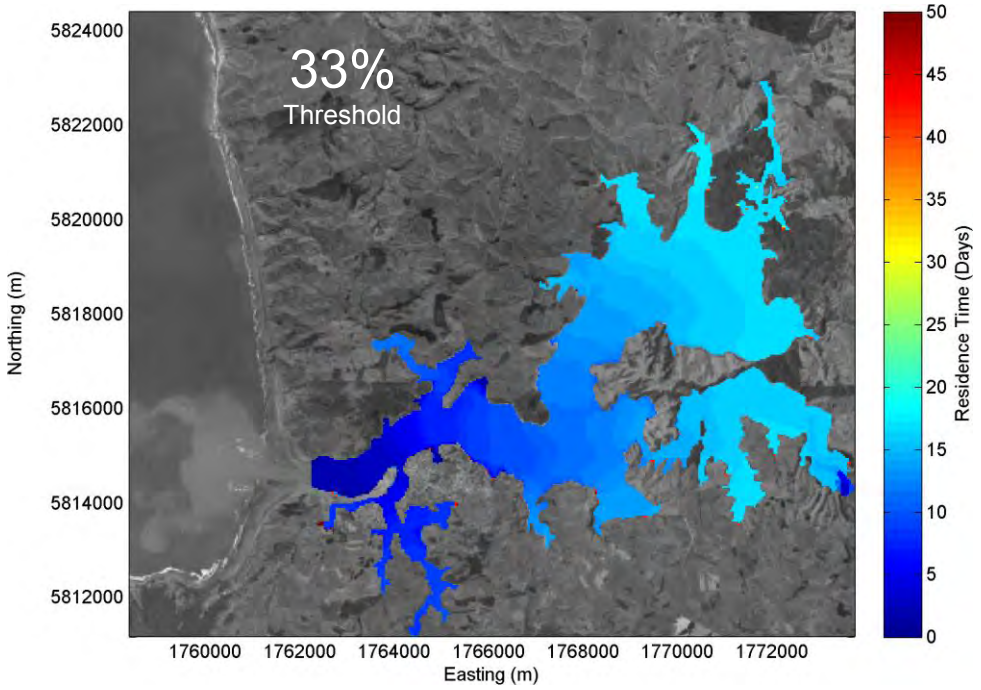

Figure 3.8: Residence time for Whaingaroa Harbour calculated using medium flow. The tracer was released at high tide during mid-range tides. The threshold at a cell was considered flushed was taken to be 33% of the original tracer concentration.

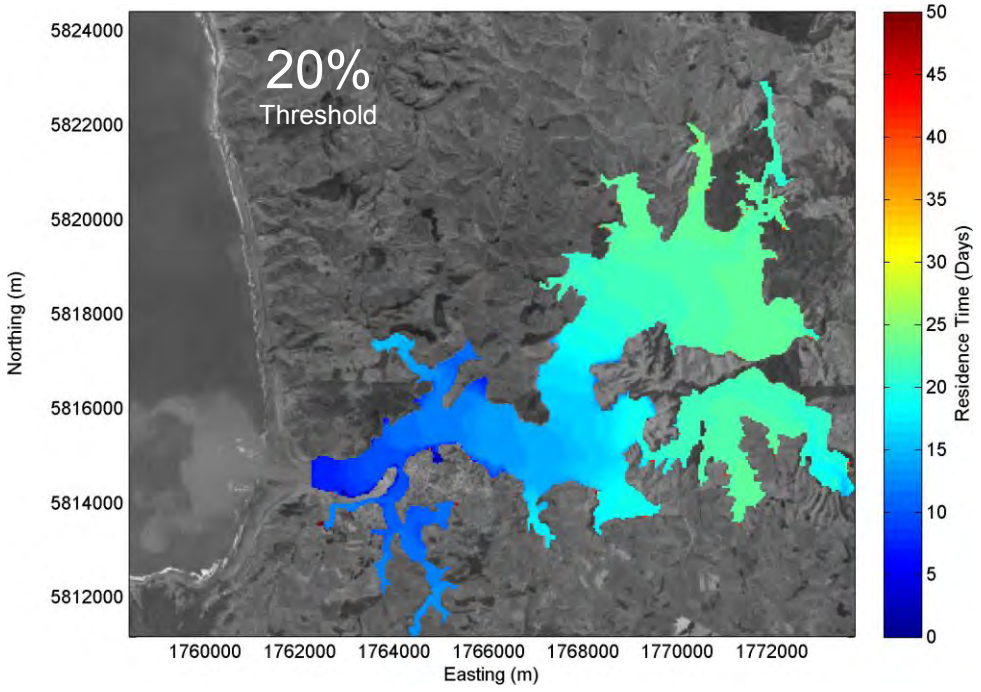

Figure 3.9: Residence time for Whaingaroa Harbour calculated using medium flow. The tracer was released at high tide during mid-range tides. The threshold at a cell was considered flushed was taken to be 20% of the original tracer concentration.

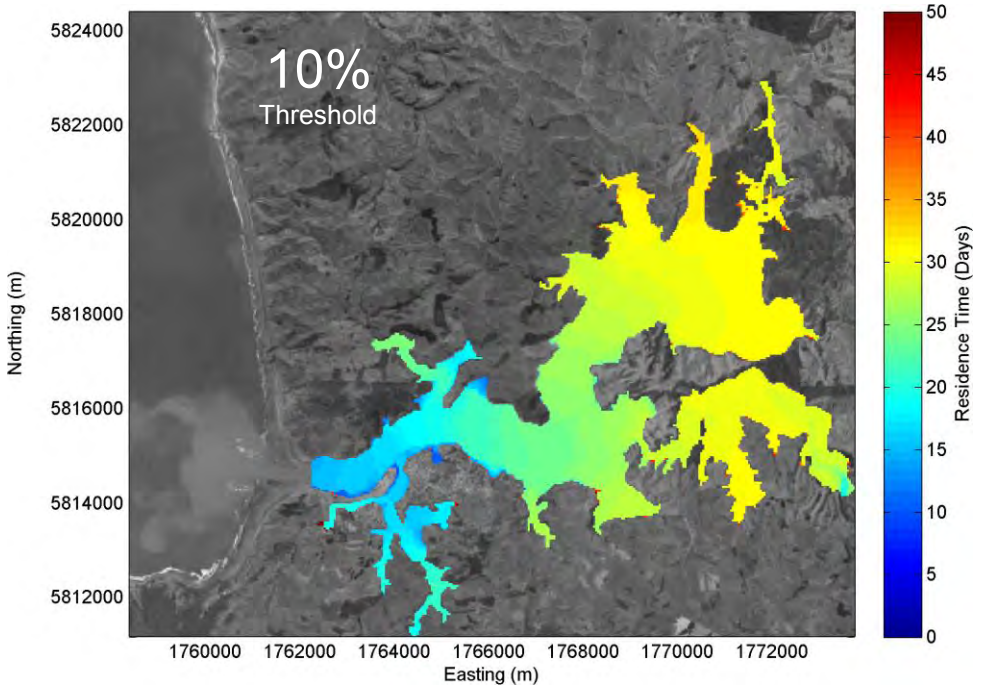

Figure 3.10: Residence time for Whaingaroa Harbour calculated using medium flow. The tracer was released at high tide during mid-range tides. The threshold at a cell was considered flushed was taken to be 10% of the original tracer concentration.

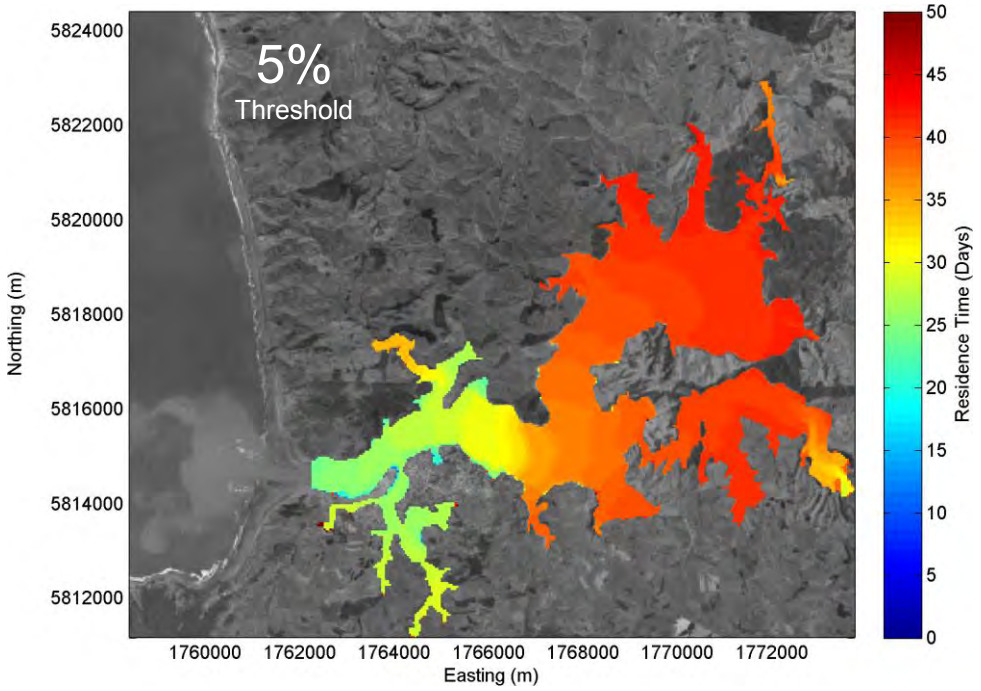

Figure 3.11: Residence time for Whaingaroa Harbour calculated using medium flow. The tracer was released at high tide during mid-range tides. The threshold at a cell was considered flushed was taken to be 5% of the original tracer concentration.

4 Discussion

The methodology for calculating residence times here has successfully been used to characterise the spatial variability of residence time throughout the seven estuaries on the west coast of the Waikato Region using partially calibrated hydrodynamic models. The modelling shows that residence time is longer for larger, more dendritic estuaries. Residence time increases towards the head of the estuaries except in high flow conditions where inflowing river water causes a reduction in residence time. Tidal river estuaries behave quite differently to tidally dominated estuaries with residence time being more heavily influenced by increased river flow and showing more uniform and lower residence times in the former. The work presented here provides a tool for comparing the relative residence times of different estuaries and establishing the residence time variability within estuaries.

The spatially variable residence times presented in Section 2 were analysed to calculate single value median residence times for each estuary for each flow rate. The results are presented in Table 4.1. This illustrates the longer residence times in the drowned river valley estuaries compared with tidal river estuaries, and how increased flow rates reduce residence time.

Table 4.1: Median residence time for whole estuary under different conditions

Estuary	low Flow (days)	Medium Flow (days)	High Flow (days)
Waikato River estuary	1.8	1.1	0.6
Whaingaroa (Raglan) Harbour	38.9	39.4	26.8
Aotea harbour	11.8	11.8	10.2
Kawhia Harbour	27.3	30.0	22.3
Marokopa River estuary	1.6	0.6	0.1
Awakino River estuary	2.2	0.7	0.2
Mokau River estuary	3.4	1.1	0.2

There are many different methodologies for calculating residence time using numerical models (Aikman and Lanerolle, 2004), and all have strengths and limitations. The method used here describes the rate at which water in the harbour is replaced by water introduced either from the sea or from inflowing rivers. This method is also useful for understanding how different meteorological and oceanographic conditions affect the residence time. However, it does not differentiate between river and ocean water.

A sensitivity analysis investigated the effect of wind, tidal releases times, and residence time thresholds on residence times in Whaingaroa Harbour. Prevailing south-westerly and north-easterly winds resulted in decreased residence times, and the choice of residence time threshold had a marked effect on estimated residence time. This sensitivity analysis highlights that the residence times estimated in this study should be interpreted with caution. Whilst the results are likely to be useful for assessing the relative difference in residence time between

estuaries and between different parts of the estuaries, further work is required to assess the validity of the results as absolute measures of residence times.

It would be beneficial to extend this work to examine the dilution of river water in the estuary as this would be less sensitive to the upstream location of the model open boundary. This could be achieved by releasing conservative tracers from the rivers and investigating the dilution patterns of the pollutant under different flow conditions specific to different rivers. This would provide the capacity to gain a thorough understanding of how individual rivers affect different parts of the harbours. An example of this approach is shown for the Waingaro River in Whaingaroa Harbour in Figure 4.1. Using this approach, it may also be useful to explore the effect of event based high river flow events rather than the constant flows used in the results presented here.

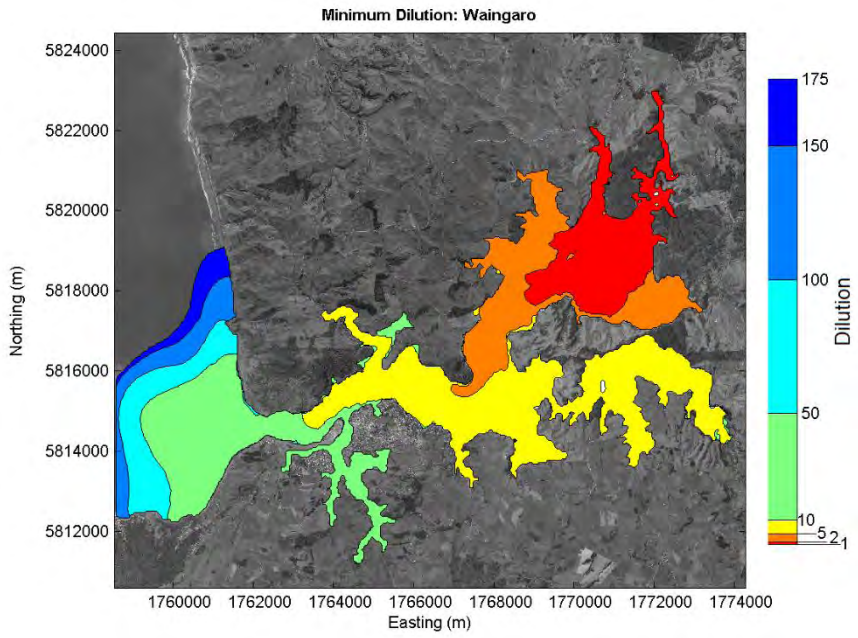

Figure 4.1: Minimum dilution of river water in Whaingaroa Harbour during a large flood event from the Waingaro River.

There are technical issues relating to the hydrodynamic modelling which could be addressed were this work to be extended. The models are currently 2D and model performance (Appendix B) may be improved by extending the models to 3D. An MSc project currently underway (R. McIntosh Pers. Comm., 2016) is aimed at recalibrating a 3D model of Whaingaroa harbour. The results of this study (due in 2016) will establish the value of extending the modelling to 3D. It may be more computationally efficient to use curvilinear grids or unstructured meshes when extending the model to 3D.

It would also be useful to address shortfalls in the catchment models used for the estuaries. For example, there are no gauged rivers in Aotea harbour, and gauging of one or more of the larger rivers in this catchment would be of great benefit in calibrating the catchment model. Additionally, the catchment model used for the drowned river valley estuaries produces daily flow rates, and it would be beneficial to increase the resolution of this model to an hourly time step.

For the tidal river estuaries, model performance may also be significantly improved if the model domains were extended upstream to a location where the main inflowing rivers are no longer tidal. This would require additional bathymetric surveying in order to generate the bathymetry grids, and in addition it would likely be necessary to employ a different gridding scheme (curvilinear or unstructured) to achieve this. The residence times for the tidal river estuaries will be sensitive to the extent of the model domain in the upstream direction. Moving the riverine open boundary up stream and extending the model domain accordingly would also result in longer estimated residence times.

All seven of the estuary models would benefit from further calibration and validation. This would require the collection of additional measured data from each estuary.

5 Conclusions

Using the partially calibrated hydrodynamic models from Appendix B, a methodology has been successfully implemented to calculate spatially variable residence times in seven estuaries along New Zealand's west coast in the Waikato Region. The method has identified the within estuary harbour variability in residence time as well as intra-estuary variability.

The study found that in drowned river valley estuaries there is a gradient in residence times from the mouth to the head of the estuaries with longer residence times in the estuary heads. Larger estuaries had longer residence times in general as would be expected. In Whaingaroa and Aotea Harbour increased river flow led to an increase in residence time close to the estuary mouths though this was not the case for Kawhia Harbour. Increased river flow led to an overall decrease in residence time. Tidal river estuaries had lower residence times overall and residence times were more sensitive to river flow than in drowned river valley estuaries. The calculation of residence time for tidal river estuaries is also sensitive to the upstream location of the model boundary, and it may be appropriate to address this in future development of the models.

Sensitivity analysis was carried out using the model of Whaingaroa Harbour to investigate the effect of wind and different tidal releases on residence times as well as using different residence time thresholds. Prevailing SW and NE winds were found to decrease residence time over all and the choice of residence time threshold had a marked effect on estimated residence time. This sensitivity analysis highlights that the residence times estimated in this study should be interpreted with caution. Whilst the results are likely to be useful for assessing the relative difference in residence time between estuaries and between different parts of the estuaries, further work is required to assess the validity of the results as absolute measures of residence times.

It is important to note that this study provides a proof-of-concept only for mapping residence times in estuaries. The hydrodynamic models were relatively simple and only partially calibrated. As such, the results are considered indicative, but the models and methodology can be refined in the future to improve the accuracy of the residence time estimates. For example, the hydrodynamic models could be refined by extending the models to 3D (particularly in estuaries where stratification is likely to be an important process), and by further model calibration and validation, which would require the collection of more field data. Furthermore, refining the catchment models (e.g. by measuring river flow in ungauged catchments) would improve estimates of freshwater inputs to the estuaries, which would likely improve the residence time estimates. Further work is also required to investigate methodologies that use alternative definitions of residence times and/or the dilution of

freshwater in estuaries, and to place each of these different definitions of residence times in the appropriate context(s) for resource management.

6 Acknowledgements

eCoast would like to thank all of the Kaitiaki of the west coast harbours along the Waikato west coast for their time and for sharing knowledge and experience of the estuaries. Thanks also to Malibu Hamilton and Danielle Hart for their support in the process of consultation.

We would also like to thank the staff at WRC for their support in delivering large amounts of data in short time frames (Debbie Eastwood, Aaron Jefferies, Howard Ettema and Heather Braybrook), and to Hannah Jones and Steve Hunt for their support throughout this project.

Finally, we would also like to thank Shawn Harrison for time, advice and access to data for Whaingaroa Harbour.

7 References

Aikman, F. I., & Lanerolle, L. W. J. (2004). Report on the National Ocean Service Workshop on Residence / Flushing Times in Bays and Estuaries. NOS Workshop on Residence/Flushing Times in Bays and Estuaries, 1–25.

Becker, J. J., D. T. Sandwell, W. H. F. Smith, J. Braud, B. Binder, J. Depner, D. Fabre, J. Factor, S. Ingalls, S-H. Kim, R. Ladner, K. Marks, S. Nelson, A. Pharaoh, R. Trimmer, J. Von Rosenberg, G. Wallace, P. Weatherall., (2009), Global Bathymetry and Elevation Data at 30 Arc Seconds Resolution: SRTM30_PLUS, Marine Geodesy, 32:4, 355-371, DOI: 10.1080/01490410903297766.

Defne, Z., & Ganju, N. K. (2014). Quantifying the Residence Time and Flushing Characteristics of a Shallow, Back-Barrier Estuary: Application of Hydrodynamic and Particle Tracking Models. Estuaries and Coasts. doi:10.1007/s12237-014-9885-3

Deltares, 2013. User Manual Delft3D-FLOW. version: 3.15.2789, May 2013 Published and printed by: Deltares, 706 p. available online: http://oss.deltares.nl/web/delft3d/manuals.

Lee, H. W., & Park, S. S. (2013). A hydrodynamic modeling study to estimate the flushing rate in a large coastal embayment. Journal of Environmental Management, 115, 278–286. doi:10.1016/j.jenvman.2012.10.055.

Liu, W. C., Chen, W. B., & Hsu, M. H. (2011). Using a three-dimensional particle-tracking model to estimate the residence time and age of water in a tidal estuary. Computers and Geosciences, 37(8), 1148–1161. doi:10.1016/j.cageo.2010.07.007

Miller, R. L., & McPherson, B. F. (1991). Estimating estuarine flushing and residence times in Charlotte Harbor, Florida. via salt balance and a box model. Limnology and Oceanography, 36(3), 602–612. doi:10.4319/lo.1991.36.3.0602.

Pokavanich, T., & Alosairi, Y. (2014). Summer Flushing Characteristics of Kuwait Bay. Journal of Coastal Research, 297, 1066–1073. doi:10.2112/JCOASTRES-D-13-00188.1.

Sheldon, J. E. and Alber, M. (2002). A Comparison of Residence Time Calculations Using Simple Compartment Models. Coastal and Estuarine Research Federation, Part B: Dedicated Issue: Freshwater Inflow: Science, Policy, Management: Symposium Papers from the 16th Biennial Estuarine Research Federation Conference (Dec., 2002), 25(6), 1304–1317.

Zimmerman, J. T. F. (1976). Mixing and flushing of tidal embayments in the western Dutch Wadden Sea part I: Distribution of salinity and calculation of mixing time scales. Netherlands Journal of Sea Research, 10(2), 149–191. doi:10.1016/0077-7579(76)90013-2.

Appendix A. **Fieldwork**

Mapping Residence Times in West Coast Estuaries of the Waikato Region: Fieldwork and Data Collection

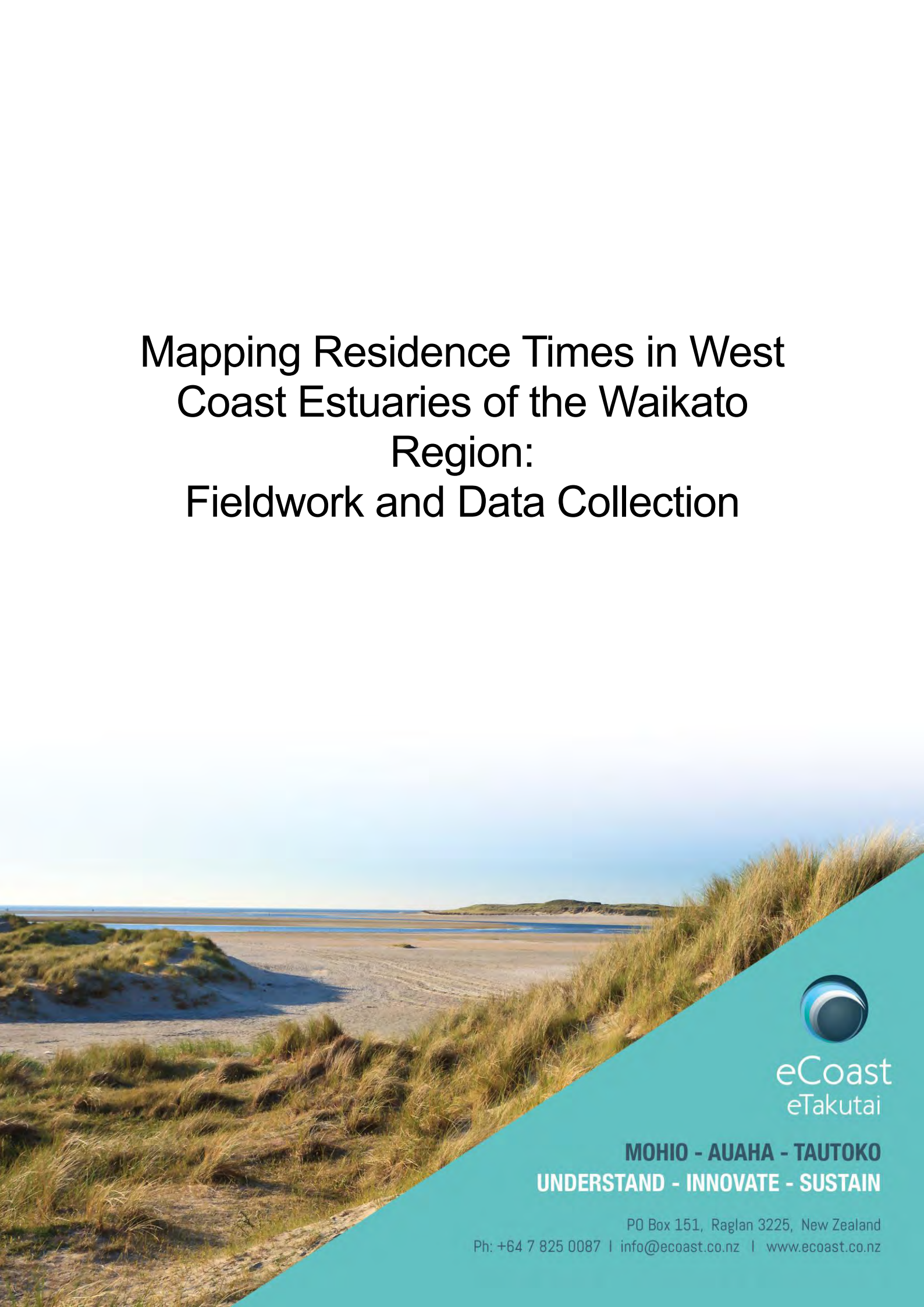

eCoast
eTakutai

MOHIO - AUAHA - TAUTOKO
UNDERSTAND - INNOVATE - SUSTAIN

PO Box 151, Raglan 3225, New Zealand
Ph: +64 7 825 0087 | info@ecoast.co.nz | www.ecoast.co.nz

Mapping Residence Times in West Coast Estuaries of the Waikato Region: Fieldwork and Data Collection

Report Status

Version	Date	Status	Approved by
V1	16/01/2016	Draft	STM
V2	25/05/2016	Final	DG

It is the responsibility of the reader to verify the version number of this report.

Authors

Ed Atkin, *HND, MSc (Hons)*

Dougal Greer, *MSc*

Shaw Mead *BSc, MSc (Hons), PhD*

Tim Haggitt *BSc, MSc (Hons), PhD*

Sam O'Neill *BSc, MSc (Hons)*

Table of Contents

Table of Figures

Table of Tables

1 Introduction

This document presents the fieldwork methodology and data collected as part of a study aimed at developing a methodology to map residence times in west coast estuaries. The fieldwork was undertaken between the 17th of August 2015 and 16th of December 2015 and consisted of instrument deployments and survey work in each estuary. Figure 1.1 provides a timeline showing when each component of the fieldwork was undertaken. Kaitiaki local to each estuary were consulted as part of this project. This included meetings, phone calls and sending out information packs describing the purpose of the project.

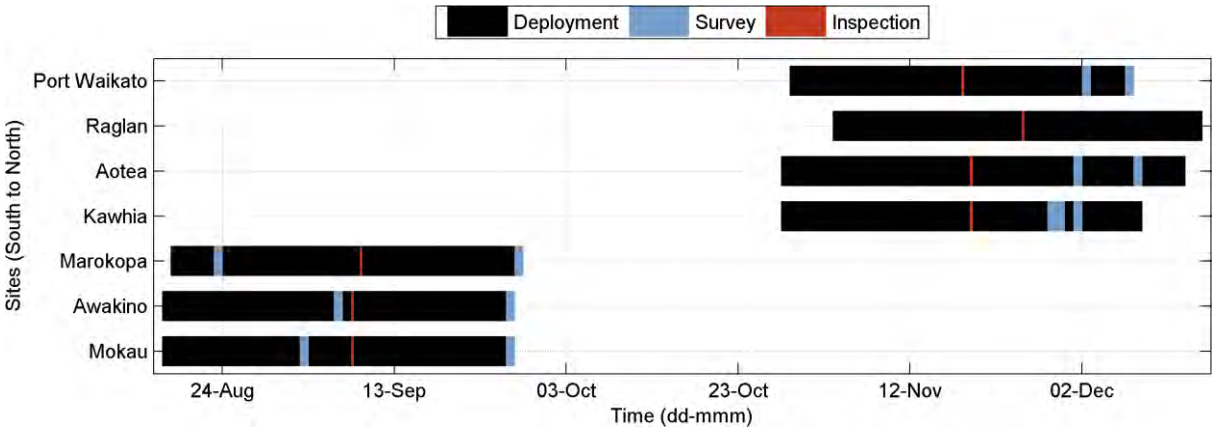

Figure 1.1: Fieldwork Gantt chart.

This document consists of three main sections following the introduction, namely, Instrument Deployments, Survey and Site Observations. Within each of the three main sections seven subsections describe the work undertaken at each site.

2 Instrument Deployments

Within each study site instruments were deployed at 2 locations for ~6 weeks with a midway (~3 week) inspection. With the exception of Raglan, the instruments collected current speed and direction, water level, temperature and conductivity (salinity). At Raglan only temperature and conductivity were recorded since sea level, current and bathymetric data already exist from tide gauges and previous field work campaigns (Greer *et al*., 2015). Instruments used to record current and water level data were deployed on the river/estuary bed secured to aluminium or stainless steel frames (Figure 2.1). The frames were secured in place with concrete block outriggers. At each deployment location a single Temperature-Salinity (TS) gauge was attached to the frame and another attached to a surface marker buoy.

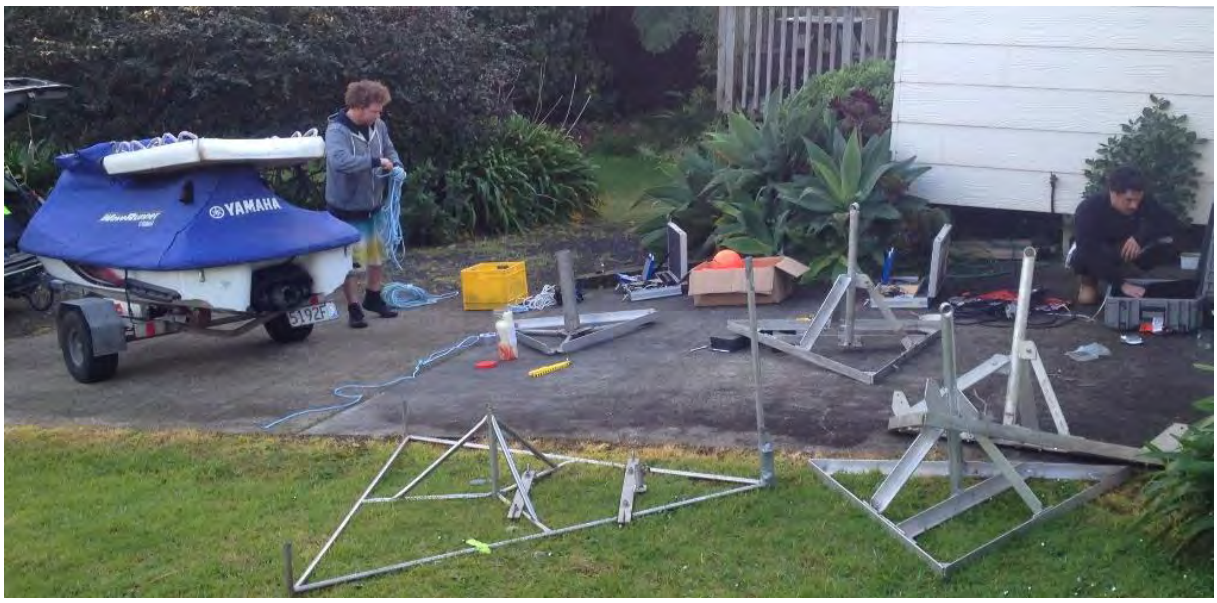

Figure 2.1: Preparing instrumentation and the mounting frames for use in the fieldwork at Mokau.

The 2 deployment locations at each study site are named “Upper” and “Lower”, relative to their location within the river/estuarine system. The exceptions are Raglan and Kawhia, where the deployments were made at intermediate locations within the harbours, more detail for these locations is provided in 2.2 and 2.4, respectively.

Pre-deployment checks were made of every instrument including compass and pressure calibrations for instruments collecting current and water level data using the instrument manufactures methods and proprietary software. Compass calibrations for current directions yielded accuracies of 1° or less. Water level is derived from pressure which is measured with a piezoresistive pressure sensor. Calibration involves resetting the pressure readings to zero in air. Prior to and following deployments, TS gauges collected data in a container of water sampled from the study sites. Salinity and electrical conductance of the sample were recorded

either by a sub sample being retained for laboratory analysis, or in situ with a high accuracy probe. In addition, surface samples for laboratory analysis were taken in-situ during midway inspections. Laboratory analysis follows APHA (2012) standard methods for the examination of water. The laboratory and probe data collected before and after deployments were used to calibrate TS gauges during post-processing.

All water levels and current profile data have been adjusted to depth above reference bed level, which in most cases is consistent throughout the deployment. At Port Waikato and Aotea subsidence was significant and depths and reference levels for currents have been adjusted accordingly to reflect depth above bed level.

The pressure record from each of the deployment locations was corrected for the Inverse Barometer Effect (IBE), using the sea level barometric pressure record from the Whaingaroa (Raglan) Harbour Automatic Weather Station (AWS). The sea/river water density is calculated with the IBE corrected pressure record and in-situ salinity and temperature records using the international equation of state (Millero *et al*., 1980; Fofonoff and Millard, 1983). The obtained density values (ρ) are used with the IBE corrected pressure record (p) and acceleration due to gravity (g) as a function of latitude (φ) to calculate depth (z) using the hydrostatic equation:

$$\mathrm{p}(z) = \int_{-h}^{0} g(\varphi, z)\rho(z)dz$$

The equation was applied under the assumption that ρ is constant with depth. It should be noted that a pressure record is not an output from the RDI Sentinel Workhorse (used at Mokau and Aotea Lower sites). Depths are calculated by the instrument based on an estimated salinity and measured pressure. The pressure record was calculated using the depth record as an approximation of pressure (<0.5 % difference) and the constant salinity set internally in the instrument. The “raw” pressure record obtained was then processed as described previously.

Each of the following subsections is broken down in to 2 further subsections relating to the 2 deployment locations within each study site, i.e. Upper and Lower. Table 2.1 summarises the instruments deployments, noting what type of instruments were used, how often data were collected, notes relevant to data collection, and in some cases multiple deployment positons. The reader should however refer to the detailed description provided in the following subsections.

Table 2.1: Summary of instrument deployments.

	Waikato		Raglan		Aotea		Kawhia		Marokopa		Awakino		Mokau	
Sub site	**Upper**	**Lower**	**Waitetuna**	**Opotoru**	**Upper**	**Lower**	**Township**	**Te Waitere**	**Upper**	**Lower**	**Upper**	**Lower**	**Upper**	**Lower**
Location (Lat/Long)	37.2801S 174.8456E	37.3850S 174.7330E	37.7967S 174.9284E	37.8171S 174.8715E	37.9318S 174.8524E	38.0056S 174.8286E	38.0688S 174.8195E	38.1338S 174.8243E	38.2926S 174.7460E	38.3005S 174.7207E	38.6635S 174.6466E	38.6489S 174.6254E	38.7057S 174.6510E	38.6998S 174.6274E
Dates	29/10/2015 to 8/12/2015		3/11/2015 to 16/12/2015		28/11/2015 to 14/12/2015		28/11/2015 to 9/12/2015		18/08/2015 to 28/09/2015		17/08/2015 to 27/09/2015		17/08/2015 to 27/09/2015	
Current Speed and Direction and depth (depth not measured by Sontek ADP)														
Instrument Make / Model	Nortek / Aquadopp / Current Meter	Nortek / Aquadopp / Profiler	NA	NA	Nortek / Aquadopp / Current Meter	RDI / Sentinel Workhorse	Sontek / ADP	Nortek / Aquadopp / Current Meter	Nortek / Aquadopp / Current Meter	Sontek / ADP	Nortek / Aquadopp / Current Meter	Nortek / Aquadopp / Profiler	Nortek / Aquadopp / Current Meter	RDI / Sentinel Workhorse
Sampling Interval	15 minutes	15 minutes	NA	NA	15 minutes	15 minutes	30 minutes	15 minutes	15 minutes	30 minutes	15 minutes	15 minutes	15 minutes	15 minutes
Averaging interval	5 minutes	5 minutes	NA	NA	5 minutes	5 minutes	5 minutes	5 minutes	5 minutes	5 minutes	5 minutes	5 minutes	5 minutes	5 minutes
Type	Single Bin	Profiler	NA	NA	Single Bin	Profiler	Profiler	Single Bin	Single Bin	Profiler	Single Bin	Profiler	Single Bin	Profiler
Bin size	0.3 m	0.5 m	NA	NA	0.3 m	0.5 m	1 m	0.3 m	0.3 m	1 m	0.3 m	0.5 m	0.3 m	0.5 m
Temperature/Salinity (Depth measured by YSI / EXO Sonde II)														
Surface Make / Model	Onset HOBO / U24-002-C	Onset HOBO / U24-002-C	Onset HOBO / U24-002-C	Onset HOBO / U24-002-C	Onset HOBO / U24-002-C	Onset HOBO / U24-002-C	Onset HOBO / U24-002-C	Onset HOBO / U24-002-C	Onset HOBO / U24-002-C	Onset HOBO / U24-002-C	Onset HOBO / U24-002-C	Onset HOBO / U24-002-C	Onset HOBO / U24-002-C	Onset HOBO / U24-002-C
Bed Make / Model	Onset HOBO / U24-002-C	Onset HOBO / U24-002-C	Onset HOBO / U24-002-C	Onset HOBO / U24-002-C	Onset HOBO / U24-002-C	Onset HOBO / U24-002-C	YSI / EXO Sonde II	Onset HOBO / U24-002-C	Odyssey / TS Recorder	YSI / EXO Sonde II	Odyssey / TS Recorder	YSI / EXO Sonde II	Onset HOBO / U24-002-C	Onset HOBO / U24-002-C
Sampling Interval	15 minutes	15 minutes	15 minutes	15 minutes	15 minutes	15 minutes	15 minutes	15 minutes	15 minutes	15 minutes	15 minutes	15 minutes	15 minutes	15 minutes
Comment	Unable to retrieve bed level TS data	Subsidence of instrument frame; TS gauge severely damage, data irretrievable	Significant biofouling of bed level instrument; data poor after ~4 weeks	Significant biofouling of bed level instrument; data poor after ~4 weeks	Instrument sensor head breaching surface during low waters	Surface TS Gauge retrieved on 9/12/2015; ADCP buried, data poor after ~4 weeks	NA	NA	NA	Multiple locations: Position 2: 38.3006S 174.7208E	NA	NA	NA	Multiple locations: Position 1: 38.7001S 174.6279E Position 2: 38.6997S 174.6274E

2.1 Waikato River estuary

Figure 2.2 shows the two deployment locations at Waikato River estuary, the instruments were deployed on the 29th of October 2015. The instruments were inspected on the 18th of November 2015, and retrieved on the 8th of December 2015. The Upper site, at 37.28005°S/174.84562°E, is central to the Waikato River, opposite the Elbow Waterski Club. The Lower site, at 37.38501°S/174.73304°E, is ~100 m north-northeast of Port Waikato Wharf.

At the Upper site a Nortek Aquadopp was deployed in ~3 m of water collecting current speed and direction at a fixed height ~ 0.8 m from the bed, and depth from a pressure sensor located ~ 0.6 m from the bed. At the Lower site a Nortek Aquadopp Profiler was deployed in ~4.5 m of water measuring depth above the instrument pressure sensor, and current speed and current direction in 0.5 m bins from 0.6 m above the seabed to the surface. Onset U24-002-C loggers were used to collect TS data at the surface and just above the bed at both sites. The sampling interval for all of the instruments was 15 minutes, with current measurements averaged over 5 minute intervals. The surface U24-002-C logger at the Lower site was destroyed during the deployment at an unknown date from an acute impact that was evident both on the surface marker buoy and the logger. The data were irretrievable. The bed level logger at the upper site failed to collect any data, likely due to a software malfunction.

Figure 2.2: Waikato River estuary deployment locations.

2.1.1 Upper site

Figure 2.3 shows the depths recorded during the deployment period. Tidal modulation is clearly apparent with a range of ~1 m. A longer period modulation of water level signal is apparent, particularly in the last third of the times series.

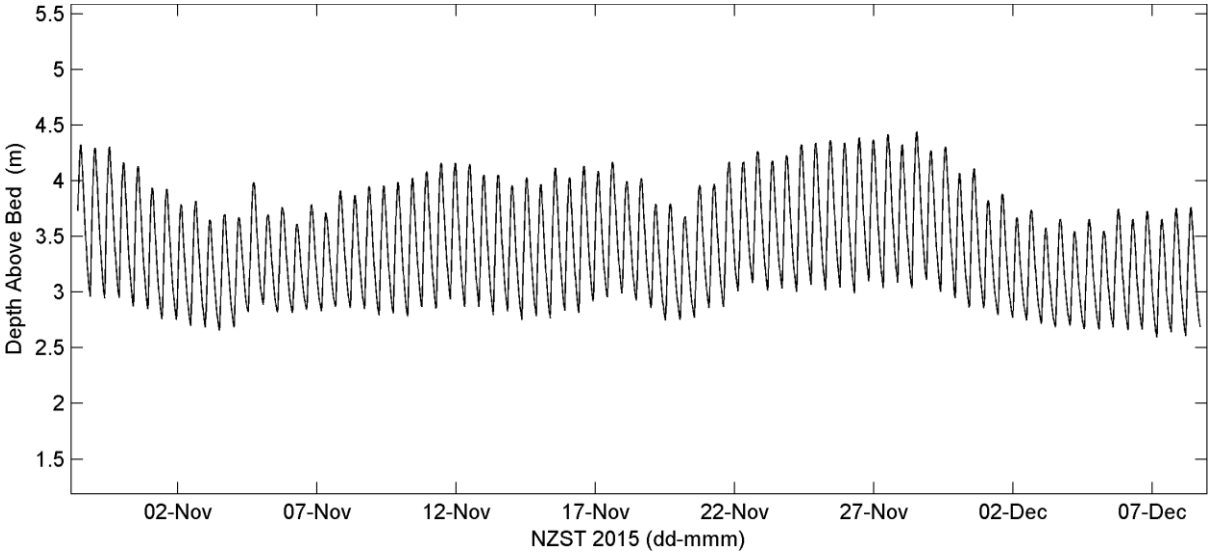

Figure 2.3: Waikato River estuary, Upper site, water depth.

Figure 2.4 and Figure 2.5 present current data at a fixed height 0.7 m above the bed. Current speed rarely exceeded 0.5 ms^{-1}. Current direction was dominated by downstream flow, around 200°T. However, reversals in direction do occur occasionally during the flooding tide for short periods of time and at low velocities.

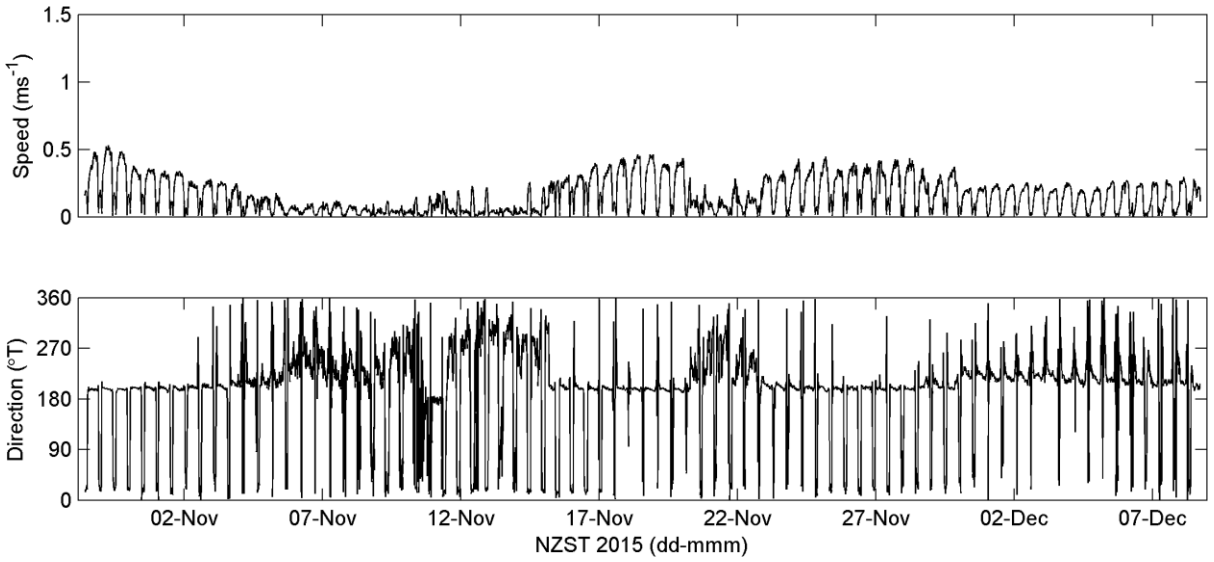

Figure 2.4: Waikato River estuary, Upper site, current speed (top) and direction (bottom).

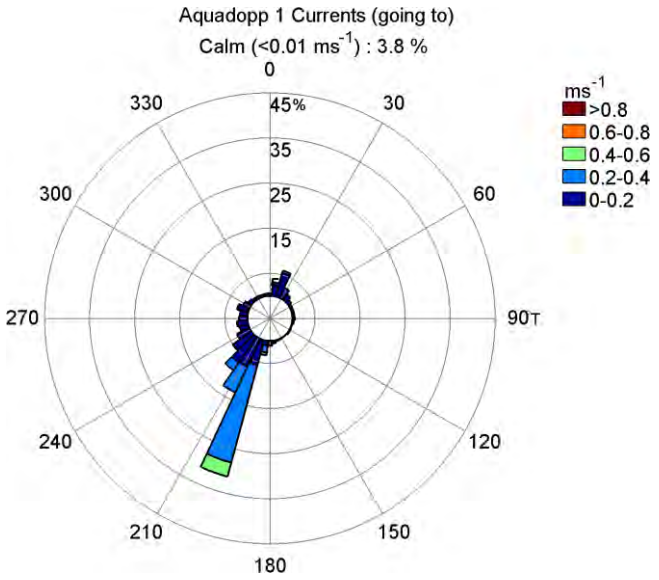

Figure 2.5: Waikato River estuary, Upper site, current speed and direction rose plot.

Figure 2.6 shows TS data collected at the surface. Temperatures range between ~17°C and ~22°C. Salinity readings were not observed above 0.1 psu for the entire deployment period. Figure 2.7 presents the temperature record from the Aquadopp's on-board thermistor (0.7 m form the bed). Temperatures also range between ~17°C and ~22°C.

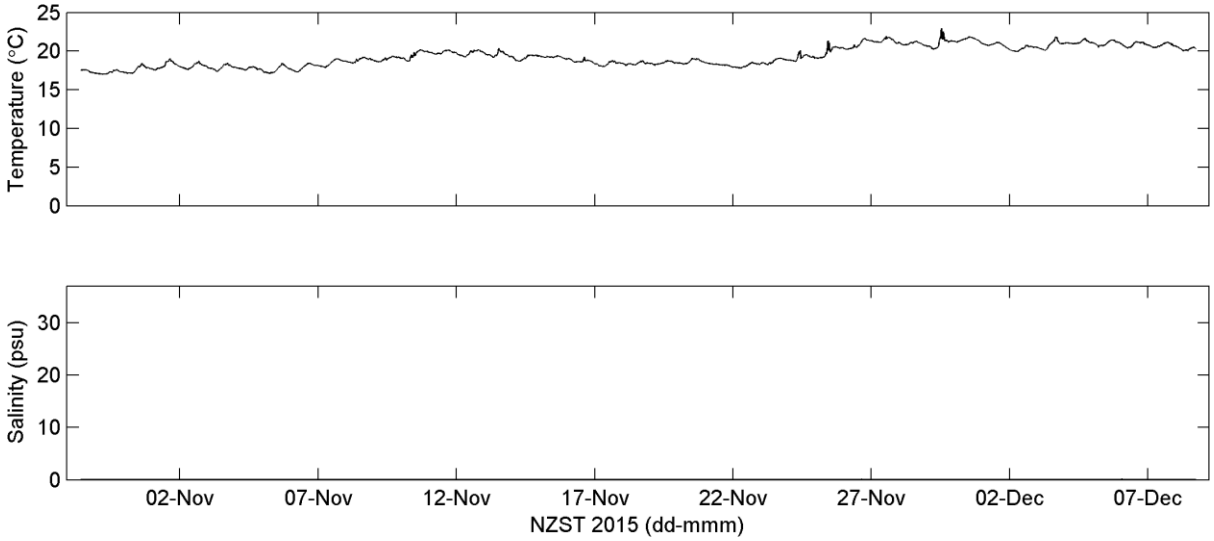

Figure 2.6: Waikato River estuary, Upper site, surface temperature (top) and surface salinity (bottom).

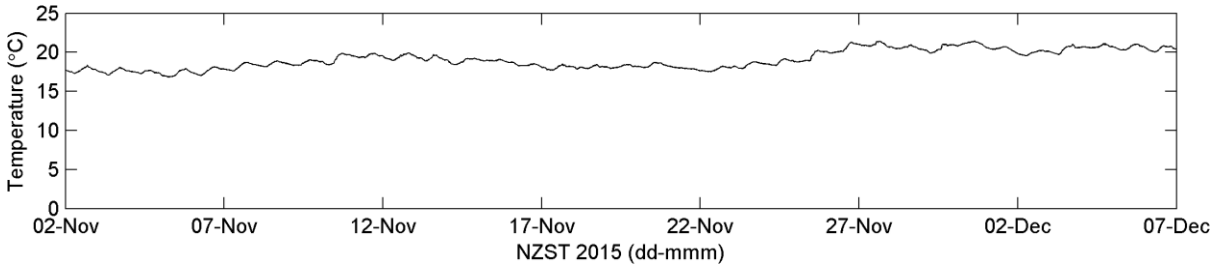

Figure 2.7: Waikato River estuary, Upper site, surface temperature.

2.1.2 Lower site

Figure 2.8 shows a time series of depth recorded at the Lower site. The data indicates that the reference level of the instrument changed over time. This is most likely due to bed level changes associated with subsidence which was observed during midway servicing and instrument retrieval. Water levels and the heights of profiling bins have been adjusted by linear de-trending.

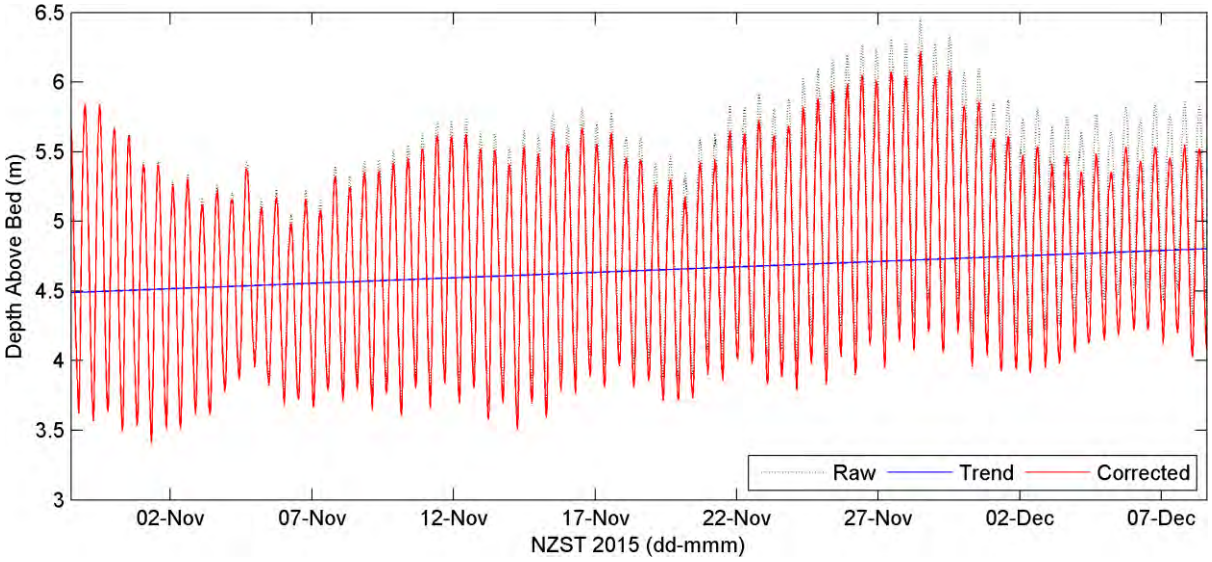

Figure 2.8: Waikato River estuary, Lower site, water depth. Black dotted: recorded data; Blue Line: trend/adjustment; Red line: adjusted data.

Figure 2.9 and Figure 2.10 present the current speed and direction through the water column in 0.5 m bins, and water level. Figure 2.11 presents snap shots of current speed and direction through the water column toward the end of the deployment. Figure 2.12 and Figure 2.13 present the depth averaged current speed and direction as line plots and rose plots respectively. Currents speeds were not observed in excess of 1.5 ms^{-1}. Current directions were approximately orientated along an east-west axis.

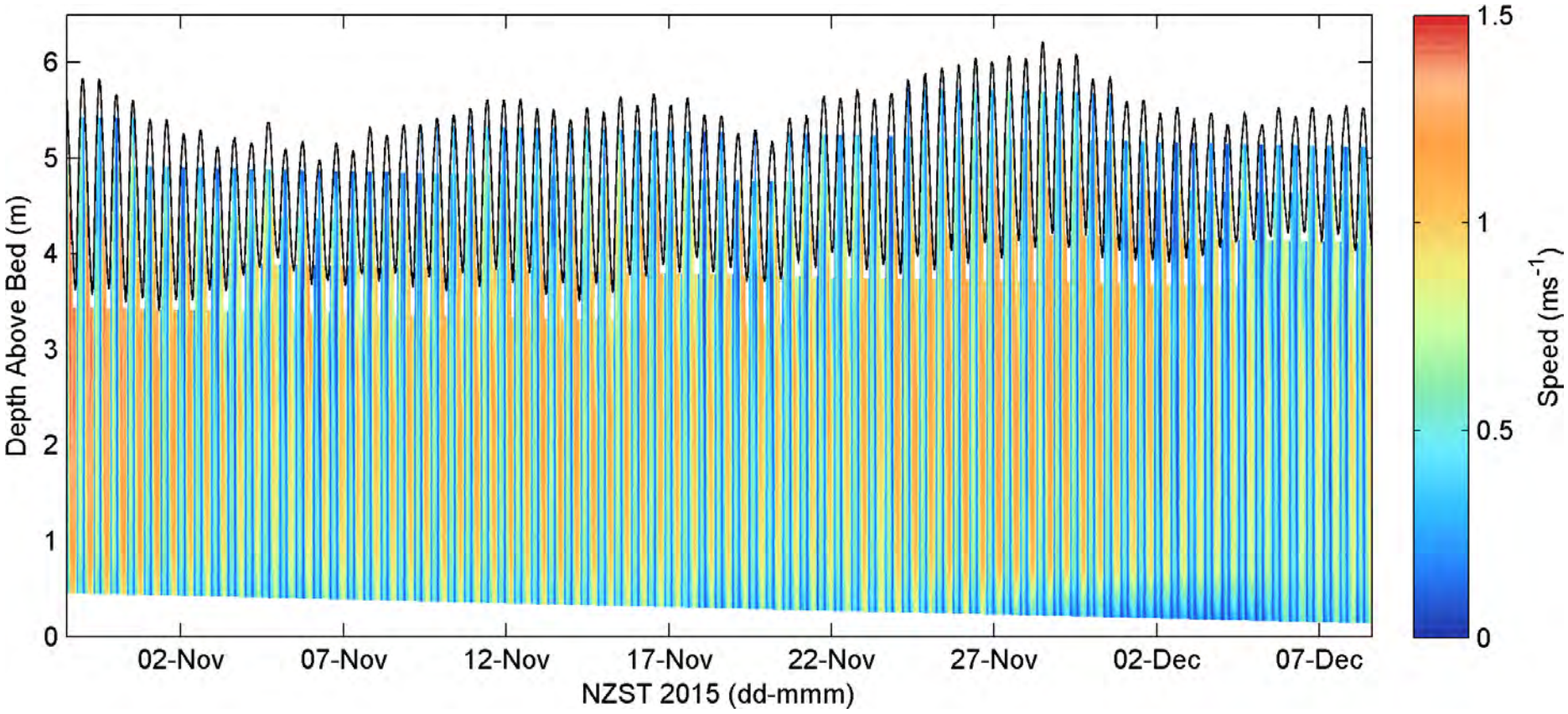

Figure 2.9: Waikato River estuary, Lower site, Current speed profile data; Black line: water level.

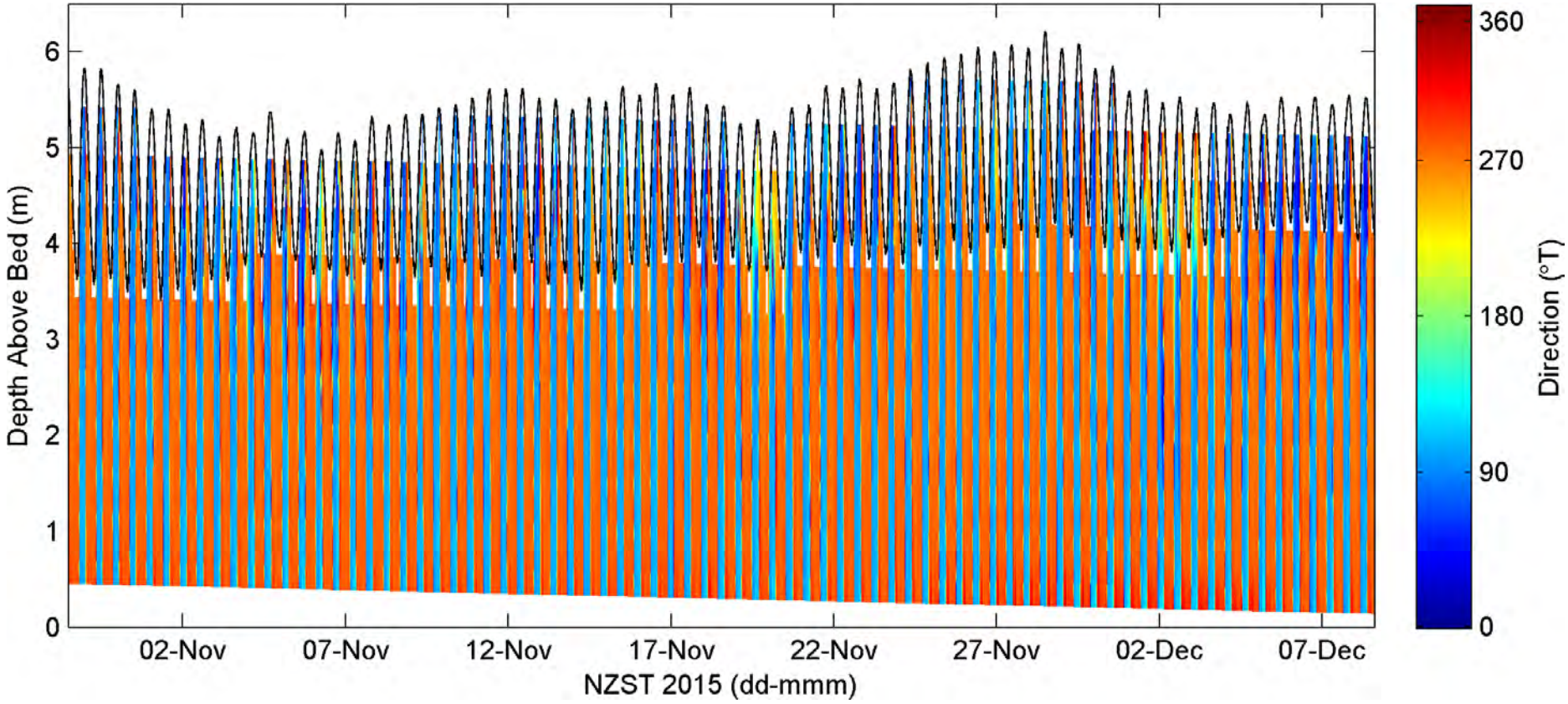

Figure 2.10: Waikato River estuary, Lower site, Current direction profile data; Black line: water level.

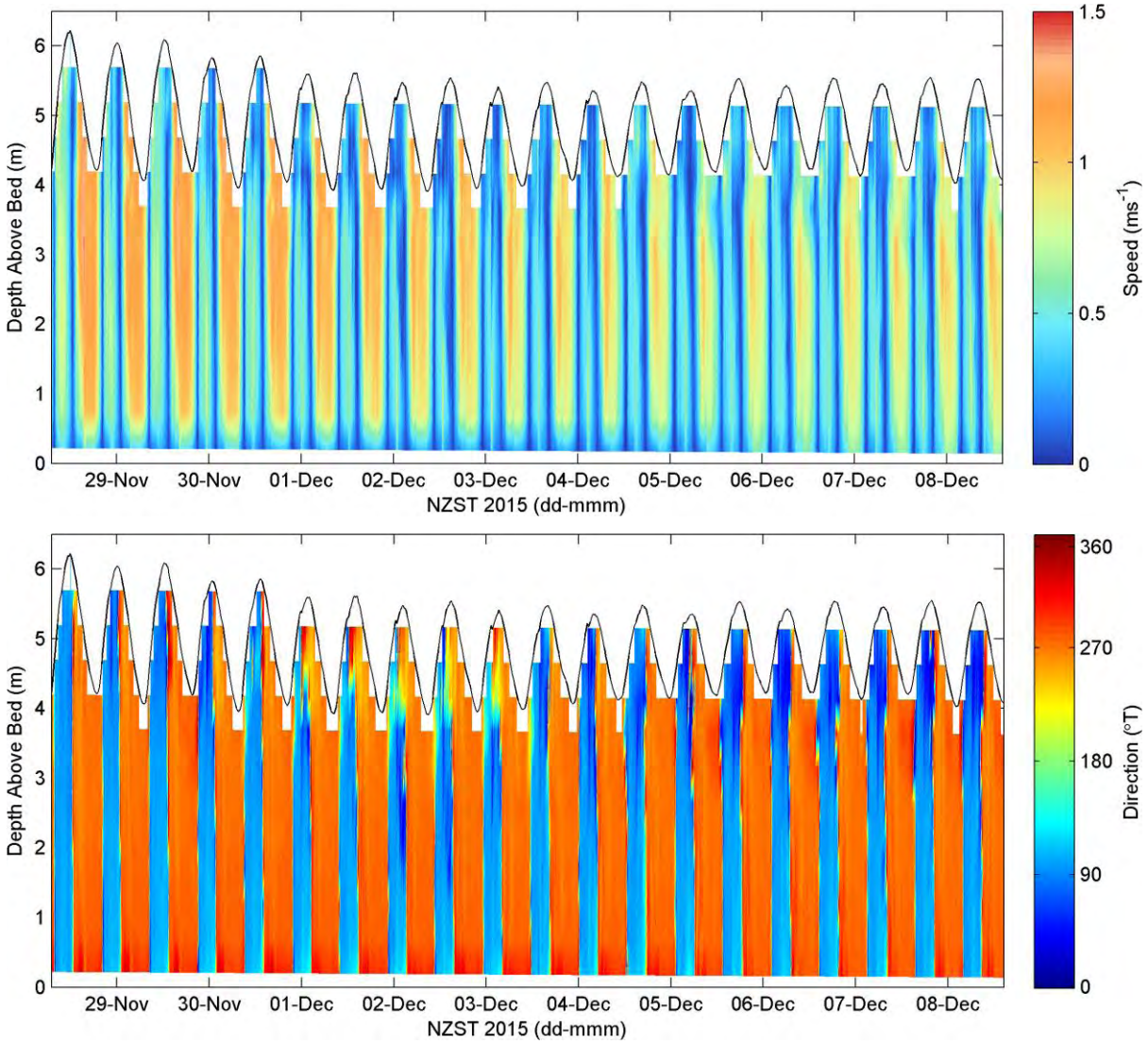

Figure 2.11: Waikato River estuary, Lower site, Current speed (top) and direction (bottom) profile data snap shot from the end of the deployment period.

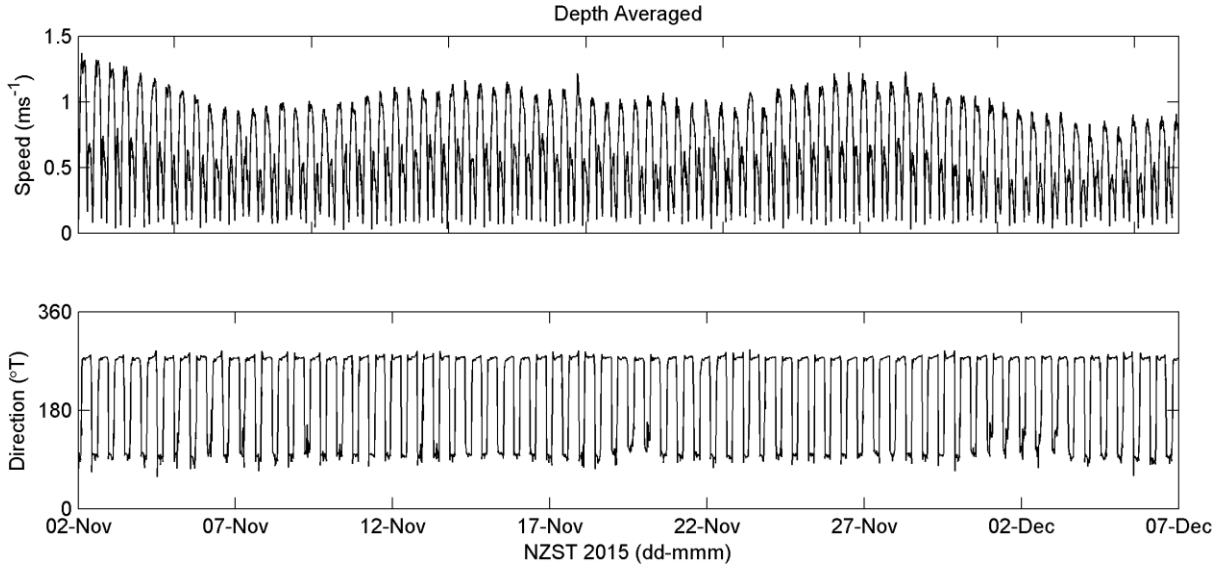

Figure 2.12: Waikato River estuary, Lower site, Depth averaged current speed (top) and direction (bottom) data.

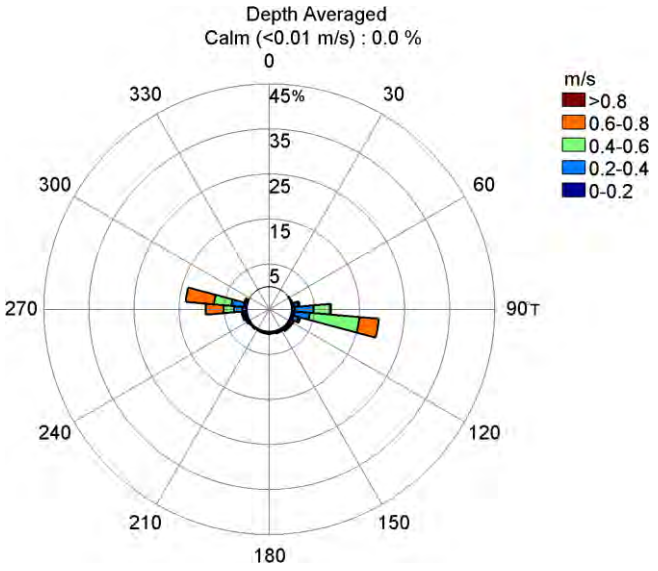

Figure 2.13: Waikato River estuary, Lower site, Depth averaged current as a rose plot.

Figure 2.14 presents the TS data collected near to the bed. Temperatures ranged between ~15°C and ~21.5°C. Salinity readings were observed from almost 0 psu to ~28 psu, or from fresh to saline.

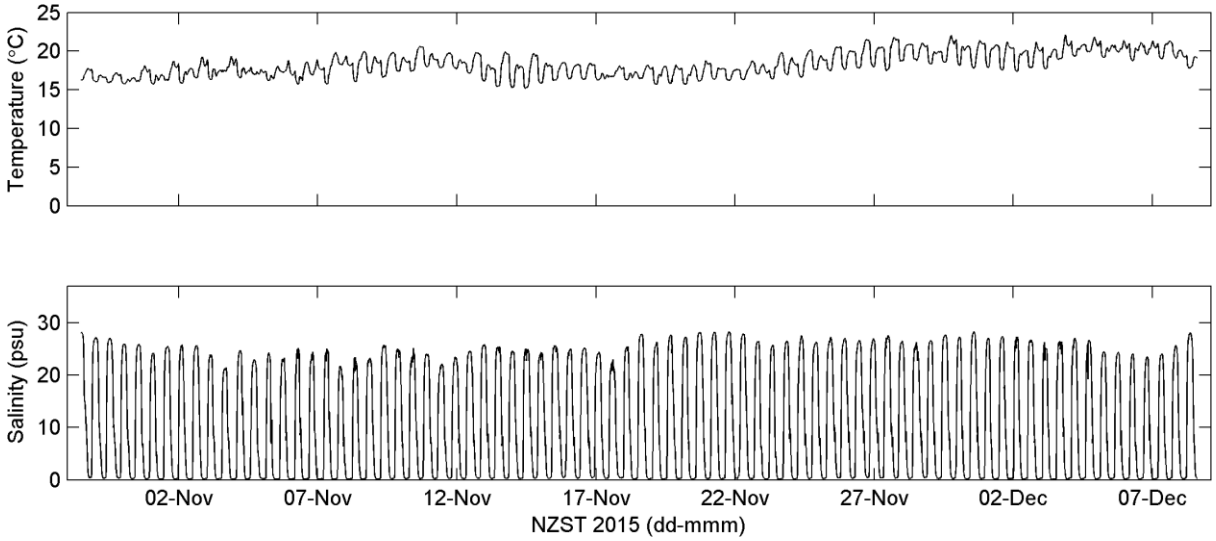

Figure 2.14: Waikato River estuary, Lower site, surface temperature (top), salinity (bottom).

2.2 Whaingaroa (Raglan) Harbour

Figure 2.15 shows the locations of the two deployments made at Whaingaroa (Raglan) Harbour, Opotoru and Waitetuna. The instruments were deployed on the 3rd of November 2015. The instruments were inspected on the 24th of November 2015, and were retrieved on the 16th of December 2015. The Waitetuna site, 37.79667°S/174.92839°E, is upstream of a natural constriction in the harbour known colloquially as “The Narrows”. The Opotoru site, 37.81713°S/174.87151°E, is ~30 m downstream of an unnamed constriction. At both sites temperature and salinity were collected using Onset U24-002-C loggers. The instruments at Waitetuna and Opotoru were deployed in ~3 m and ~8 m of water, respectively.

Conductivity sensors rely on uninterrupted contact with the medium being sampled. Both the bed level TS gauges suffered from a level of biofouling that compromised the capacity of the sensors to sample effectively. After ~4 weeks of deployment, around the 27th of November 2015 the data became unusable despite post processing efforts and this data has been removed from the record. The salinity records still show some signs of drift, despite repeat calibration efforts particularly in the surface gauge at Opotoru. In terms of the suitability of the data for use in model calibration, the data still shows clear short term fluctuations which will be useful for model assessment. The resilience of thermistors means that temperature data were recorded throughout the deployment.

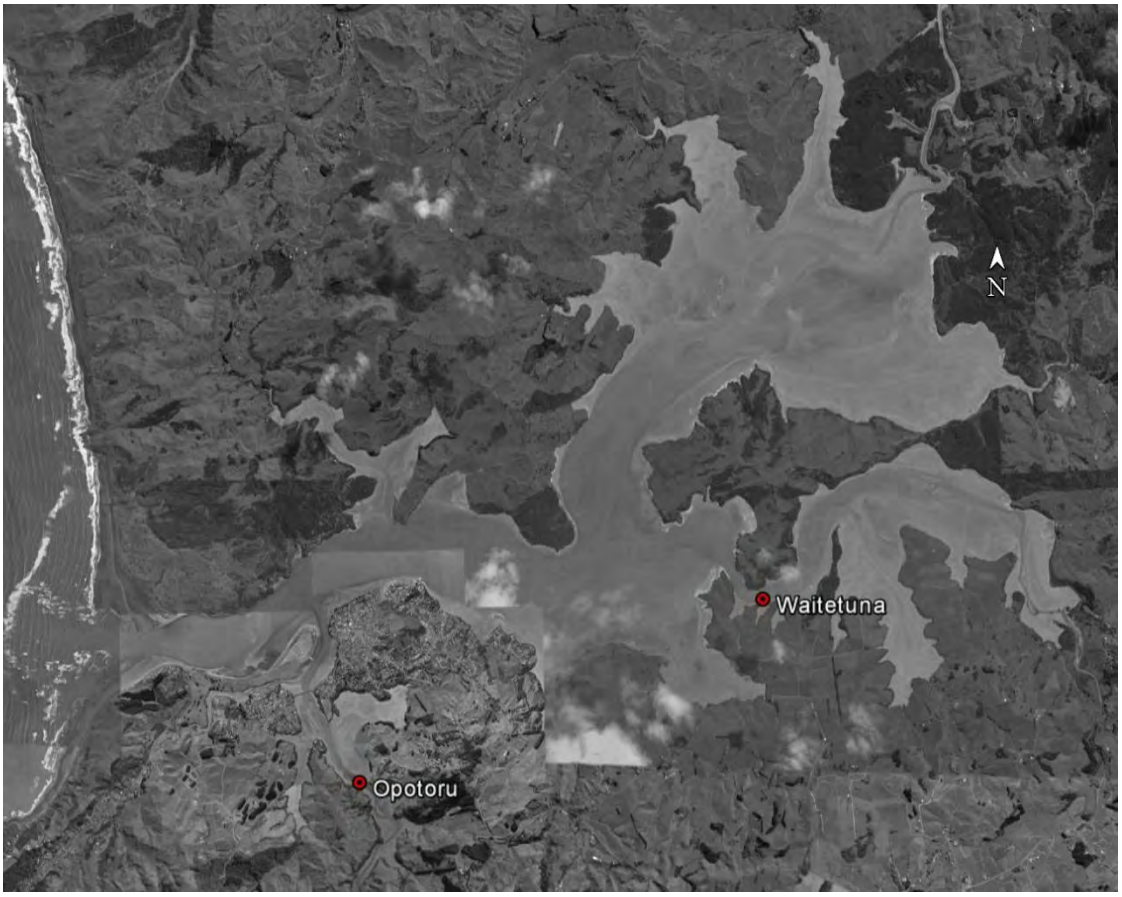

Figure 2.15: Whaingaroa (Raglan) Harbour deployment locations.

2.2.1 Waitetuna site

Figure 2.16 and Figure 2.17 present the TS data from the Waitetuna site collected at the surface and bed level, respectively. Temperatures ranged between ~16°C and ~21.5°C. Salinity readings were generally >25 psu but were consistently higher at the bed level. At least two distinct freshwater flow events were recorded between the ~16th and ~23rd of November 2015 and are marked on the figures.

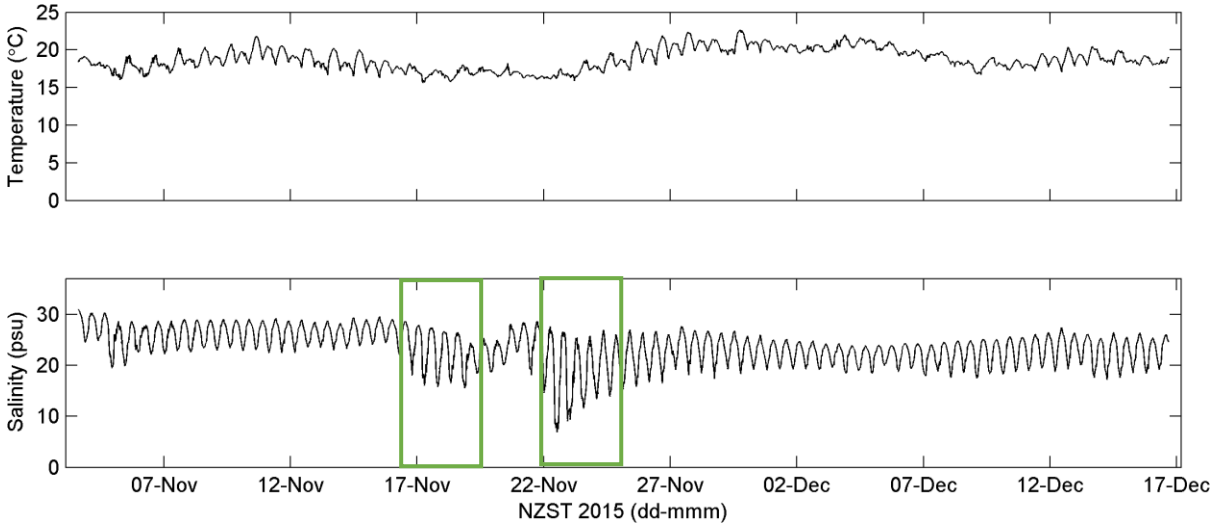

Figure 2.16: Raglan, Waitetuna site, surface temperature (top), salinity (bottom).

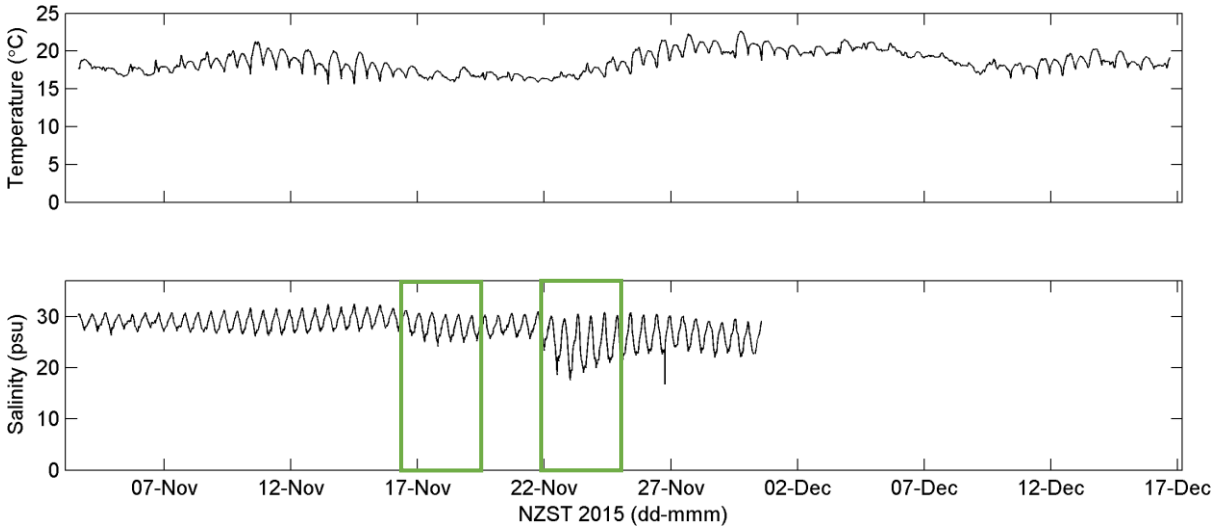

Figure 2.17: Raglan, Waitetuna site, bed level temperature (top), salinity (bottom). Green boxes mark freshwater events.

2.2.2 Opotoru site

Figure 2.18 and Figure 2.19 present the TS data from the Opotoru site collected at the surface and bed level, respectively. Temperatures ranged between ~11°C and ~23°C. Salinity readings exhibit fluctuations from almost 0 to ~29 psu at the surface, and almost 0 to more than 30 psu at the bed.

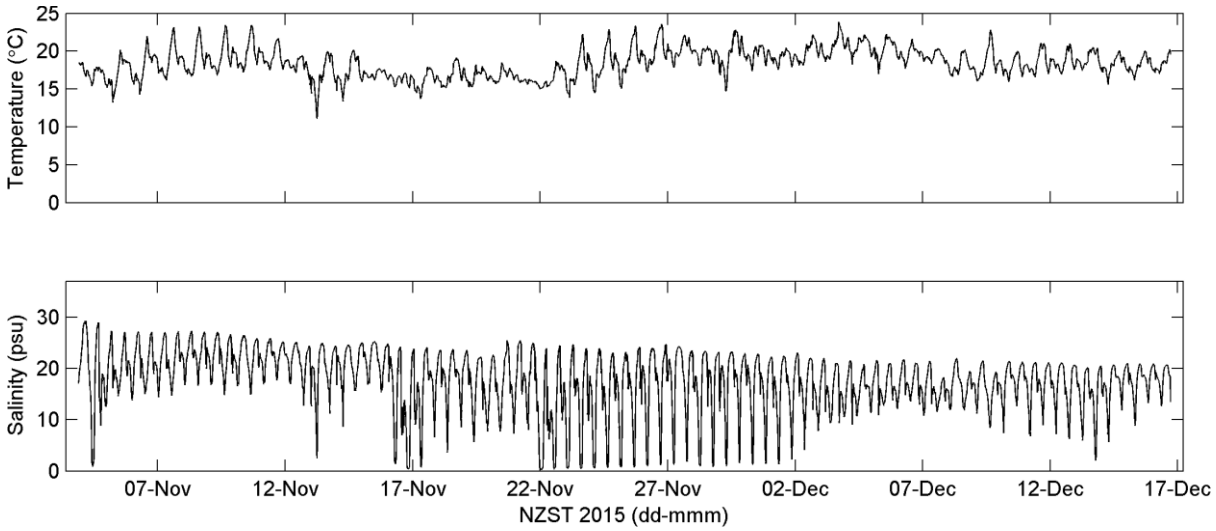

Figure 2.18: Raglan, Opotoru site, surface temperature (top), salinity (bottom).

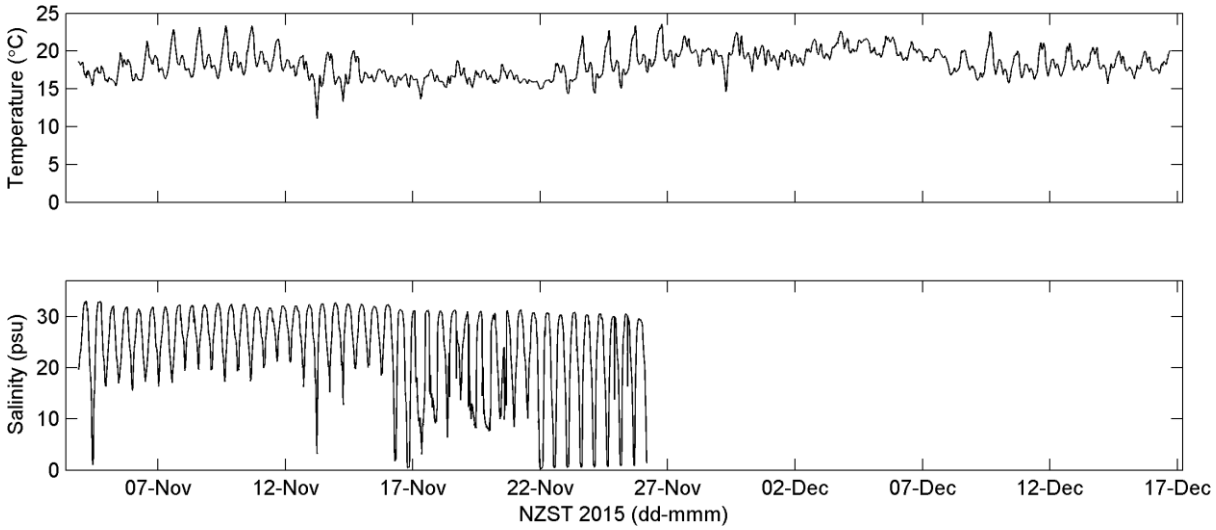

Figure 2.19: Raglan, Opotoru site, bed level temperature (top), salinity (bottom).

2.3 Aotea Harbour

Figure 2.20 shows the locations of the two deployment locations at Aotea Harbour. The Upper site is in the Pakoka River that flows in to the Aotea Harbour from the north and east. The instruments were deployed under the Te Papatapu Rd Bridge at 37.93183°S/174.85235°E. The Lower site is on the north-western edge of the mussel spat farm in the southern part of the estuary, adjacent to Tahuri Point and Pourewa Point at, 38.00559°S/174.82857°E. At the Upper site a Nortek Aquadopp was deployed collecting current speed and direction (at a fixed height of 0.7 m from the bed), and water level. The site is extremely shallow with ~1.5 m of water.

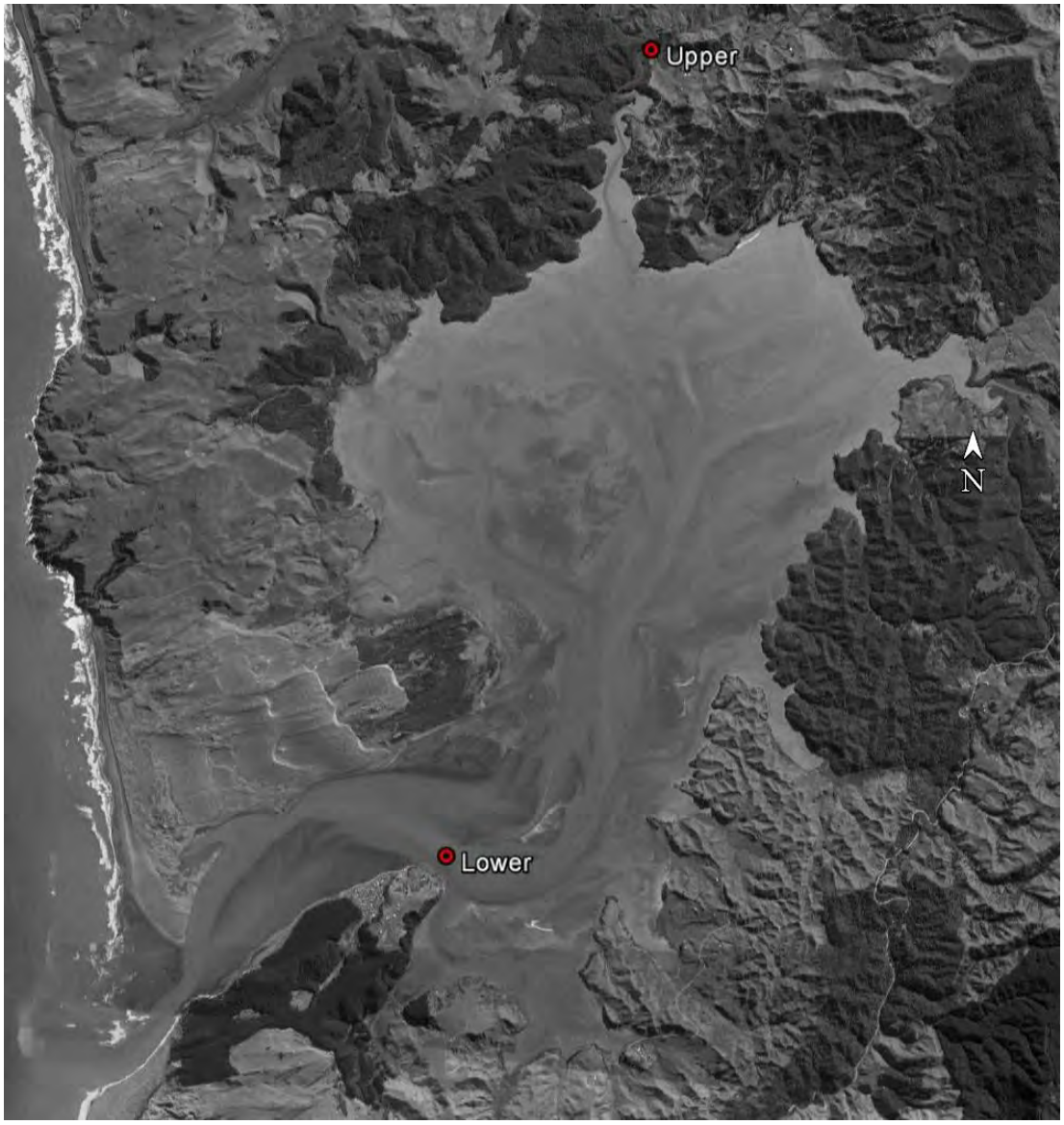

Figure 2.20: Aotea Harbour instrument deployment locations.

At the Lower site a Teledyne RDI Workhorse Sentinel ADCP was deployed in ~5.5 m measuring water level as well as current speed and current direction in 0.5 m bins from 1 m above the bed to the surface. Onset U24-002-C loggers measured temperature and salinity at the surface and just above the seabed at both sites. At the Upper site only a single TS logger was deployed due to the shallow water at this location. The sampling interval for all instruments was 15 minutes, with current measurements averaged over 5 minutes.

The instruments were deployed on the 28th of October 2015 and were serviced on the 19th of November 2015. At the Lower site in Aotea the concrete block outriggers, stainless steel frame, Sentinel Workhorse and TS gauge were all covered with seabed sediment after ~4 weeks of deployment. The degraded data has been removed from the current, water level and TS records. The data collected by the surface TS gauge was of good quality and was retrieved on the 9th of December. Both the bed level instruments at the Lower site and the instruments at the Upper site were retrieved on the 14th of December 2015.

2.3.1 Upper site

The shallow water at the site meant that during periods of low water level the Nortek Aquadopp sensor became exposed, above the water level, resulting in invalid data points during these times. The data has been filtered to remove data points recorded during these low water periods. Figure 2.21 shows the depths recorded during the deployment period. Regardless of the loss of data points, tidal modulation of water level can still be observed.

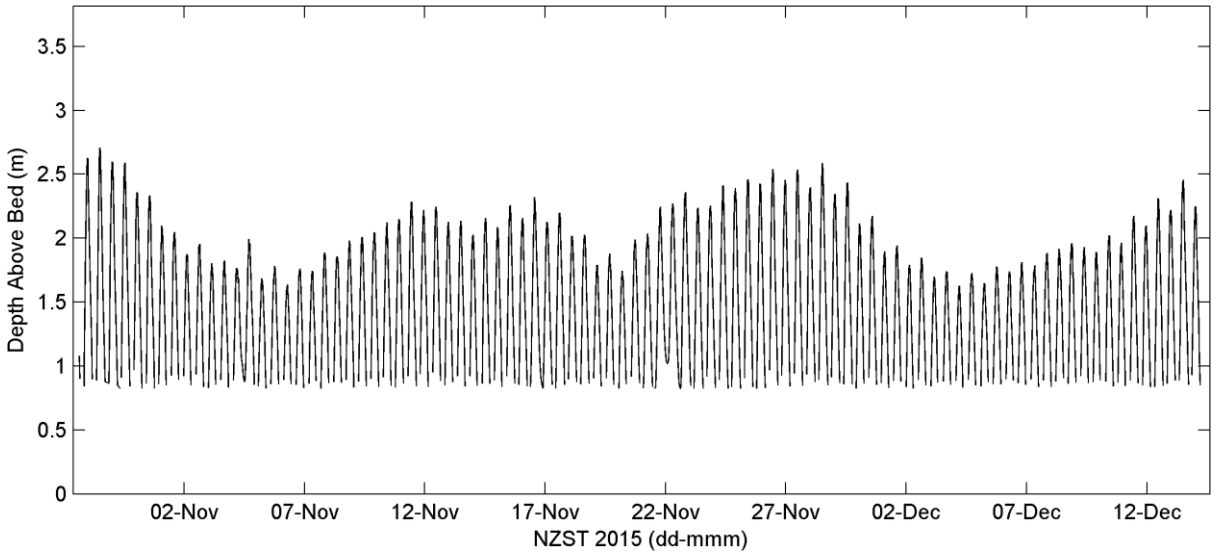

Figure 2.21: Aotea Harbour, Upper site, water depth.

Figure 2.22 and Figure 2.23 present current data recorded at a fixed height above the seabed. Current speed was rarely in excess of 0.25 ms^{-1}. Current direction was orientated along the

thalweg[1] of the stream bed and is ebb/river flow dominant. Figure 2.24 shows the bed level TS data, temperatures ranged from ~13°C to ~20°C, and salinity from fresh to 30 psu.

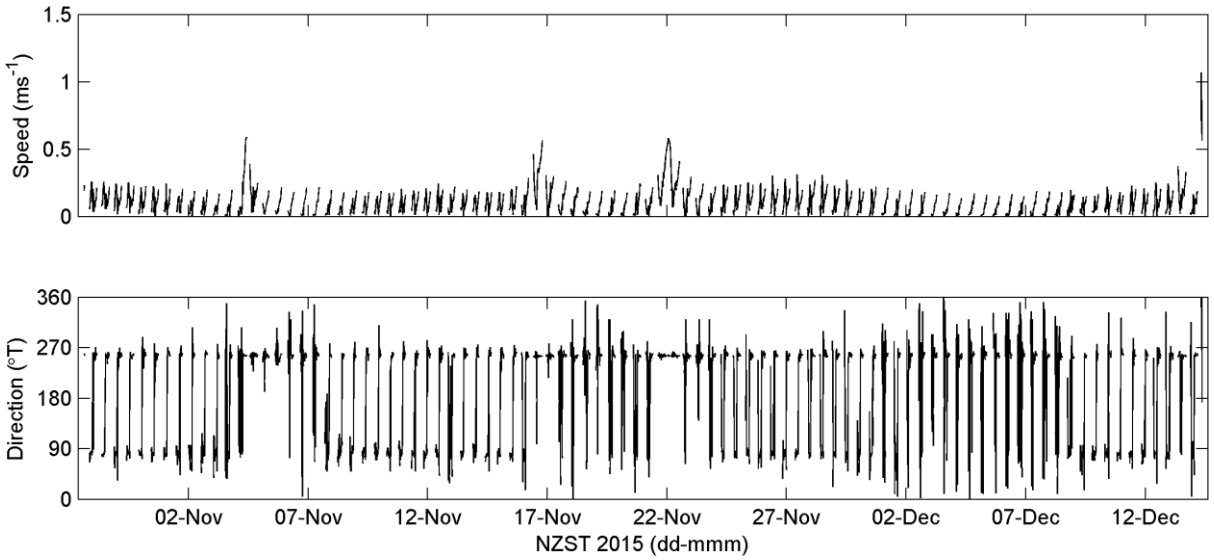

Figure 2.22: Aotea Harbour, Upper site, Current speed (top) and direction (bottom) 0.7 m above bed.

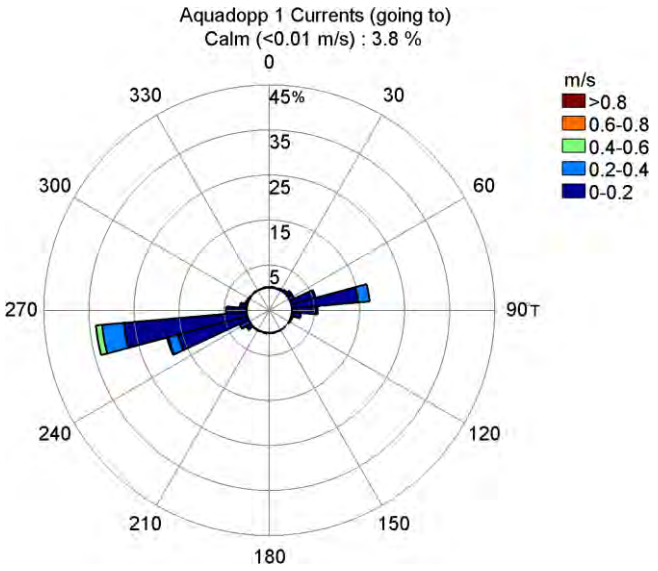

Figure 2.23: Figure 2.21: Aotea Harbour, Upper site, current rose plot.

[1] The thalweg is a line drawn to join the lowest points along the entire length of a stream bed or valley in its downward slope, defining its deepest channel

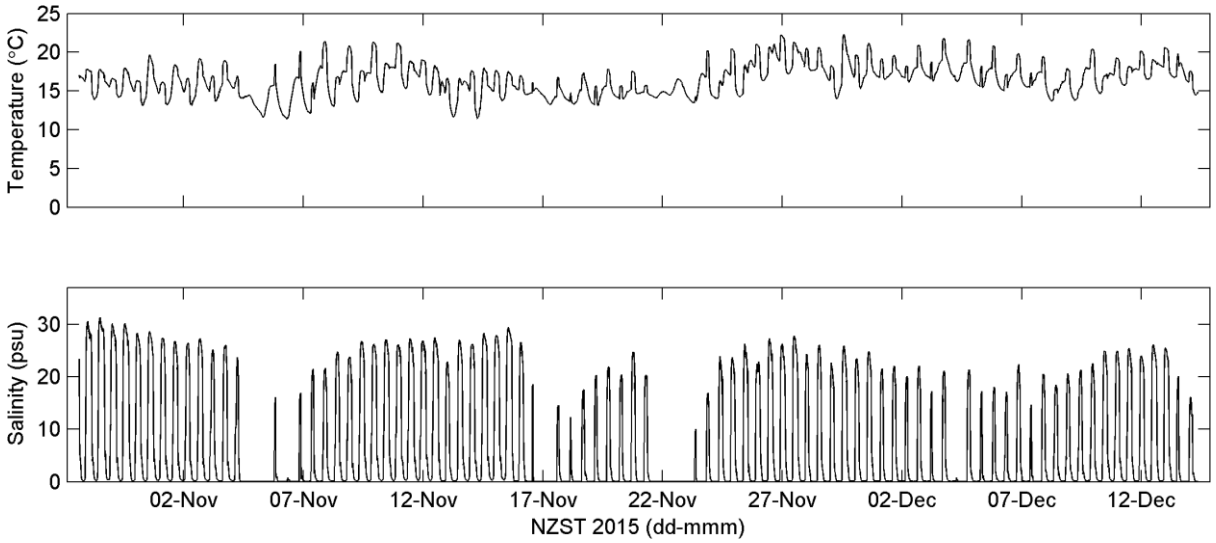

Figure 2.24: Aotea Harbour, Upper site, bed level temperature (top), salinity (bottom).

2.3.2 Lower site

Figure 2.25 shows the water depth recorded at the lower site, the water depths are strongly dominated by the tidal signal. The tidal range is approximately 3 m during spring tides and 2 m during the neap tides.

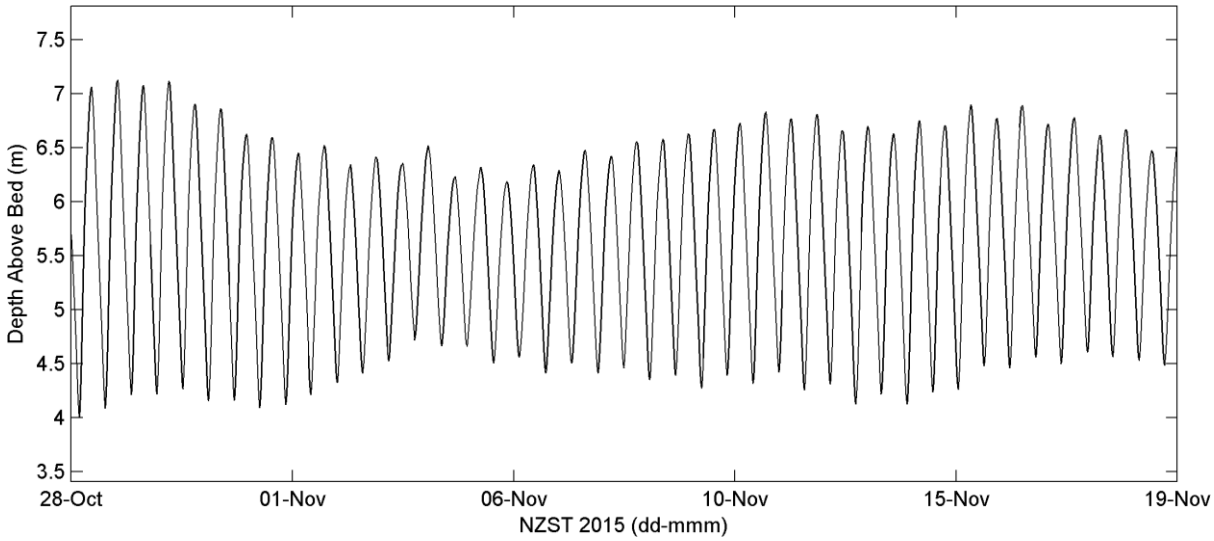

Figure 2.25: Aotea Harbour, Lower site, water depth.

Figure 2.26 and Figure 2.27 present water level and the current speed and direction through the water column in 0.5 m bins. Figure 2.28 and Figure 2.29 show the depth averaged current speed and direction as line plots and rose plots, respectively. Currents speeds reach a maximum of ~1.7 ms^{-1} during ebb flow. Salinity and temperature data from the top and bottom of the water column are shown in Figure 2.30 and Figure 2.31 respectively. Both show evidence of tidal modulation with variability increasing during spring tides.

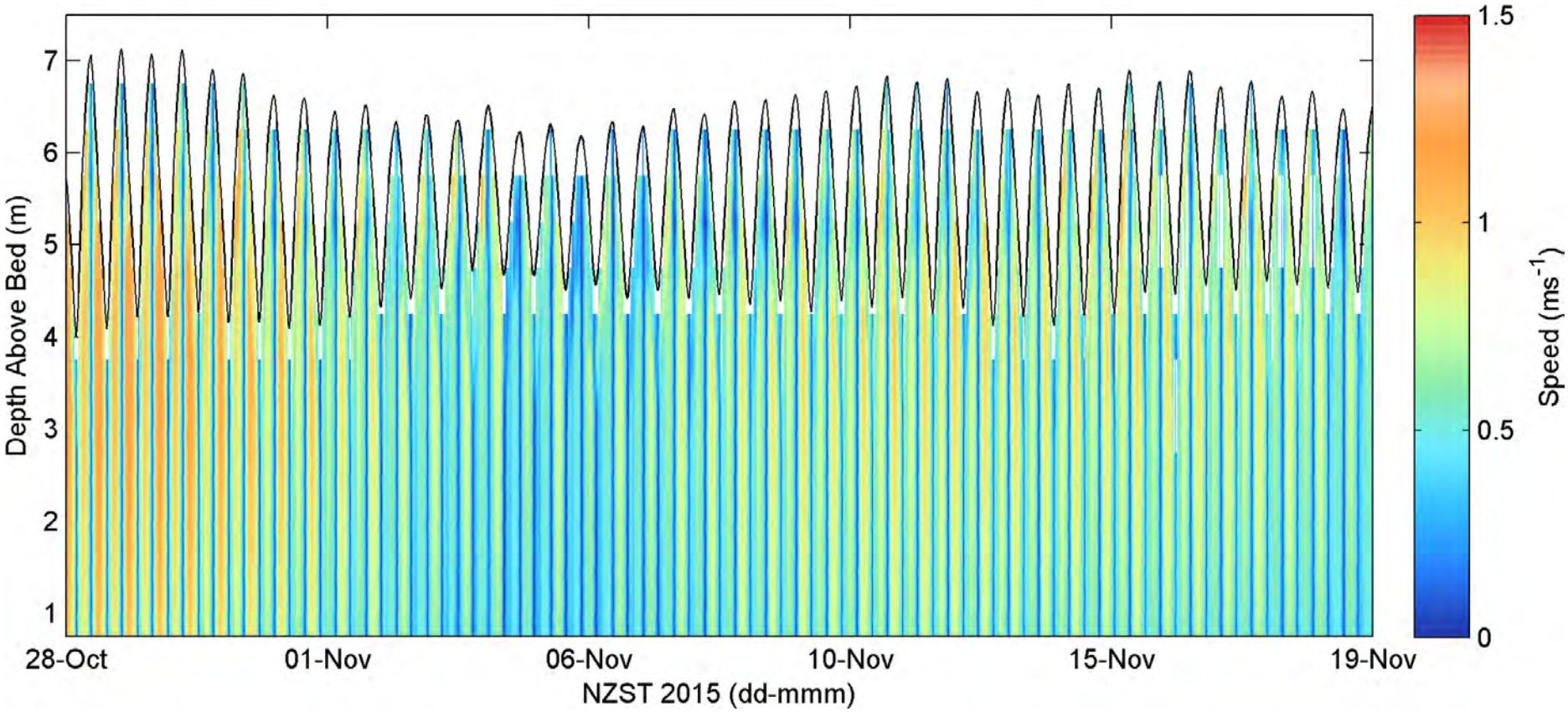

Figure 2.26: Aotea Harbour, Lower site, Current speed profile data; Black line: water level.

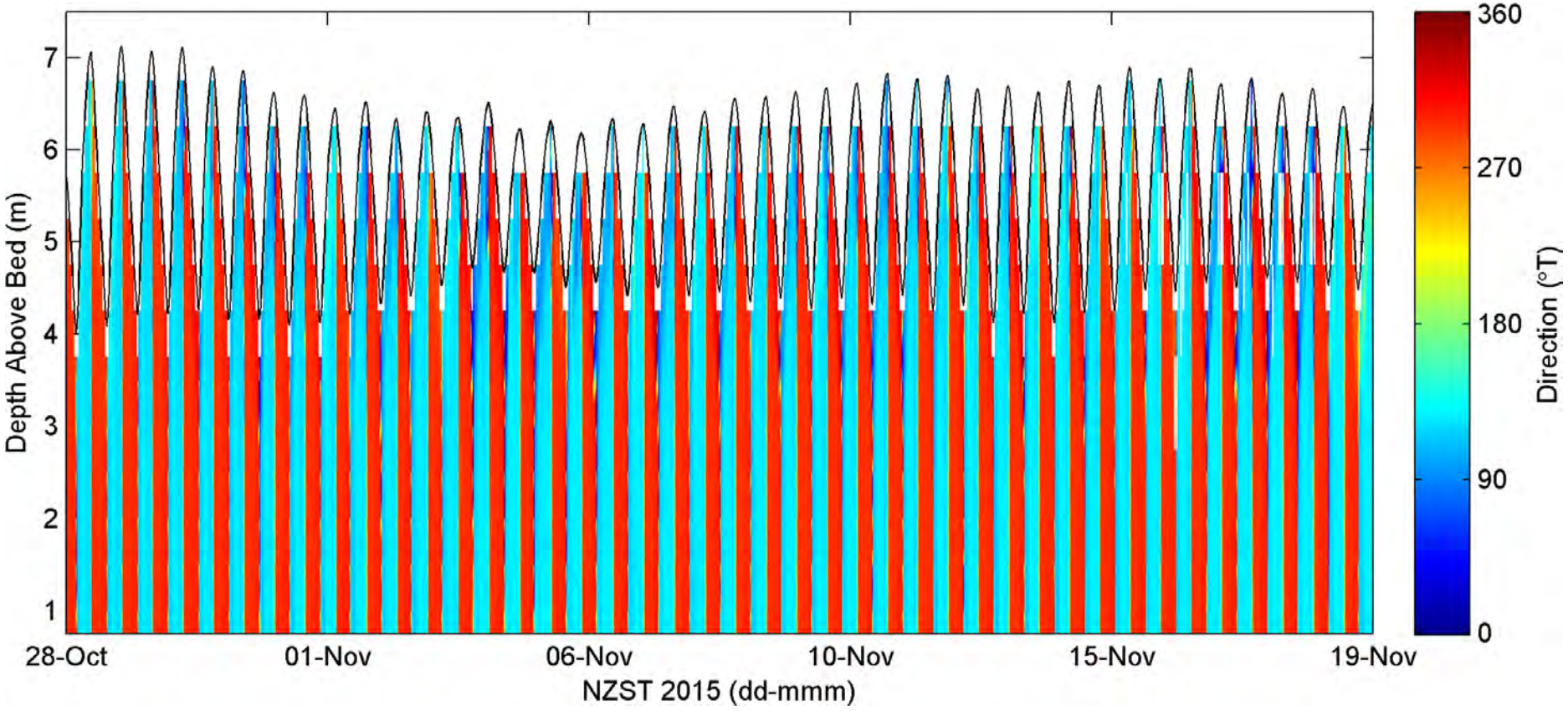

Figure 2.27: Aotea Harbour, Lower site, Current direction profile data; Black line: water level.

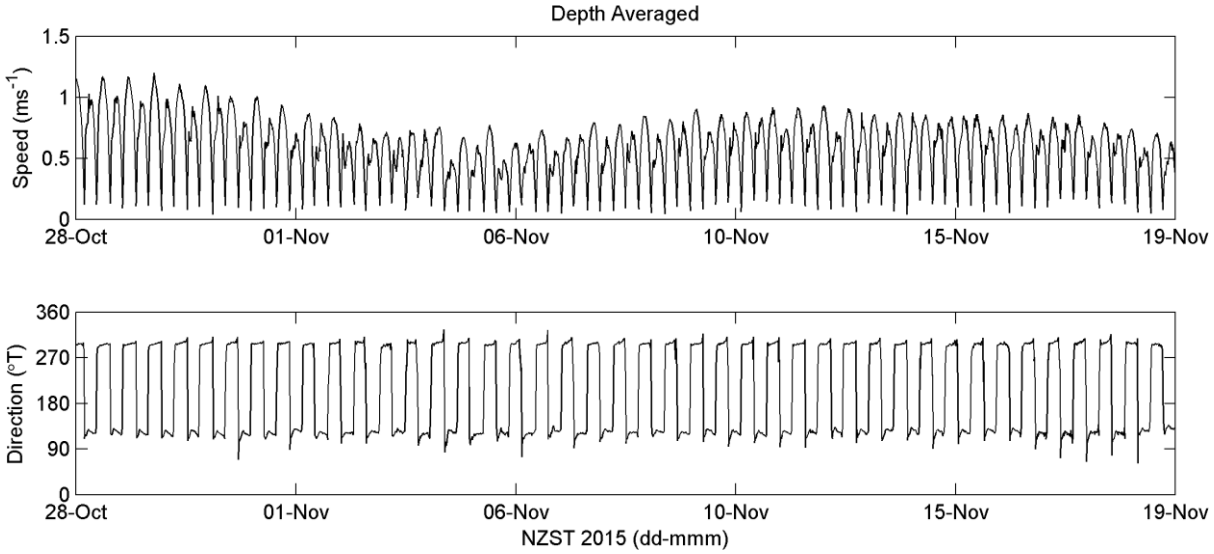

Figure 2.28: Aotea Harbour, Lower site, Depth averaged current speed (top) and direction (bottom) data.

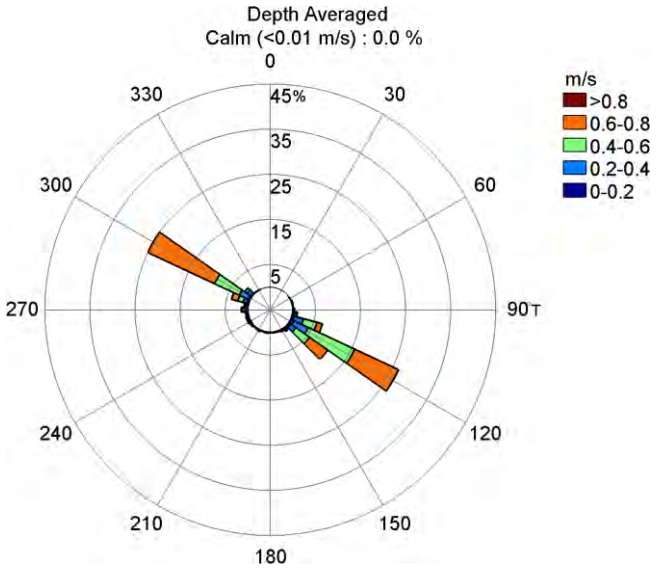

Figure 2.29: Aotea Harbour, Lower site, Depth averaged current rose plot.

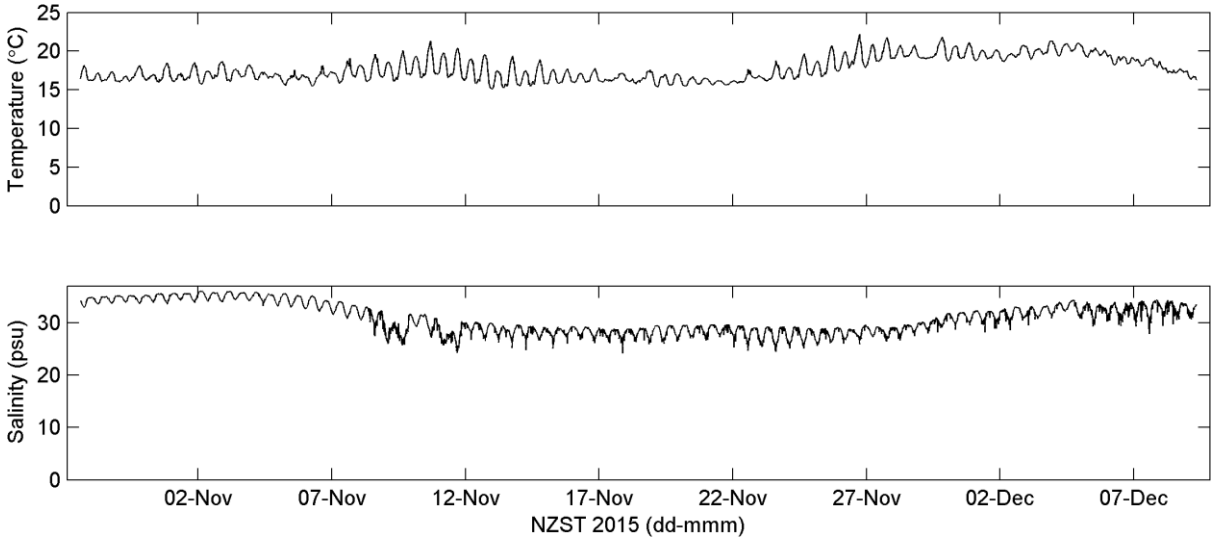

Figure 2.30: Aotea Harbour, Lower site, surface temperature (top), salinity (bottom).

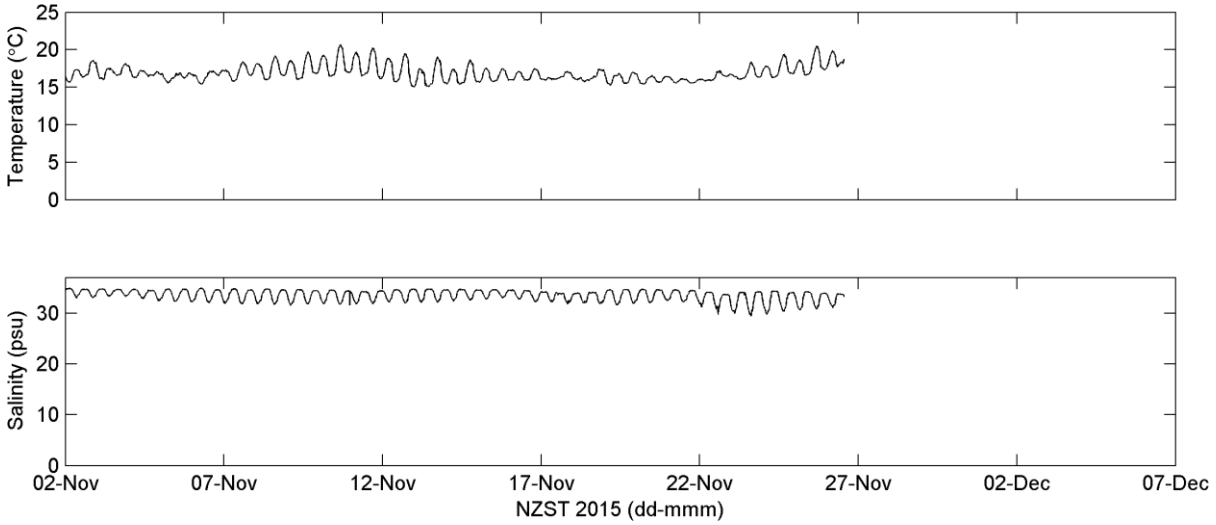

Figure 2.31: Aotea Harbour, Lower site, bed level temperature (top), salinity (bottom).

2.4 Kawhia Harbour

Figure 2.32 shows the locations of the two deployments made at Kawhia harbour, namely, Township and Te Waitere. The instruments were deployed on the 28th of October 2015. They were serviced on the 19th of November 2015, and retrieved on the 9th of December 2015. The Township site is adjacent to a foreshore structure known as the triangle and just to the side of the main estuarine channel, at 38.06879°S/174.81949°E. The Te Waitere site is in the southern part of the estuary adjacent to the Te Waitere boat ramp and jetty, at 38.13381°S/174.82431°E.

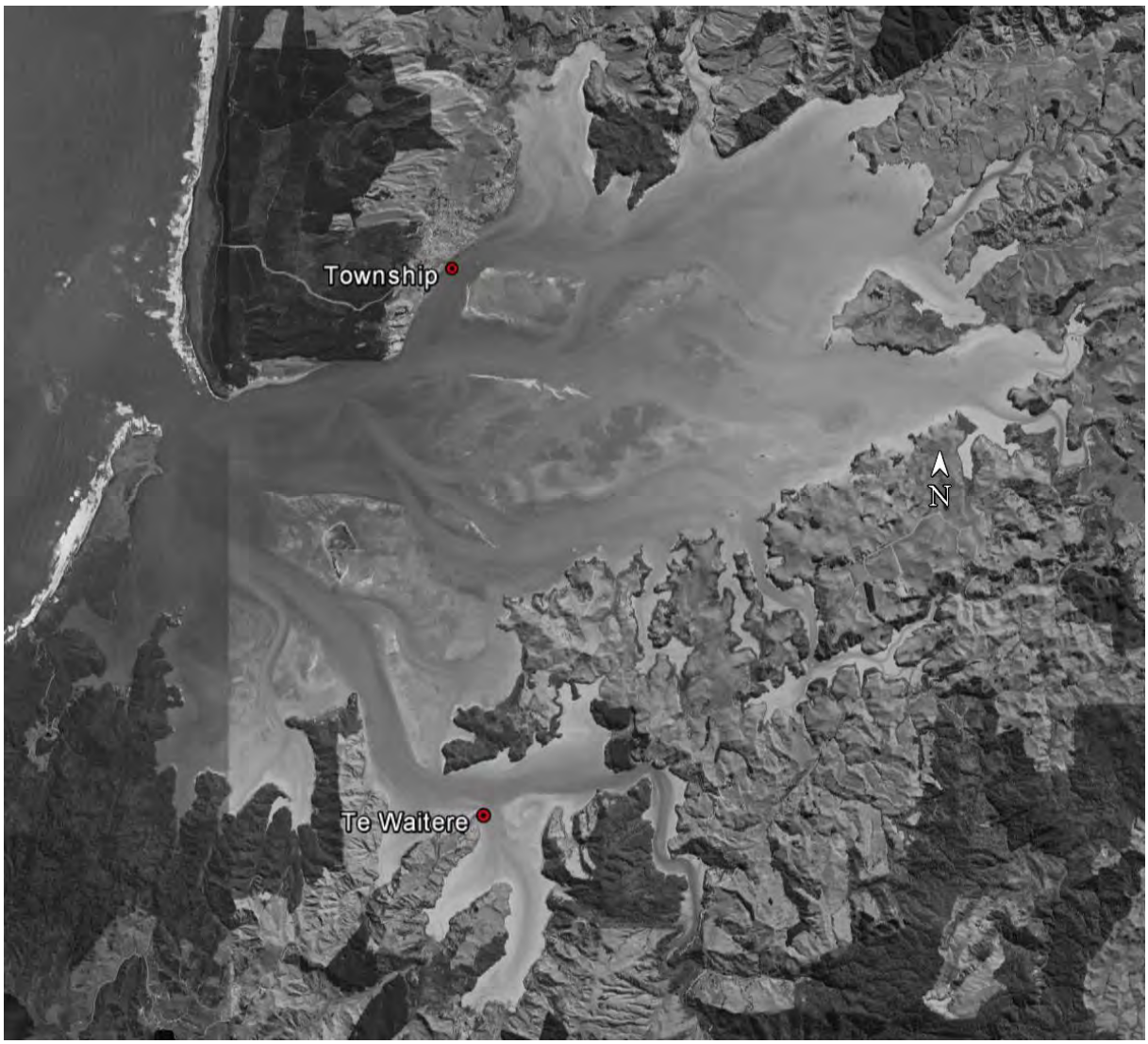

Figure 2.32: Kawhia deployment locations.

At the Te Waitere site a Nortek Aquadopp was deployed in ~5 m (MSL) measuring water level and current speed and direction at a fixed height 0.7 m above the seabed. At the Township site a 500 KHz Sontek ADP was deployed in ~5.5 m (MSL) collecting water level and current

speed and current direction in 1 m bins from 1.5 m above the bed to the surface. Onset U24-002-C loggers collected temperature and salinity measurements at the surface at both sites, and at the surface at the Township site. A YSI EXO II Sonde collected temperature and salinity data at the seabed at the Township site. The sampling interval for all instruments, with the exception of the Sontek ADP, was 15 minutes, with current measurements averaged over 5 minutes. The Sontek ADP (Township) collected data at 30 minute intervals.

2.4.1 Township site

Figure 2.33 shows the depths recorded at the Township Site, the tidal range was approximately 3.5 m during spring tides. Figure 2.34 and Figure 2.35 present water depth and current speed and direction through the water column in 1 m bins. Figure 2.37 and Figure 2.38 present the depth averaged current speed and direction as line plots and rose plots respectively. Currents speeds reach a maximum of ~1 ms^{-1} during ebb flow.

Salinity and temperature are shown at the surface and bed level in Figure 2.39 and Figure 2.40 respectively. Both temperature and salinity are similar at the top and bottom of the water column indicating that the water is well mixed at this site.

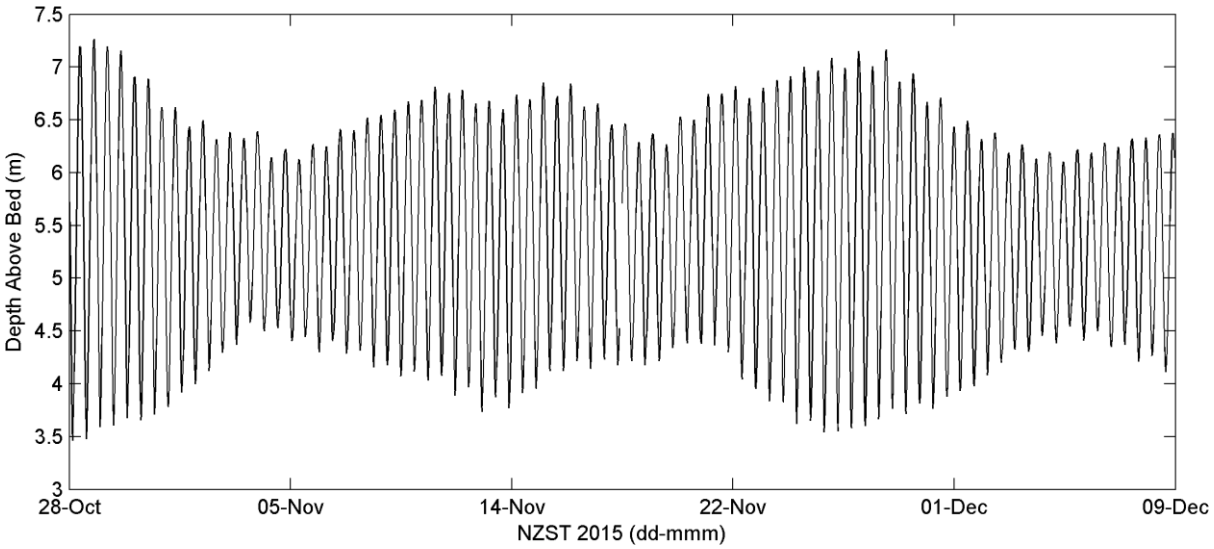

Figure 2.33: Kawhia Harbour, Township site, water depth.

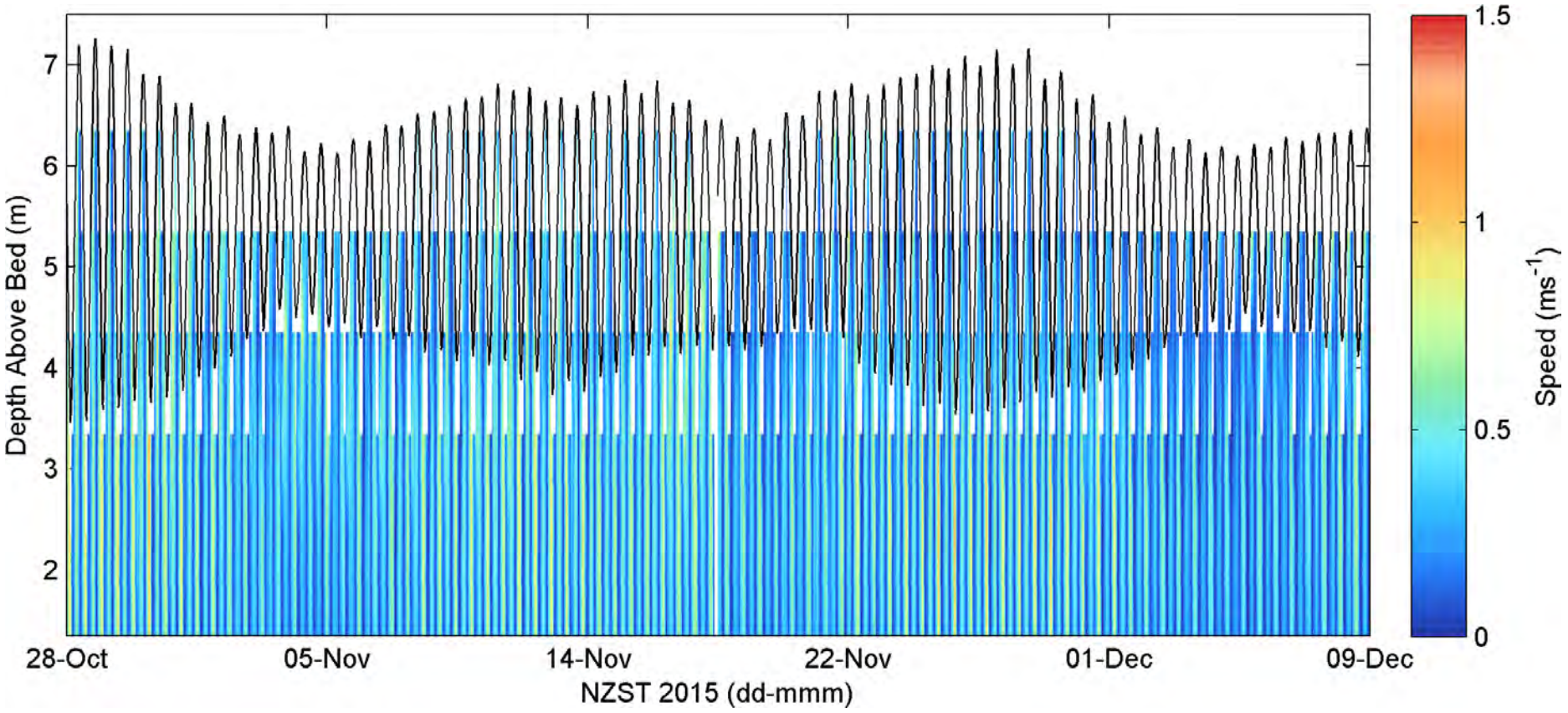

Figure 2.34: Kawhia Harbour, Township site, Current speed profile data; Black line: water level.

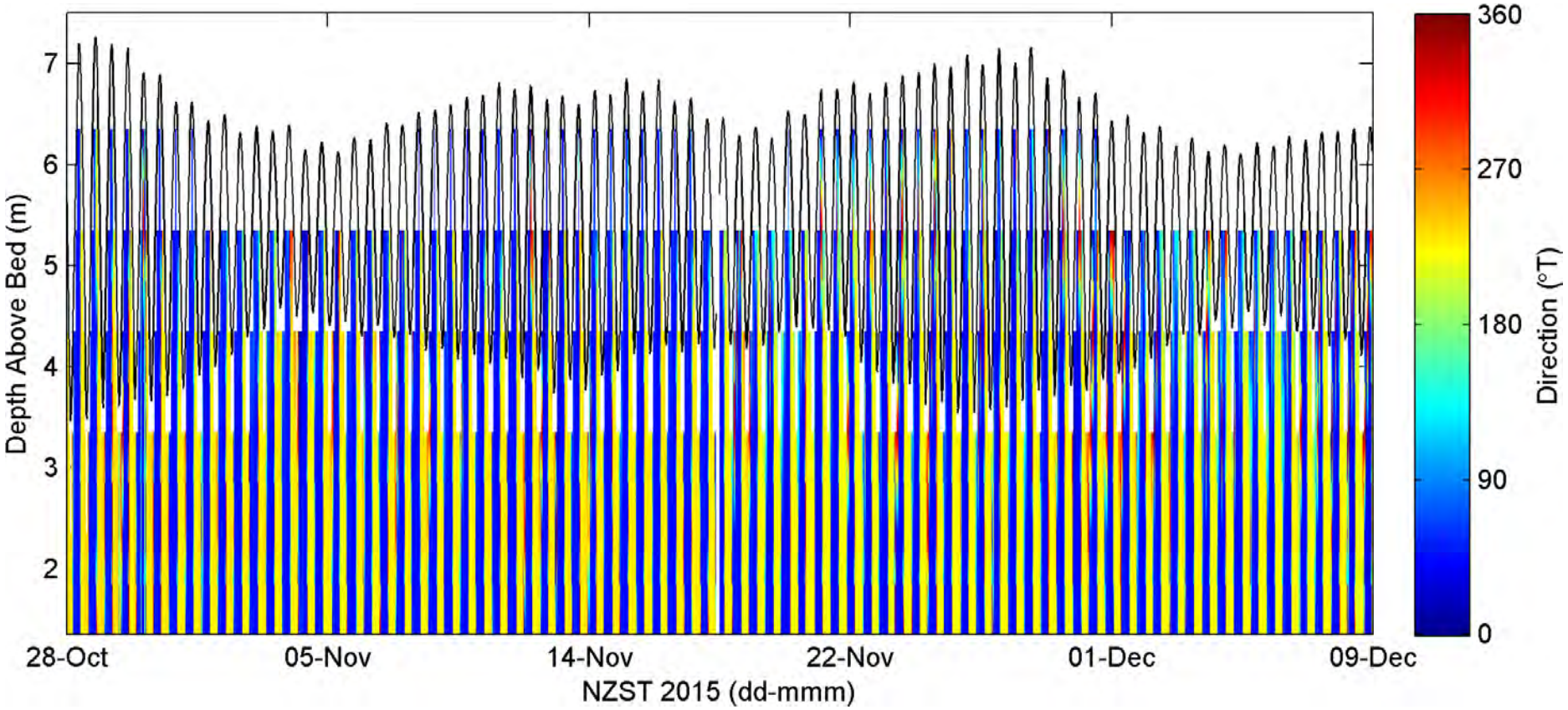

Figure 2.35: Kawhia Harbour, Township site, Current direction profile data; Black line: water level.

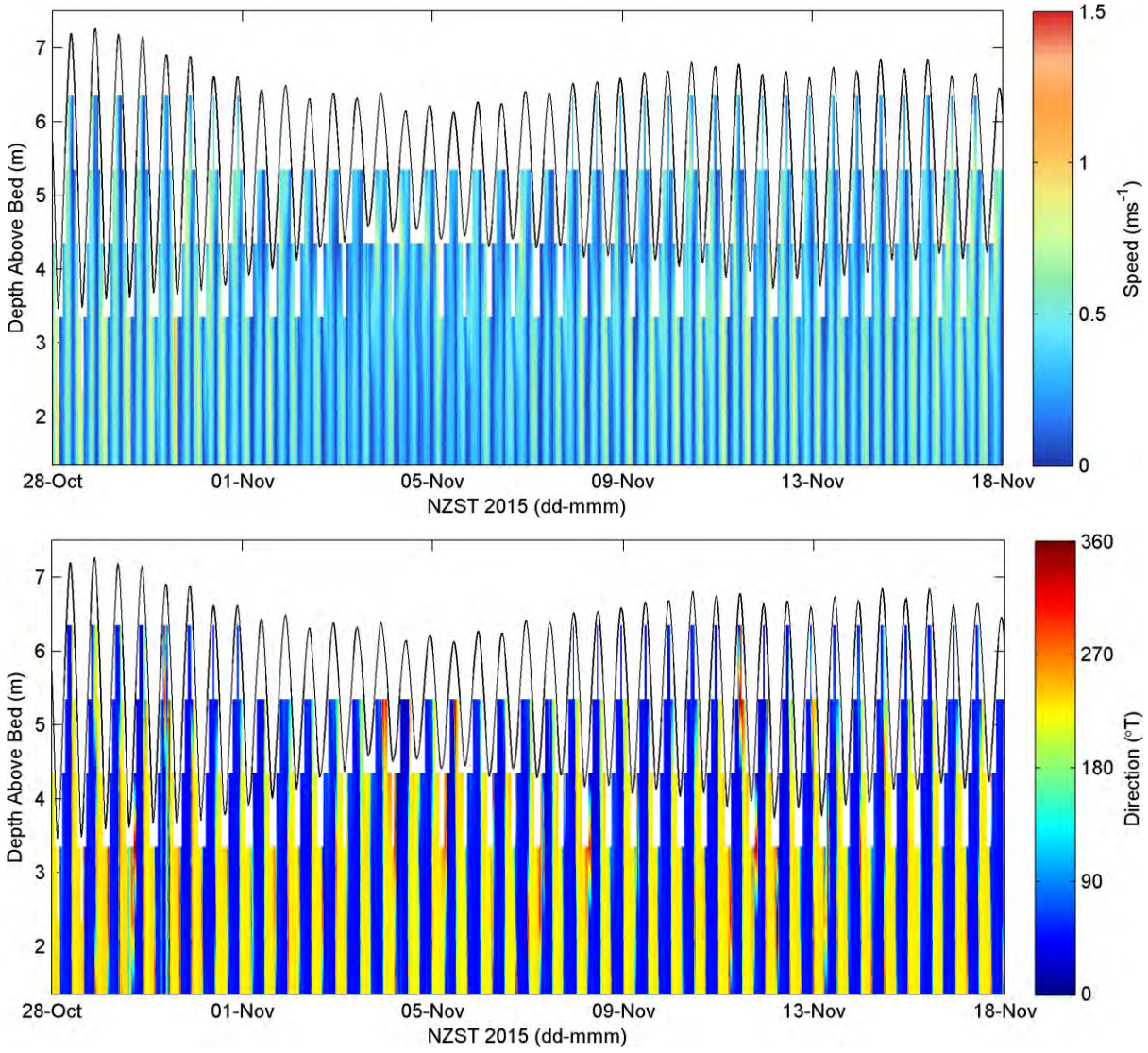

Figure 2.36: Kawhia Harbour, Township site, Current speed (top) and direction (bottom) profile data snap shot from the start of the deployment period.

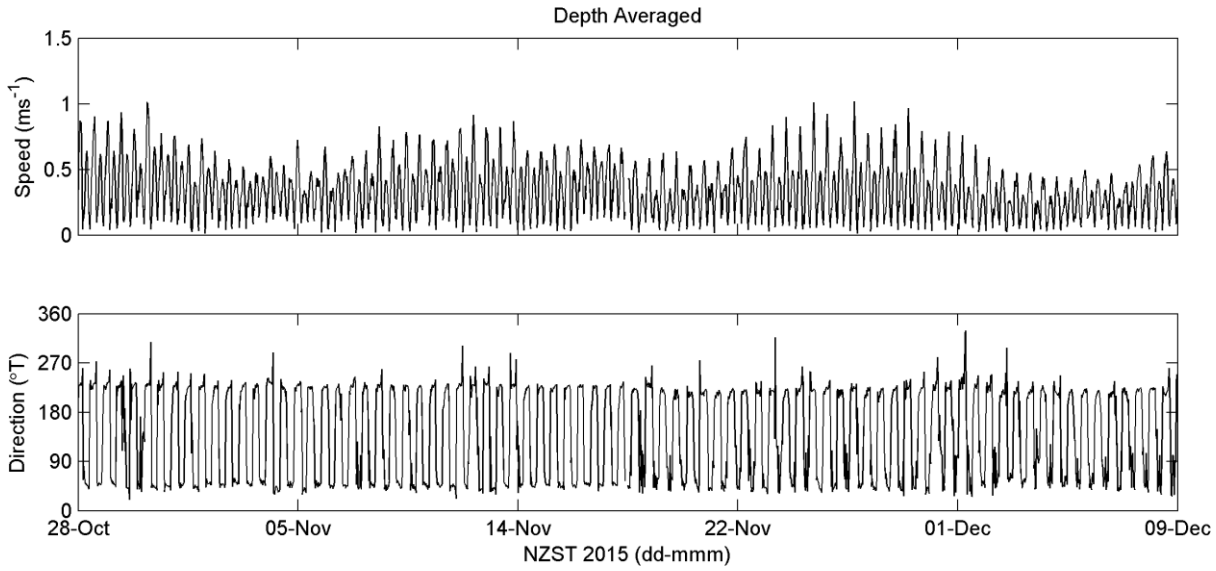

Figure 2.37: Kawhia Harbour, Township site, Depth averaged current speed (top) and direction (bottom) data.

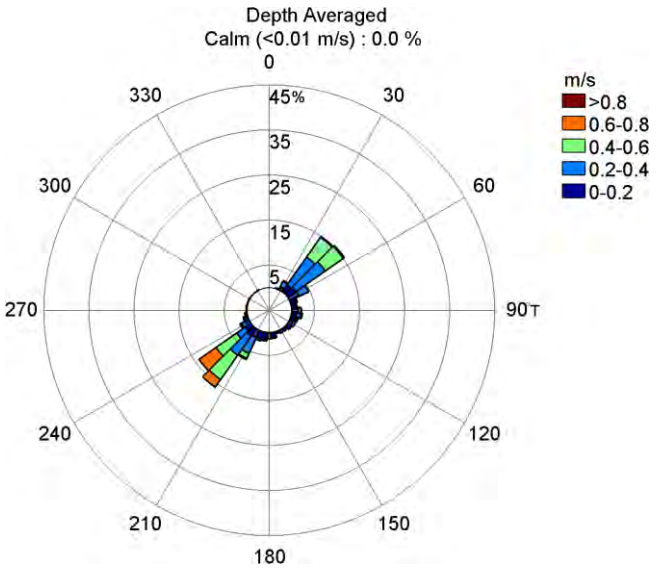

Figure 2.38: Kawhia Harbour, Township site, Depth averaged currents rose plot.

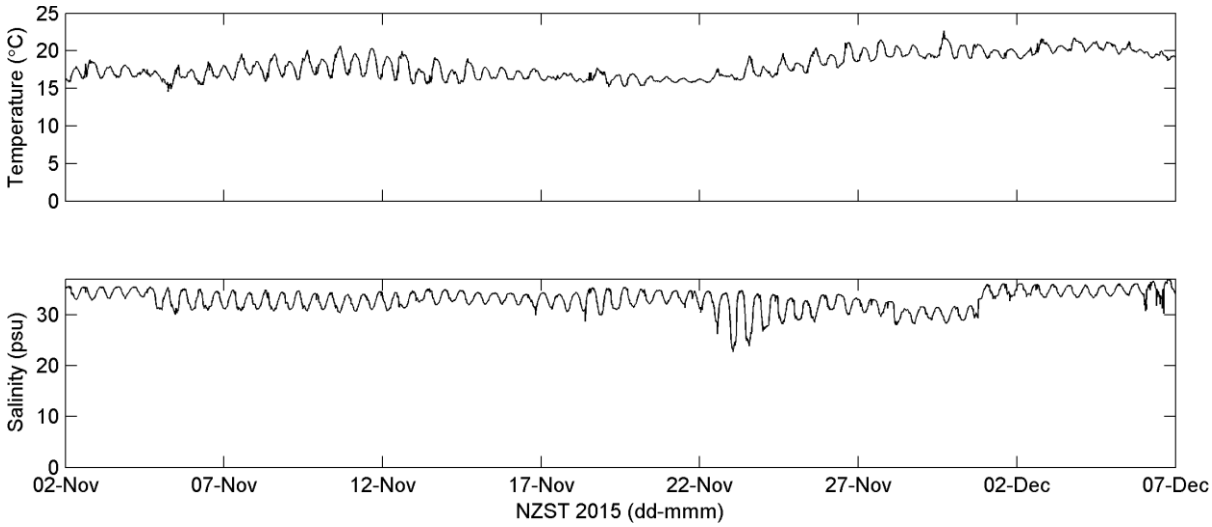

Figure 2.39: Kawhia Harbour, Township site, surface temperature (top), salinity (bottom).

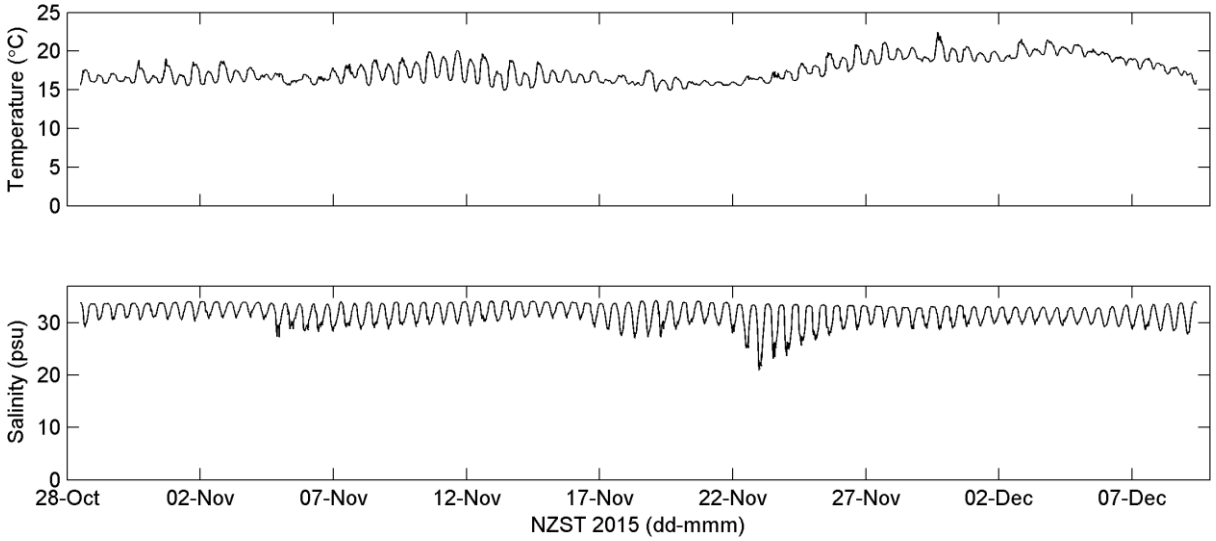

Figure 2.40: Kawhia Harbour, Township site, bed level temperature (top), salinity (bottom).

2.4.2 Te Waitere site

Figure 2.41 shows the depths recorded at the Te Waitere site, the tidal range is approximately 3.5 m during spring tides. Figure 2.42 and Figure 2.43 present current data recorded at a fixed height 0.7 above the seabed. The maximum recorded current speed during the deployment was 0.85 ms^{-1}. Figure 2.44 and Figure 2.45 show surface and bed level TS data, respectively. Temperatures ranged from ~15°C to ~25°C, and salinity ranged from approximately 10 psu to 30 psu. Both surface and bed level salinity data show occasional drops of up to 10 psu. One such drop on the 13th of November recorded by both instruments and another on 23rd/24th of November was only observed by the bed level instrument and may be a spurious observation. There was greater variability in the salinity at the surface than at the sea bed. Fresh water is more buoyant than saltwater so the intrusion of a freshwater wedge onto a saltwater body frequently causes greater variability at the surface than at the seabed.

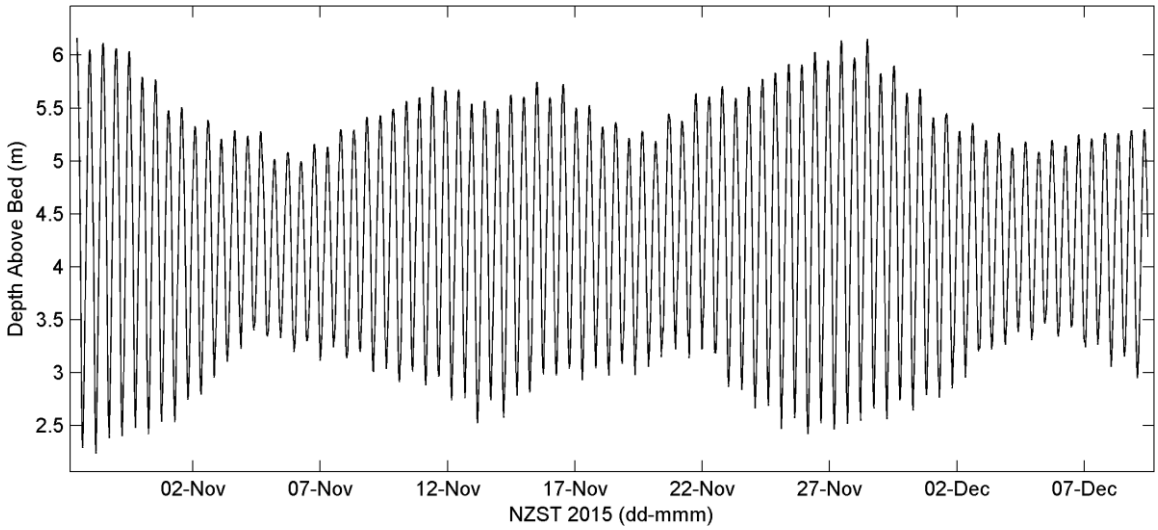

Figure 2.41: Kawhia Harbour, Te Waitere site, water depth.

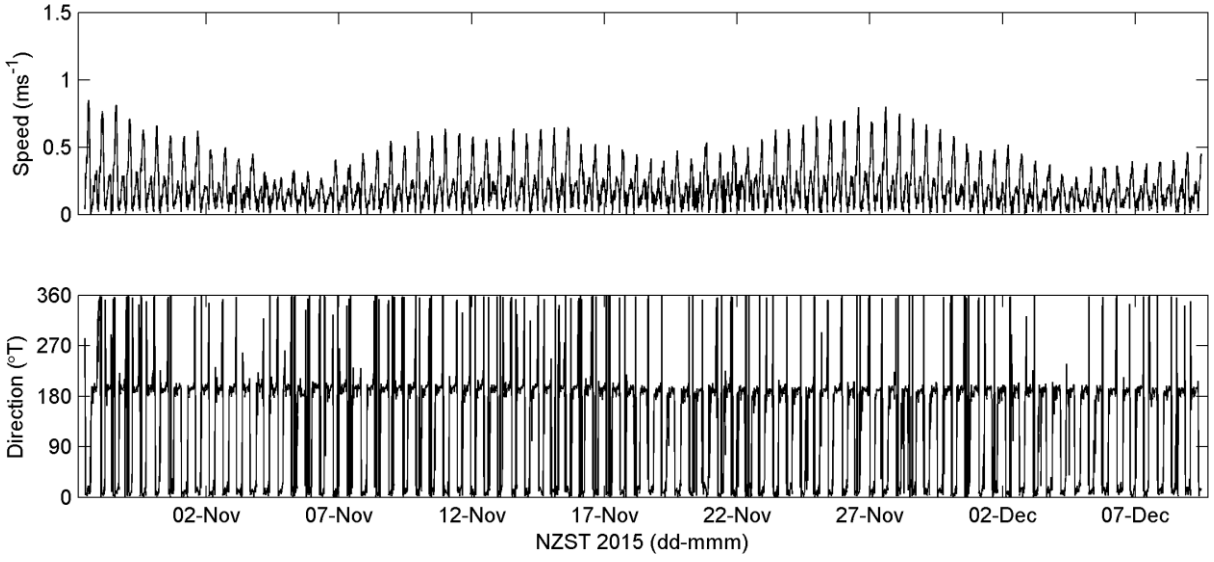

Figure 2.42: Kawhia Harbour, Te Waitere site, Current speed (top) and direction (bottom) 0.7 m above bed.

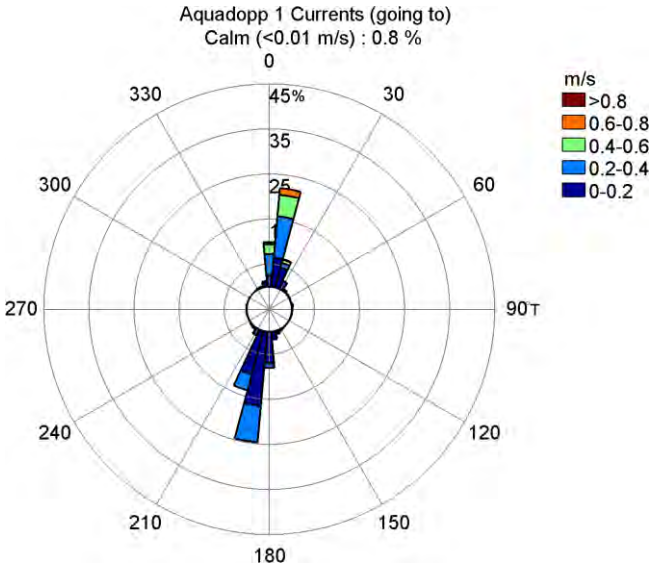

Figure 2.43: Kawhia Harbour, Te Waitere site, Current rose plot.

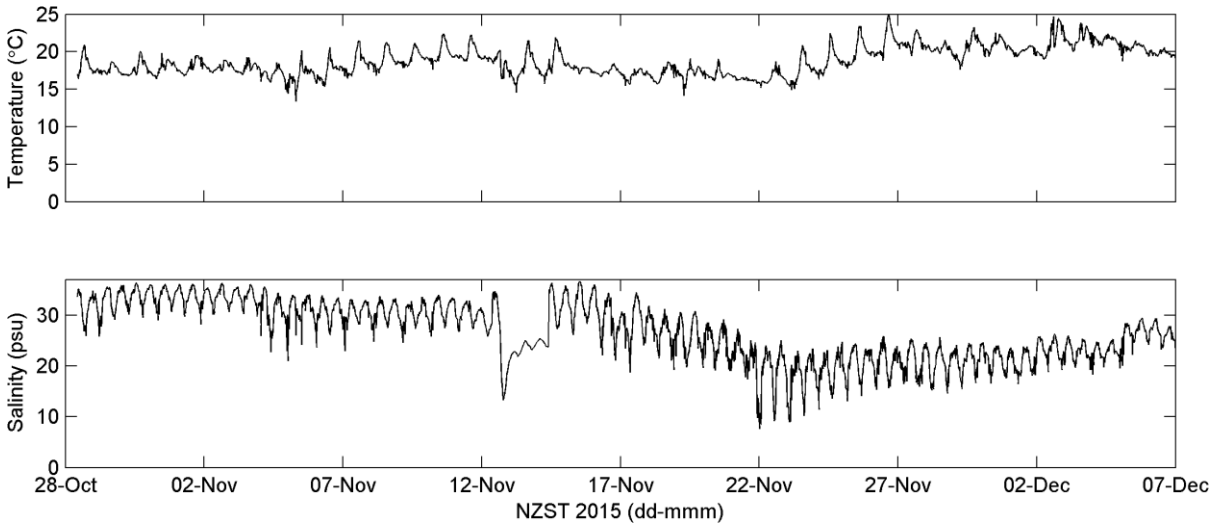

Figure 2.44: Kawhia Harbour, Te Waitere site, surface temperature (top), salinity (bottom).

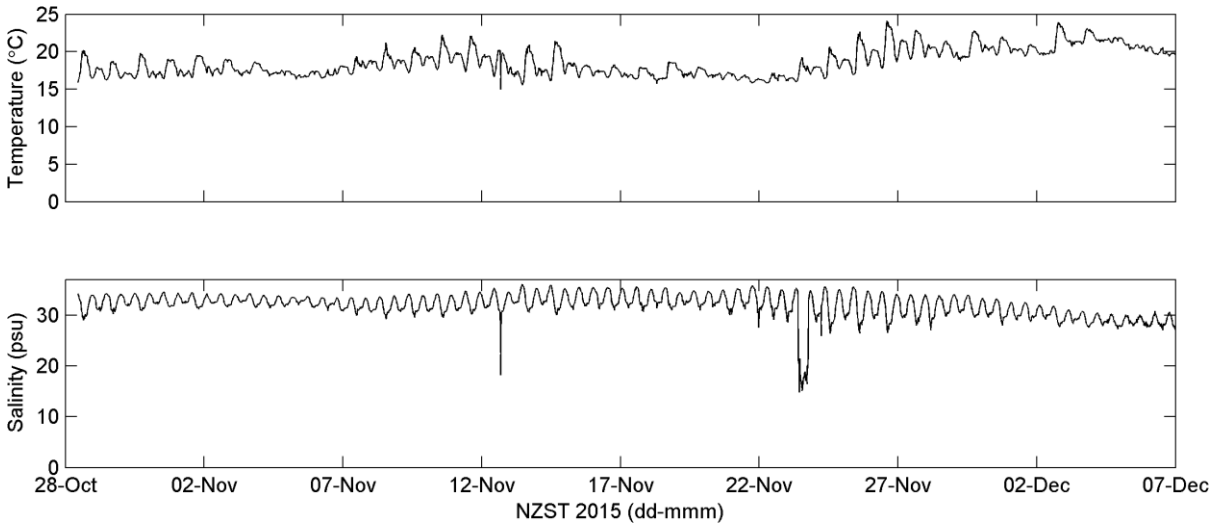

Figure 2.45: Kawhia Harbour, Te Waitere site, bed level temperature (top), salinity (bottom).

2.5 Marokopa River estuary

Figure 2.46 shows the locations of the two deployments made at Marokopa River estuary. The deployments were made on the 18th of August 2015. The instruments were inspected on the 9th of September 2015, and retrieved on the 28th of September 2015. The Upper site is approximately ~5 km upstream from the estuary mouth at 38.29262°S/174.74599°E. The Lower site is approximately ~2 km upstream from the estuary mouth; see Section 2.5.2 for further details on geographical positioning.

At the Upper site a Nortek Aquadopp was deployed in ~3.5 m of water and measured water level, current speed and current direction at a fixed height 0.7 m above the seabed. At the Lower site a 500 KHz Sontek ADP was deployed in ~2 m collecting current speed and current direction in 1 m bins from 1.5 m above the bed to the surface, and water level. At both the Upper and Lower sites Onset U24-002-C loggers collected TS data at the surface. At the Upper site an Odyssey TS Recorder was used at the bed level. At the Lower site a YSI EXO II Sonde was used at the bed level. The sampling interval for all instruments, with the exception of the Sontek ADP, was 15 minutes with current measurements averaged over 5 minutes. The Sontek ADP (Lower) collected data at 30 minute intervals.

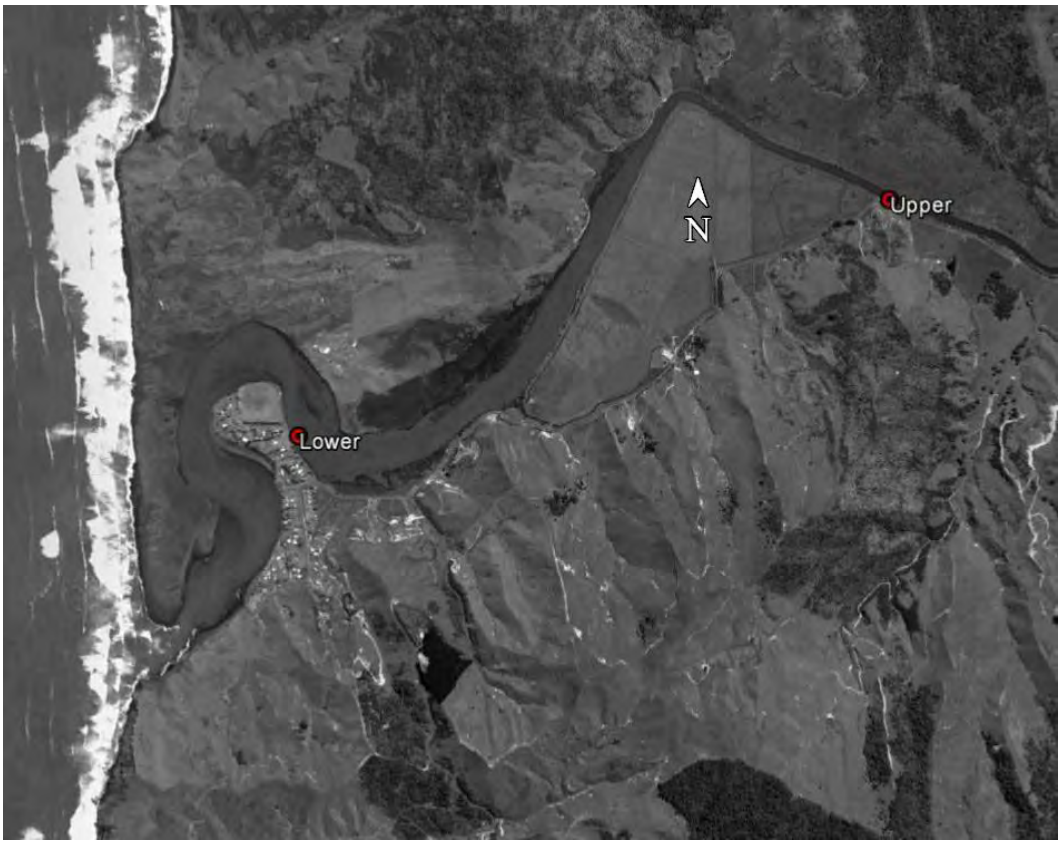

Figure 2.46: Marokopa River estuary deployment locations.

2.5.1 Upper site

Figure 2.47 shows the depths recorded at the Upper site. Tides are clearly evident in the record, along with episodic periods of elevated water level where the tidal signal is less apparent. Currents recorded at a fixed height 0.6 m above the seabed are shown in Figure 2.48 and Figure 2.49. The maximum current speed observed during the deployments was 0.9 ms^{-1} coincident with the periods of elevated water level (Figure 2.47). Current directions were almost entirely unidirectional in the ebb (downstream) direction (around 290°T). Figure 2.50 and Figure 2.51 show surface and bed level TS data, respectively. In both surface and bed level data, temperatures range from ~10°C to ~13°C, and salinity was consistently very low, less than 1 psu.

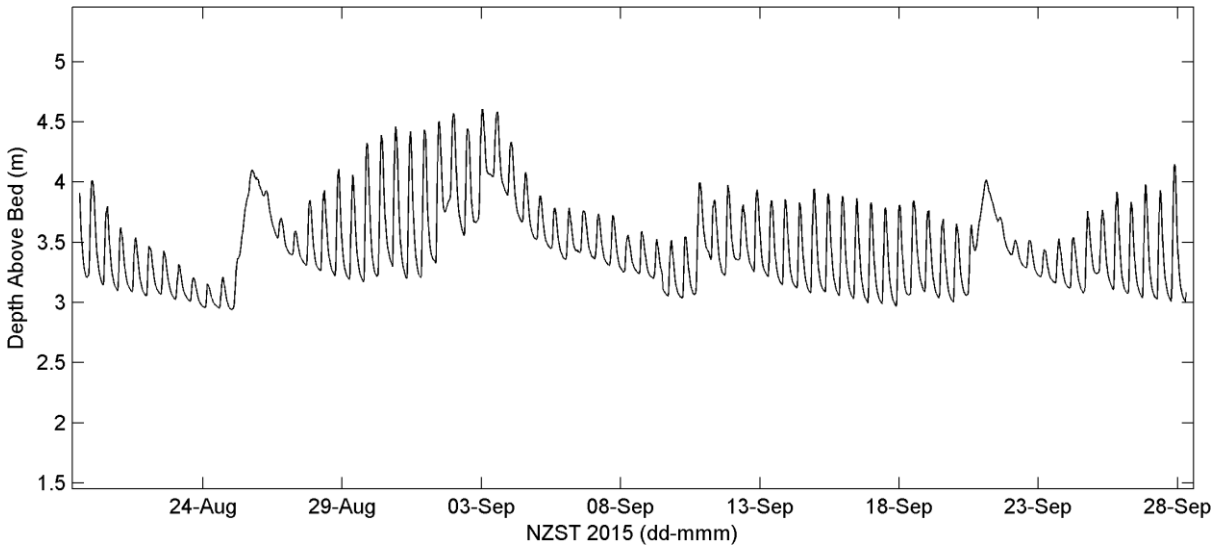

Figure 2.47: Marokopa River estuary, Upper site, water depth.

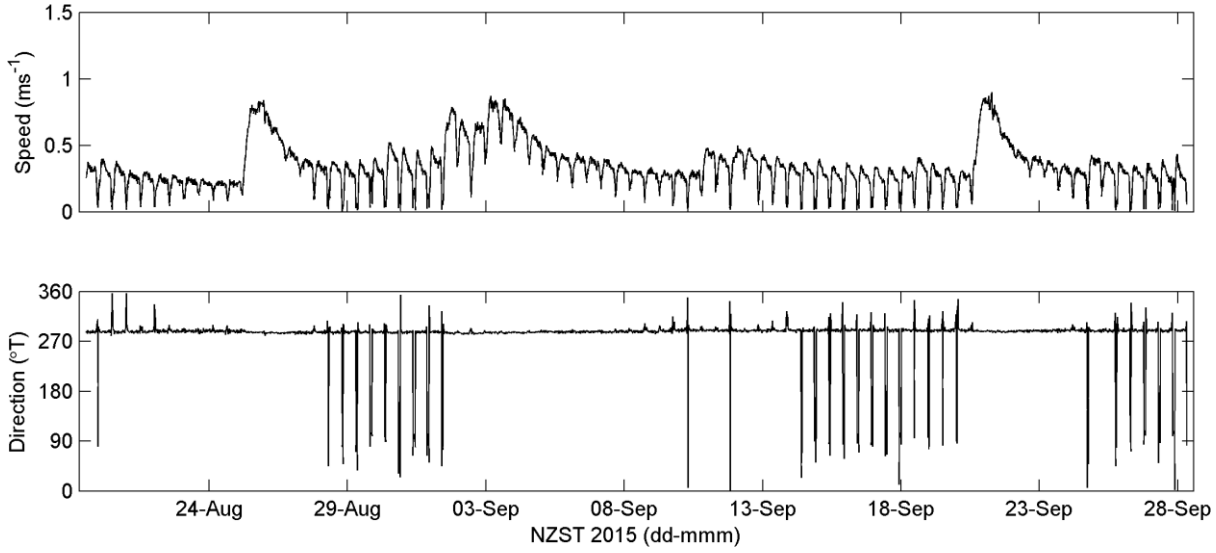

Figure 2.48: Marokopa River estuary, Upper site, Current speed (top) and direction (bottom) 0.7 m above bed.

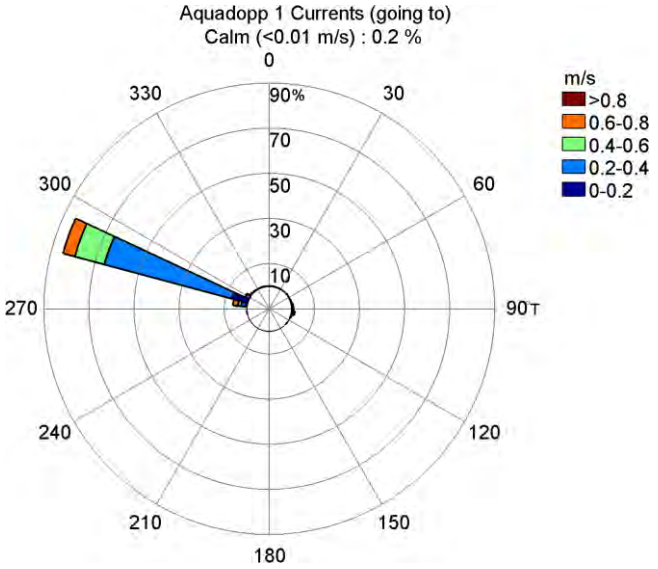

Figure 2.49: Marokopa River estuary, Upper site, Current rose plot.

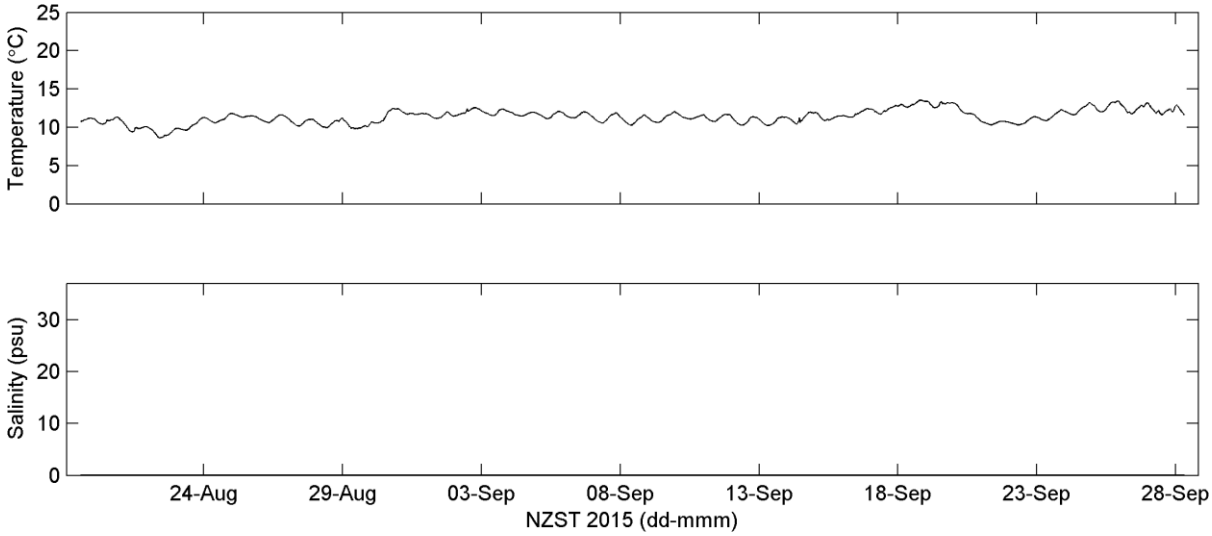

Figure 2.50: Marokopa River estuary, Upper site, surface temperature (top), salinity (bottom).

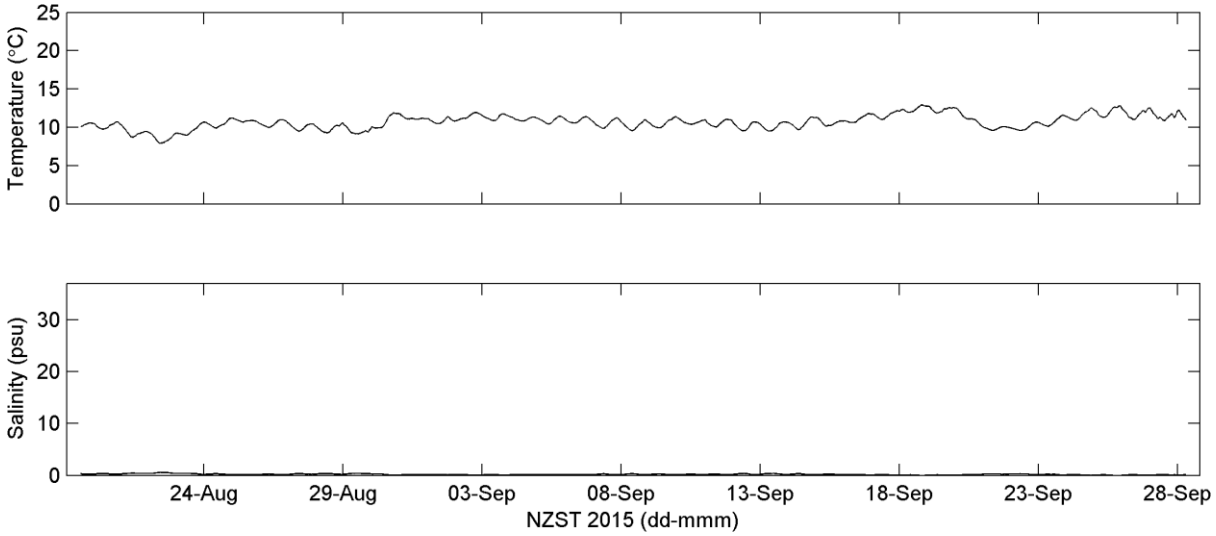

Figure 2.51: Marokopa River estuary, Upper site, bed level temperature (top), salinity (bottom).

2.5.2 Lower site

The frame and attached instruments at the Lower site were tampered with shortly after its deployment on the 18th of August at 38.30049°S/ 174.72072°E (Position 1). eCoast was informed by members of the public that the deployed equipment was seen being dragged from its deployed location to the stream bank. eCoast's fieldwork team travelled to Marokopa on Saturday 22nd August to check on the condition of the instruments. The equipment was found on the stream bank, but there was no damage to either the frame or to the instruments. The equipment was redeployed at 38.30056°S/174.72083°E (Position 2), further from the bank to deter any more tampering. Analysis of the data indicates that no further tampering occurred.

The collected data has been split for the two different deployment locations and the data collected while the equipment remained on the river bank was removed from the data set. The current data is presented on 2 sets of plots, while the TS data remains on a single set of plots.

In addition to the unfortunate circumstances described above, the Sontek ADP deployed to collect current speed and direction, became exposed at low water. Public consultation indicated that only a limited area was suitable for instrument deployment due to boat traffic. Although a thorough search was conducted to find the deepest location for deployment in this area, the area was all very shallow.

The exposure of the instrument resulted in low-confidence measurements at times when the water was particularly low. The current speed and direction data presented here, like that presented for the Aotea Harbour Upper site, have been filtered to identify and remove measurements where insufficient water depth was available for accurate readings.

Figure 2.52 and Figure 2.53 present depth readings during the deployments at Position 1 and 2, respectively. Both show a small tidal range of little more than approximately 1.5 m during spring tides. Figure 2.54, Figure 2.55 and Figure 2.56 present the current data, current speeds averaged round ~0.5 ms^{-1}, with peak velocities up to 0.8-1 ms^{-1}. Current directions were almost unidirectional in an ebb (downstream) direction, centred around 325°T.

Figure 2.57 and Figure 2.58 show surface and bed level TS data, respectively. Temperatures ranged between ~9°C and ~14°C and salinity from 0 to 30 psu. The salinity data shows saltwater intrusion into a predominantly freshwater environment. This happened more often during spring tides. Periods of saltwater intrusion were seen more often at the bed level than at the surface. The lack of data in Figure 2.58 centred on the 29th of August is the period during which the equipment was tampered with and left on the stream bank until eCoast redeployed the instrument.

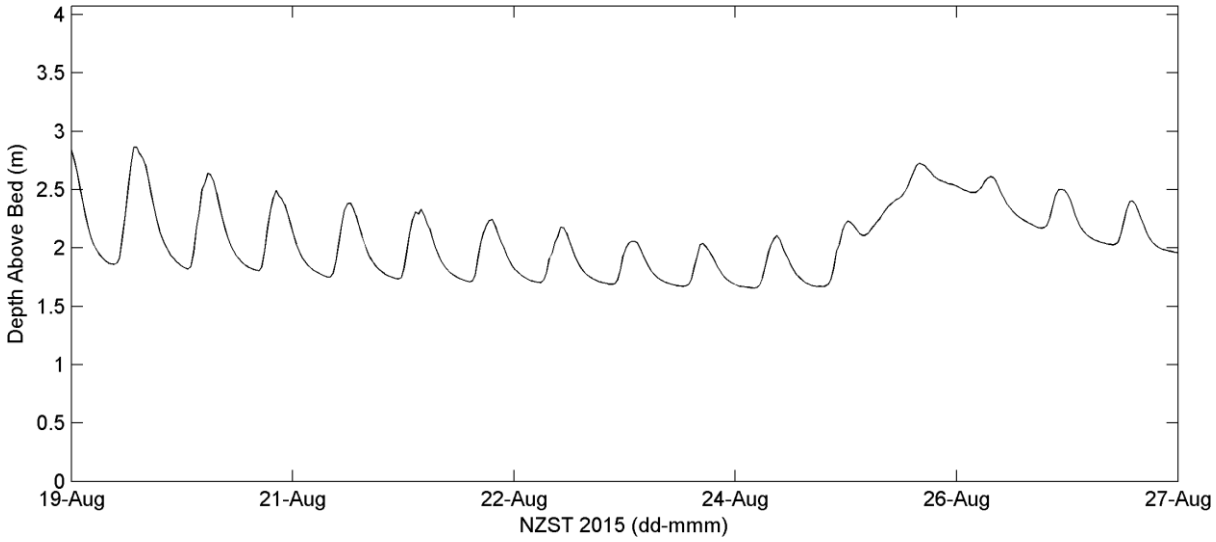

Figure 2.52: Marokopa River estuary, Lower site, Position 1, water depth.

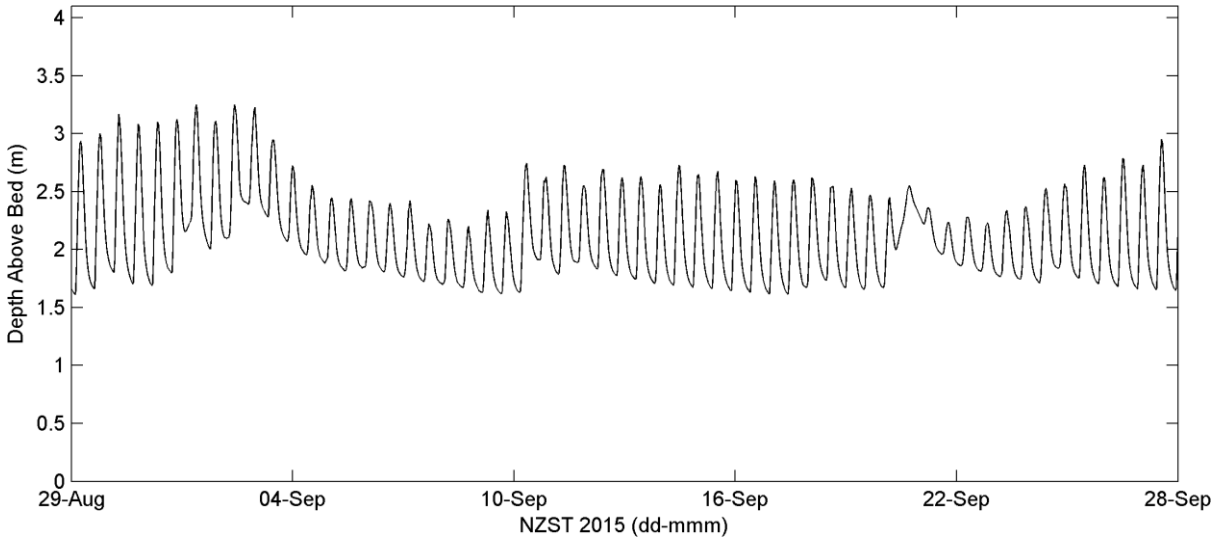

Figure 2.53: Marokopa River estuary, Lower site, Position 2, water depth.

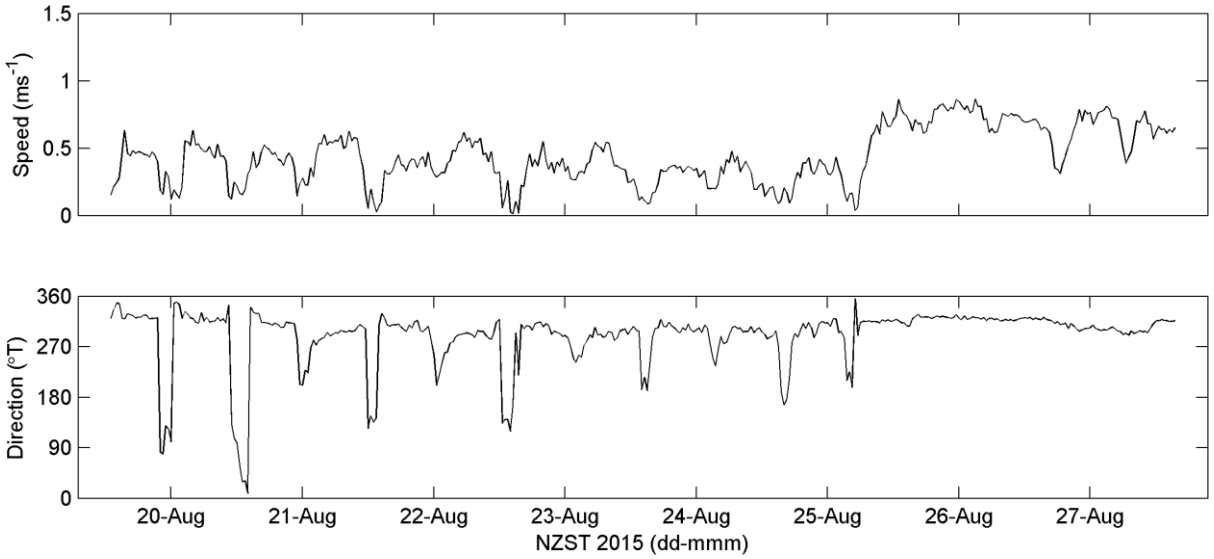

Figure 2.54: Marokopa River estuary, Lower site, Position 1, Current speed (top) and direction (bottom) 1.5 m above bed.

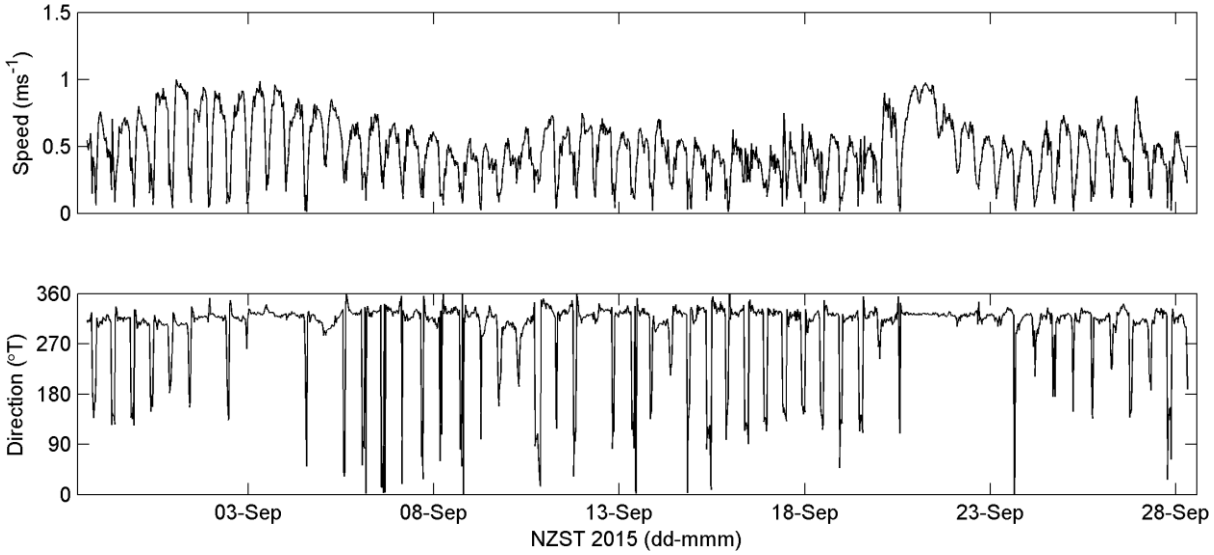

Figure 2.55: Marokopa River estuary, Lower site, Position 2, Current speed (top) and direction (bottom) 1.5 m above bed.

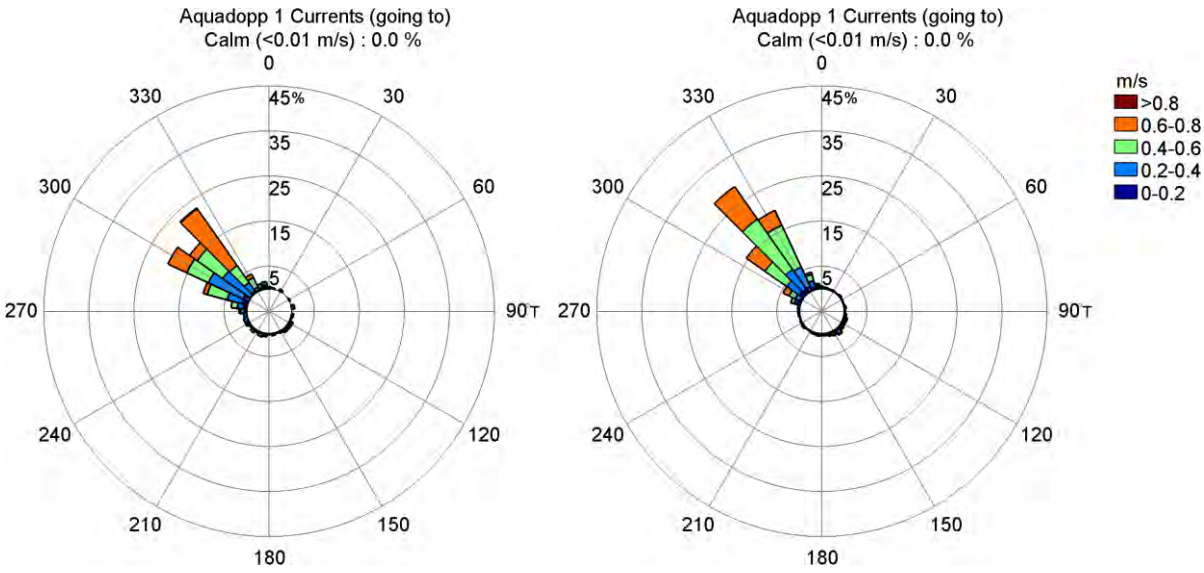

Figure 2.56: Marokopa River estuary, Lower site, Current rose plots for Position 1 (left) and Position 2 (right) 1.5 m above bed.

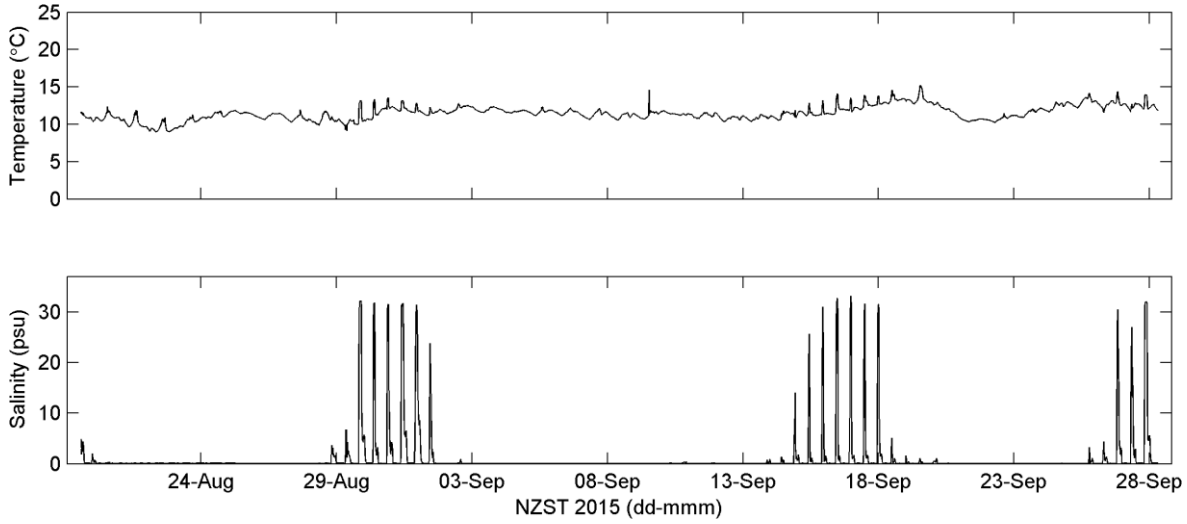

Figure 2.57: Marokopa River estuary, Lower site, surface temperature (top), salinity (bottom).

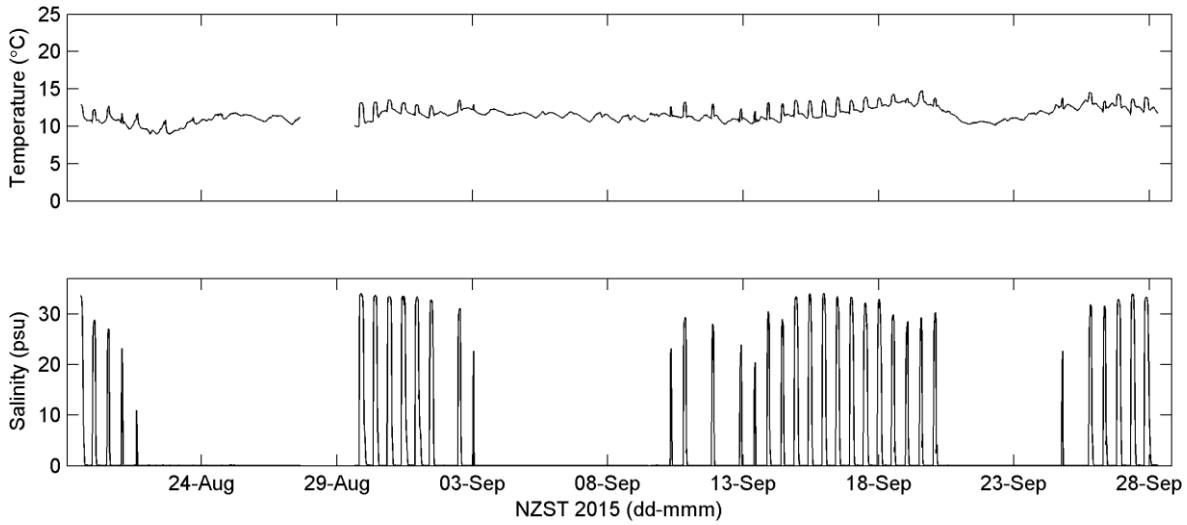

Figure 2.58: Marokopa River estuary, Lower site, bed level temperature (top), salinity (bottom).

2.6 Awakino River estuary

Figure 2.59 shows the locations of the two deployments at Awakino River estuary. The instruments were deployed on the 17th of August 2015. The instruments were inspected on the 8th of September 2015, and retrieved on the 27th of September 2015. The Upper site is approximately ~5 km upstream from the estuary mouth at 38.66350°S/174.64657°E. The Lower site is approximately ~2 km upstream from the estuary mouth at 38.64893°S/174.62538°E.

At the Upper site a Nortek Aquadopp was deployed in ~7 m of water measuring water level and current speed and direction at a fixed height 0.7 m above the seabed. At the Lower site a Nortek Aquadopp Profiler was deployed in ~3.5 m of water measuring water level as well as current speed and current direction in 0.5 m bins from 1 m above the bed to the surface. At the Upper site an Onset U24-002-C logger collected TS data at the surface, and an Odyssey TS Recorder was used at the bed. At the Lower site, TS data were recorded by a YSI EXO II Sonde and a U24-002-C logger at the bed level and surface respectively. The sampling interval for all instruments was 15 minutes, with current measurements averaged over 5 minutes.

Figure 2.59: Awakino River estuary deployment locations.

2.6.1 Upper site

Figure 2.60 presents depth readings at the Upper site during the deployment. The tidal signal is evident in the water depth record, along with periods of sustained high water levels, the most notable event occurred around the 27th of August which coincided with a riverine flood event.

Figure 2.61 and Figure 2.62 present current data. Current speeds were generally less than 0.4 ms^{-1} for much of the deployment period. The riverine flood event on the 17th of August caused an increase in downstream current speeds up to almost 1 ms^{-1} at its peak. A smaller riverine flood event around the 4th of September also led to increased downstream current speeds in excess of 0.5 ms^{-1}. Current directions are almost unidirectional in an ebb (downstream) direction, centred around 30°T, however two short lived periods towards the start and end of the deployment period indicate current reversal in a flood (upstream) direction. These periods both occurred during spring tides and possibly low flow conditions.

Figure 2.63 and Figure 2.64 show surface and bed level TS data, respectively. Temperatures ranged between ~9°C and ~14°C. The salinity values indicate that during the deployment the Upper site was almost exclusively fresh water. However the data recorded at the bed level (Figure 2.64) show increased salinity values, up to and in excess of 20 psu at the start and end of the deployment period, coincident with the current direction reversal which indicates that salt water does occasionally reach this point in the river.

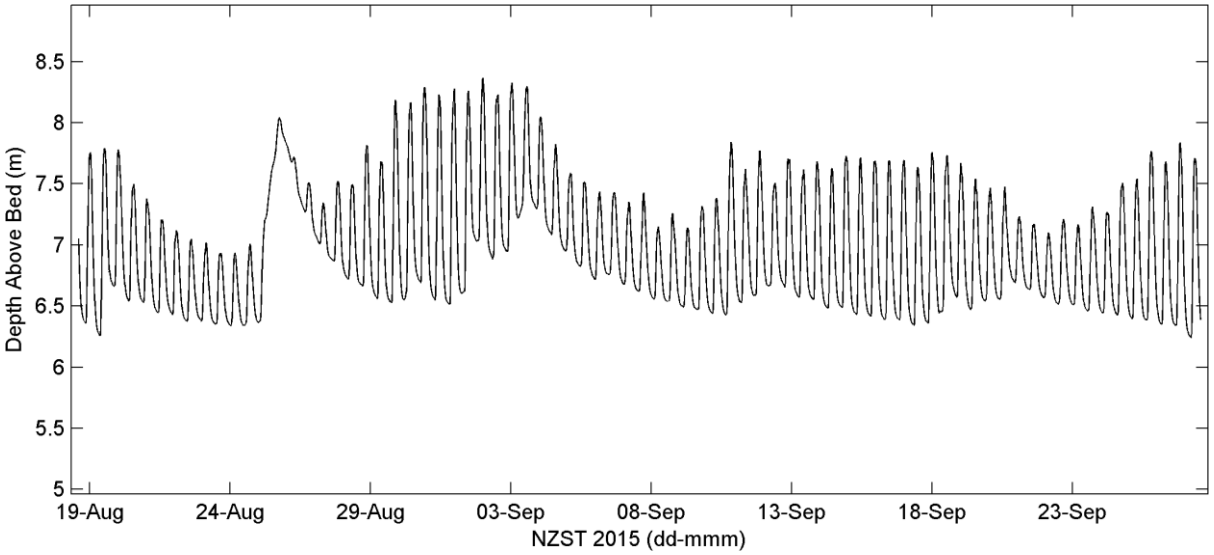

Figure 2.60: Awakino River estuary, Upper site, Water depth.

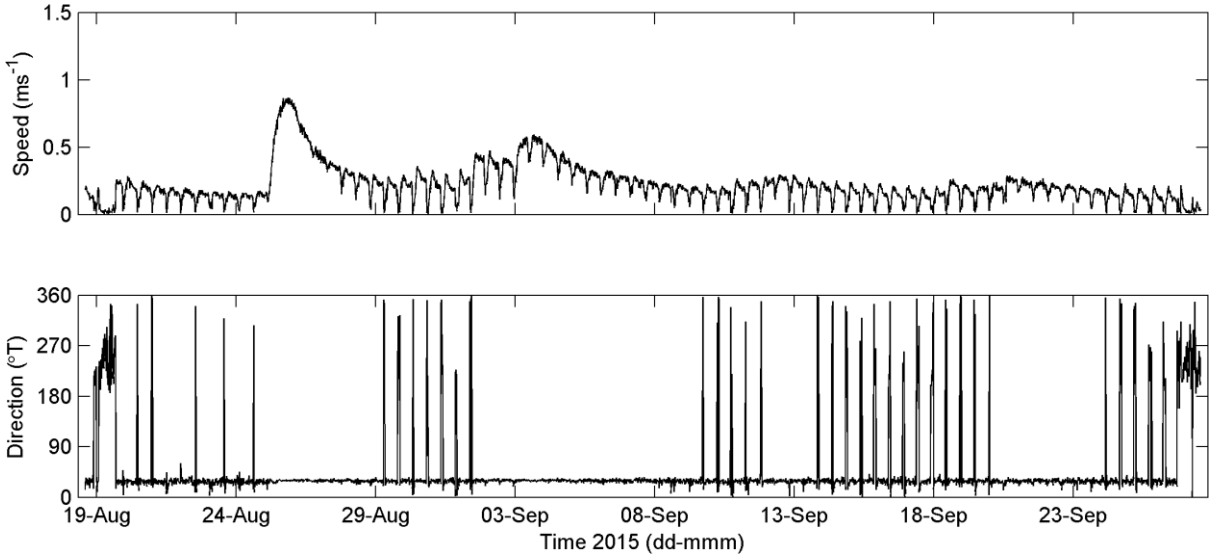

Figure 2.61: Awakino River estuary, Upper site, Current speed (top) and direction (bottom) 0.7 m above bed.

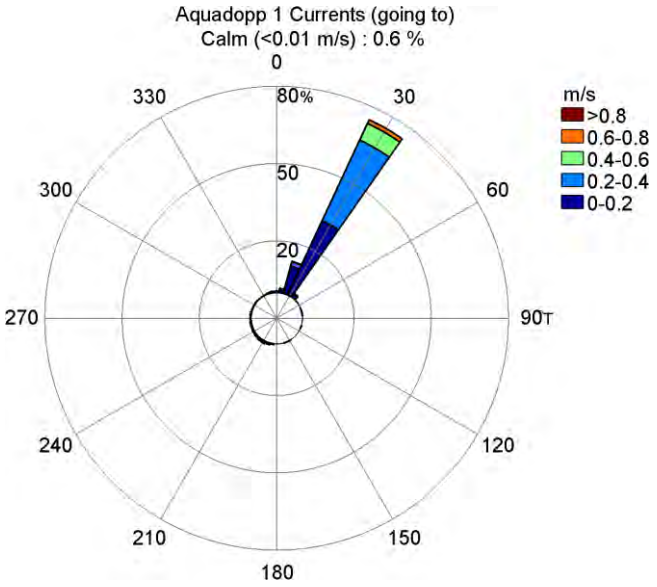

Figure 2.62: Awakino River estuary, Upper site, Current rose plot.

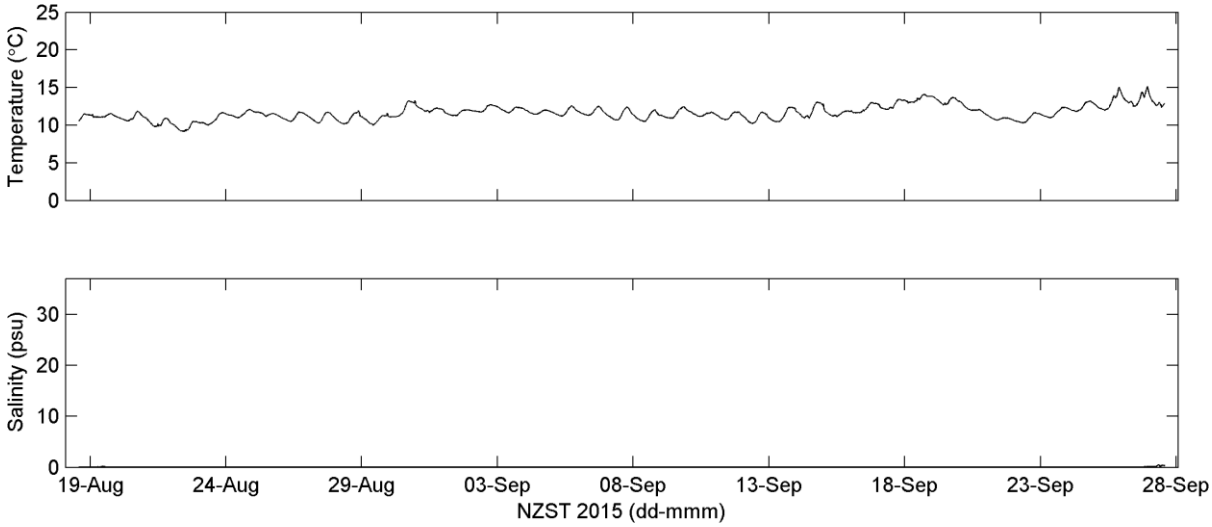

Figure 2.63: Awakino River estuary, Upper site, surface temperature (top), salinity (bottom).

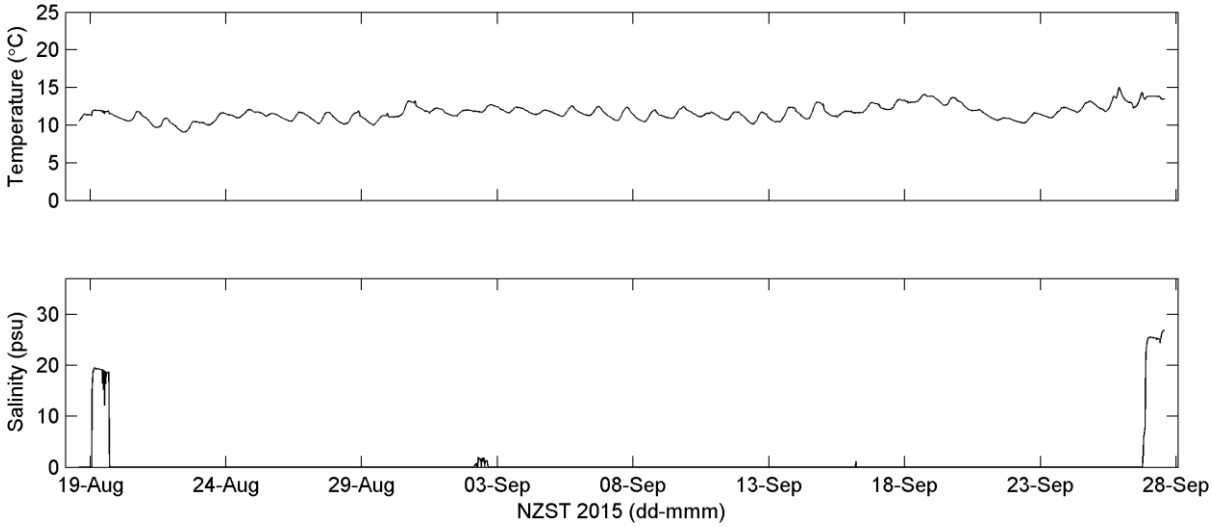

Figure 2.64: Awakino River estuary, Upper site, bed level temperature (top), salinity (bottom).

2.6.2 Lower site

Figure 2.65 presents the water depth. Figure 2.66 and Figure 2.67 present the current speed and direction through the water column in 0.5 m bins, and water level. Figure 2.68 and Figure 2.69 present the depth averaged current speed and direction as line plots and rose plots, respectively. Currents speeds reach a maximum of ~1 ms^{-1}. Current directions are dominated by flow to 260°T in the ebb (downstream) direction, but show multiple reversals in the flood (upstream) direction, interspersed with periods of up to 3 days of downstream unidirectional flow.

Figure 2.70 and Figure 2.71 show surface and bed level TS data, respectively. Temperatures range between ~9°C and ~15°C at the surface and ~9°C and ~14°C at bed level. Both surface and bed level salinity data show oscillations with variation between 0 and more than 30 psu. High salinity readings are coincident with spring tides and may also be affected by varying river flow. These oscillations are interspersed with periods of several days of salinity readings of 0 psu.

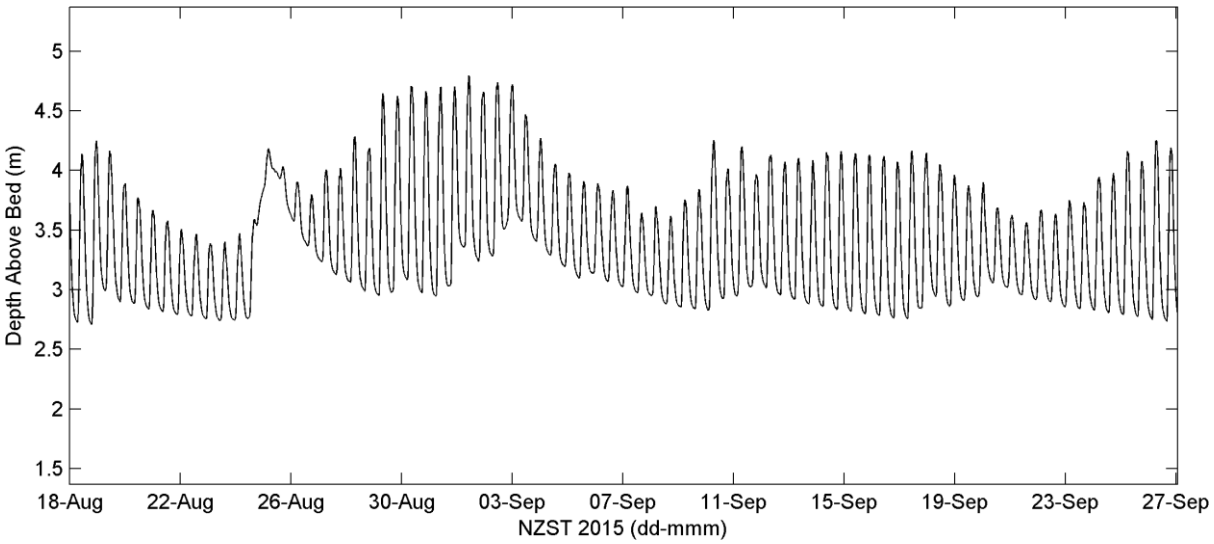

Figure 2.65: Awakino River estuary, Lower site, Water depth.

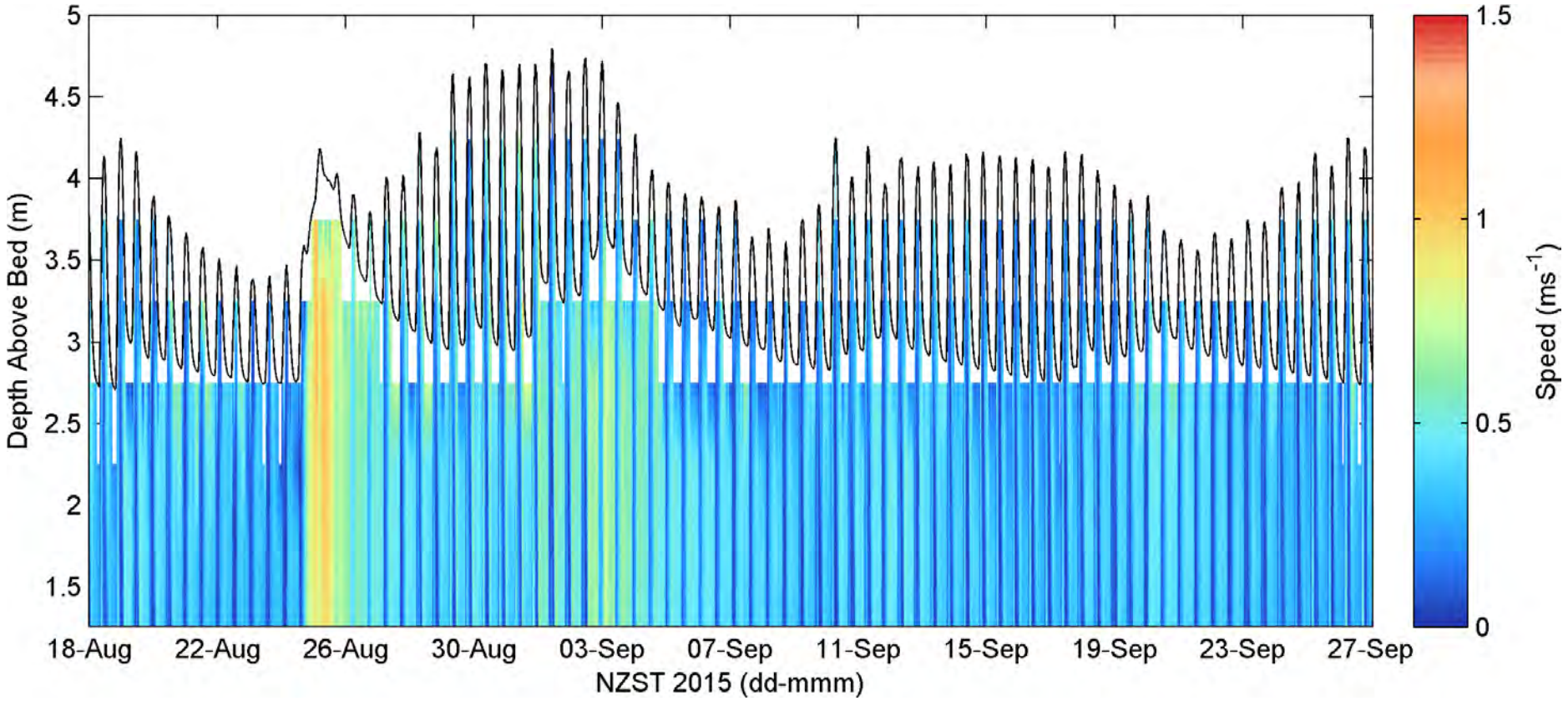

Figure 2.66: Awakino River estuary, Lower site, Current speed profile data: Black line: water level.

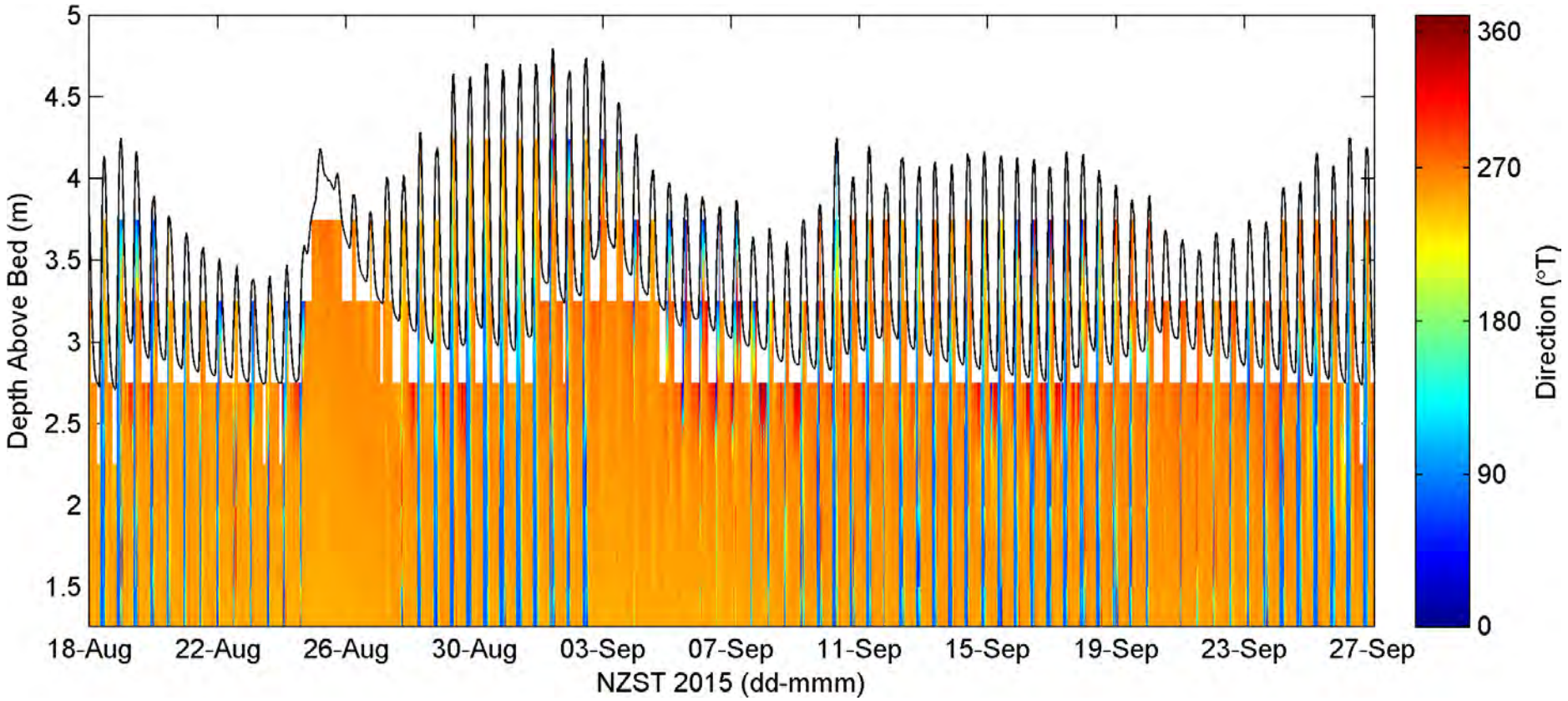

Figure 2.67: Awakino River estuary, Lower site, Current speed profile data: Black line: water level.

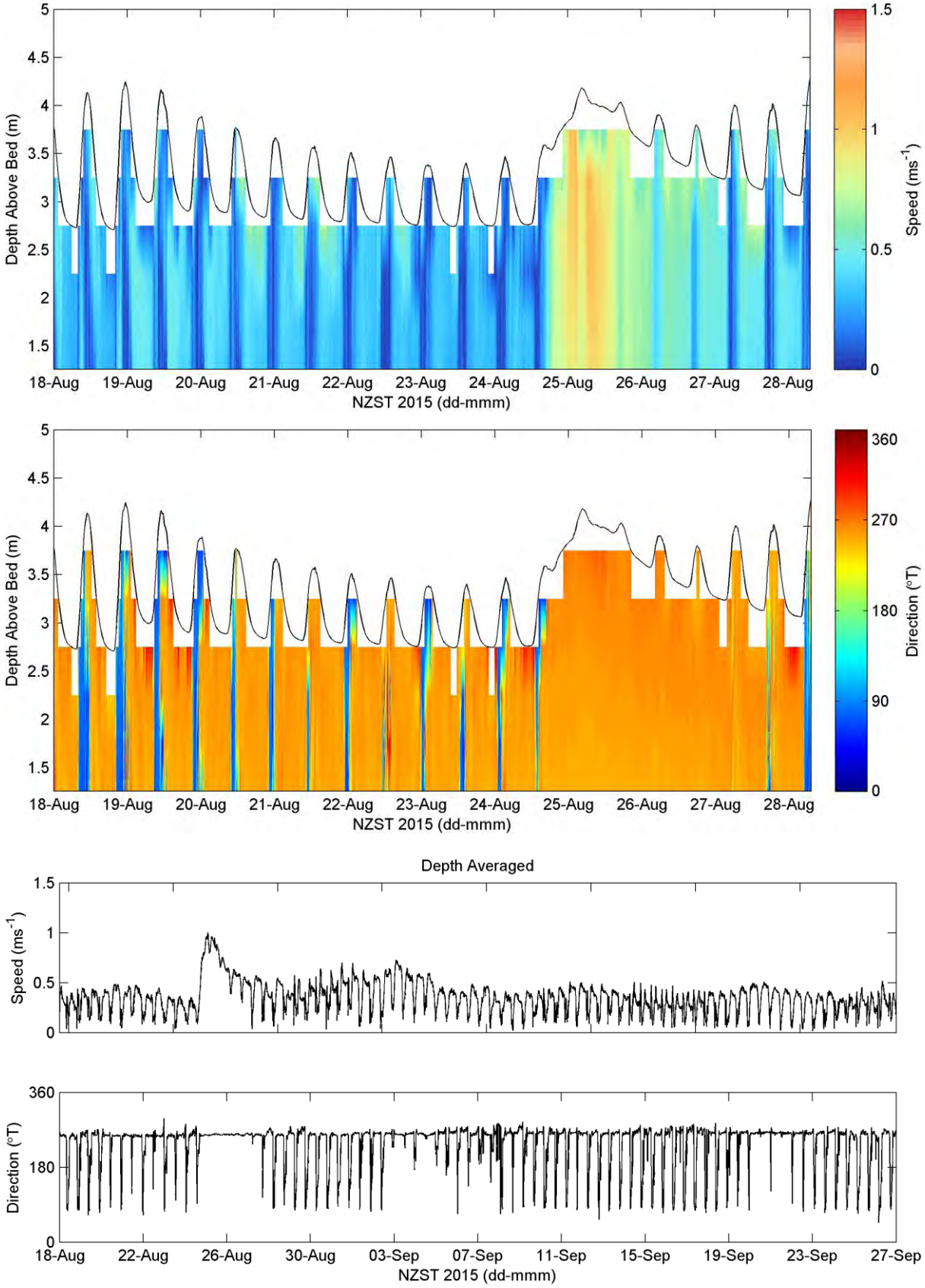

Figure 2.68: Awakino River estuary, Lower site, Depth averaged current speed (top) and direction (bottom).

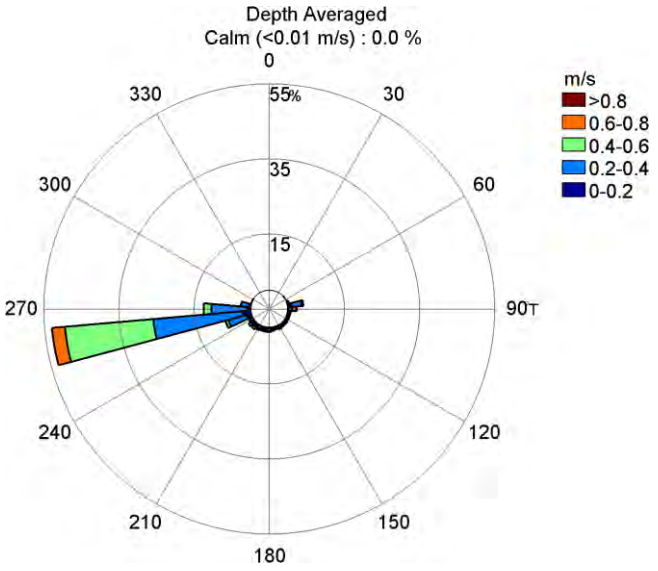

Figure 2.69: Awakino River estuary, Lower site, depth averaged current rose plot.

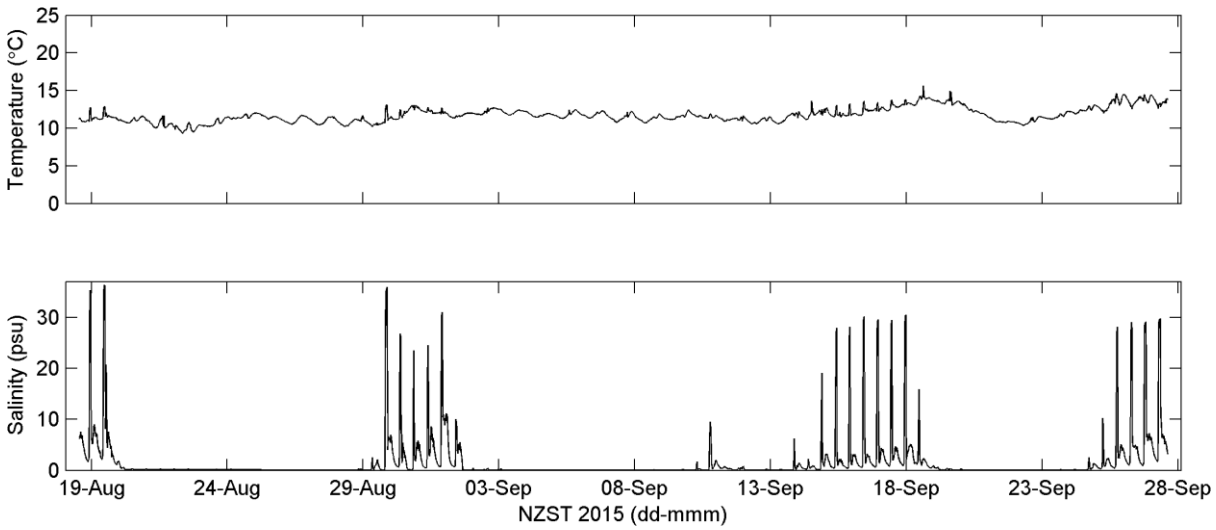

Figure 2.70: Awakino, Lower site, surface temperature (top), salinity (bottom).

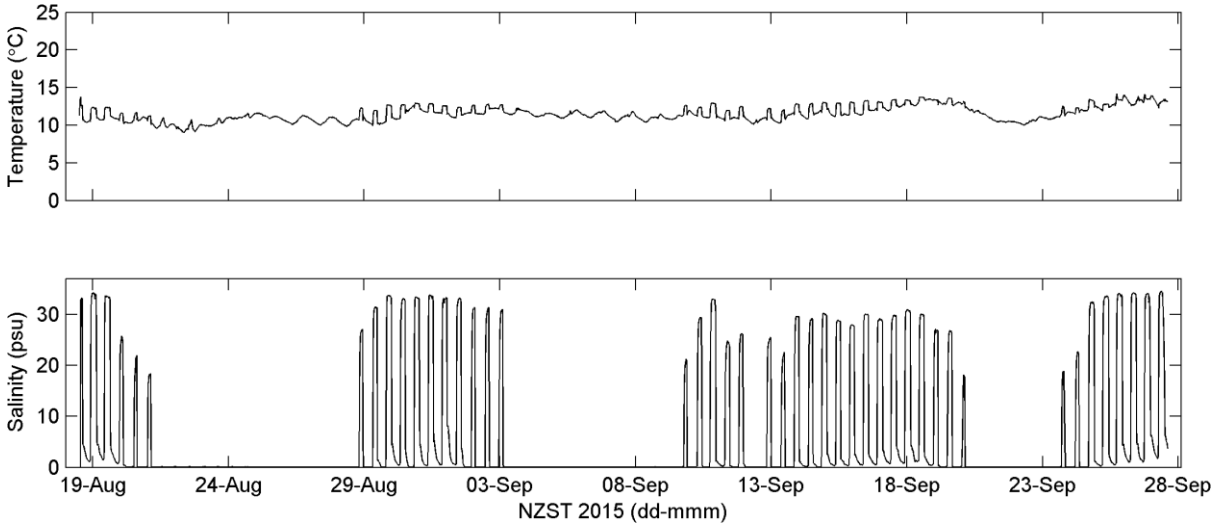

Figure 2.71: Awakino, Lower site, bed level temperature (top), salinity (bottom).

2.7 Mokau River estuary

Figure 2.72 shows the locations of the two deployments made at Mokau River estuary. The deployments were made on the 17th of August 2015. The instruments were inspected on the 8th of September 2015, and retrieved on the 27th of September 2015.

The Upper site is ~ 7 km upstream from the entrance at 38.70569 °S/174.65104°E. On the 4th of September the deployed equipment was tampered with. The frame was flipped onto its side; however the frame was not moved beyond this position.

At the Mokau River estuary Lower site the equipment was initially deployed east of the SH3 bridge at 38.70006°S/174.62788°E. On the 21st of August 2015, 29th of August 2015 and 2nd of September 2015, the deployed equipment was tampered with. All evidence suggests attempts were made to haul the equipment out of the water. The data shows that the instrument was deposited on the seabed upside down during the first interference, righted on the second and flipped again on the third. After the first interference the equipment was moved 30 m to the west. On the 8th of September 2015, during an inspection, eCoast's field team retrieved the equipment from 38.69974°S/174.62740°E. After downloading the data, the equipment was redeployed at 38.69976 °S/174.62739°E.

Figure 2.72: Mokau River estuary deployment locations.

At the Upper site a Nortek Aquadopp was deployed in ~5.5 m collecting current speed and direction at a fixed height 0.7 m above the seabed, and water level. At the Lower site a Teledyne RDI Workhorse Sentinel ADCP was deployed in ~3.5 m of water collecting current speed and current direction in 0.5 m bins from 1 m above the bed to the surface, and water level.

Onset U24-002-C loggers collected TS data at the surface and just above the bed at both sites, with the exception of the Upper site bed level gauge being an Odyssey TS recorder. The sampling interval for all instruments was 15 minutes, with current measurements averaged over 5 minutes.

2.7.1 Upper site

The instrument at the Upper site was tampered with a few days before the midway inspection and consequently ~4 days of current data were unsalvageable. Depth data remained usable with a simple offset applied to correct for the vertical displacement of the pressure sensor when the instrument/frame was tipped over. Figure 2.73 shows the depths recorded during the deployment period. There was a ~2.5 m range in depth during spring tides with an apparent attenuation of the tidal signal during periods of high river flow.

Figure 2.74 and Figure 2.75 present the current speed and direction 0.7 m above the bed. The blank section in the speed and direction plot is the period during which the equipment was tampered with prior to the midway inspections. Both speeds and direction show strong tidal influence throughout the deployment period. However, tidal oscillations were strongly attenuated during a period of high river flow around the 27th of August. At this time unidirectional currents in an ebb (downstream) direction reached speeds of ~0.75 ms^{-1}.

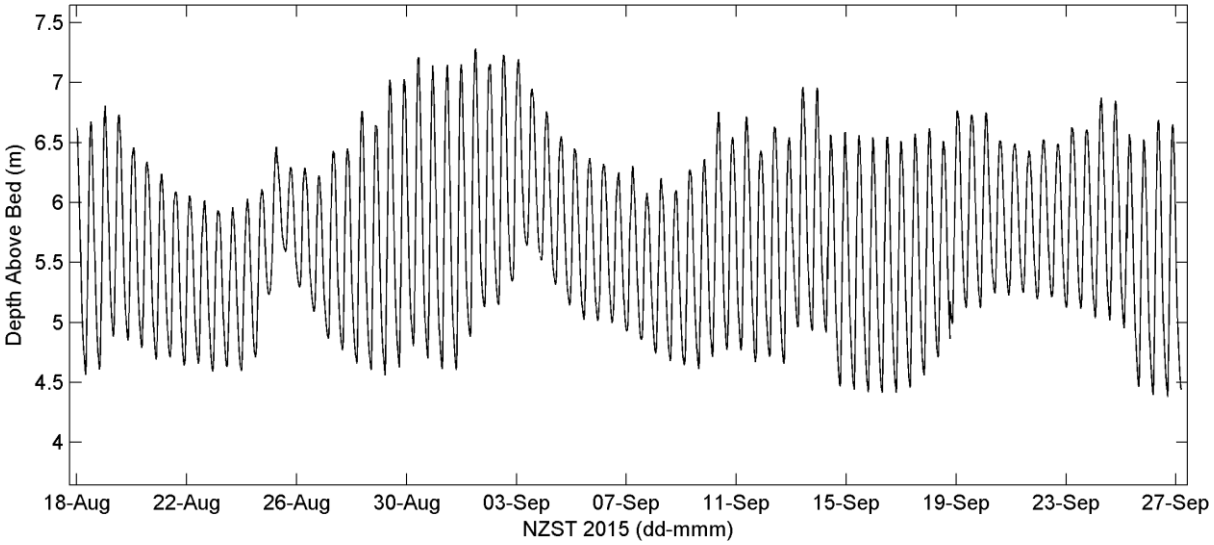

Figure 2.73: Mokau River estuary, Upper site, water depth.

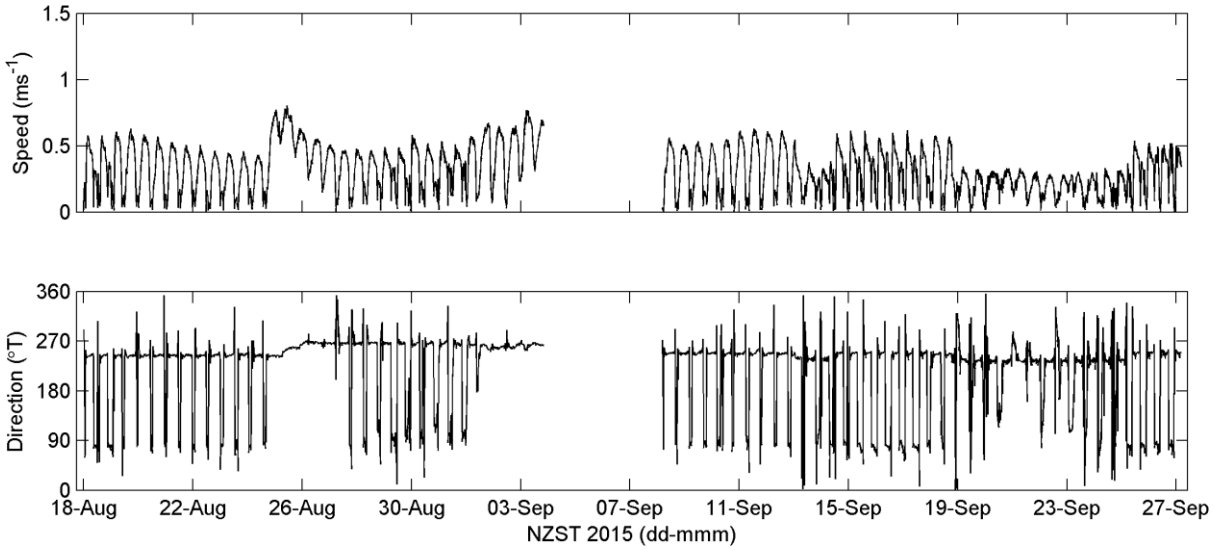

Figure 2.74: Mokau River estuary, Upper site, Current speed (top) and direction (bottom).

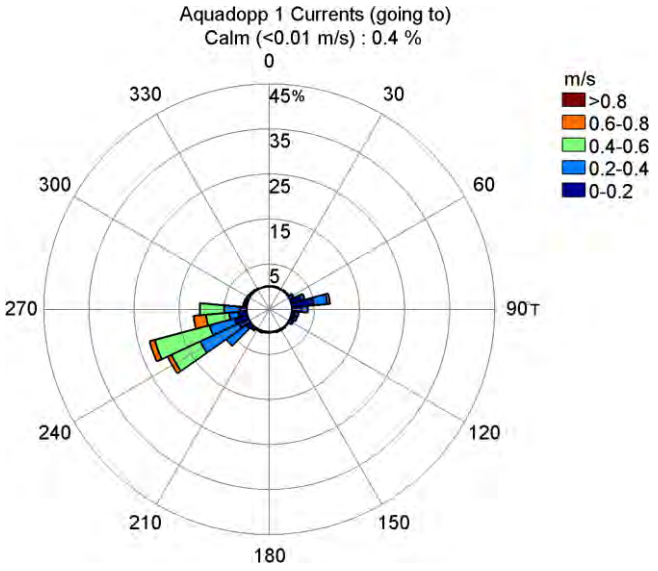

Figure 2.75: Mokau River estuary, Upper site, current rose plot.

Figure 2.76 and Figure 2.77 present the TS data from surface and bed level respectively. Temperatures ranged from ~9°C to ~13°C in both surface and bed level records. The surface salinity record shows that the water is consistently fresh during the deployment period. The bed level data exhibits periods of significant salt water intrusion with salinity values undergoing periods of oscillations between 0 and ~30 psu on a number of occasions.

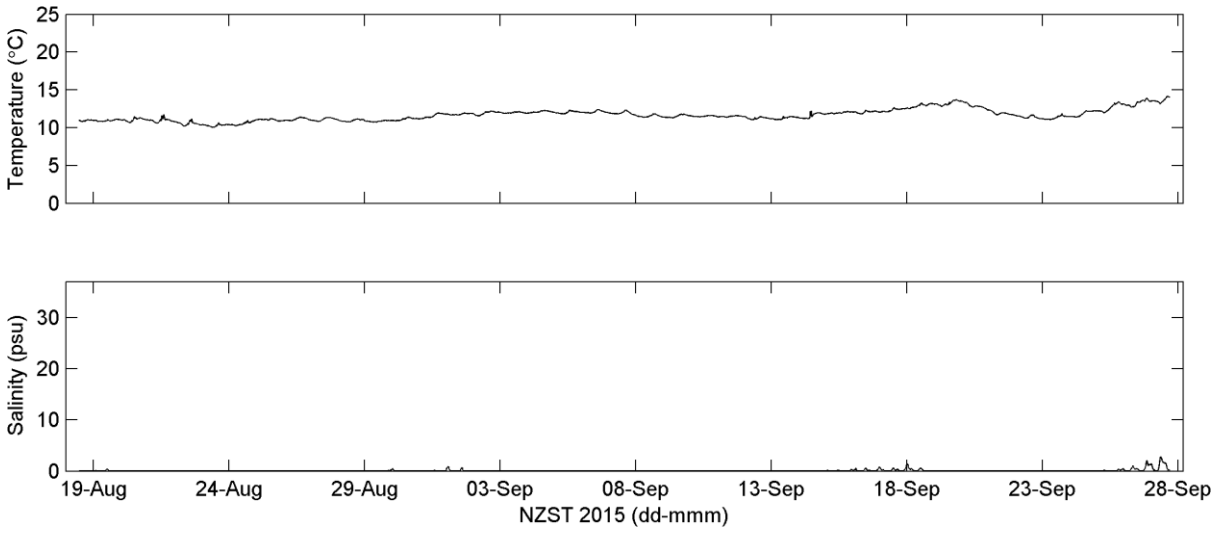

Figure 2.76: Mokau River estuary, Upper site, surface temperature (top), salinity (bottom).

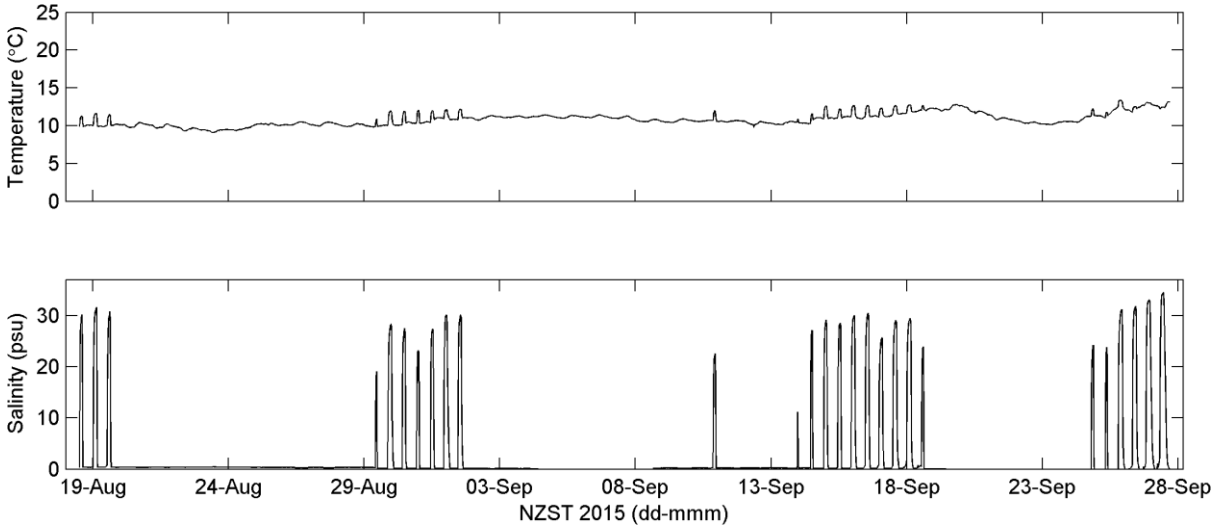

Figure 2.77: Mokau River estuary, Upper site, bed level temperature (top), salinity (bottom).

2.7.2 Lower site

As described previously, the instrument was tampered with during the first half of the deployment period. Only two short sections of data were salvageable from the first half, the second half of the deployment was completed without disturbance. The result is 3 sets of data from 3 different positions within the same general area. The current data is presented as 3 separate plots. The TS data remain on a single plot for the deployment duration.

Figure 2.78 presents water depth data for Positions 1 to 3. The tidal range at Position 1 was ~2 m, while at Position 2 it increased to ~2.7 m. The data from Position 3 includes spring and neap tides with ranges of ~2.3 m and ~1.35 m, respectively.

Figure 2.79 and Figure 2.80 present current data for all three positions for speed and direction respectively. Figure 2.81 and Figure 2.82 present depth averaged current data for all 3 positions. Maximum current speeds reached 1.30 ms^{-1} at Position 1, 1.27 ms^{-1} at Position 2, and 1.25 ms^{-1} at Position 3. Currents flowed in a 330°T direction during the ebb and 120°T direction during the flood tide.

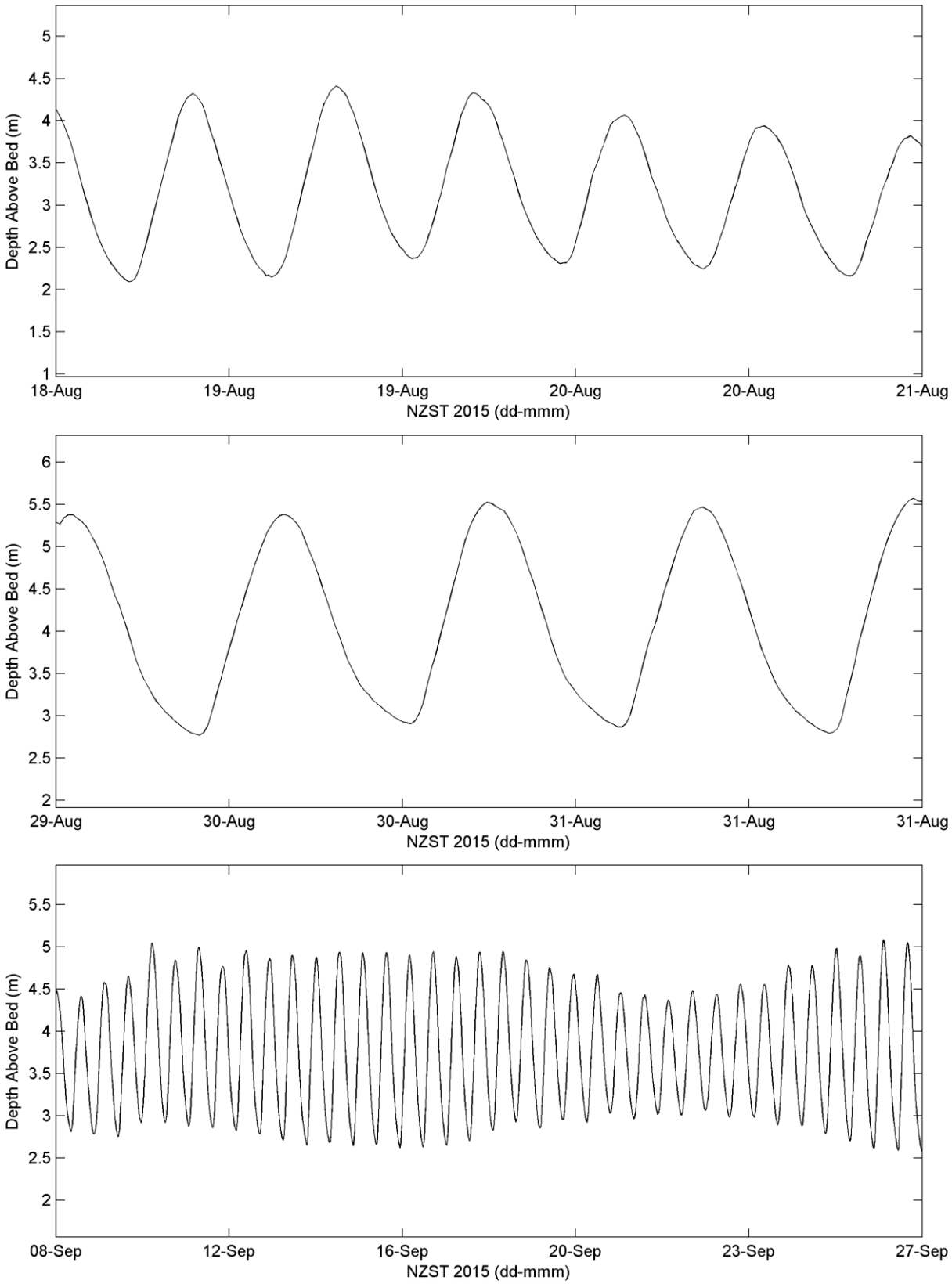

Figure 2.78: Mokau River estuary, Lower site, Depth plots for Position 1 (top), Position 2 (middle), and Position 3 (bottom).

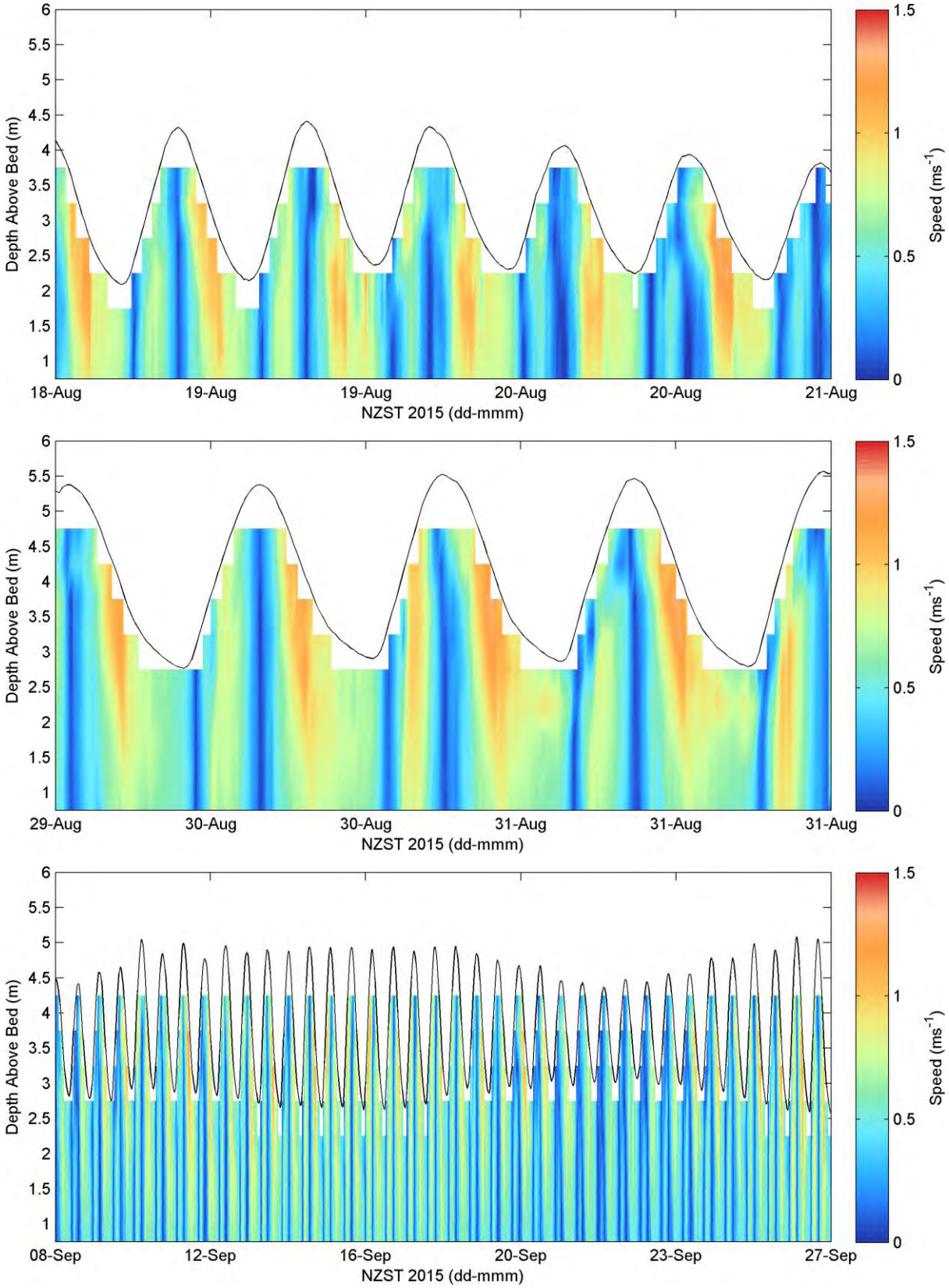

Figure 2.79: Mokau River estuary, Lower site, Current speed profiles for Position 1 (top), Position 2 (middle), and Position 3 (bottom).

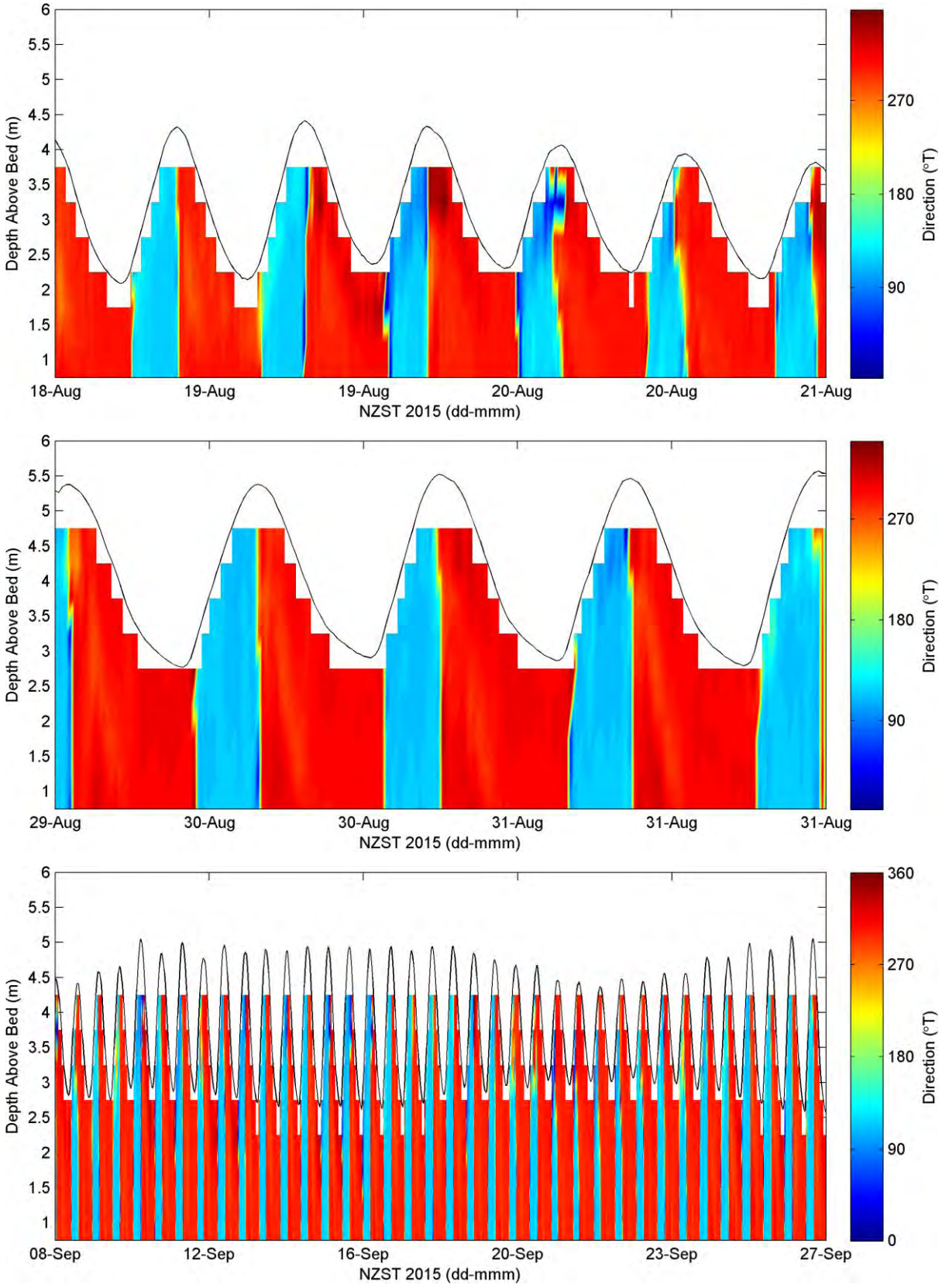

Figure 2.80: Mokau River estuary, Lower site, Current direction profiles for Position 1 (top), Position 2 (middle), and Position 3 (bottom).

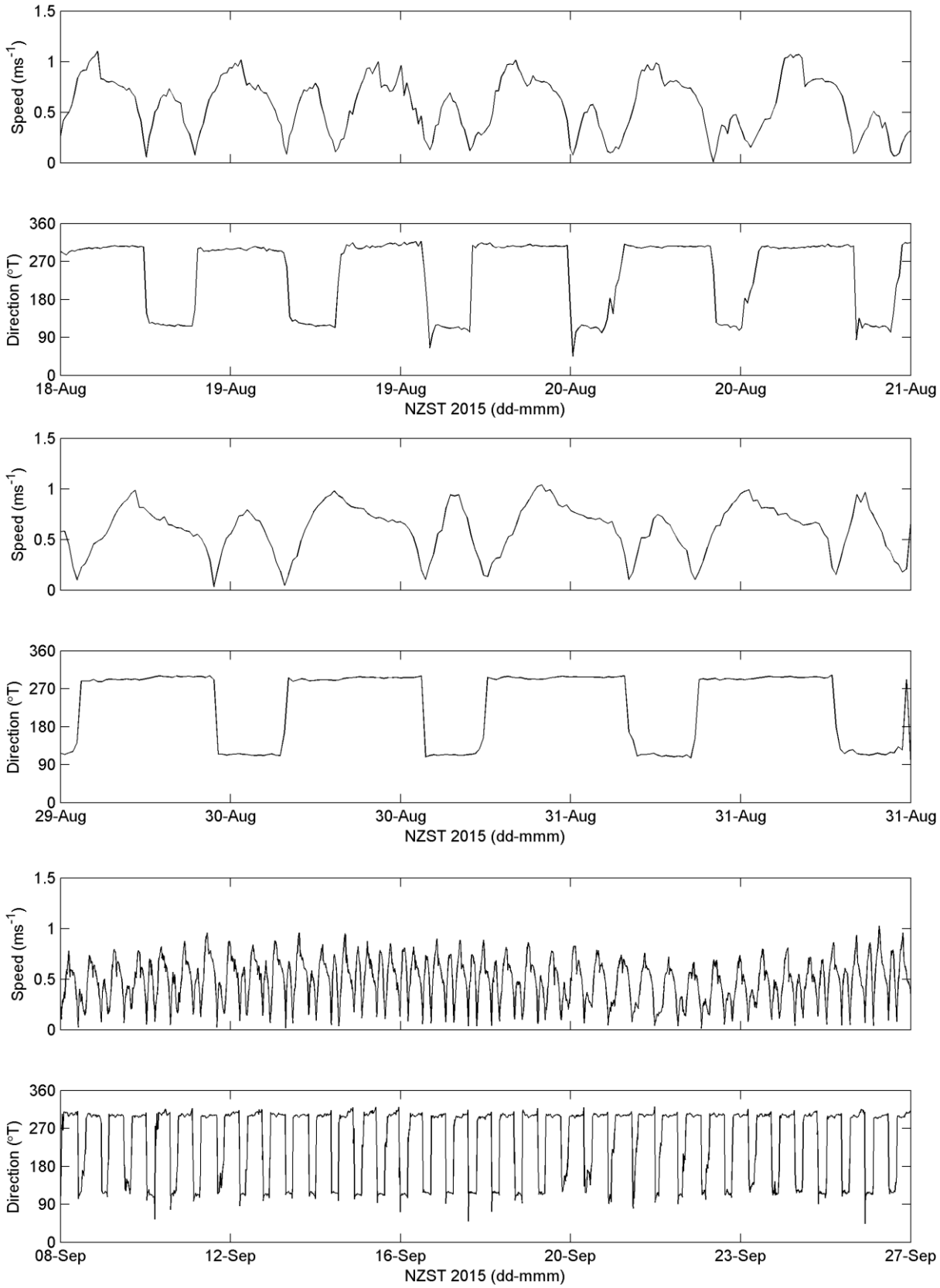

Figure 2.81: Mokau River estuary, Lower site, Depth averaged current data for Position 1 (top), Position 2 (middle), and Position 3 (bottom).

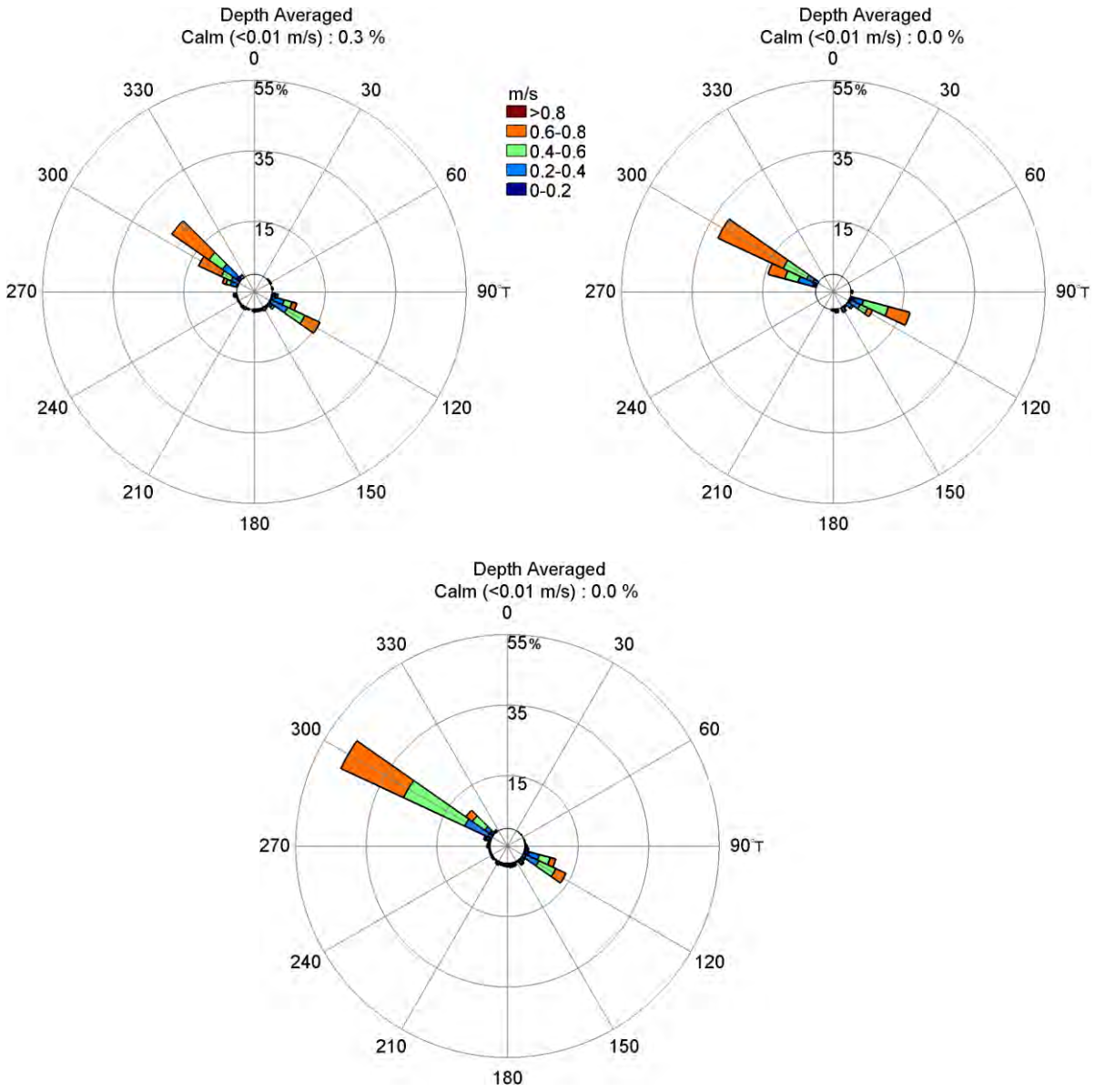

Figure 2.82: Mokau River estuary, Lower site, Depth averaged current rose plots for Position 1 (top left), Position 2 (top right), and Position 3 (bottom).

Figure 2.83 and Figure 2.84 present the TS data for surface and bed level gauges, respectively. Temperatures ranged between 10 and 15°C in both the surface and bed level records. Salinity records in both the surface and bed level exhibited oscillations between fresh and saline water, periodically fluctuating from 0 to ~30 psu or more. Both records showed sustained periods of low salinity, most evident around the 27th August concurrent with a period of high river flow. The high river flow events are less evident in the bed level record than the surface record, with high salinity values observed at the bed when surface values are less than 10 psu (e.g. 8th September)..

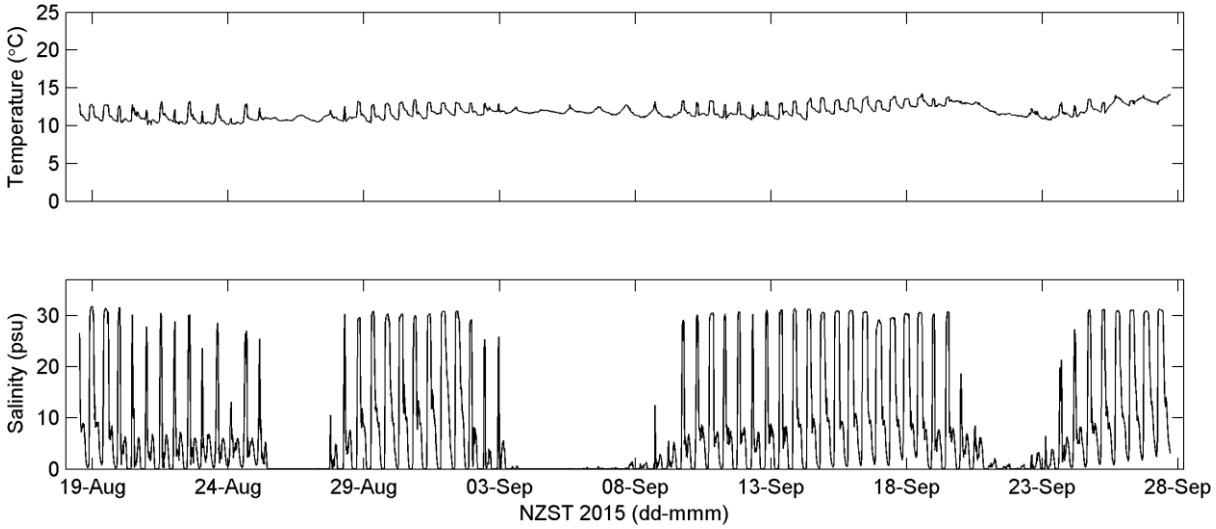

Figure 2.83: Mokau River estuary, Lower site, surface temperature (top), salinity (bottom).

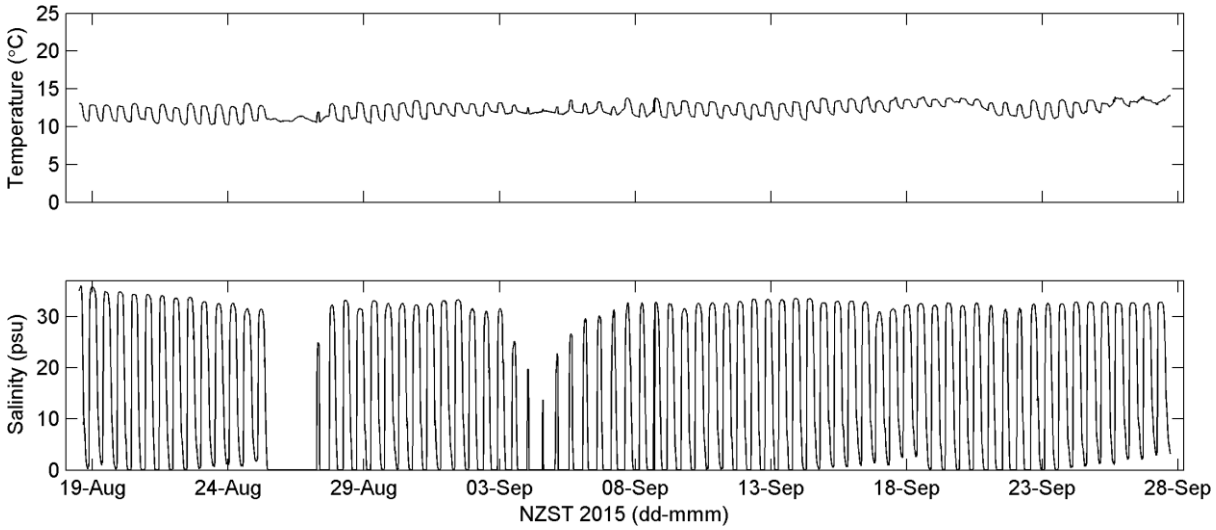

Figure 2.84: Mokau River estuary, Lower site, bed level temperature (top), salinity (bottom).

3 Bathymetric and Topographic Survey

With the exception of Whaingaroa (Raglan) Harbour, surveys were undertaken at all sites to collect data to develop Digital Elevation Models (DEMs) for hydrodynamic modelling. At Whaingaroa (Raglan) Harbour, bathymetric and topographic datasets have been previously collected and will be used for DEM development (Greer *et al*., 2015).

Both bathymetric and topographic data were collected. Bathymetric data were collected using eCoast's jet ski "Red Rocket" (Figure 3.1). Topographic data were collected on foot at Marokopa, Awakino and Mokau River estuaries. Topographic survey was not collected at Waikato River estuary, Aotea Harbour and Kawhia Harbour as terrestrial LiDAR data, held by WRC, is available.

A Real Time Kinematic (RTK) Global Positioning System (GPS) device collected horizontal position (WGS84) and elevation (Ellipsoidal) data at 1 Hz for the bathymetric survey and every metre for the topographic survey. Before each survey a base station was established above a Land Information New Zealand (LINZ) geodetic mark, the base station provides real time corrections of horizontal and vertical position to a roving GPS receiver used in the field to collect data points. Data points are collected in World Geodetic System 1984 (WGS84).

The Red Rocket is equipped with an Airmar in-hull, 200 kHz Single Beam Echo Sounder. Calibration of the sounder showed that measurements provide an accuracy of ± 0.1 m or better. Depth data are collected simultaneously with RTK-GPS horizontal position and elevation data. Depth data, the distance between the RTK-GPS receiver and the depth sounder (transducer) and the receiver's elevation relative to the ellipsoid were used to reduce the elevation recorded at water level to a value at the bed level.

Each RTK-GPS data point collected has an associated 3 Dimensional Quality Control (3DCQ) value. Where 3DCQ values exceeded 0.05 m an elevation value was assigned from the nearest points in time using a spring metaphor interpolation. The accuracy of the system is multifactorial but the majority of horizontal measurements have an accuracy of ± 0.1 m.

Using LINZ's Concord conversion software and the New Zealand Quasigeoid (NZGeoid2009), corrected in the horizontal from WGS84 to New Zealand Transverse Mercator (NZTM); and corrected in the vertical from WGS84 ellipsoidal heights to New Zealand Vertical Datum (NZVD), which approximates Mean Sea Level (MSL). The following steps show the data flow process:

- Data collected in WGS84
- Converted with Concord to New Zealand Geodetic Datum (NZGD)
- Converted NZGD ellipsoid heights to NZVD

- Converted NZGD Latitudes and Longitudes to New Zealand Transverse Mercator

The following information relates to data points collected that are an exception to the survey procedure described previously:

- At Kawhia Harbour there were 3 zones that did not achieve very high horizontal accuracy during the survey period for differing reasons, namely: the southern reaches of the harbour due to a lack of geodetic marks; the very north east arm due to atmospheric interference on the day of survey; and, the chart verification lines collected over the Kawhia Harbour Bar. The depth data collected in these areas were corrected using the Kawhia tide gauge, the datum of which is set to Moturiki MSL. For each data point collected water level was derived from the tide gauge record. The water level was used as an offset to correct the data points to a common vertical datum. The LINZ prescribed offset between Moturiki MSL and NZVD of 0.24 m was applied. Horizontal accuracy for the areas described here is less than 3 m.
- The ebb tidal deltas and exposed coasts of Marokopa, Awakino and Mokau River estuaries were surveyed with standard GPS. The conditions, while safe to undertake the survey for eCoast's Red Rocket, were not deemed suitable for the RTK-GPS equipment. Depths were corrected with predicted tides and an atmospheric pressure offset. Predicted water levels were generated from the TPXO wave atlas (Egbert and Erofeeva, 2002) Pacific Ocean model which provides the 11 most influential constituents, as well as two long period (Mf, Mm) harmonic constituents at 1/12 degree resolution (approx. 10 km). Atmospheric pressure is retrieved from the NOAA NCEP reanalysis model (see Section 7.3). Corrections due to atmospheric pressure were based on the assumption that an increase in atmospheric pressure of 1 decibar is equivalent to a 0.01 m decrease in sea level. The corrected data points were further processed by co-locating data points with the RTK-GPS data points, and establishing and applying any offset, if required.

While it would have been ideal to have every data point collected with RTK-GPS, the data points collected with the method described above were collected where horizontal accuracy is less relevant. For example outside of the shallow narrow channels of the inner estuaries or across broad scale features (ebb tidal delta, large channels, open coast beach- planar beach or long-shore bar trough). Therefore the data collected with this method are more than sufficient for modelling purposes.

Table 3.1 provides the dates of the surveys and the number of data points collected at each site after processing and editing.

Table 3.1: Survey metadata

Site	No. of Points	Survey Dates
Port Waikato	17,915	3/12/15, 8/12/15
Aotea	33,100	1/12/15. 2/12/15, 9/12/15
Kawhia	52,516	28/11/15, 29/11/15, 23/11/15, 2/12/15
Marokopa	33,012	23/8/15, 24/8/15, 28/9/15
Awakino	28,538	6/915, 7/9/15, 27/9/15
Mokau	37,301	2/9/15, 3/9/15, 27/9/15

Figure 3.1: Selection of images from work undertaken at Awakino River estuary: Top, RTK Base Station established at Awakino Heads overlooking the bar, entrance and lower reaches; Middle, eCoast's Red Rocket being prepared for (left) and undertaking (right) survey work; Bottom, RTK Base station set up over a geodetic survey mark in Awakino township

3.1 Waikato River estuary

For Waikato River estuary recent survey data exists from the lower reaches up to the now decomissioned Elbow Road aggregate processing site (Jones and Hamilton, 2014). Survey work undertaken as part of this project included two areas (Figure 3.2); one extending the existing survey to to the north to fill the gap between the end of the existing data and the deployed instuments adjacent to Elbow Road Waterski Club (Figure 3.3); and the lower part of the estuary including the entrance and bar area (Figure 3.4).

Transect line spacing ranged from 50 m in the inner harbour to 75 m, 100m and 150 m over different parts of the spit surrounding the inlet channel to 400 m on the ebb tidal delta. The survey lines at the Elbow Road site were spaced at 150 m.

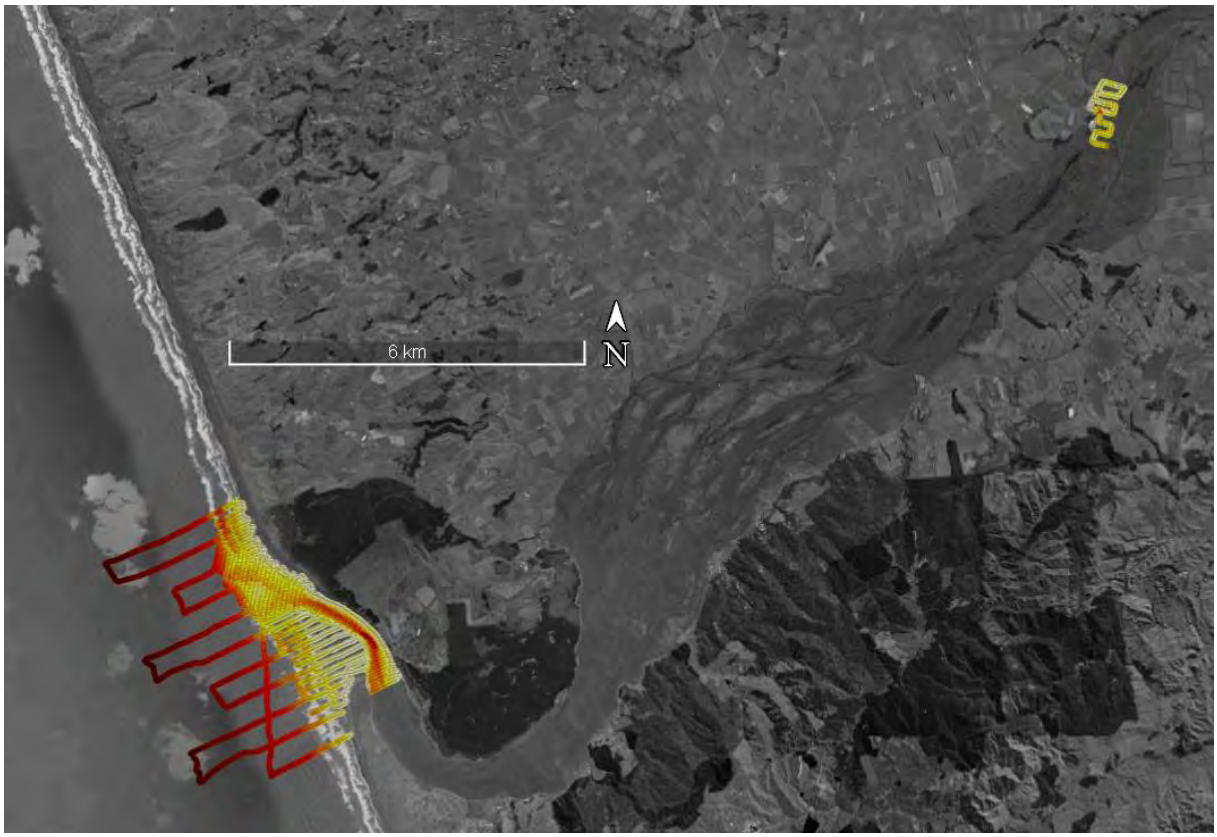

Figure 3.2: Overview of the 2 survey areas in Waikato River estuary: the bar and entrance area (left side) and the Elbow Road water ski area (right side).

Figure 3.3: Processed survey data points at the Elbow Road site, Waikato River estuary. Depths to Moturiki MSL.

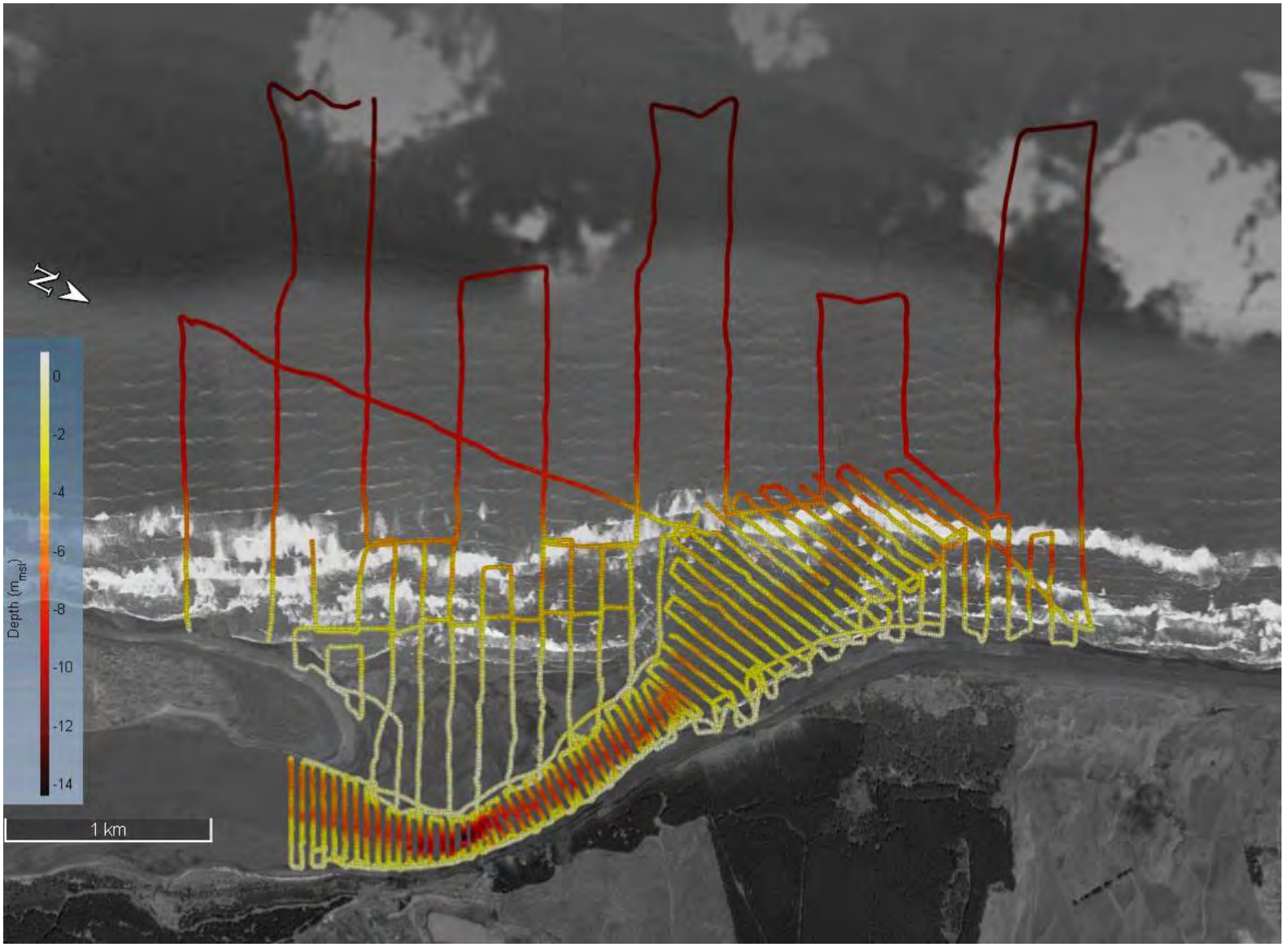

Figure 3.4: Processed survey data points at Waikato River estuary entrance. Depths are referenced to Moturiki MSL.

3.2 Aotea Harbour

At Aotea Harbour the surveyed area included the ebb tidal bar, the entrance, the main ebb and flood channels, the intertidal bars and multiple navigable channels. This data set will be supplemented with LiDAR data to fill the gaps over the intertidal areas not surveyed during this project. In the inner harbour the spacing of the transect lines ranged from 75m up to 200 m. Transect spacing over the ebb tidal bar was 200 m in the near shore and 400 m further offshore.

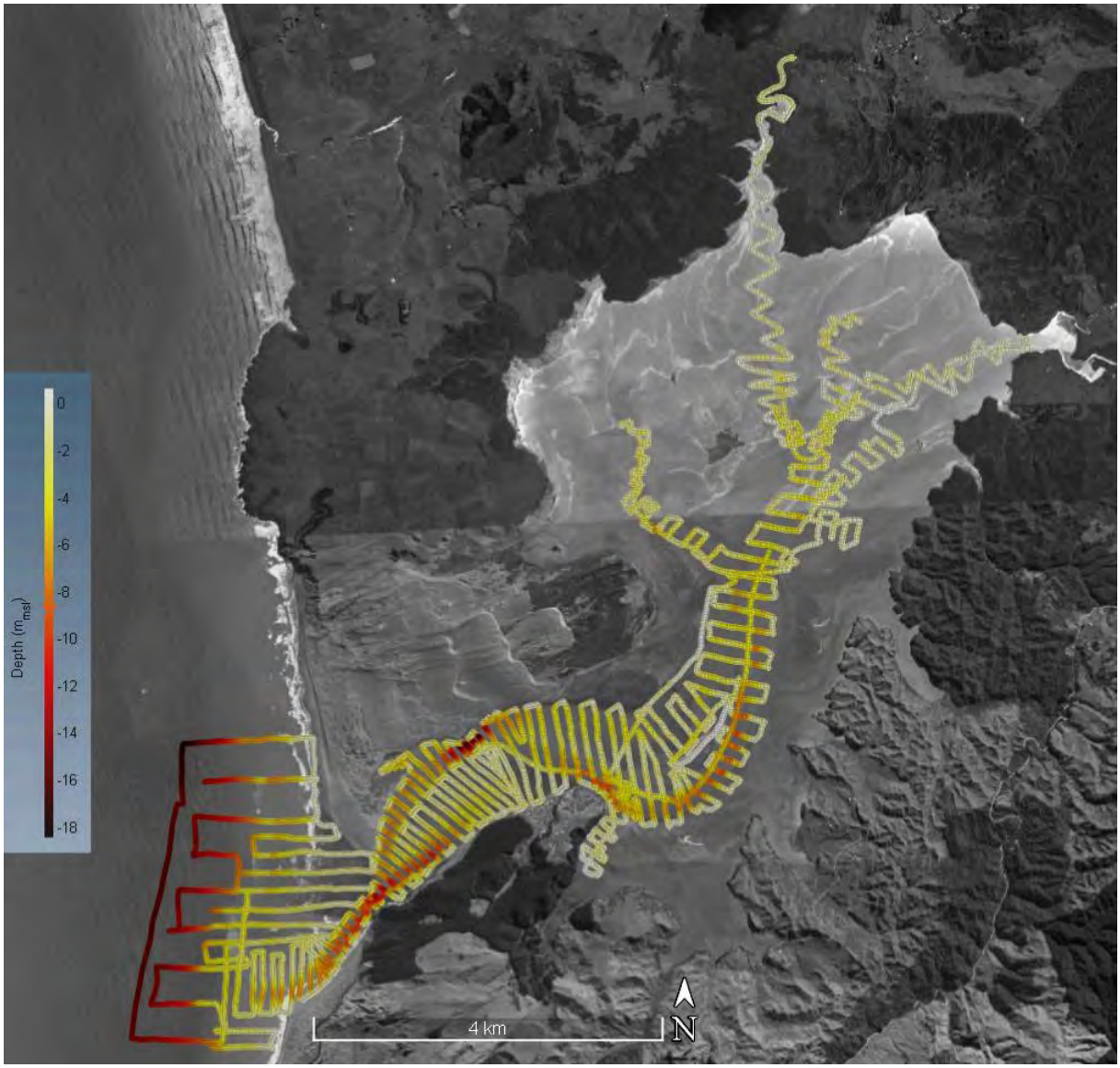

Figure 3.5: Processed survey data points at Aotea Harbour. Depths to Moturiki MSL

3.3 Kawhia Harbour

At Kawhia Harbour there is an existing nautical chart of the ebb tidal delta and the harbour entrance extending up to the wharf in the north and down to the entrance of the Te Waitere arm in the south. The surveyed area included the main ebb and flood channels, the intertidal bars and multiple navigable channels including many of the multiple smaller rivers and streams entering Kawhia Harbour (Figure 3.6). In addition, chart verification lines of the bar, and harbour entrance where also undertaken. This data set will be supplemented with LiDAR data to fill the gaps over the intertidal areas not surveyed during this project. Transect spacing in the inner harbour ranged from 100 m to 200 m depending on the size of the scale of the bathymetric features being resolved.

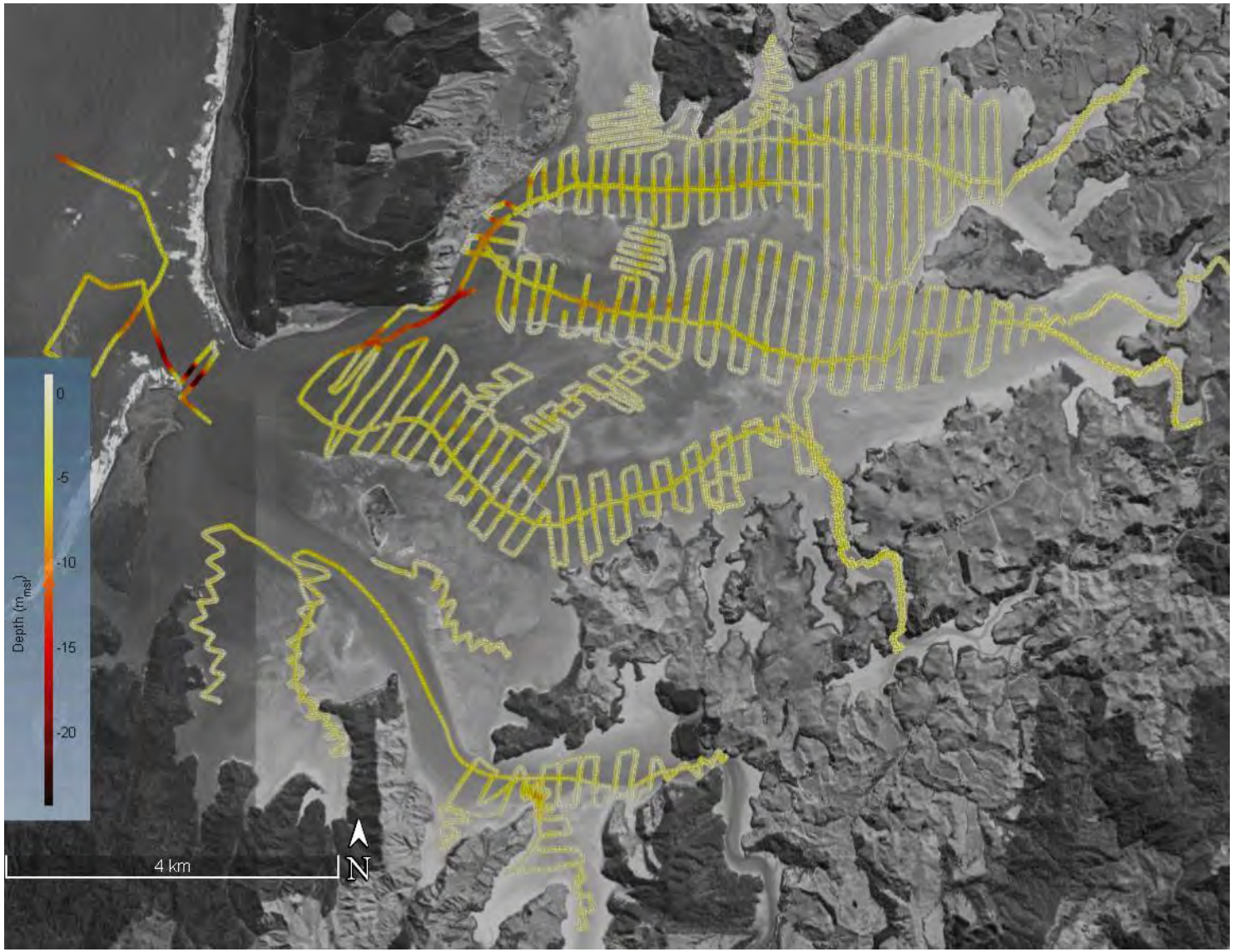

Figure 3.6: Processed survey data points in Kawhia Harbour. Depths are referenced to Moturiki MSL.

3.4 Marokopa River estuary

At Marokopa River estuary both bathymetric and topographic data were collected. The survey included the ebb tidal delta, the entrance and the lower reaches and also extended some ~6 km inland along the Marokopa River (Figure 3.7). Survey transect spacing was 25 m in the inner harbour and 75 m over the ebb tidal bar.

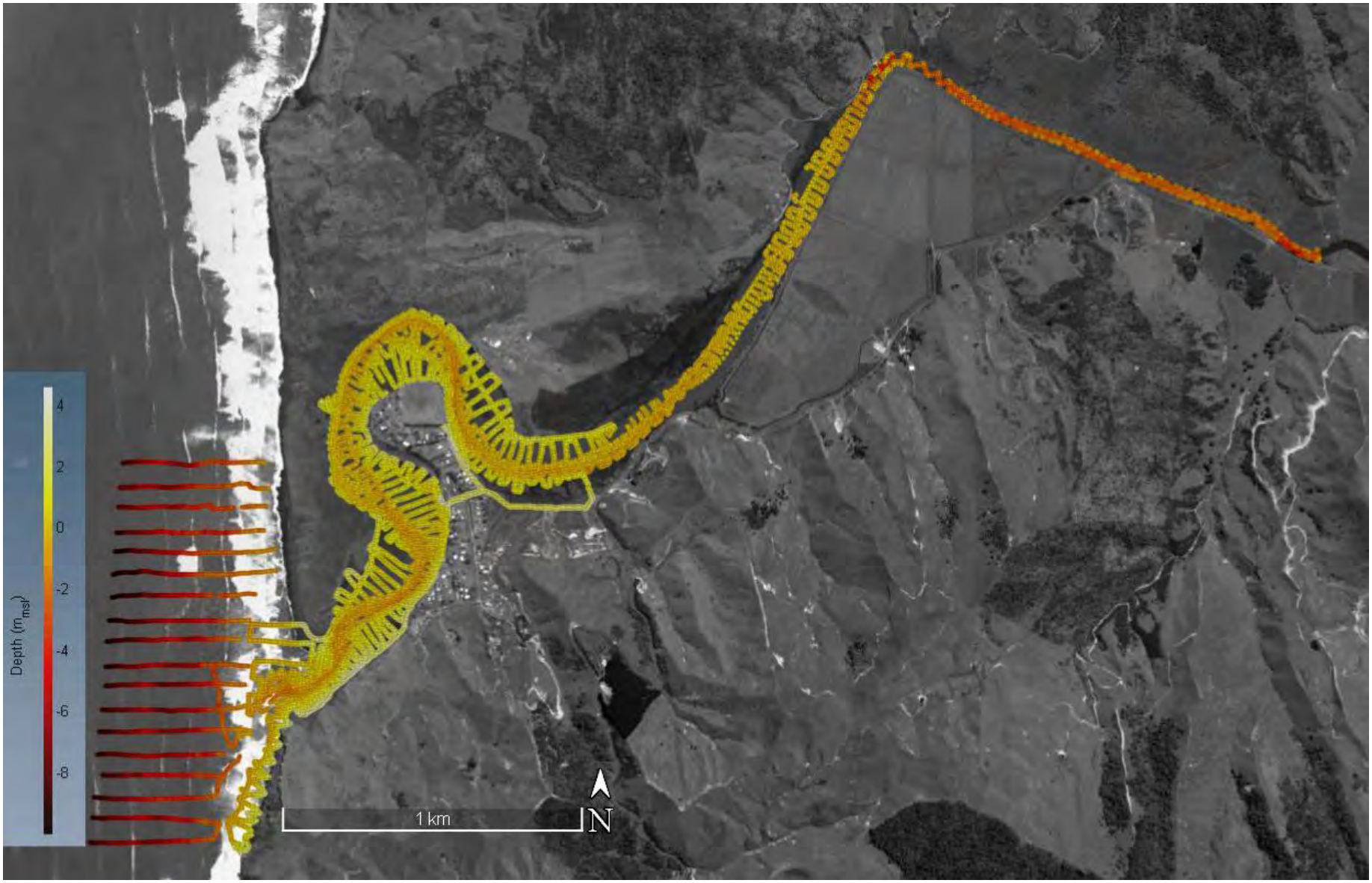

Figure 3.7: Processed survey data points at Marokopa River estuary. Depths were referenced to Moturiki MSL.

3.5 Awakino River estuary

At Awakino River estuary both bathymetric and topographic data were collected. The survey included the ebb tidal delta, the entrance, the lower reaches and extended some ~5 km inland along the Awakino River (Figure 3.8). The data from one of the transect lines over the ebb tidal delta was irretrievable during post-processing. However sufficient data were acquired for modelling purposes. Survey transect spacing was 25 m in the inner harbour and 75 m over the ebb tidal bar.

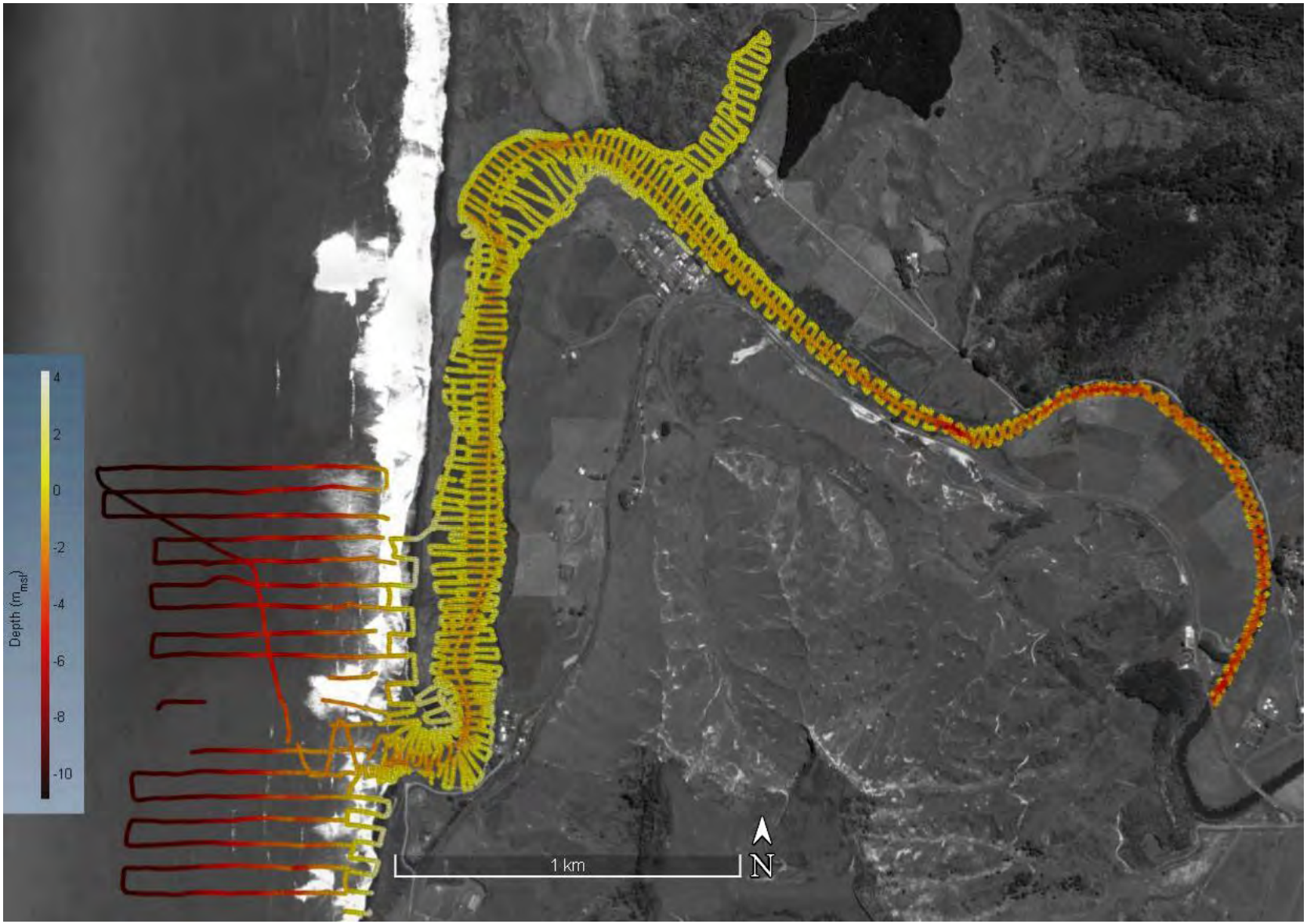

Figure 3.8: Processed survey data points at Awakino River estuary. Depths are referenced to Moturiki MSL.

3.6 Mokau River estuary

At Mokau River estuary both bathymetric and topographic data were collected. The survey included the ebb tidal delta, the entrance and the lower reaches and also extended ~11 km inland along the Mokau River (Figure 3.9). Survey transect spacing was 25 m in the inner harbour and 75 m over the ebb tidal bar.

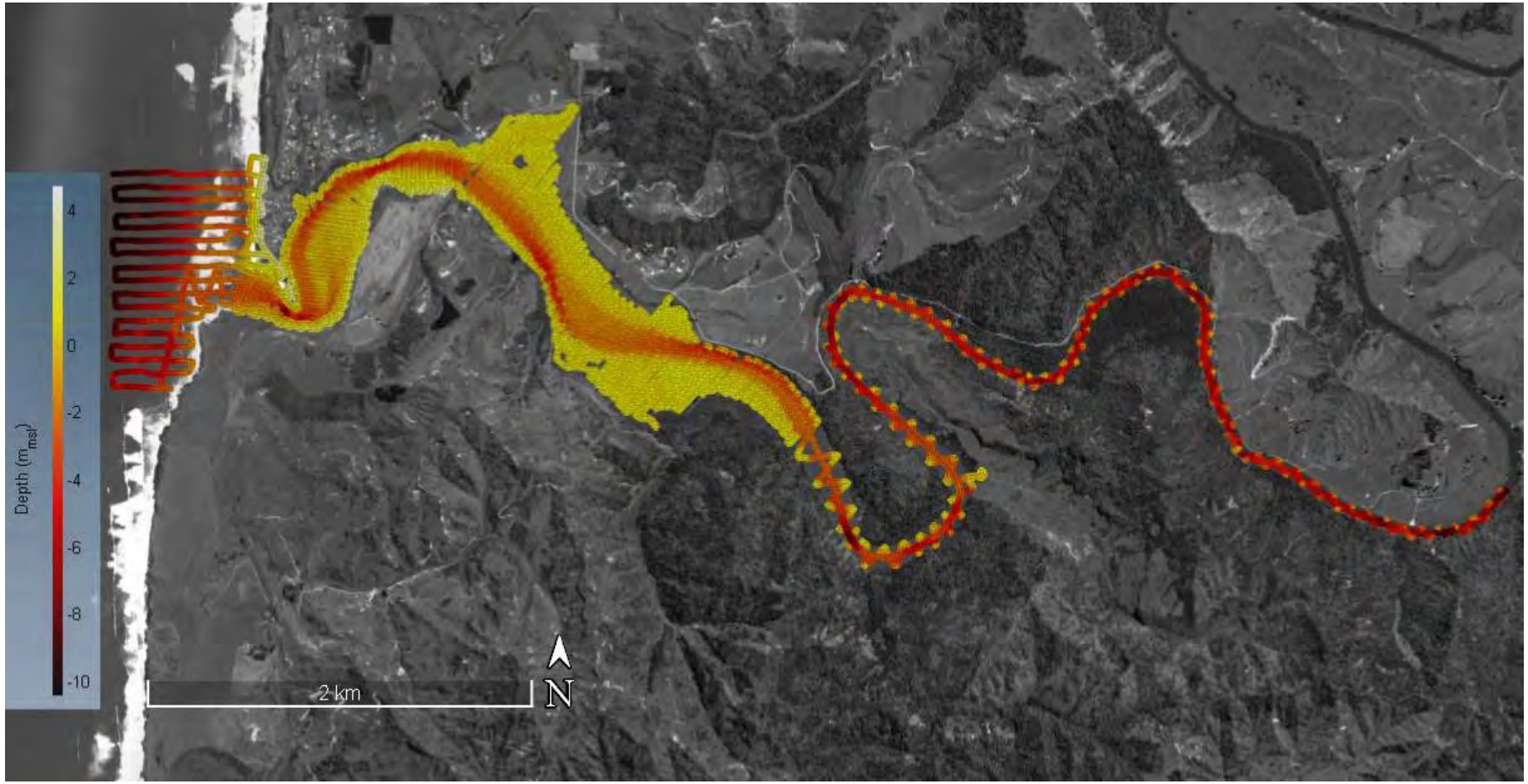

Figure 3.9: Processed survey data points at Mokau River estuary. Depths are referenced to Moturiki MSL.

4 References

APHA, 2012. Standard Methods for the Examination of Water and Wastewater, 22nd Ed. American Public Health Organisation, Washington, DC.

Egbert, G.D., and Erofeeva, S.Y., 2002. Efficient inverse modeling of barotropic ocean tides, J. Atmos. Oceanic Technol., 19(2), 183-204

Fofonoff, P. and Millard, R.C. Jr., 1983. Algorithms for computation of fundamental properties of seawater. _Unesco Tech. Pap. in Mar. Sci._, No. 44, 53 pp.

Greer, S. D, McIntosh, R., Harrison, S., Phillips, D., and Mead, S., 2015. Understanding Water Quality in Raglan Harbour, Australasian Coasts & Ports Conference 2015.

Jones, H. F. E. and Hamilton, D. P., 2014. Assessment of the Waikato River estuary and delta for whitebait habitat management: field survey, GIS modelling and hydrodynamic modelling, Waikato Regional Council Technical Report 2014/35

Millero, F.J., Chen, C.T., Bradshaw, A., and Schleicher, K., 1980. A new high pressure equation of state for seawater. Deap-Sea Research., Vol 27A, pp255-264.

Appendix B. **Hydrodynamic Modelling**

Mapping Residence Times in West Coast Estuaries of the Waikato Region: Model Calibration

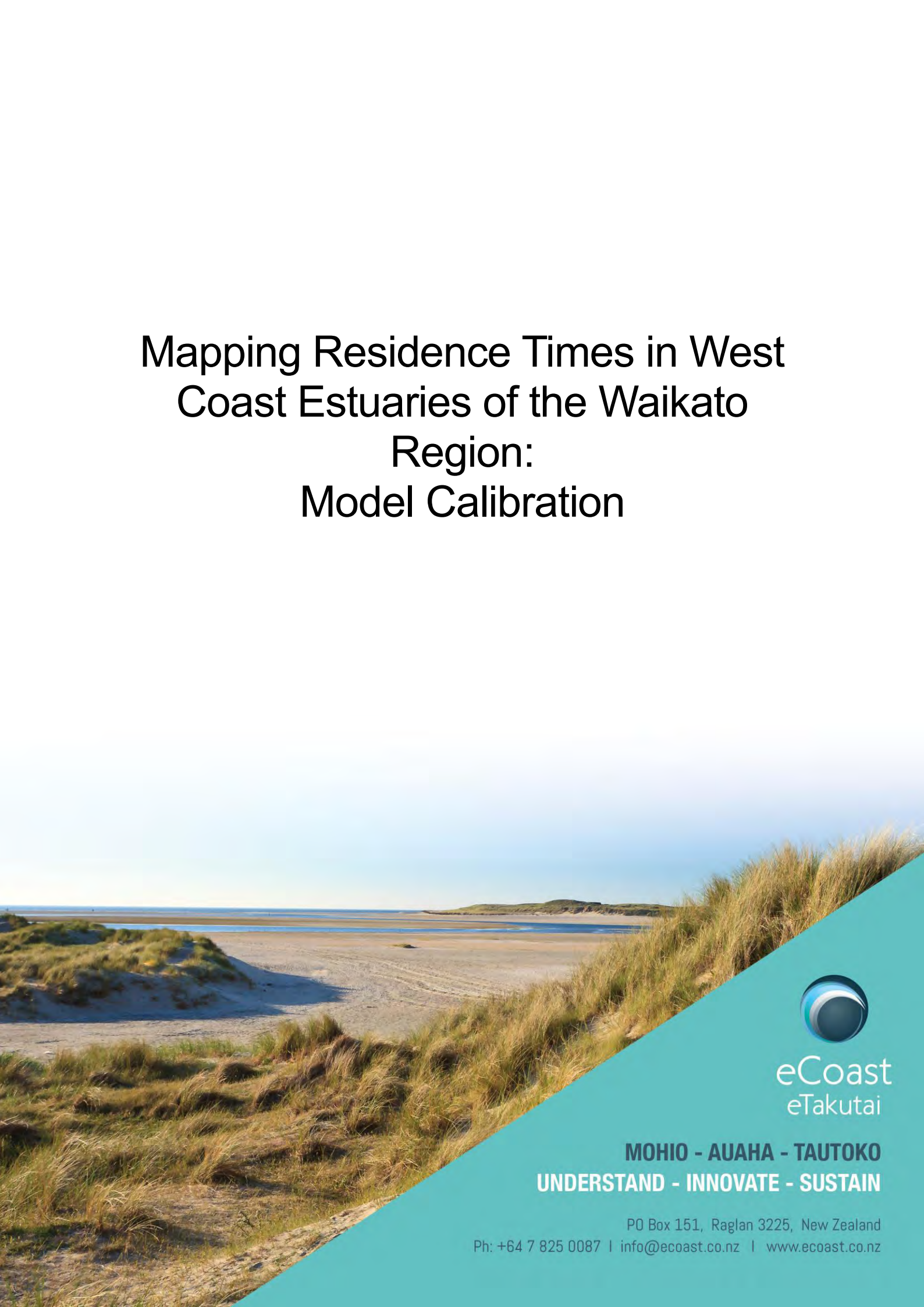

eCoast
eTakutai

MOHIO - AUAHA - TAUTOKO
UNDERSTAND - INNOVATE - SUSTAIN

PO Box 151, Raglan 3225, New Zealand
Ph: +64 7 825 0087 | info@ecoast.co.nz | www.ecoast.co.nz

Mapping Residence Times in West Coast Estuaries of the Waikato Region: Model Calibration

Report Status

Version	Date	Status	Approved by
V1	9/05/2016	Draft	STM
V2	6/05/2016	Draft	SDG
V3	25/05/2016	Final	EA

It is the responsibility of the reader to verify the version number of this report.

Authors

Dougal Greer, *MSc*

Ed Atkin, *HND, MSc (Hons)*

Shaw Mead *BSc, MSc (Hons), PhD*

Tim Haggitt *BSc, MSc (Hons), PhD*

Sam O'Neill *BSc, MSc (Hons)*

Contents

Figures

Tables

1 Introduction

This report describes the development and partial calibration of hydrodynamic models of 7 estuaries on the west coast of New Zealand's Waikatio (Figure 1.1). The models simulated the spatial and temporal variability in salinity throughout the model domains and have been used as the basis for calculating residence times in each estuary. The report also describes the development of associated catchment modelling which was used to provide riverine inputs into the hydrodynamic models.

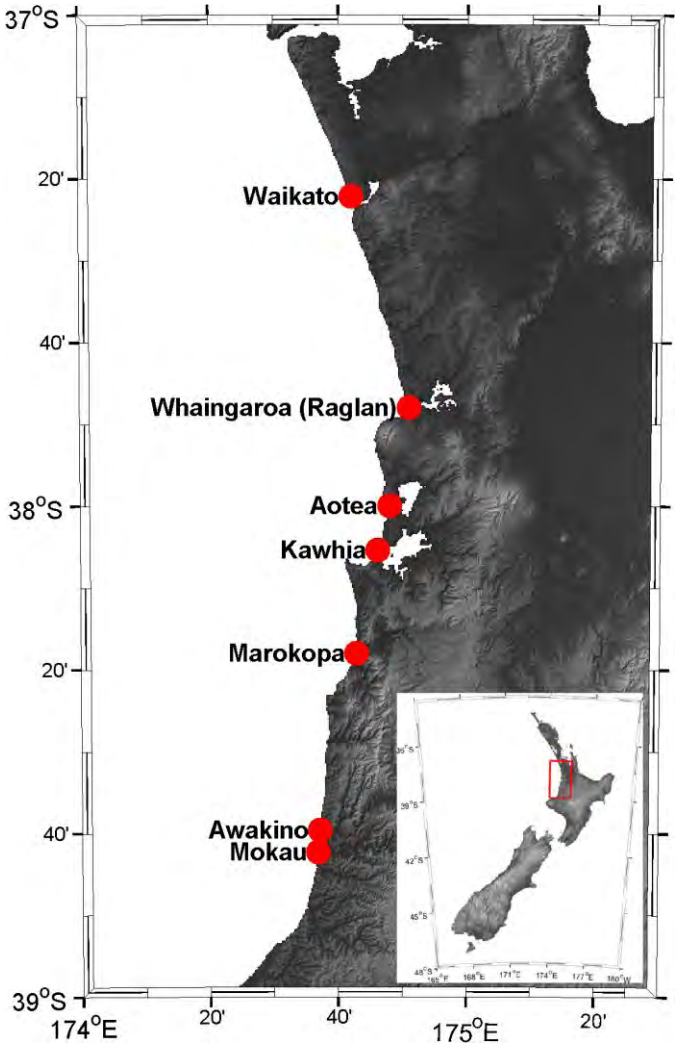

Figure 1.1: Locations of the seven estuaries modelled in this study (image: Courtesy NASA/JPL-Caltech).

2 Accuracy Measurement

Comparisons between modelled and measured data are presented throughout this report and they are compared as time series of modelled output compared with time series of measured data. These provide a valuable qualitative overview of model performance which can be used to assess the ability of the model to simulate physical processes in broad terms.

A range of quantitative methods have also been applied to assess the performance of the hydrodynamic models. Skill Scores, described by Van Rijn *et al*. (2003) and Sutherland *et al*. (2004), have been used to assess model performance. Skill scores are required to be:

- easy to understand;
- agree with expert opinion;
- "honest" (e.g. cannot be biased by changing model domain sizes or arbitrary aspects of the models), and;
- transferable between datasets and take intuitive values that show skill rather than accuracy.

Sutherland *et al*. (2004) conclude that the most effective skill score measure is the Briar Skill Score (BSS) when compared with the Root Mean Skill Score (RMSS) and the Mean Absolute Skill Score (MASS). It gives higher values for positive skill scores and lower values for negative skill scores. The error derived from the BSS can easily be decomposed into phase (α), amplitude (β), and bias (γ) which is a major advantage over other skill scores. The BSS and its decomposed components can be interpreted as follows:

- BSS: A measure of model skill. Perfect modelling gives a BSS of 1.
- α: A measure of phase error – perfect modelling gives α = 1.
- β: A measure of amplitude error – Perfect modelling of phase and amplitude gives β= 0.
- γ: A measure of bias. Perfect modelling gives γ= 0.

This BSS has been used to assess the modelled sea level, current speeds and salinity and is defined as follows:

$$BSS = 1 - \frac{\langle (Y-X)^2 \rangle}{\langle (B-X)^2 \rangle} \quad (1)$$

Where Y and X are time series of predictions and observations and B is a baseline value chosen to represent a skill-less model. A full description of how to decompose this into its constituent parts can be found in Sutherland *et al*. (2004). The γ term is not applicable for the

sea level calibrations when they are not referenced to a known vertical datum, for example sea level data recorded by the Nortek Aquadopp current meters, but it can be used for vertically referenced tide gauges. For tide gauges MLOS (as defined in Section 4.2) was used as a vertical reference datum. For salinity calibrations a baseline value of 35 psu was used, sea level calibrations used the mean of the measured sea level record and current speed calibrations used 0 m s^{-1}.

Linear regression was also used to compare measured and modelled signals. The r^2 from this analysis has been used to describe the amount of variance in the measured signal which was accounted for by the model.

Ultimately however, model performance needs to be related back to accuracy in real units to be considered acceptable, and so Root Mean Squared Error (RMSE) is also presented for each calibration.

For comparison with modelled currents, measured currents at fixed depths were converted to depth averaged values assuming a logarithmic vertical velocity profile Soulsby (1997).

Where possible modelled salinity was compared with measured salinity at the top and bottom of the water column. There is usually some difference between the two with the salt wedge intruding from the open ocean being more pronounced at the bed than at the surface. Since these are 2D models, it is not possible for it to accurately replicate vertical variability in salinity recorded in the measured data set. Instead the top and bottom salinity measurements can be usefully viewed as upper and lower bounds for modelled salinity.

3 Catchment Modelling of River Inflows

A different approach was used modelling riverine input flow for the tide dominated estuaries (i.e. the drowned river valley-type estuaries - Whaingaroa, Kawhia and Aotea Harbours) than for the river dominated estuaries (i.e. the tidal river-type estuaries - Waikato, Marokopa, Awakino and Mokau River estuaries). For the drowned river valley estuaries, river flow was calculated using the INCA catchment model (Whitehead *et al*. 1998a and Whitehead *et al*. 1998b) which provided daily river flow estimates. For each estuary, sub-catchments were incrementally added to the INCA model in order of size, starting with the largest, until at least 95% of the estuary catchment area was accounted for in the catchment model. Where it was practical to do so WRC river flow gauge data were used to calibrate the catchment model. The locations of these gauges are shown in Figure 3.1. Model performance was assessed using skill scores and other metrics which are discussed more fully in Section 2.

For the remaining estuaries, data from river flow gauges, provided by WRC, were used to estimate multiple year river flow rates for use in model boundary conditions.

Figure 3.1. River flow gauges used in this study.

3.1 INCA Catchment Model

The INCA-N module is specifically designed to model nitrogen fluxes within catchments (Whitehead *et al*. 1998a and Whitehead *et al*. 1998b), but it was only used to model river discharge for this project which it produced as daily average flow. All of the nitrogen-related parameters were removed from the model. To calculate river discharge, INCA required boundary conditions in the form of time series of daily actual precipitation, Soil Moisture Deficit (SMD), temperature and Hydrological Effective Rainfall (HER), as well as a range of other parameters specific to each catchment. Measured quantities were sourced from Waikato Regional Council and NIWA's Cliflo service[1]. Actual precipitation and SMD values were taken from local climate stations (Figure 3.2). Temperature has no effect on river flow within INCA so an arbitrary constant temperature of 20°C was used in the model. A HER time-series was created using the equation:

$$\text{HER} = \text{actual precipitation} - \text{evaporation} - \text{SMD}$$

Evaporation values used for the HER calculation were also taken from local climate stations (Figure 3.3). Climate stations used for the catchment model were chosen based on their proximity to the sub-catchment being modelled. The choice of station also took into account its surrounding terrain. For example, a station located in a mountainous area would not have been used for simulating flow on a largely flat sub-catchment.

[1] http://cliflo.niwa.co.nz/

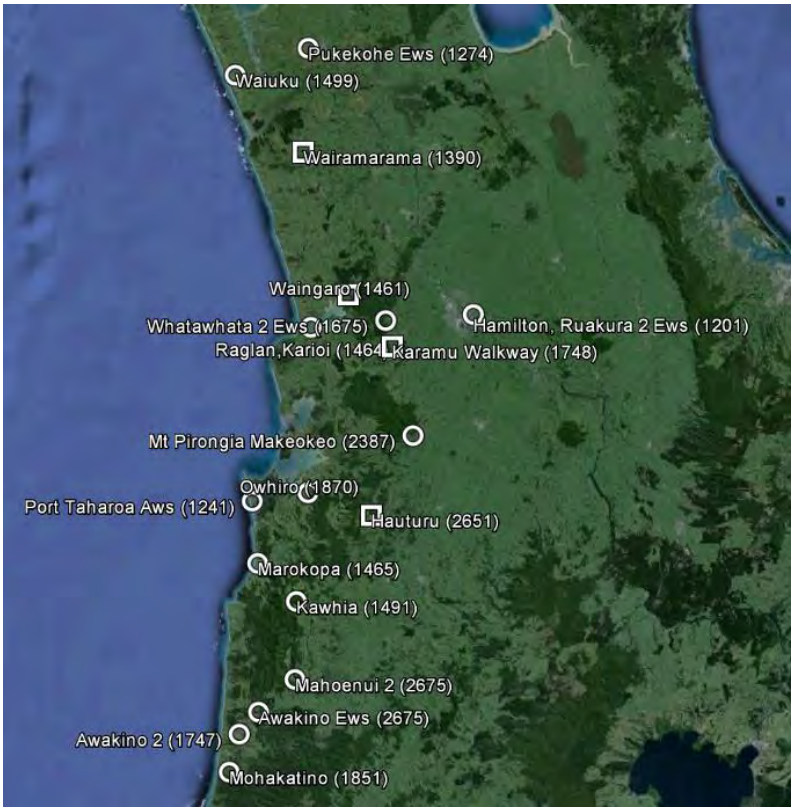

Figure 3.2. Locations of 18 West Coast climate stations with available rainfall data, mean annual cumulative rainfall in mm between 2008 and 2013 for each station is given in brackets. Squares indicate WRC stations while circles indicate CliFlo stations. Note that all CliFlo stations have available SMD data in addition to rainfall data.

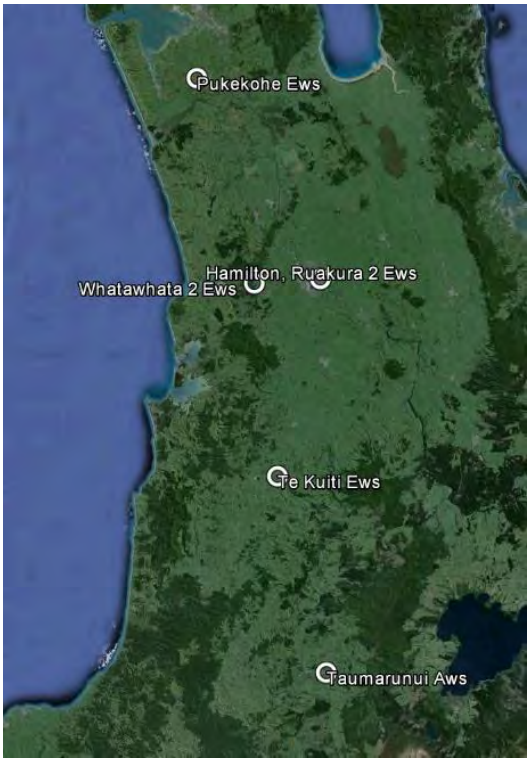

Figure 3.3. Locations of 5 West Coast climate stations with available evaporation data. All of these stations can be accessed through the CliFlo database.

3.2 Waikato River Estuary

The Waikato River estuary is fed by a large catchment which covers approximately 14,500 km^2 to the east and south of the estuary[2], shown in Figure 3.4. The majority of the catchment is upstream of the Mercer flow gauge (Figure 3.1) and therefore much of the flow is measured by this instrument, which provides a flow record from January 2000 until present. Consequently, the Mercer flow gauge data were used to create the flow boundary for the Waikato River in the Waikato River estuary model. Flow data were also available from the Whakapipi Stream and Mangatawhiri River, these gauges record much smaller flows than those recorded at Mercer (Jones and Hamilton, 2015). Nevertheless, flow from the Whakapipi gauge was added to the flow from the Mercer gauge to create the flow boundary conditions for use in the hydrodynamic model. The flow boundary time series is shown in Figure 3.5 and includes detailed plots of the time series for the calibration periods which are discussed further in Section 5. At this location the flow is affected by the tidal intrusion into the estuary and this can be seen in the detailed plots of the river flow boundary condition. However, the Mercer gauge is located approx. 30 km upstream from the upstream model boundary, and the tidal effects on flow may be underestimated by this flow boundary condition.

[2] Source: shape files provided by WRC

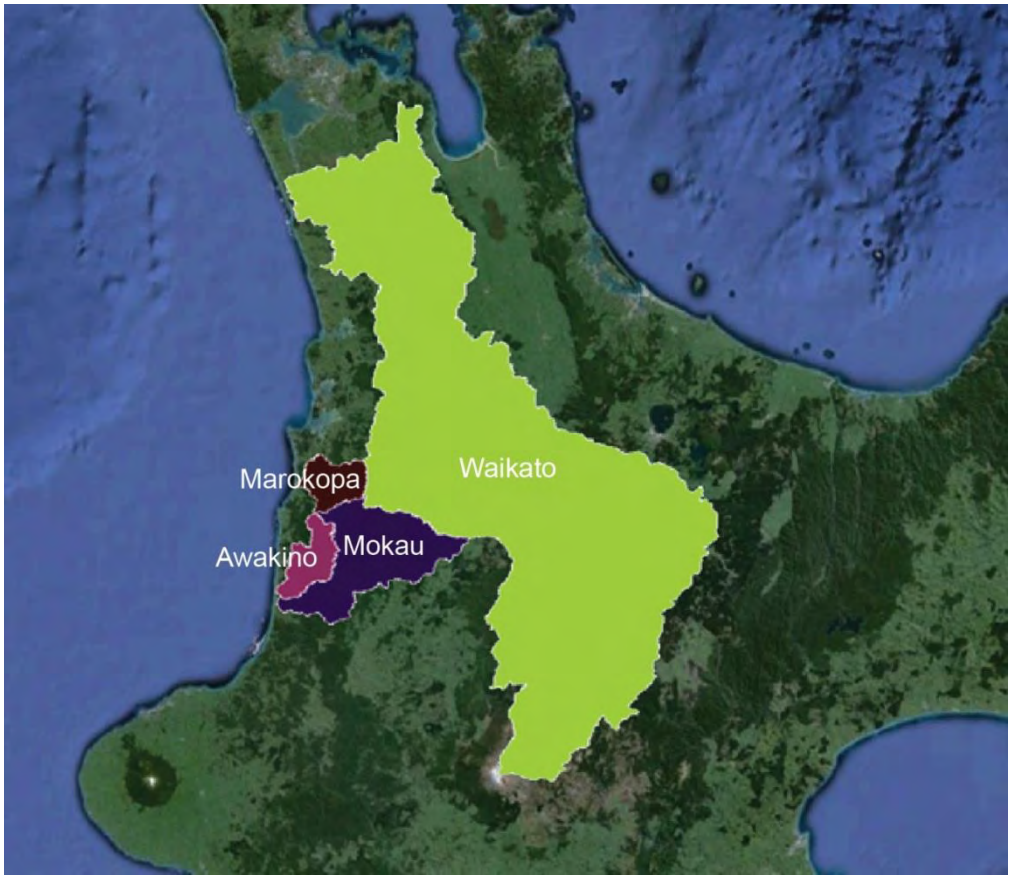

Figure 3.4. Catchments of tidal river estuaries on the Waikato west coast included in this study (source: WRC).

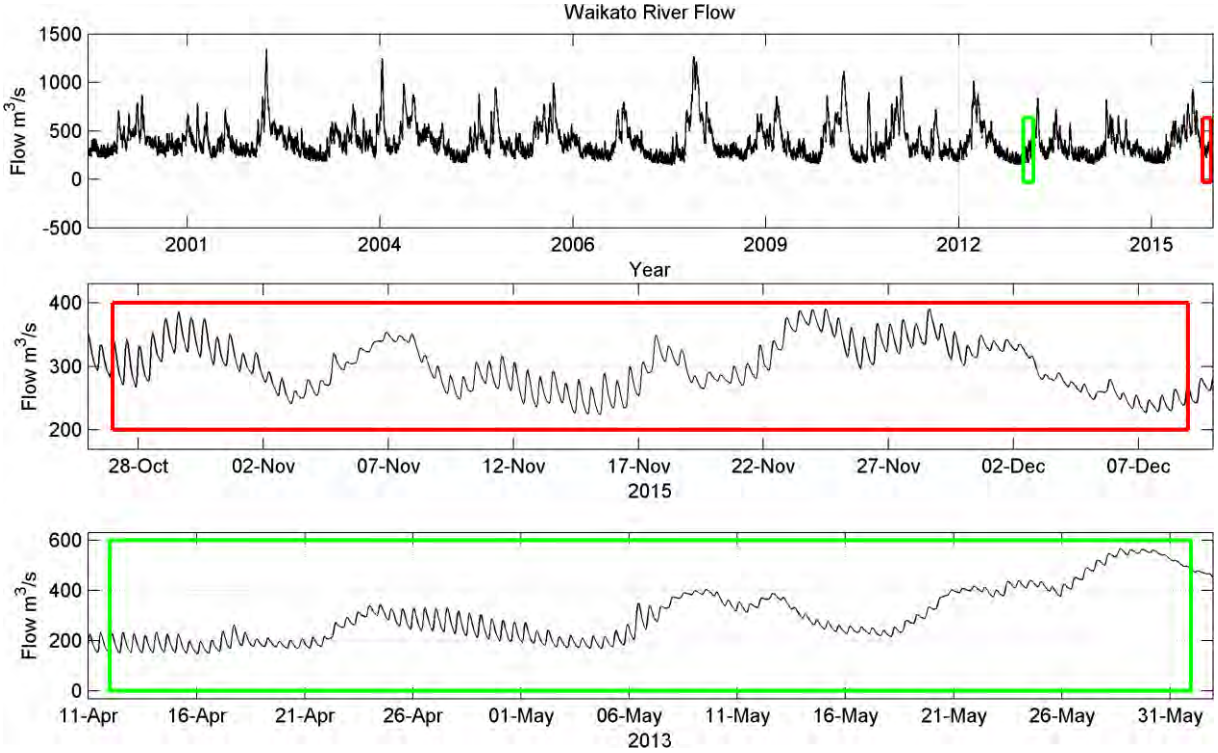

Figure 3.5. Half hourly river flow generated for the Waikato river from 2000 until 2015 (upper panel). The region bounded by the red box outlines the first calibration period and the box in green shows the second calibration period.

3.3 Whaingaroa (Raglan) Harbour

The flow of 15 streams and rivers feeding into Whaingaroa Harbour were modelled based on their individual catchment sizes and land use percentages, as provided by WRC (Figure 3.6 and Table 3.1). The combined area of these catchments accounts for 95.1% of the total Whaingaroa Harbour catchment area.

There are two flow gauges within the Whaingaroa Harbour catchment, on the Waingaro and Waitetuna Rivers operated by WRC. The catchment area upstream of the Waingaro flow gauge accounts for 96.4% of the total Waingaro sub-catchment area, while the sub-catchment area upstream of the Waitetuna flow gauge only accounts for 51.6% of total Waitetuna sub-catchment area[3]. The catchment model was calibrated using both of these gauges.

Recorded precipitation data for Waingaro were sourced from the Waingaro Automatic Weather Station (AWS) (see Figure 3.2 for locations). SMD data were sourced from the Whatawhata 2 Electronic Weather Station (EWS), with gaps in the data infilled with Raglan Karioi AWS SMD data. Evaporation data were sourced from the Whatawhata 2 EWS infilled using data from Hamilton, Ruakura 2 EWS (see Figure 3.3 for locations). The INCA model was used to generate output time-series from 01 January 2005 to 14 December 2014.

A comparison of the INCA output with measured flow data from the Waingaro flow gauge showed that the catchment model constantly overestimated Waingaro cumulative water load by approximately 20%, so a multiplier of 0.9 was applied to the HER to account for this. Model parameters were adjusted within INCA until a satisfactory calibration had been reached (Figure 3.7). Model performance statistics for this calibration are shown in Table 3.2. The INCA model performed reasonably well with a BSS of 0.72 and an RMSE of 2.66. The final cumulative load calibration gave an overestimation of 3.7% (Figure 3.8).

The input file used to model the Waitetuna catchment flow used actual precipitation from Karamu Walkway, SMD from Mt Pirongia Makeokeo supplemented with Whatawhata 2 EWS data and evaporation data from Whatawhata 2 EWS supplemented with data from the Hamilton, Ruakura 2 EWS.

Parameters were adjusted within INCA until an optimal calibration was reached (Figure 3.9). Performance metrics presented in Table 3.2 show that the INCA prediction of Waitetuna flow was not as accurate as for Waingaro (BSS = 0.43 and RMSE = 3.72). However, the final cumulative load calibration gave an underestimation of only 0.5%. All of the northern catchments (u682, Te Tarata, u712, u646, Kerikeri, Waingaro and Ohautira) were modelled using INCA with the Waingaro parameterisation while all southern catchments (Waitetuna,

[3] Source: WRC

u598, Okete, Bridal, u607, Opotoru, Omahina and Wainui) were modelled using INCA with the Waitetuna parameterisation. For modelling purposes, Waingaroa and Waitetuna were replaced with scaled measured hourly flow in the catchment model. The Waitetuna flow gauge accounts for 51% of the Waitetuna River catchment so a multiplier of 100/51 was applied to the flow data to account for the catchment area downstream from the flow gauge. The Waingaro flow gauge accounts for 96.4% of the Waingaro River catchment area so a multiplier of 100/96.4 was applied to the flow data in this instance.

Figure 3.6. The 15 largest Whaingaroa Harbour sub-catchments as used in this study (Source: WRC).

Table 3.1: Sub-catchments of the Whaingaroa catchment included in the catchment model (Source: WRC).

Catchment	Catchment Area (km^2)	% of Catchment Area	ID	% Farm	% Forest	% Urban	% Other
Waitetuna	167	35.0	768	48	42	0	10
Waingaro	123	25.8	766	54	37	0	9
Ohautira	50	10.5	755	36	50	0	14
Okete	41	8.6	749	68	18	0	14
Opotoru	36	7.5	748	74	13	0	13
Kerikeri	19	4.0	735	68	27	0	5
Wainui	13	2.7	724	53	30	1	16
Unknown Catchment	9	1.9	712	96	1	0	3
Unknown Catchment	6	1.3	682	94	5	0	1
Bridal	5	1.0	674	60	1	0	39
Unknown Catchment	2	0.4	646	90	1	0	9
Te Tarata	2	0.4	599	93	3	0	4
Unknown Catchment	1.6	0.3	598	75	1	0	24
Unknown Catchment	1.5	0.3	607	91	2	0	7
Omahina	1	0.2	591	67	12	0	21

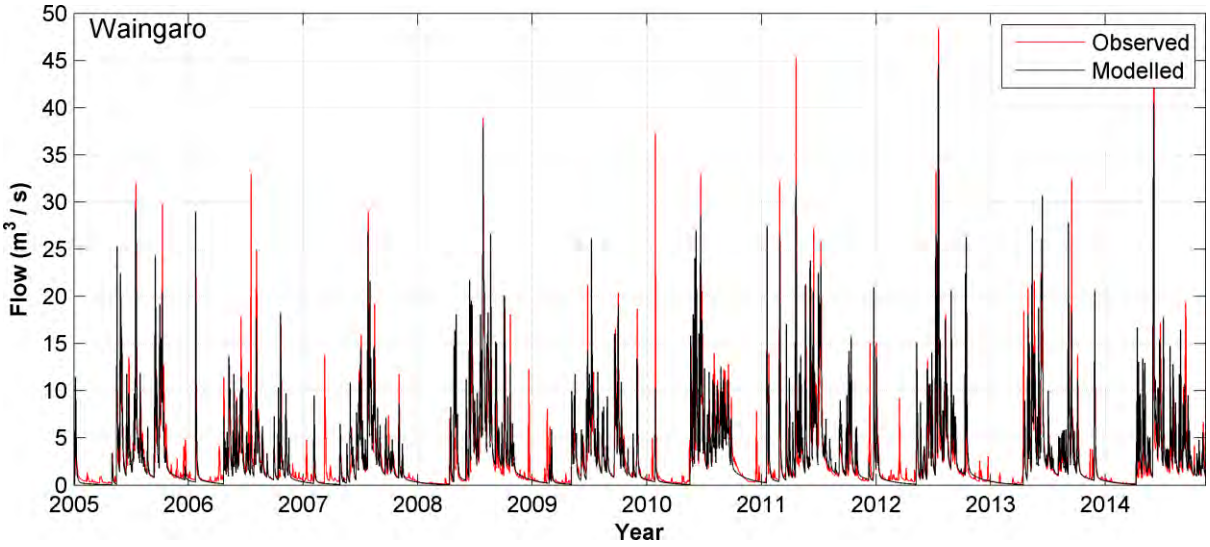

Figure 3.7. Waingaro River calibration: observed Waingaro flow against Waingaro flow from the INCA catchment model between 2005 and 2014.

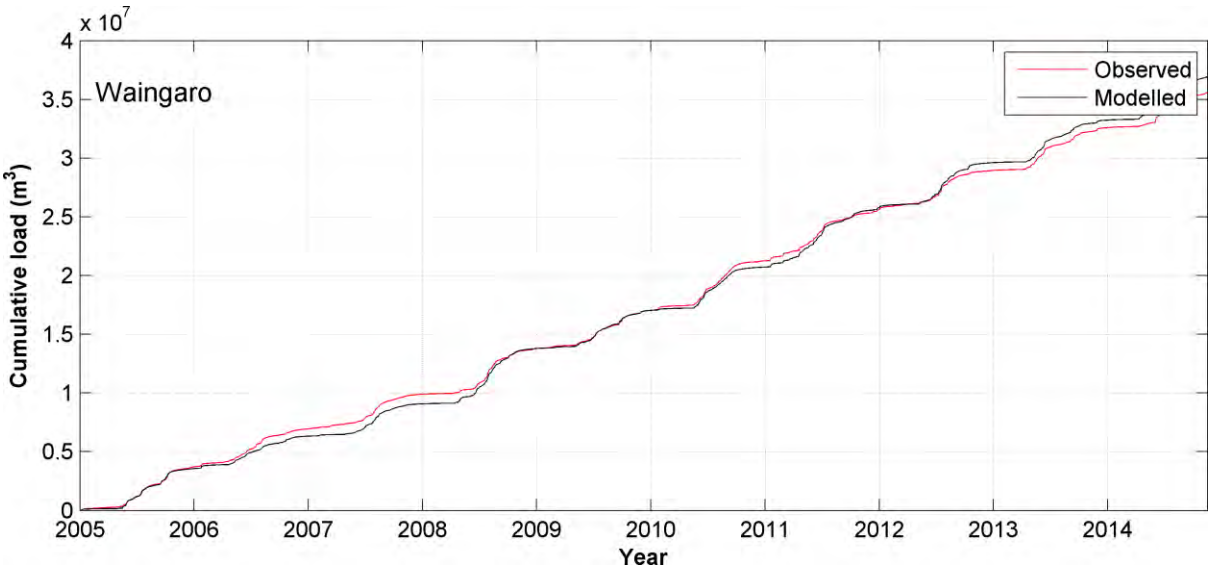

Figure 3.8. Observed Waingaro cumulative freshwater load against Waingaro cumulative water load from the INCA catchment model between 2005 and 2014. By the end of the model the cumulative load was overestimated by 3.7%.

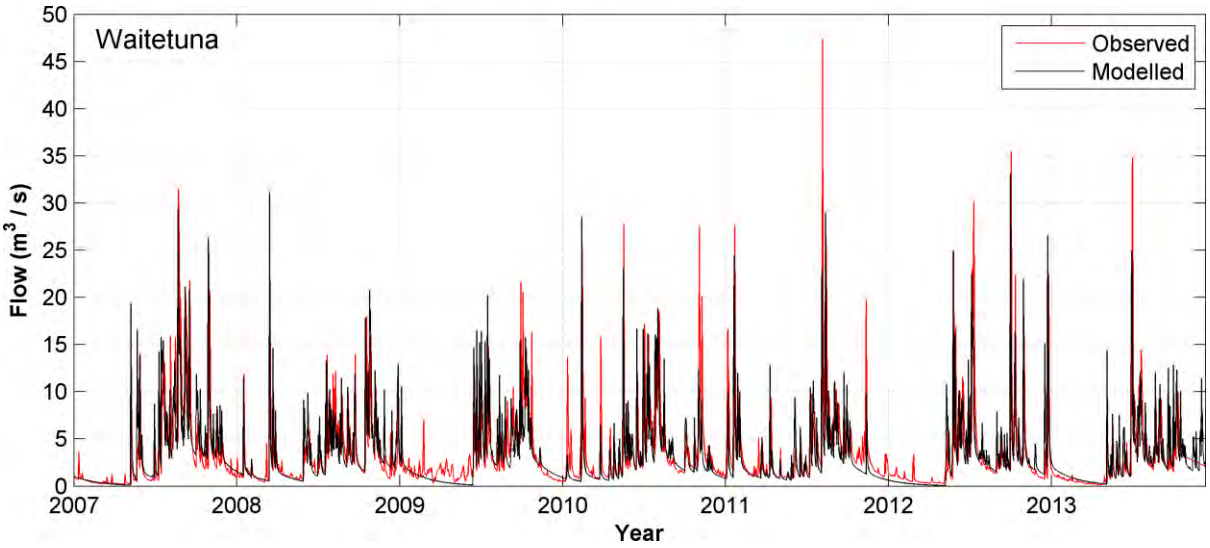

Figure 3.9. Waitetuna River calibration: observed Waitetuna flow against Waitetuna flow from the INCA catchment model between 2007 and 2013.

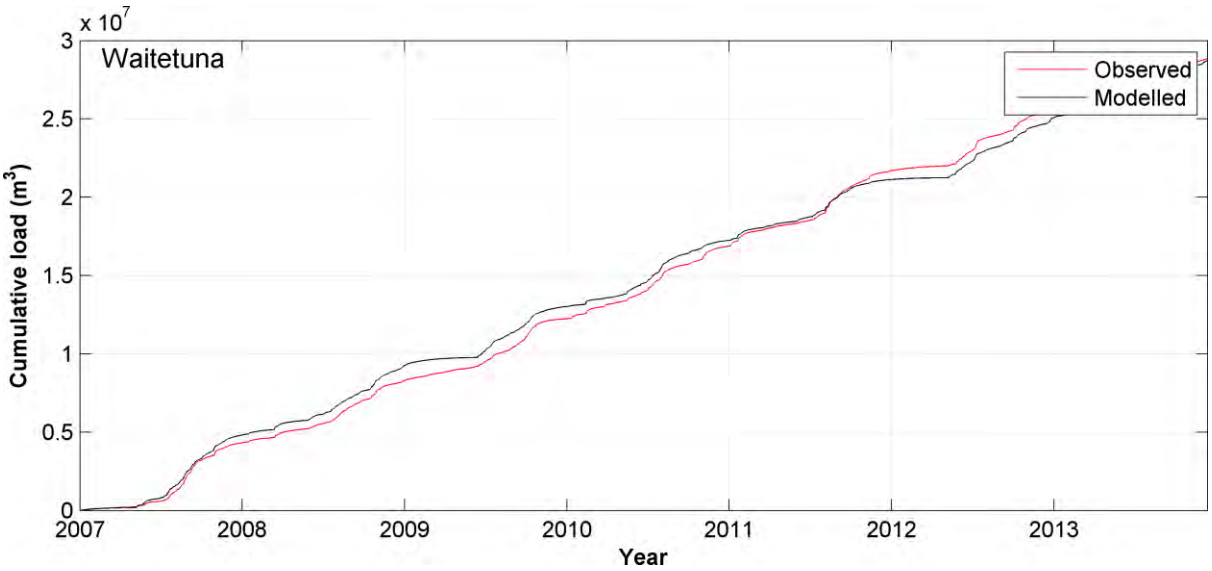

Figure 3.10. Observed Waitetuna cumulative freshwater load against Waitetuna cumulative water load from the INCA catchment model between 2007 and 2013. By the end of the model the cumulative load was underestimated by 0.5%.

Table 3.2: Skill scores for the INCA calibrations for Whaingaroa Harbour.

Variable	Briar Skill Score (BSS)	α	β	γ	R^2	RMSE
Waingaro Flow	0.72	0.65	0.05	0.00	0.65	2.66 $m^3 s^{-1}$
Waitetuna Flow	0.43	0.27	0.21	00	0.27	3.72$m^3 s^{-1}$

3.4 Aotea Harbour

The flow of 25 streams and rivers feeding into Aotea Harbour were modelled, accounting for 95.4% of the total Aotea Harbour catchment area (Figure 3.11 and Table 3.3). The Aotea catchment is characterised by four large sub-catchments accounting for 80% of the total catchment area and many smaller sub-catchments. There were no flow gauges available for any of the Aotea Harbour rivers, so modelled flow could not be calibrated. Instead it was assumed that Aotea catchments would have similar properties to Kawhia catchments due to their proximity, so the parameters and input files used for the calibration of the Kawhia catchment model (Section 3.5) were used for the Aotea rivers.

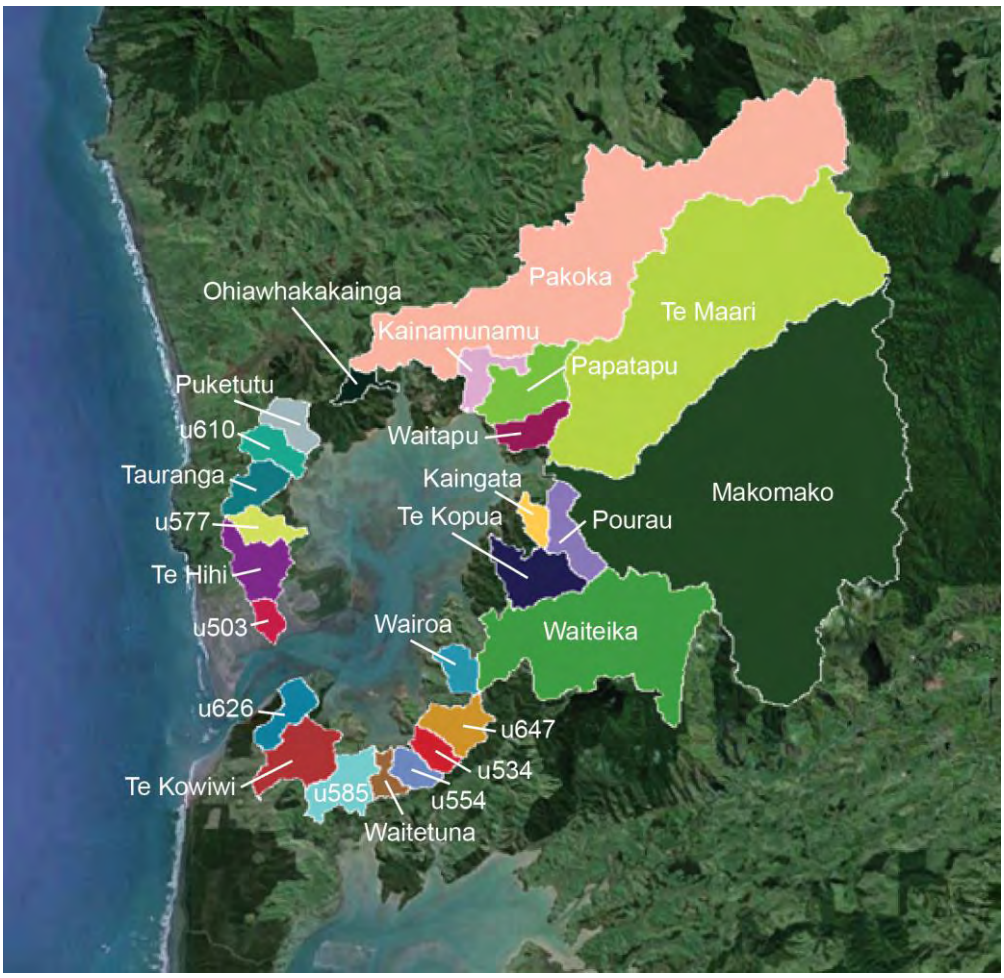

Figure 3.11. The 25 largest catchments of the Aotea Harbour to be modelled in this study (Source: WRC).

Table 3.3: Sub-catchments of the Aotea catchment included in the catchment model (Source: WRC).

Catchment	Catchment Area (km^2)	% of Catchment Area	ID	% Farm	% Forest	% Urban	% Other
Makomako	50	32.5	753	45.6	49.85	0	4.55
Te Maari	30	19.5	744	54.03	30.29	0	15.68
Pakoka	29	18.8	743	40.18	26.67	0	33.15
Waiteika	14	9.1	726	65.73	33.46	0	0.81
Papatapu	3	1.9	777	53	41.2	0	5.8
Te Kowiwi	3	1.9	671	63.91	21.5	0	14.59
Te Kopua	3	1.9	658	24.6	15.44	0	59.96
Te Hihi	2	1.3	615	13.26	0	0	86.74
Unknown Catchment	2	1.3	585	76.61	9.21	0	14.18
Pourau	2	1.3	624	31.78	13.46	0	54.76
Unknown Catchment	2	1.3	647	93.94	4.54	0	1.52
Tauranga	1	0.6	592	16.47	11.9	0	71.63
Kainamunamu	1	0.6	643	92.79	4.24	0	2.97
Waitapu	1	0.6	642	61.73	33.91	0	4.36
Unknown Catchment	1	0.6	626	0	64.44	6.72	28.84
Unknown Catchment	1	0.6	610	16.13	0	0	83.87
Puketutu	1	0.6	596	14.97	4.48	0	80.55
Unknown Catchment	1	0.6	577	18.46	0	0	81.54
Wairoa	1	0.6	567	95.94	1.82	0	2.24
Unknown Catchment	1	0.6	554	98.61	1.05	0	0.34
Unknown Catchment	1	0.6	534	93	2.87	0	4.13
Waitetuna	1	0.6	522	92.7	0.87	0	6.43
Kaingata	1	0.6	515	73.27	21.09	0	5.64
Ohiawhakakainga	1	0.6	509	81.48	5.81	0	12.71
Unknown Catchment	1	0.6	503	0	0	0	100

3.5 Kawhia Harbour

The flow from 21 streams and rivers feeding into Kawhia Harbour were modelled, accounting for 95.2% of the total Kawhia Harbour catchment area (Figure 3.12 and Table 3.4). There are two flow gauges within the Kawhia Harbour catchment on the Awaroa and Oparau Rivers maintained by WRC. The sub-catchment upstream of the Awaroa flow gauge accounts for

64.4% of the total Awaroa sub-catchment area[4]. The sub-catchment upstream of the Oparau flow gauge accounts for 48.9% of total Oparau sub-catchment area. The catchment model was calibrated and validated using these gauges.

Actual precipitation data for Awaroa were sourced from Owhiro, with gaps in the data infilled with Port Taharoa AWS and Hauturu (see Figure 3.2 for locations). SMD was sourced from Owhiro, infilled with Port Taharoa AWS and Mt Pirongia Makeokeo. Evaporation data were sourced from Whatawhata 2 EWS infilled with Te Kuiti EWS (see Figure 3.3 for locations).

The model parameters were adjusted within INCA until a satisfactory calibration had been reached with Awaroa River flow (Figure 3.13). Model performance statistics for this calibration are shown in Table 3.5. The INCA model performed reasonably well with a BSS of 0.73 and an RMSE of 2.76. The final cumulative load calibration gave an underestimation of 0.7% (Figure 3.14). The same parameterisation was then applied to the Oparau River as validation. Figure 3.15 shows that the Awaroa parameterisation accurately represents the Oparau River catchment, confirmed by the small Oparau River cumulative load overestimation of 0.9% (Figure 3.16) and a BSS of 0.73 and RMSE of 2.28 (Table 3.5). This validation gives confidence that these parameters can be applied to the remaining Kawhia catchments.

The Oparau flow gauge accounts for 48.9% of the Oparau River catchment so a multiplier of 100/48.9 was applied to the flow data to account for catchment area downstream from the flow gauge. The Awaroa flow gauge accounts for 64.4% of the Awaroa River catchment area so a multiplier of 100/64.4 was applied to the flow data in this instance.

The Kawhia Harbour model parameters were also used in the Aotea Harbour catchment model (see Section 3.4), due to their close proximity and the lack of recorded flow data in the rivers flowing into Aotea Harbour.

[4] Source: WRC

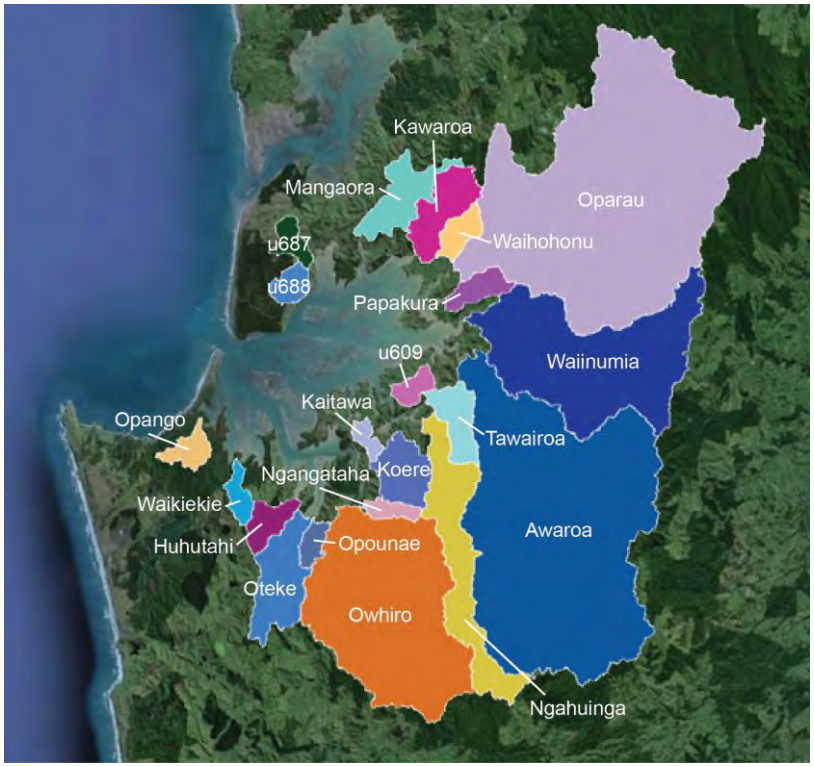

Figure 3.12. Kawhia Harbour's 21 largest sub-catchments modelled in this study (Source: WRC).

Table 3.4: Sub-catchments of the Kawhia catchment included in the catchment model (Source: WRC).

Catchment	Catchment Area (km^2)	% of Catchment Area	ID	% Farm	% Forest	% Urban	% Other
Oparau	120	28.0	765	60.94	36.41	0.07	2.58
Awaroa	109	25.4	764	37.97	53.15	0	8.88
Ngangataha	58	13.5	757	31.43	64.73	0	3.84
Waiinumia	50	11.7	754	55.85	39.59	0	4.56
Ngahuinga	21	4.9	736	30.71	50.74	0	18.55
Oteke	12	2.8	720	88.87	6.56	0	4.57
Kawaroa	8	1.9	701	30.71	68.26	0	1.03
Mangaora	8	1.9	700	48.01	44.08	0	7.91
Koere	7	1.6	693	55.58	25.99	0	18.43
Tawairoa	6	1.4	684	60.95	25.11	0	13.94
Huhutahi	4	0.9	663	73.56	20.82	0	5.62
Papakura	4	0.9	659	90.72	7.29	0	1.99
Waihohonu	3	0.7	781	68.91	28.37	0	2.72
Opango	3	0.7	776	9.02	42.32	0	48.66
Unknown Catchment	3	0.7	688	44.97	23.44	16.79	14.8
Unknown Catchment	3	0.7	687	76.78	13.23	0.5	9.49
Waikiekie	2	0.5	632	36.92	30.4	0	32.68
Unknown Catchment	2	0.5	609	87.39	6.61	0	6
Opounae	2	0.5	652	66.7	25.72	0	7.58
Owhiro	2	0.5	651	45.24	51.19	0	3.57
Kaitawa	2	0.5	644	91.84	3.31	1.11	3.74

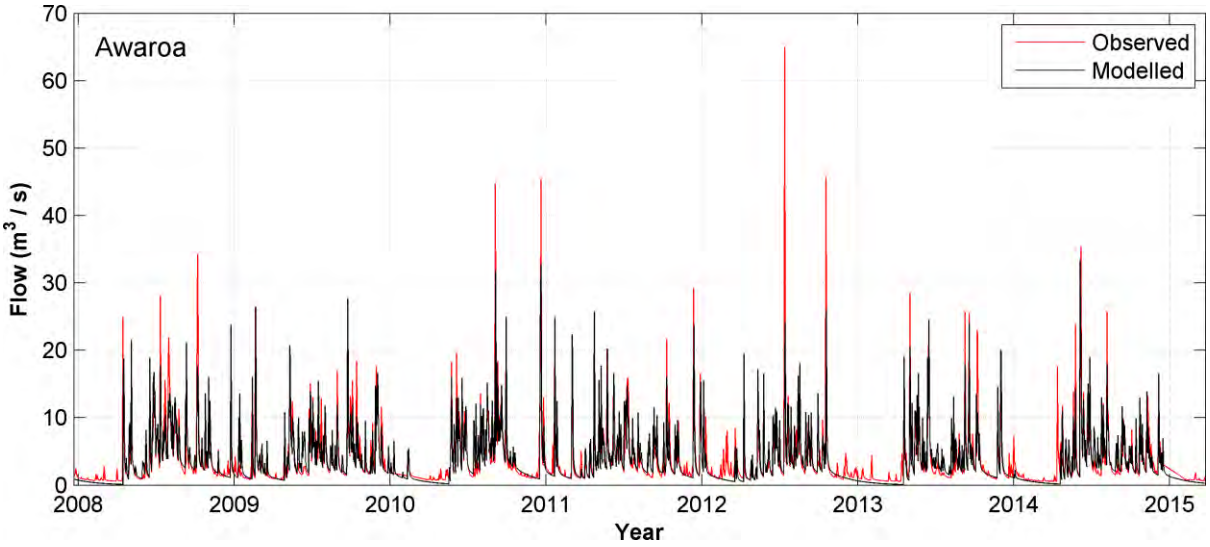

Figure 3.13. Awaroa River calibration: observed Awaroa flow against Awaroa flow from the INCA catchment model between 2008 and 2015.

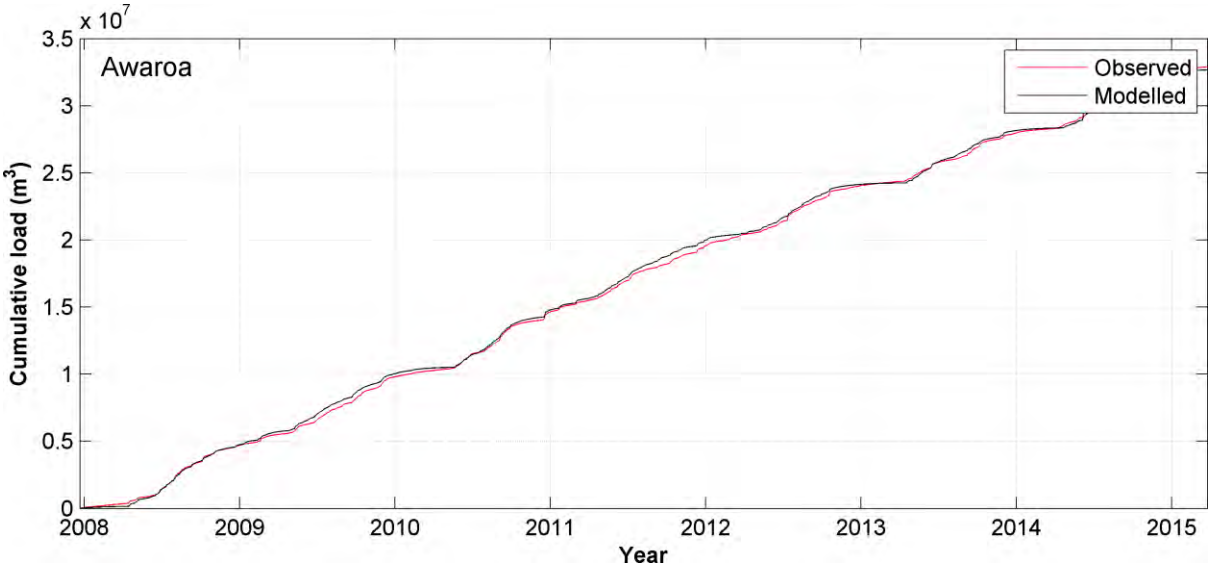

Figure 3.14. Observed Awaroa cumulative freshwater load against Awaroa cumulative water load from the INCA catchment model between 2008 and 2015. By the end of the model the cumulative load was underestimated by 0.7%.

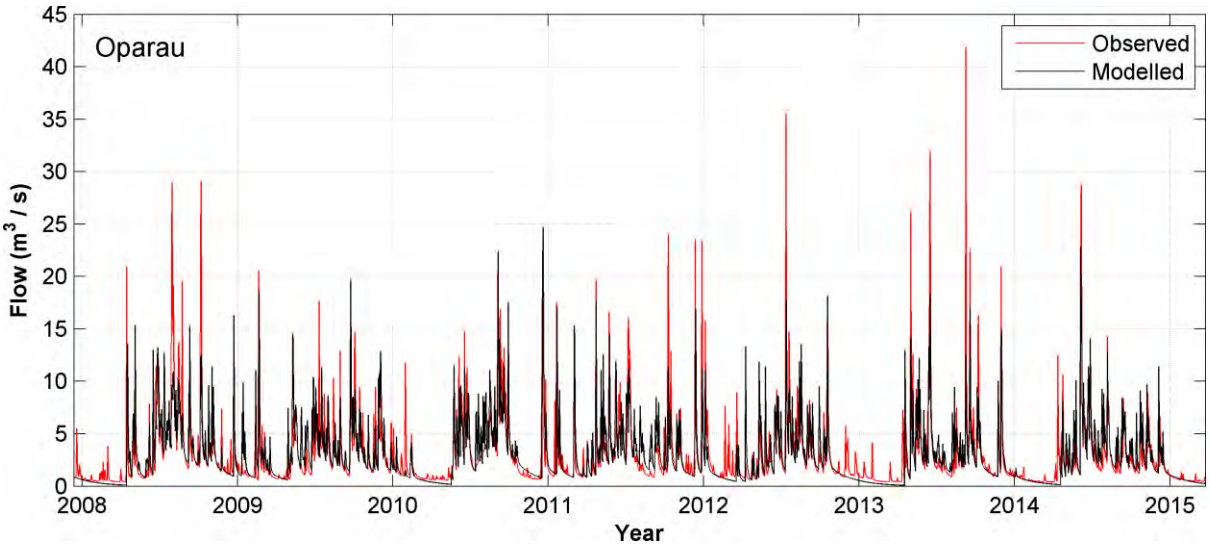

Figure 3.15. Oparau River calibration: observed Oparau flow against Oparau flow from the INCA catchment model between 2008 and 2015.

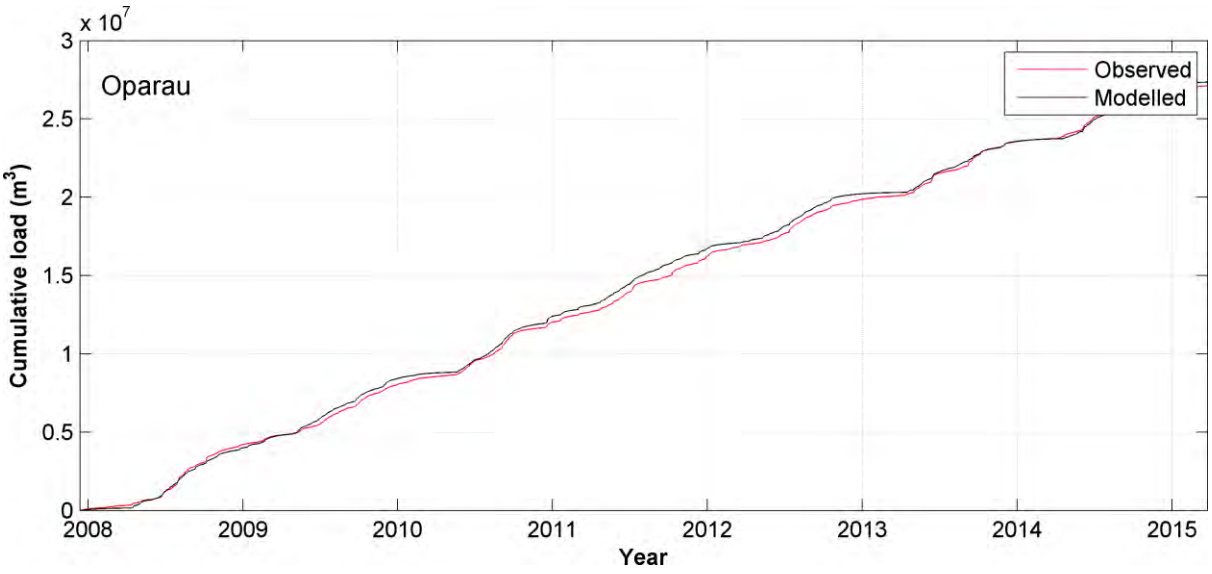

Figure 3.16. Observed Oparau cumulative freshwater load against cumulative water load from the INCA catchment model between 2008 and 2015. By the end of the model the cumulative load was overestimated by 0.9%.

Table 3.5: Skill scores for the INCA calibrations for Kawhia Harbour.

Variable	Briar Skill Score (BSS)	α	β	γ	R^2	RMSE
Awaroa Flow	0.73	0.58	0.04	0.00	0.58	2.76 $m^3 s^{-1}$
Oparau Flow	0.73	0.55	0.02	0.00	0.55	2.28 $m^3 s^{-1}$

3.6 Marokopa, Awakino and Mokau Rivers

River flow boundary conditions for Marokopa, Awakino and Mokau River estuaries were created using measured flow data from the Marokopa flow gauge (for Marokopa River) and the Awakino flow gauge for the Awakino and Mokau Rivers. Both the Awakino and Marokopa flow gauges contain flow records from 2006 until present. Since the gauges are located some distance upstream from the river mouths, they do not account for the total land derived flow. To account for this the gauged flow data were adjusted using measurements of catchment area upstream and downstream from the gauges[5] as well as using flow data near the river mouths derived from data recorded as part of the field work component of this project (Atkin *et al*., 2015).

In each estuary, the current meters deployed in the upper reaches of the estuaries recording current and sea level data for 6 weeks in each location. These data were combined with cross sectional areas from the river transects to calculate the flux of water at the deployment location. Flow was calculated with a temporal resolution of 15 minutes. Since the flow was recorded at a single height in the water column a scaling factor was applied to convert the flow at that location to a depth averaged flow. For each river a scaling factor of 1.4 was used corresponding to a point in the water column between 10 and 20% of the total depth (Hulsing *et al.*, 1966).

The method for calculating river flow for from the gauged flow differed between estuaries depending on the data available for each location. The methodology used for each estuary is described below.

The catchment of the Marokopa River has a total area of 36,440 km^2, but the Marokopa flow gauge is located some distance upstream from the river mouth such that only 26% (9,295 km^2) of the total catchment feeds into the river upstream from the gauge. Nonetheless the gauged data provides a valuable source of data describing the pattern of flow for the Marokopa River. These gauged data were adjusted using a scaling factor to account for the additional catchment area downstream from the flow gauge. For this estuary, the scaling factor of 2.15 was established by comparing the flow gauge data with flow rates derived from the current meter deployment using a linear regression (r^2 = 0.47).

The Awakino River catchment has a total area of 38,301 km^2 of which 54% (20,723 km^2) Since the Awakino River flow gauge is located much closer to the river mouth than the Marokopa gauge a different approach was taken for scaling the gauged flow. In this instance the flow

[5] Source: WRC.

was increased by 46% (100%-54%) to account for the catchment area downstream from the flow gauge.

There is no flow gauge in the Mokau River. The nearest available flow gauge is the Awakino flow gauge and this was used to generate flow boundary conditions for the Mokau River estuary model. Cumulative flows were calculated for the Mokau and Awakino Rivers for the 6-week field work period. And the ratio of the two were used to scale the Awakino River flow to estimate the flow for the Mokau River. The scaling factor found using this method to alter the Awakino river flow data was 2.43.

Time series comparisons between flow data calculated using the river gauge data and the deployed current meter data are shown for each of the three rivers in Figure 3.17.

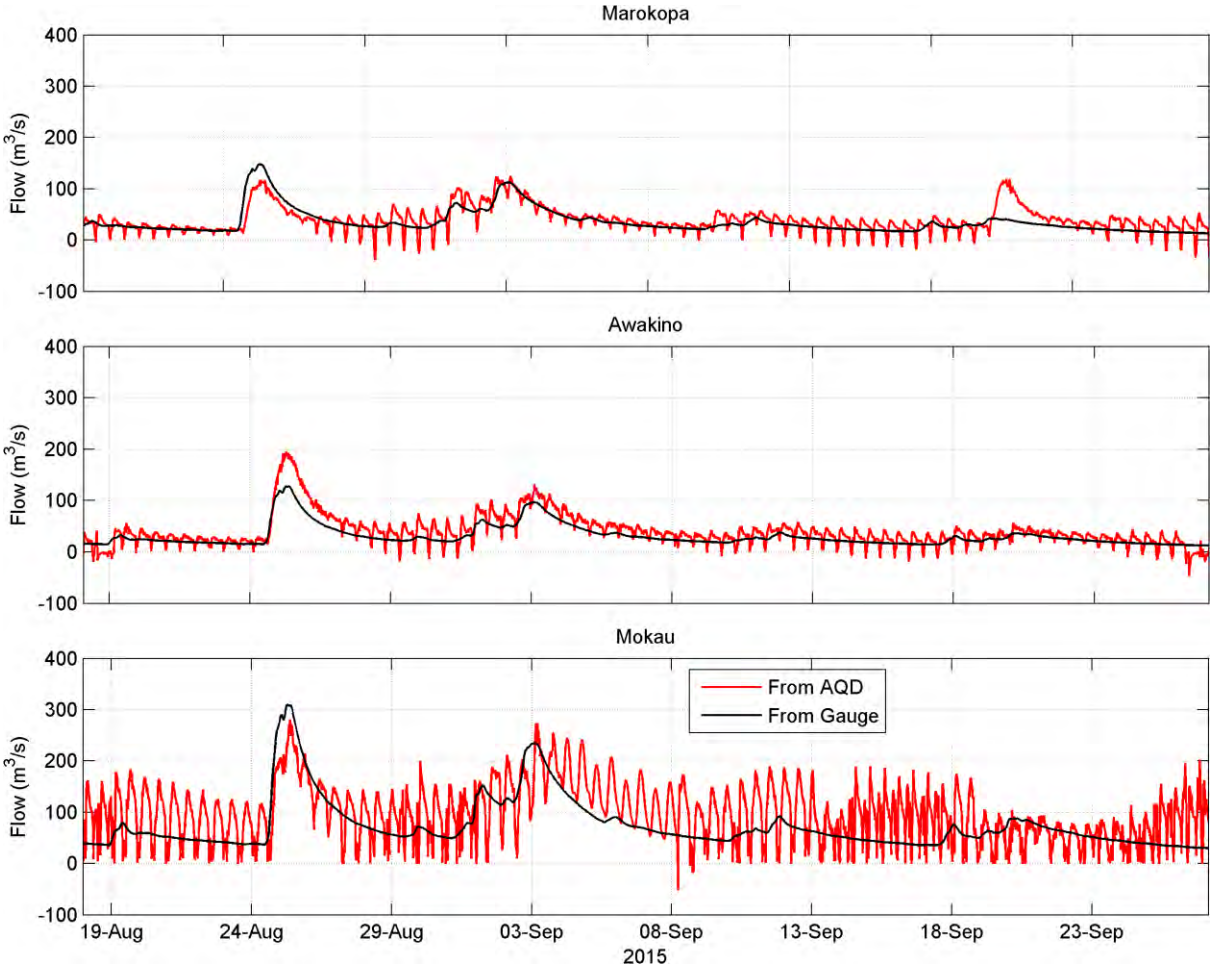

Figure 3.17: River flow for Marokopa River (upper panel), Awakino River (middle panel) and Mokau River (lower panel) estimated using data from the current meters (AQD) and the flow gauges.

4 Hydrodynamic Modelling Methodology

The hydrodynamic modelling used an open source hydrodynamic model called Delft3D-Flow. Details of the modelling package can be found in the Delft-Flow user manual (Deltares, 2013).

4.1 Modelling Method

The hydrodynamic models presented here are 2D and simulate sea level, currents and salinity (the models do not include temperature). The models were driven by tides, wind, atmospheric pressure and salinity boundaries. The development of these boundary conditions is described in the following sections. The modelling setup used a system of nested rectilinear model grids using a process known as Domain Decomposition (DD). Standard nesting procedures use a coarse model run over a large model domain, and nested boundary conditions are extracted from this to run higher resolution models covering a smaller area contained within the domain of the coarse grid. DD is a dynamically coupled nesting system whereby the coarser and finer grids are run simultaneously and information is passed between the domains. This means that trace substances can pass seamlessly between the two grids in a way that is not possible using standard nesting. Furthermore, information pertaining to other hydrodynamic processes is not lost between domains in the nesting process, as it is using standard nesting.

The system of bathymetric grids starts with a common large scale west coast grid which covered the Waikato west coast in its entirety. Within this, a series of nested grids were embedded which led to high-resolution local bathymetric grids of each of the 7 estuaries. These grids are referred to throughout the rest of the document as the local grids. The local grids were designed to be at a high enough resolution to represent features that could influence broad scale circulation patterns. Table 4.1 presents the system of nesting showing how the grids become increasingly fine with each nest. More details of the grids are given in Table 4.2. The generation of the bathymetry files for each of these grids is more fully described in Section 4.2.

The decision was made by WRC to use 2D models in order to create a fast and efficient system of hydrodynamic models for exploring measurements residence time. We recognise that this modelling methodology may be an oversimplification for simulating estuaries where stratification can be a significant feature, but this methodology is a proof of concept, and the models can be extended to 3D should this be required at later date.

Table 4.1: The system of nests used to create hydrodynamic models of each of the 7 estuaries with numbers referring to the increase in resolution between nests.

<table>
<tr><td colspan="7">West Coast
(1050 m)</td></tr>
<tr><td>↓7
North</td><td colspan="3">↓5
Central</td><td colspan="3">↓5
South</td></tr>
<tr><td>↓3
Waikato River Estuary</td><td>↓5
Whaingaroa (Raglan) Harbour</td><td>↓5
Aotea Harbour</td><td>↓5
Kawhia Harbour</td><td>↓7
Marokopa Intermediate</td><td>↓5
Awakino Intermediate</td><td>↓7
Mokau Intermediate</td></tr>
<tr><td colspan="4"></td><td>↓3
Marokopa River Estuary</td><td>↓3
Awakino River Estuary</td><td>↓3
Mokau River Estuary</td></tr>
</table>

Table 4.2: Fine scale estuary resolutions including timescales. The time step of the model run is common across all of the grids and is determined by the local nest so time steps are only given for the local nests.

Harbour	Cell size (m)	Time step (s)	Min Easting	Min Northing	Max Easting	Max Northing
West Coast	1050	N/A	1591377	5649926	1778277	5935526
North	150	N/A	1736277	5852576	1768827	5876726
Central	210	N/A	1732077	5766476	1778277	5829476
South	210	N/A	1723677	5703476	1758327	5774876
Marokopa Intermediate	30	N/A	1746567	5755556	1754337	5762486
Awakino Intermediate	30	N/A	1736487	5717546	1744047	5722586
Mokau Intermediate	42	N/A	1736487	5712086	1745517	5717126
Waikato River estuary	50	0.2	1744677	5859926	1765077	5874326
Whaingaroa Harbour	42	0.5	1758537	5810576	1774287	5824436
Aotea Harbour	42	0.4	1753707	5788946	1766937	5800076
Kawhia Harbour	42	0.5	1751817	5774246	1768617	5789156
Marokopa River estuary	10	0.1	1748967	5757926	1753347	5760776
Awakino River estuary	10	0.1	1740207	5718746	1743597	5721356
Mokau River estuary	14	0.1	1739385	5712926	1744215	5716076

4.2 Bathymetry Generation

Bathymetry data for this project was gathered from a variety of sources as follows:

- Bathymetry surveys of each of the harbours undertaken as part of this project (Atkin *et al*, 2016).
- Digitised coastline data from aerial photography.
- Multibeam survey data of Whaingaroa Harbour.

- LIDAR data for the mud flats of Kawhia, Whaingaroa and Aotea Harbours[6].
- Data digitised from hydrographic charts[7].
- GEBCO (Becker *et al.* 2009).

The different bathymetry datasets were merged together into a single point cloud all using the New Zealand Transverse Mercator (NZTM) projection using the NZGD datum. Where datasets overlapped, higher resolution, or more recent datasets were chosen preferentially. The order of precedence is reflected in the above list of datasets. All of the data were converted to a common vertical datum which was the Mean Level Of the Sea (MLOS) estimated from long term averages of the Kawhia and Manu Bay tide gauges (see Figure 4.1). For both gauges MLOS was found to be 0.15 m above Moturiki vertical datum (1956).

The bathymetry maps were generated using Kriging interpolation in SURFER® software. Kriging is a geostatistical gridding method that produces contour and surface plots from irregularly spaced data. Kriging attempts to express trends that are suggested in the data, so that, for example, high points might be connected along a ridge, rather than isolated by bull's-eye type contours. Kriging always uses the measured value exactly (known as an “exact” interpolator) when it coincides with the grid node in the gridded data file. Survey track lines were mostly perpendicular to seabed gradients, as a result channels in the estuary seabed are well represented in the bathymetry. Within the drowned river valley estuary model bathymetries some river channels were deepened so that freshwater inputs did not become trapped in the hydrodynamic models at lower tides.

The arrangement of nested grids used in this project are shown in Figure 4.2 which also shows the extent of the broad scale model grid. The seven local bathymetries are shown in Figure 4.3 to Figure 4.9.

[6] Source: WRC
[7] Source: Land Information New Zealand (LINZ)

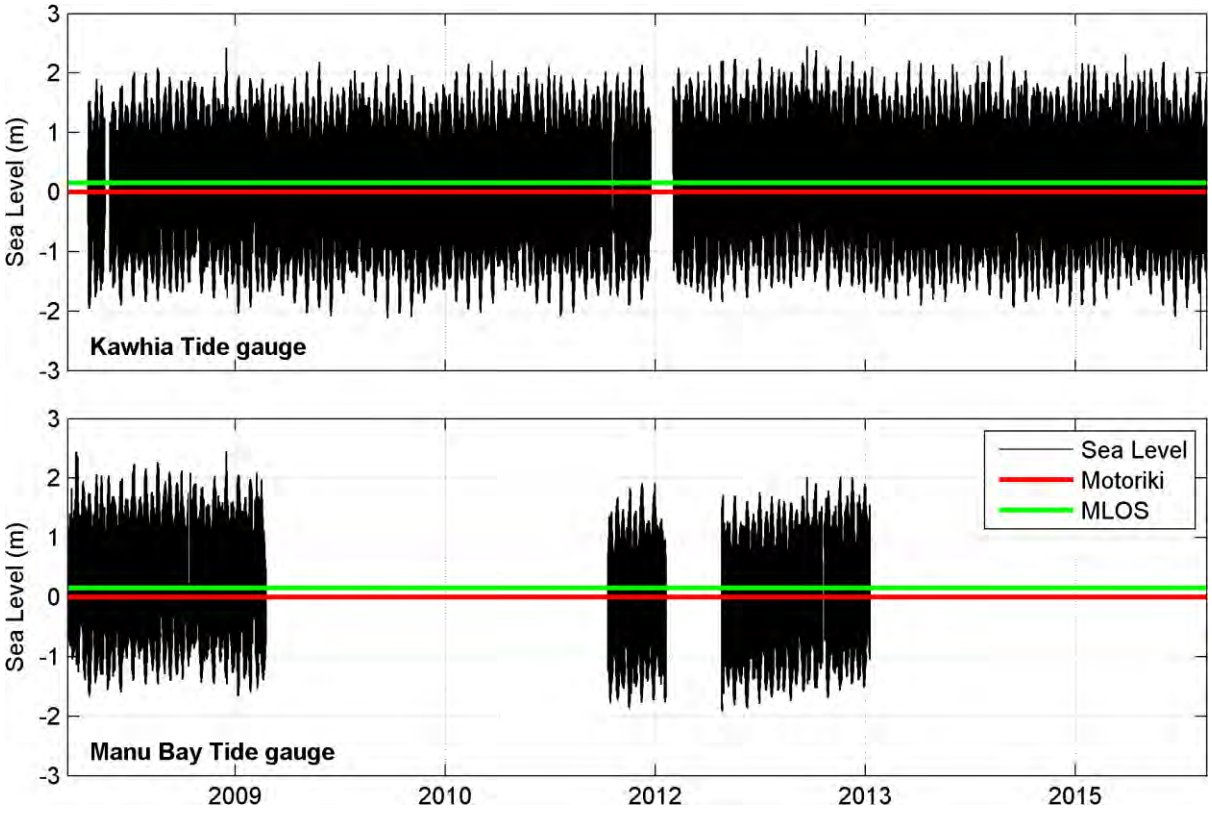

Figure 4.1: Analysis of the Kawhia (upper panel) and Manu Bay (lower panel) tide gauges to determine MLOS relative to Moturiki Datum.

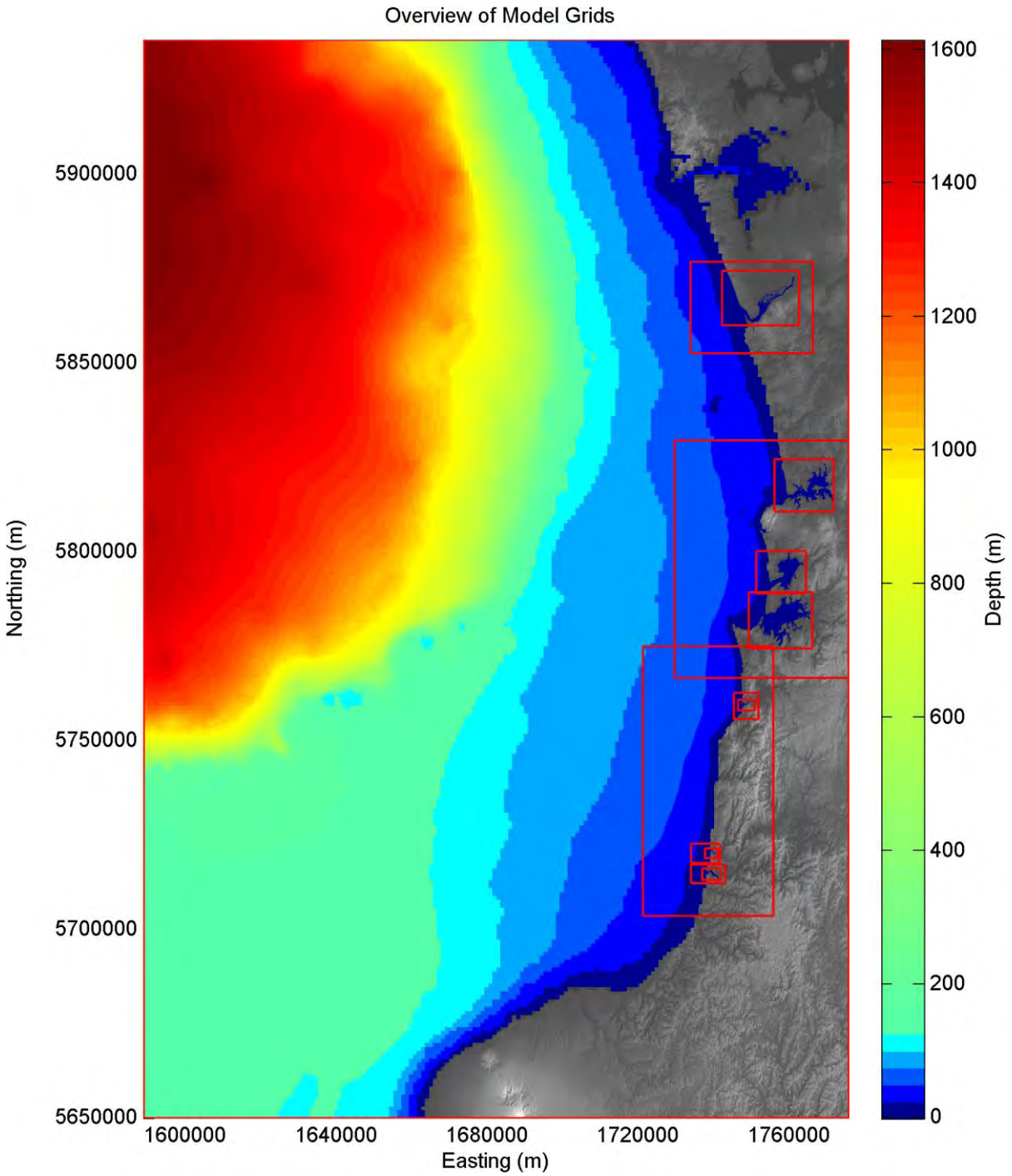

Figure 4.2: Overview of all the model domains used in this project.

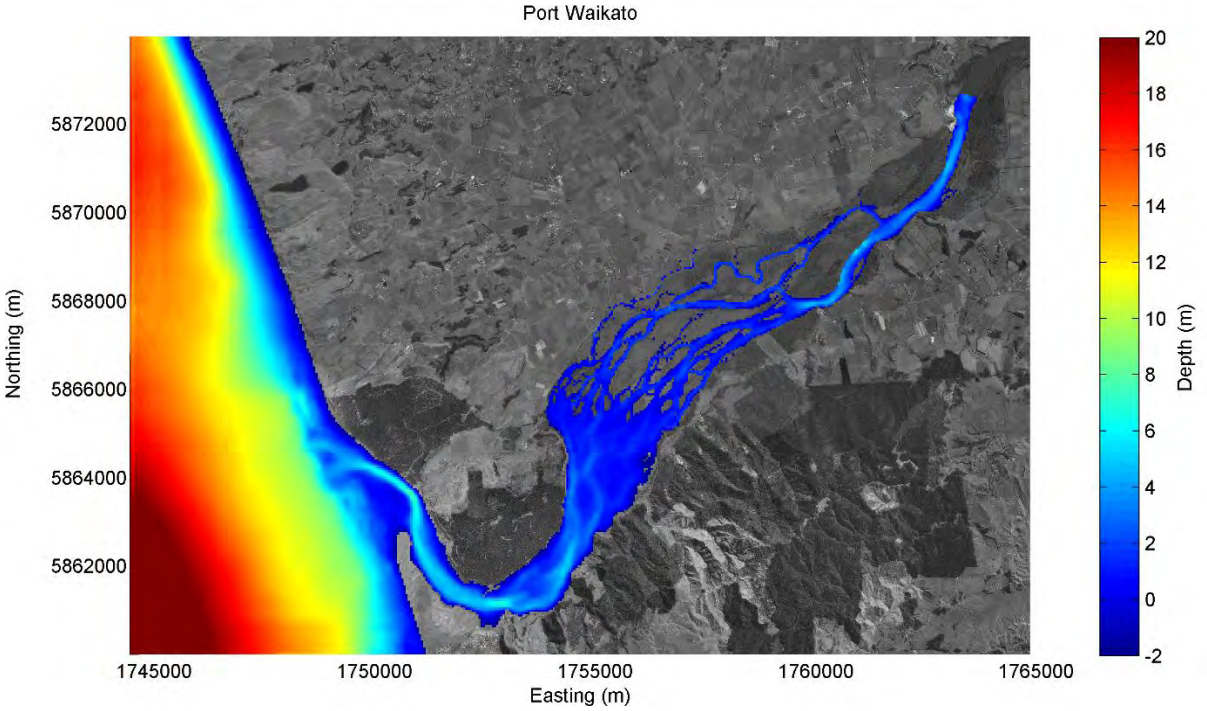

Figure 4.3: Waikato River estuary bathymetry.

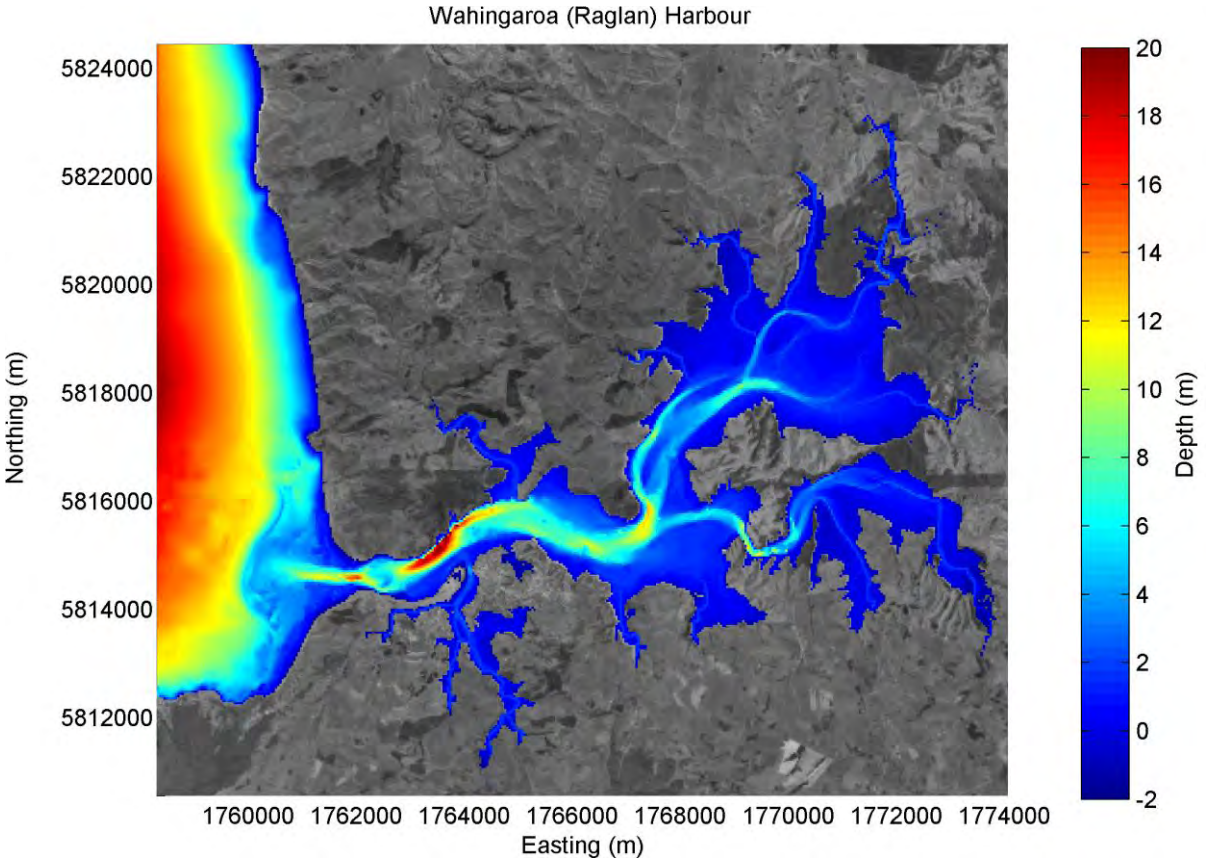

Figure 4.4: Whaingaroa (Raglan) Harbour bathymetry.

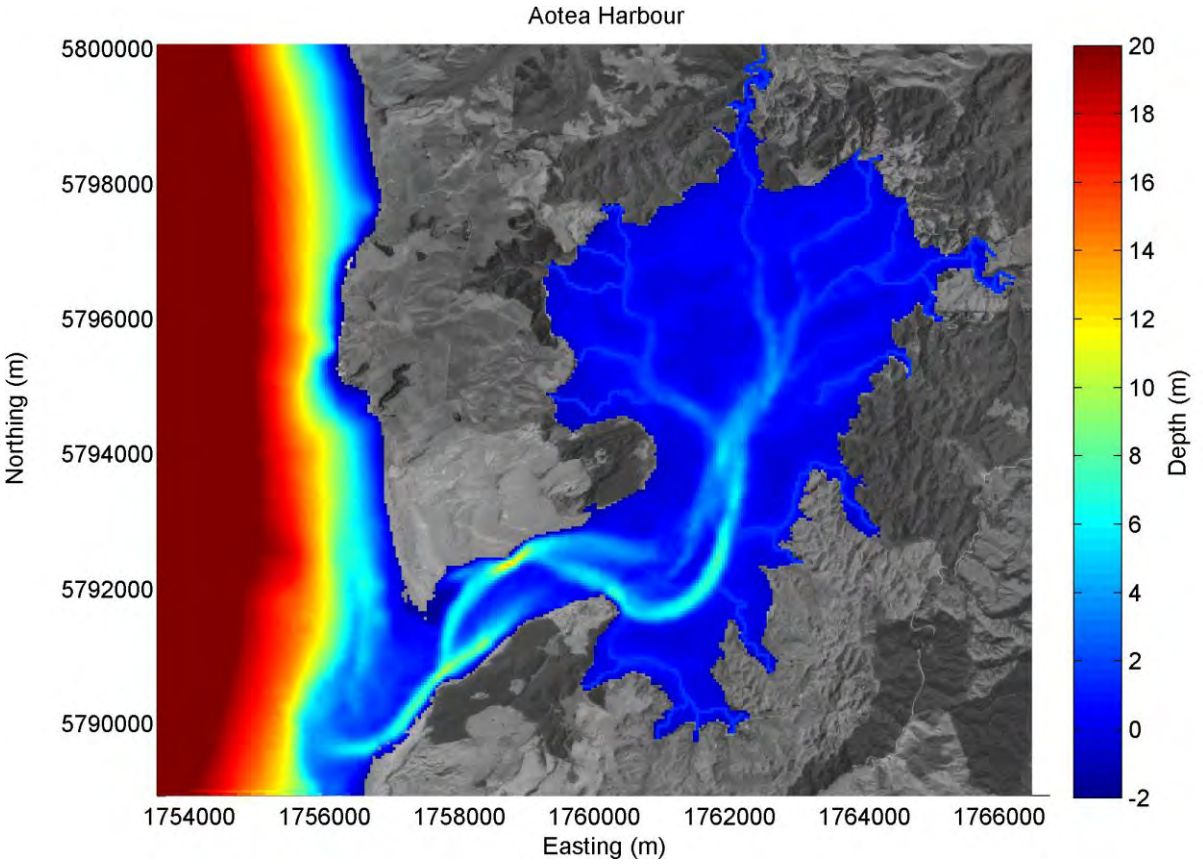

Figure 4.5: Aotea Harbour bathymetry.

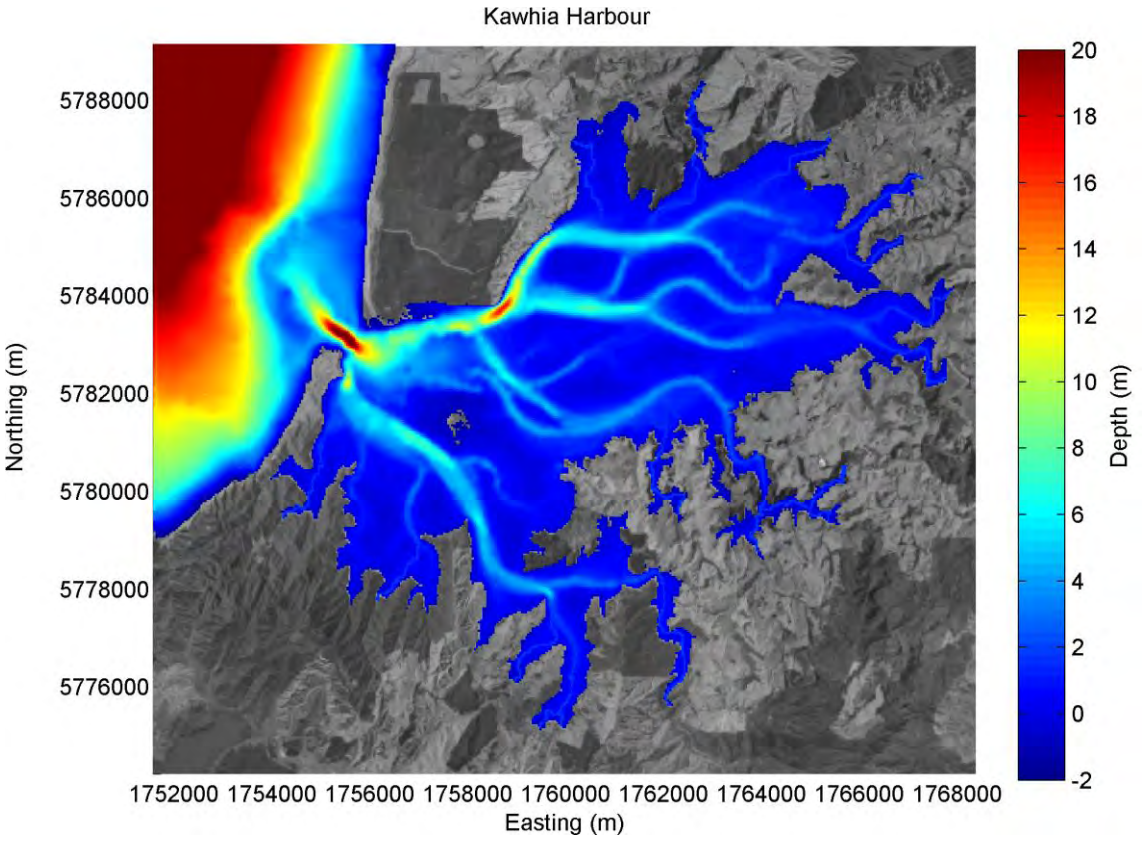

Figure 4.6: Kawhia Harbour bathymetry.

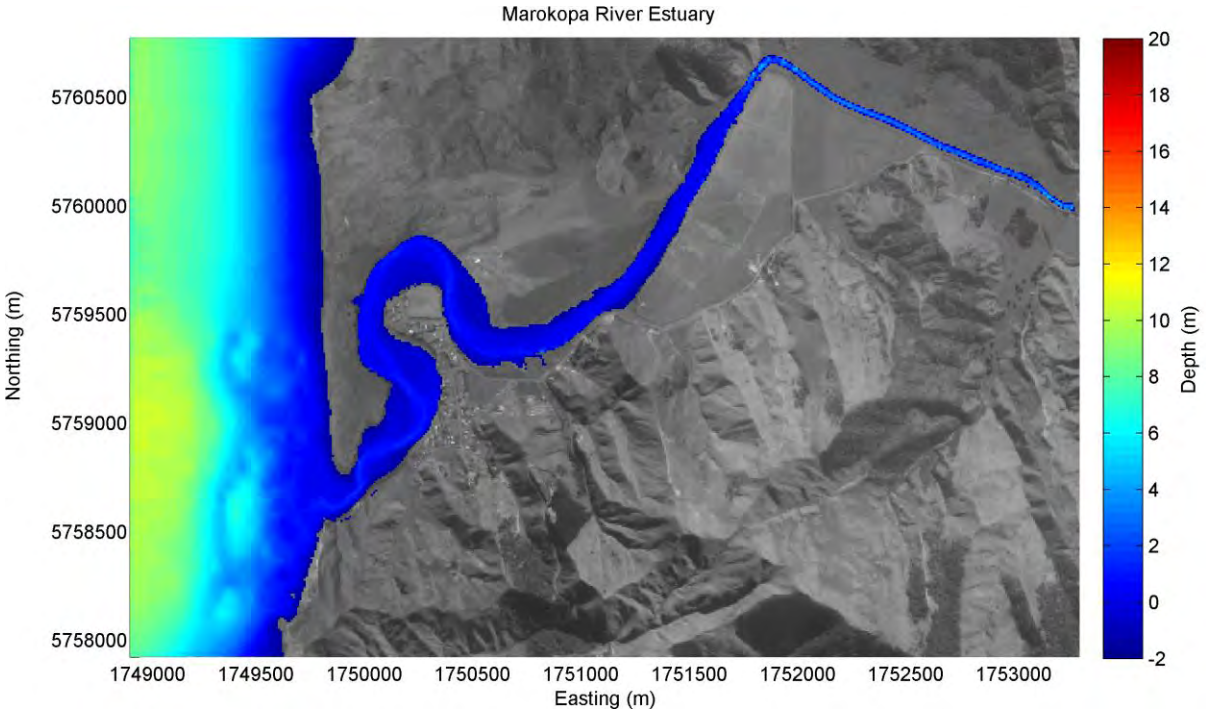

Figure 4.7: Marokopa River estuary bathymetry.

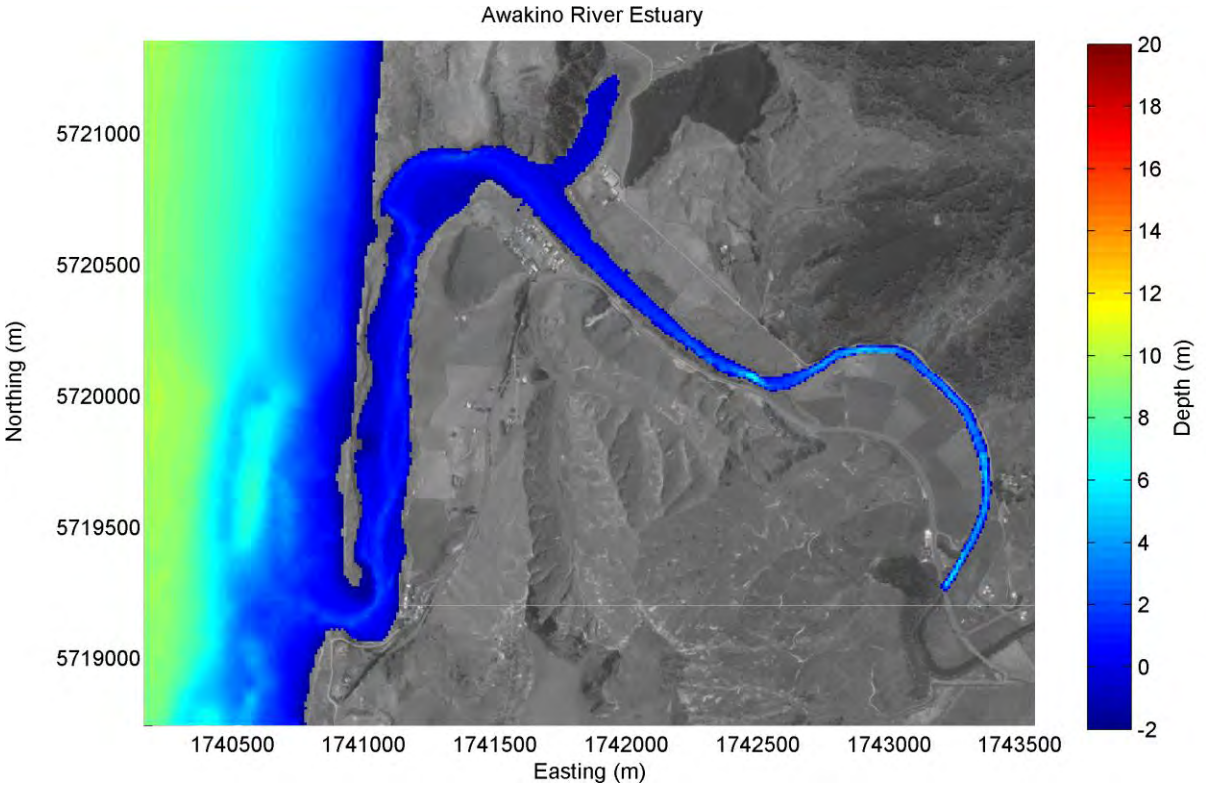

Figure 4.8: Awakino River estuary bathymetry.

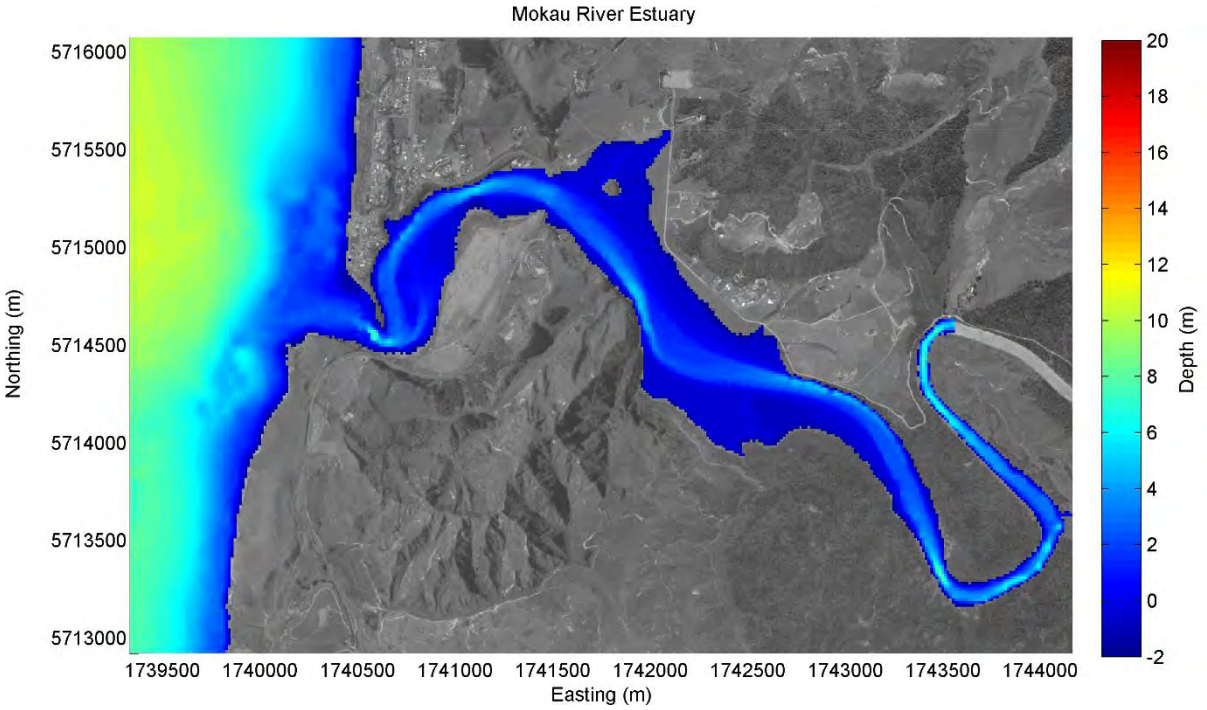

Figure 4.9: Mokau River estuary bathymetry.

4.3 Boundary Conditions

The models were all depth averaged and were driven by tides, atmospheric pressure, wind, salinity and river flow.

Tidal boundary conditions on the open ocean boundaries of the large scale West Coast model were extracted from the TPXO tide atlas (Egbert and Erofeeva, 2002). This global model of ocean tides was developed by the Oregon State University using along track averaged altimeter data from the TOPEX/Poseidon and Jason satellites since 2002. The methodology applied in the global tide models and has been refined to create regional models at higher resolution. For this project we used the Pacific Ocean model with a resolution of 1/12 degree. The model provided the 11 most influential constituents, as well as two long period (Mf, Mm) harmonic constituents. Each constituent is a sinusoid which represents the gravitational influence of a particular aspect of a planetary body or of several bodies. Each sinusoid was described in the model by a phase and amplitude. Tidal constituents were described at 144 (the maximum allowed by Delft-Flow) evenly spaced locations around the model boundary.

For the broad scale models, MSL atmospheric pressure data and 10 m wind data were sourced from the NOAA's global NCEP reanalysis model (Kalnay *et al*. 1996). The atmospheric pressure model is available at a resolution of 0.5 by 0.5 degrees. The wind model

resolution is 0.312 by 0.312 degree resolution from 1979 until 2011 and 0.205 by 0.204 from 2011 onwards.

The local models used hourly wind data recorded by land-based AWSs made available by WRC and NIWA's Cliflo service. Substantial gaps exist in all of the wind data records so multiple AWSs were used to create continuous wind time series (see Figure 4.10). This was achieved by choosing a primary AWS for wind data and then using secondary stations to fill in any gaps. So that the wind records remained as consistent as possible, a linear regression was used to create a relationship between the primary and secondary time series (using u and v wind components) where records overlapped. This relationship was used to modify secondary wind data prior to using them to fill in gaps.

The 4 northern estuaries (Waikato River estuary, Whaingaro Harbour, Kawhia Harbour and Aotea Harbour) used data from Raglan AWS (Figure 4.11) with gaps filled in using the Whatawhata AWS (u-component $r^2 = 0.64$, v-component $r^2 = 0.46$). Any remaining gaps were filled with data from the Awakino AWS (u-component $r^2 = 0.65$, v-component $r^2 = 0.23$). The 3 estuaries to the south (Marokopa, Awakino and Mokau River estuaries) used wind data from the Awakino AWS (Figure 4.12) with gaps filled in using the Whatawhata AWS data (u-component $r^2 = 0.61$, v-component $r^2 = 0.31$).

To reduce model spin-up time, spatially variable sea level initial condition files were created for each domain using the same TPXO tide atlas model used to create the tidal boundary conditions. The salinity was initialised in each model at 35 psu, and this value was applied as a constant value around the open boundaries of the West Coast model domain throughout all of the model runs.

The river boundary conditions are described in Section 3. These were applied in the model as flux boundaries with a salinity of 0 psu.

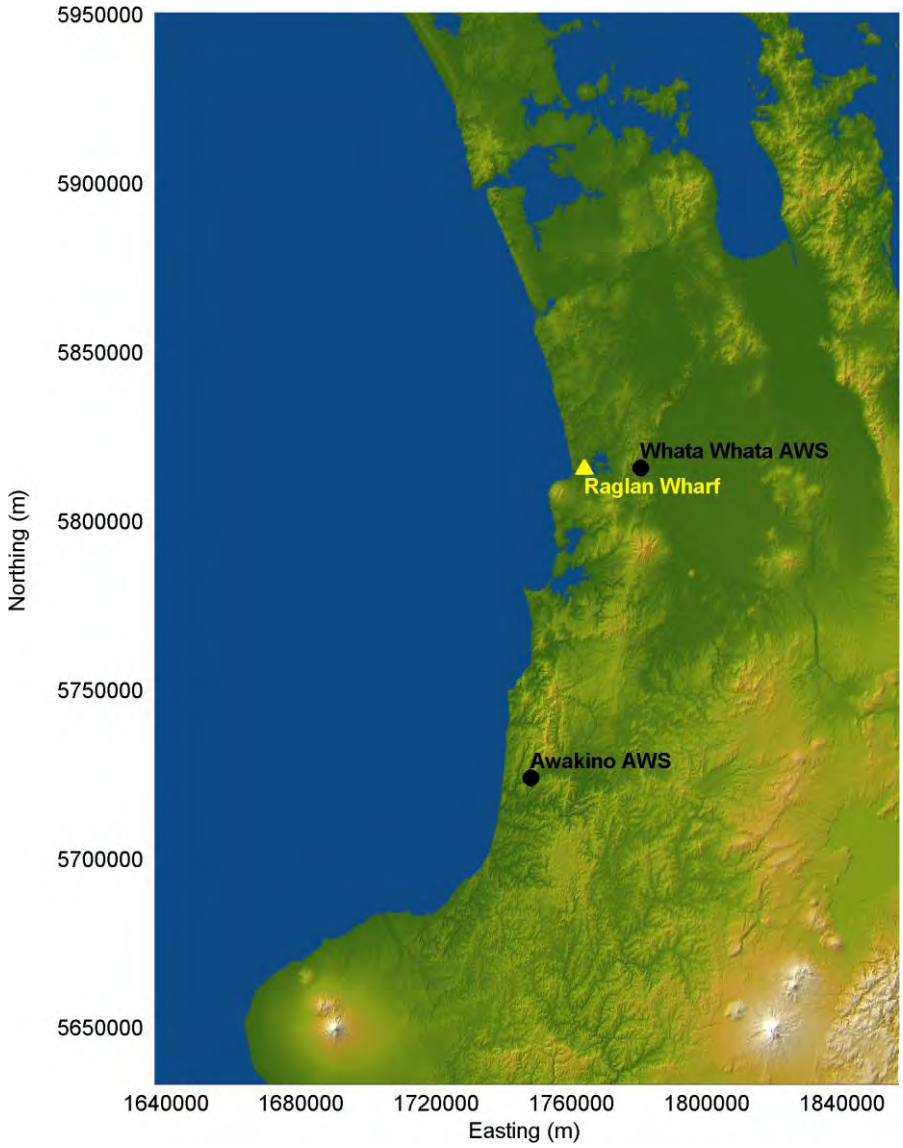

Figure 4.10: Automatic weather stations providing wind data for the model development. The yellow triangle indicates a station maintained by WRC and the black circles are stations obtained from Cliflo.

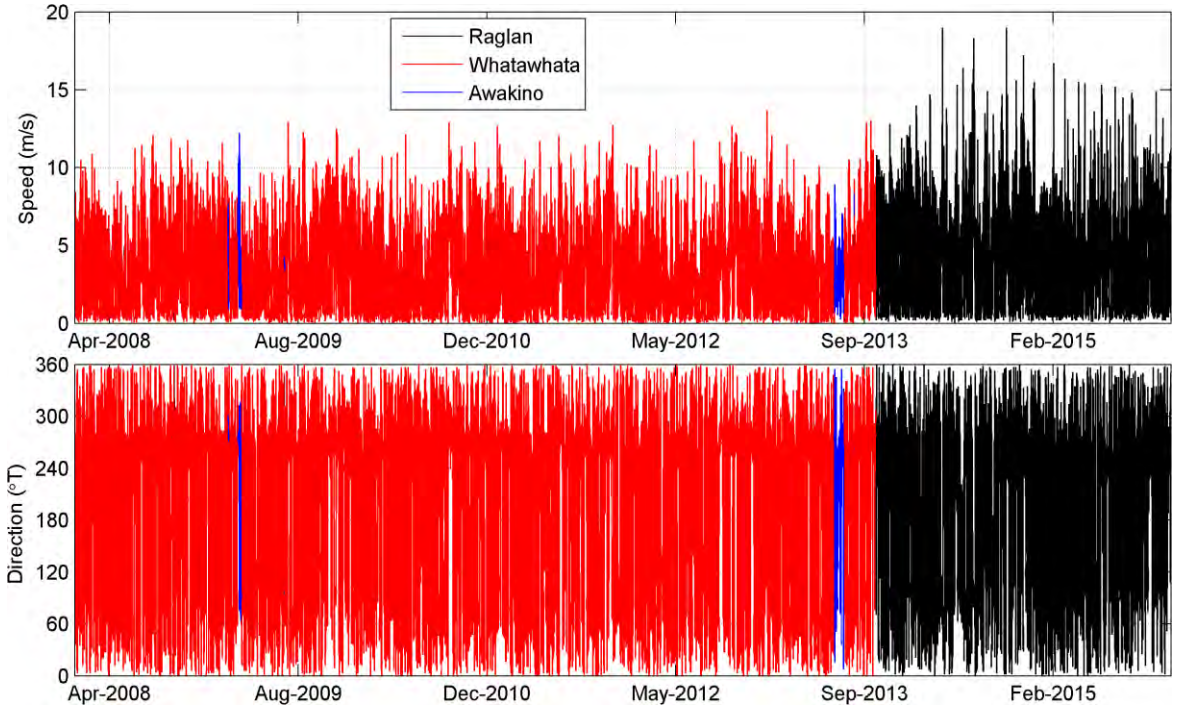

Figure 4.11: Wind boundary conditions time series using Raglan AWS as the primary wind source'

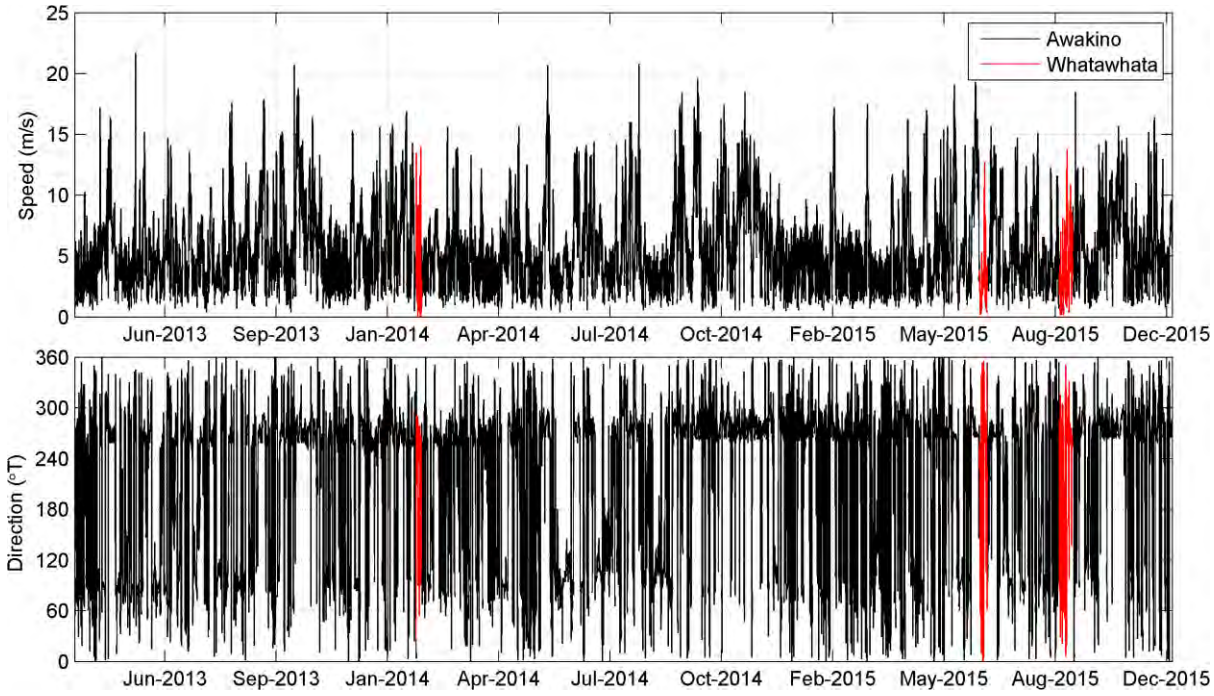

Figure 4.12: Wind boundary conditions time series using Awakino AWS as the primary wind source'

5 Calibration and Analysis

The hydrodynamic models have been calibrated by comparing model output with measured sea levels, current data and salinity time series. Much of these data were taken from the field work component of this project which is described in full in Atkin *et al*. (2016). Data from tide gauges and other field work projects were used where they were available. Considerably more data existed for some estuaries than for others. These data are described for each estuary throughout this section.

For each location, peak flood and ebb velocities are presented. Peak flows do not occur at the same time throughout the model domains. For each estuary model output was examined visually to identify times when outgoing and incoming tides were occurring over the entire model domains.

The models were calibrated by adjusting Horizontal Eddy Viscosity (HEV), diffusion and the Chézy bed roughness coefficient. The broad scale model grids all used a HEV of 30 $m^2 s^{-1}$, a diffusion coefficient of 10 $m^2 s^{-1}$ and a Chézy Bed Roughness Coefficient of 65 $m^{1/2} s^{-1}$. The final values for these parameters, for the local scale grids, are shown in Table 5.1.

Table 5.1: Model parameters for local models.

Estuary	HEV $m^2 s^{-1}$	Diffusion $m^2 s^{-1}$	Chezy Coefficient $m^{1/2} s^{-1}$
Waikato River estuary	10	10	50
Whaingaroa (Raglan) Harbour	10	10	50
Aotea Harbour	5	10	80
Kawhia Harbour	5	10	55
Marokopa River estuary	5	10	80
Awakino River estuary	5	10	80
Mokau River estuary	5	10	80

5.1 Waikato River Estuary

The field work component of this project provided sea level, current and salinity data at two locations in the estuary ('Lower') in the lower reaches of the estuary and ('Upper') in the upper reaches of the estuary (Atkin *et al*., 2015).

Additionally, data were available from a previous study (Jones and Hamilton 2014) including 3 sites where salinity was recorded and 6 sites where sea level data were recorded. The data collection locations are shown in Figure 5.1. At the Upper location the salinity gauges recorded a constant salinity of approximately 0 psu at the surface (the sea bed salinity gauge failed to

collect data). The model reproduced this faithfully, but since there was very little fluctuation in either the measured or modelled signals, comparisons of measured and modelled salinity at this location were excluded from the calibration results below.

Time series comparisons between modelled and measured data are presented in Figure 5.2 to Figure 5.4 for sea level, in Figure 5.6 and Figure 5.7 for currents and Figure 5.9 for salinity.

The sea level calibration at the Upper and Lower locations indicate that the model has represented the attenuation of the tidal signal in the upper reaches of the estuary (BSS = 0.91 for both locations). During spring tides the measured data shows a tidal range of approximately 2.2 m during spring tides which is reduced to 1.5 m at the Upper location.

The calibration against sea level data recorded by the Hoods Landing tide gauge shows considerable low frequency sea level variability (approximately 4 to 7-day period) which has not been replicated by the model (BSS = 0.67). Though some low frequency variability can be explained by fluctuations in atmospheric pressure much can be explained by examination of wave characteristics extracted from a global wave model maintained by NOAA[8] from this period (see Figure 5.5). The periods of elevated sea level in the Hoods Landing sea level record coincide with periods of elevated wave height. However, comparison between the river flow record (Figure 3.5) and the sea levels recorded at the Upper location, for a different period of time, illustrate that river flow also influences low period sea level variability and this is well represented in the model.

Additional sea level calibrations were undertaken at 5 locations around the estuary using the data from Jones and Hamilton (2014) and the results are presented in Appendix B. The measured sea level records from location WR9 appear to be badly degraded and were omitted from the calibration. In general, the measured and modelled sea level records are in good agreement and illustrate that the progressive sea level attenuation with distance upstream was well captured by the model. An exception to this is location WRX in the lower reaches. At this location the model overestimated the tidal range by up to a meter during spring tides.

At the lower location, the model correctly estimated the phase of current speeds including spring neap variability. The model also picked up the tidal asymmetry in current speeds with stronger current speeds occurring on the outgoing tide. However current speeds in the model were underestimated by approximately 50%. Altering the boundary conditions and model parameters such as HEV and bed friction did not improve the current calibration. The bathymetry survey from this region of the model domain was undertaken in June 2013 (Jones and Hamilton, 2014) whereas the current speed and direction data were recorded in

[8] http://polar.ncep.noaa.gov/waves/nopp-phase1/

November 2015. It is possible that in this time the bathymetry has changed leading to altered current patterns. Additionally, this is a 2D model and the misrepresentation of current speeds in the model may have been due in part to the absence of 3D processes in the model. At the Upper location the currents were poorly represented by the model. The extent of tidal variability greatly underestimated by the model and this is reflected in the performance statistics (BSS = 0.43). This is likely due to the lack of tidal variability in the river boundary condition. Plots of peak flood and ebb currents are presented in Figure 5.8.

The salinity calibration illustrates that the salt water intrusion into the estuary was underestimated by the model especially during neap tide conditions centred around 7 November 2015. The measured salinity at this location was located at the bottom of the water column where the intruding salt wedge was likely to be strongest. Unfortunately, the surface salinity gauge at this location was destroyed during the deployment; however, it is likely that the surface salinity values would be lower than at the bed. Salinity profiles collected by Jones and Hamilton (2014) observed lower salinity at the surface than at depth in some locations in the Waikato River estuary as would be expected in this environment. Additionally, the river flow boundary conditions were based on flow records from the Mercer flow gauge and these likely underestimate the tidal component of flow variability since the Mercer flow gauge is approx. 30 km upstream from the model boundary. Therefore, it is possible that the tidal excursion at the Lower location is underestimated by the model which may explain the lack of intrusion by salt water in the model.

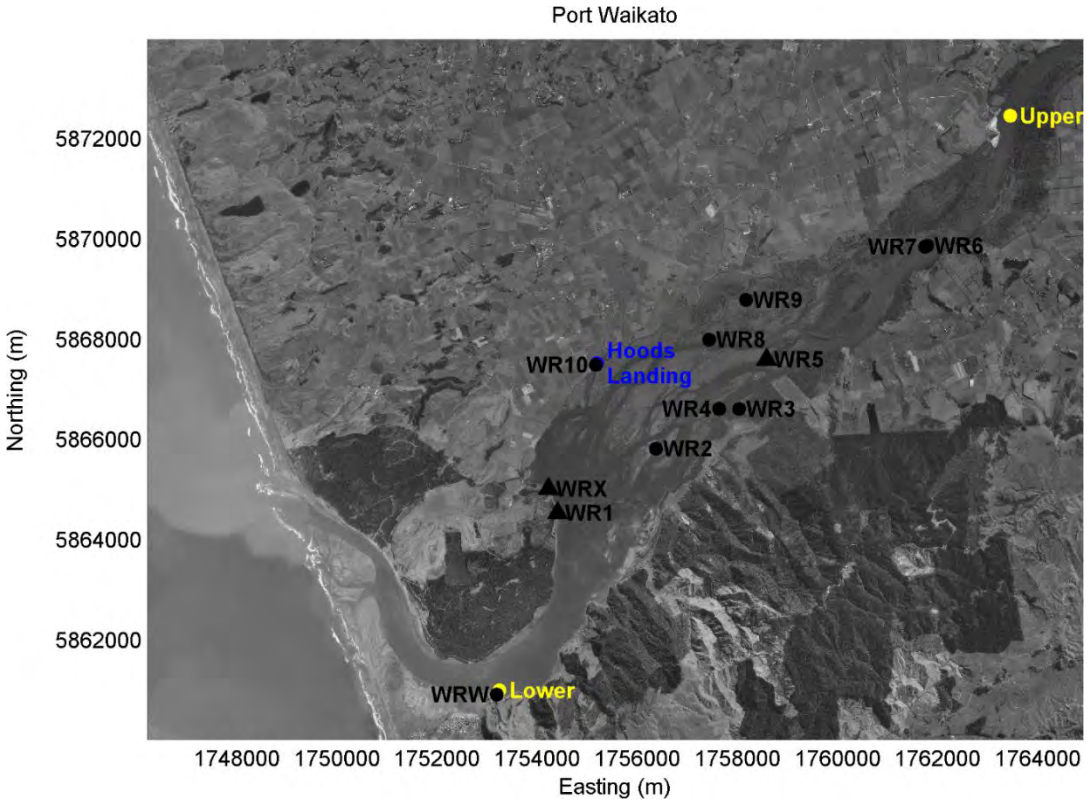

Figure 5.1: Waikato River estuary calibration locations. Locations in yellow were from the fieldwork component of this project. Those in black are from the study by Jones and Hamilton (2014) with circles indicating locations where only sea level was recorded and triangles indicating locations where sea level and salinity were recorded. The location in blue is a tide gauge.

Table 5.2: Skill scores for the Waikato River estuary calibrations.

Variable	Briar Skill Score (BSS)	α	β	γ	R^2	RMSE
Sea Level (Upper)	0.91	0.91	0.00	N/A	0.92	0.12 m
Sea Level (Lower)	0.91	0.91	0.00	N/A	0.91	0.19 m
Sea Level (Hoods Landing)	0.67	0.87	0.00	0.20	0.87	0.27 m
Currents (Upper)	-0.43	0.19	0.00	2.84	0.19	0.24 m s^{-1}
Currents (Lower)	0.85	0.76	0.10	0.32	0.19	0.26 m s^{-1}
Salinity (Lower: Bed)	0.89	0.71	0.07	0.34	0.72	8.9 psu

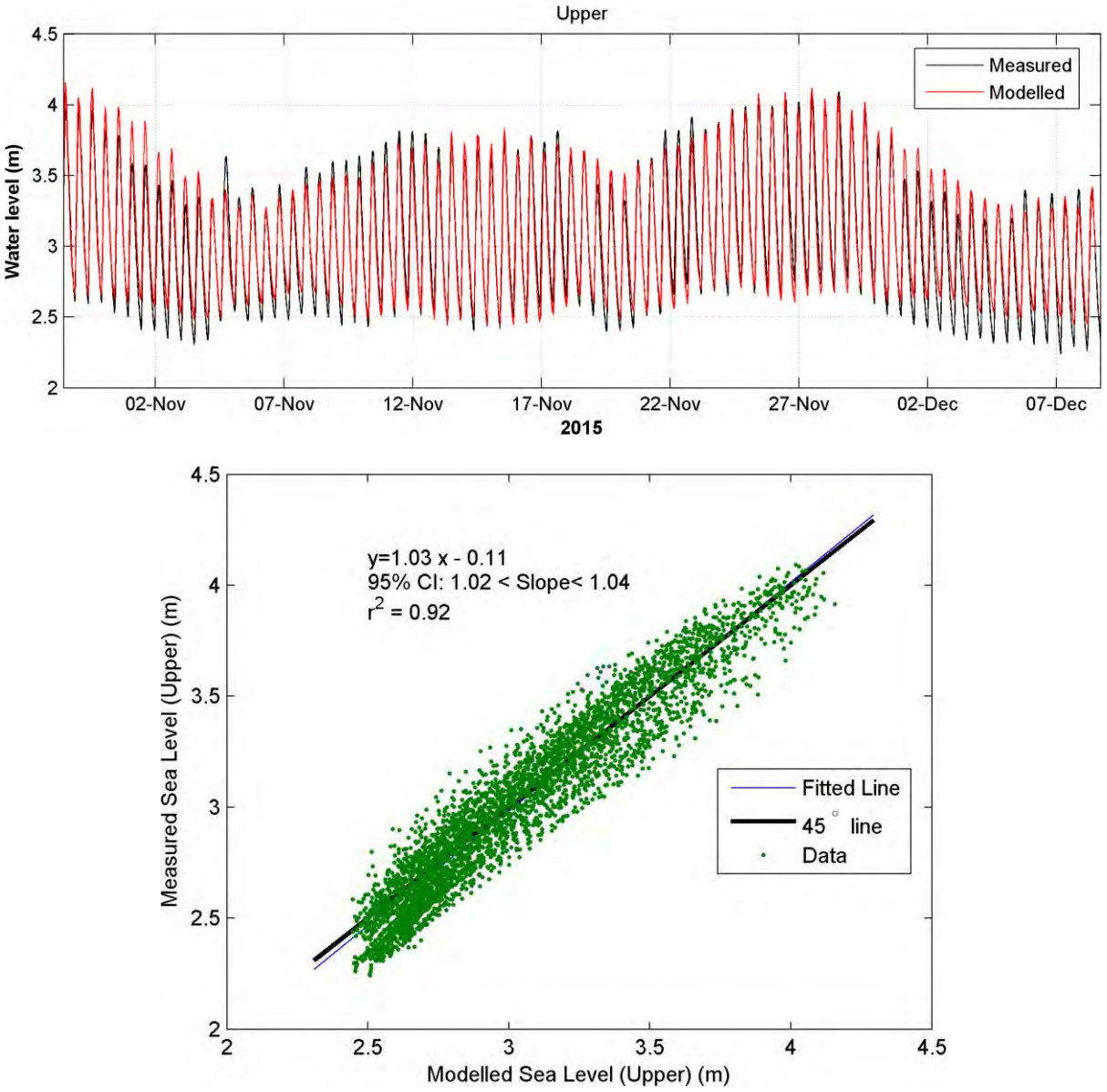

Figure 5.2: Sea level calibration at the 'Upper' location in the Waikato River estuary as a time series (upper panel) and as a linear regression (lower panel).

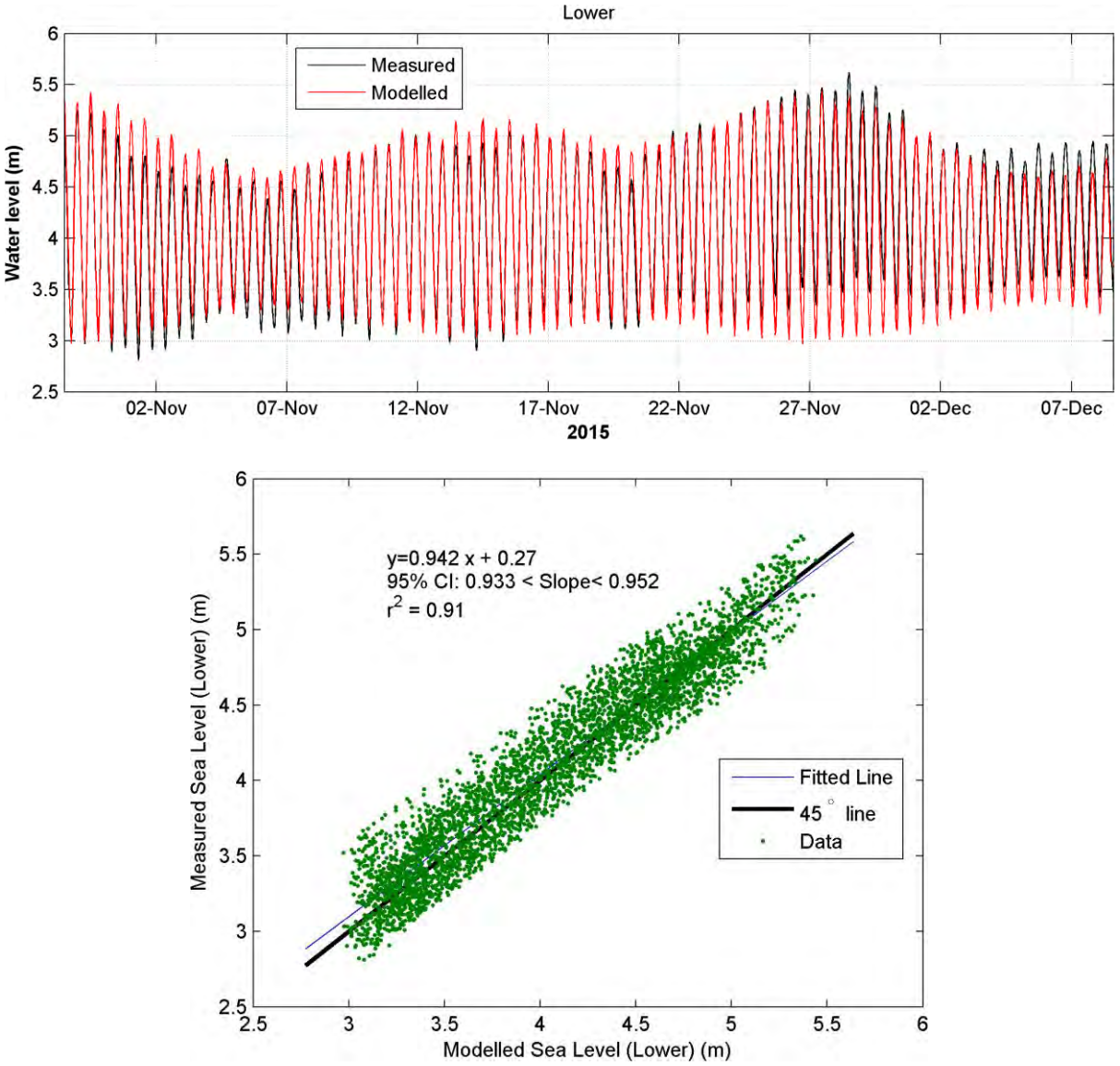

Figure 5.3: Sea level calibration at the 'Lower' location in the Waikato River estuary as a time series (upper panel) and as a linear regression (lower panel).

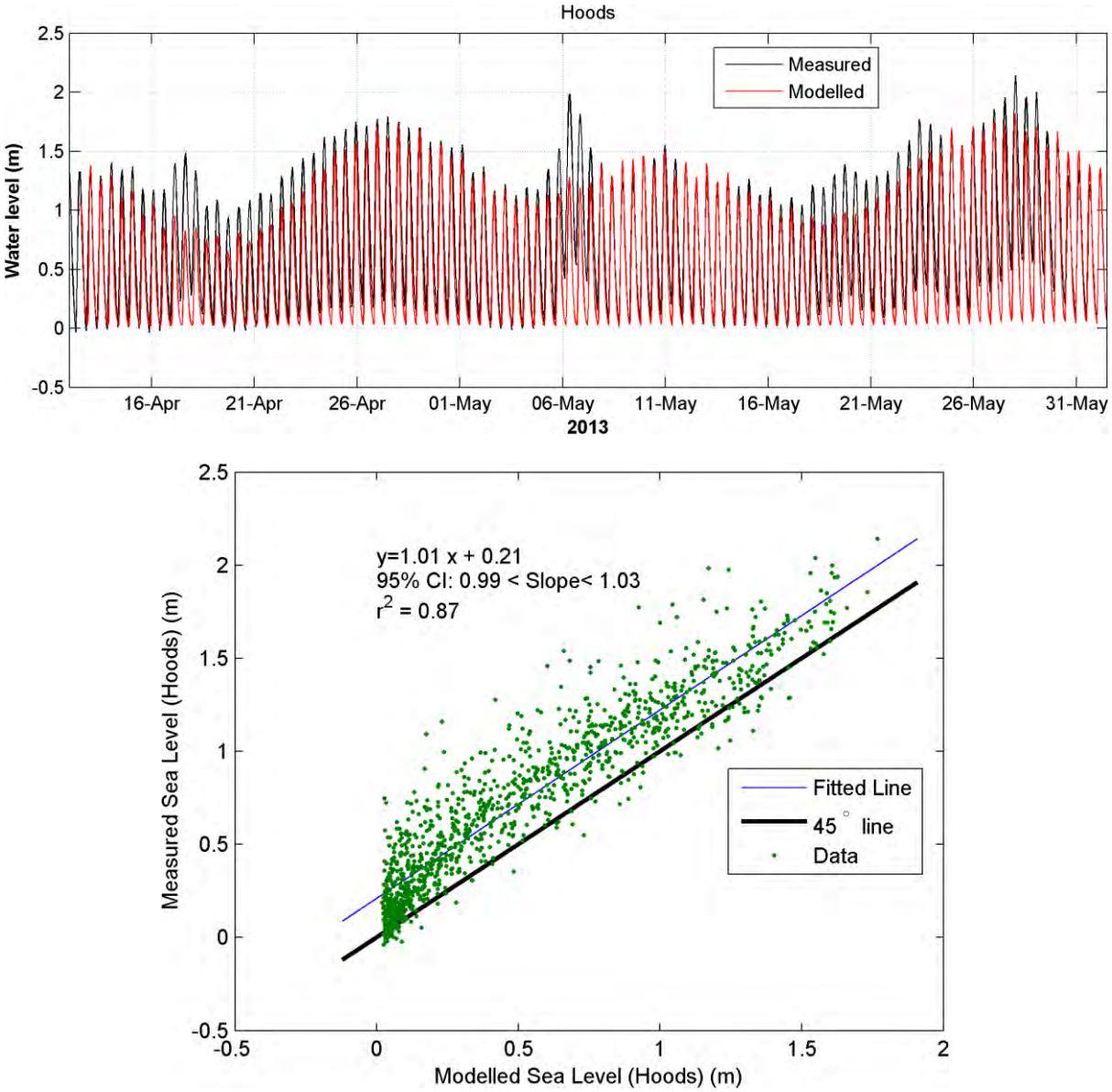

Figure 5.4: Sea level calibration at the Hoods Landing tide gauge in the Waikato River estuary as a time series (upper panel) and as a linear regression (lower panel).

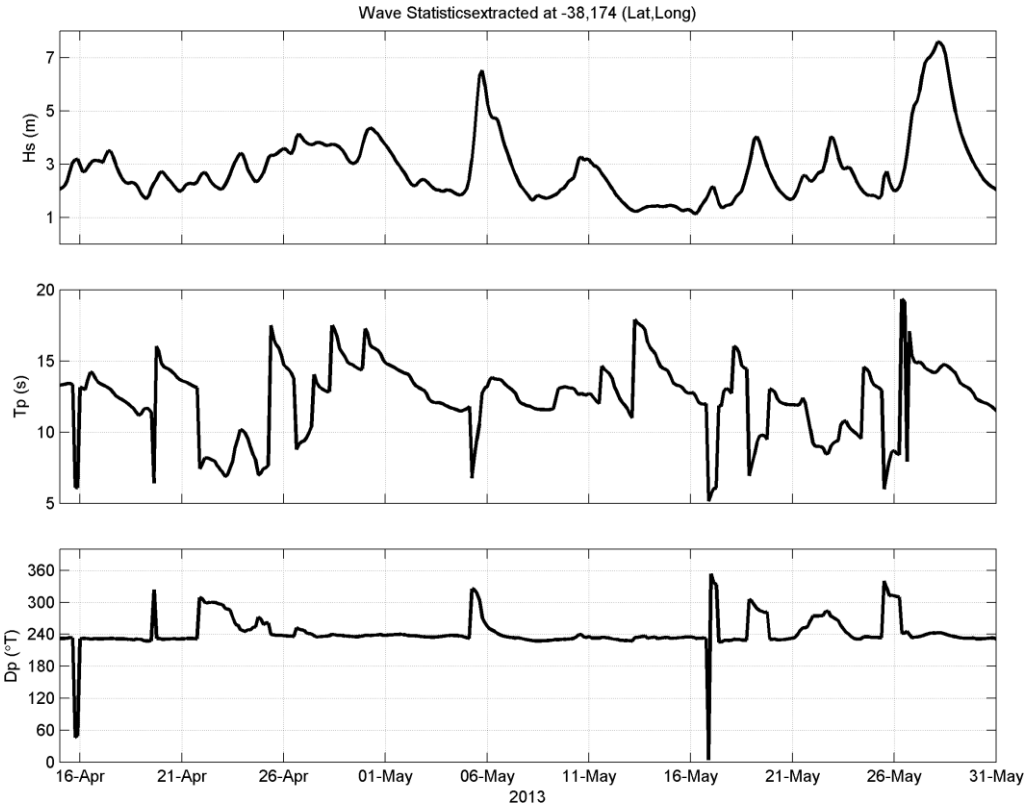

Figure 5.5: Wave characteristics on the west coast of the Waikato (Source: NOAA) during the deployment period for the data collected by Jones and Hamilton (2014).

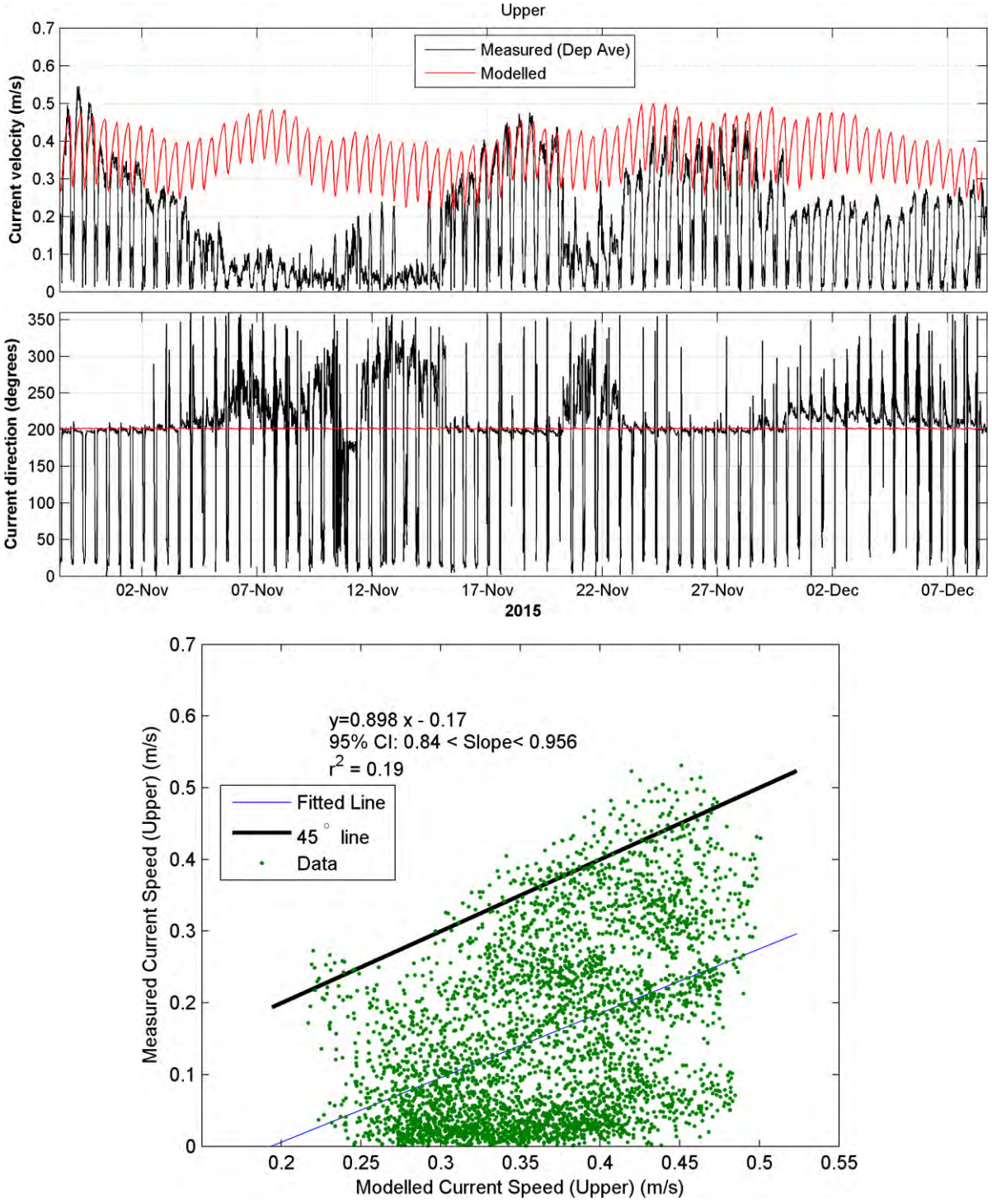

Figure 5.6: Waikato River estuary current calibration at the 'Upper' deployment location as a time series (upper panel) and as a linear regression of modelled versus measured current speed (lower panel).

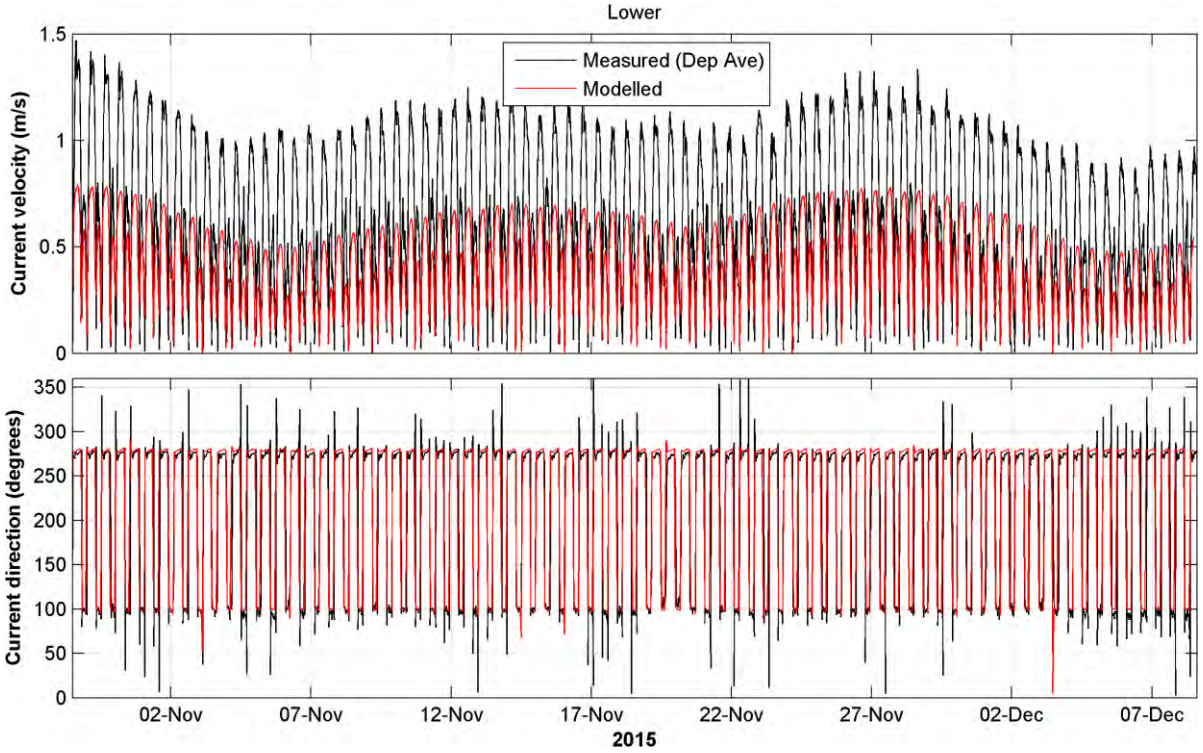

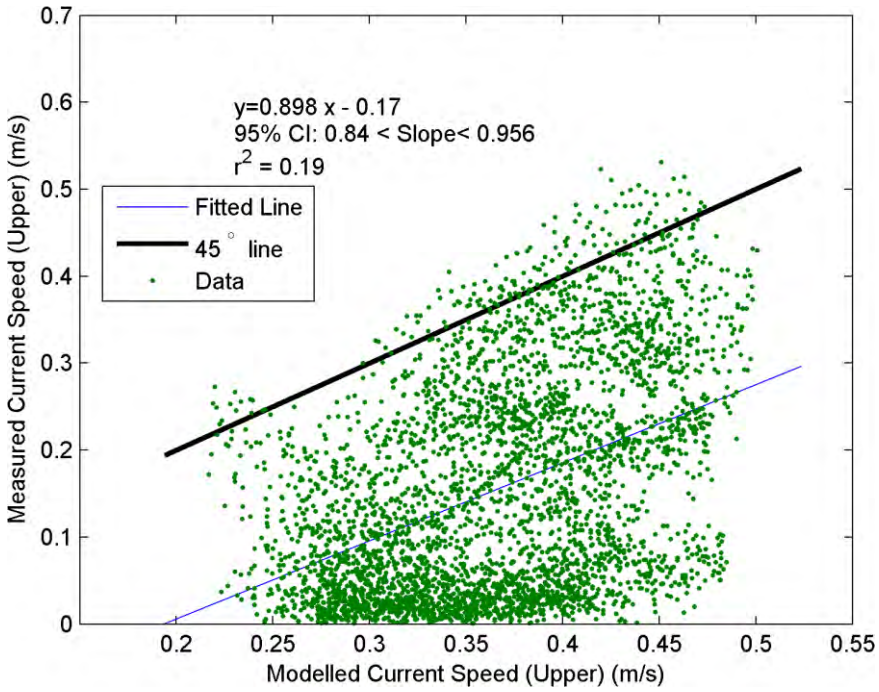

Figure 5.7: Waikato River estuary current calibration at the 'Lower' deployment location as a time series (upper panel) and as a linear regression of modelled versus measured current speed (lower panel).

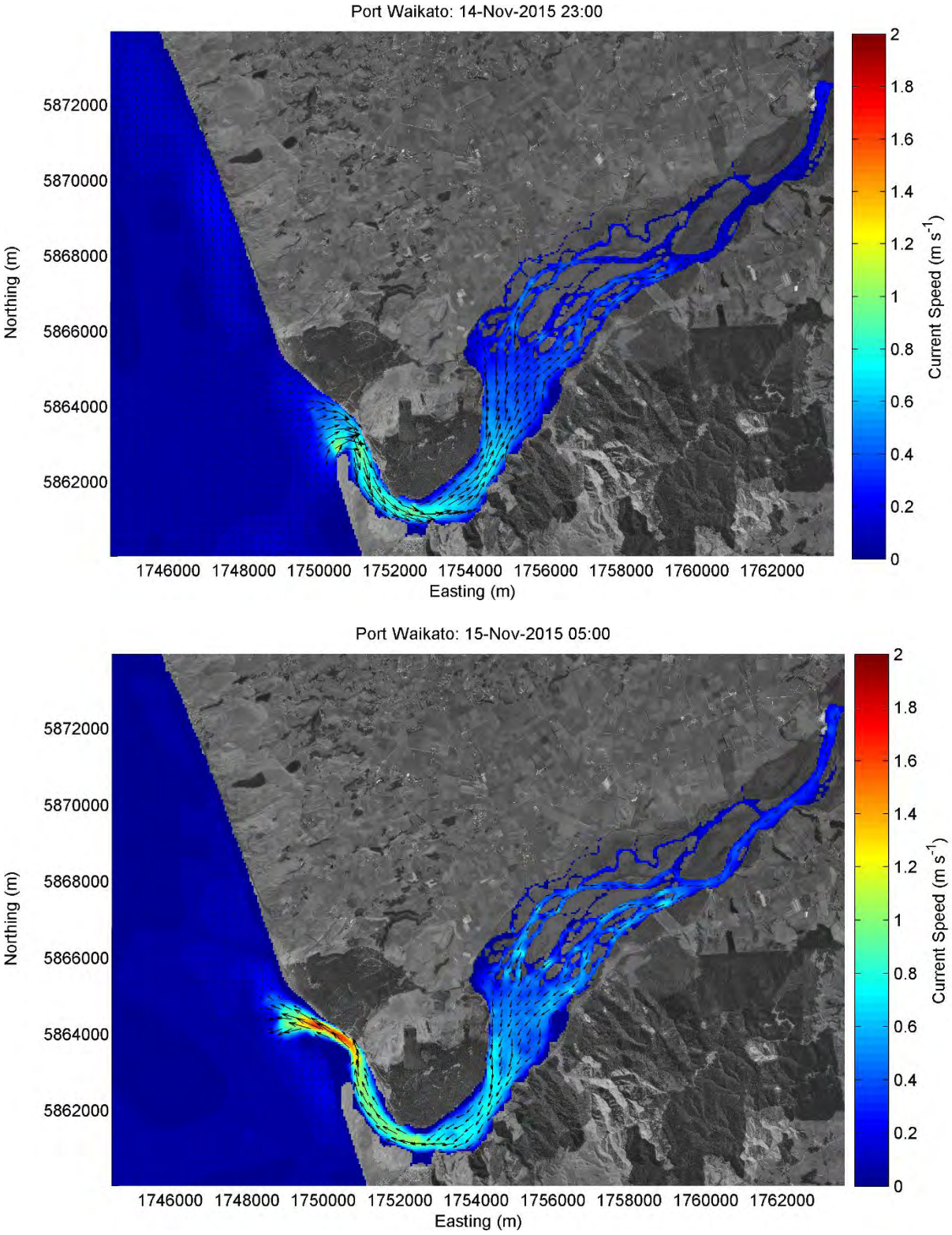

Figure 5.8: Waikato River estuary peak flood (upper panel) and ebb (lower panel) currents.

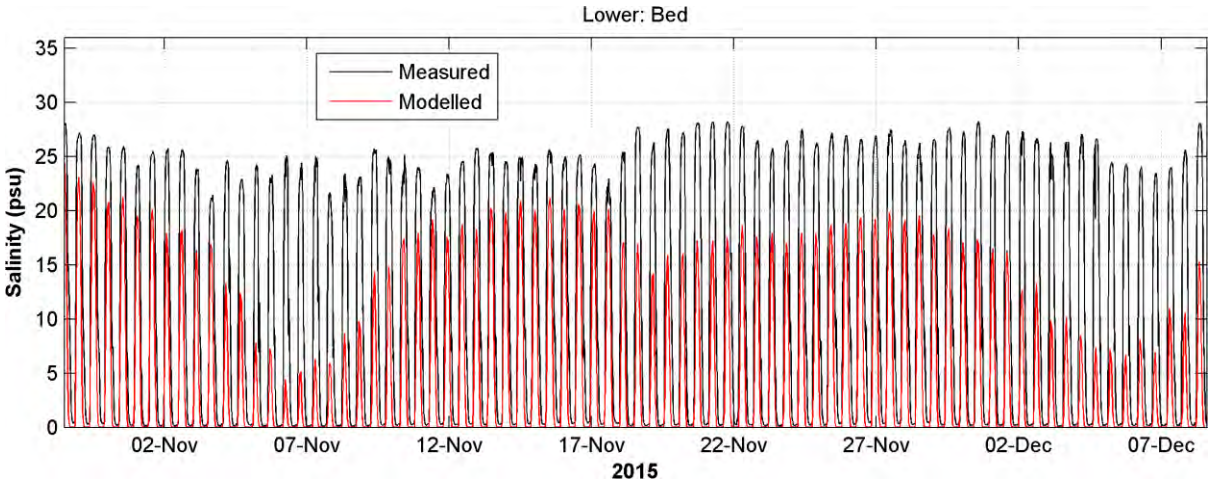

Figure 5.9: Waikato River estuary salinity calibration at the Lower deployment location.

5.2 Whaingaroa (Raglan) Harbour

Whaingaroa Harbour has been the focus of many studies in the past (e.g. Stark *et al*., 2010, Harrison, 2015, Greer *et al*., 2015) and as a consequence a reasonable amount of data already exists, and was available for the calibration of the model described here. Five datasets from different studies were used in this project for model calibration purposes:

1. As part of the field work component of this project, salinity gauges were deployed for a 6-week period between 3 November and 16 December 2015 within the Opotoru arm of the harbour and in the Waitetuna arm of the harbour. At each location, salinity data were recorded at the top and bottom of the water column for the duration of the deployment.
2. Two Nortek Aquadopps were deployed between 17 March and 4 April 2009 at one location in the channel inside the harbour mouth and at another location outside the harbour mouth on the ebb tidal delta. The instruments recorded currents, sea level data and wave characteristics. This data has previously been used in several studies for the development of water quality models of Whaingaroa harbour (Phillips *et al*., 2009 and Greer *et al*., 2015)
3. Between 14 Feb and 29 Feb 2008, a single Nortek Aquadopp was deployed in three locations around in the Opotoru arm of the harbour recording current speed and direction and water level (Mead and Greer, 2007). Deployment lengths were approximately 3-4 days at each location.
4. On 14 April 2014 a downward looking Sentinel workhorse was used to undertake 24 transects through the harbour mouth recording current speed and direction at 0.25 m bins through the water column (Harrison, 2015).

5. Two tide gauges exist at Manu Bay and at the Raglan Wharf which provide hourly sea level data.

The locations of these instrument deployments are shown in Figure 5.10. Calibrations against these datasets are discussed in this section in the order of the above list. While this represents a comprehensive number of datasets, much of the data is focused on the estuary mouth and ebb tidal bar. This is very useful for model calibration, but more data collected in the larger arms of the estuary would increase confidence in model performance.

Modelled salinity was calibrated against measured salinity in the Opotoru and the Waitetuna arms of the harbour. Plots of hourly flow rate from the Waingaro and Waitetuna Rivers (Figure 3.1) over the calibration period are shown in Figure 5.11. This illustrates when the main high river flow events occurred during this model period. There were two notable high river flow events during the deployment period on 16 and 22 Nov 2015.

For this calibration, the model was started on 12 October 2015 allowing 3 weeks of spin up time to allow the salinity in the harbour to reach equilibrium. Comparisons between measured and modelled salinity at the two instrument deployment locations are shown in Figure 5.12 and Figure 5.13 and calibration metrics are presented in Table 5.3. At both locations the tidal modulation of the salinity signal was replicated by the model, and the high river flow events can also be seen in the model output. The variability in salinity is over-predicted by the model at Waitetuna. The model under-predicts salinity variability at the Opotoru site. There appears to be some sensor drift, especially in the surface sensor, in Opotoru and to a lesser degree in the bed sensor at Opotoru and Waitetuna. This is reflected in the γ component of the skill scores. The BSS was highest at Waitetuna (0.73 to 0.94) than at Opotoru (0.58 to 0.74). This may be explained by the smaller Opotoru arm being more poorly resolved in the model than the Waitetuna arm, and also by of the sensor drift at the surface at Opotoru.

The current and sea level data recorded at the Inside and Outside locations were useful for calibration of the model over the mouth of the estuary since strong flood and ebb currents in this region are very sensitive to parameterisation of HEV and bed roughness. Overall the model performed well against these measurements with sea level skill scores showing high α (0.96 and 0.98 for the Inside and Outside locations respectively) and low β (0.00 for both the Inside and Outside locations) indicating good agreement for phase and amplitude between modelled and measured values. For currents, the model performed well inside the entrance although outside on the bar, performance was worse. This is most likely because the currents over the bar are highly turbulent and affected by waves. Furthermore, the bar is highly mobile (Stark *et al*., 2010) and while the currents were recorded in April 2009, the multibeam bathymetric survey of the bar was undertaken in November 2013. However, the currents at

the Outside location showed strong tidal asymmetry with peak current speeds 2 to 3 times as strong on the outgoing tide than on the incoming tide. This feature was reproduced reasonably well in the model.

For the Nortek Aquadopp data collected in February 2008 in the Opotoru arm of the harbour, only the data from locations AQD 1 and AQD 3 were used as the deployment at AQD 2 suffered extreme subsidence which affected the data quality. Sea level and current calibrations are shown in Figure 5.19 and Figure 5.20 respectively. Skill metrics are presented in Table 5.5. The model performed well for sea level at both locations (BSS of 0.97 and 0.91) illustrating that bed friction and HEV were well parameterised in the model, and it correctly simulates the attenuation of the tidal signal into this arm of the harbour. The currents at AQD 1 were also well represented by the model although at AQD 3 the measured current speeds were highly variable and this was not picked up in the model. Plots of peak flood and ebb currents are presented in Figure 5.18.

The downward looking ADCP transects from 14 April 2014 were converted to depth averaged speed and direction and compared to modelled currents. All of the tracks covered by this survey are shown in Figure 5.23. Separate calibration plots are shown for each of the transects and are presented in Appendix C. They provide a valuable overview of the models ability to replicate observed currents throughout the harbour mouth and over the bar. Skill metrics were not calculated for these transects, rather the images provide a qualitative overview of model performance. Broadly, the model performs well for most of the transects with the exception of one (Transect 1) where the current speed is over predicted by the model by a factor of approximately 2 over the ebb tidal bar.

Finally, the model was compared with two tide gauges located at Manu Bay outside the harbour and the Raglan Wharf located inside the harbour. These are particularly valuable since unlike the other sea level gauges, these are referenced to vertical datums (Moturiki vertical datum). The sea level comparisons for Manu Bay and Raglan Wharf are shown in Figure 5.21 and Figure 5.22 respectively and the skill metrics are presented in Table 5.6. In the model the sea levels are referenced to MLOS which is 0.15 m above Moturiki vertical datum, as discussed in Section 4.2. The amplitude and phase of the model fits well with the measured record, and this is reflected in the BSS, α and β values. The Raglan Wharf calibration achieves a γ of 0.00 indicating that there is very little bias in the modelled water level inside the harbour. However, at Manu Bay the linear regression indicates that there is a 0.17 m offset between the Manu Bay tide gauge and the modelled sea level which is reflected in the γ score of 0.04.

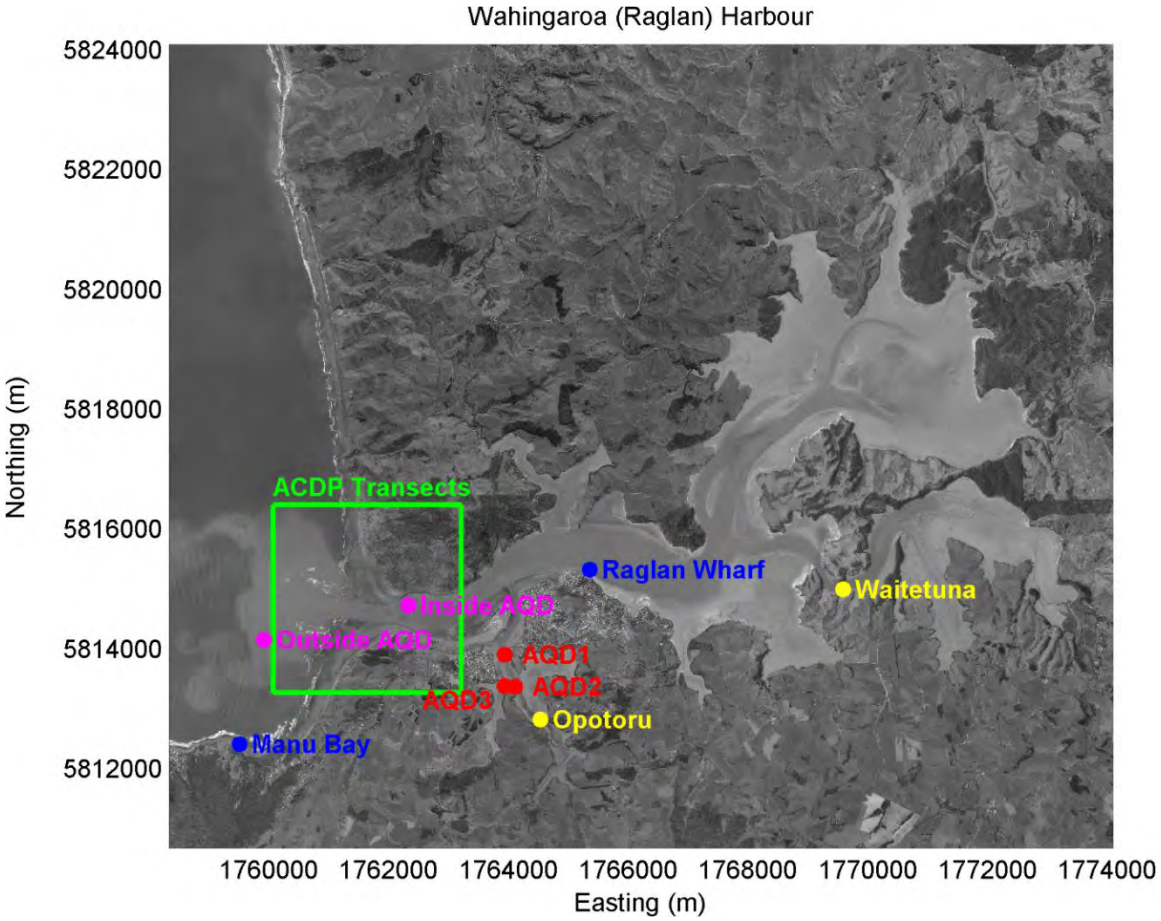

Figure 5.10: Measurement locations for datasets used in the calibration of the hydrodynamic model of Whaingaroa Harbour.

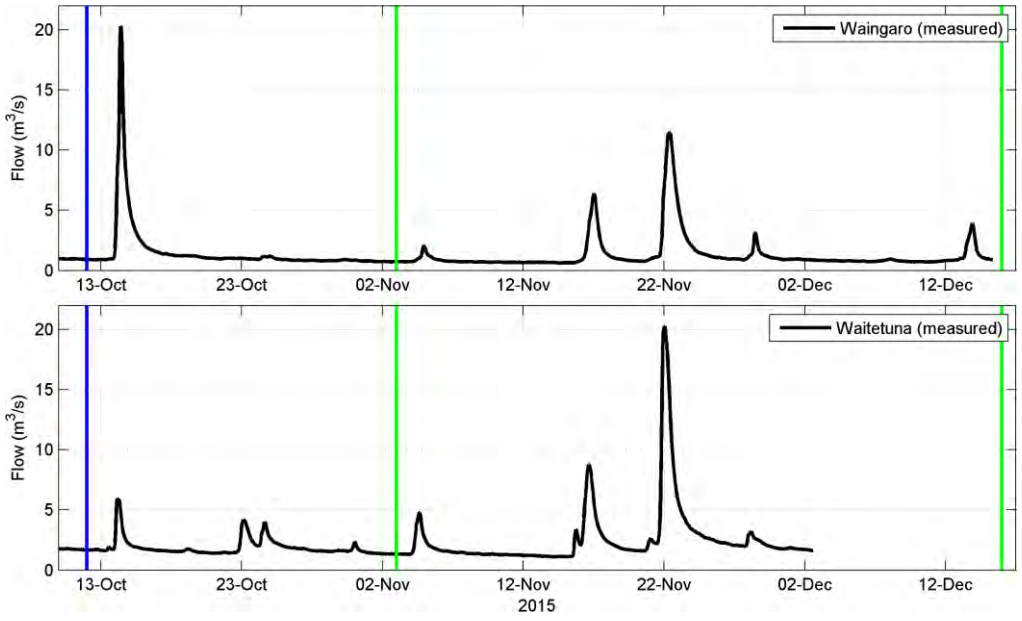

Figure 5.11: Hourly flow from Waingaro (upper panel) and Waitetuna (lower panel) flow gauges (see Figure 3.1) during the period when salinity data were collected in Whaingaroa Harbour. The blue line indicates the start time of the model run for this model calibration and the green lines indicate the start and end times of the collection of salinity data.

Table 5.3: Skill and accuracy metrics for salinity measurements in the Waitetuna and Opotoru Arms of Whaingaroa Harbour.

Variable	Briar Skill Score (BSS)	α	β	γ	R^2	RMSE
Salinity (Waitetuna: Mean)	0.92	0.87	0.65	0.01	0.87	2.8 psu
Salinity (Waitetuna: Surface)	0.94	0.81	0.21	0.29	0.81	2.9 psu
Salinity (Waitetuna: Bed)	0.73	0.83	1.62	0.77	0.83	4.0 psu
Salinity (Opotoru: Mean)	0.69	0.68	0.02	1.13	0.69	8.7 psu
Salinity (Opotoru: Surface)	0.58	0.57	0.00	3.6	0.57	11.9 psu
Salinity (Opotoru: Bed)	0.74	0.69	0.06	0.36	0.69	7.2 psu

Table 5.4: Skill and accuracy metrics for sea level and current measurements at two locations around the Whaingaroa harbour mouth.

Variable	Briar Skill Score (BSS)	α	β	γ	R^2	RMSE
Sea Level (Inside)	0.95	0.96	0.00	N/A	0.96	0.17 m
Currents (Inside)	0.89	0.75	0.11	0.13	0.75	0.24 m s^{-1}
Sea Level (Outside)	0.98	0.98	0.00	N/A	0.98	0.12 m
Currents (Outside)	0.62	0.39	0.29	0.16	0.39	0.07 m s^{-1}

Table 5.5: Skill and accuracy metrics for sea level and current measurements at two locations in the Opotoru arm of Whaingaroa harbour.

Variable	Briar Skill Score (BSS)	α	β	γ	R^2	RMSE
Sea Level (AQD 1)	0.97	0.98	0.01	N/A	0.98	0.11 m
Currents (AQD 1)	0.87	0.67	0.01	0.38	0.67	0.11 m s^{-1}
Sea Level (AQD 3)	0.91	0.91	0.00	N/A	0.91	0.23 m
Currents (AQD 3)	0.72	0.11	0.11	0.25	0.11	0.14 m s^{-1}

Table 5.6: Skill and accuracy metrics for sea level recorded by tide gauges at Manu Bay and the Raglan Wharf.

Variable	Briar Skill Score (BSS)	α	β	γ	R^2	RMSE
Sea Level (Manu Bay)	0.95	0.99	0.00	0.04	0.99	0.19 m
Sea Level (Raglan Wharf)	0.99	0.99	0.00	0.00	0.99	0.09 m

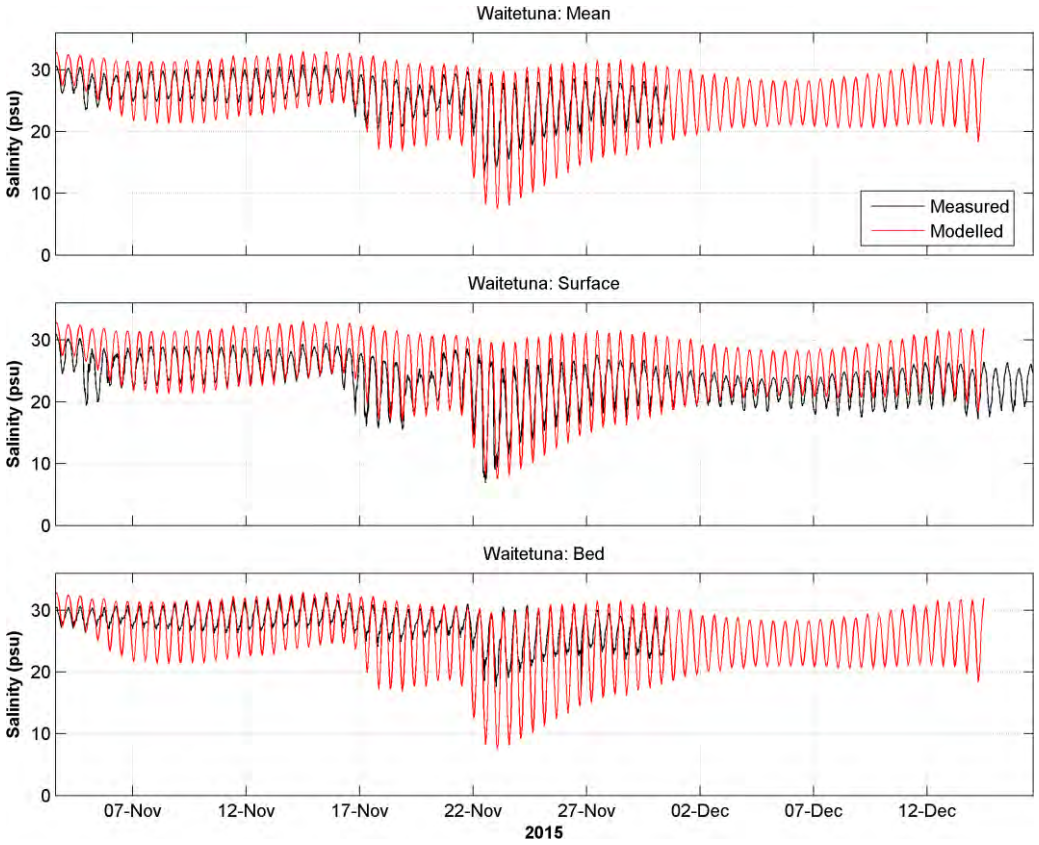

Figure 5.12: Salinity calibration in the Waitetuna arm of Whaingaroa Harbour.

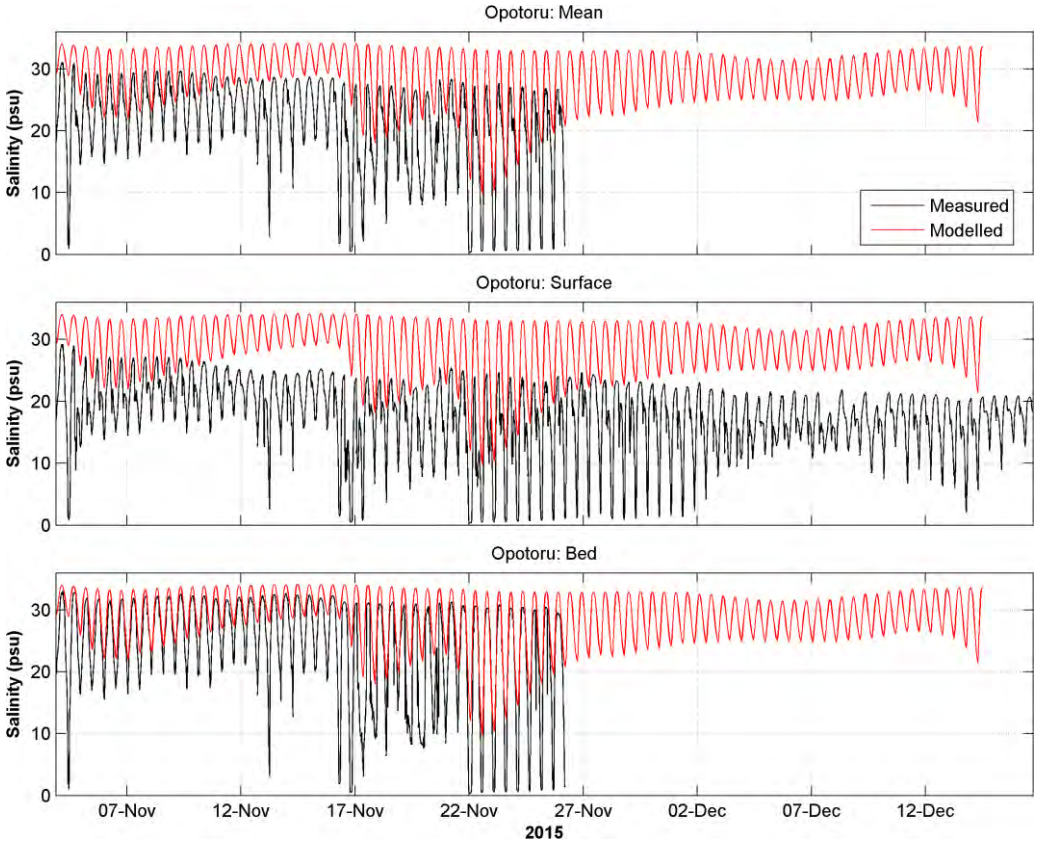

Figure 5.13: Salinity calibration in the Opotoru arm of Whaingaroa Harbour.

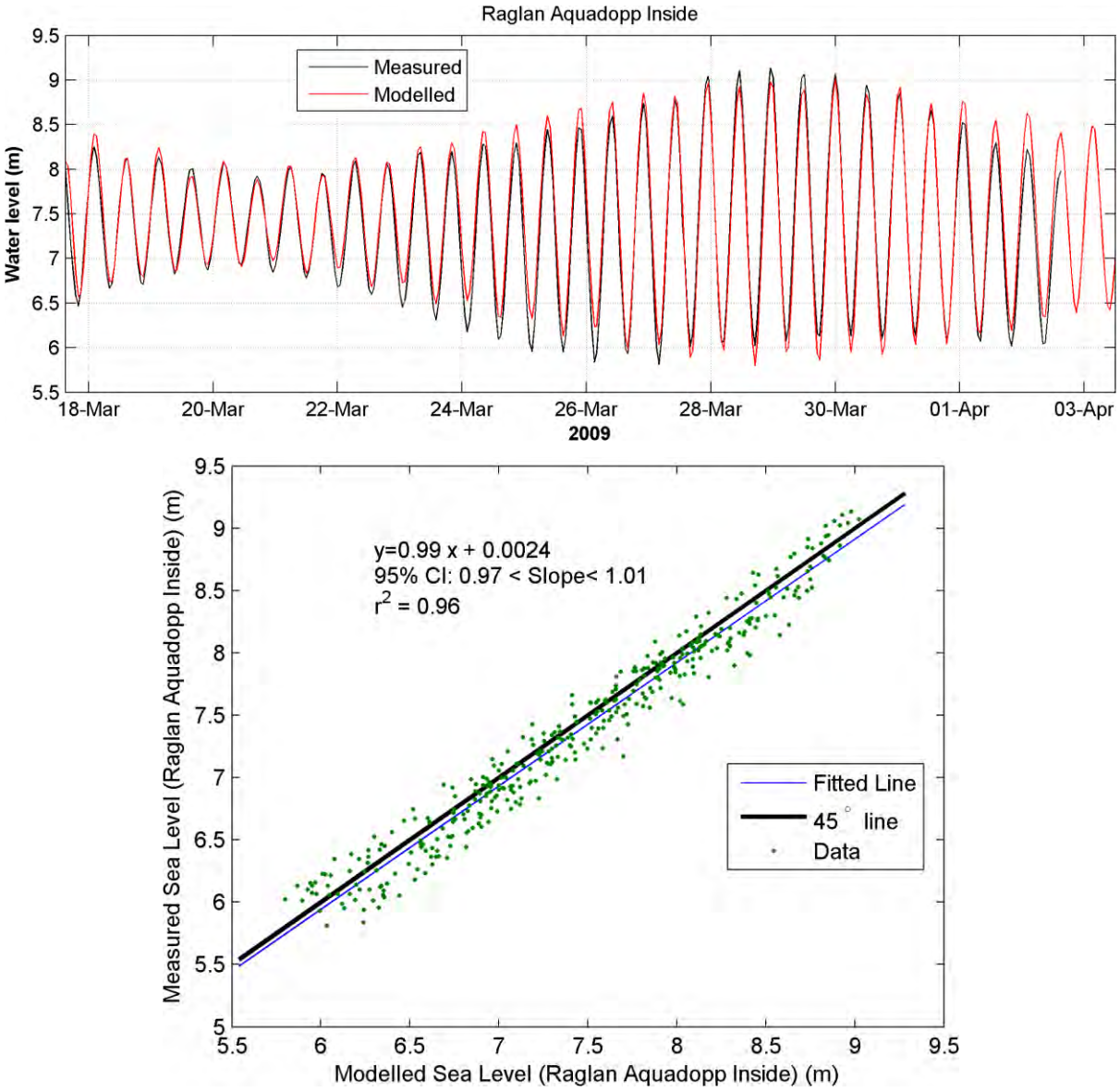

Figure 5.14: Sea level calibration at the 'Inside' location in Whaingaroa Harbour as a time series (upper panel) and as a linear regression (lower panel).

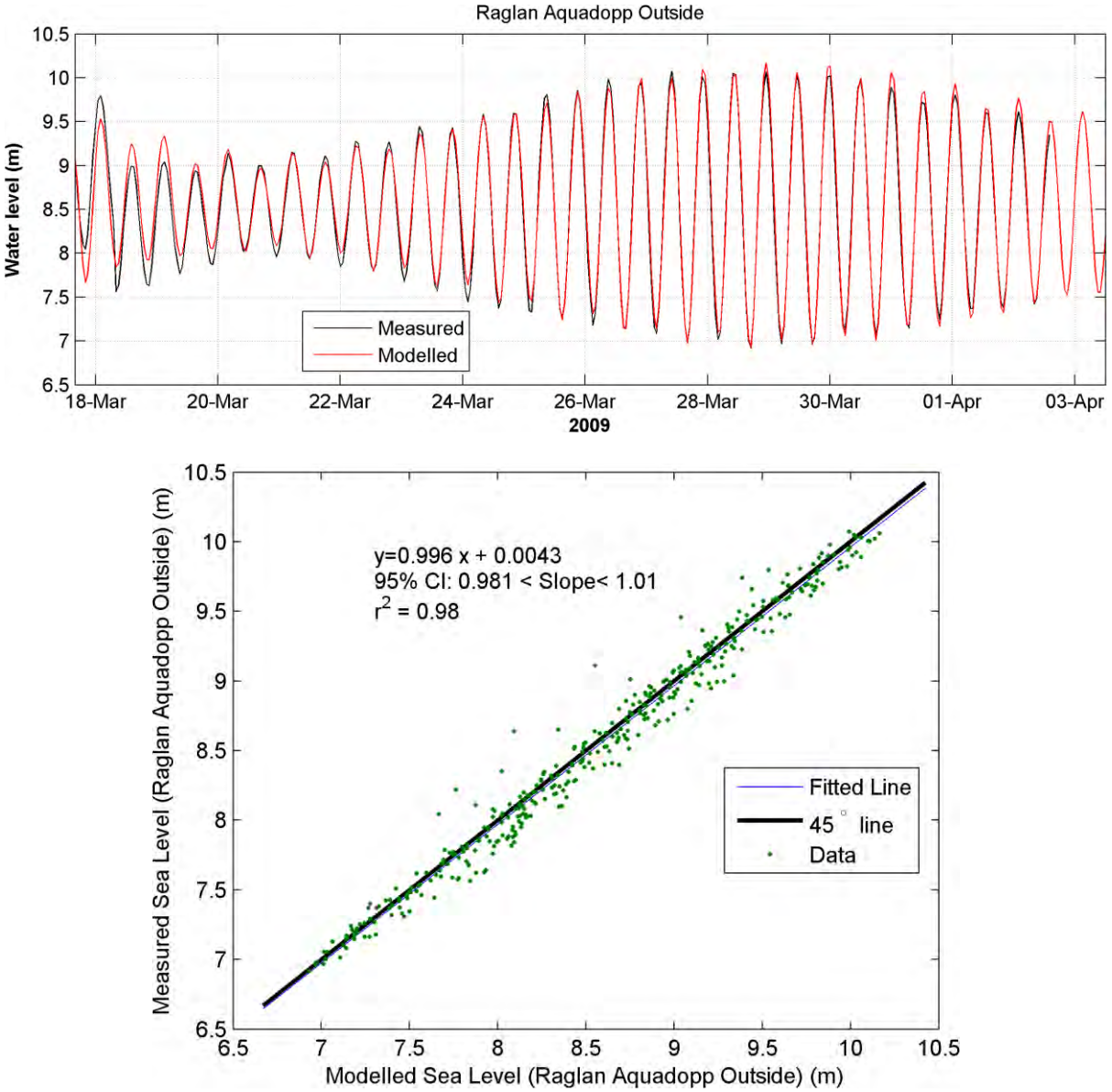

Figure 5.15: Sea level calibration at the 'Outside' location in Whaingaroa Harbour as a time series (upper panel) and as a linear regression (lower panel).

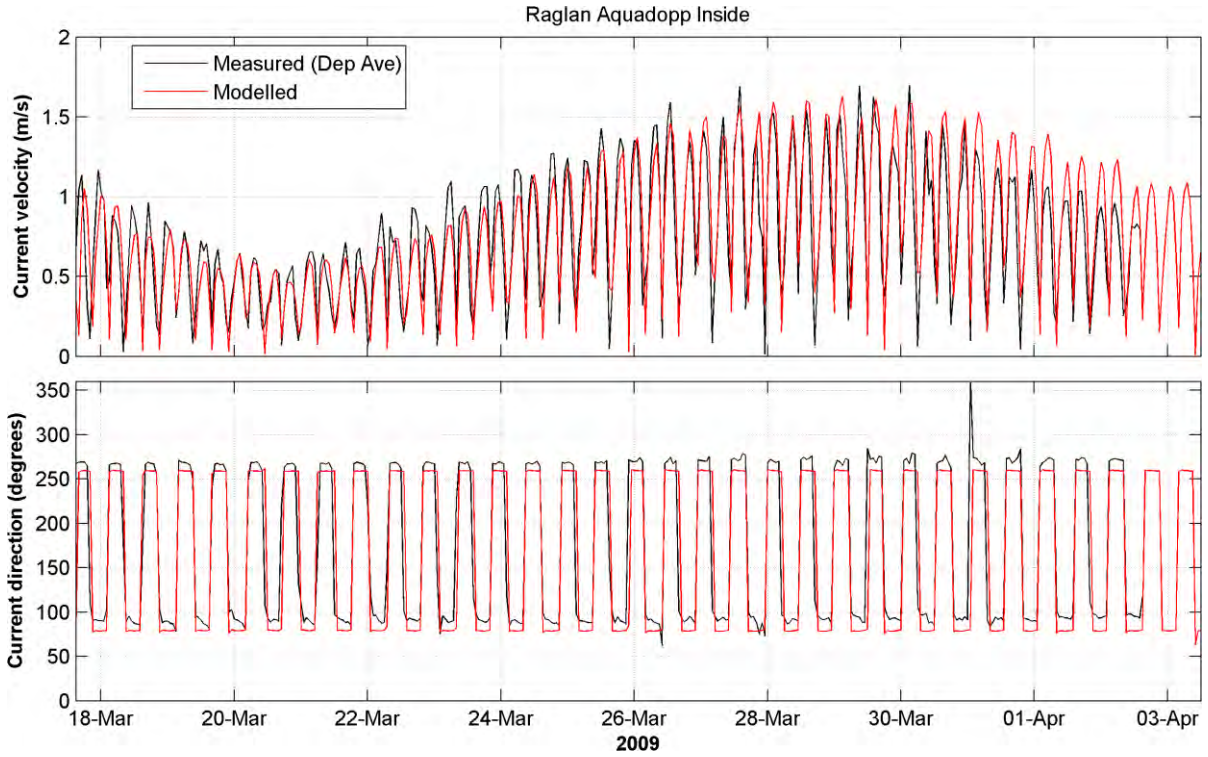

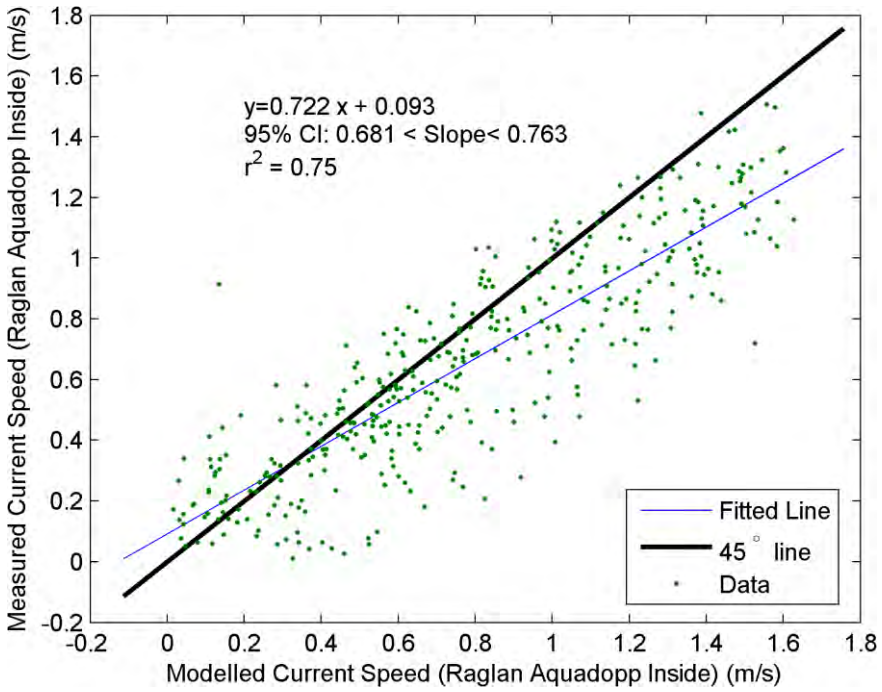

Figure 5.16: Currents calibration at the 'Inside' location in Whaingaroa Harbour as a time series (upper panel) and as a linear regression (lower panel).

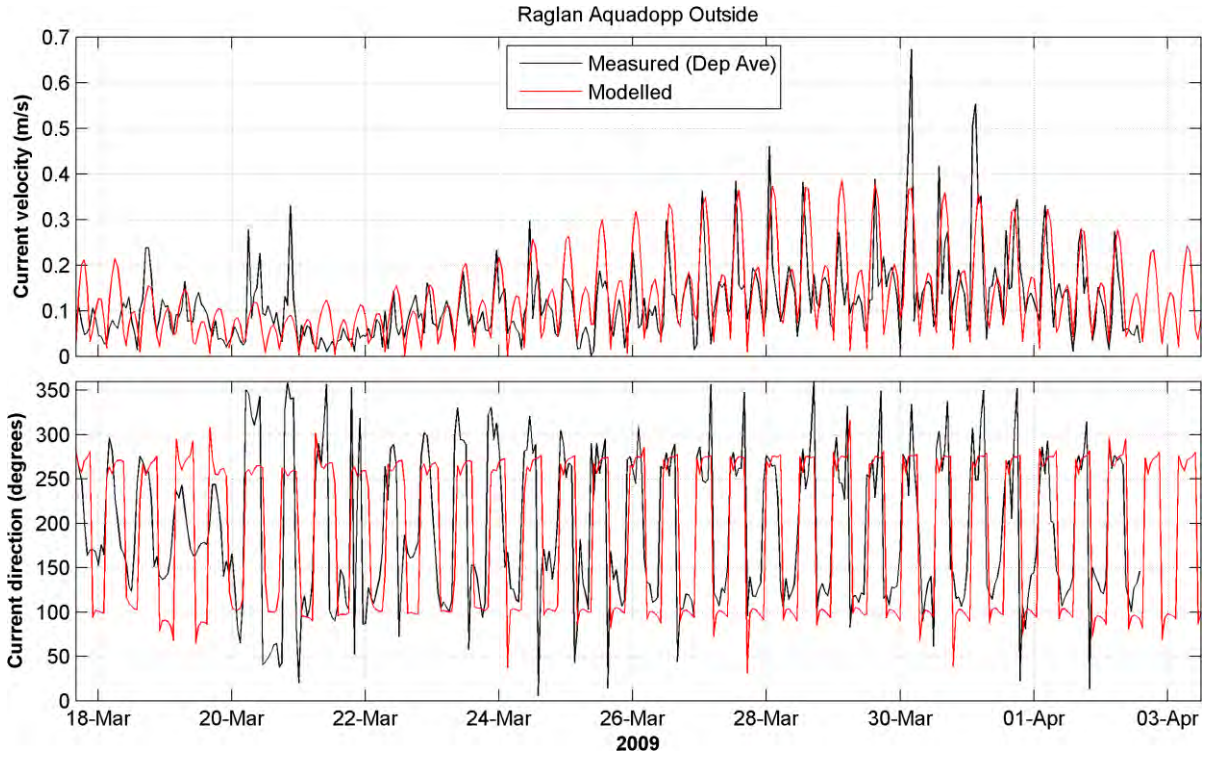

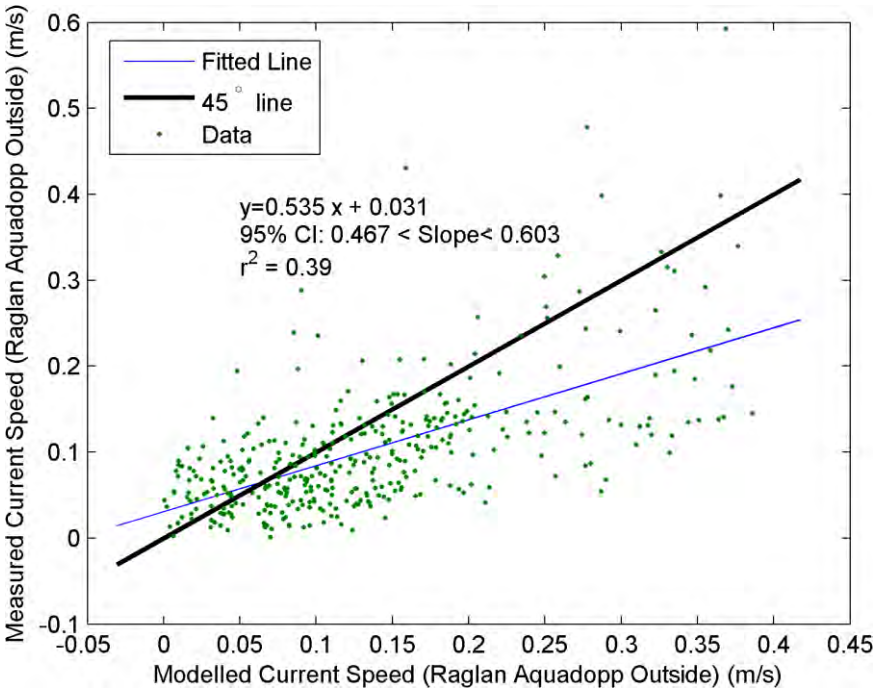

Figure 5.17: Currents calibration at the 'Outside' location in Whaingaroa Harbour as a time series (upper panel) and as a linear regression (lower panel).

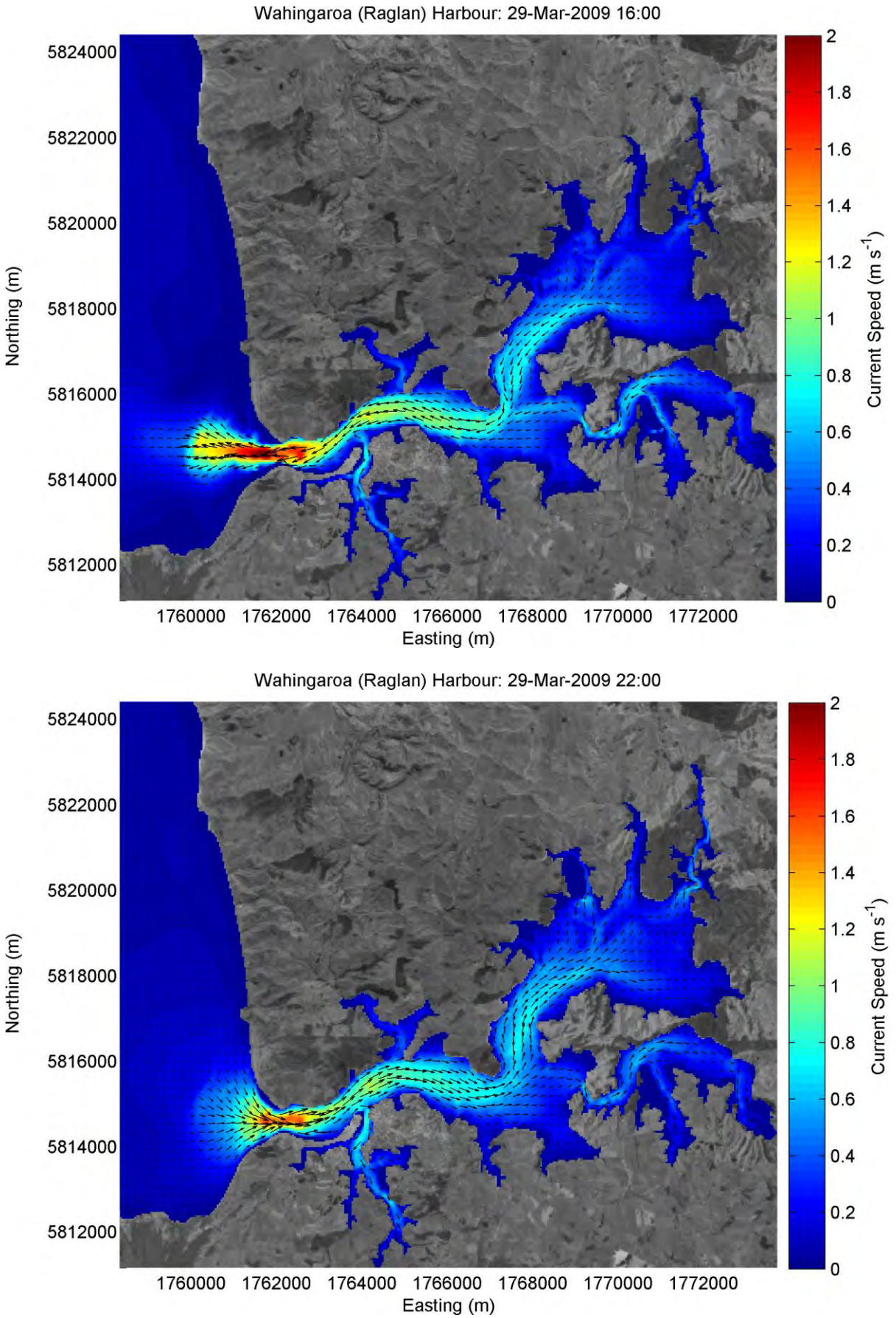

Figure 5.18: Whaingaroa Estuary peak flood (upper panel) and ebb (lower panel) currents.

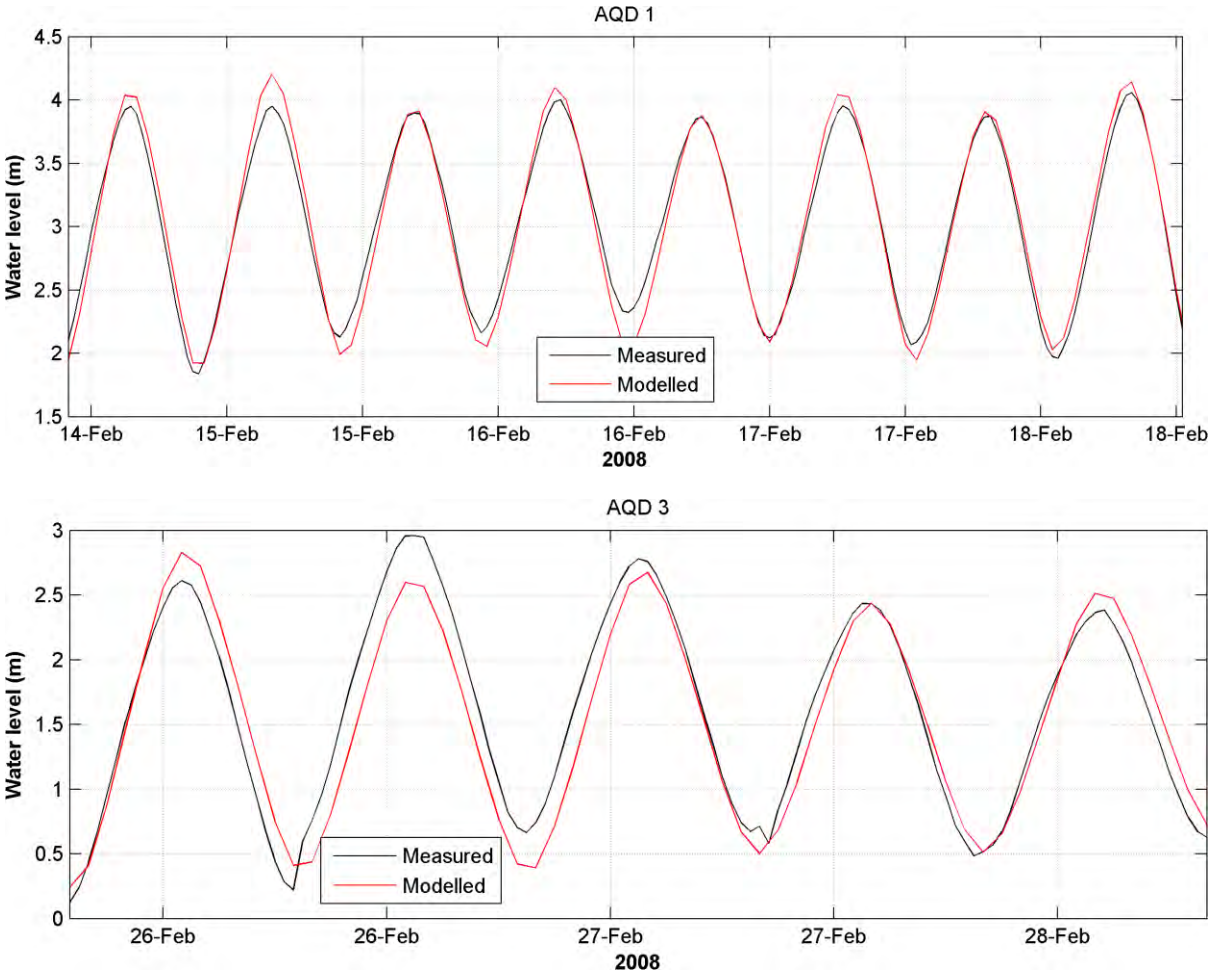

Figure 5.19: Sea level calibration at the 'AQD 1' location (upper panel) and at the 'AQD 2' location (lower panel) in Whaingaroa Harbour.

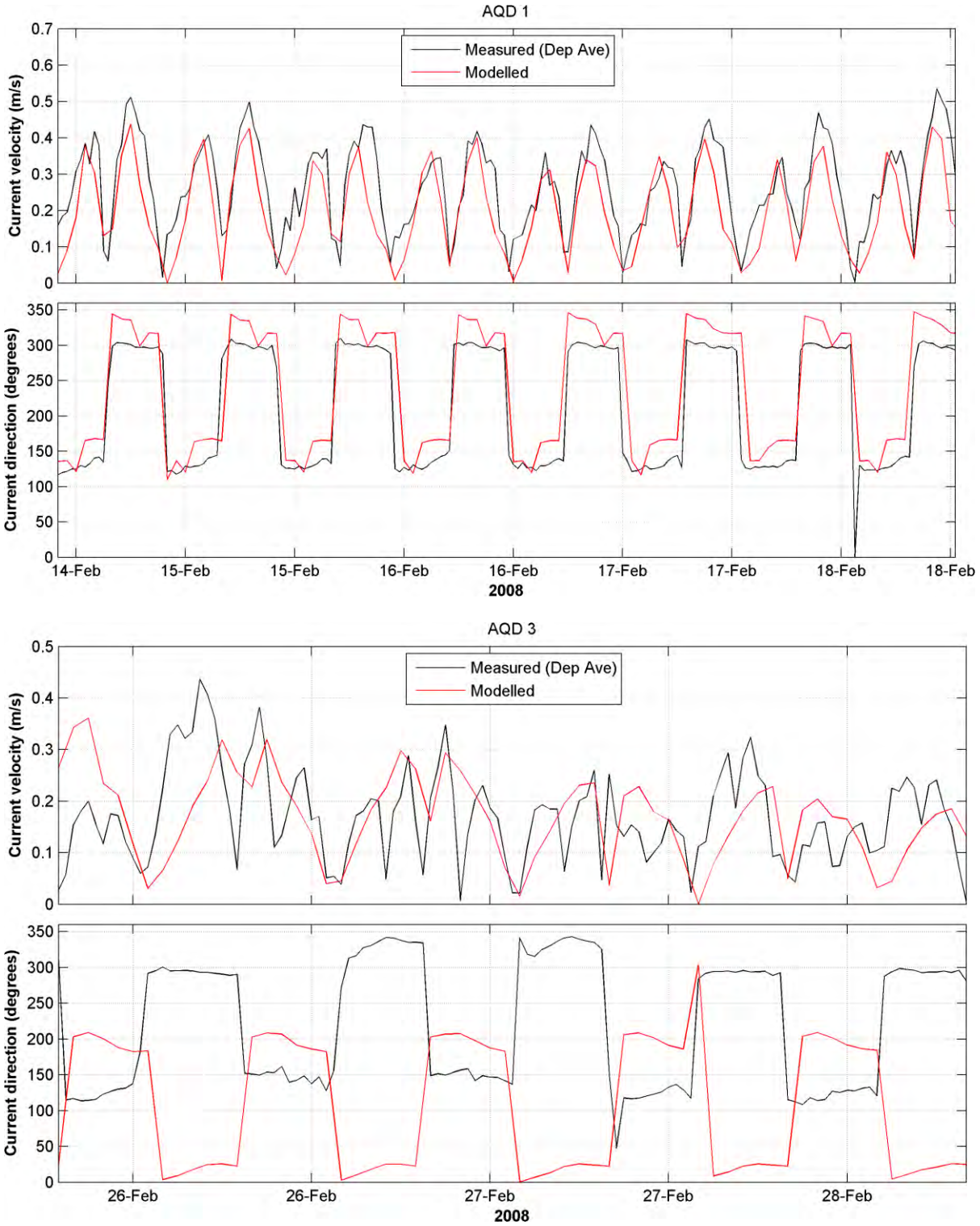

Figure 5.20: Current speed and direction calibration at the 'AQD 1' location (upper panel) and at the 'AQD 2' location (lower panel) in Whaingaroa Harbour.

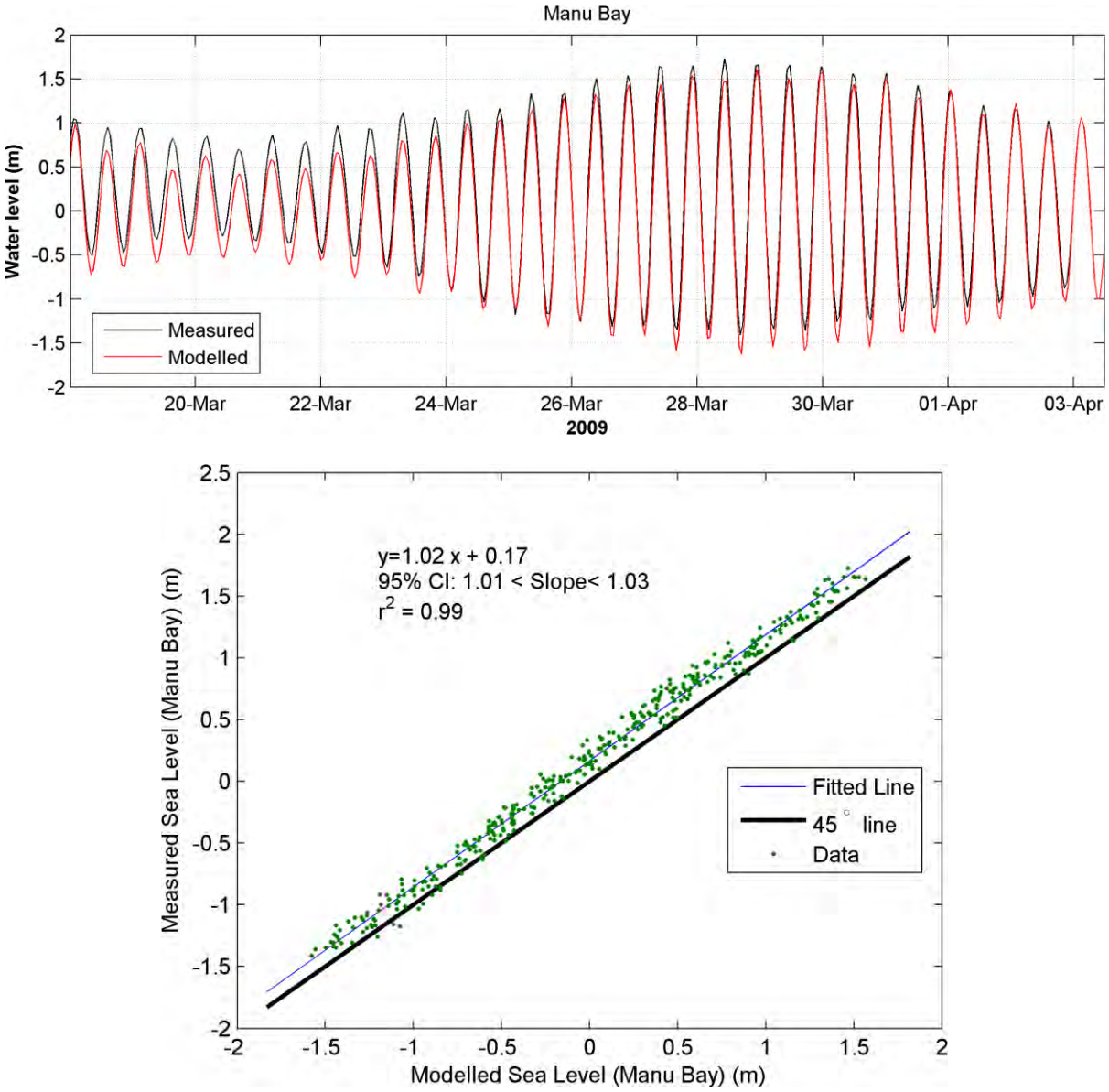

Figure 5.21: Sea level calibration at the Manu Bay tide gauge.

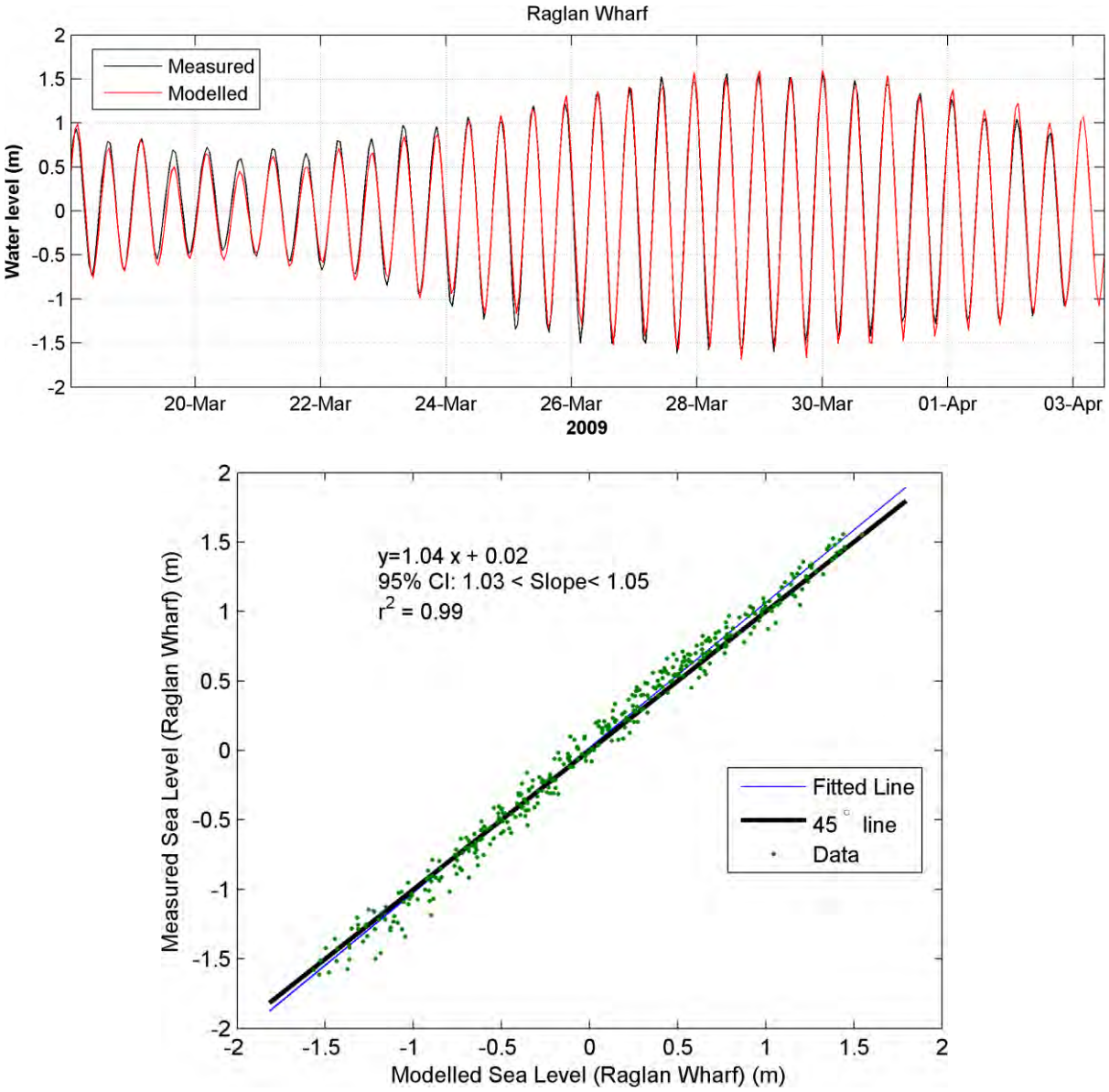

Figure 5.22: Sea level calibration at Raglan Wharf tide gauge.

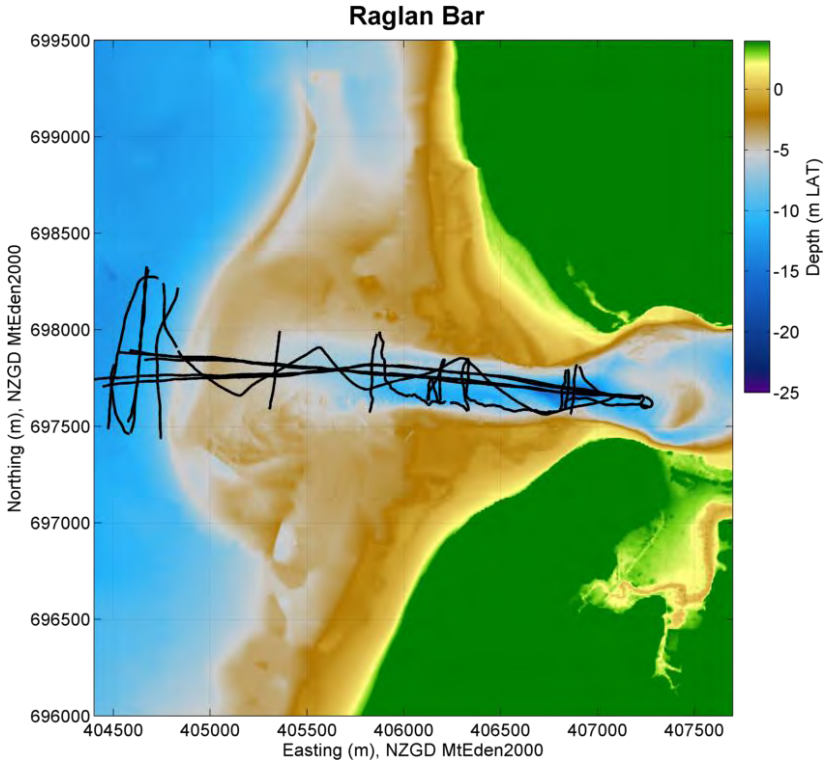

Figure 5.23: The tracks of the downward looking ADCP profiles in Whaingaroa Harbour.

5.3 Aotea Harbour

Aotea Harbour has not historically been the subject many scientific studies. However, an MSc thesis by Willet (1983) presented physical observations focusing on the morphology of the estuary and highlighted the morphological mobility of the sand spit, particulary at the harbour mouth.

As part of the fieldwork component of the present study, sea level, current and salinity data were collected at 2 locations within the harbour. The instrument deployment locations are shown in Figure 5.24. There is relatively little infrastructure around Aotea, and for health and safety reasons finding suitable locations for deploying instruments was more challenging here than in the other estuaries. Consequently, the Upper deployment location was up inside the Pakoka River and was not suitable for model calibration at this resolution. However, the instrument deployment at the Lower location was in the main channel of the harbour and therefore is suitable for model calibration. The sea level, current and salinity calibration plots are shown in Figure 5.25, Figure 5.26 and Figure 5.28 respectively. Skill metrics are presented in Table 5.7. It should be noted that the current meter became engulfed by a large sand wave 3 weeks into the deployment although the recorded data is sufficient for assessing model performance at this location. Comparison between measured and modelled data at a single

location represents reasonably sparse dataset for model calibration, and that this is something that could be improved upon in future.

The model performed well against measured sea level using all measurement statistics: BSS = 0.97 α = 0.98 and β = 0. This indicates that the phase and amplitude of the modelled output is in good agreement with the measured data.

Currents speeds in the model were broadly consistent with the measured data with the phase (α = 0.78) of the tidal oscillations being similar to measured values. Maximum current speeds were also similar to measured values as was spring neap variability in current speed. However, during reverses in tidal direction, modelled current speeds remained higher than the almost slack currents in the observed record. Plots of peak flood and ebb currents are presented in Figure 5.27.

The measured data from the surface salinity gauge also showed signs of drift past 7 November and therefore the bottom salinity gauge measurements are more reliable and more appropriate for comparison with the model. The modelled salinity record showed tidal modulation in line with that of the measured data although the magnitude was consistently less than that in the observed record and this is reflected in the model skill scores (α = 0.74, β = 0.3 and γ=1.43). Since none of the major catchments in Aotea harbour are gauged there is uncertainty around the fresh water inputs into the model.

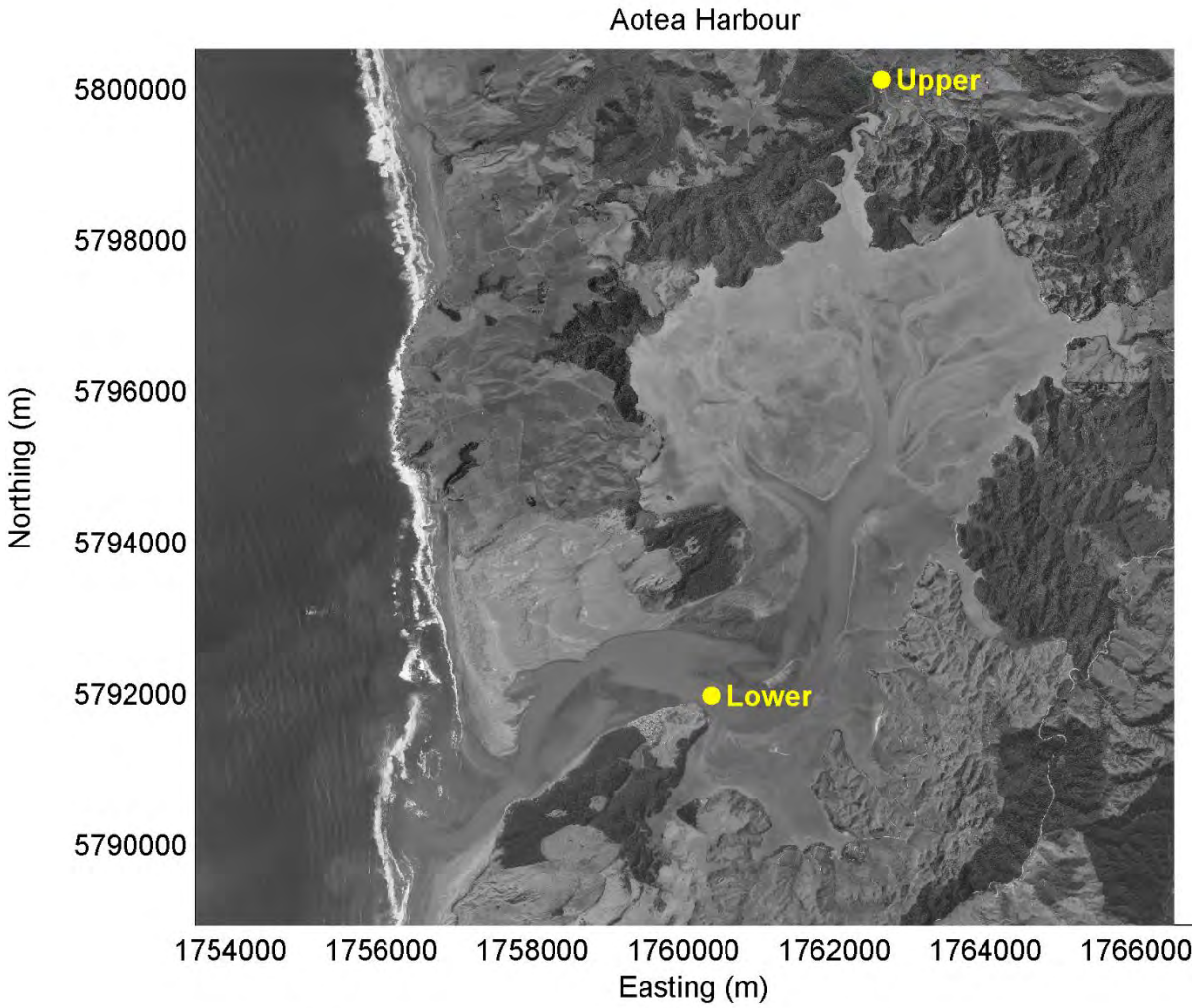

Figure 5.24: Aotea Harbour instrument deployment locations.

Table 5.7: Skill scores for the Aotea Harbour calibrations.

Variable	Briar Skill Score (BSS)	α	β	γ	R^2	RMSE
Sea Level (Lower)	0.97	0.97	0.00	N/A	0.97	0.13 m
Currents (Lower)	0.94	0.78	0.03	0.16	0.78	0.16 m s^{-1}
Salinity (Lower: Mean)	0.15	0.31	0.15	2.03	0.31	3.24 psu
Salinity (Lower: Surface)	0.09	0.15	0.08	1.76	0.15	5.21 psu
Salinity (Lower: Bed)	0.33	0.74	0.30	1.43	0.74	1.46 psu

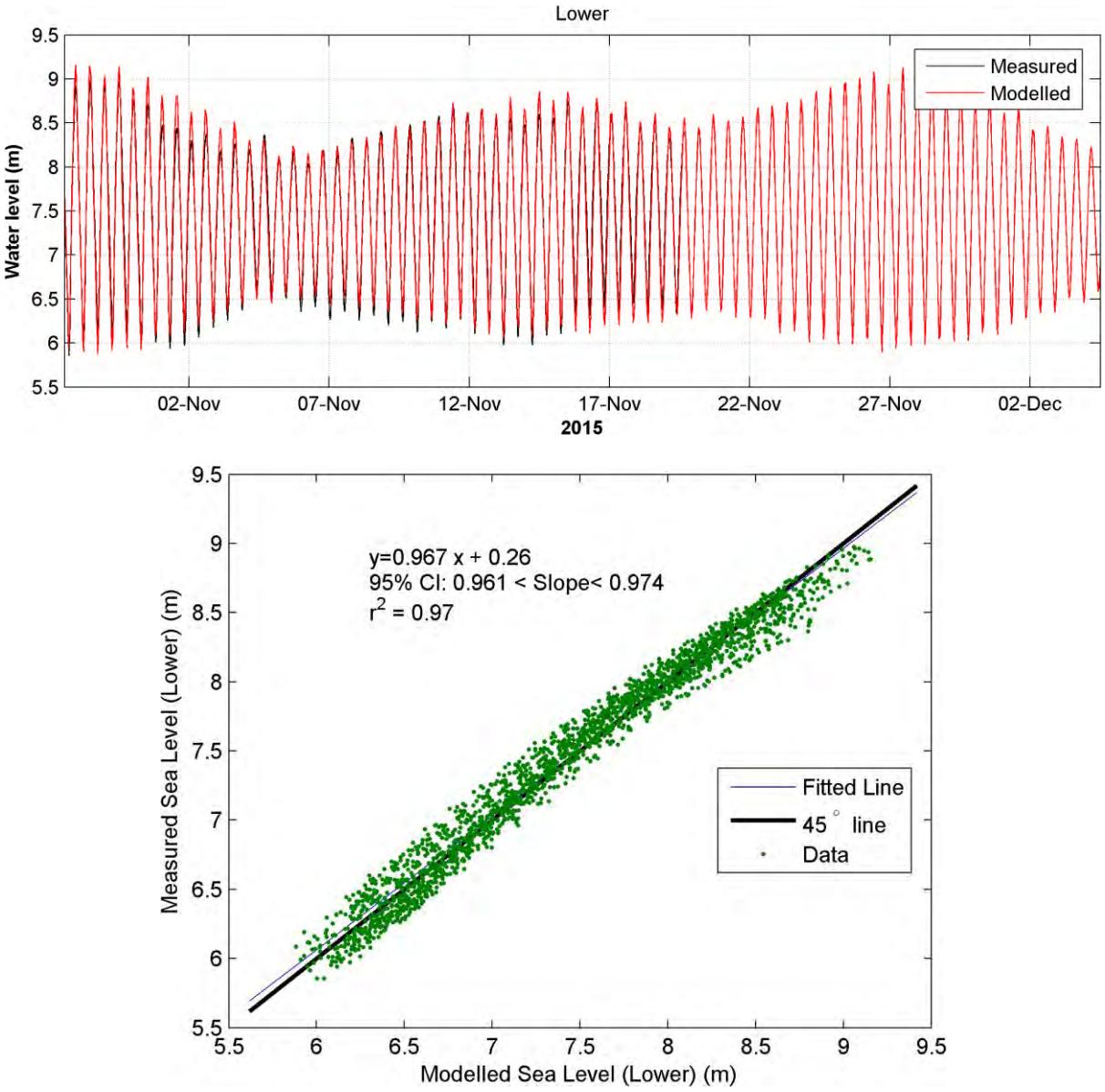

Figure 5.25: Aotea Harbour sea level calibration at the Lower deployment location as a time series (upper panel) and as a linear regression (lower panel).

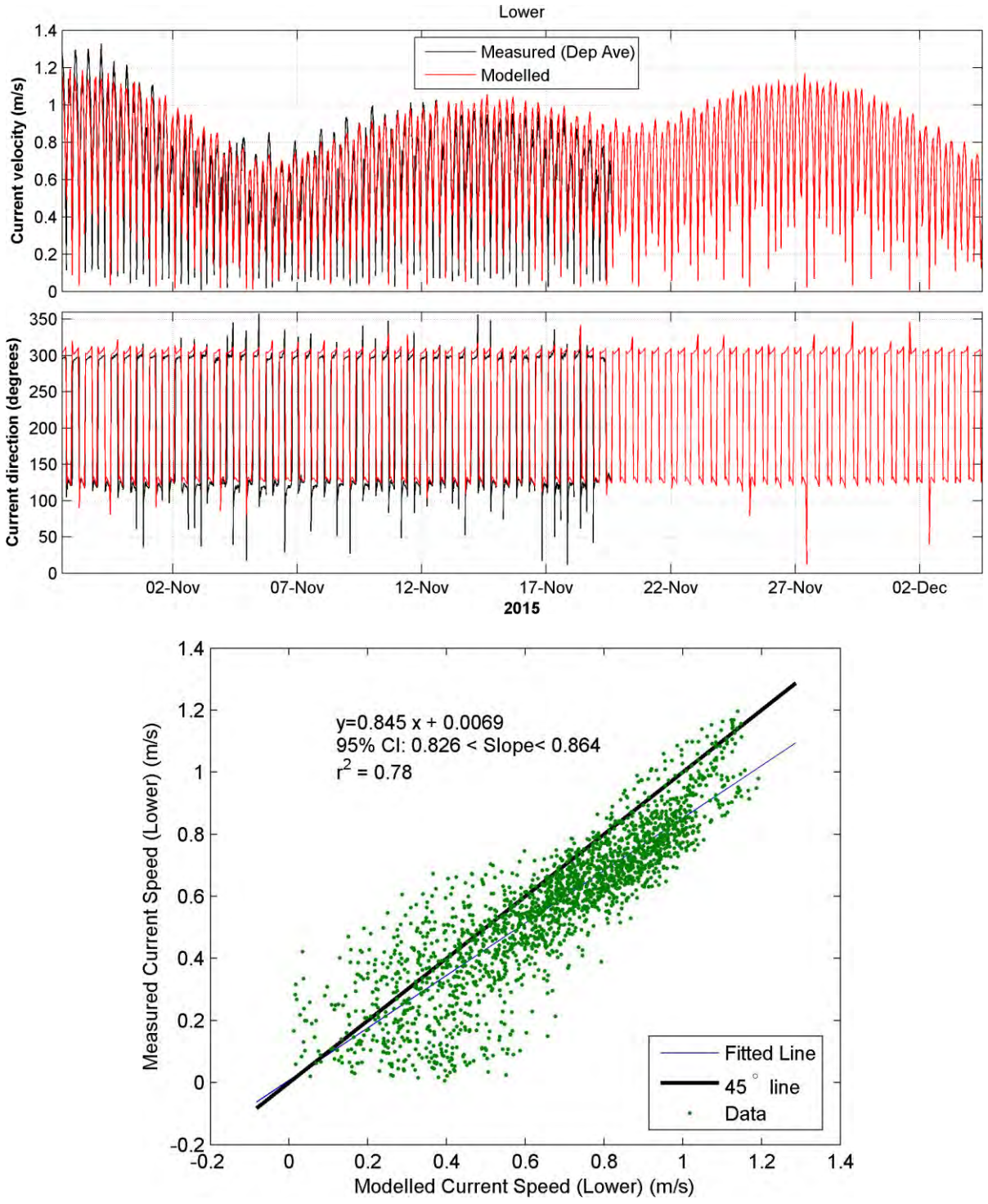

Figure 5.26: Aotea Harbour current calibration at the Lower deployment location as a time series (upper panel) and as a linear regression of modelled versus measured current speed (lower panel).

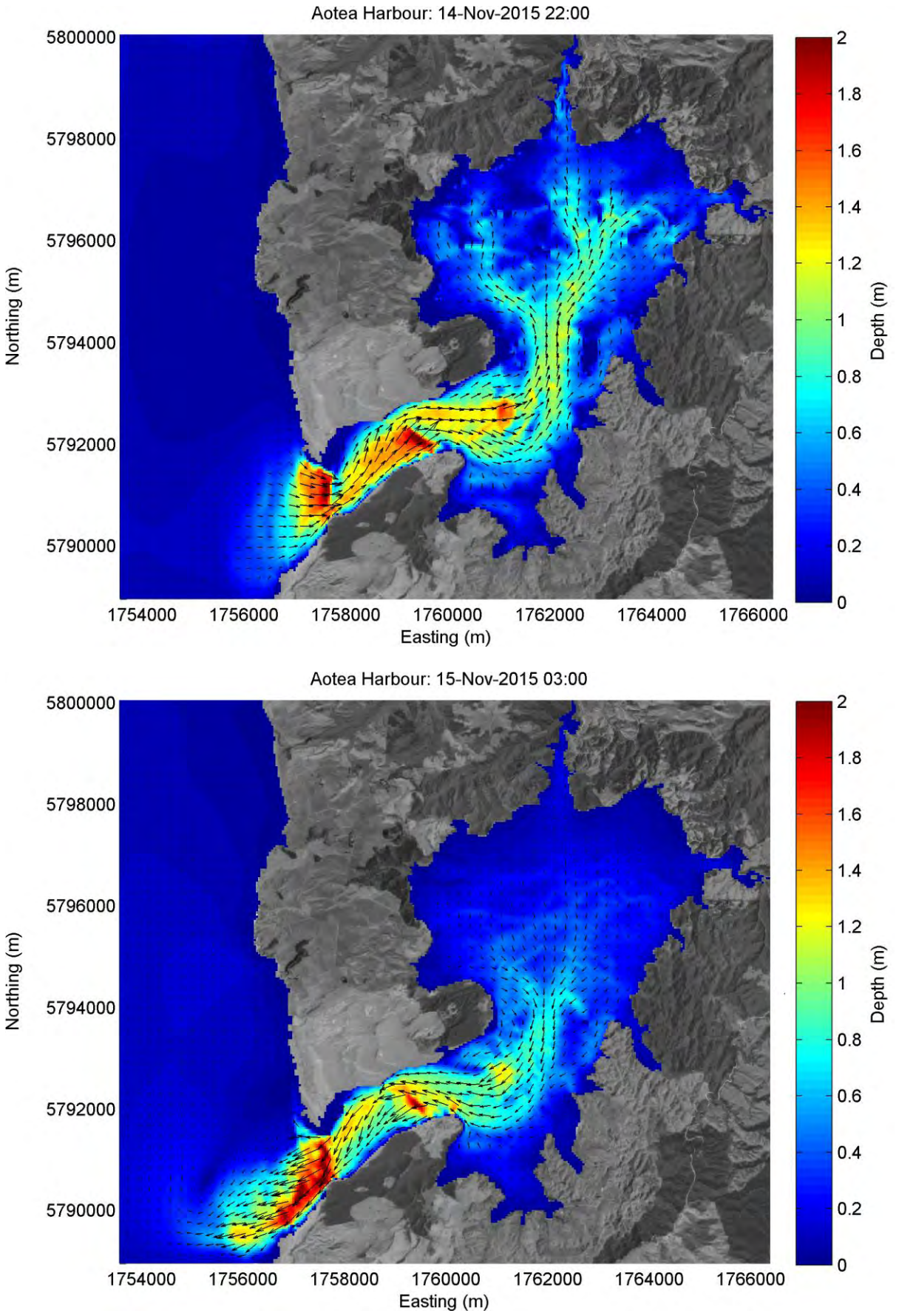

Figure 5.27: Aotea Estuary peak flood (upper panel) and ebb (lower panel) currents.

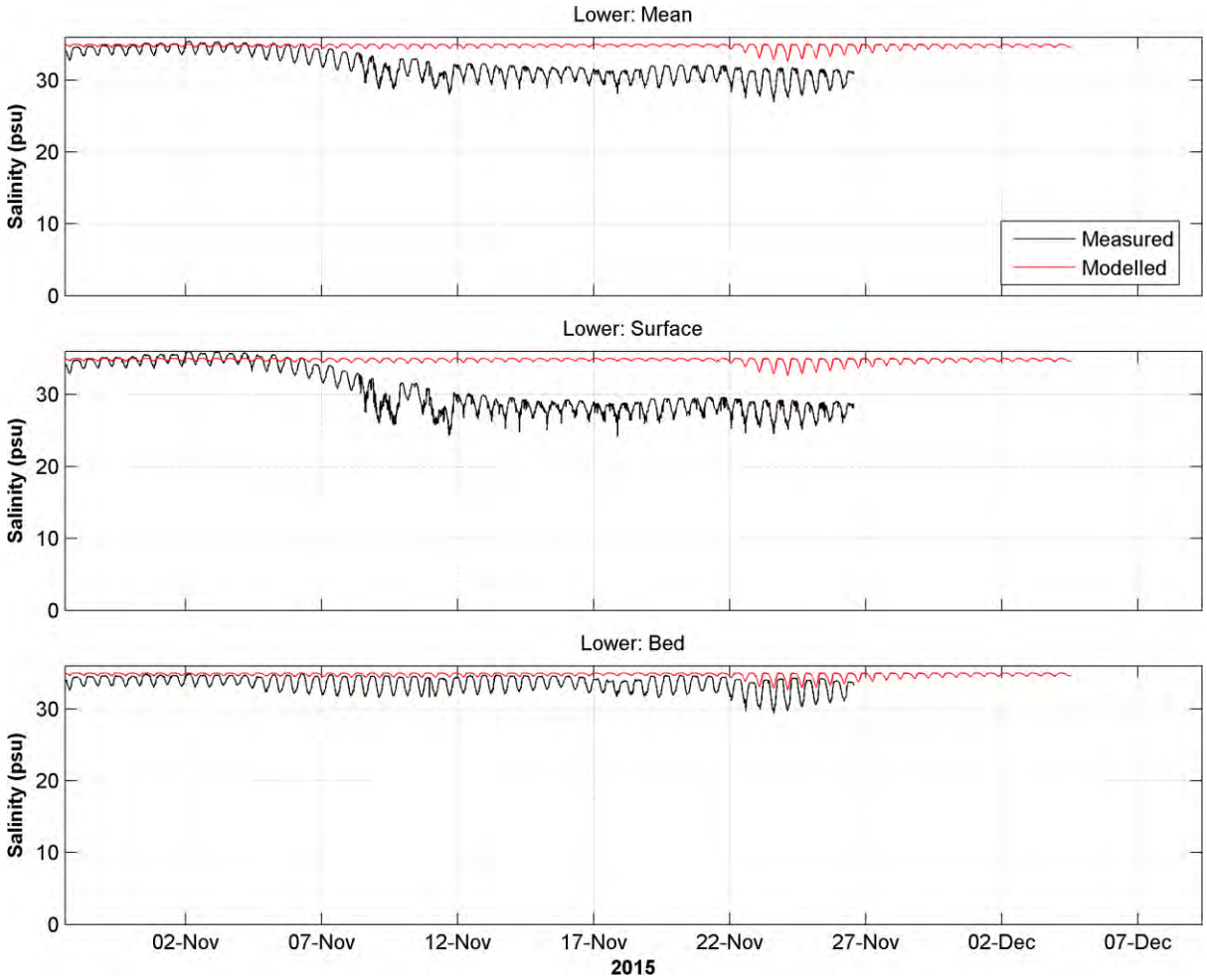

Figure 5.28: Aotea Harbour salinity calibration at the Lower deployment location.

5.4 Kawhia Harbour

The Kawhia Harbour model was calibrated against sea level, current and salinity data recorded at two locations in the estuary (Atkin *et al*., 2015). The locations of the instruments (Township and Te Waitere) are shown in Figure 5.29. Time series comparison between modelled and measured sea level, current and salinity data are shown in Figure 5.31, Figure 5.34 and Figure 5.37 for Township and Figure 5.32, Figure 5.35 and Figure 5.38 for Te Waitere. The model was also compared with sea level data recorded by the Kawhia Wharf tide gauge (Figure 5.33). Model performance statistics are shown in Table 5.8 for sea level and currents and Table 5.9 for salinity.

The estuary is strongly dominated by tides and at the 3 locations where sea level was recorded, the model performed well accurately predicting the phase and amplitude of spring and neap tides. All locations scored BSS ≥ 0.97, $\alpha = 0.98$, and $\beta = 0$.

Measured currents at township and Te Waitere are approximately twice as fast on the outgoing tide than on the incoming tide during spring tides though this asymmetry is less pronounced on neap tides. The model replicated this asymmetry though to a reduced degree at Te Waitere. The asymmetric effect on currents was not apparent in the model at the township location. However, tidal current speeds were in the correct range and modelled current directions lined up will with those in the measured record. Plots of peak flood and ebb currents are presented in Figure 5.36.

Plots of hourly flow rate from the Awaroa and Oparau Rivers (Figure 2.1) over the calibration period are shown in Figure 5.30. This illustrates when the main high river flow events that occurred during this model periodwhich were on 16 and 22 Nov 2015. Salinity data at the Township location was only available at the surface. The modelled salinity reproduced tidal variability in salinity in the correct range, and also picked up the decreased salinity on 18 November and 23 November (BSS = 0.84, α = 0.71, β = 13, γ =0.15). However, after the second high river flow event the model did not reduce in the model as quickly as it did in the measured data. Salinity data were available at the Te Waitere location at the surface and at the bed although the surface signal appeared to suffer some degradation early in the deployment. The modelled salinity at this location compared well to measured data at the bed although the variability of the modelled signal was less than that in the measured signal (BSS = 0.71, α = 0.32, β = 0.00, γ =0.03). As with the Township location however, the model also picked up the high river flow event on 23 November.

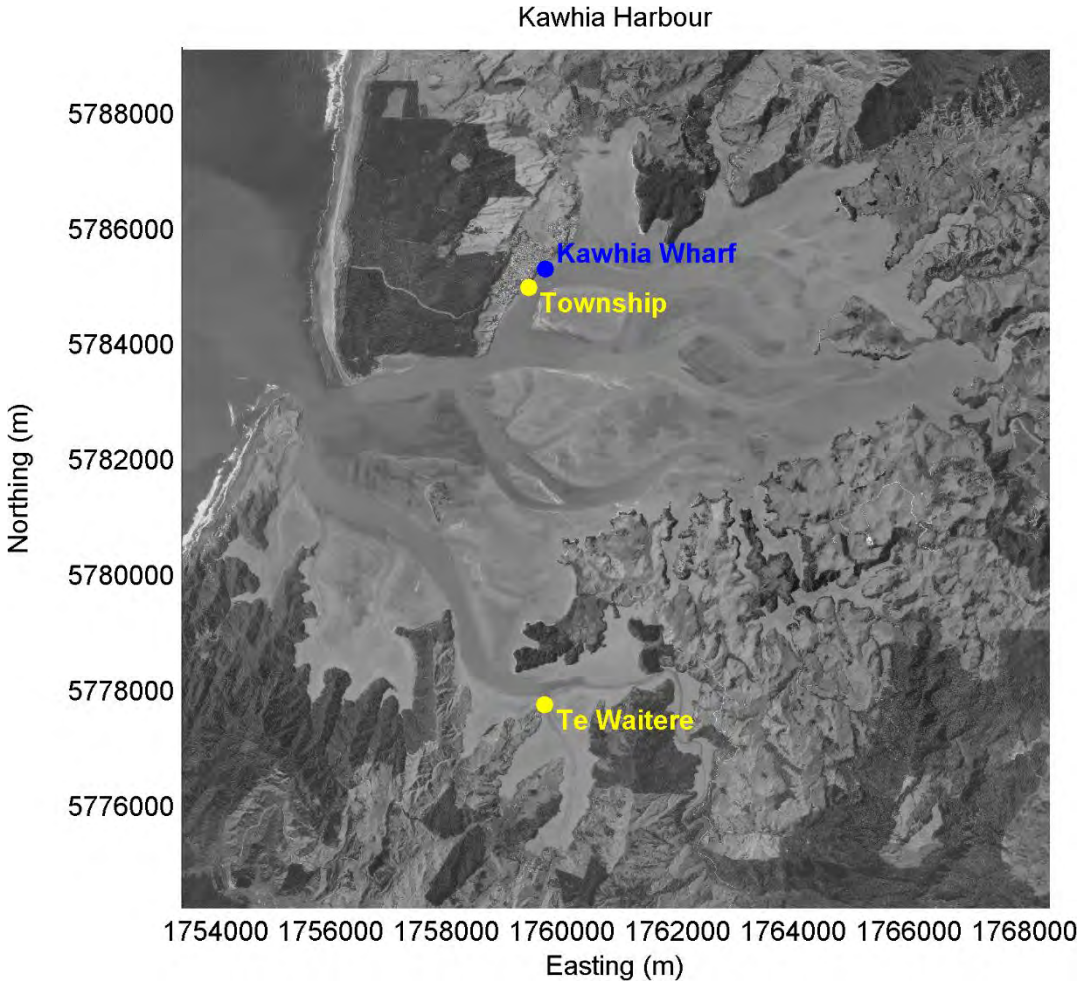

Figure 5.29: Measurement locations for datasets used in the calibration of the hydrodynamic model of Kawhia Harbour.

Table 5.8: Skill scores for the Kawhai Harbour calibrations.

Variable	Briar Skill Score (BSS)	α	β	γ	R^2	RMSE
Sea Level (Township)	0.98	0.98	0.00	N/A	0.98	0.13 m
Sea Level (Te Waitere)	0.98	0.98	0.00	N/A	0.98	0.12 m
Sea Level (Kawhia Wharf)	0.97	0.98	0.00	0.00	0.98	0.14 m s^{-1}
Currents (Township)	0.88	0.66	0.00	0.08	0.66	0.13 m s^{-1}
Currents (Te Waitere)	0.60	0.49	0.11	0.53	0.49	0.16 m s^{-1}

Table 5.9: Skill and accuracy metrics for salinity measurements at Township and Te Waitere in Kawhia Harbour.

Variable	Briar Skill Score (BSS)	α	β	γ	R^2	RMSE
Salinity (Township: Mean)	0.84	0.71	0.13	0.15	0.71	1.53 psu
Salinity (Te Waitere: Mean)	0.61	0.71	0.22	0.66	0.71	3.92 psu
Salinity (Te Waitere: Surface)	0.43	0.66	0.34	0.84	0.66	7.37psu
Salinity (Te Waitere: Bed)	0.71	0.32	0.00	0.03	0.32	1.9 psu

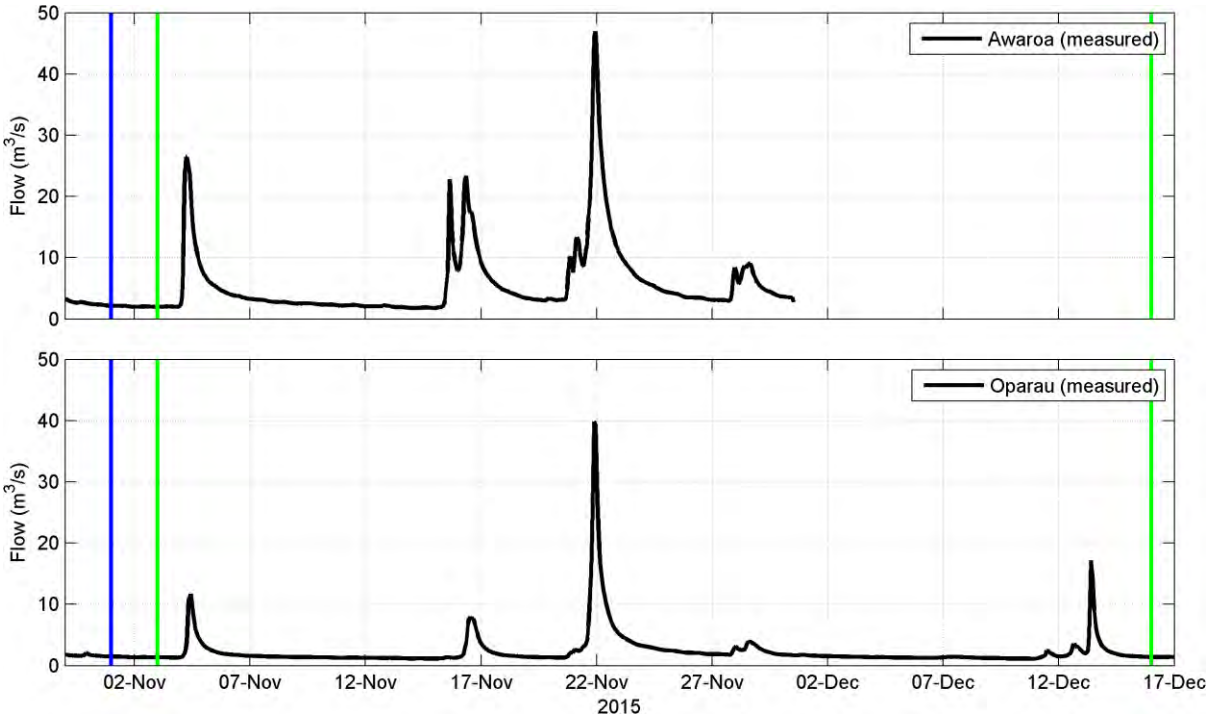

Figure 5.30: Hourly flow from Awaroa (upper panel) and Oparau (lower panel) flow gauges (see Figure 3.1) during the period when salinity data were collected in Kawhai Harbour. The blue line indicates the start time of the model run for this model calibration and the green lines indicate the start and end times of the collection of salinity data.

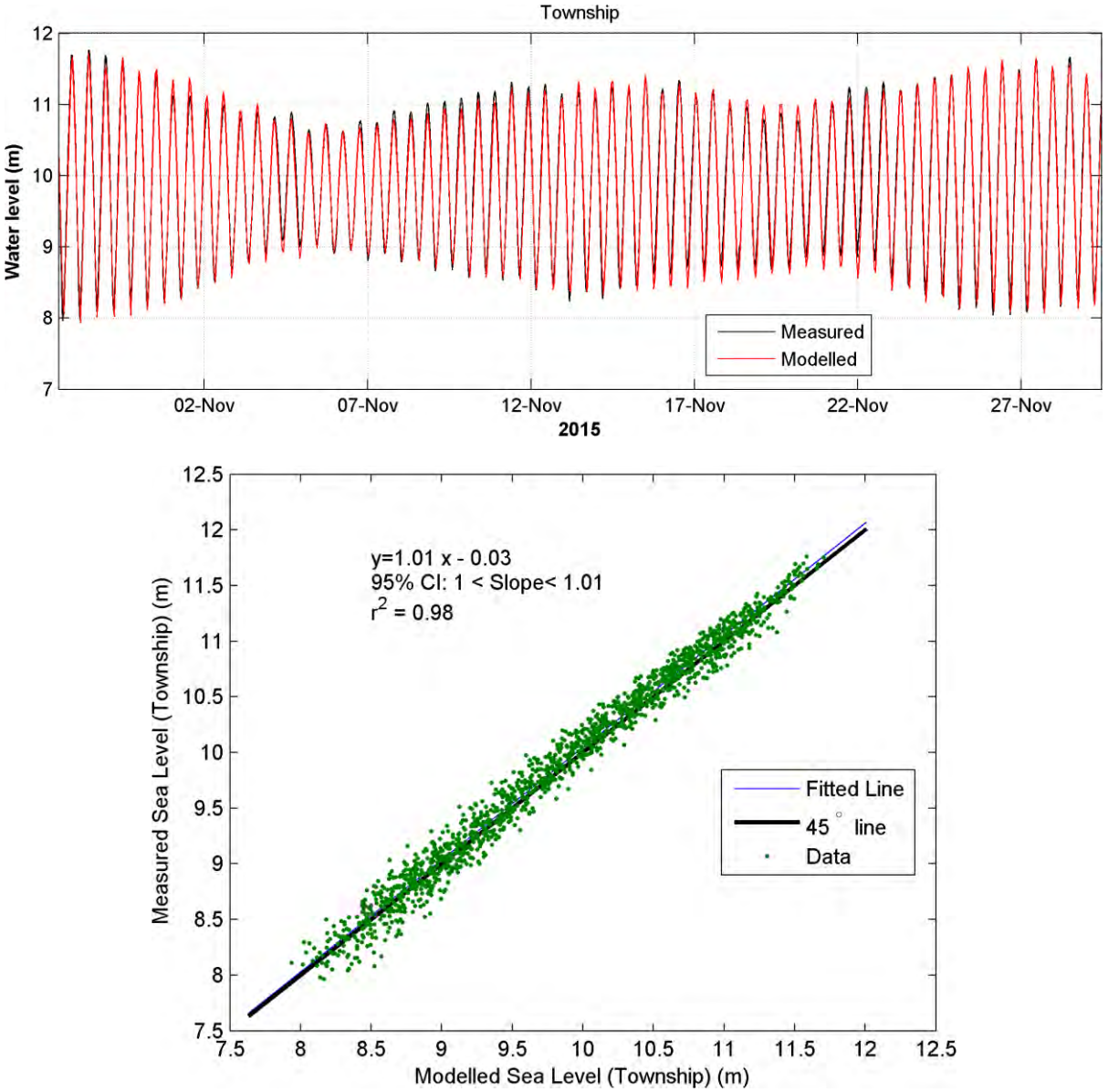

Figure 5.31: Kawhai Harbour sea level calibration at the Township deployment location as a time series (upper panel) and as a linear regression (lower panel).

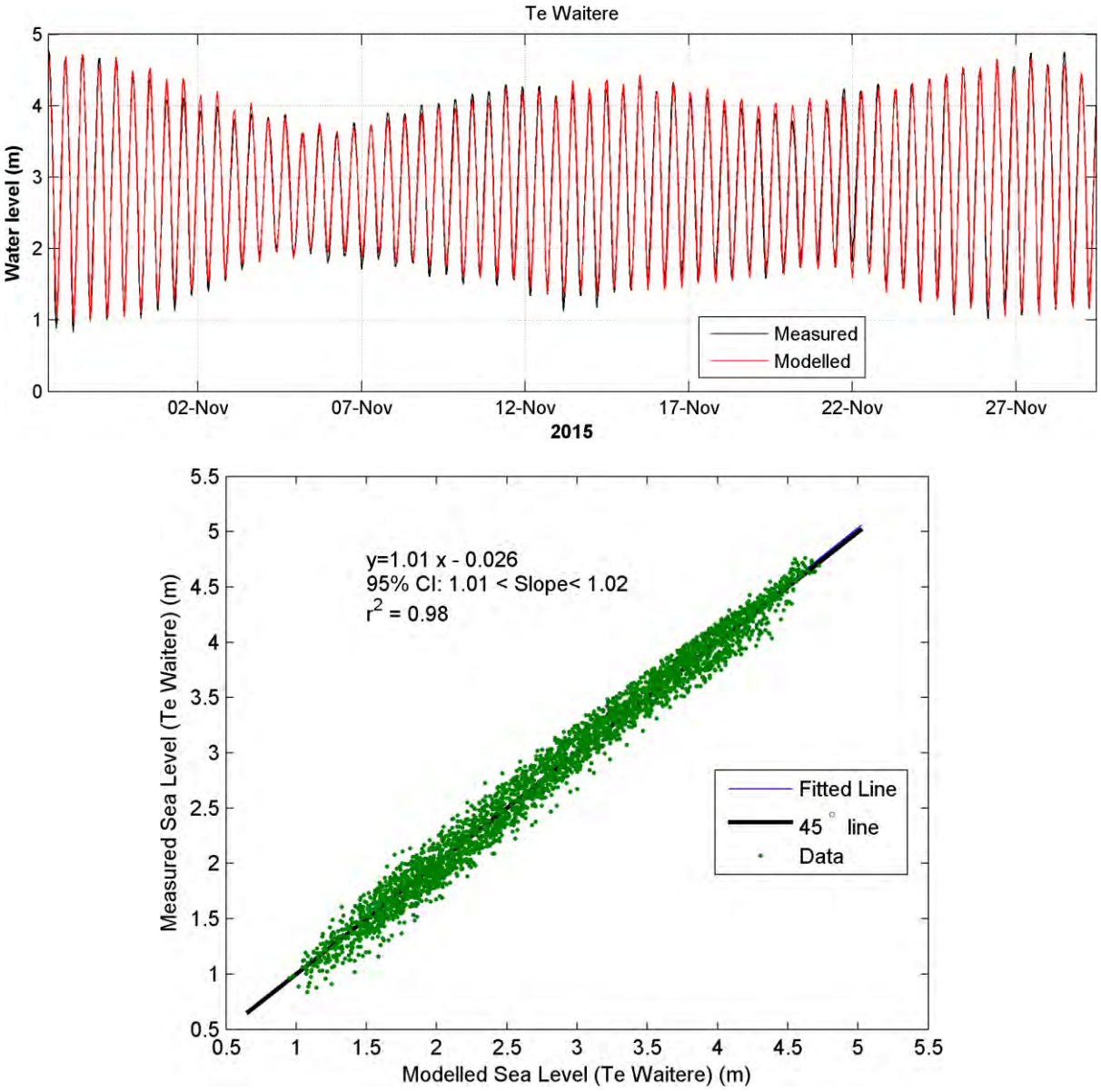

Figure 5.32: Kawhai Harbour sea level calibration at the Te Waitere deployment location as a time series (upper panel) and as a linear regression (lower panel).

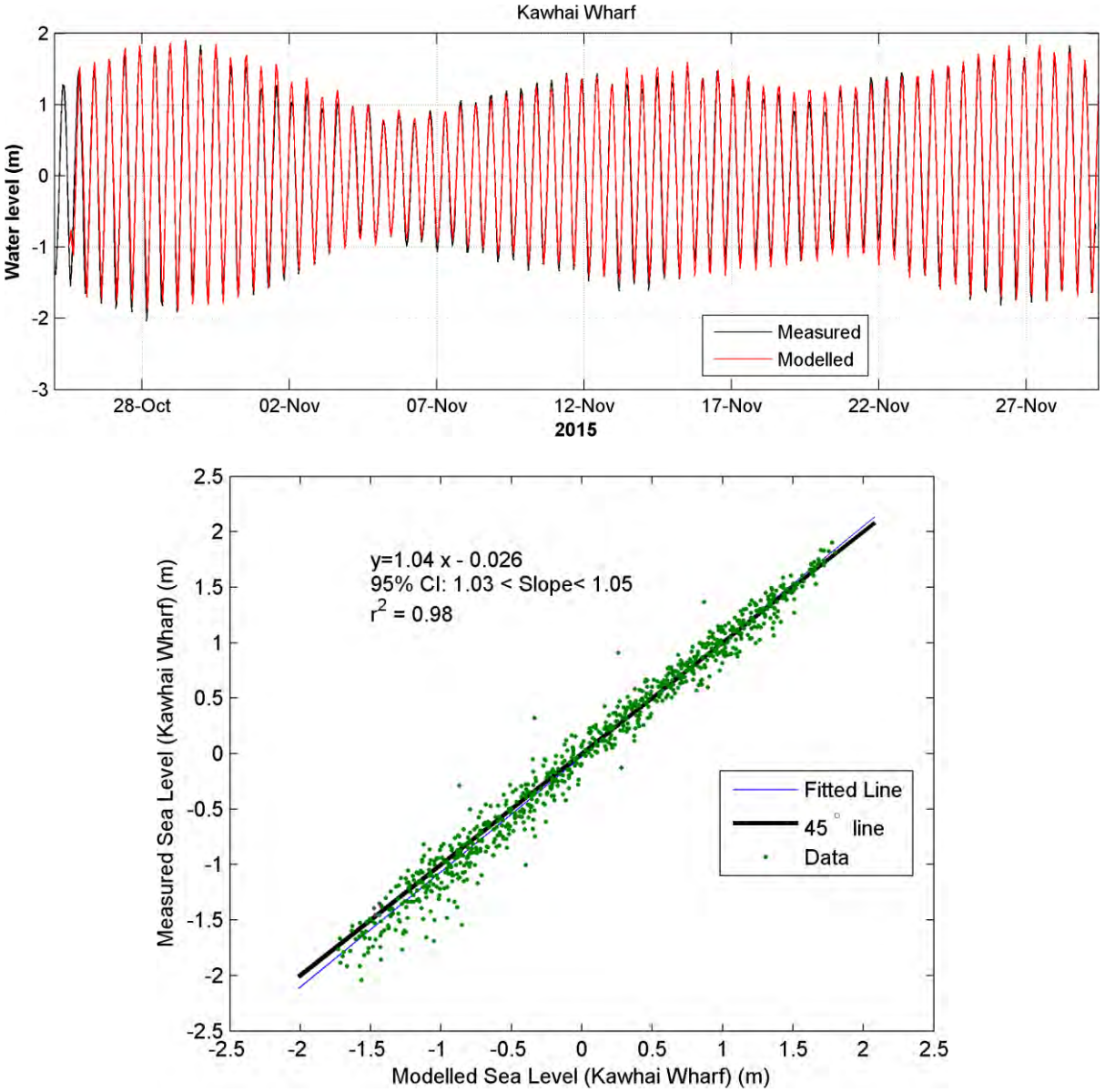

Figure 5.33: Kawhai Harbour sea level calibration at the Kawhai Wharf tide gauge as a time series (upper panel) and as a linear regression (lower panel).

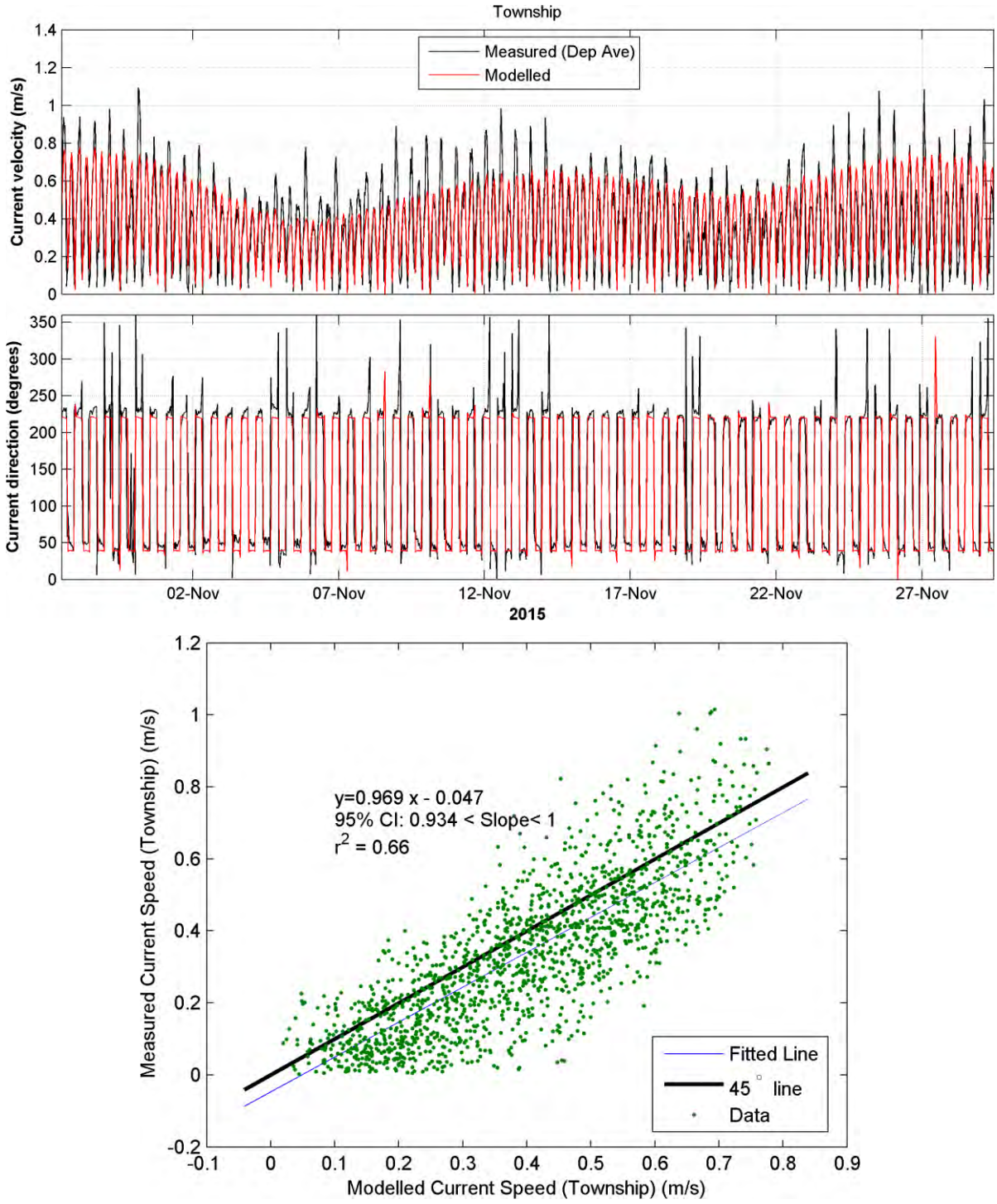

Figure 5.34: Kawhia Harbour current calibration at the Township deployment location as a time series (upper panel) and as a linear regression of modelled versus measured current speed (lower panel).

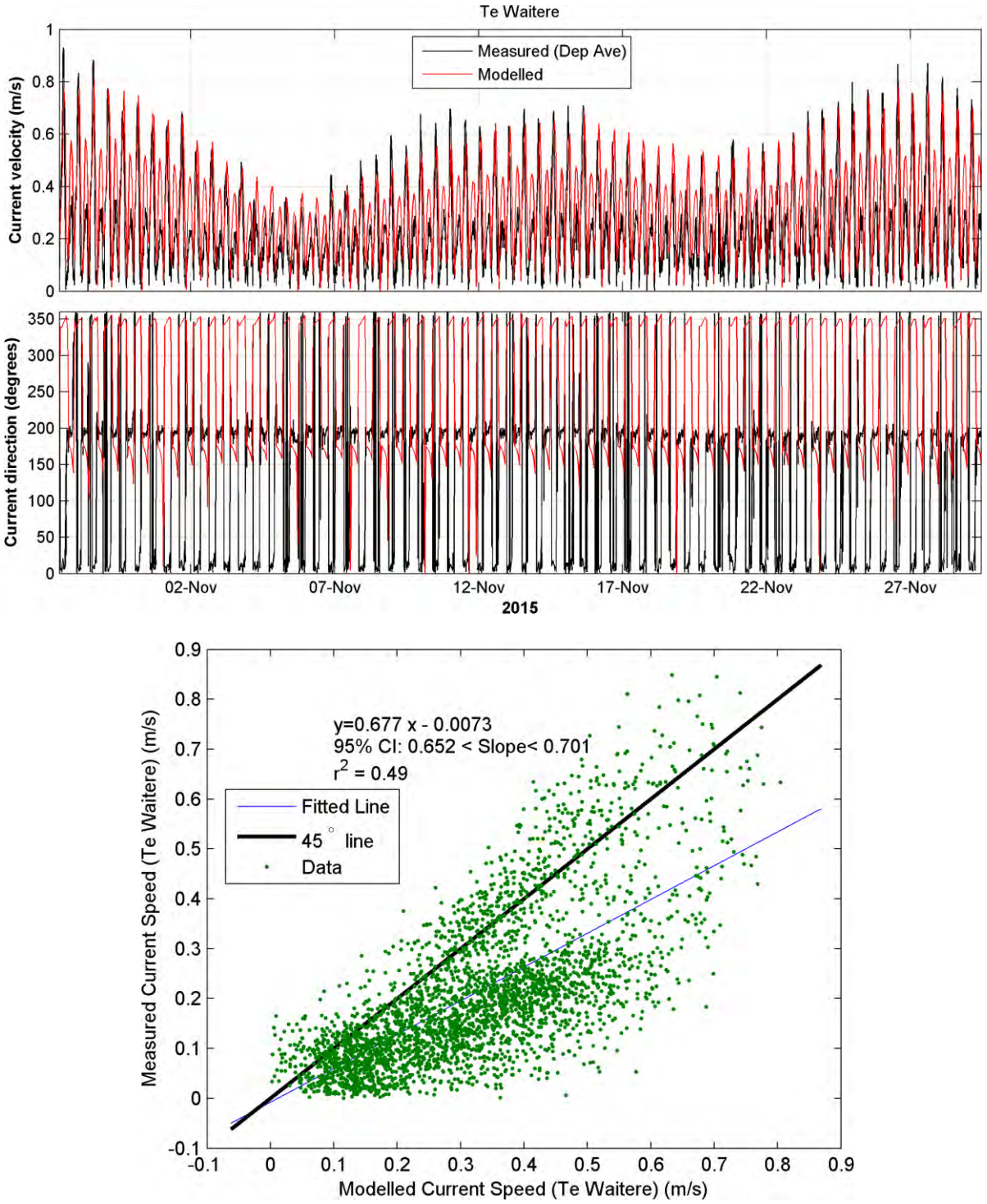

Figure 5.35: Kawhia Harbour current calibration at the Te Waitere deployment location as a time series (upper panel) and as a linear regression of modelled versus measured current speed (lower panel).

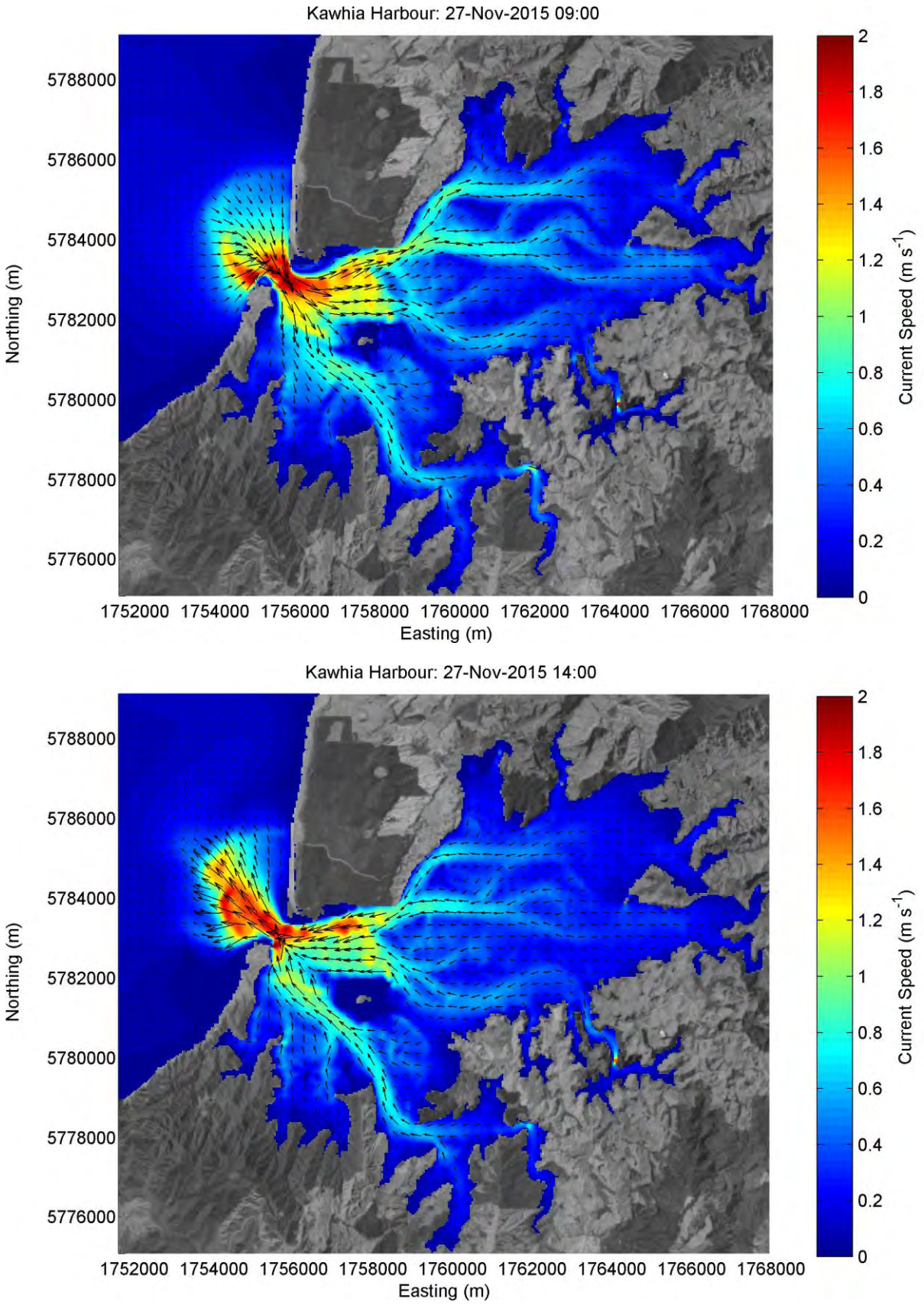

Figure 5.36: Kawhia Estuary peak flood (upper panel) and ebb (lower panel) currents.

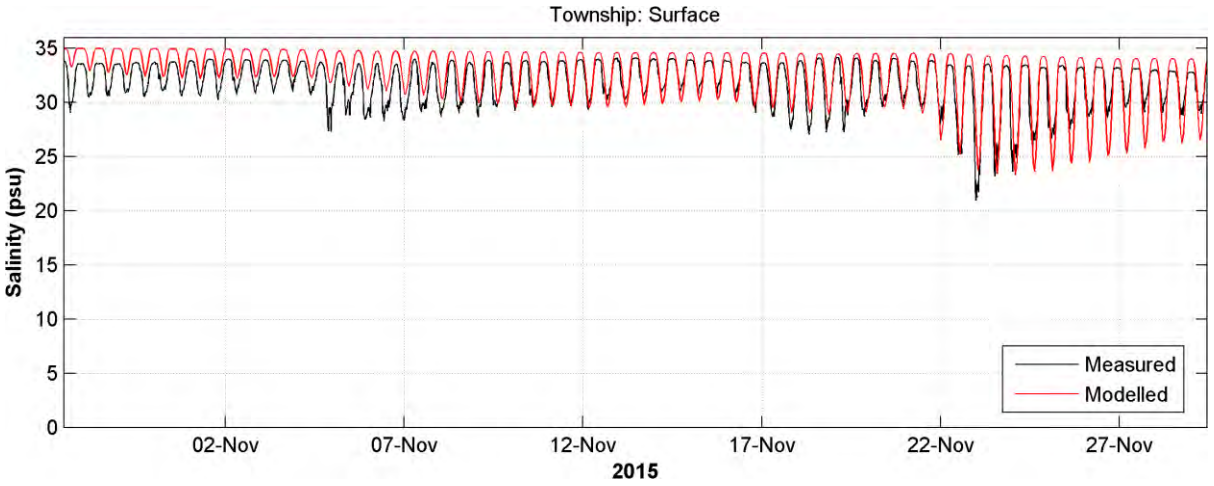

Figure 5.37: Kawhia Harbour salinity calibration at the Township deployment location.

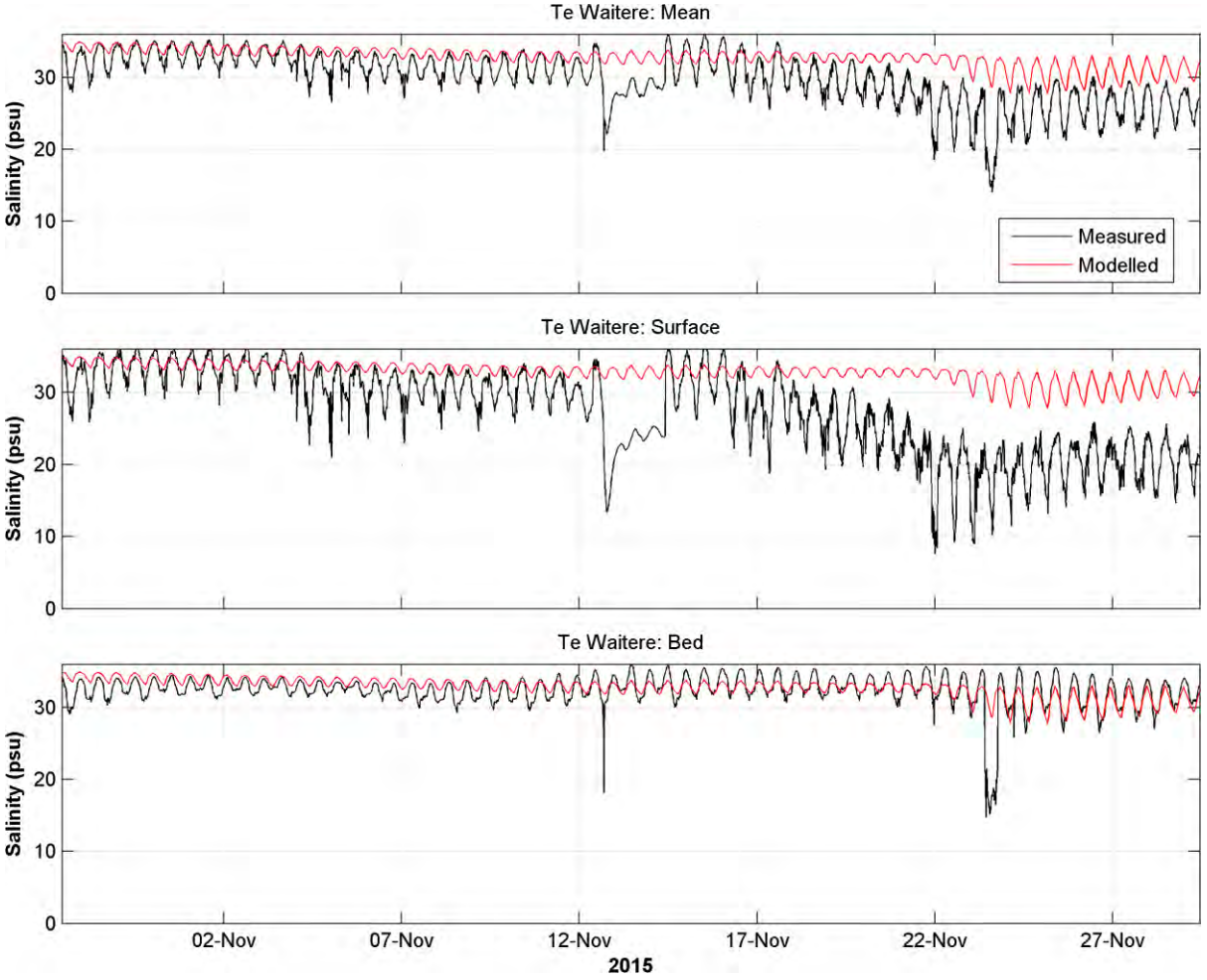

Figure 5.38: Kawhia Harbour salinity calibration at the Te Waitere deployment location.

5.5 Marokopa River Estuary

The Marokopa River estuary model was calibrated against currents, sea level and salinity data recorded at a location ('Lower') in the lower reaches of the estuary and another location ('Upper') in the upper reaches of the estuary (Atkin *et al.*, 2015). The two locations are shown in Figure 5.39. Time series comparisons between modelled and measured data are presented in Figure 5.40 and Figure 5.41 for sea level, in Figure 5.42 and Figure 5.43 for currents and Figure 5.45 for salinity. Peak flood and ebb currents are shown in Figure 5.44. Model performance statistics are shown in Table 5.10.

At the Upper location the salinity gauges recorded a constant salinity of approximately 0 psu both at the surface and at the seabed. The model reproduced this faithfully, but since there was very little fluctuation in either the measured or modelled signals, comparisons of measured and modelled salinity at this location were excluded from the calibration results below. It should also be noted that analysis of the sea level and current data recorded at the Upper location was used to adjust the river flow boundary conditions and consequently interpretation of the sea level and current calibrations at this location should be treated with caution.

Modelled sea level in the Upper and Lower locations captured tidal and non-tidal oscillations which were observed in the measured data. The magnitude of the tidal signal was over-estimated by the model at both locations. One of the most prominent high river flow events of the calibration period was centred on 25 August 2015 and was well represented by the model at the Lower location. However, the rise in sea level associated with this event was overestimated by the model at the Upper location. During this event the high river flow coincided with reduced tidal oscillations, presumably due to the high flow attenuating the tidal signal, and this was well represented in the model. Another prominent high flow period occurred over a longer period of time (between 1 and 8 September) and was captured by the model at the Upper and Lower locations. A final high flow event, centred on 21 September 2015, was not well represented in the model as it was not captured in the flow data recorded by the Marokopa flow gauge (see Figure 3.17) which was used to make the model boundary conditions. Model performance is reflected in the BSS (0.48 Upper and 0.83 Lower), α (0.75 for Upper and 0.88 for Lower) and β (0.25 for Upper and 0.04 for Lower).

The current speeds in the model were consistently underestimated in the model when compared with measured values. The modelled current speeds at the Lower location picked up some but not all of the brief direction reversals associated with the incoming tide. Notably the model failed to replicate these between 3 and 13 September 2015. Tidal reversals were

not seen at all in the model output at the Upper location. This is most probably because the river flow boundary conditions were unidirectional and did not include tidal oscillations. As with the sea level, the model picked up the elevated current speeds associated with the high river flow events, and this was particularly well represented in the model during the first large flow event (25 August 2015). Subsequent high river flow events were captured by the model although, current speeds were consistently underestimated by the model.

The model performance is reflected in the BSS (0.89 for Upper and 0.87 for lower) and β (0.00 for both Upper and Lower) with the reduced α value (0.59 and 0.62 for Upper and Lower respectively).

At the Lower location the model correctly picked up the timing of saline intrusions into the estuary between 29 August and 3 September and again between 13 and 20 September and after 25 September though peak salinity values were underestimated by the model. The salinity signal was most closely matched to the salinity gauge at the surface with the sea bed gauge showing more frequent saline intrusion. This may be in part due to the fact that the model is 2D, but additionally the flow boundary condition does not contain the tidal oscillations which may reduce the intrusion of saline water during the flooding tide.

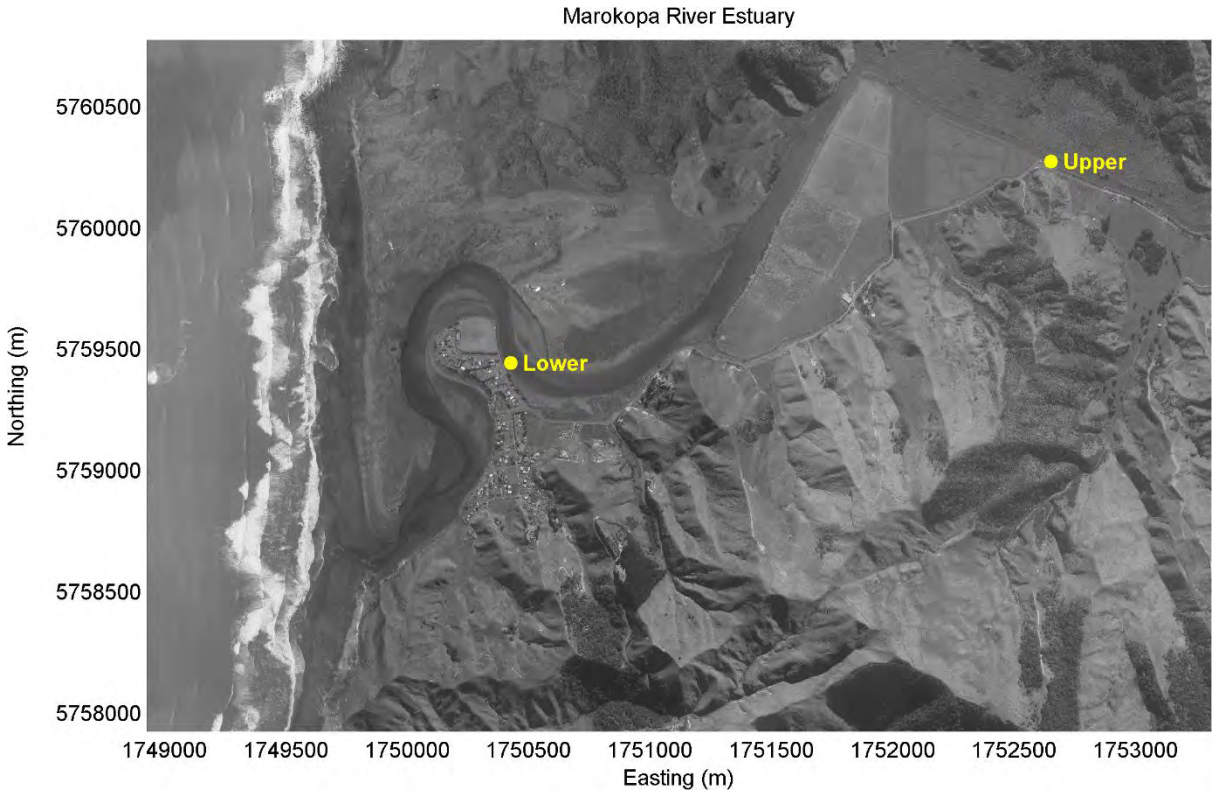

Figure 5.39: Marokopa River estuary deployment locations.

Table 5.10: Skill scores for the Marokopa River estuary calibrations.

Variable	Briar Skill Score (BSS)	α	β	γ	R^2	RMSE
Sea Level (Upper)	0.48	0.75	0.25	N/A	0.75	0.24 m
Sea Level (Lower)	0.83	0.88	0.04	N/A	0.88	0.14 m
Currents (Upper)	0.89	0.59	0.00	0.12	0.59	0.12 m s^{-1}
Currents (Lower)	0.87	0.62	0.00	0.035	0.62	0.19 m s^{-1}
Salinity (Lower: Mean)	0.98	0.57	0.18	0.07	0.57	4.77 psu
Salinity (Lower: Surface)	0.99	0.53	0.08	0.02	0.53	3.10 psu
Salinity (Lower: Bed)	0.95	0.045	0.20	0.09	0.45	7.65 psu

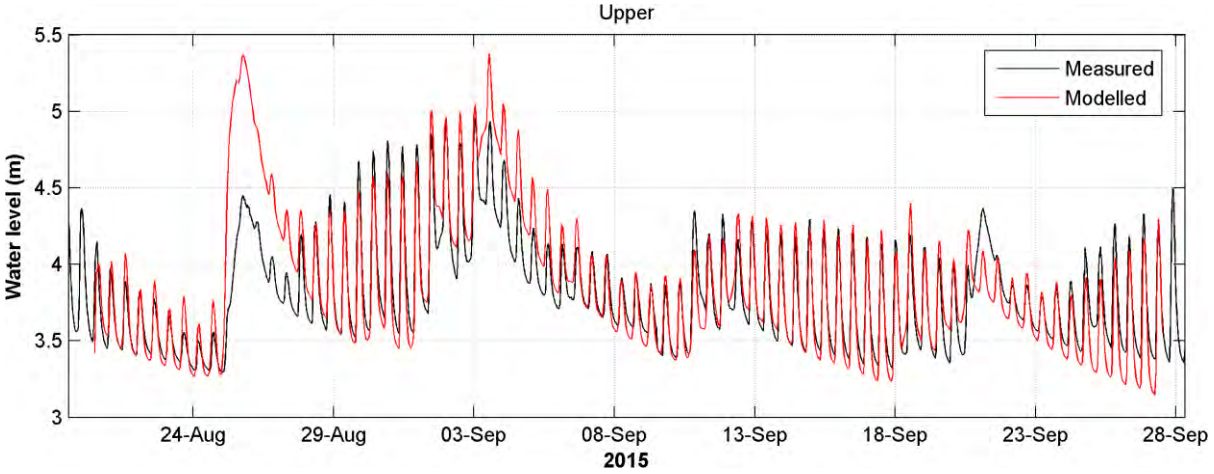

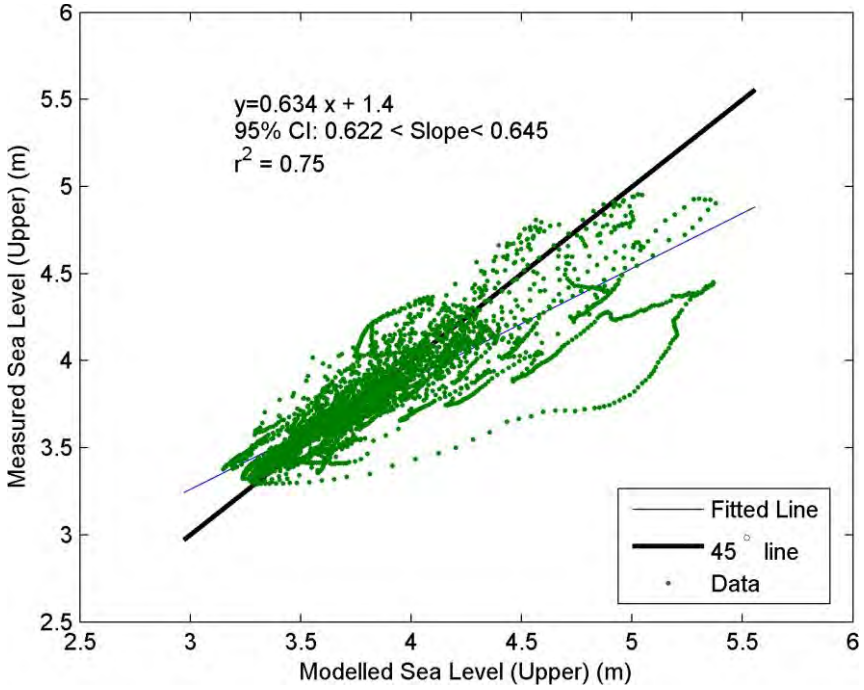

Figure 5.40: Marokopa River estuary sea level calibration at the Upper deployment location as a time series (upper panel) and as a linear regression (lower panel).

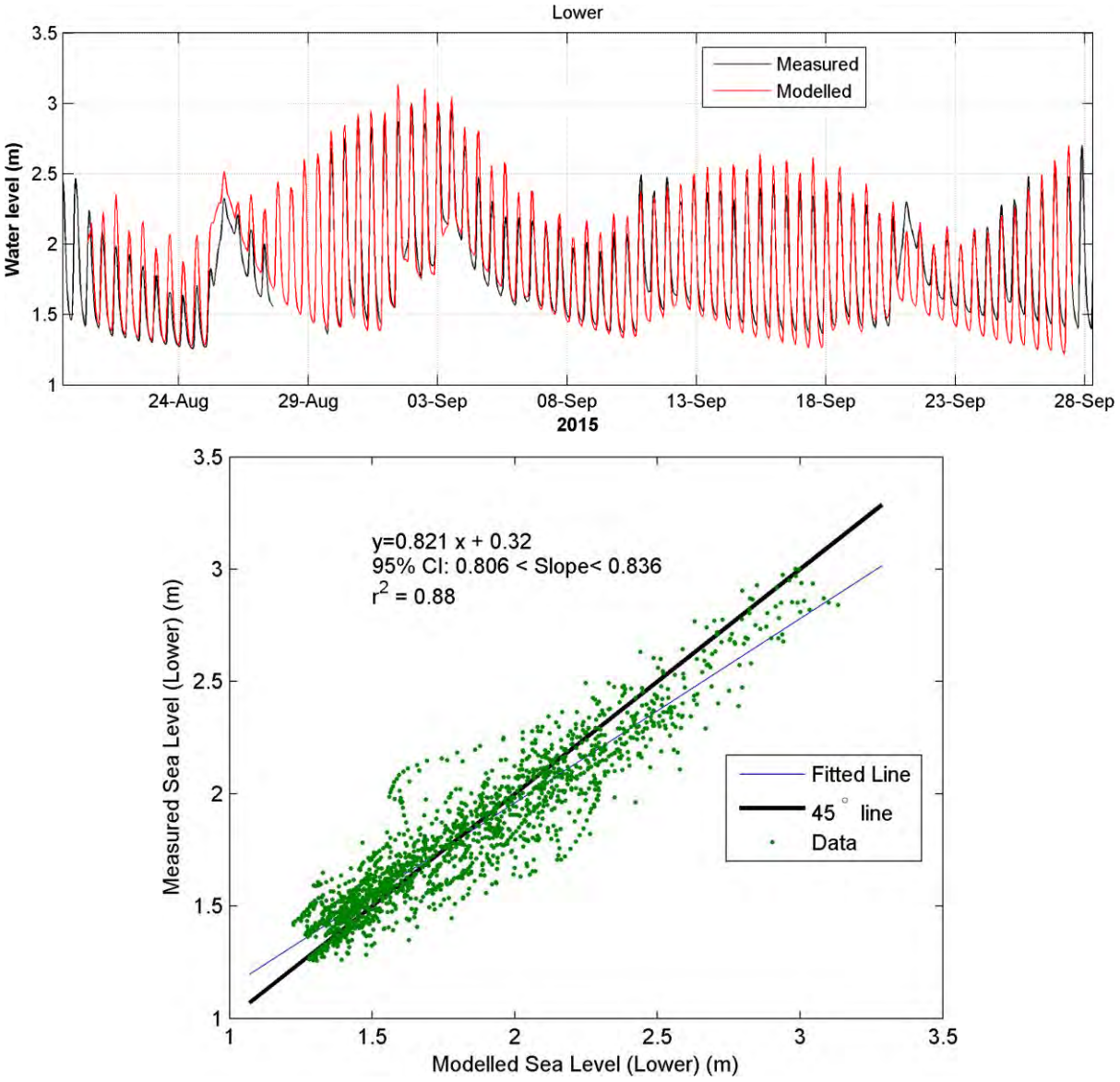

Figure 5.41: Marokopa River estuary sea level calibration at the Lower deployment location as a time series (upper panel) and as a linear regression (lower panel).

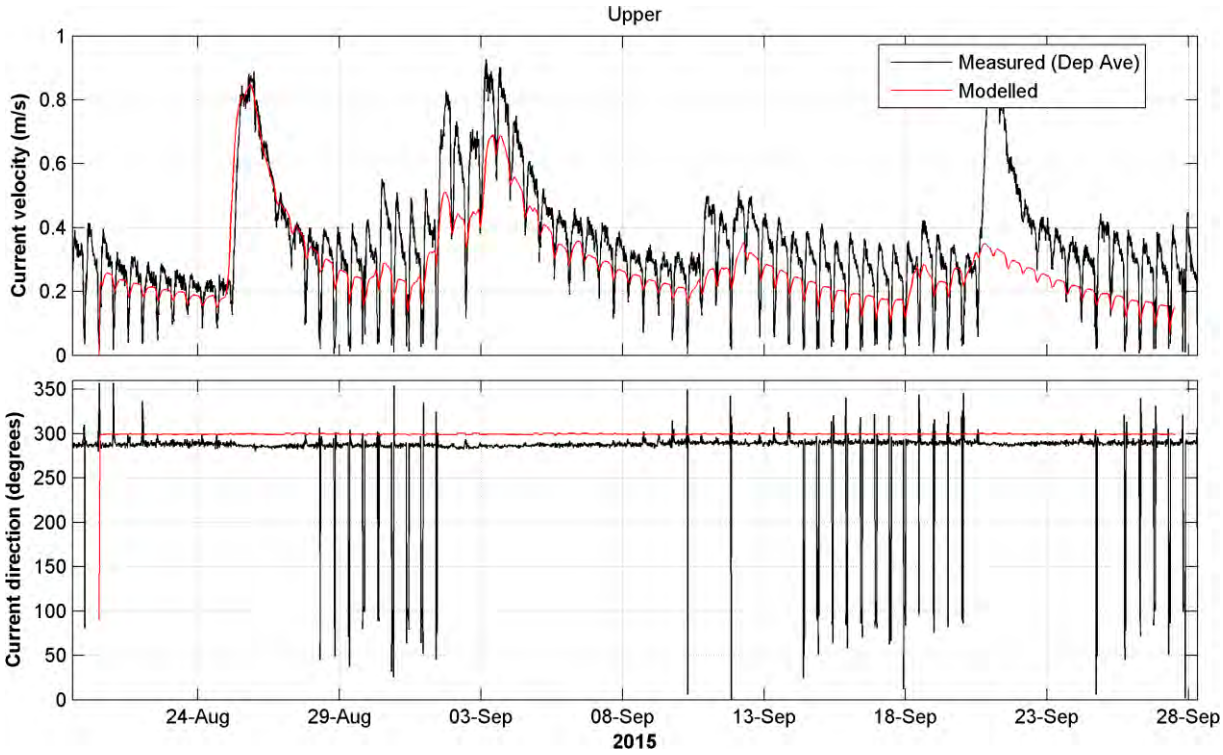

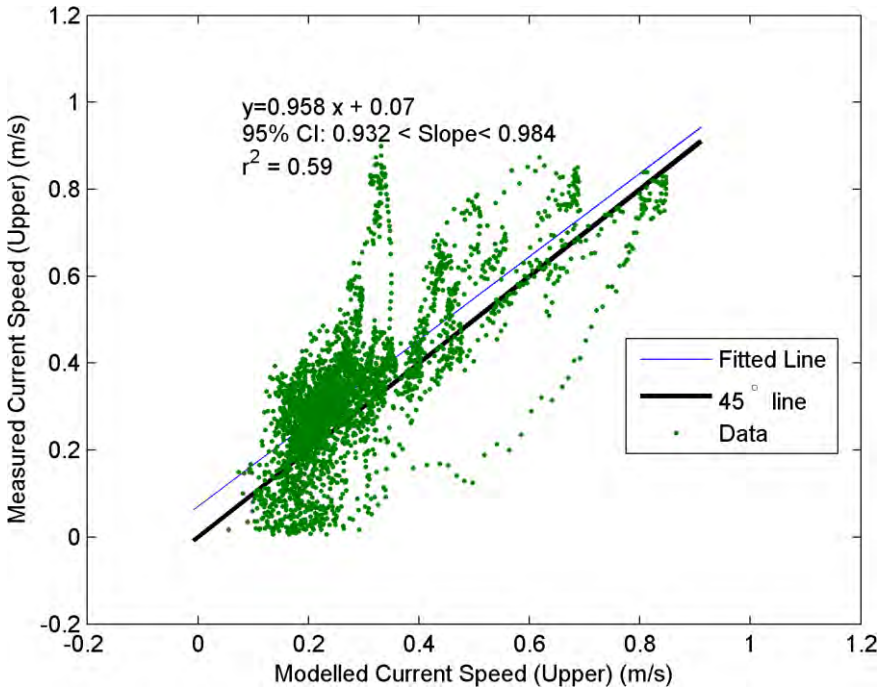

Figure 5.42: Marokopa River Estuary current calibration at the Upper deployment location as a time series (upper panel) and as a linear regression of modelled versus measured current speed (lower panel).

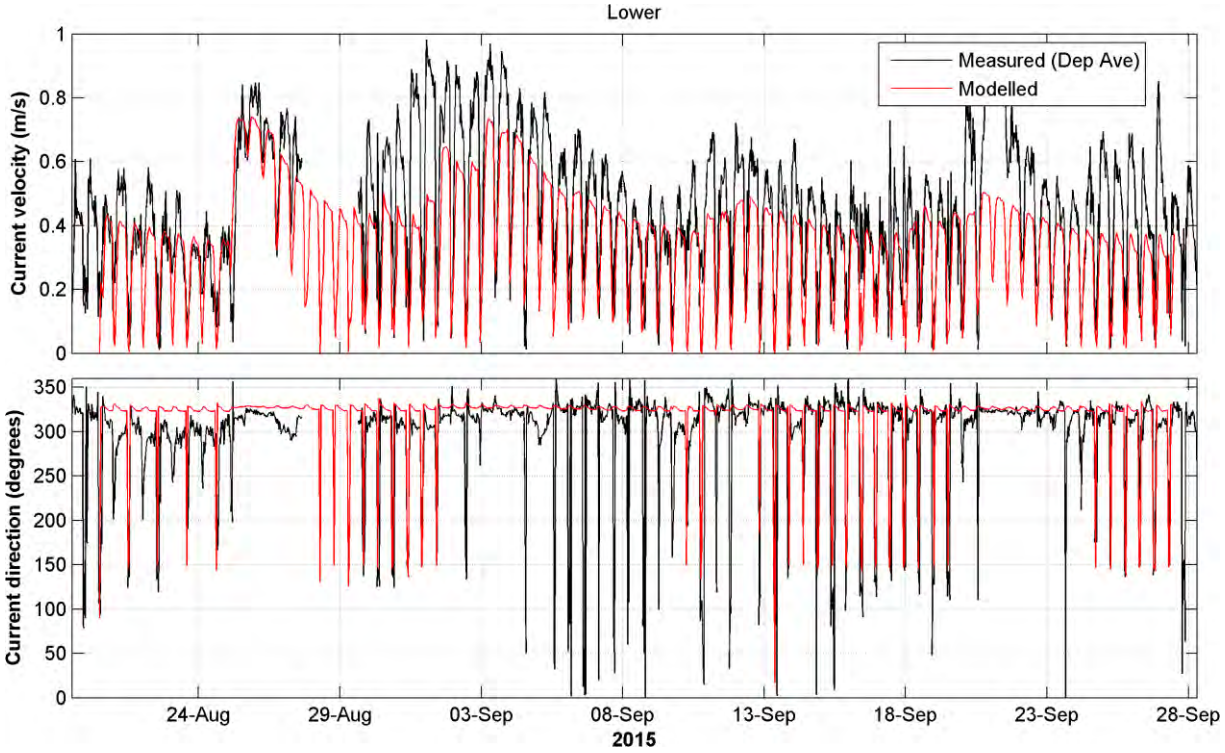

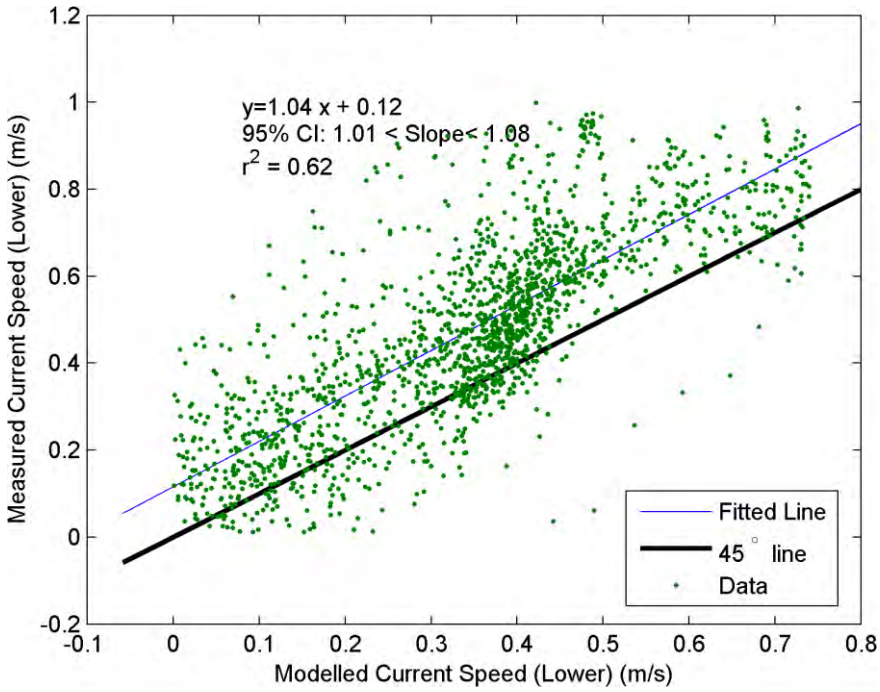

Figure 5.43: Marokopa River Estuary current calibration at the Lower deployment location as a time series (upper panel) and as a linear regression of modelled versus measured current speed (lower panel).

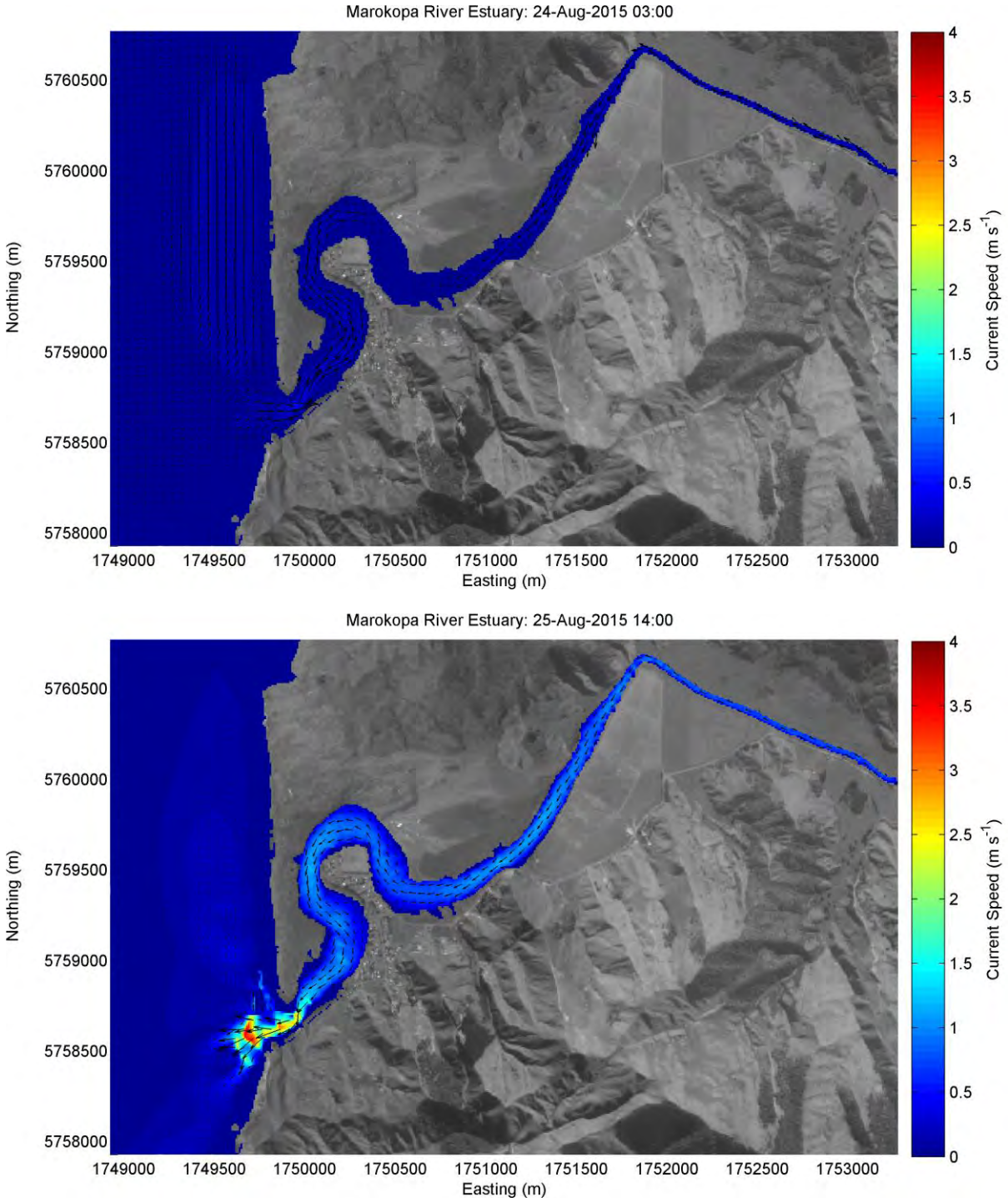

Figure 5.44: Marokopa River estuary peak flood (upper panel) and ebb (lower panel) currents.

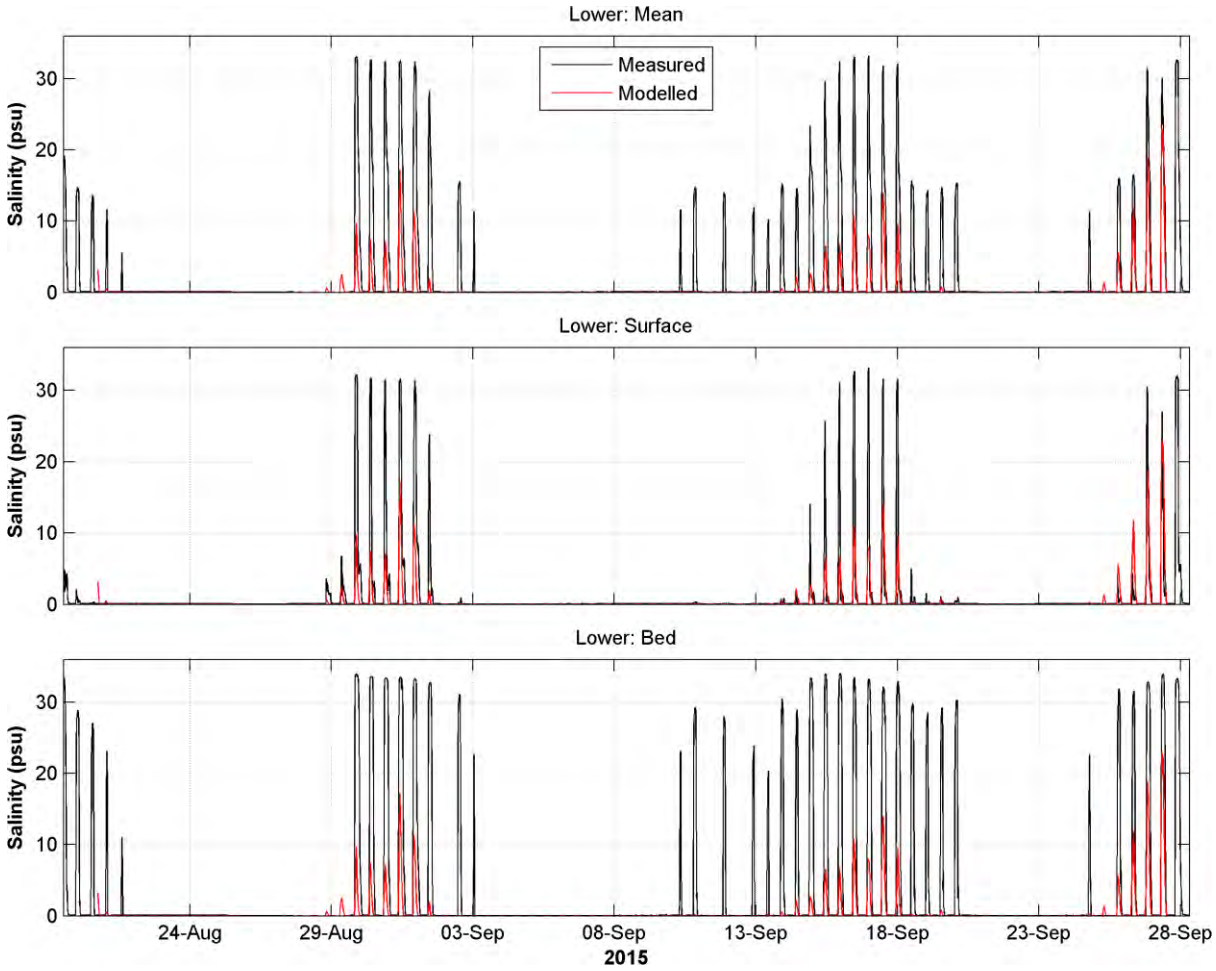

Figure 5.45: Marokopa River estuary salinity calibration at the Lower deployment location.

5.6 Awakino River Estuary

The Awakino River estuary model was calibrated against currents, sea level and salinity data recorded at a location ('Lower') in the lower reaches of the estuary and another location ('Upper') in the upper reaches of the estuary (Atkin *et al*., 2015). The instrument locations are shown in Figure 5.46. Time series comparison between modelled and measured data are shown in Figure 5.47 and Figure 5.48 for sea level, Figure 5.49 and Figure 5.50 for currents and Figure 5.52 for salinity. Model performance statistics are shown in Table 5.11.

As with Marokopa the Upper location salinity gauges recorded a constant salinity of approximately 0 psu both at the surface and at the seabed for most of the deployment. The model reproduced this faithfully, apart from at the beginning and end of the calibration period, but since there was very little fluctuation in either the measured or modelled signals, comparisons of measured and modelled salinity at this location were excluded from the calibration results below.

Overall the model broadly reproduced tidal sea level variability, although at the Lower location the model over predicted the tidal range by approximately 0.2 to 0.3 m. The tidal range was more accurately represented in the model at the Upper location. Performance statistics showed similar levels of accuracy at both locations (BSS = 0.87, α = 0.91, β = 0.04 for Upper and BSS = 0.88, α = 0.91, β = 0.03 for Lower). The model also picked up the rise in sea level during the major high river flow events centred on 25 August 2015 and over a longer period of time between 1 and 8 September. However, the rise in sea level during these periods was somewhat over predicted at the Upper location and under predicted at the Lower location. Note that the high river flow event observed in Marokopa on 21 September 2015 is absent from the measured and modelled record in Awakino.

Modelled currents also replicated patterns in the measured data. Tidal variability was better captured by the model at the Lower location, where tidal reversals indirection were picked up reasonably consistently by the model, than at the Upper location where the model did not capture tidal reversals. This is most likely because the river flow boundary condition applied at the upstream open boundary of the model was unidirectional and was not modulated by the tides. The model achieved a BSS of 0.94 an α of 0.82 and a β of 0.01 at the Upper location and a BSS of 0.93 an α of 0.79 and a β of 0.01 at the Lower location. Plots of peak flood and ebb currents are presented in Figure 5.51 and show that currents are considerably stronger on the ebbing tide due to the influence of river flow.

At the Lower location the salinity data were recorded at the top and the bottom of the water column and there were considerable differences between the two records; however, spikes in salinity were more frequent and occurred for a longer duration in the salinity data recorded at the bed compared to at the surface. The model captured many of the spikes in salinity associated with spring tides and low flow conditions when oceanic saline water protruded further into the harbour. The model matched the measured salinity data better at the surface than at depth though it achieved the best model performance against the mean of the two (BSS = 0.97, α = 0.55, β = 0.06).

At the end of the record the Aquadopp at the Upper location recorded very low currents (<0.1 m s^{-1}) moving slowly up stream for approximately 20 hours. This was ongoing at the time when the instrument was removed from the water. At that time, the sea level continued to show normal tidal modulation. Coincident with this, the salinity gauge at the Upper location (Figure 5.53) showed a sustained elevated salinity of approximately 23 psu over the same period. In the model, the slack currents in the river boundary condition at this time caused a rapid decrease in sea level which was not recorded by the Aquadopp pressure sensor. The time period of the model only included the final second of these events although the phenomenon

was not replicated by the model. At present it is unclear why this was observed in the measured data.

Table 5.11: Skill scores for the Awakino River estuary calibrations.

Variable	Briar Skill Score (BSS)	α	β	γ	R^2	RMSE
Sea Level (Upper)	0.87	0.91	0.04	N/A	0.91	0.17 m
Sea Level (Lower)	0.88	0.91	0.03	N/A	0.91	0.16 m
Currents (Upper)	0.94	0.82	0.01	0.02	0.82	0.06 m s^{-1}
Currents (Lower)	0.93	0.79	0.01	0.11	0.79	0.10 m s^{-1}
Salinity (Lower: Mean)	0.97	0.55	0.06	0.11	0.55	5.13 psu
Salinity (Lower: Surface)	0.99	0.45	0.03	0.00	0.45	2.96 psu
Salinity (Lower: Bed)	0.90	0.44	0.03	0.15	0.44	9.77 psu

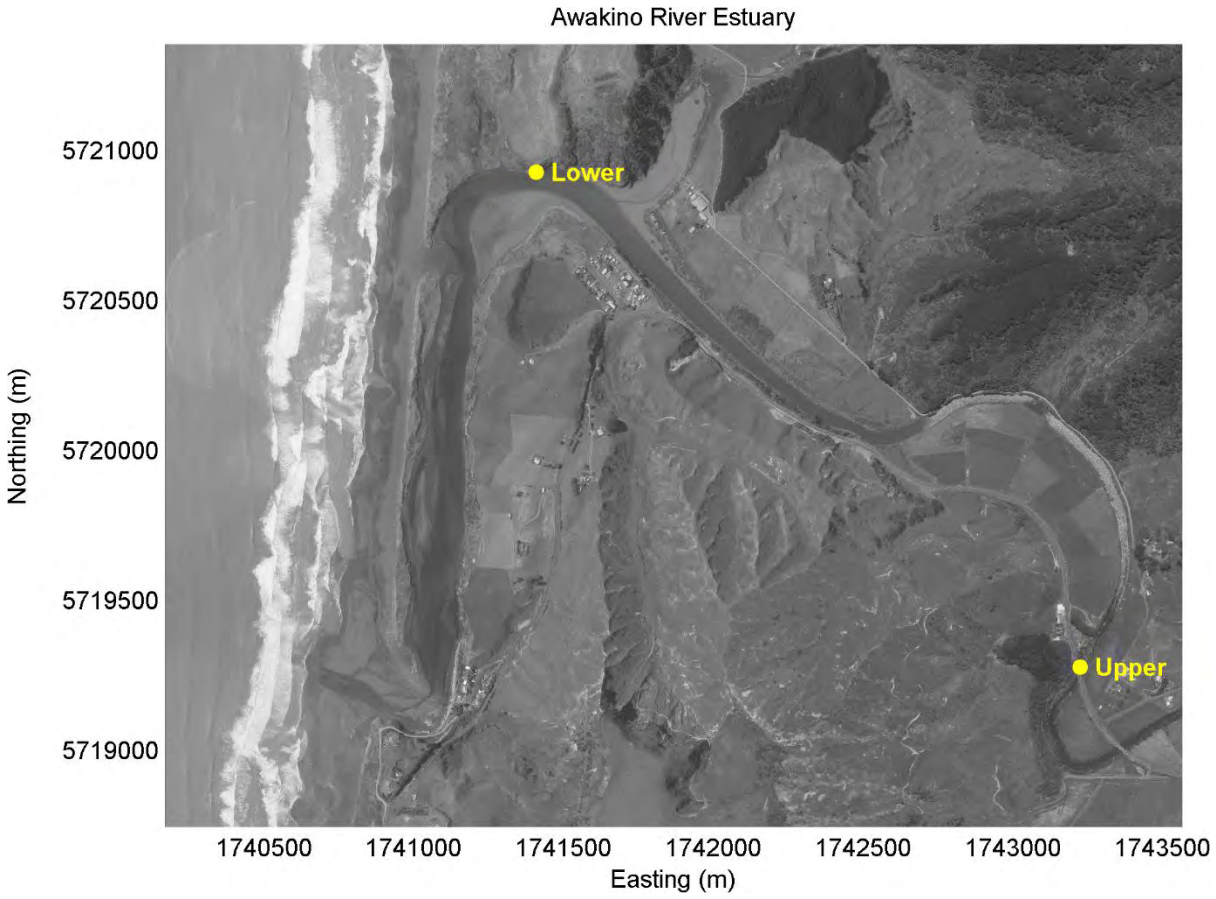

Figure 5.46: Awakino River estuary deployment locations.

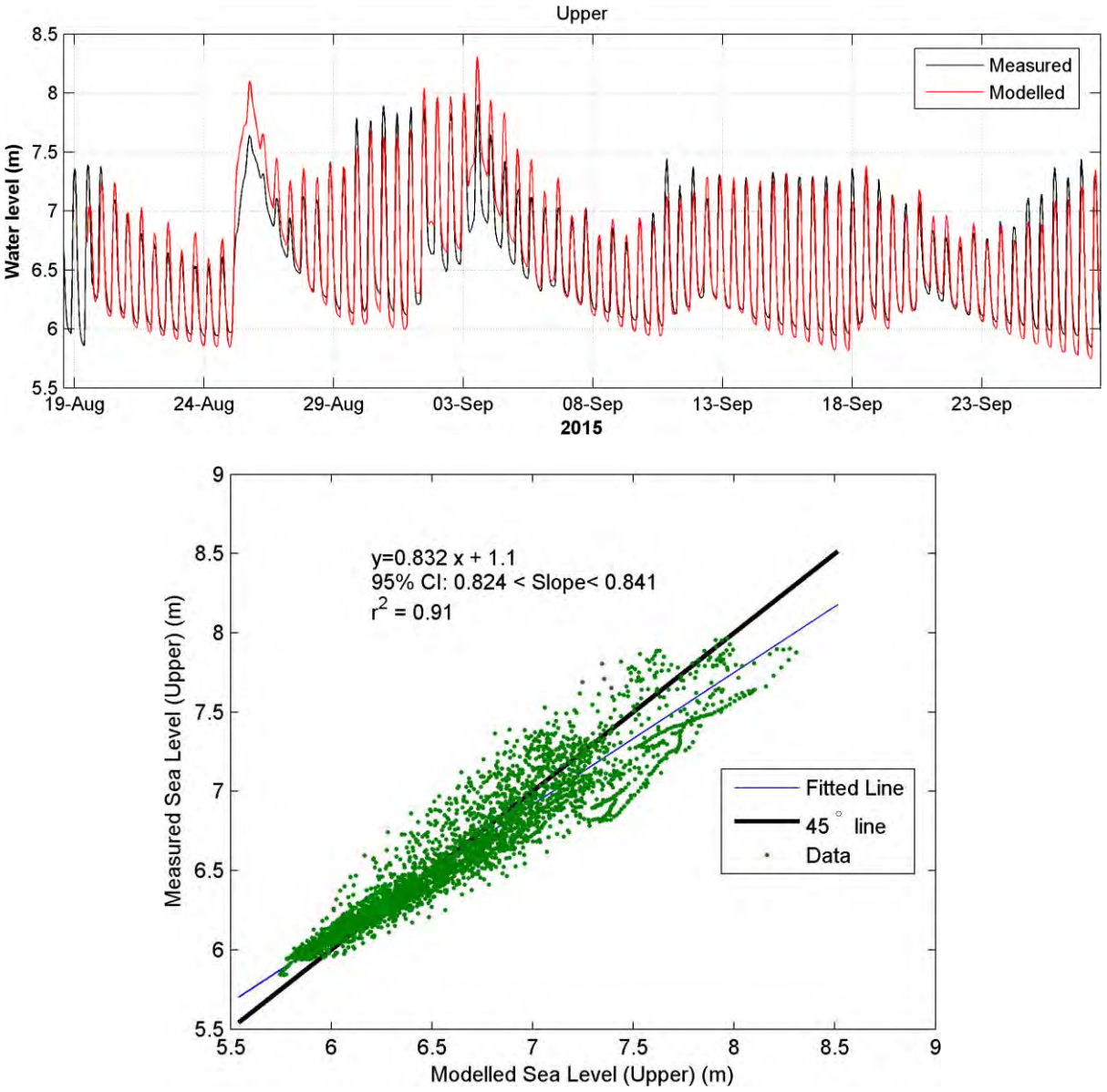

Figure 5.47: Awakino River estuary sea level calibration at the Upper deployment location as a time series (upper panel) and as a linear regression (lower panel).

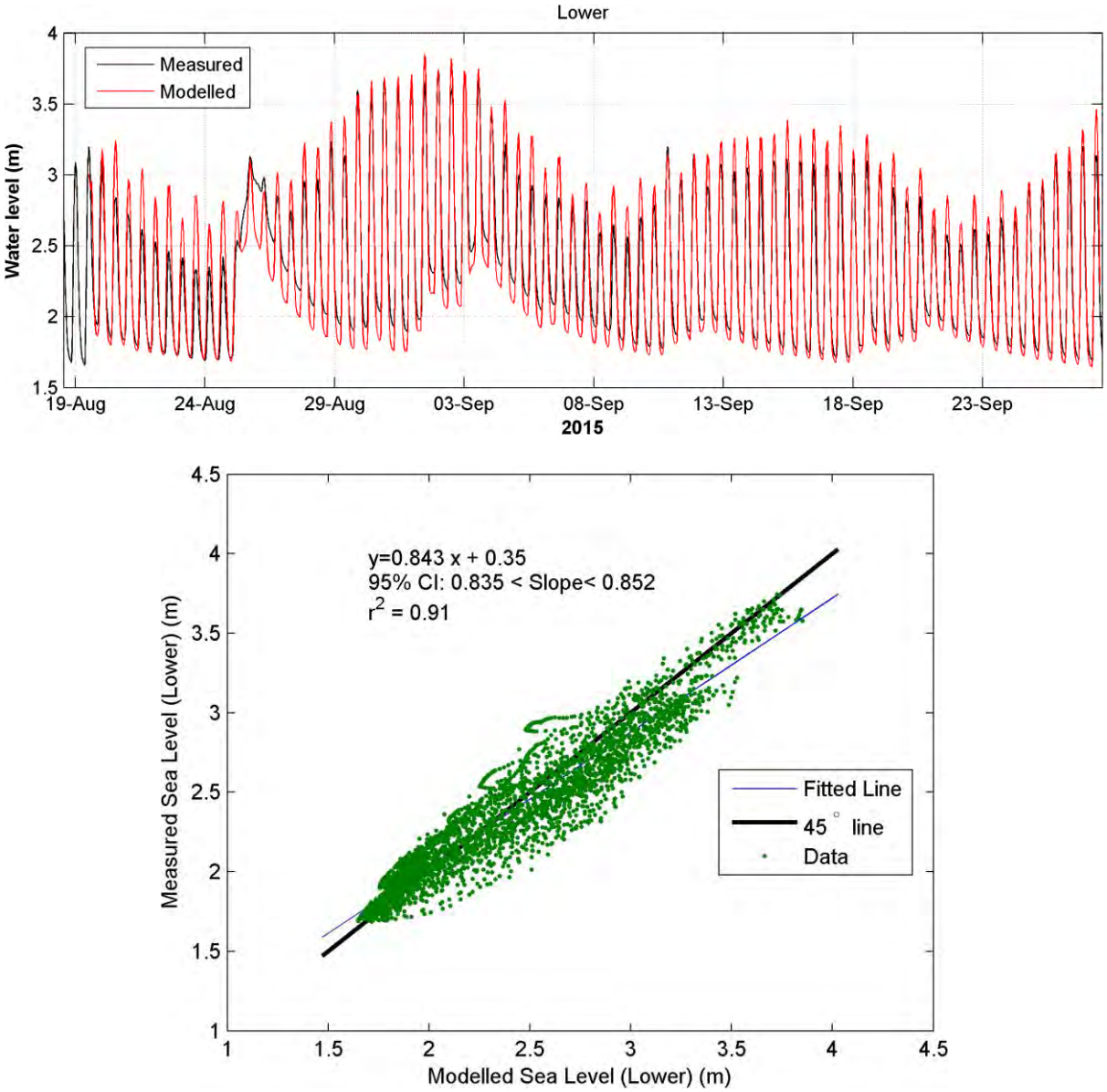

Figure 5.48: Awakino River estuary sea level calibration at the Lower deployment location as a time series (upper panel) and as a linear regression (lower panel).

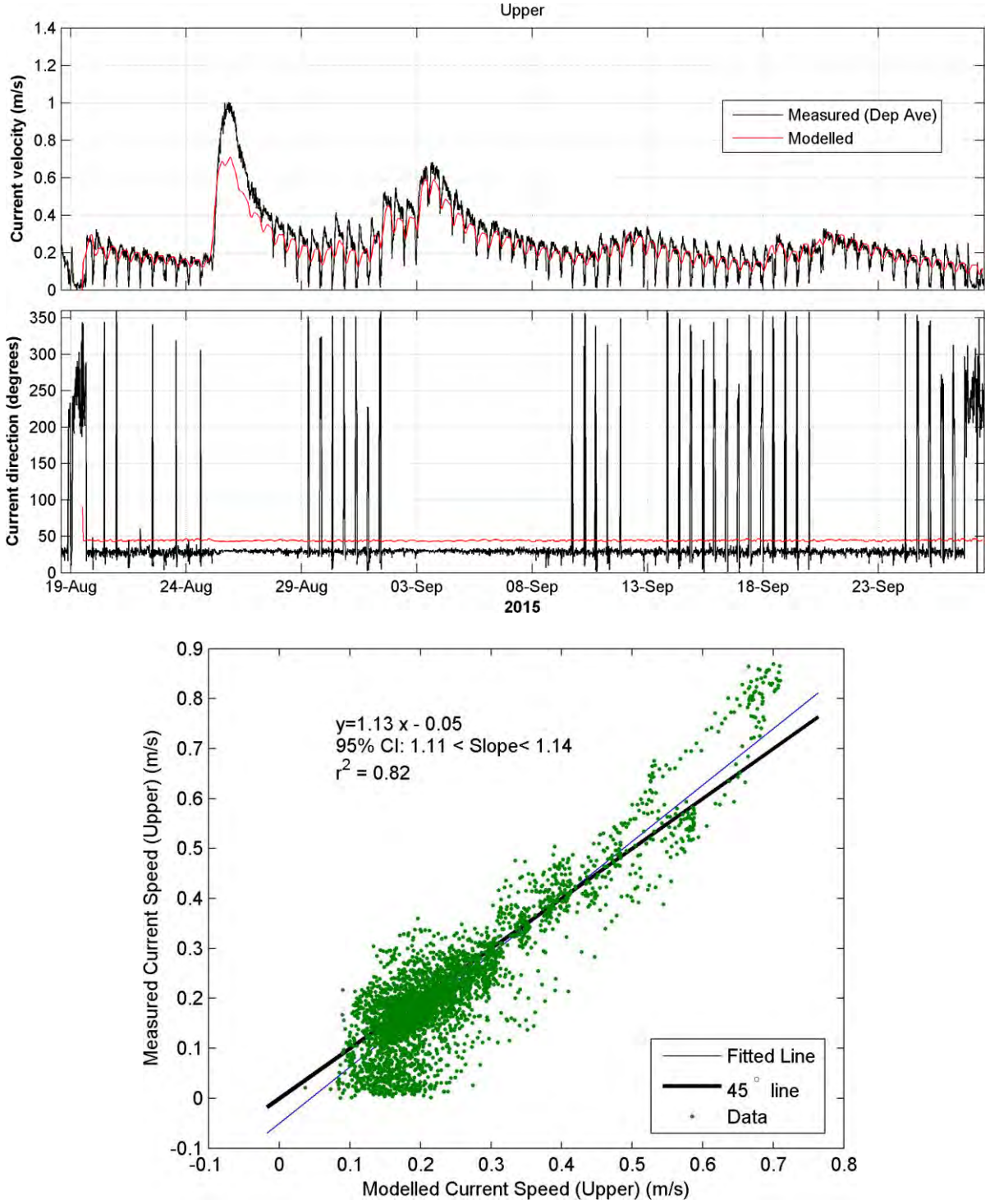

Figure 5.49: Awakino River estuary current calibration at the Upper deployment location as a time series (upper panel) and as a linear regression of modelled versus measured current speed (lower panel).

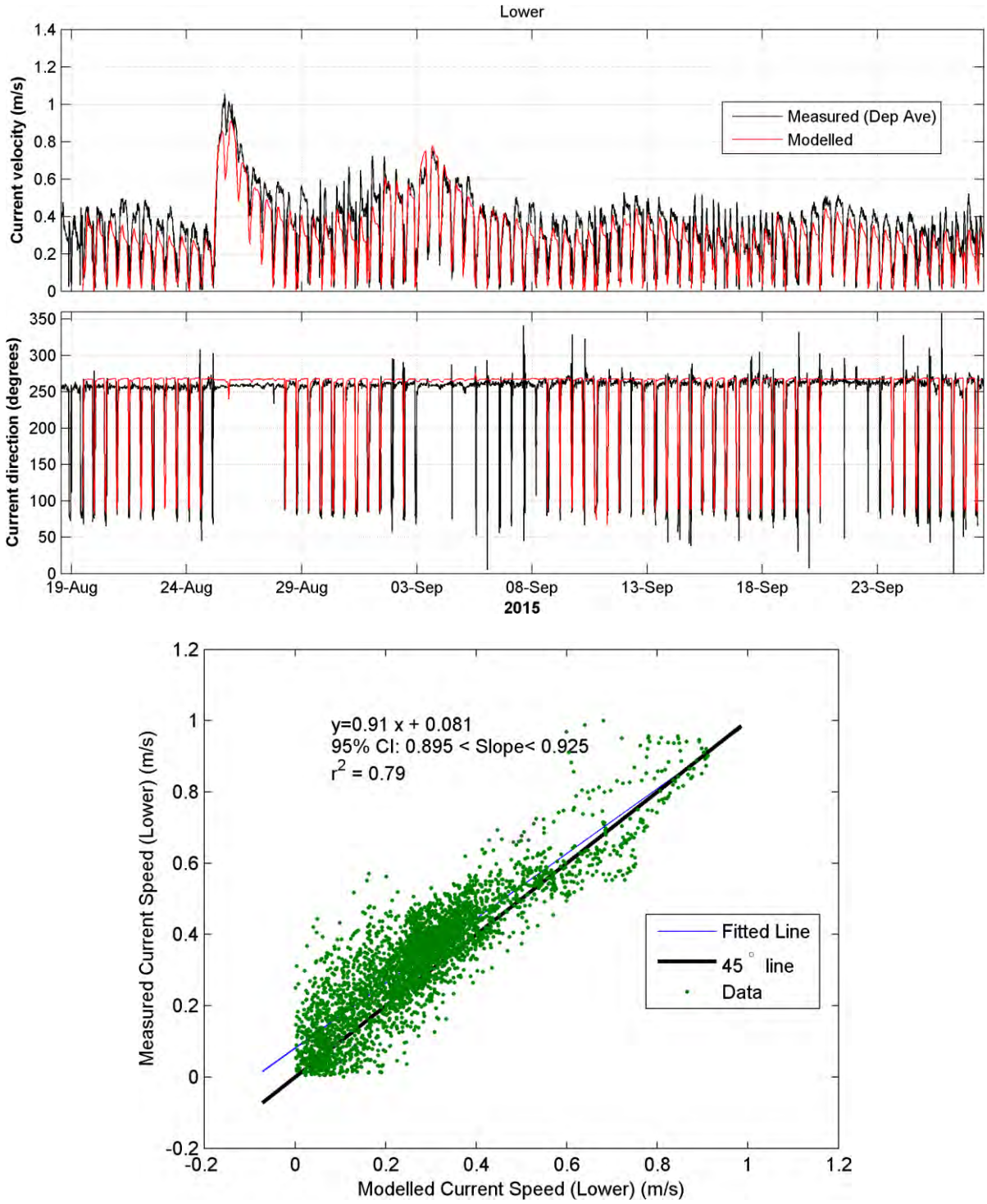

Figure 5.50: Awakino River estuary current calibration at the Lower deployment location as a time series (upper panel) and as a linear regression of modelled versus measured current speed (lower panel).

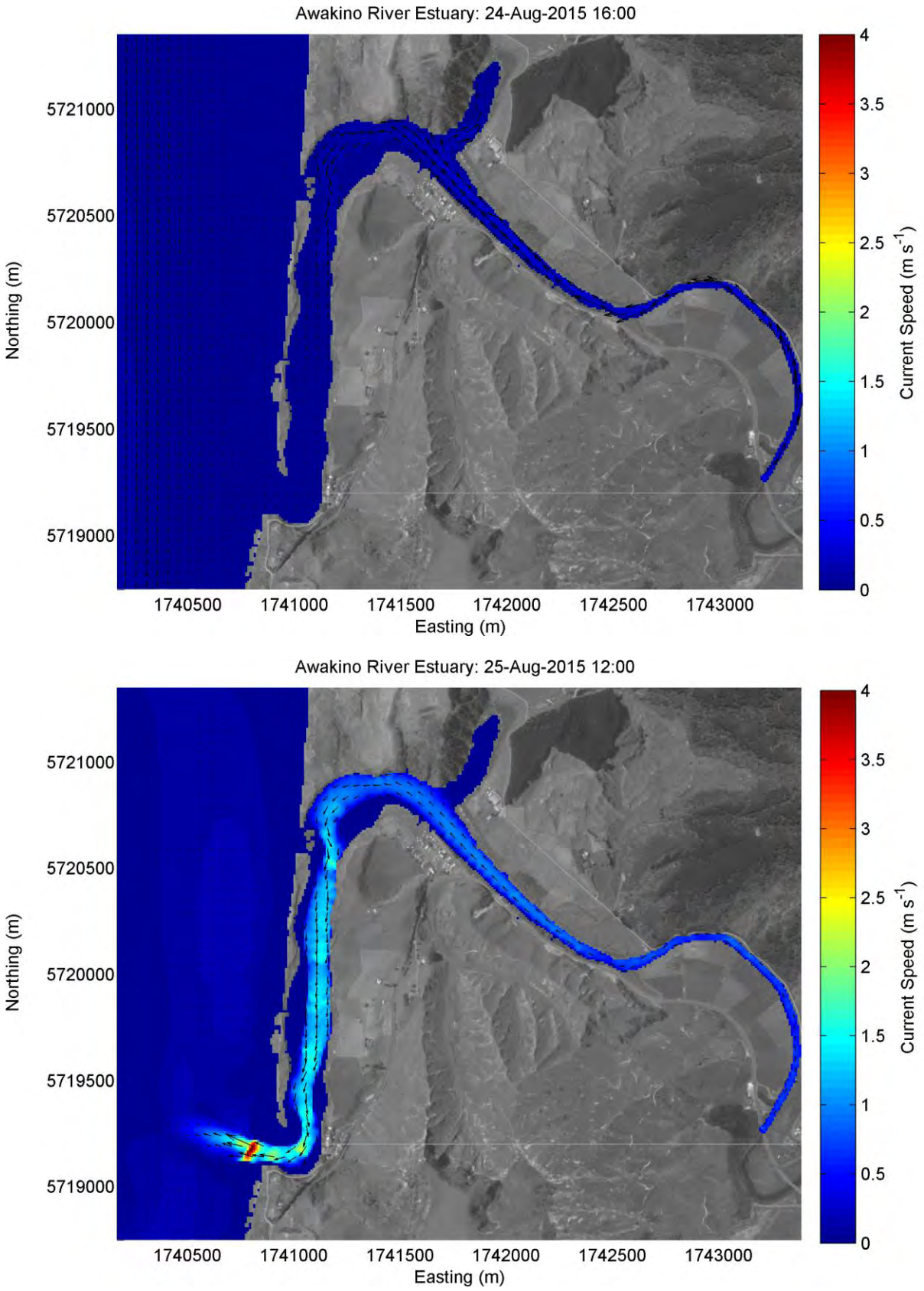

Figure 5.51: Awakino River estuary peak flood (upper panel) and ebb (lower panel) currents.

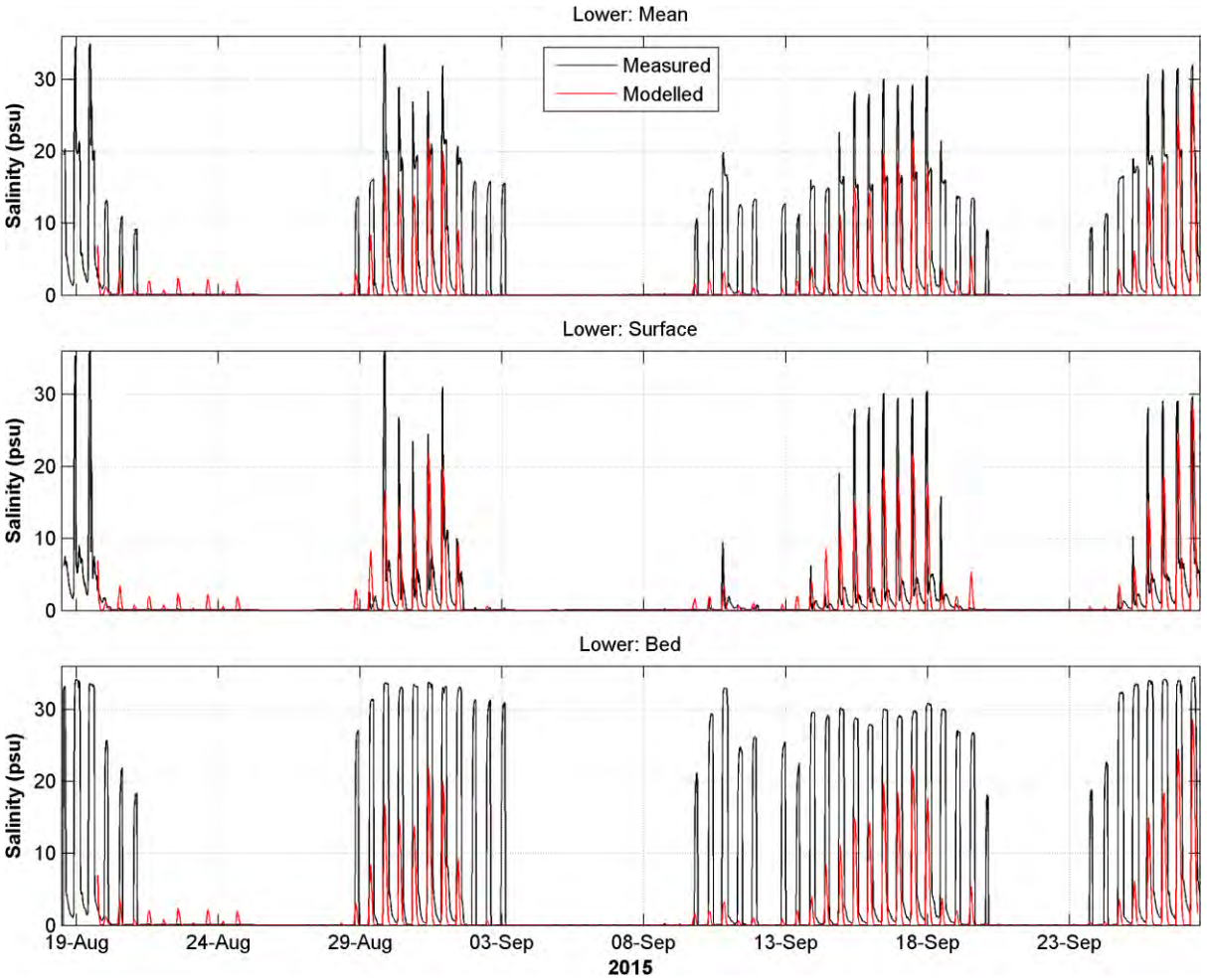

Figure 5.52: Awakino River estuary salinity calibration at the Lower deployment location.

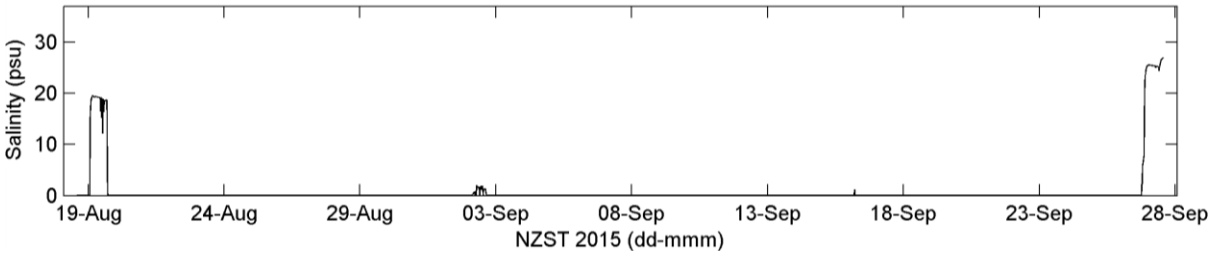

Figure 5.53: Awakino River estuary salinity recorded at the Upper location.

5.7 Mokau River Estuary

The Mokau River estuary model was calibrated against currents, sea level and salinity data recorded at a location ('Lower') in the lower reaches of the estuary and another location ('Upper') in the upper reaches of the estuary (Atkin *et al*., 2015). The location of the instrument in the Lower location is shown in Figure 5.54 and is located near to the bridge over the Mokau River. Due to interference with the instrument during its deployment, there are two periods of missing data from the Aquadopp record. The remaining data are still sufficient for model

calibration, although unfortunately the high river flow events on 25 August was not captured by the instrument. Time series comparison between modelled and measured data are shown in Figure 5.55 and Figure 5.56 for sea level, Figure 5.57 and Figure 5.58 for currents and Figure 5.60 and Figure 5.61 for salinity. Peak ebb and flood currents are shown spatially in Figure 5.59. Model performance statistics are shown in Table 5.12. It should also be noted that the sea level and current data recorded at the Upper location was used to adjust the river flow boundary conditions and consequently interpretation of the sea level and current calibrations at this location should be treated with caution.

The Mokau River estuary is similar in nature to both Marokopa and Awakino River estuaries. However, it is the receiving environment for a larger catchment (see Section 3.6) and tidal variability in sea level, current speed and salinity were more apparent at the Upper location in the Mokau River estuary than in the Awakino or Marokopa River estuaries. High river flow events also had a less pronounced effect on the tidal signal at the Lower location. Unlike Awakino and Marokopa River estuaries, the calibration of Mokau river estuary included a comparison between the modelled and measured salinity at the Upper location.

The measured sea level at the Upper and Lower locations were dominated by tidal oscillations during the deployment period, and this was reproduced by the model. There were gaps in the data for the Lower location which coincided with the two high flow periods events. The first was centred on 25 August 2015 and the second occurred between 1 and 8 September. However, these events were recorded by the instrument at the Upper location. The flood event was captured by the model although the rise in sea level during these events was over predicted by the model. Over all the sea level calibration scored better at the Lower location (BSS = 0.94, α = 0.96, β = 0.00 and RMSE = 0.18 m) than at the Upper location (BSS = 0.83, α = 0.87 and a β = 0.04 and RMSE = 0.27 m) though this may have been partly due to the absence of measured data at the Lower location during the high flow periods.

Currents were more difficult to capture in the model with flood tidal current speeds underrepresented by the model at the Lower location. At the Upper location the modelled tidal oscillations were considerably smaller than in the measured signal. Overall the calibration was better at the Lower location (BSS = 0.86) than at the Upper location (BSS = 0.52). Plots of peak flood and ebb currents (Figure 5.59) show stronger currents on the ebb tide due to the effect of river flow.

Modelled salinity at the Lower location most closely matched the surface measurements. It also performed well against the mean salinity record, but several salt water intrusion events recorded by the sea bed salinity gauge were not seen in the model. At the Upper location tidal

salinity intrusions were observed in the measured data, but the model produced values of approximately 0 psu throughout the model run at this location.

Figure 5.54: Mokau River estuary deployment locations.

Table 5.12: Skill scores for the Mokau River estuary calibrations.

Variable	Briar Skill Score (BSS)	α	β	γ	R^2	RMSE
Sea Level (Upper)	0.83	0.87	0.04	N/A	0.87	0.27 m
Sea Level (Lower)	0.94	0.97	0.02	N/A	0.96	0.17 m
Currents (Upper)	0.52	0.30	0.05	1.23	0.3	0.25 m s^{-1}
Currents (Lower)	0.86	0.44	0.28	0.06	0.44	0.21 m s^{-1}
Salinity (Lower: Mean)	0.87	0.55	0.00	0.32	0.55	9.7 psu
Salinity (Lower: Surface)	0.93	0.75	0.00	0.07	0.48	7.54 psu
Salinity (Lower: Bed)	0.66	0.44	0.02	0.49	0.45	14.7 psu
Salinity (Upper: Mean)	0.99	0.00	0.00	0.10	0.00	3.47 psu
Salinity (Upper: Surface)	0.99	0.00	0.00	0.27	0.00	0.23 psu
Salinity (Upper: Bed)	0.96	0.00	0.00	0.09	0.00	6.8 psu

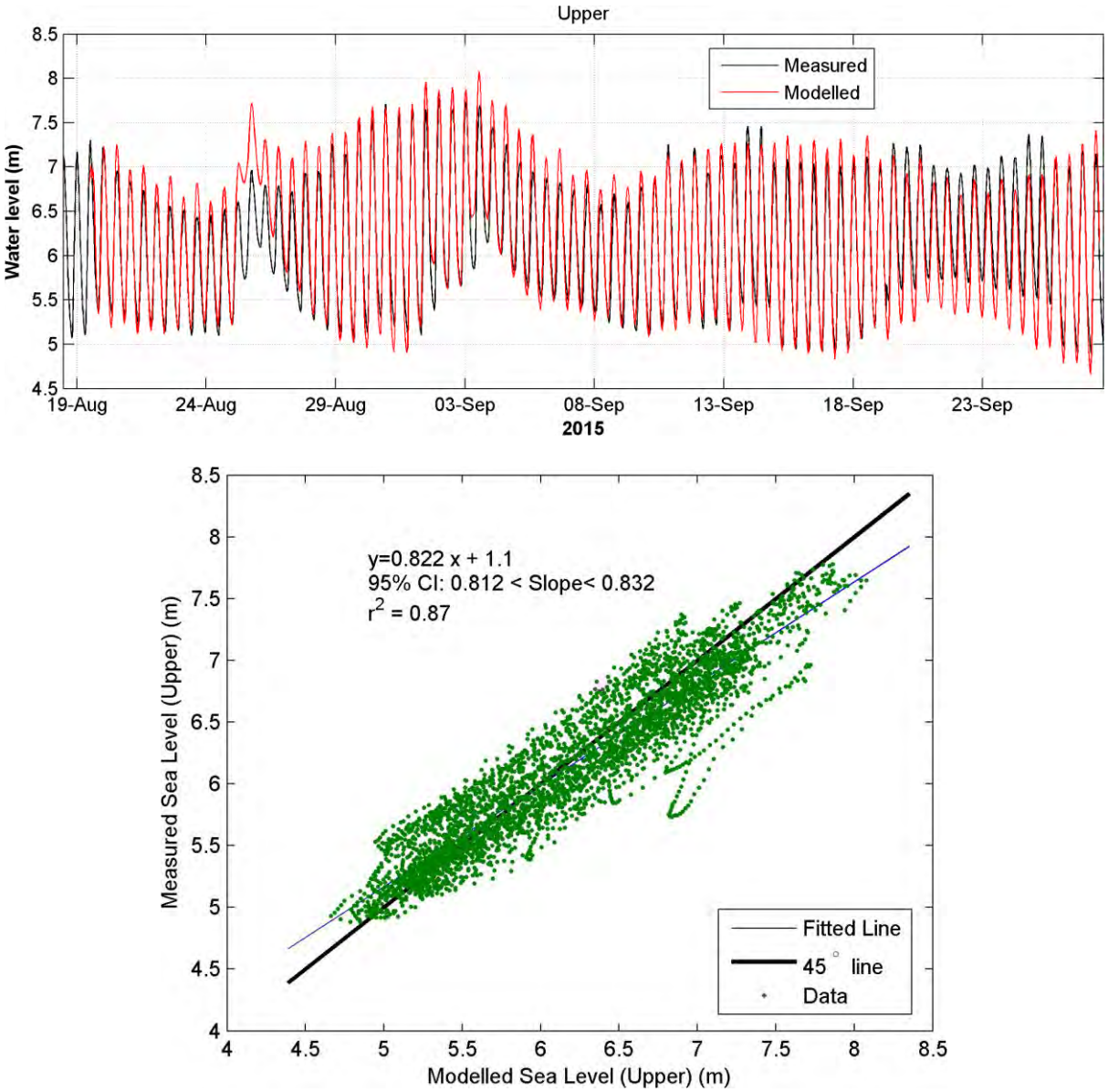

Figure 5.55: Mokau River Estuary sea level calibration at the Upper deployment location as a time series (upper panel) and as a linear regression (lower panel).

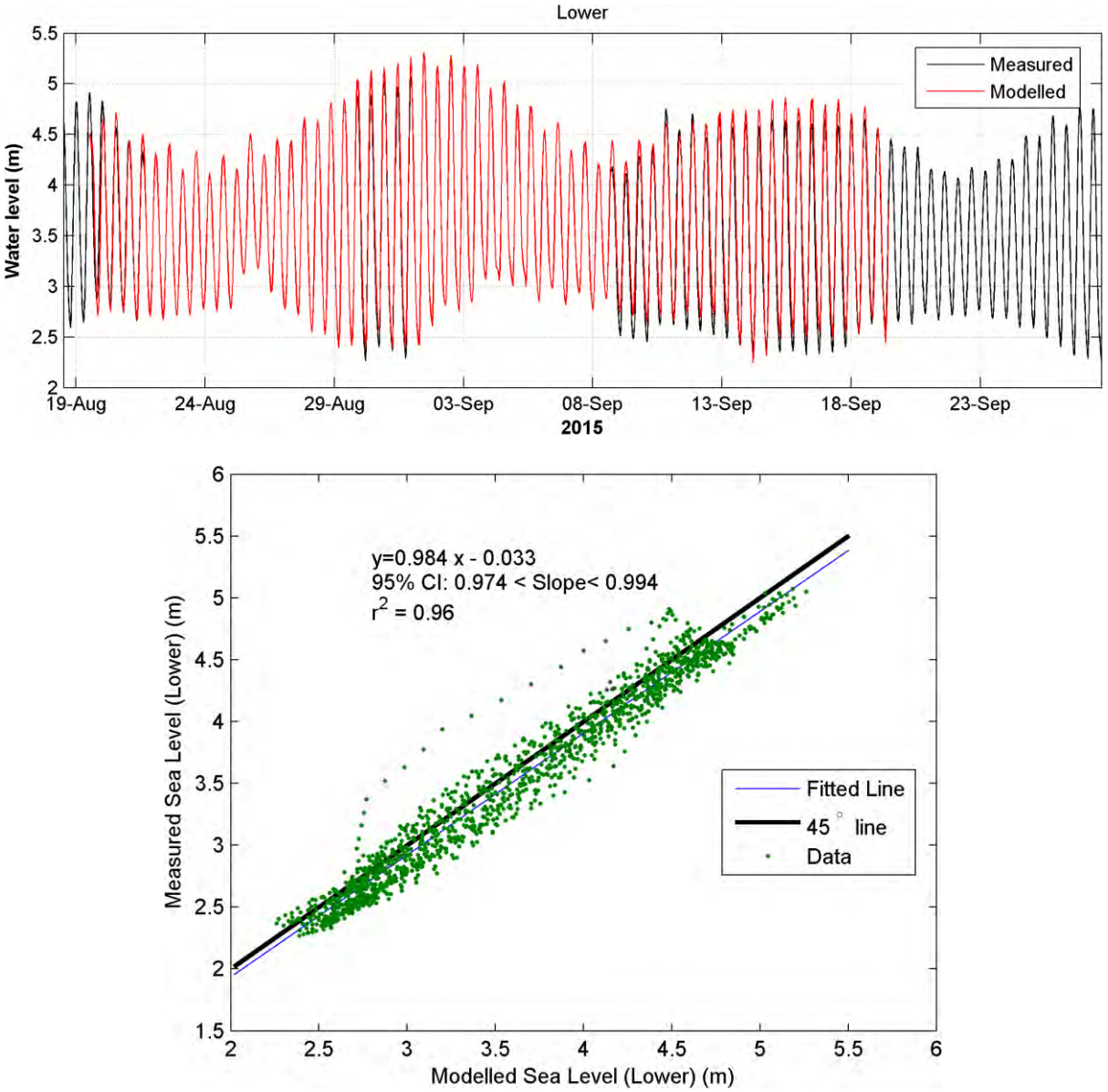

Figure 5.56: Mokau River Estuary sea level calibration at the Lower deployment location as a time series (upper panel) and as a linear regression (lower panel).

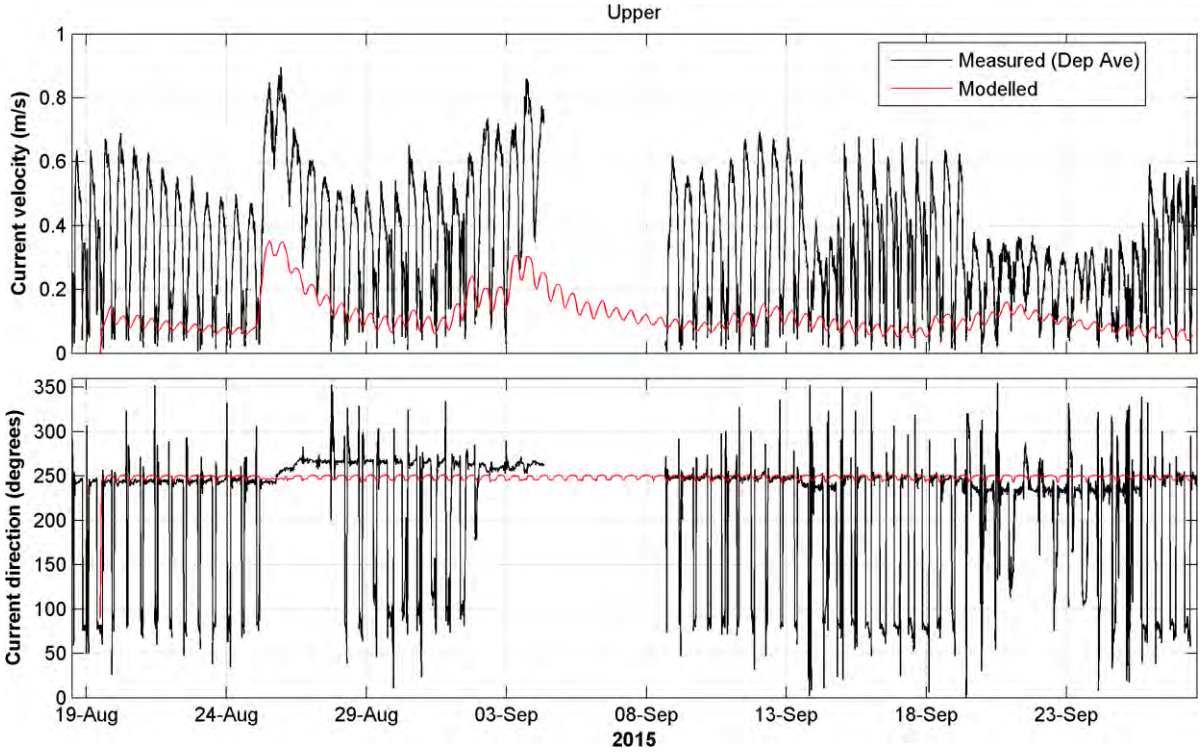

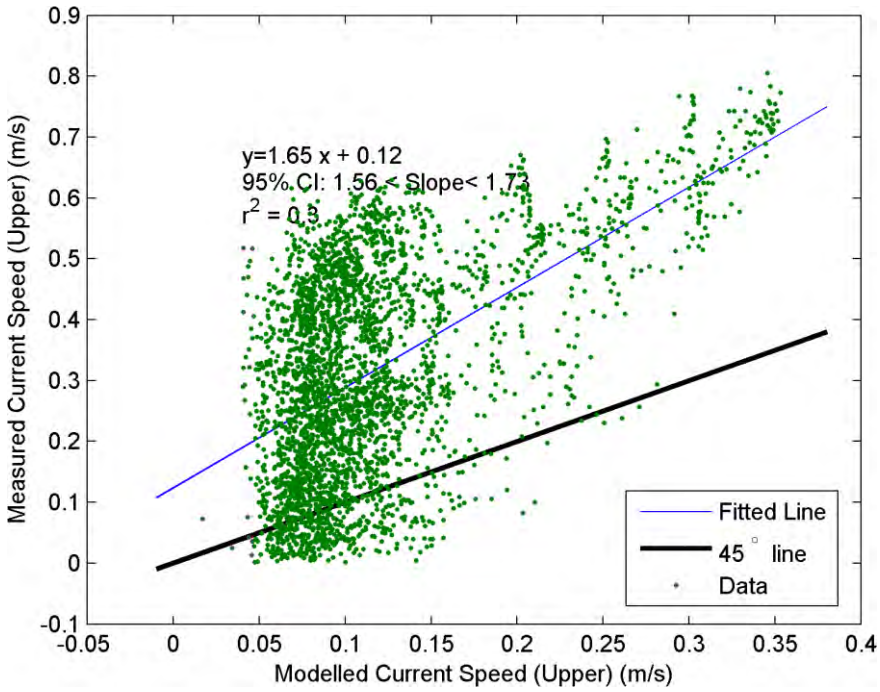

Figure 5.57: Mokau River Estuary current calibration at the Upper deployment location as a time series (upper panel) and as a linear regression of modelled versus measured current speed (lower panel).

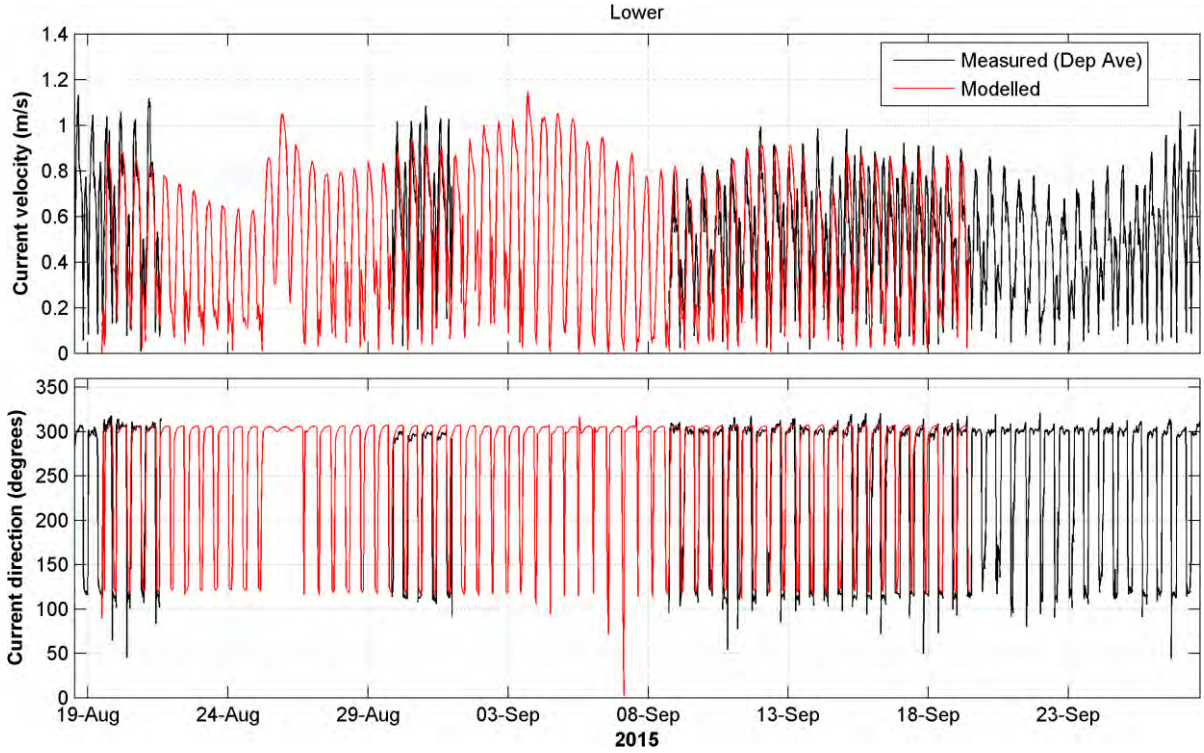

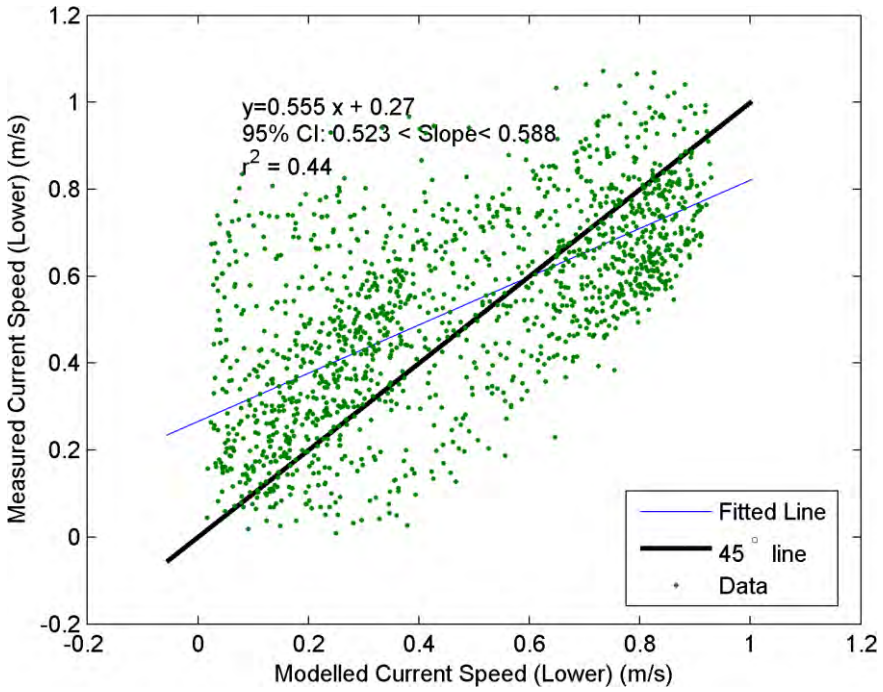

Figure 5.58: Mokau River Estuary current calibration at the Lower deployment location as a time series (upper panel) and as a linear regression of modelled versus measured current speed (lower panel).

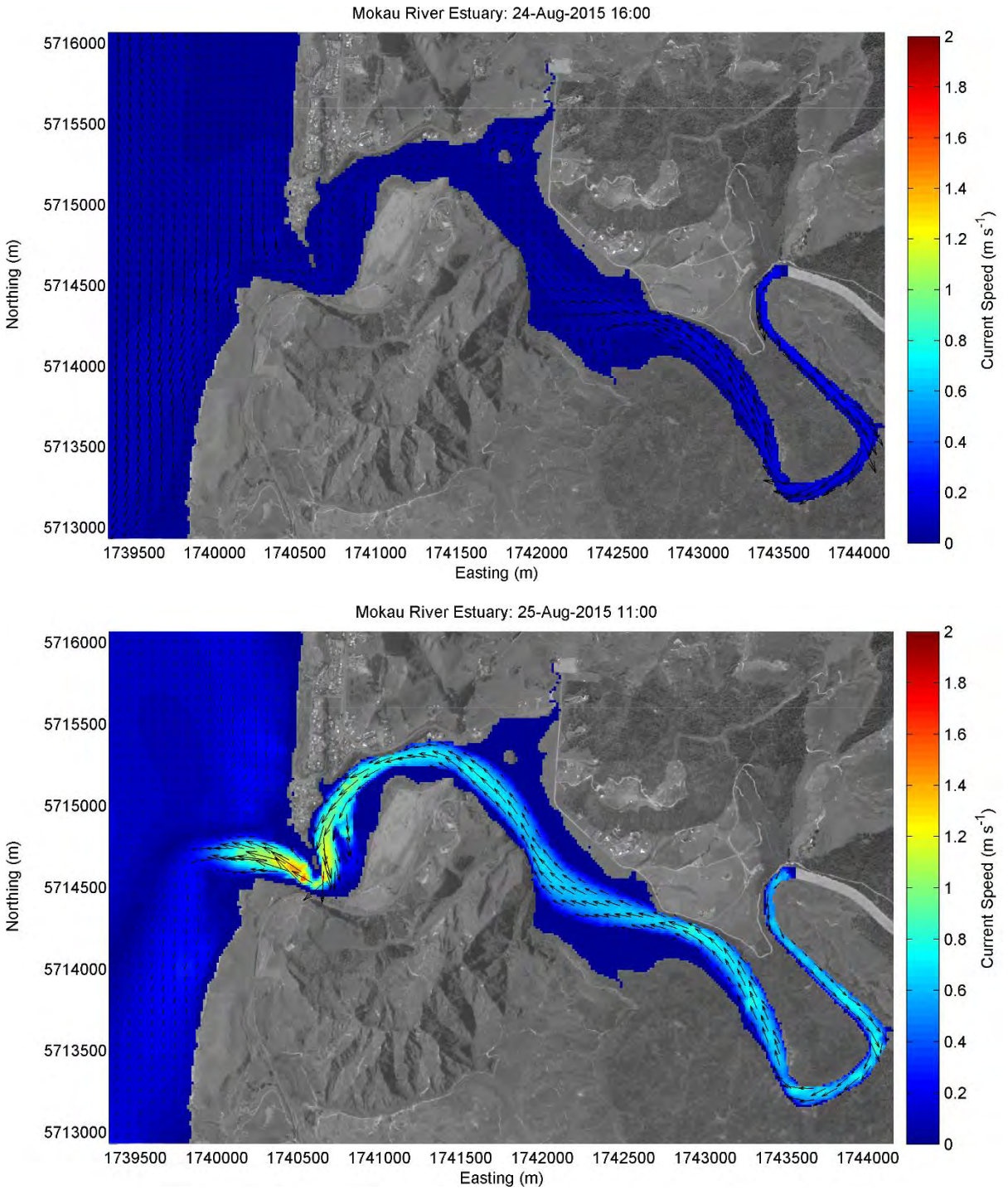

Figure 5.59: Mokau River estuary peak flood (upper panel) and ebb (lower panel) currents.

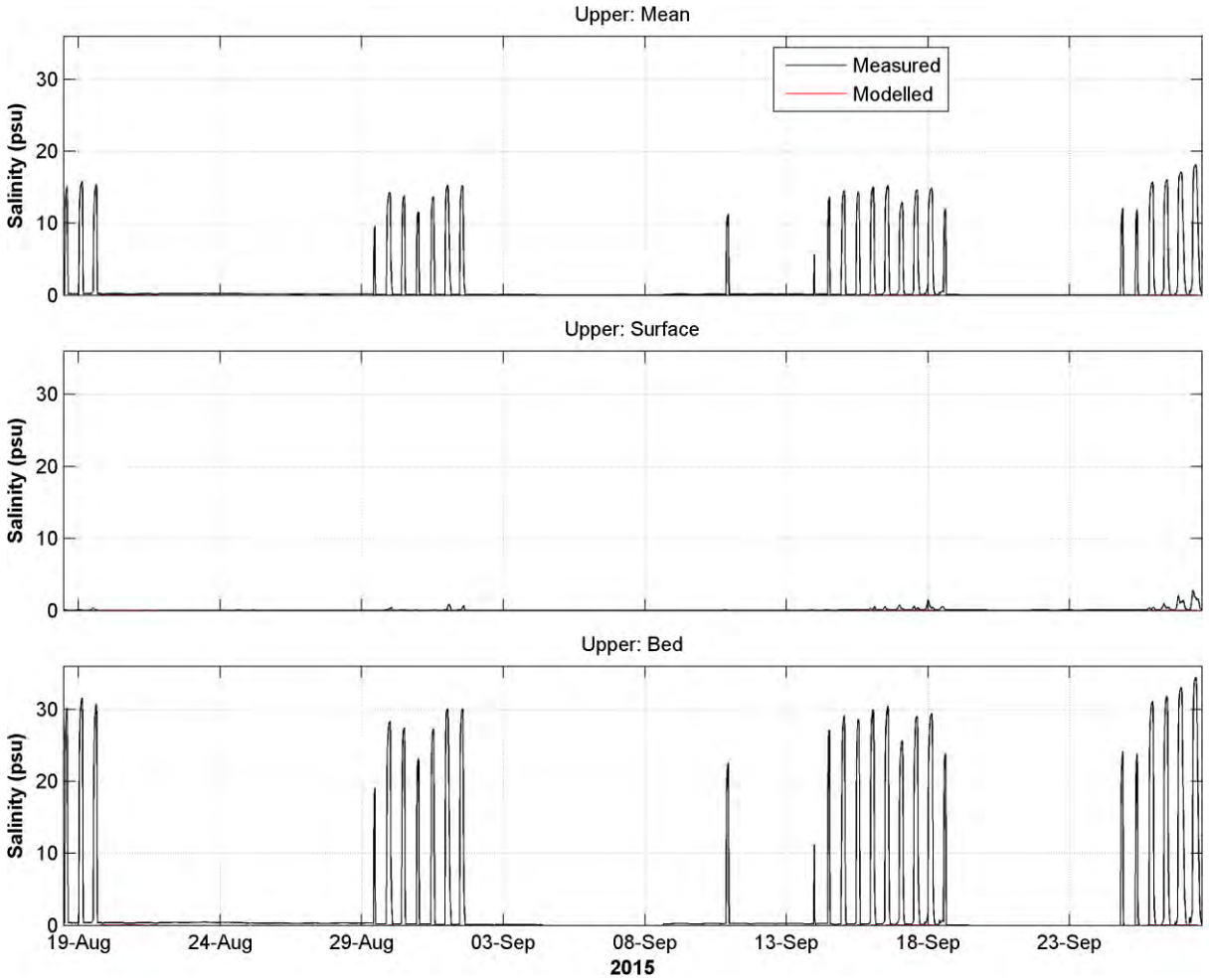

Figure 5.60: Mokau River Estuary salinity calibration at the Upper deployment location.

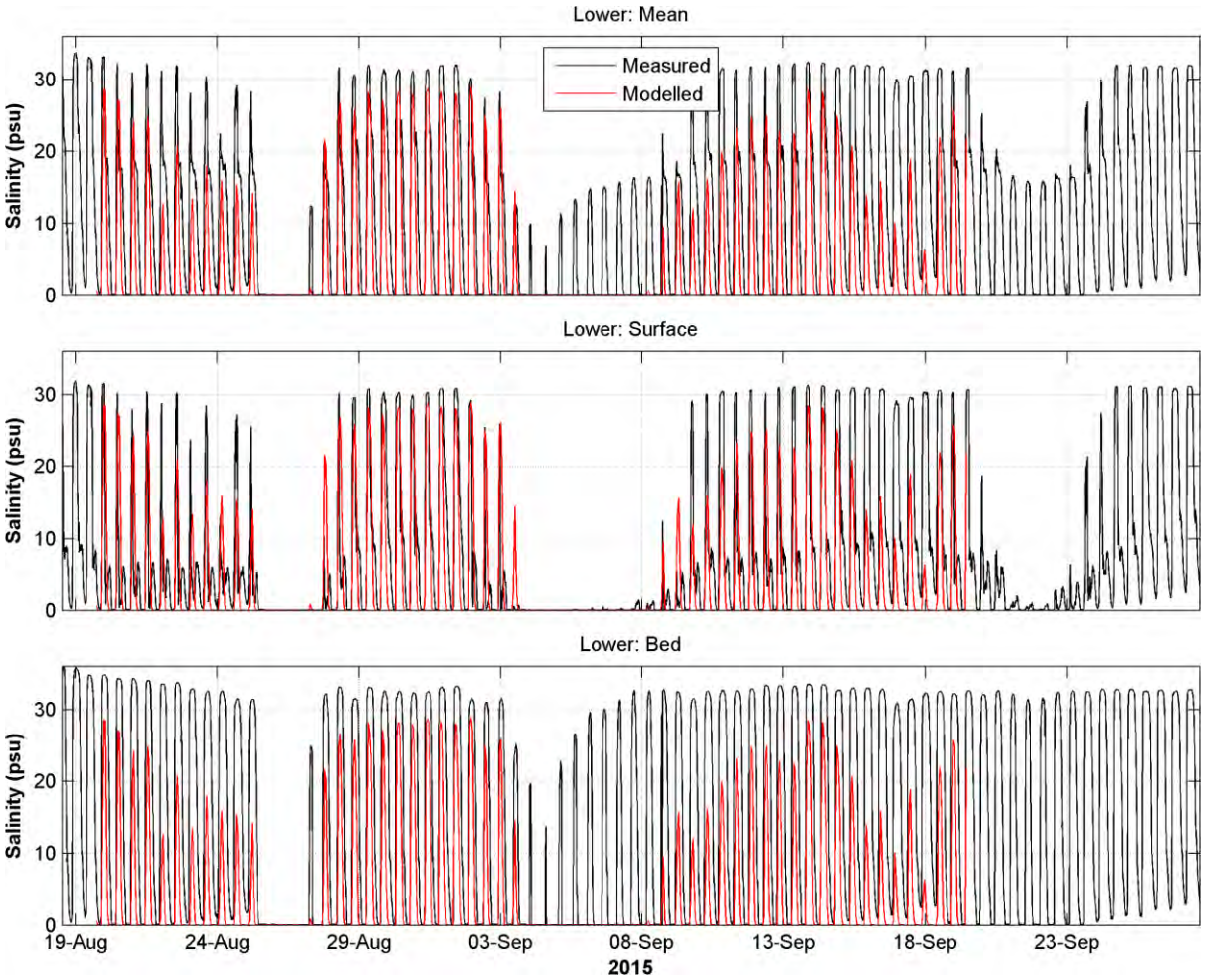

Figure 5.61: Mokau River Estuary salinity calibration at the Lower deployment location.

6 Model Limitations

The modelling and associated calibrations presented here provide hydrodynamic models which take into account the dominant physical processes and major freshwater inputs for the 7 estuaries. However, the calibration process identified areas where model performance could be improved. In particular, the present modelling approach seemed to have limited success in the Waikato River estuary where current speed and salinity were poorly represented in the model. In Aotea harbour, the model was calibrated to sea level, current and salinity data at a single location. Additional field data would be beneficial for gaining a better understanding of model performance in this estuary.

The models are 2D at present, and this limits the physical processes that can be represented by the models such as salinity stratification, stratified hydrodynamic flow and vertical mixing. At some locations the pattern of measured salinity differed between the surface and the sea bed (Atkin et *al.*, 2015) indicating the presence of a salt wedge or some degree of stratification. In the tidal river estuaries in particular, the model tended to underrepresent the extent of saline intrusion into the estuaries. If the models were extended to 3D they would be capable of simulating stratification and this would likely improve model performance. An MSc project currently underway (R. McIntosh Pers. Comm., 2016) aimed at recalibrating a 3D model of Whaingaroa harbour. It should be noted the 3D modelling is more computationally intensive than 2D modelling.

The current model grids are cartesian (square model cells). While this is simple and intuitive to interpret, it does not allow for variable cells sizes throughout an individual model domain. Other methodologies for the representation of bathymetries include the use of curvilinear and unstructured grids which allow for changing resolution in areas where it is needed such as within dendritic estuary arms and through harbour mouths. Using these methodologies also allows for a more efficient use of space and can result in fewer model cells being used. This can result in reduced model run times which would be beneficial if the models were to be extended to 3D.

For each of the tidal river estuaries, measured sea level, current and salinity data were collected at a location corresponding the upstream open boundary of the estuary model domains. In each case, evidence of tidal effects was seen in the sea level, current and in some cases the salinity data. The flow boundary conditions used in the models were unidirectional and did not incorporate tidal modulation that was observed in the measurements. This could be addressed either by incorporating tidal modulation into the flow boundary conditions or by extending the model domains upstream to locations where tidal effects are no longer evident.

The former option is difficult to achieve as the tidal effects appear to be attenuated by high flow conditions (see Section 5.5) possibly in a non-linear way. The latter option would require the extension of the bathymetry surveys upstream to the non-tidal regions of the estuaries and alteration of the model domains to incorporate this region of the rivers. This would be considerably easier to achieve using a curvilinear or unstructured approach to creating model grids.

Finally, the ability of the models to correctly represent variability in salinity was largely dependent on the fresh water inputs, and it would be useful to address shortfalls in the catchment modelling. For example, there are no gauged rivers in Aotea harbour, and gauging of one or more of the larger rivers in this catchment would be of great benefit in calibrating the catchment model. Additionally, the catchment model used for the drowned river valley estuaries produced daily flow rates, and it would be beneficial to increase the resolution of this model to an hourly time step. For the tidal river estuaries the river flow was calculated using gauged river flow but it would be useful to validate this process at locations closer to the river mouths

7 Conclusions and Recommendations

We have developed partially calibrated 2D hydrodynamic models for seven estuaries on the west coast of the Waikato region. These estuaries are: The Waikato River estuary, Whaingaroa (Raglan) Harbour, Aotea Harbour, Kawhia Harbour, Marokopa River estuary, Awakino River estuary and Mokau River estuary.

Catchment modelling to generate river inflows for the estuary models used a different approach for the drowned river valley estuaries (Whaingaroa Harbour, Aotea Harbour and Kawhia Harbour) than for the tidal river estuaries (the Waikato River estuary, Marokopa River estuary, Awakino River estuary and Mokau River estuary). For the drowned river valley estuaries, the INCA catchment model was used which simulated daily river flow based on measured meteorological data and land use specific to each sub-catchment. The catchment models were calibrated against available gauged flow data. Both Whaingaroa and Kawhia estuaries have permanent flow gauges in their two largest rivers, but none of the rivers in Aotea Harbour have gauge records that could be used for model calibration. Where it was available modelled river flow was replaced with gauged data. The three tidal river estuaries to the south (Marokopa, Awakino, and Mokau river estuaries) were fed by single rivers and flow data from the Marokopa and Awakino flow gauges were used to estimate long term flow for each of these rivers.

The hydrodynamic modelling was undertaken using Delft-Flow and used a nesting procedure known as Domain Decomposition (DD). For each estuary, all available measured data were used to calibrate the modelled hydrodynamics. Modelled sea level and salinity were assessed using skill scores and other calibration metrics.

The Waikato River estuary was the most challenging of the estuaries to simulate. The riverine effect on sea level is well represented and currents were in phase, but current speeds were underestimated in the model. Analysis of measured data identified that the open ocean wave climate appears to have a strong impact on sea level variability within the estuary with large waves events coincident with an increase in sea level.

The three drowned river valley estuaries (Whaingaroa, Kawhia and Aotea Harbours) calibrated quite well for currents and sea level. Modelled salinity picked up tidal variability and decreased salinity due to high river flows, but there is considerable scope for improvement. In particular, there was only one calibration site in Aotea Harbour and so there is limited confidence in the model. In the three tidal river estuaries to the south, agreement between measured and modelled data for sea level, currents and salinity varied at different locations. Broadly, the models correctly identified patterns in salinity intrusion, but overall

underestimated the amount of salt water entering the estuaries. Sea level was reasonably well represented although at upstream locations modelled sea level elevation was overestimated during high flow events.

Improvements to the model and methodology could be achieved by:

- Further calibration and validation of the models. This would require the collection of further field data.
- Extending the model to 3D. Using the current model framework, this may increase the computational time by up to an order of magnitude.
- Extending the model domain of tidal river estuaries further upstream to the point where the tidal influence is completely attenuated. This may involve additional bathymetric surveys.
- Using curvilinear or unstructured gridding schemes. This may be useful to do when extending the models to 3D.
- Improving freshwater inputs by gauging river flow in one or more of the major rivers feeding into Aotea Harbour and increasing the output time step of the catchment model to hourly instead of daily.

8 References

Atkin, E., Greer, D., Mead S., Haggitt, T., O'Neill, S., (2016), Hydrodynamic Model and Residence Times of the Waikato West Coast: Fieldwork and Data Collection. Prepared for Waikato Regional Council.

Becker, J. J., D. T. Sandwell, W. H. F. Smith, J. Braud, B. Binder, J. Depner, D. Fabre, J. Factor, S. Ingalls, S-H. Kim, R. Ladner, K. Marks, S. Nelson, A. Pharaoh, R. Trimmer, J. Von Rosenberg, G. Wallace, P. Weatherall., (2009), Global Bathymetry and Elevation Data at 30 Arc Seconds Resolution: SRTM30_PLUS, Marine Geodesy, 32:4, 355-371, DOI: 10.1080/01490410903297766

Deltares, 2013. User Manual Delft3D-FLOW. version: 3.15.2789, May 2013 Published and printed by: Deltares, 706 p. available online: http://oss.deltares.nl/web/delft3d/manuals.

Egbert, G.D., and S.Y. Erofeeva, (2002), Efficient inverse modeling of barotropic ocean tides, J. Atmos. Oceanic Technol., 19(2), 183-204.

Greer, S. D, McIntosh, R., Harrison, S., Phillips, D., and Mead, S., (2015) Understanding Water Quality in Raglan Harbour, Australasian Coasts & Ports Conference 2015.

Harrison, S. R. (2015), Morphodynamics of Ebb-Tidal Deltas (Thesis, Doctor of Philosophy (PhD)). University of Waikato.

Hulsing, H., Smith, W., & Cobb, E. D. (1966). Velocity-Head Coefficients in Open Channels. Technical Report, Geological Survey Water-Supply, United States Government Printing Office, Washington, U.S.A.

Jones, H. F. E., and Hamilton, D. P., (2014), Assessment of the Waikato River estuary and delta for whitebait habitat management: field survey, GIS modelling and hydrodynamic modelling. Prepared for Waikato Regional Council, TR 2014/35.

Kalnay, E., M. Kanamitsu, R. Kistler, W. Collins, D. Deaven, L. Gandin, M. Iredell, S. Saha, G. White, J. Woollen, Y. Zhu, A. Leetmaa, R. Reynolds, M. Chelliah, W. Ebisuzaki, W. Higgins, J. Janowiak, K. C. Mo, C. Ropelewski, J. Wang, R. Jenne, D. Joseph, (1996), The NCEP/NCAR 40-year reanalysis project, Bull. Amer. Meteor. Soc., 77, 437-470,

Mead, S. T. and Greer, D., (2007), Extreme Water Elevations in Raglan Harbour. Prepared for C & M Planning

Phillips, David; Mead, Shaw; Harrison, Shawn; Frazerhurst, James; Dodet, Guillaume; Klinginger, Chris and Borrero, Jose C. Oceanography in the public interest: Tales from Raglan. Coasts and Ports 2009.

Stark, N., Greer, D., Phillips, D., Borrero, J., Harrison, S., and Kopf, A. (2010). In-situ Geotechnical Investigation of Sediment Dynamics over 'The Bar', Raglan, New Zealand, American Geophysical Union, Fall Meeting 2010, abstract #OS43C-02

Soulsby, R. (1997), Dynamics of marine sands - A manual of practical applications, Thomas Telford.

Sutherland, J.and Peet, A.H. and Soulsby, R.L., (2004), Evaluating the performance of morphological models. Coastal Engineering, 51 (8-9). 917-939.

Van Rijn, L. C., Walstra D.J.R., Grasmeijer, B., Sutherland, J., Pan, S. and Sierra, J. P., (2003), The predictability of cross-shore bed evolution of sandy beaches at the time scale of storms and seasons using process-based profile models, Coastal Engineering 47 (3), 295-327.

Willet, R. N., (1983), Erosion-accretion and sedimentology of Aotea Harbour with reference to the erosion at Pourewa Point.

Whitehead, P.G., Wilson, E.J. and Butterfield, D. (1998a), A semi-distributed Integrated Nitrogen Model for Multiple source assessment in Catchments (INCA): Part I - Model Structure and Process Equations. Science of the Total Environment, 210/211: 547-558.

Whitehead, P.G., Wilson, E.J., Butterfield, D. and Seed, K. (1998b), A Semi-distributed Integrated Nitrogen Model for Multiple source assessment in Catchments (INCA): Part II Application to large River Basins in South Wales and Eastern England. Science of the Total Environment, 210/211: 559-583.

Appendix A. **INCA: Sensitivity Analysis**

As described above, the INCA catchment model was developed using available data from nearby AWSs. To assess the potential impact of this on model performance a sensitivity analysis was undertaken on the rainfall input into the Awaroa catchment within Kawhia Harbour.

The Awaroa catchment was chosen as the best catchment for sensitivity analysis as it gave strong flow calibration results with Owhiro rainfall input (Figure 3.13 and Figure 3.14), as well as strong flow validation results when the same inputs were applied to the Oparau catchment (Figure 3.15 and Figure 3.16).

Three rain gauges near the Awaroa catchment were chosen for analysis: Hauturu, Owhiro (the original gauge used for calibration) and Port Taharoa Aws. Figure 3.2 shows that these rain gauges range from mountainous (Hauturu) to intermediate (Owhiro) to coastal (Port Taharoa Aws), which is reflected in their extreme range in five-year mean annual cumulative rainfall (2651 mm, 1870 mm and 1241 mm respectively). The input files with these rain gauges were converted to flow through INCA-N with the same SMD and evaporation inputs, as well as INCA-N parameters, as the Awaroa calibration in Section 3.5. The flow results were then converted to cumulative loads for ease of analysis. The sensitivity analysis of each rain gauge ran from 22 December 2007 to 24 November 2014.

The extreme range in five-year mean annual cumulative rainfall was reflected in the extreme range in cumulative load results. The Hauturu rain gauge gave a final cumulative overestimation of 30.3% (Figure A.1), Owhiro overestimated by 0.1% (Figure A.2) and Port Taharoa Aws underestimated by 37.7% (Figure A.3). This suggests that, despite each rain gauge being within 20 km of the Awaroa catchment, the environment that the rain gauge is in may be just as important as its proximity to the catchment.

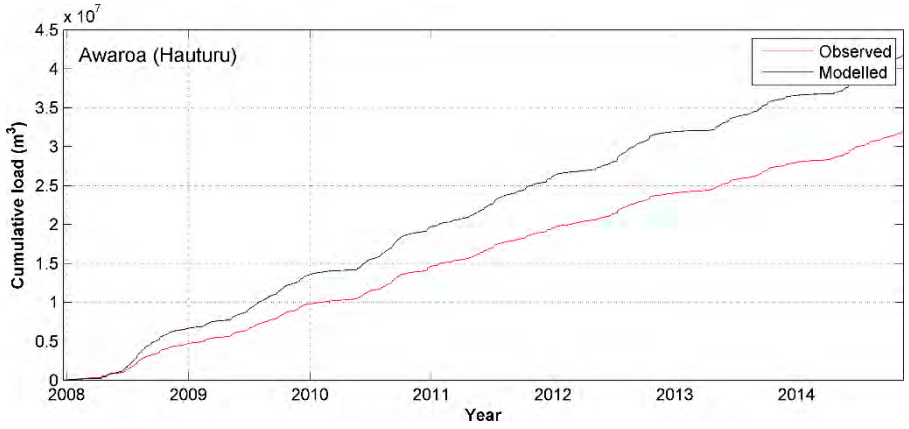

Figure A.1. Awaroa catchment sensitivity analysis using Hauturu rain gauge input: observed Awaroa cumulative water load against INCA-N catchment-modelled Awaroa cumulative water load between 2008 and 2014. By the end of the model the cumulative load was overestimated by 30.3%.

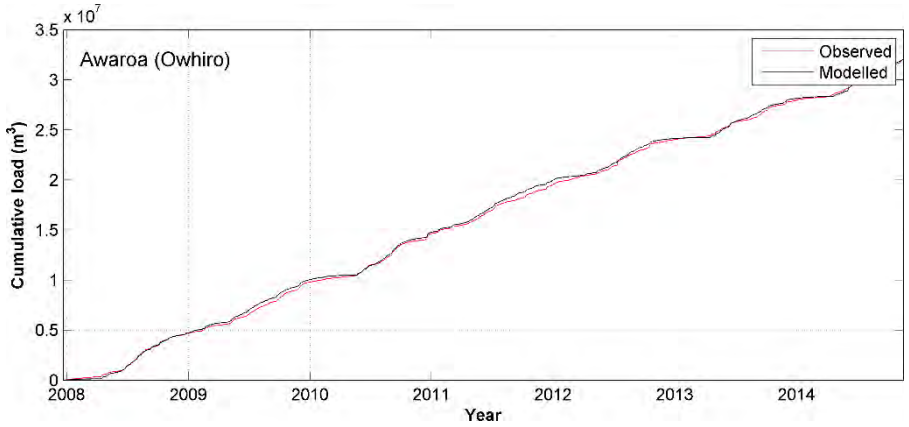

Figure A.2. Awaroa catchment sensitivity analysis using Owhiro rain gauge input: observed Awaroa cumulative water load against INCA-N catchment-modelled Awaroa cumulative water load between 2008 and 2014. By the end of the model the cumulative load was overestimated by 0.1%.

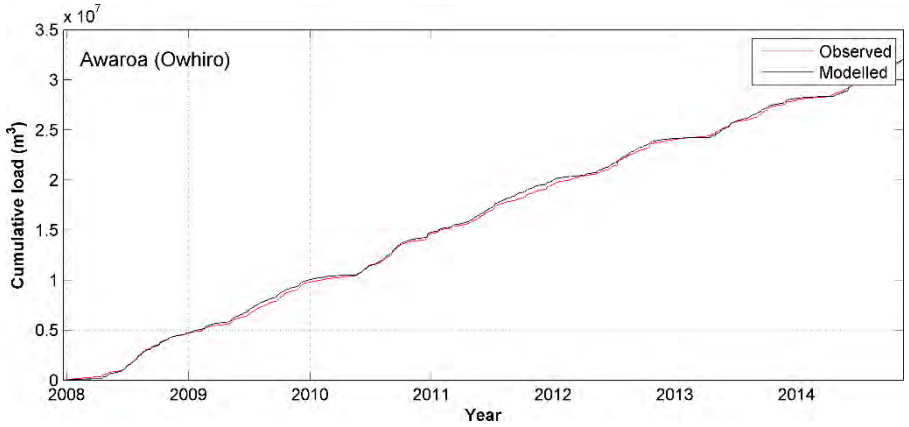

Figure A.3. Awaroa catchment sensitivity analysis using Port Taharoa Aws rain gauge input: observed Awaroa cumulative water load against INCA-N catchment-modelled Awaroa cumulative water load between 2008 and 2014. By the end of the model the cumulative load was underestimated by 37.7%.

Appendix B. Waikato River Estuary Sea Level Calibration Plots

This Appendix presents the sea level calibrations referred to in Section 5.1. The measured sea level data were recorded by Jones and Hamilton (2014) as part of a separate study which also creating a hydrodynamic model of the Waikato River estuary.

Figure B.1 to Figure B.5 present time series comparisons between measured and modelled sea level as well as linear regressions relating the two using modelled sea level as the independent variable.

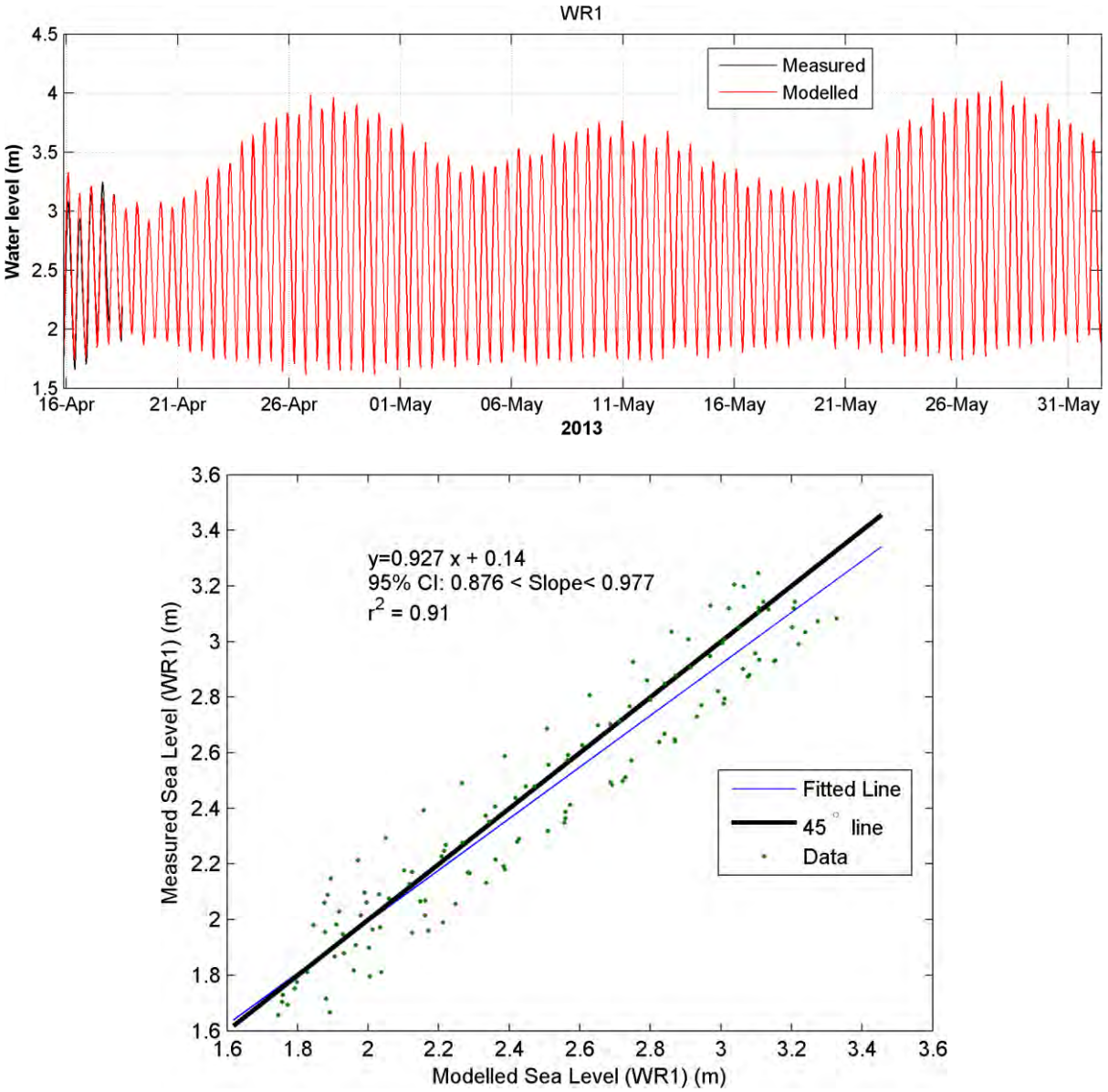

Figure B.1: Sea level calibration at the 'WR1' location in the Waikato River estuary as a time series (upper panel) and as a linear regression (lower panel).

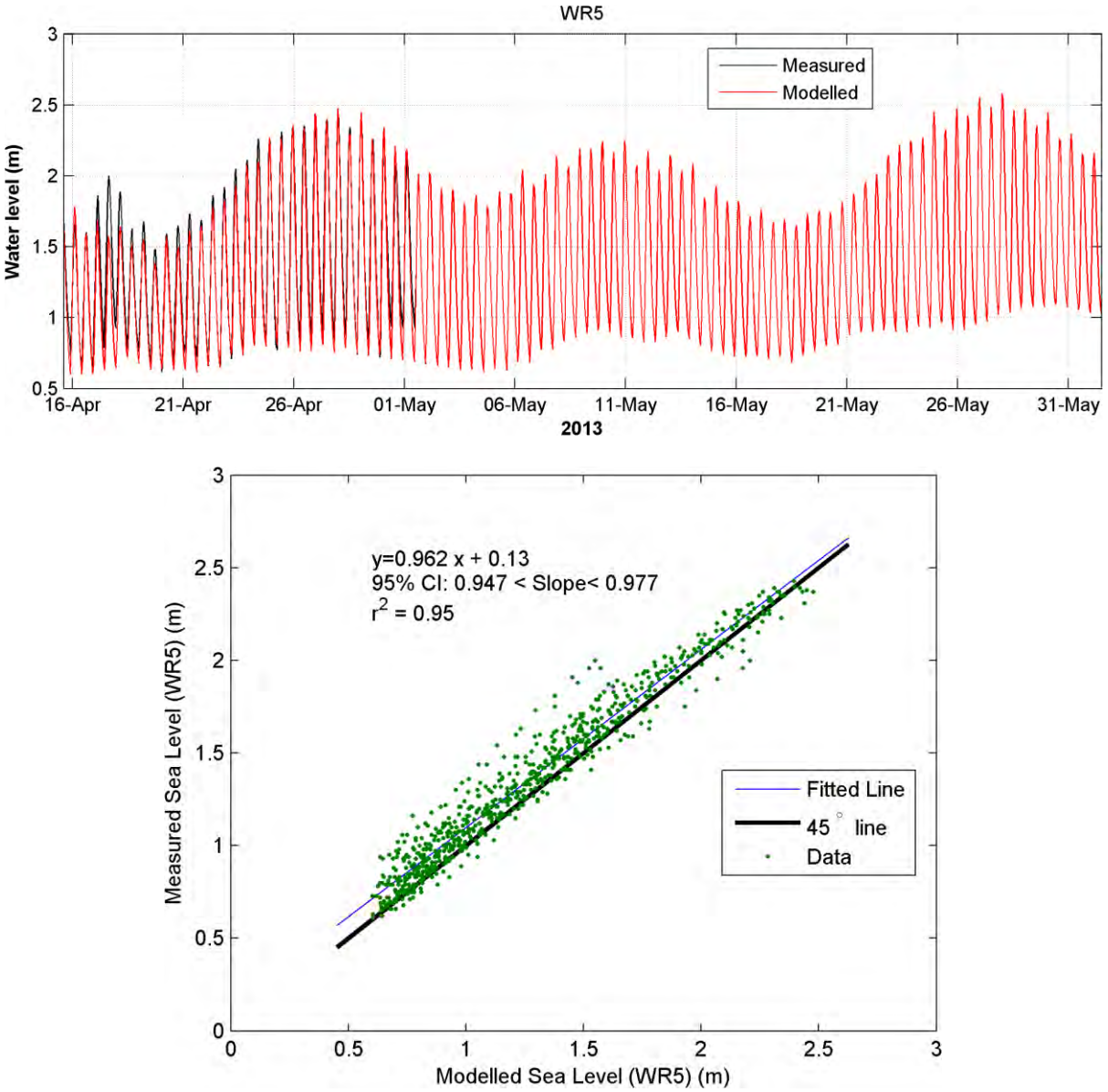

Figure B.2: Sea level calibration at the 'WR5' location in the Waikato River estuary as a time series (upper panel) and as a linear regression (lower panel).

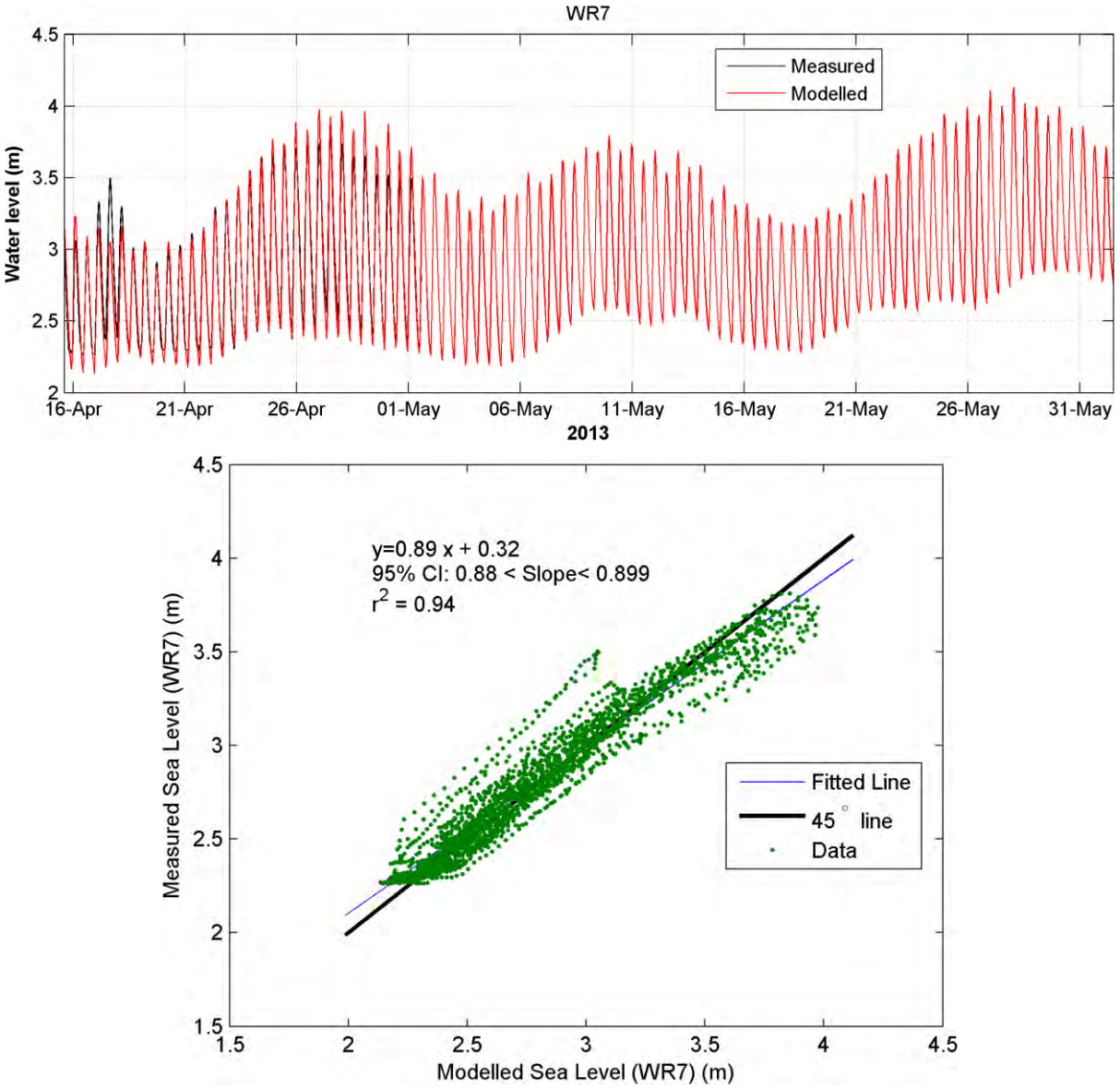

Figure B.3: Sea level calibration at the 'WR7' location in the Waikato River estuary as a time series (upper panel) and as a linear regression (lower panel).

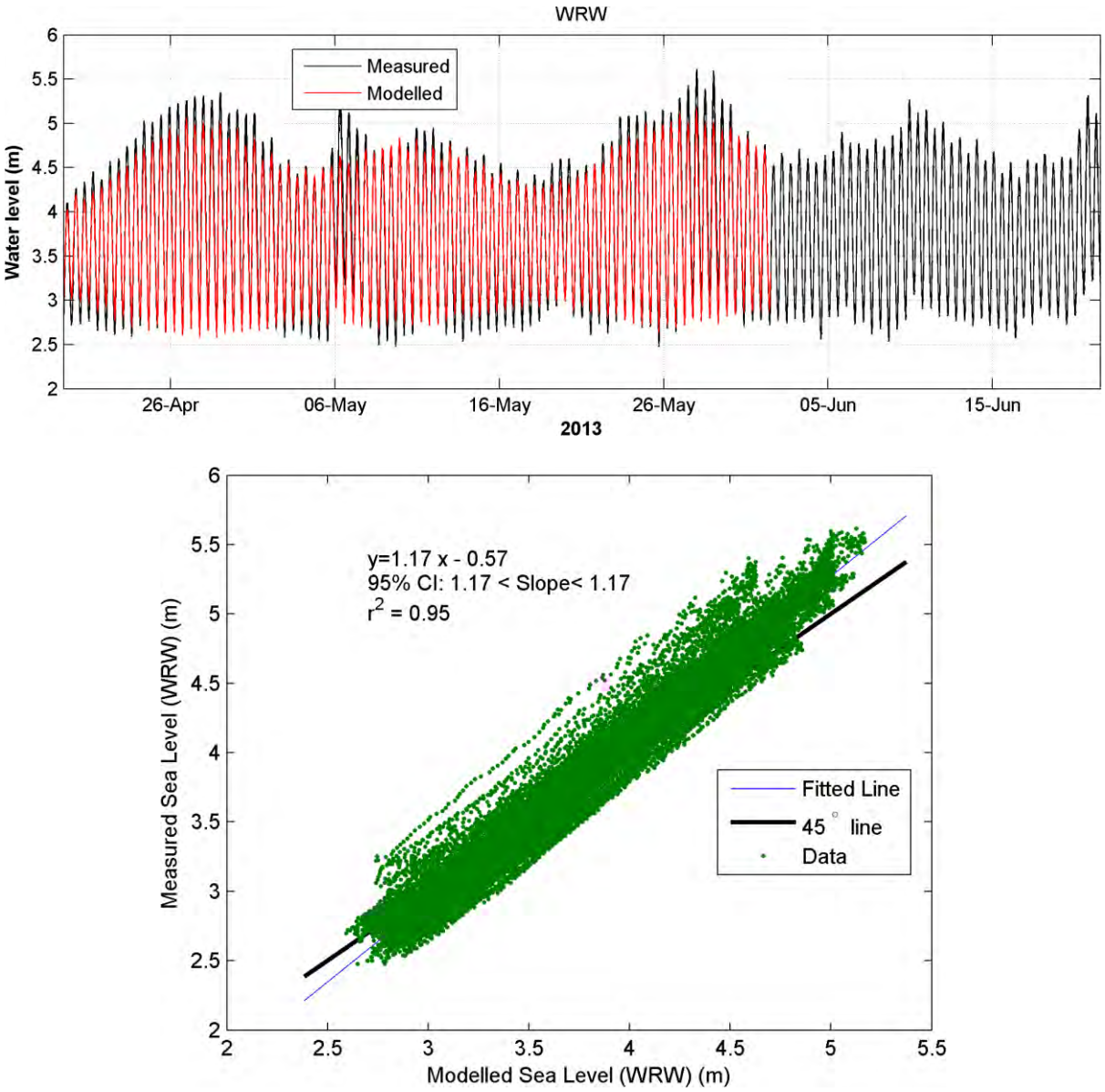

Figure B.4: Sea level calibration at the 'WRW' location in the Waikato River estuary as a time series (upper panel) and as a linear regression (lower panel).

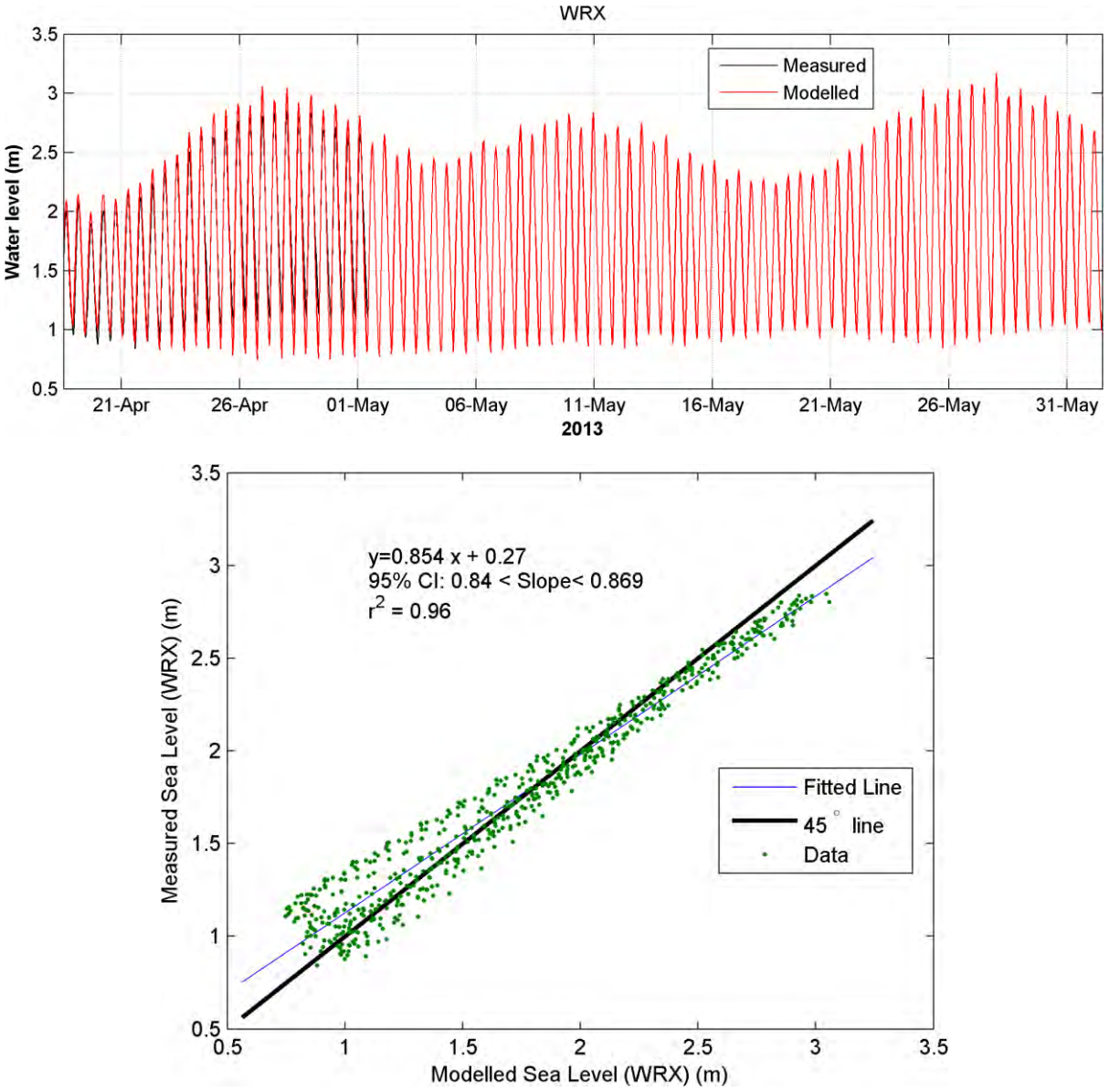

Figure B.5: Sea level calibration at the 'WRX' location in the Waikato River estuary as a time series (upper panel) and as a linear regression (lower panel).

Appendix C. **Whaingaroa ADCP Transects**

This Section presents the calibrations of current speed and velocity recorded bu a downward looking ADACP on 14 April 2014 by presented more fully in Harison (2015). The ADCP was used to undertake 24 transects through the harbour mouth measuring current speed and direction at 0.25 m bins through the water column (Harrison, 2015). The currents were vertically averaged for comparison with modelled data. A separate plot is shown for each comparison in Figure C.1 to Figure C.24. Skill scores have not been calculated for each of these, rather they provide a qualitative comparison between modelled and measured data to assess model performance over the ebb tide delta and the entrance to Whaingaro Harbour.

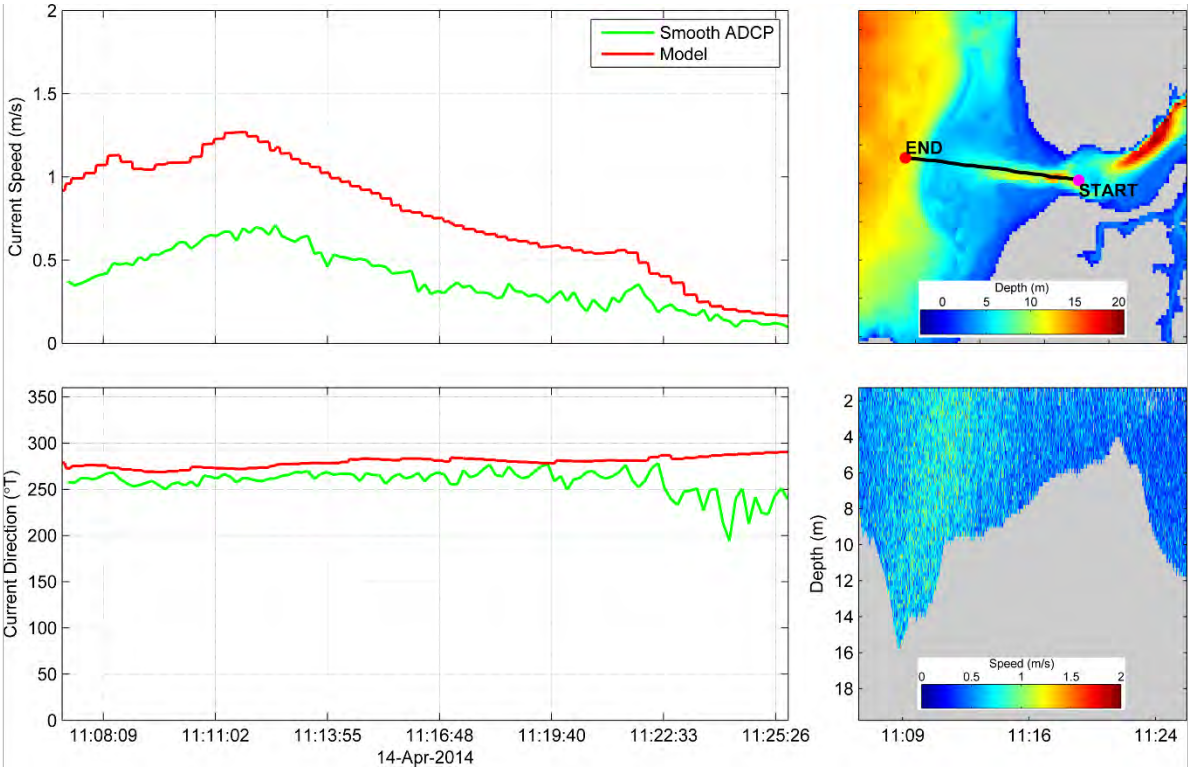

Figure C.1: ADCP Transect 1.

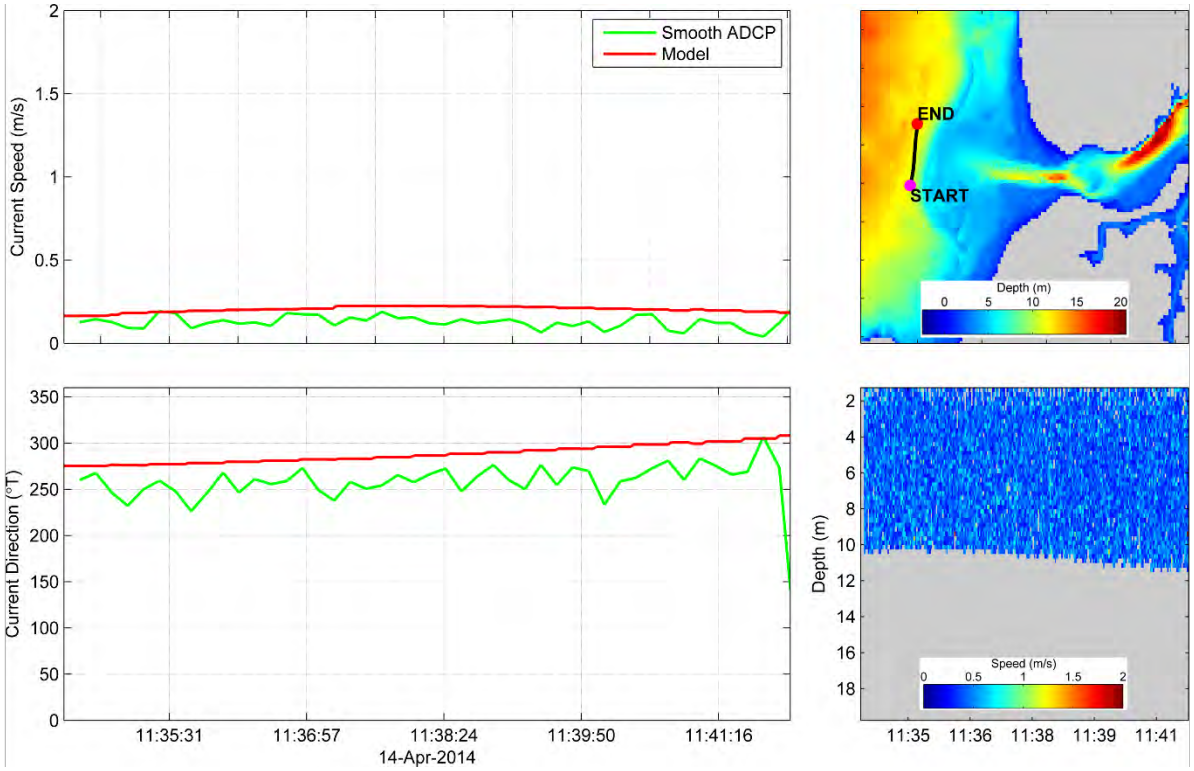

Figure C.2: ADCP Transect 2.

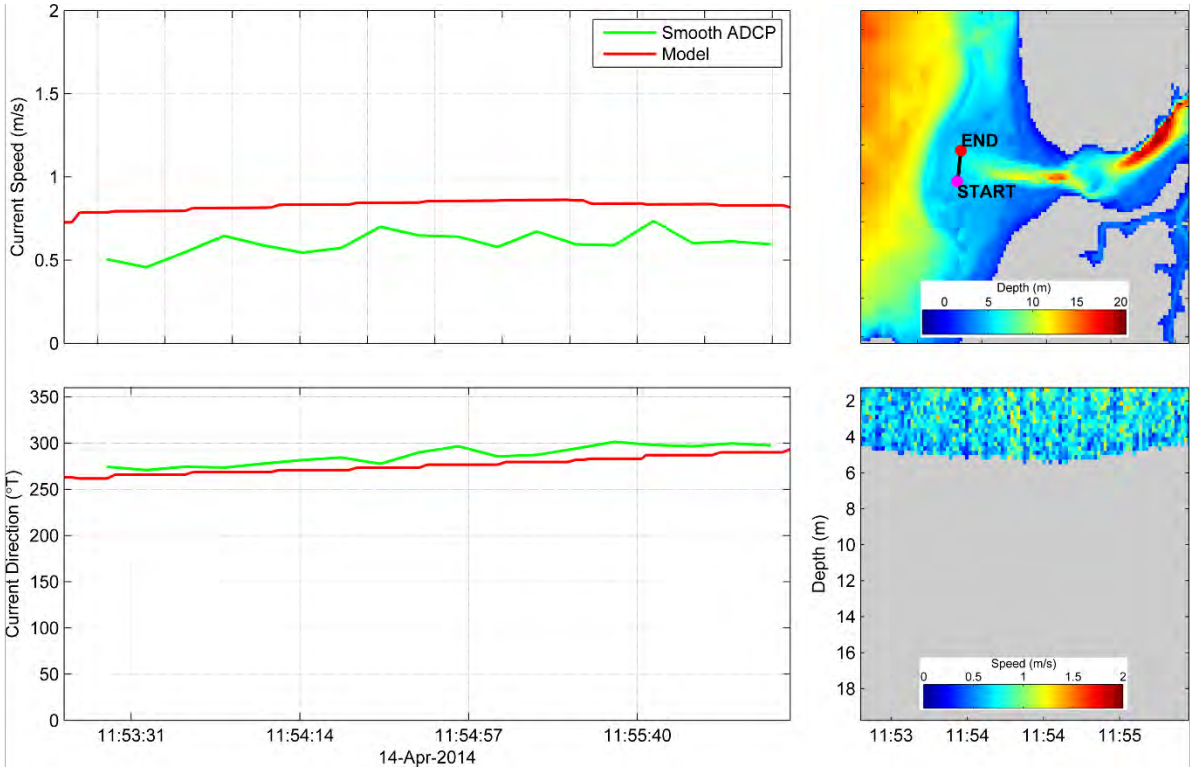

Figure C.3: ADCP Transect 3.

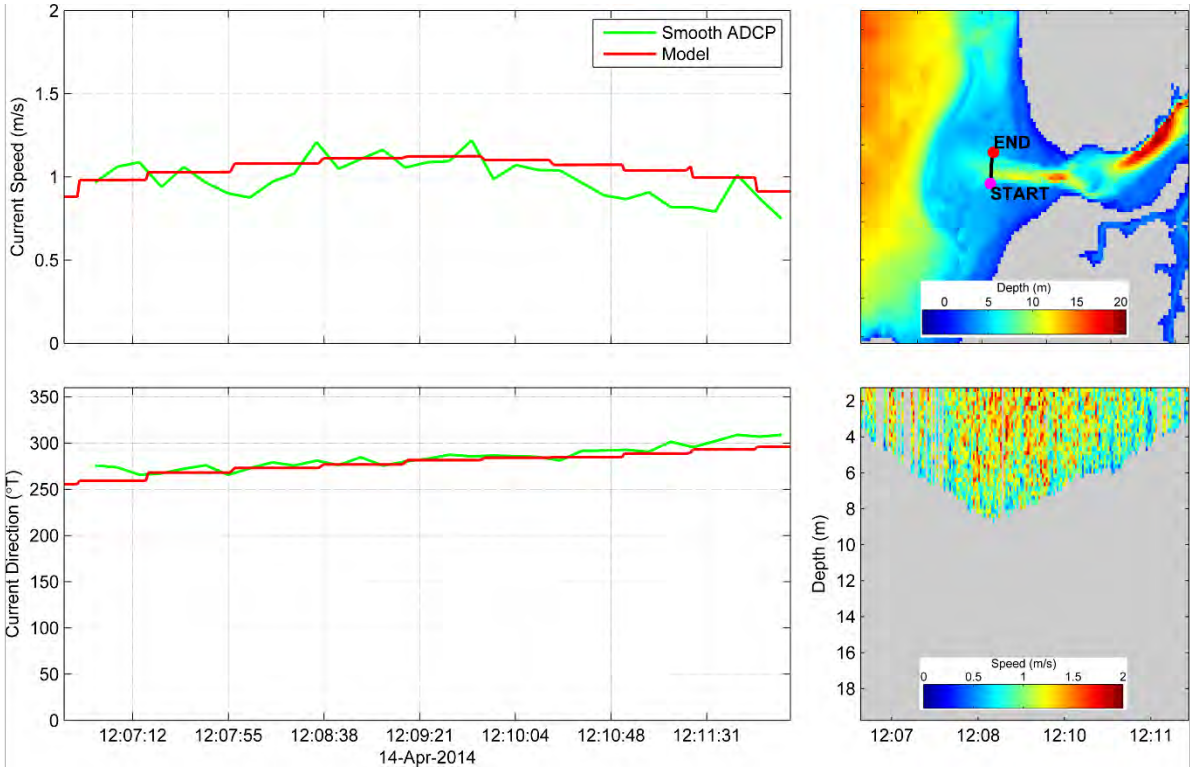

Figure C.4: ADCP Transect 4.

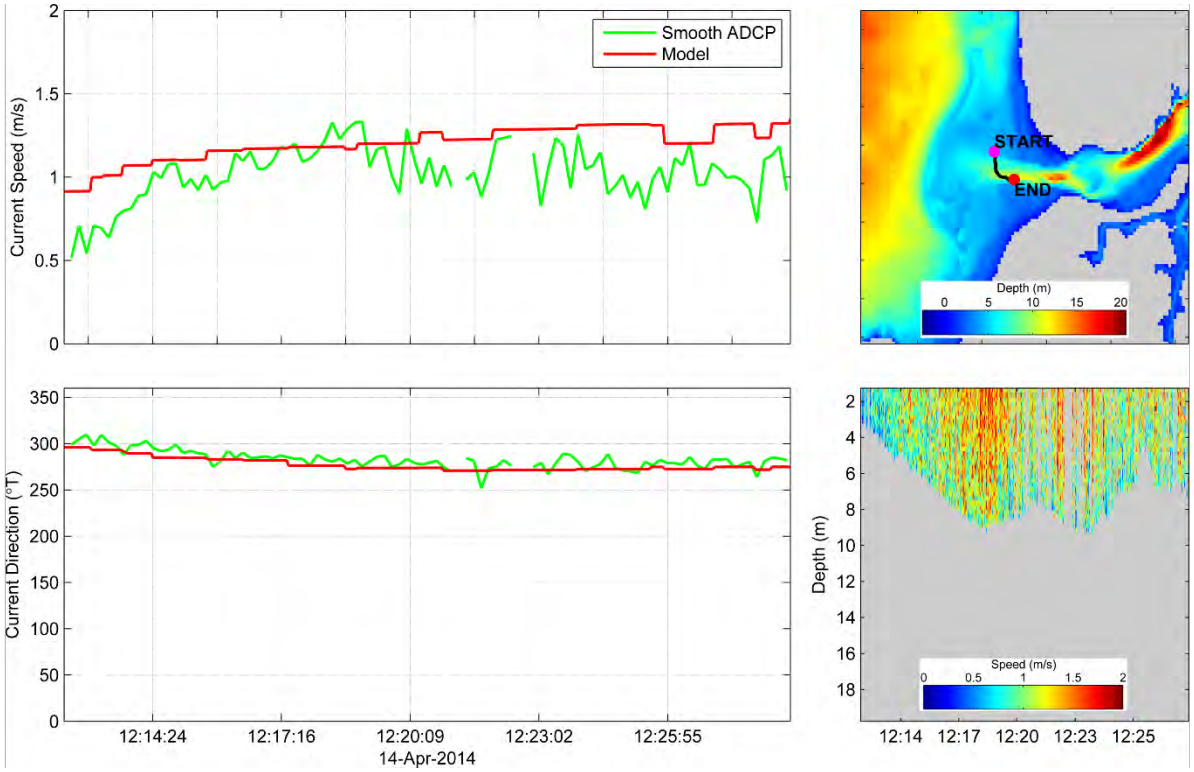

Figure C.5: ADCP Transect 5.

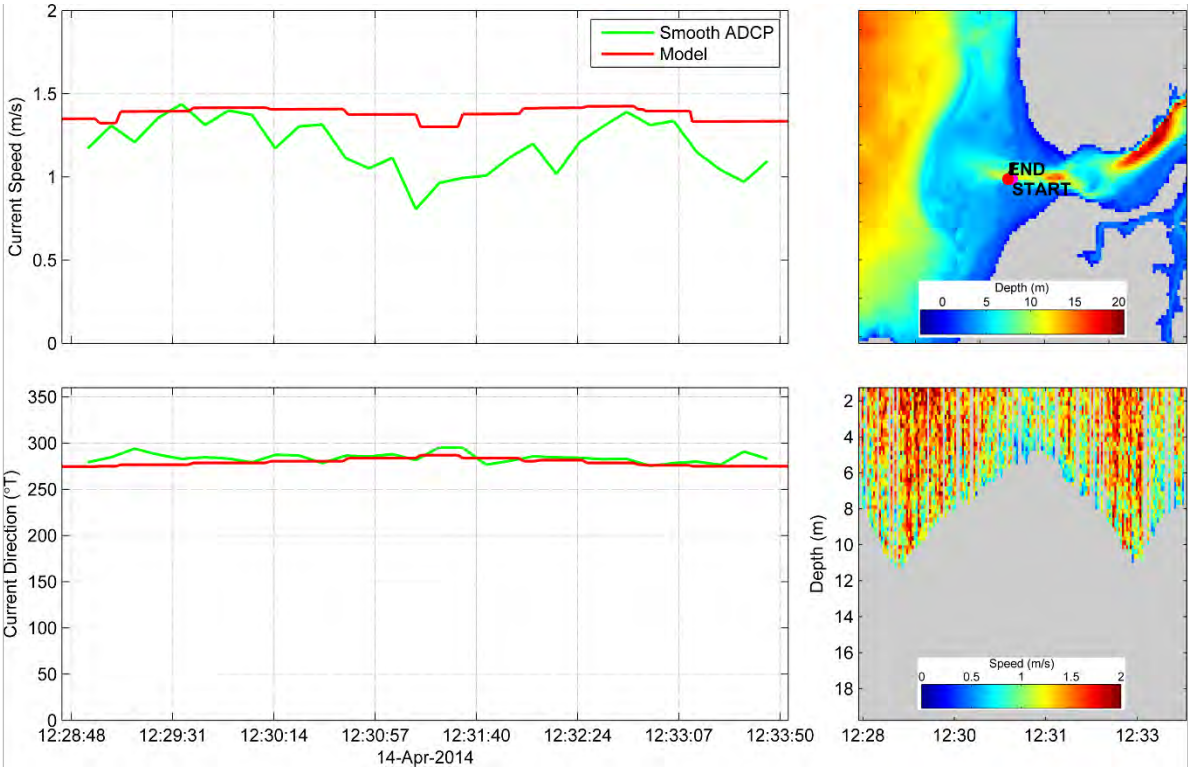

Figure C.6: ADCP Transect 6.

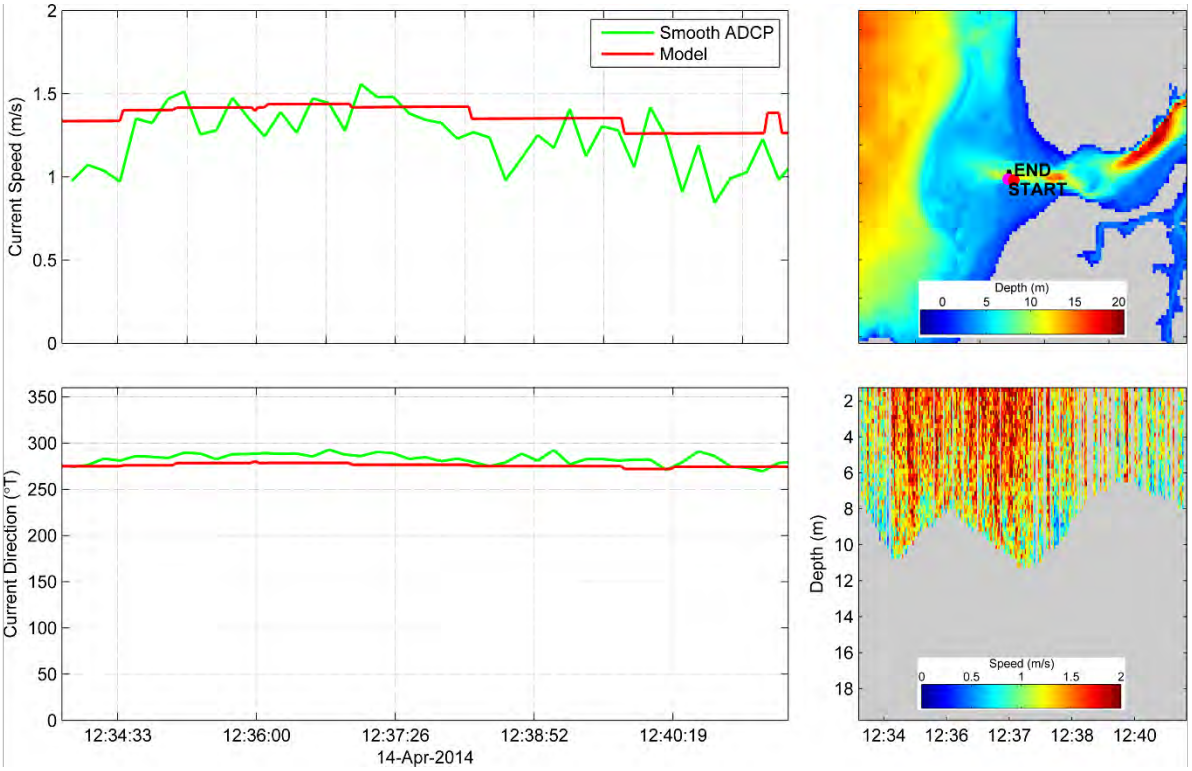

Figure C.7: ADCP Transect 7.

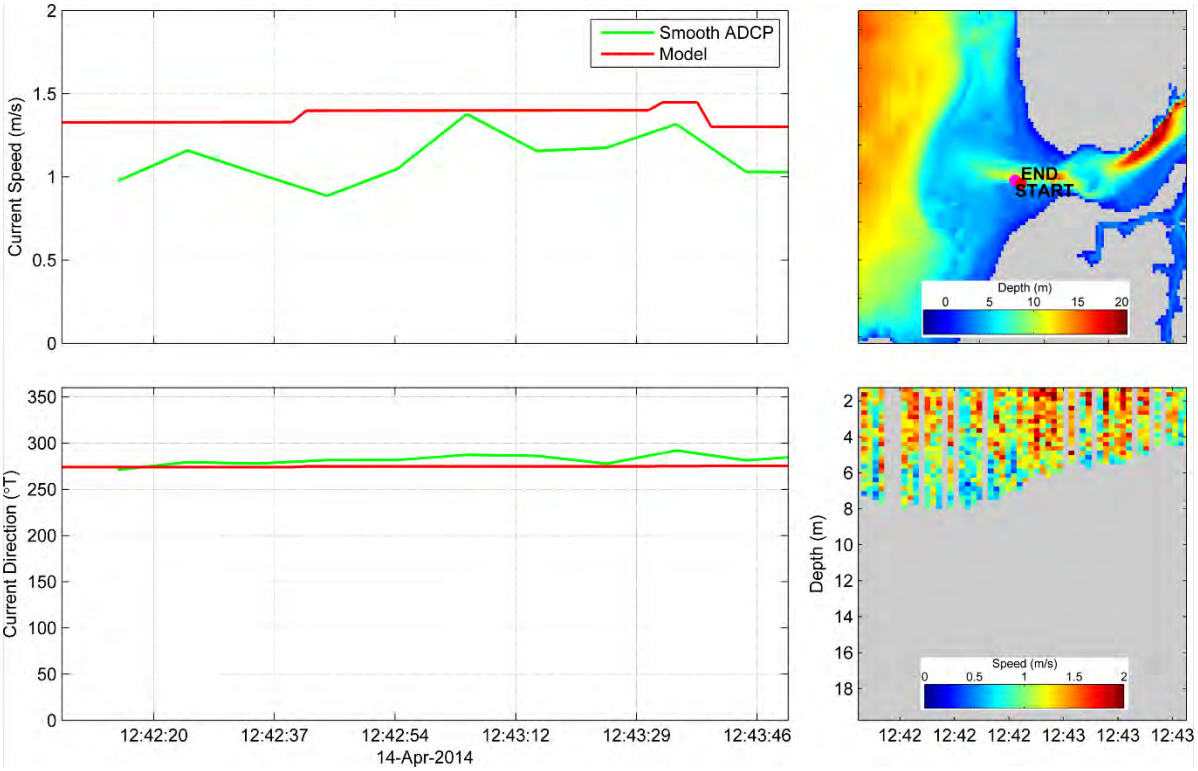

Figure C.8: ADCP Transect 8.

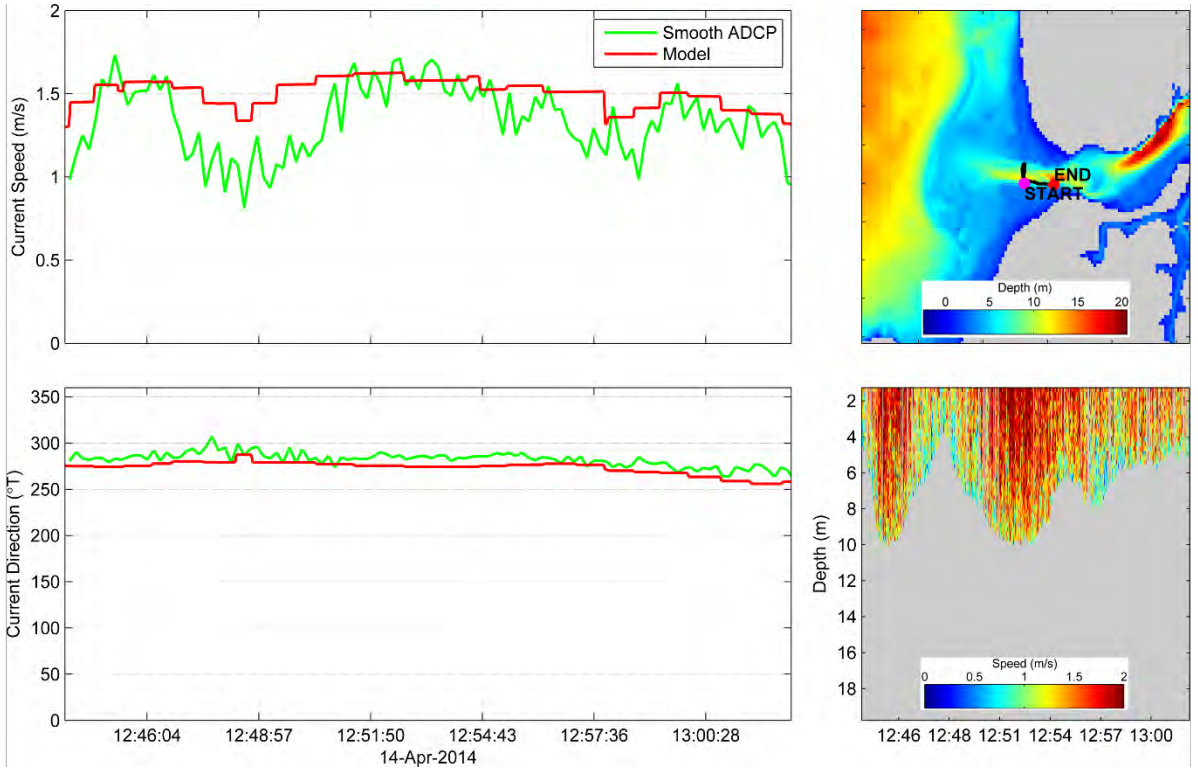

Figure C.9: ADCP Transect 9.

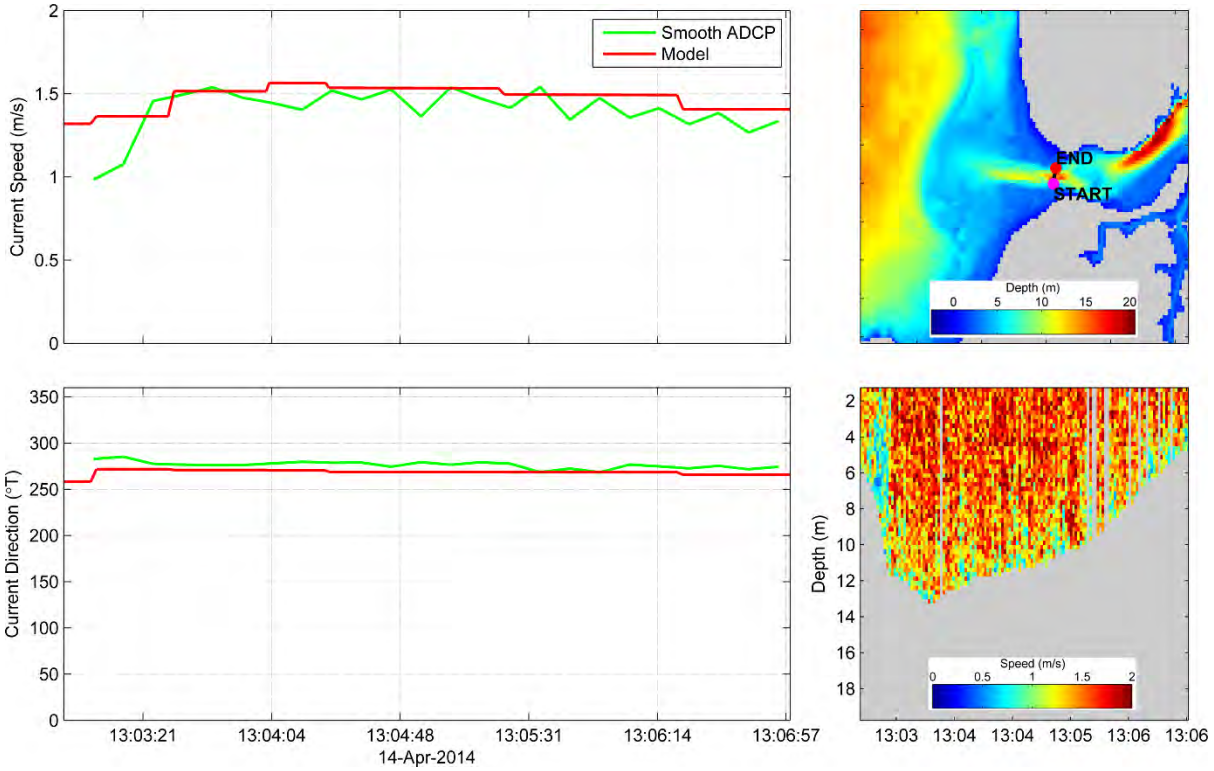

Figure C.10: ADCP Transect 10.

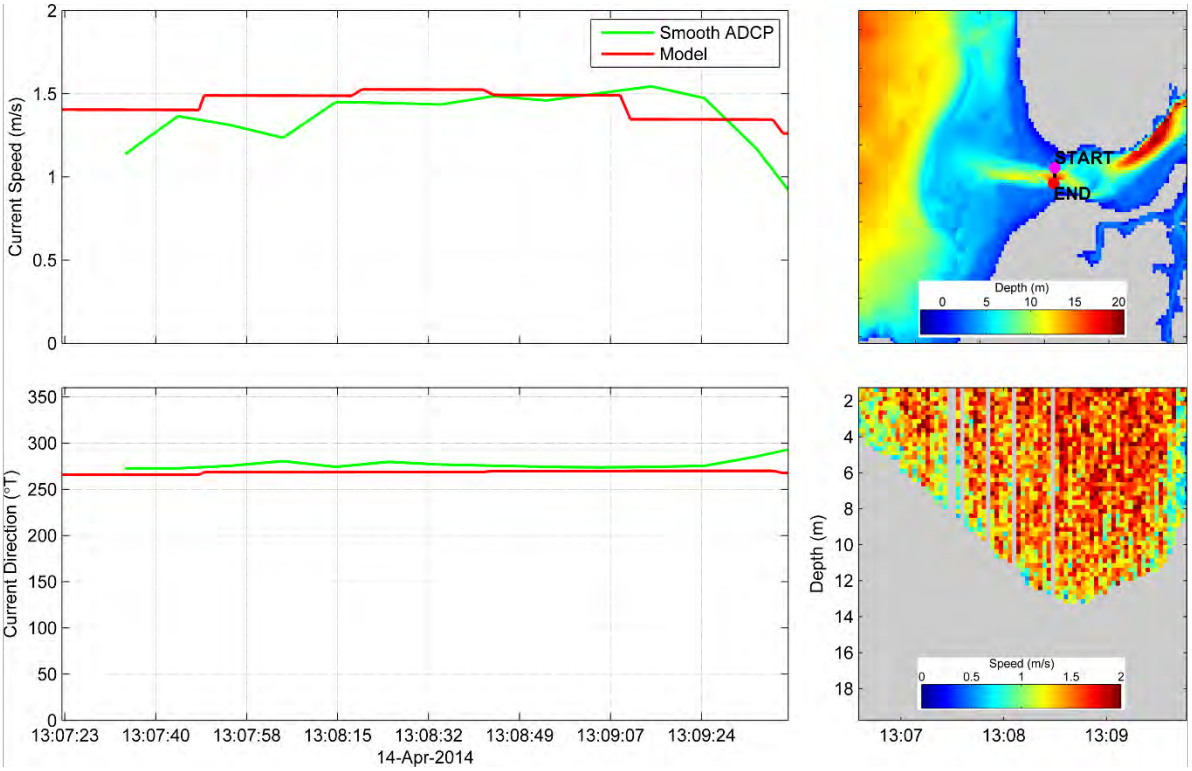

Figure C.11: ADCP Transect 11.

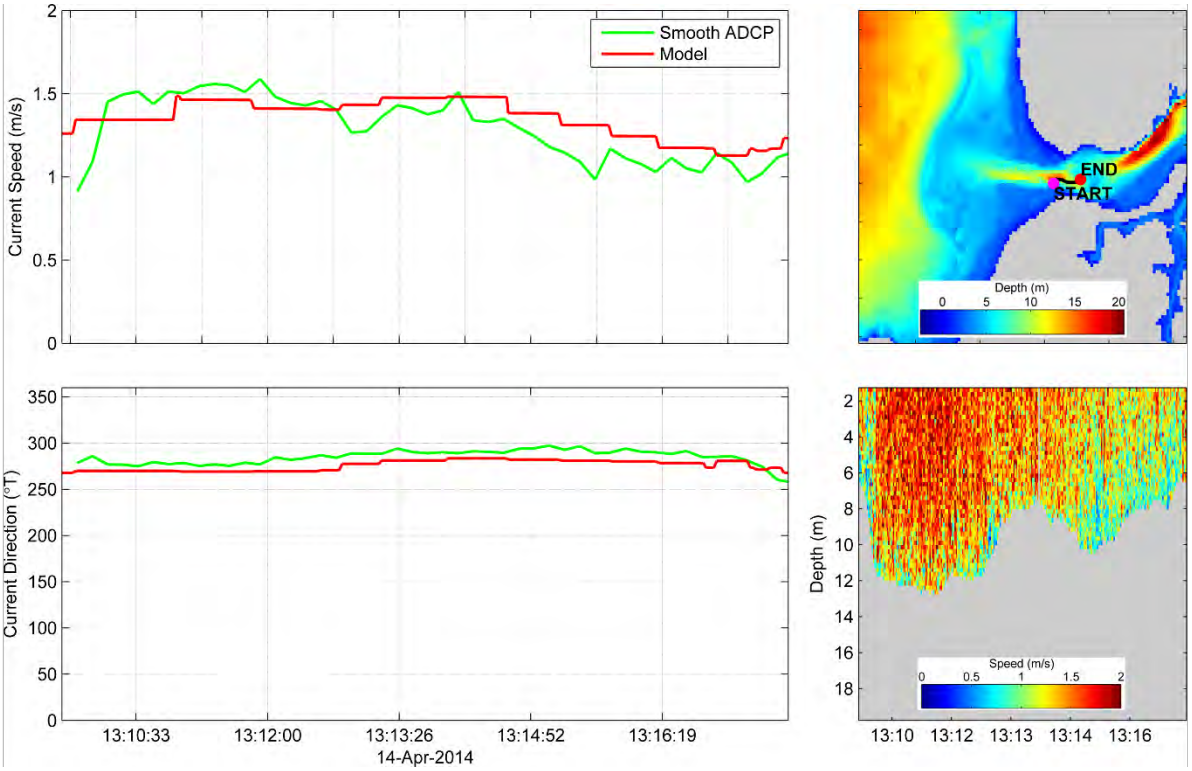

Figure C.12: ADCP Transect 12.

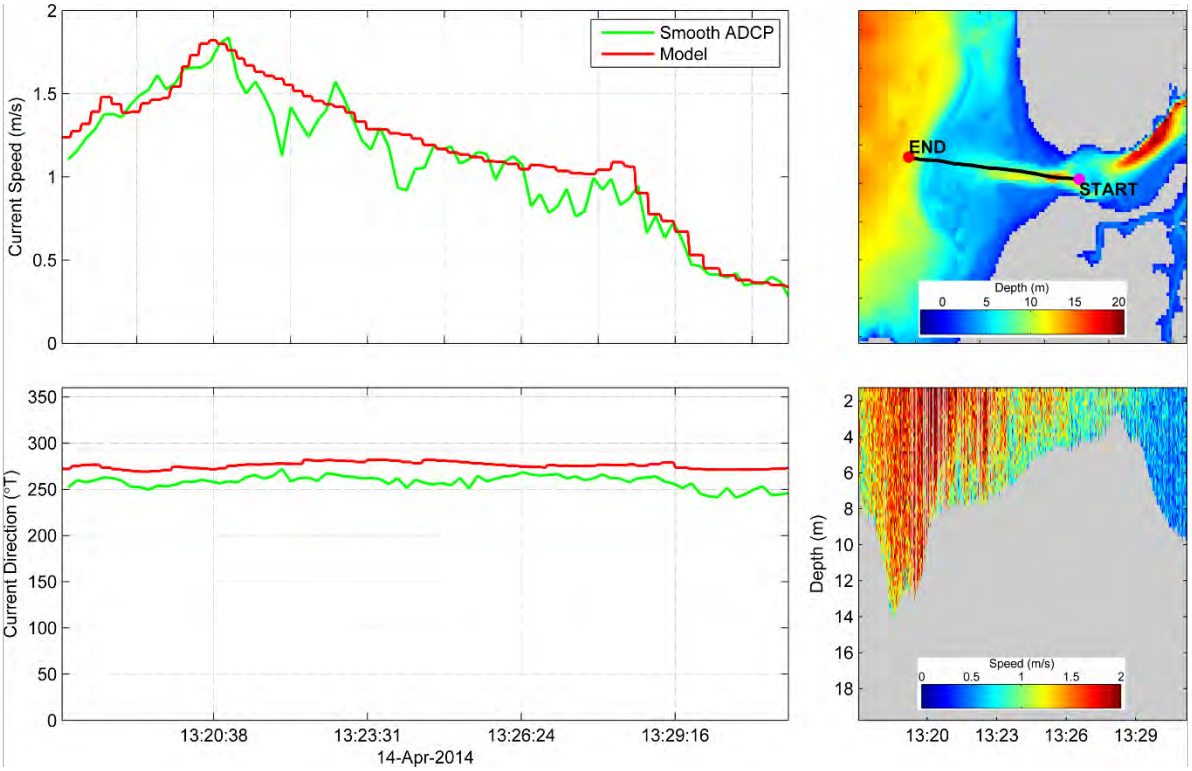

Figure C.13: ADCP Transect 13.

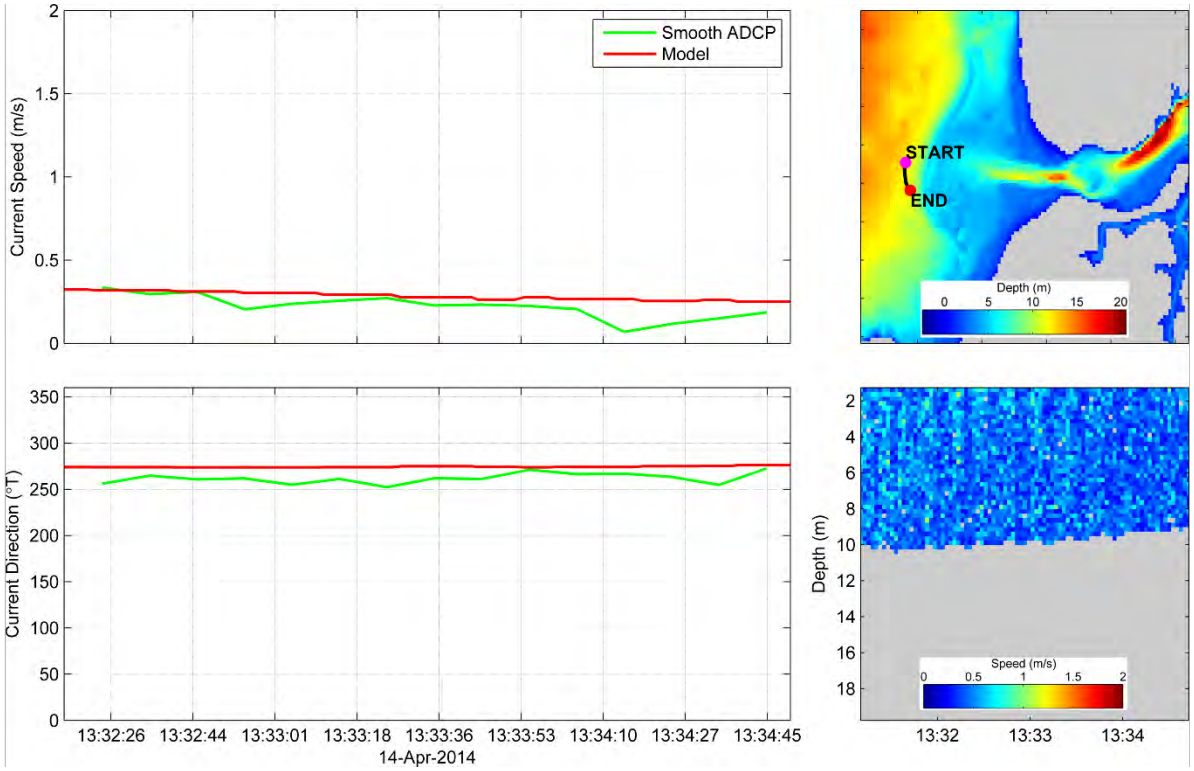

Figure C.14: ADCP Transect 14.

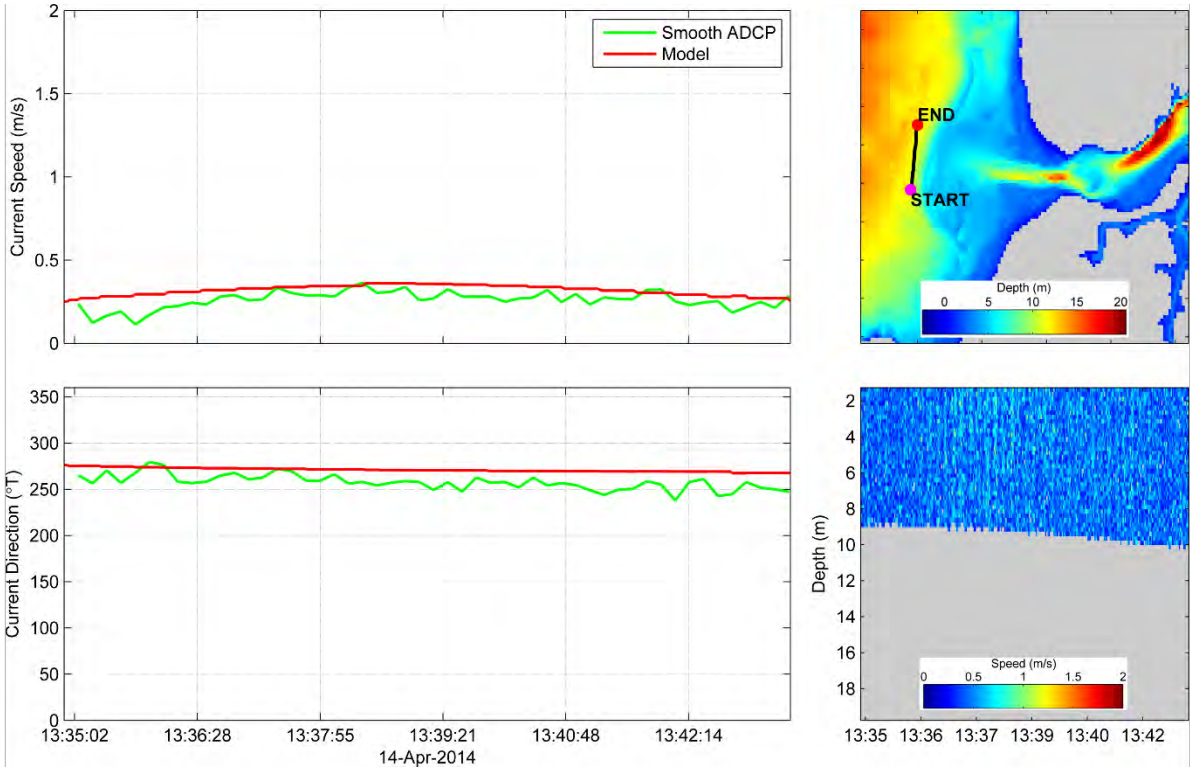

Figure C.15: ADCP Transect 15.

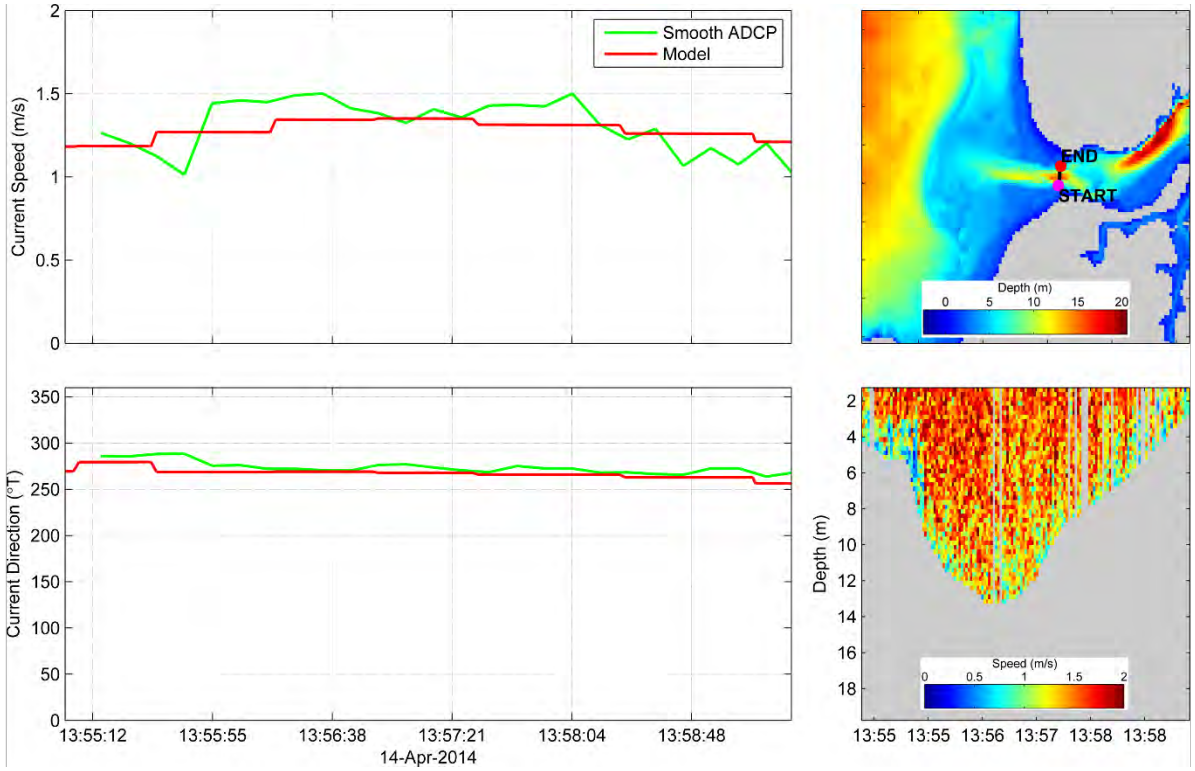

Figure C.16: ADCP Transect 16.

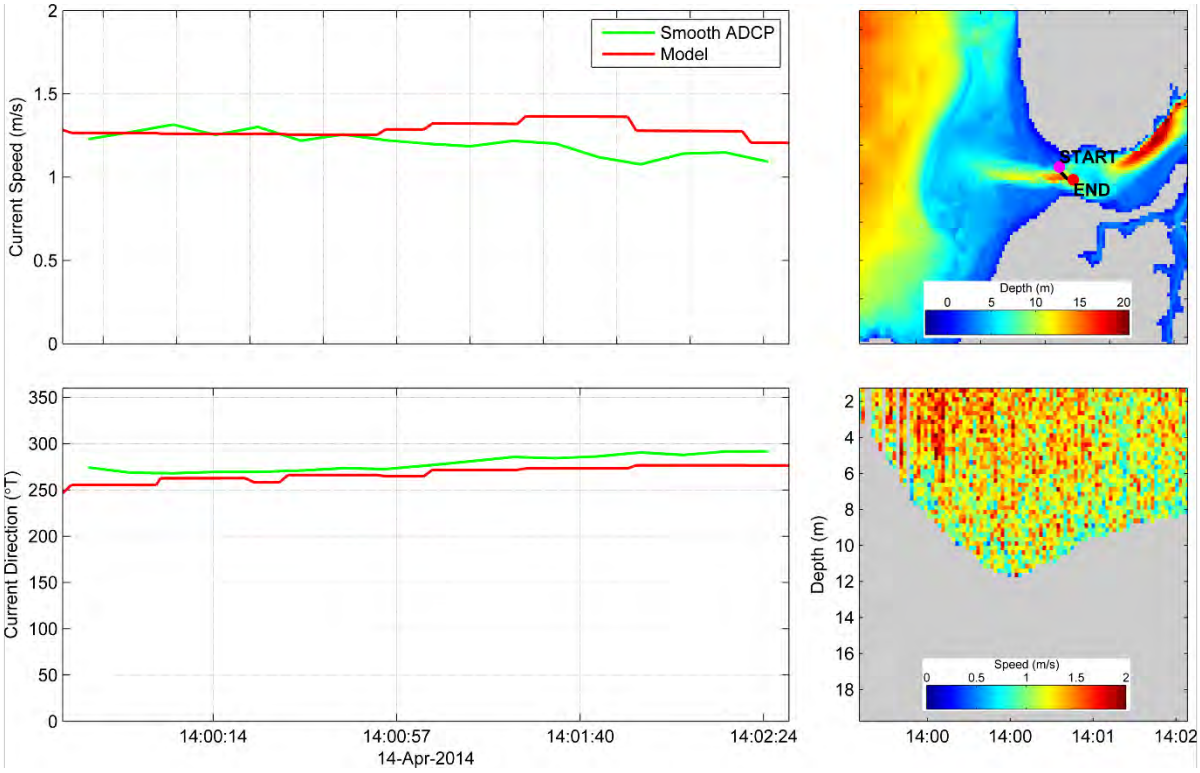

Figure C.17: ADCP Transect 17.

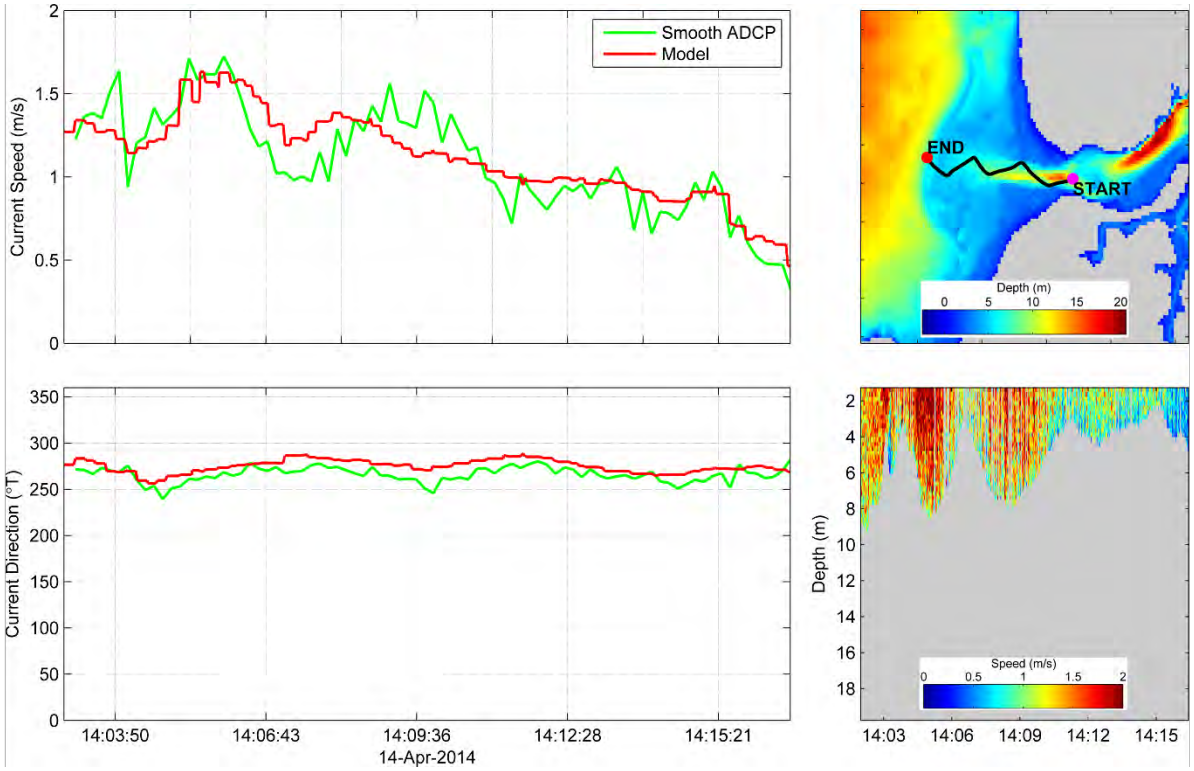

Figure C.18: ADCP Transect 18.

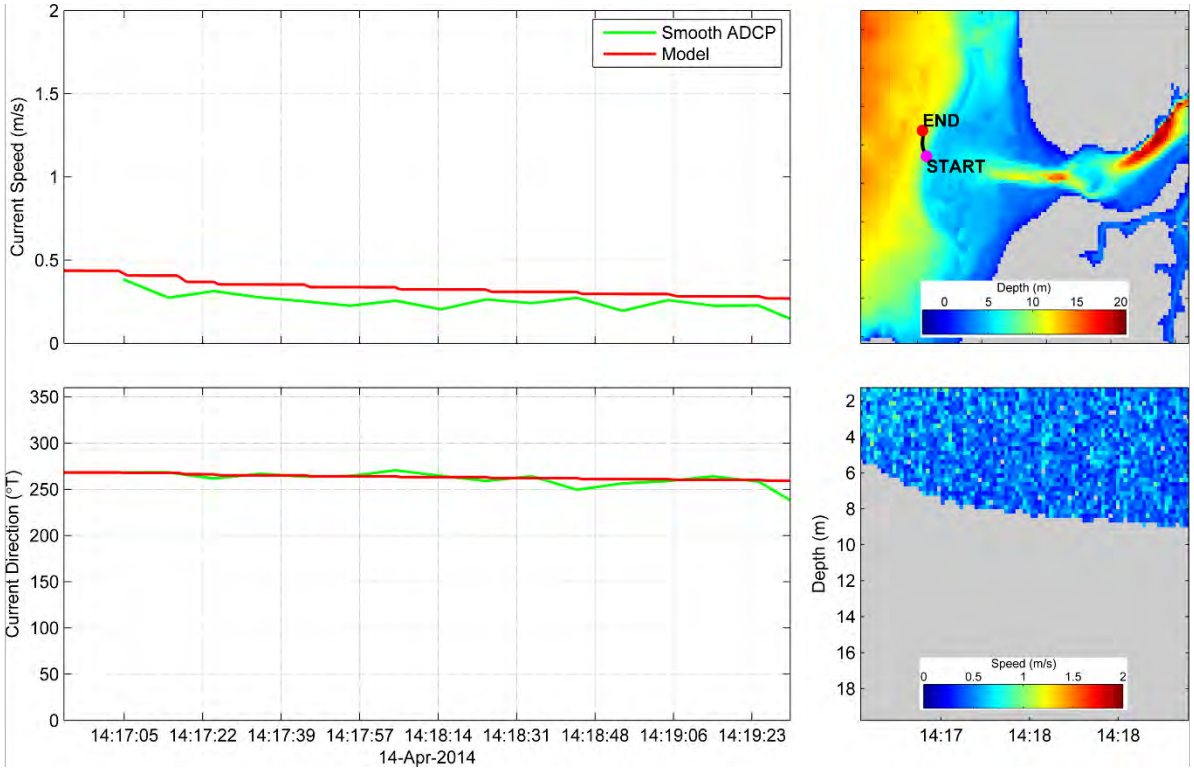

Figure C.19: ADCP Transect 19.

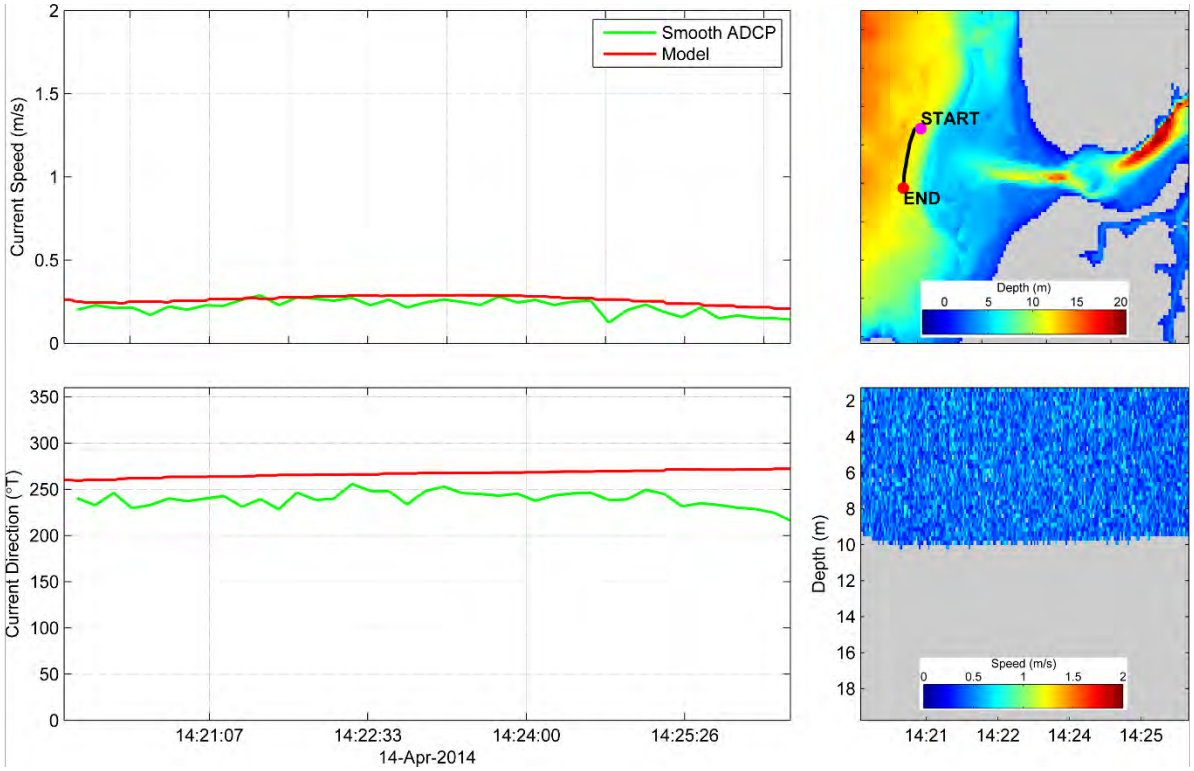

Figure C.20: ADCP Transect 20.

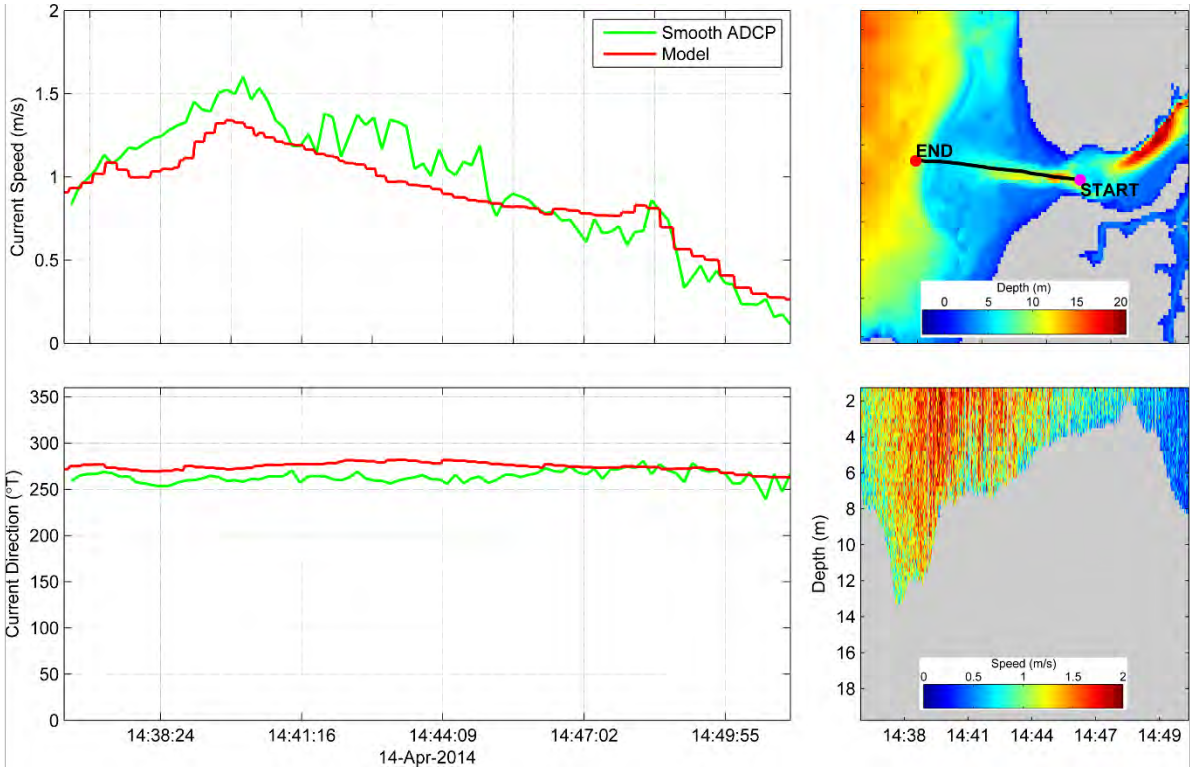

Figure C.21: ADCP Transect 21.

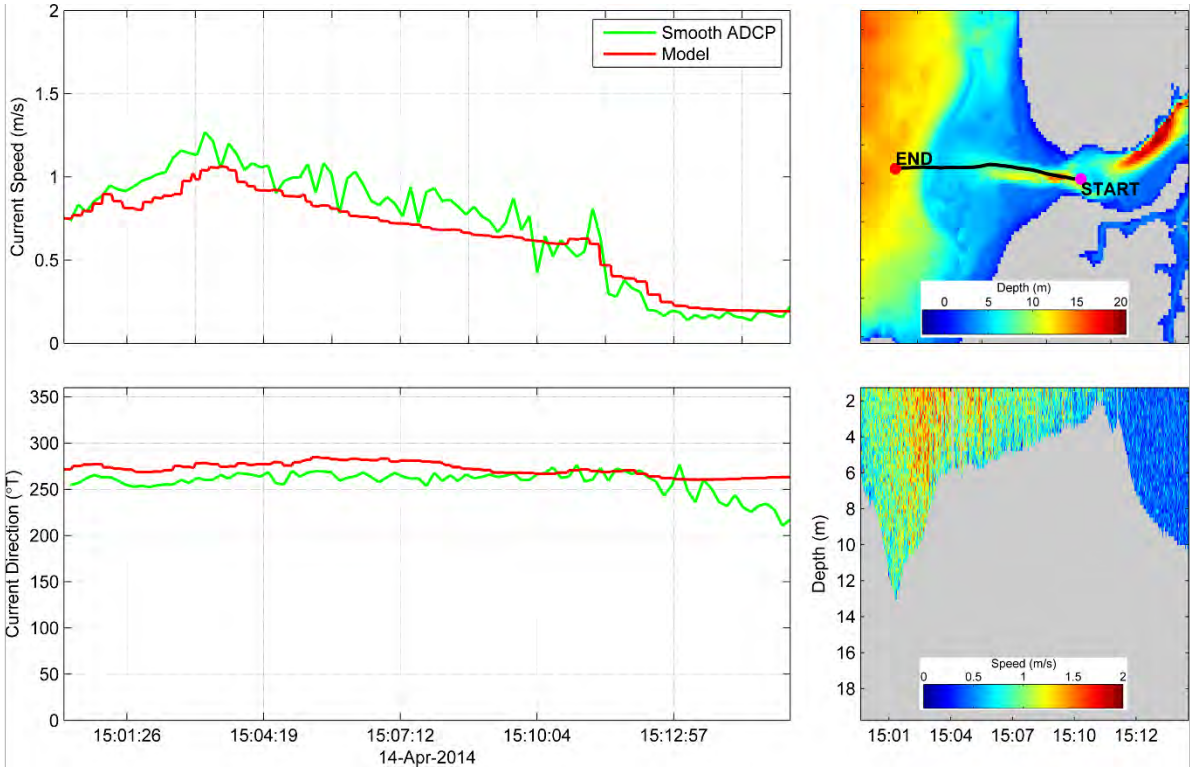

Figure C.22: ADCP Transect 22.

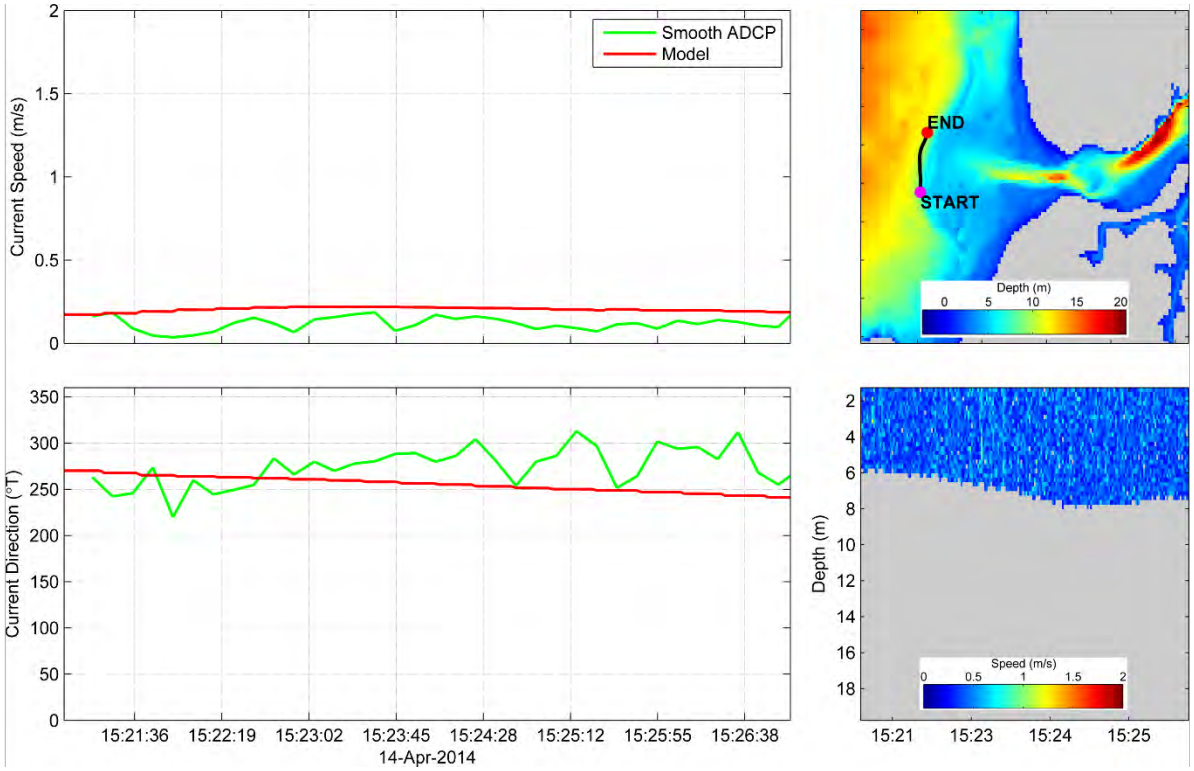

Figure C.23: ADCP Transect 23.

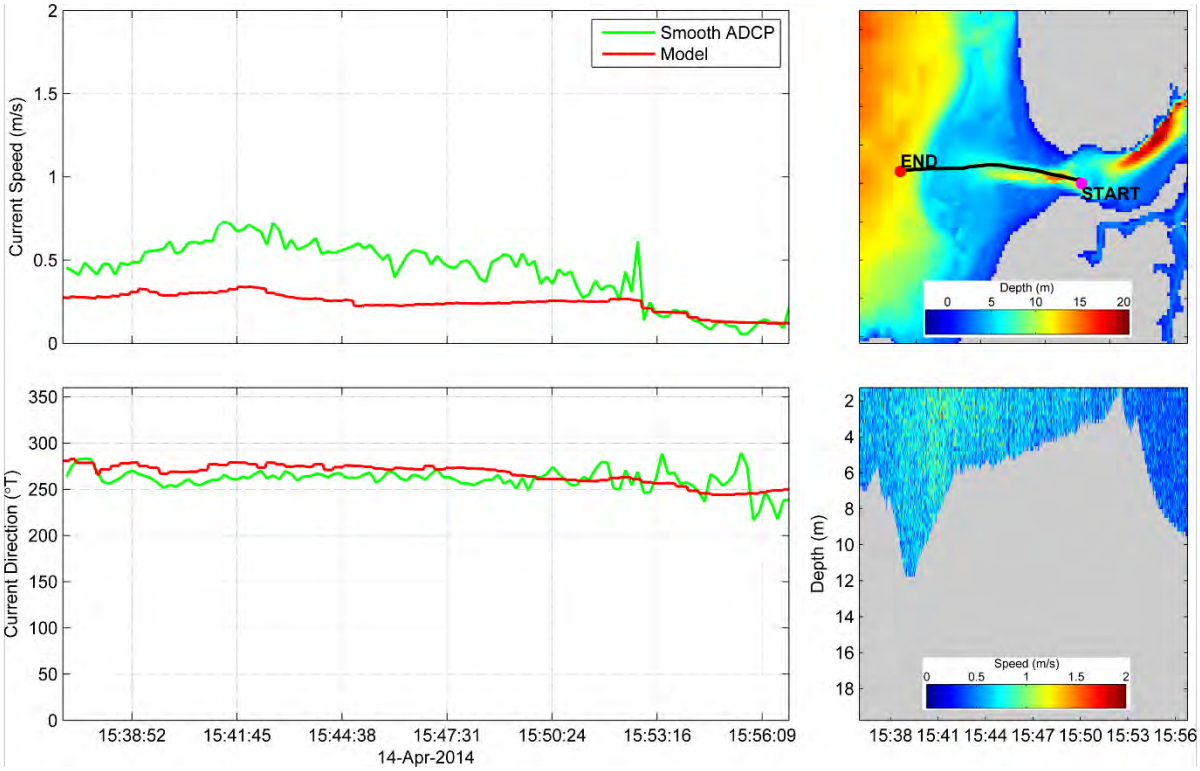

Figure C.24: ADCP Transect 24.